1990

Electrical Strengthening Of Soft Sensitive Clays (volumes I And Ii)

Kai Sing Ho

ELECTRICAL STRENGTHENING OF SOFT SENSITIVE CLAYS

Volume I

by

Kai Sing Ho

Faculty of Engineering Science

Submitted in partial fulfilment

of the requirements for the degree of

Doctor of Philosophy

Faculty of Graduate Studies

The University of Western Ontario

London, Ontario

September 1990

ISBN 0-315-59108-0

ABSTRACT

The damages brought by landslides of soft sensitive clay are so extensive that the safety of existing structures are threatened and new constructions are hindered. Traditional methods of soil improvement are usually inadequate, expensive and in some cases impossible. New method of soil improvement is therefore needed. With the advancing technology of electrostatics, two methods of electrical strengthening of soft sensitive clay are developed towards this goal. Electro-osmosis, the first method, is a phenomenon involving the transport of pore water in capillaries under the influence of a direct current electric potential. An electro-osmotic cell was developed to investigate this process in the laboratory and the results showed that the shear strength of the treated clay was increased by 172 % with the concurrent reduction of moisture content by 30 % under an applied voltage up to 6 volts. The physical and chemical properties are significantly improved.

A novel technique of electrical strengthening of soil is the application of dielectrophoresis. The process employs an alternating current high voltage, generating a converging electric field towards the electrode by which a net resultant movement of water in the clay mass is produced towards the direction of stronger electric field intensity. The water extraction caused the shear strength to increase drastically as much as 996 % with a corresponding moisture content reduction of 22 % , under an applied potential of 20 kV.

A field test was then undertaken to assess the effectiveness of these two

methods in strengthening the soft sensitive (Leda) clay in Gloucester test fill site. Specially designed copper electrodes were installed for electro-osmotic treatment to prevent gas accumulation around electrodes and to allow pore water in the soil to flow out from the cathodes without pumping. Field vane test results showed that the undrained shear strength increased uniformly by approximately 50 % throughout the depth of the electrodes in 32 days of treatment. The soft clay is shown to be "over-consolidated" and the strength in terms of effective stresses also increased. This improved version of electro-osmosis demonstrated its application in engineering practice.

The dielectrophoretic treatment was less effective due to water surrounding electrodes and electric short circuit problem. Nevertheless, this pioneer research enables the accumulation of experience that contributes to the foreseeable success of the process in the future.

ACKNOWLEDGEMENTS

The author wishes to express his sincere gratitude to Dr. K. Y. Lo and Prof. I. I. Inculet, his chief and co-advisers respectively, for their guidance, constant encouragement and support throughout the duration of this research program, and to Dr. R. M. Quigley for his continuous concern and interest.

The project was supported by the research grant of the National Science and Engineering Research Council of Canada. Additional funding was granted by Ontario Hydro to the field test in Gloucester test fill site and Ontario Graduate Scholarship to the author.

The author wishes to express his special thanks to Dr. M. Bozozuk of the Geotechnical Section, National Research Council of Canada, for his initiation, guidance, advice and discussion of the field test, and to Dr. J. H. L. Palmer and Dr. K. T. Law for their co-operation of conducting the field test, and to their Technical Staff for the assistance of installation of electrodes and soil sampling.

Sincere thanks are given to Mr. Dave Woytowich and the Technical Staff of the Store, Machine Shop and Electronic Workshop of the University of Western Ontario for their excellent work in building the laboratory apparatus and field equipment.

The author is indebted to Messrs. Gary Lusk, Kiny Kaniaru, Jiang-An Huang, Ting C. Yu, Edward K. W. San and Ms. Qiulin Shang of the Geotechnical Research Centre of the University of Western Ontario, for their assistance,

encouragement and discussion in the field test and they made the work effective and enjoyable. Thanks are also due to Mr. Wilbert Logan for carrying out part of the chemical tests for this research and to Mr. Gary Lusk in the preparation of part of the figures of this thesis.

Finally, the author wants to express his loving thanks to his wife, Helen, for her patience, understanding, support and encouragement throughout the work, and to his energetic four-year old son, Humphrey, for his participation and co-operation in the research work.

TABLE OF CONTENTS

VOLUME I

LIST OF TABLES

LIST OF FIGURES

APPENDIX

NOMENCLATURE

A	area (m^2)
A_o	concentration of wall charge of clay (ionic equivalents/unit volume of pore fluid)
C	constant
CIU	isotropically consolidated undrained triaxial test
c_v	coefficient of consolidation (m^2/year)
DP	dielectrophoresis
E	electric field (V/m)
E(x)	electric field at position x (V/m)
EO	electro-osmosis
F	force (N)
F_e	dielectrophoretic force (N)
F_o	Faraday constant (9.648456×10^4 C-mol^{-1})
h	hydraulic head (m)
i_e	electrical potential gradient (V/m)
i_h	hydraulic gradient
J	current density (A/m^2)
K	dielectric constant
k_e	electro-osmotic permeability (m^2/s-V)

k_h	hydraulic permeability (m/s)
L	sample length (m)
n	porosity
N	number of capillaries
p	dipole moment (coulomb-m)
pwp	pore water pressure (kPa)
q, q_1, q_2	charges (coulomb)
q_e	flow rate due to applied electric potential (m^3/s)
q_h	flow rate due to hydraulic gradient(m^3/s)
r	radius (m)
t	time (second)
T_v	time factor in one dimensional consolidation theory
u	pore water pressure (kPa)
u_o	constant
U(t)	degree of consolidation
V	electric potential (V)
V(x)	electric potential at position x (V)
V_e	velocity of water induced by applied electric potential gradient (m/s)
V_h	velocity of water induced by hydraulic gradient (m/s)
V_t	total velocity of water induced by electric potential and hydraulic gradients (m/s)

x	distance (m)
α	polarizability, constant
β	constant
γ_w	unit weight of water (kN/m^3)
ϵ	permittivity of the dielectric (Farad/m)
ϵ_o	permittivity of free space = $1/36\pi \times 10^9$ (Farad/m)
ζ	zeta potential (V)
η	fluid viscosity (kg/m-s)
ν	pore radius (m)
$P(x)$	resistivity at position x (ohm-m)
σ_c	preconsolidation pressure (kPa)

CHAPTER 1

INTRODUCTION

It was 130 years after the discovery of electro-osmosis that the process was first applied in geotechnical engineering by L. Casagrande in 1939. Since then its application was demonstrated in a number of projects for the stabilization and improvement of soils (Casagrande 1947, 1949, 1952a,b, Soderman and Milligan 1961, Bjerrum et al 1967, Fetzer 1967, Wade 1976). A wide variety of soil was treated such as sensitive silt, soft clay and very sensitive clay. In most cases electro-osmosis was only used for temporary stabilization such as excavation or dewatering. However, unsuccessful application was also reported (Caron 1971a,b). It has often been considered that, in spite of the successful case histories, the process was economically impractical and retained as the last resort until field problem was encountered.

A number of laboratory experiments was carried out to study the fundamentals of electro-osmosis (Esrig et al 1967, Gray and Mitchell 1967, Mitchell and Wan 1977, Johnston and Butterfield 1977, Banerjee and Vitayasupakorn 1984) but no full scale field test was then conducted to support the investigation. On the other hand, most past field applications were performed urgently when problems were encountered and the project engineers were not interested in correlating the field work with laboratory study. In view

of this deficiency, a systematic research program was proposed to investigate the process in greater details and to develop a new version of electro-osmotic process for field treatment.

The treatment was focused on the strengthening of soft sensitive clay (Champlain Sea or Leda clay) in Eastern Canada. Deposits of soft sensitive clay covers a large proportion of the lowlands of the St. Lawrence River and Ottawa Valleys. Extensive networks of past and future constructions such as highway embankments, bridges, earth dams of major hydro-electric generating facilities are located in this area. It is therefore of engineering and economic importance to improve the soil properties of the soft sensitive clay.

Due to the advancement of the application of electrostatics, a novel approach of electrical strengthening of soil by dielectrophoresis was also studied. In contrast to electro-osmosis in which a high direct current and a uniform electric field are applied, dielectrophoresis is an electrical phenomenon resulting from the application of low alternating current and a high nonuniform electric field. The theory was first developed by Phol (1951) with significant physical, chemical and biological applications but no work has been done in the application of dielectrophoresis to soils. Theoretically, this process was found (Inculet and Lo 1988) to be possible to remove water (as particle) from the clay medium and its power consumption would be low. It was therefore decided to explore this novel technique and to investigate the feasibility of its application in electrical strengthening of soft sensitive clay.

This thesis consists of three parts. The first part is the laboratory investigation of electro-osmosis that focused on the investigation of the mechanism of soil strengthening by this process and the development of an improved method of treatment. This included the development of a new electro-osmotic cell for laboratory tests and a new electrode design for field application. It is followed by a series of laboratory investigations for the better understanding of the process of dielectrophoresis and its possibility of soil strengthening. The experimental results lead to the development of high voltage electrode for field application. Finally a full scale field test in Gloucester test fill site was carried out to assess the effectiveness of these two processes in strengthening the soft sensitive clay and the performance of the two new electrode designs. It is hoped that, with the improved version of electro-osmosis and the novel technique of dielectrophoresis, the experience gained in this study will contribute to a solution to the stabilization and improvement of properties of soft sensitive clay. It is also expected that these two electrical strengthening methods may receive wider application as a result of these studies.

PART I

LABORATORY INVESTIGATION OF ELECTRO-OSMOSIS

CHAPTER 2

INTRODUCTION

The electrical induced flow across porous material was first noticed by Reuss in 1809 and the first field application of electro-osmosis in soil was successfully demonstrated by Casagrande in 1939 (Casagrande 1941). Since then, the process has been applied to different type of soils, ranging from sensitive silt (Wade 1976), to soft clay (Fetzer 1967), to very sensitive clay (Bjerrum 1967). Interesting case of application of electro-osmosis include increasing the bearing capacity of H-piles in loose silt (Soderman and Milligan 1961). Three piles were re-tested 10 years after driving and the treatment was proven to be permanent (Ministry of Transportation Report 1981). Bozozuk and Labrecque (1969) applied the process in a reversed manner to reduce the negative skin friction of long composite steel and concrete pile in soft sensitive clay.

In spite of the success in the past, the process has not received wider application, probably due to the high operation costs and some remaining uncertainties about the process. A research program to explore improvement of the process and the relationships between electrical and soil parameters was therefore undertaken.

In the first part of this thesis, the objectives are;

(a) to investigate the mechanism of soil strengthening by electro-osmosis,

(b) to assess the applicability of the available theoretical solution particularly on the prediction of the development of pore water pressure, and

(c) to develop an improved method of treatment.

The preliminary investigation consisted of an extensive review of past experimental work and case history of the subject, followed by the development of an electro-osmotic cell. The experimental stage involved the study of electro-osmosis on clays in the electro-osmotic cell under different sample lengths, various applied voltages, and with or without electrodes reversal. Model tests were also included as to investigate the process under simulated field situation. Laboratory tests were performed to study the variation of parameters before and after treatment.

CHAPTER 3

THEORETICAL BACKGROUND

3.1 Theories of Electro-Osmosis

The electrical induced flow across porous material was first discovered by Reuss (1809). In 1879, Helmholzt developed a mathematical model in trying to explain the phenomenon. The model was further refined in later years by Smoluckowski (1914). The model indicates that there exists a double layer immediately adjacent to the capillary wall in a capillary tube as shown in Figure 3.1 (Casagrande 1952a). The inner layer, which is relatively thin as compared to the outer layer consists of negative ions strongly attached to the wall. The outer layer contains movable positive ions. Immediately adjacent to the double layer is a portion of free water. Due to the application of electric current, the mobile positive ions will be attracted toward the cathode, dragging along with them the free water molecules and resulted in the general movement of water from anode to cathode.

The velocity of water moved under the influence of applied potential according to Helmholtz-Smoluchowski theory is,

$$V_e = \frac{\zeta K}{4\pi\eta} \frac{\Delta V}{\Delta L} \qquad (3.1)$$

where $\frac{\Delta V}{\Delta L}$ = electrical potential gradient

ζ = potential across the capillary (zeta potential[1])

K = dielectric constant

η = fluid viscosity

In a cross sectional area A of N number of capillaries with each having an area a, the flow will be,

$$q_e = \frac{\zeta K}{4\pi\eta} \frac{\Delta V}{\Delta L} Na \qquad (3.2)$$

Since Na is equal to nA, where n is the porosity for the given mass, therefore equation (3.2) becomes,

$$q_e = \left(\frac{\zeta Kn}{4\pi\eta}\right) \left(\frac{\Delta V}{\Delta L}\right) A = k_e i_e A \qquad (3.3)$$

in which k_e is the electro-osmotic permeability and i_e is the electrical potential gradient, in analogy to Darcy's law of fluid flow.

In contrast to the hydraulic permeability k_h, the electro-osmotic permeability k_e is independent of pore size. Since the porosity of soils varies within a relatively narrow limit, it is expected that the electro-osmotic permeability will lie in a close range as well. As reported by Casagrande (1952a) and Mitchell (1976) the range in which k_e would expect to fall is within 1×10^{-4} and 1×10^{-5}

[1] Zeta or electrokinetic potential is the electric potential in the double layer at the interface between a particle which moves in an electric field and the surrounding medium (Mitchell 1976). The zeta potential is not the same as the surface potential of the double layer, although factors that give hign values of surface potential also give high values of zeta potential. A common interpretation is that the actual slip plane in electrokinetic processes is located some small, unknown distance from the surface of particles; thus zeta potential should be less than surface potential (see Figure 3.5). Values of zeta potential in the range of 0 to -50 mV are typical for clays, with the lowest values associated with high pore water salt concentration.

^{5} cm^2/V-s, as shown in Table 3.1. Casagrande (1952a) suggested that for most practical applications, k_e of 5 x 10^{5} cm^2/V-s would be sufficient.

Schmidt (1950, 1951) proposed another theory describing the electro-osmotic mechanism by assuming a uniform distribution of positive ions throughout the entire pore space of a much smaller pore diameter. The flow according to Schmidt model is,

$$q_e = \frac{A_o F_o \nu^2}{8\eta} n i_e A \qquad (3.4)$$

or,

$$q_e = k_e i_e A \qquad (3.4a)$$

where,

ν = pore radius

A_o = concentration of wall charge

F_o = Faraday constant.

with n and η are the same as before.

The relation described by equation (3.4) implies that k_e varies as square of pore radius ν. Both Schmidt and Helmholzt-Smoluchowski theory are applicable to their own capillary size. The former is to a coarser pore while the latter is to a finer pore.

Spiegler (1958) introduced a totally different concept of electro-osmotic flow which based on the relative degree of frictional interaction between the ions and the wall of pores. Spiegler model is conceptually useful but

analytically, it requires complicated and lengthy computations and this model will not be discussed here.

The significant difference between electro-osmotic flow and the hydraulic flow can be illustrated by comparing Figure 3.2 and Figure 3.1. In hydraulic flow, due to the stationary double layer, only the middle portion of the capillary will contribute to the flow whereas in electro-osmotic flow (Figure 3.1), the entire cross-sectional area will contribute to the flow.

3.2 Development of Mathematical Models

In order to simplify the derivation of the mathematical equations, the following assumptions are made,

(1) soil is isotropic and saturated

(2) physical-chemical properties of soil are uniform and remain constant with time

(3) electrophoresis and electrolysis do not occur

(4) electric field remains constant with time

(5) the flow due to electrical potential gradient and hydraulic gradient can be superimposed.

In one-dimensional combined electrically and hydraulically induced flow, the total velocity can be written as,

$$V_t = V_e + V_h \qquad (3.5)$$

where,

V_e = velocity of water induced by electrical potential gradient

V_h = velocity of water induced by hydraulic gradient.

According to Darcy's Law,

$$V_h = k_h (\partial h/\partial x)$$

And similarly, there is a proportionality between V_e and the electrical potential gradient $(\partial V/\partial x)$ such that,

$$V_e = k_e (\partial V/\partial x)$$

Therefore, equation (3.5) can be rewritten as

$$V_t = k_e \frac{\partial V}{\partial x} + k_h \frac{\partial h}{\partial x} \qquad (3.6)$$

Considering a system with sealed anode (anode with drainage line closed) and drained cathode (cathode with drainage line opened), at equilibrium, the electro-osmotic flow is equal to the counter flow caused by the electrically induced hydraulic gradient in which the net flow will be zero. With $\partial h=(\partial u/\gamma_w)$, where γ_w is the unit weight of water and ∂u is the change in pore water pressure, then, equation (3.6) becomes,

$$\frac{k_h}{\gamma_w}\frac{\partial u}{\partial x} = - k_e \frac{\partial V}{\partial x}$$

Integrating yields

$$u = - \frac{k_e}{k_h} \gamma_w V(x) + C$$

At cathode, $u = 0$ (opened) and $V = 0$, therefore $C = 0$.

Then,

$$u = - \frac{k_e}{k_h} \gamma_w V(x) \qquad (3.7)$$

Equation (3.7) describes the electro-osmotically induced pore water pressure at equilibrium, with closed anode and opened cathode. The induced pressure will be maximum at the anode and decreases linearly to zero at the cathode as given in Figure 3.3.

Due to the fact that k_e is relatively constant for most soils and the k_h varies from 1×10^{-4} to 1×10^{-9} cm/s for different soils, it suggested that the induced negative pore water pressure at equilibrium will be high for soil having low hydraulic permeability. But the lower is the hydraulic permeability, the lower will be the rate of flow. It appears that there is a range of k_h in which the electro-osmotic process will be effective. Beyond or below that range, the treatment is either ineffective (high k_h, low induced pore water pressure) or not feasible (low k_h, long treatment time).

Esrig (1968a) showed that by using the continuity equation and applying the law of conservation of mass, the conventional one-dimensional consolidation equation will also hold true for electro-osmotic consolidation. That is,

$$\frac{\partial u}{\partial t} = c_v \frac{\partial^2 u}{\partial x^2} \qquad (3.8)$$

where c_v is the coefficient of consolidation and u=u(x,t), a function of distance from cathode and time. The equation is identical to the classical equation for one dimensional consolidation and the solutions for consolidation of clays therefore also applies to electro-osmosis consolidation with the appropriate boundary and initial conditions.

For one-dimensional electro-osmotic flow, Esrig (1968a) showed that, by applying the continuity equation and the law of conservation of mass, the conventional one-dimensional consolidation equation will also hold true for one-dimensional electro-osmotic consolidation. For the system of closed anode and opened cathode, the pore water pressure u(x,t), in kPa, at position x along the sample at time t is given by,

$$u(x,t) = -\frac{k_e}{k_h}\gamma_w V(x) + \frac{2k_e\gamma_w V}{k_h\pi^2}\sum_{n=0}^{\infty}\frac{(-1)^n}{(n+\frac{1}{2})^2}\sin\frac{(n+\frac{1}{2})\pi x}{L}\left[\exp(-(n+\frac{1}{2})^2\pi^2 T_v)\right] \qquad (3.9)$$

where,

V(x) = electric potential at position x relative to the potential at cathode at x=0 (volt)

V = maximum potential (volt)

γ_w = unit weight of water (kN/m^3)

L = length of sample (m)

x = distance from cathode (m)

T_v = time factor in one dimensional consolidation theory

k_h = hydraulic permeability (m/s)

k_e = electro-osmotic permeability (m^2/s-V).

The development of negative pore water pressure with time described by equation (3.9) is plotted in Figure 3.4. As t approaches to infinity,

$$u(x,\infty) = -\frac{k_e}{k_h}\gamma_w V(x) \qquad (3.10)$$

Equation (3.10) indicates that, for one-dimensional electro-osmotic consolidation, the induced negative pore water pressure at any point in the soil during treatment is proportional to the potential at that point relative to the potential at x=0 (cathode).

Equation (3.10) can further be developed by writing it in terms of current density and resistivity. By definition,

$$E(x) = J\rho(x) \qquad (3.11)$$

$$V(x) = -\int_0^x E(x)dx \qquad (3.12)$$

where,

$E(x)$ = electric field (V/m)

J = current density (ampere/m^2)

$\rho(x)$ = resistivity of soil at position x (ohm-m)

Combining equations (3.11) and (3.12),

$$P(x) = -\frac{1}{J}\frac{dV(x)}{dx} \tag{3.13}$$

and, equation (3.12) becomes,

$$u(x,\infty) = \frac{k_e}{k_h}\gamma_w J\int_0^x P(x)dx \tag{3.14}$$

Note that x is in opposite direction with J (x is measured in a direction from cathode to anode while current flows from anode to cathode), therefore a negative sign will result after integration to indicate that the pore pressure is negative. From equation (3.14), it may be seen that the induced negative pore water pressure at equilibrium is a function of the current density and resistivity of the soil. The reason for deriving this relationship is that the current density is the governing quantity in the process. For example, if there is no current, the process will not occur no matter how high the voltage is. It is therefore more appropriate, at least for the interest of electrical engineering study, to describe electro-osmosis in terms of current density and resistivity instead of using the term "voltage". However, the terms "voltage", "applied voltage" and "applied potential" will also be used in future discussions in order to be consistent with the past experimental work.

3.3 Electrolysis at Electrodes

In the development of electro-osmosis theories and a mathematical model as described in sections 3.1 and 3.2, the electrochemical effect is neglected in the description of the electrically induced flow through a soil mass. The explanation of electro-osmosis lies in the electrochemical nature of soil particle surfaces and the pore water. According to colloidal theory, a clay particle, when suspended in water, has a negatively charged surface. Surrounding the particle is a diffuse double layer of positive ions. Most rigidly attached to the surface is the first layer of cations, often called the Stern Layer (Figure 3.5); with greater distance from the soil particle, the attractive force between the soil particle surface and cations diminishes, giving rise to an increasingly diffuse ionic atmosphere (the double layer), where the ions are relatively free to move (Figure 3.5). Beyond the double layer, the ion concentration is equal to that of the free pore water. Because of the polar nature of water molecules they are oriented around cations. In the presence of water, the hydrated radius of an ion may thus increase to several times its original, nonhydrated dimension. Applying an electric potential to a saturated soil causes the hydrated cations to move towards the cathode, dragging free water with them. The movement is primarily generated in the diffuse double layer where the cations dominate.

During the application of current, the clay-water electrolyte system behaves like a electro-chemical cell in which cations migrate towards cathode and anions migrate towards anode. At the cathode, the principal reaction is the reduction

of hydrogen from water (Potter 1956, Conway 1965),

$$2H_2O \rightleftharpoons H_3O^+ + OH^- \quad (3.15a)$$

$$H_3O^+ + e + M \rightleftharpoons MH + H_2O \quad (3.15b)$$

$$MH + H_3O^+ + e^- \rightarrow H_2\uparrow + H_2O + M \quad (3.15c)$$

or,

$$2H_3O^+ + 2e^- \rightarrow H_2\uparrow + 2H_2O \quad (3.15d)$$

or,

$$4H_2O + 4e^- \rightarrow 2H_2\uparrow + 4OH^- \quad (3.15e)$$

where M is the metal used as electrode. The increase in hydroxide ions concentration may enhance the precipitation of metallic hydroxide. As a result, the pH at the cathode region and of the effluent will increase. At the anode, the possible oxidation reactions are the oxidation of the metallic electrode into its oxide and oxidation of hydroxide ions into oxygen. The following equations describe the chemical reactions at anode (Potter 1956, Conway 1965).

$$2H_2O \rightleftharpoons H_3O^+ + OH^- \quad (3.16a)$$

$$OH^- + M \rightarrow MOH + e^- \quad (3.16b)$$

$$MOH + OH \rightarrow MO + H_2O + e^- \quad (3.16c)$$

$$2MO \rightarrow O_2\uparrow + 2M \quad (3.16d)$$

or,

$$4OH^- \rightarrow O_2\uparrow + 2H_2O + 4e \quad (3.16e)$$

or,

$$2H_2O - 4e^- \rightarrow O_2\uparrow + 4H^+ \quad (3.16f)$$

As a result, the soil adjacent to the electrode will be impregnated with metallic oxide and the pH at the anode region will decrease.

As a consequence of reactions (3.15) and (3.16), in addition to the migration of existing anions and cations in the pore fluid of the soil sample under the electric field, two supplemental ionic species, H^+ and OH^-, are generated which can have a significant influence on the local conductance. Figure 3.6 displays this changing chemistry across the soil sample. After a period of electrolysis, concentration gradients as sketched in Figure 3.7 may exist.

The chemical reaction described by equations (3.16a) to (3.16f) depends on the type of metal used as anode. For example, if copper is used as anode, copper oxide (CuO) will be formed onto the copper anode. Hydroxides of iron will be precipitated on iron anode causing anode corrosion, with little or no evolution of oxygen. Platinum is stable and all the reactions described in equations (3.16a) to (3.16f) will be completed with the evolution of oxygen. It can be seen from these equations that the chemical reaction desired will influence the selection of material for the electrodes.

3.4 Soil Chemistry Factors Affecting Electro-Osmosis

One of the measures of effectiveness of electro-osmosis for use in soils and tailings is the amount of water transferred per unit charge passed, for example, in terms of litres/ampere-hour. Unlike the electro-osmotic permeability this

quantity may vary over several orders of magnitude depending upon such factors as exchange capacity, water content, and electrolyte concentration. A rational basis for examining the influence of these factors can be developed from thermodynamic considerations without recourse to a specific kinetic model.

In fine grained soils and negatively charged tailings, balancing cations (counter-ions) provide an excess of cations over anions in the pore water and there is a net transfer of water in the direction of counter-ion or cation movement. The rate of water r- vement depends on the applied electric field, the flow resistance of the soil, and the frictional drag of the ions on the water molecules. Thus, of fundamental importance are both the cation-anion distribution, and the water-ion distribution. The Donnan theory can be used to give the equilibrium distribution. The basis for the Donnan theory is that at equilibrium the potentials of the internal (double layer) and external solutions are equal and that electro-neutrality is required in both phases. The ratio of cation to anion in the internal phase, R, for the case of a symmetrical electrolyte is given by (Gray and Mitchell 1967),

$$R = \frac{C^+}{C} = \frac{1 + (1 + y^2)^{\frac{1}{2}}}{-1 + (1 + y^2)^{\frac{1}{2}}} \qquad (3.17)$$

where,

$$y = \frac{2C_o \pm \gamma}{B_o \pm \gamma'} \qquad (3.18)$$

where C_o is the concentration in external solution, $\pm\gamma$ is the mean molar activity

coefficient in the external solution, $\pm\gamma'$ is the mean molar activity coefficient in the internal (double layer) solution, and B_o is the surface charge density per unit pore volume. The parameter B_o is related to the exchange capacity by (Gray and Mitchell 1967),

$$B_o = \frac{cec\ \rho_w}{\omega} \times 100 \qquad (3.19)$$

where cec is the cation exchange capacity in meq/g, ρ_w is the density of water (g/cm^3), and ω is the water content in percent. The higher the R ratio, the greater the electro-osmotic transport, on assuming that all the other factors are equal.

Equations (3.17) to (3.19) show that high R ratios are favoured by a high exchange capacity (active clay), a low water content, and low salinity in the external solution. In inactive clays or media with low exchange capacity, the concentration of anions (co-ions) in the double layer builds up rapidly as the salinity of the external solution increases.

High electro-osmotic effectiveness also requires that the water to cation ratio be high. A high exchange capacity, low water content system may have good co-ion exclusion properties and be relatively insensitive to increases in external electrolyte, but there is less water per cation than in a low exchange capacity, high water content system. This effect combined with the cation-anion ratio consideration leads to the water transport-water content-soil type-electrolyte concentration prediction shown schematically in Figure 3.8. Tests

carried out by Gray and Mitchell (1967) on sodium kaolinite (inactive clay) and sodium illite (relatively more active clay) gave the results shown in Figure 3.9, which agree with the predictions of Figure 3.8.

The results of electro-osmosis measurements on a number of materials are summarized in Figure 3.10 (Gray and Mitchell 1967), which shows water flow as a function of water content. This figure may be used as a guide for prediction of electro-osmotic flow rates in other soils as well. The flow rates shown are for open systems, with solution admitted at the anode at the same time it is extracted from the cathode. Electrochemical effects and water content changes were minimized for the tests used to obtain the data shown. Thus, the values could be interpreted as upper bounds on the flow rates.

To estimate the effectiveness of electro-osmosis in a given case, values of the water content, electrolyte concentration of the pore water, and type of clay are required. The former is readily measured, the electrolyte concentration is easily determined using a conductivity cell or atomic absorption spectrometer, and the latter can be estimated on the basis of plasticity and grain size data or more accurately from the mineralogical data determined by the x-ray diffraction technique.

In the present research, the soft sensitive clay (Leda clay) in the Ottawa area (Gloucester) will be used. The clay is inactive having the low exchange capacity value of 10 to 20 meq/100g, electrolyte concentration of 10^{-3} to 10^{-1} N and moisture content of 50 to 80 %. If these values are plotted in Figure 3.8,

the possible relation can be represented by the enclosed area ABCD. This schematic prediction according to the Donnan concept indicates that the electro-osmotic treatment of the soft sensitive clay is possible.

Table 3.1 Coefficient of Electro-Osmotic Permeability
(after Casagrande 1952a and Mitchell 1976)

Material	Water Content (%)	k_e (x 10^5 cm/sec-V)
London Clay	52.3	5.8
Boston Blue Clay	50.8	5.1
Kaolin	67.7	5.7
Clayey Silt	31.7	5.0
Rock Flour	27.2	4.5
Na-Montmorillonite	170	2.0
Na-Montmorillonite	2000	12.0
Mica Powder	49.7	6.9
Fine Sand	26.0	4.1
Quartz Powder	23.5	4.3
Ås Quick Clay	31.0	2.0-2.5
Bootlegger Cove Clay	30.0	2.4-5.0
Silty Clay (West Branch Dam)	32.0	3.0-6.0
Clayey Silt (Little Pic River)	26.0	1.5

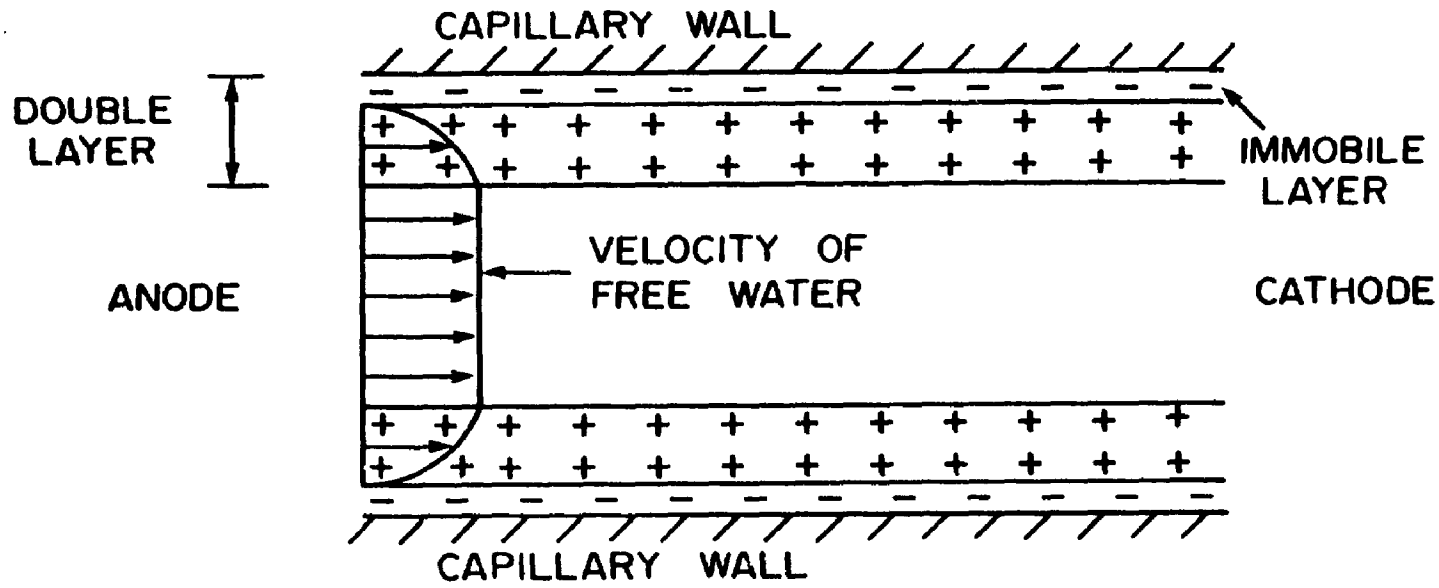

FIGURE 3.1 CROSS-SECTION OF CAPILLARY (after Casagrande 1952a)

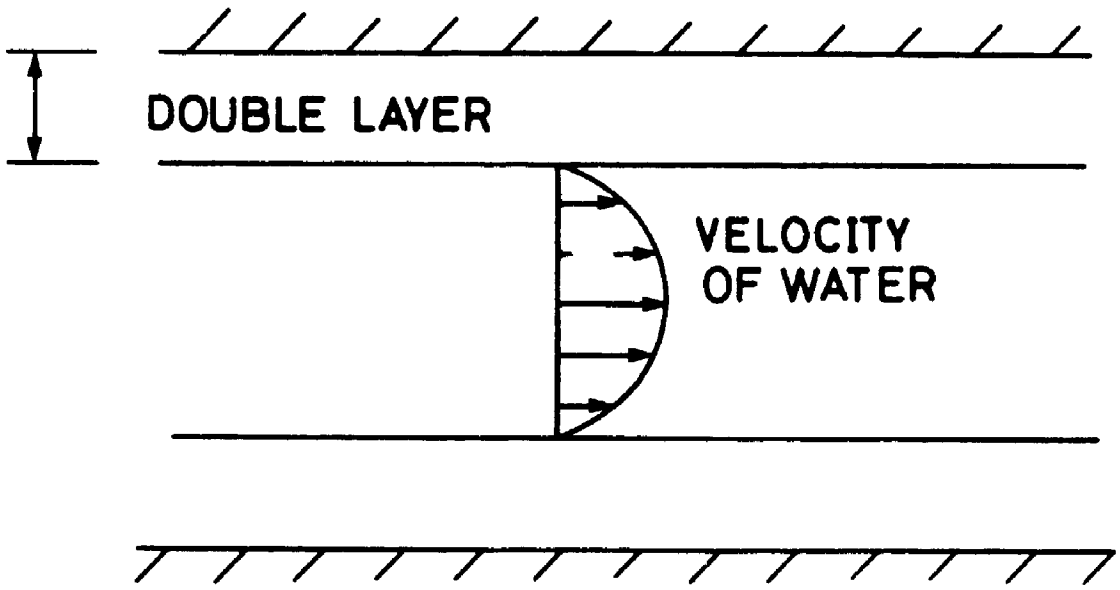

FIGURE 3.2 HYDRAULIC FLOW IN CAPILLARY
(after Casagrande 1952 a)

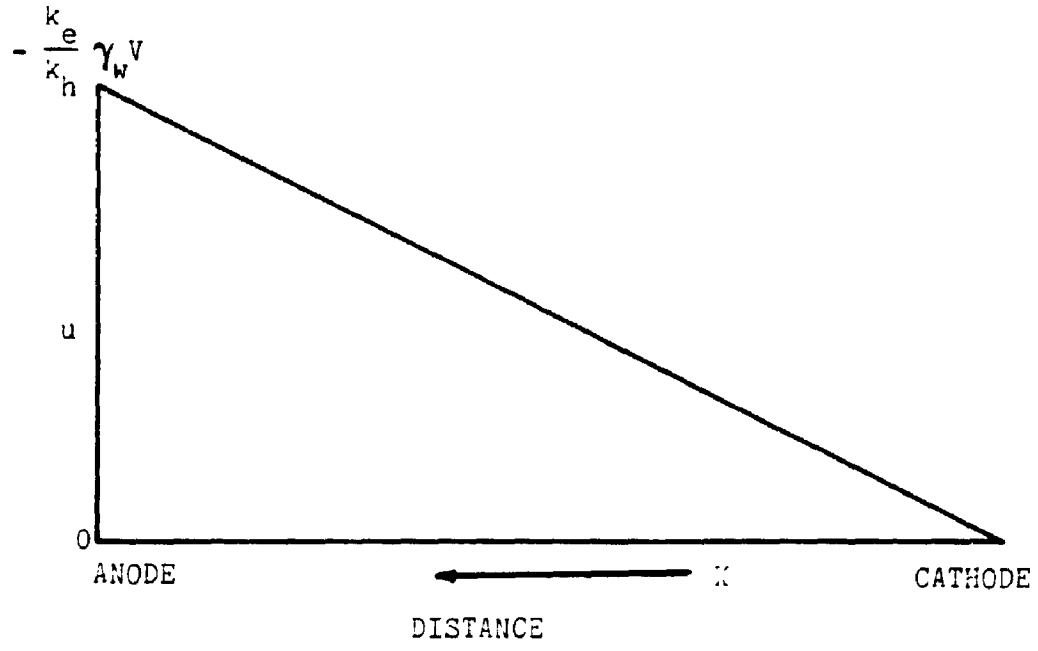

FIGURE 3.3 THE PORE WATER PRESSURE INDUCED AT EQUILIBRIUM FOR THE CASE OF OPENED CATHODE AND CLOSED ANODE (after Esrig 1968a)

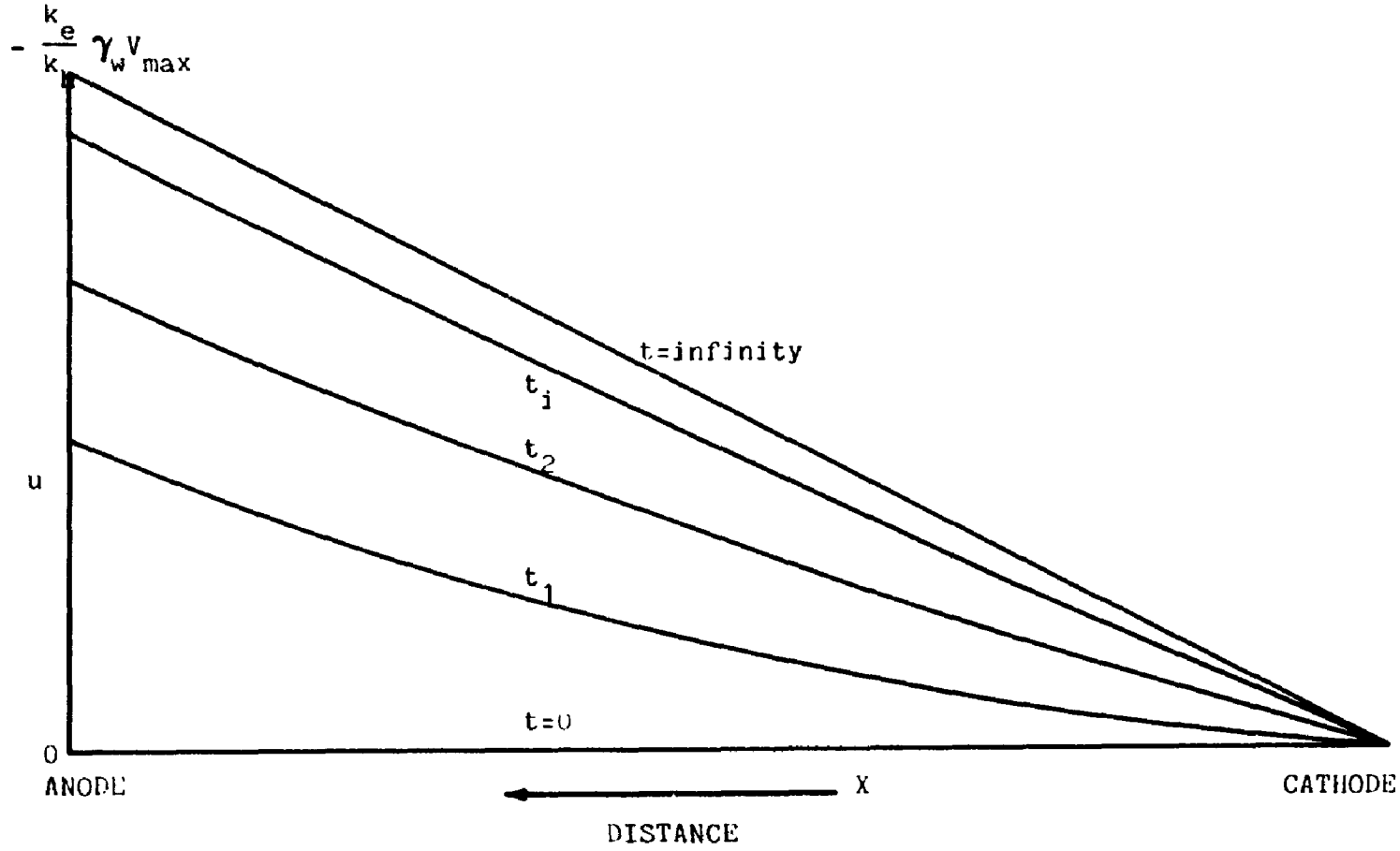

FIGURE 3.4 THE DEVELOPMENT OF PORE WATER PRESSURE WITH TIME (t) FOR THE CASE OF OPENED CATHODE AND CLOSED ANODE (after Esrig 1968a)

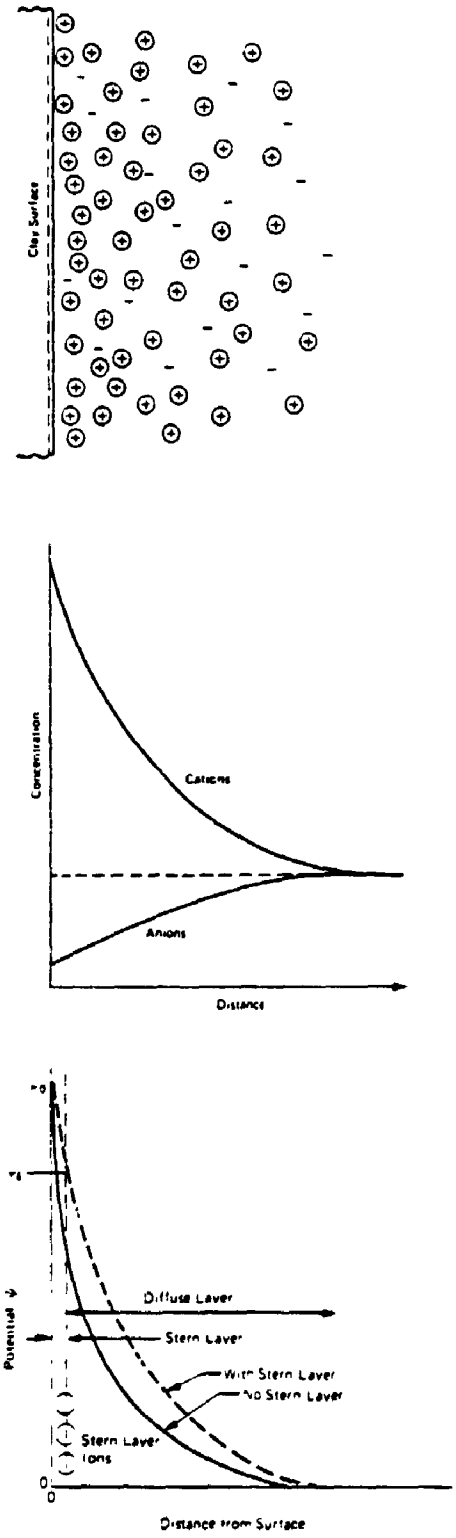

FIGURE 3.5 DISTRIBUTION OF IONS ADJACENT TO A CLAY SURFACE ACCORDING TO THE CONCEPT OF THE DIFFUSE DOUBLE LAYER (after Mitchell 1976)

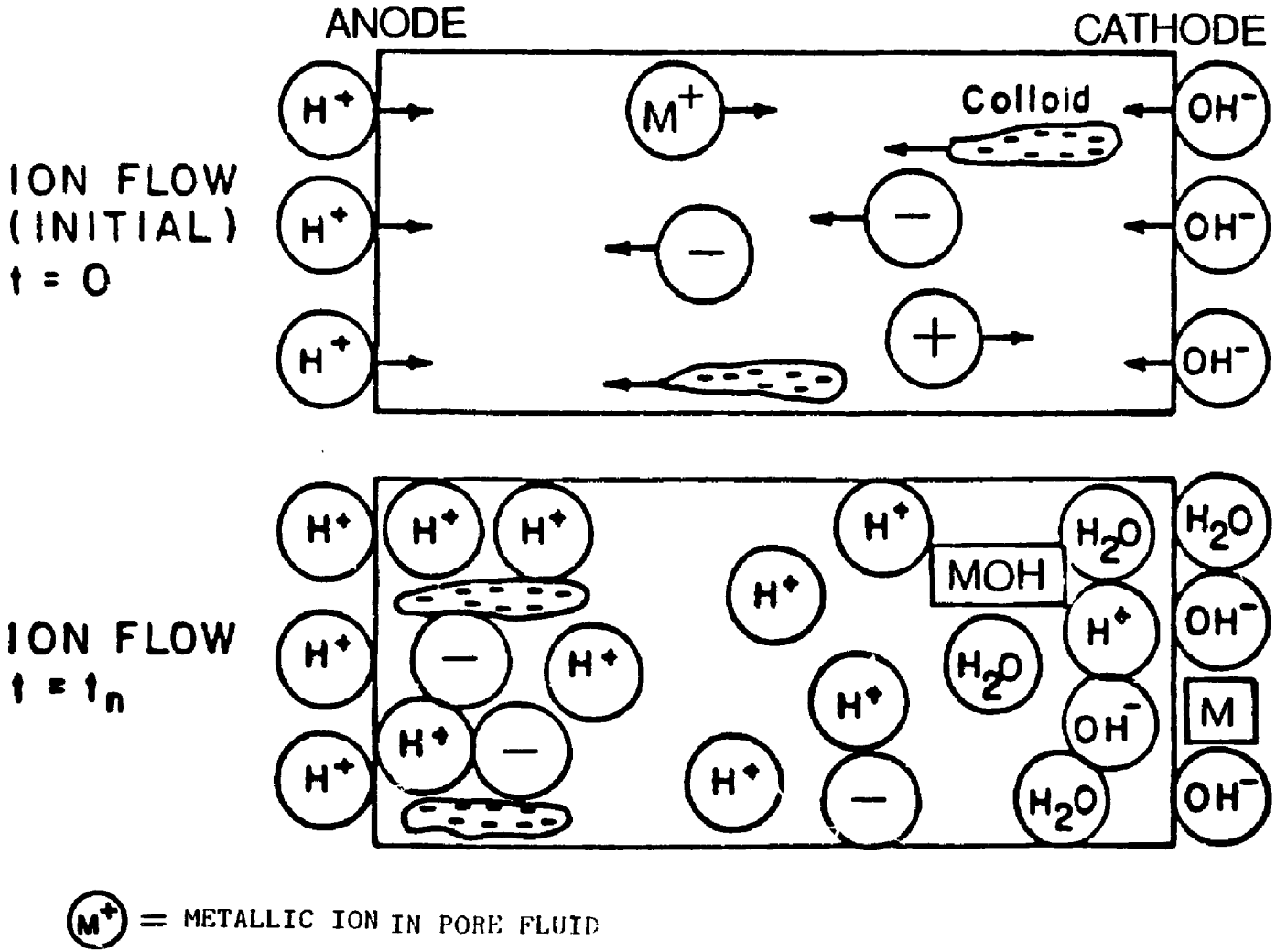

FIGURE 3.6 SCHEMATIC DIAGRAM OF ELECTROKINETIC SOIL PROCESSING AND THE ION FLOW

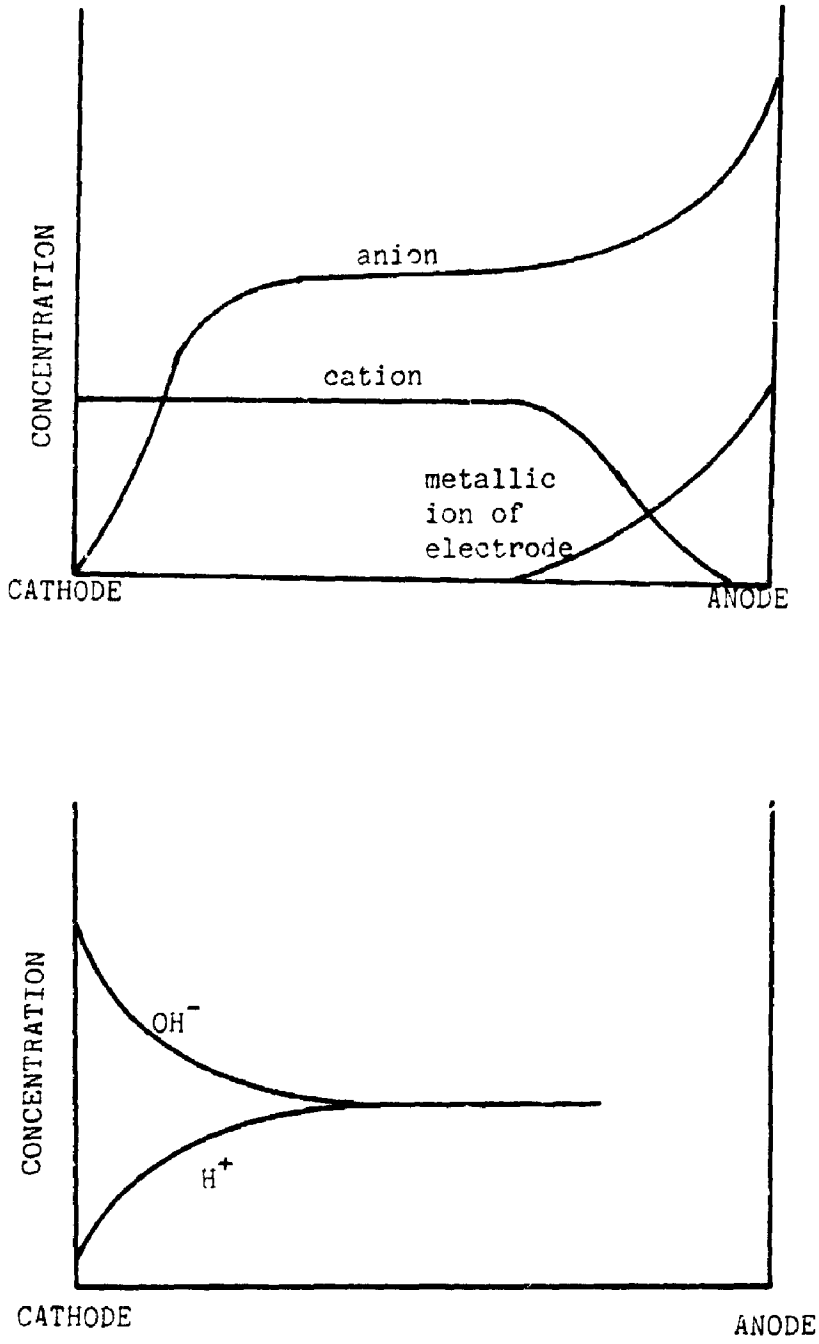

FIGURE 3.7 CONCENTRATION GRADIENTS FOR
(a) MAJOR IONS DURING ELECTROLYSIS
(b) H^+ AND OH^- NEAR THE CATHODE
(after Ferguson and Nelson)

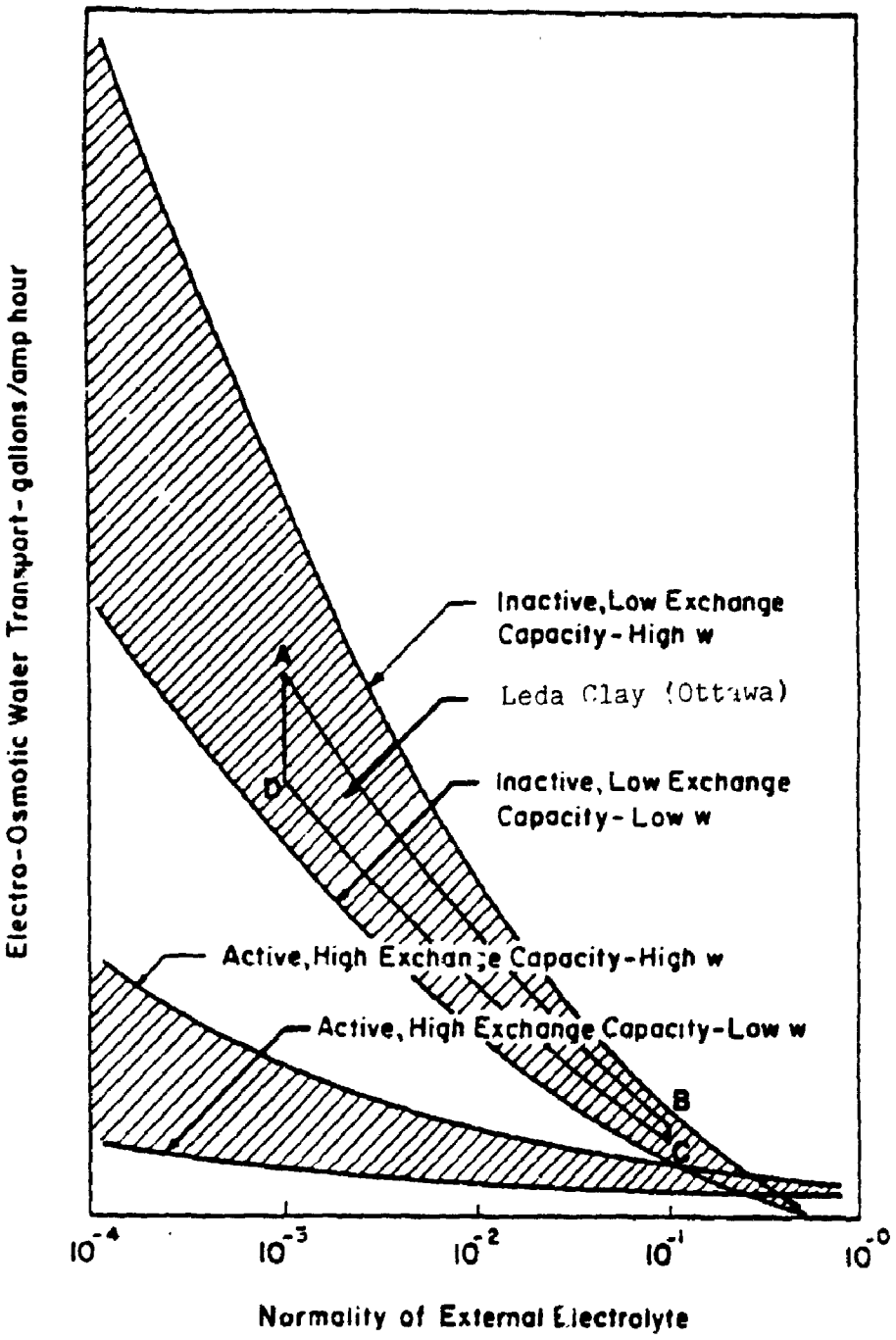

FIGURE 3.8 SCHEMATIC PREDICATION OF ELECTRO-OSMOSIS IN VARIOUS CLAYS ACCORDING TO THE DONNAN CONCEPT (after Gray and Mitchell 1967)

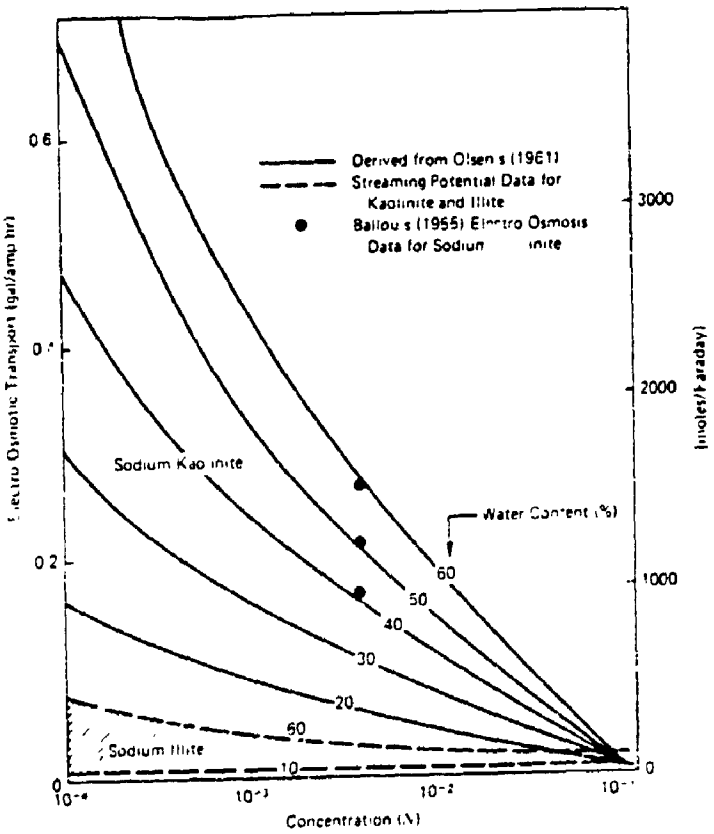

FIGURE 3.9 ELECTRO-OSMOTIC WATER TRANSPORT VS CONCENTRATION OF EXTERNAL ELECTROLYTE SOLUTION FOR HOMOIONIC KAOLINITE AND ILLITE AT VARIOUS WATER CONTENTS
(after Gray and Mitchell 1967)

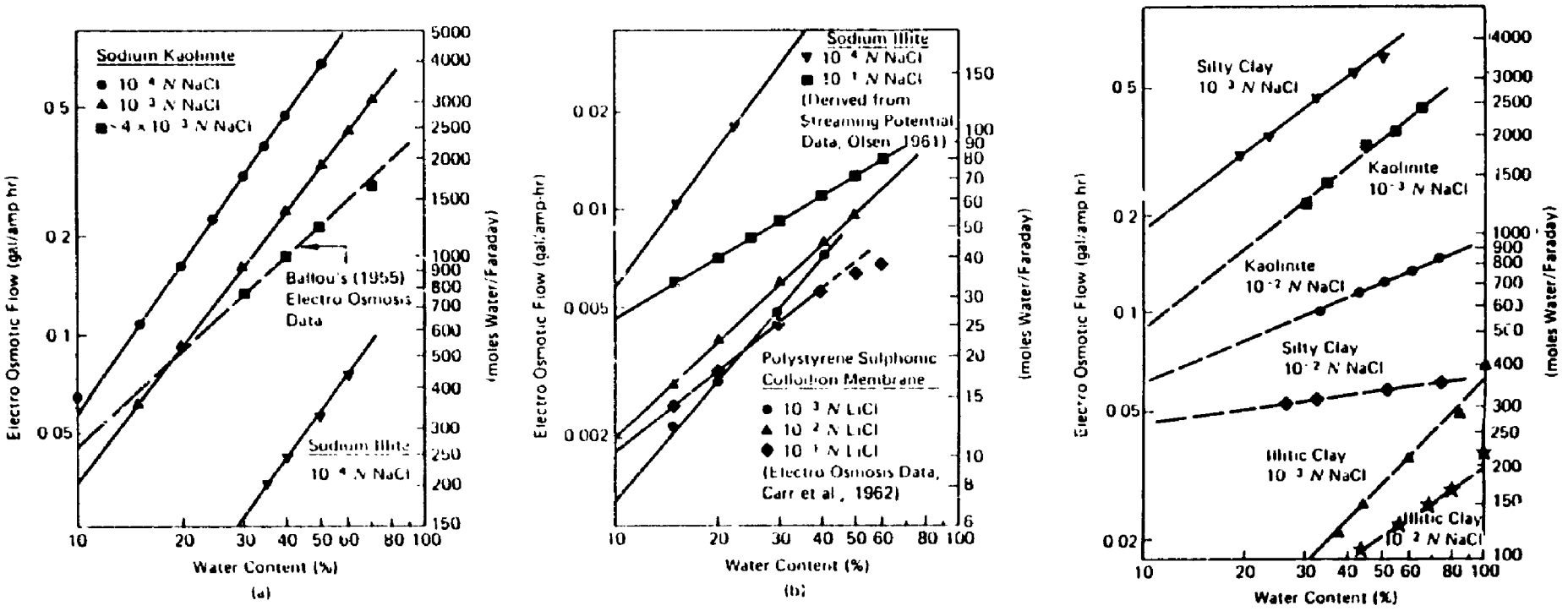

FIGURE 3.10 Electro-osmotic water transport as a function of water content, soil type, and electrolyte concentration.
(a) Homoionic kaolinite and illite
(b) Illitic clay and collodian membrane
(c) Silty clay, illitic clay, and kaolinite
(after Gray and Mitchell 1967)

CHAPTER 4

REVIEW OF PAST EXPERIMENTAL WORK AND CASE HISTORIES

In this chapter, some major experimental work and case histories are reviewed. A better experimental apparatus and procedures can then be designed after gaining the experience from the previous researchers.

4.1 Experimental Studies

(a) Wang and Vey (1953)

Direct measurement of the induced pore water pressure during electro-osmotic treatment was first performed by Wang and Vey (1953). In the experiment, silty loam was compacted inside a transparent lucite cylinder (76 mm diameter) and was enclosed by perforated steel electrode as anode on the top and perforated copper electrode as cathode on the bottom of the cylinder with both ends connected to a constant head of water. An electric potential of 115 volts was applied. During the first day of treatment, pore water pressure at the middle region was decreased to about -17 kPa. On the second day, the pressure was at -27 kPa. But the pore water pressure started to increase from then on. On the third day, the measured pressure was -7 kPa. At day 8, the pore water pressure returned to its original value. A total of about 3.8 percent settlement was measured. After treatment, 3 distinct patterns of cracks were

observed along the sample as shown in Figure 4.1.

(b) Evans and Lewis (1966)

Direct measurement of induced pore water pressure was also performed by Evans and Lewis (1966) for electro-osmotic tests on collo-kaolin for positive pore water pressure measurement and on silty clay for negative pore water pressure measurement. For the test on collo-kaolin (opened anode and closed cathode), a maximum pressure of 150 kPa was induced under 1.5 volts applied electric potential after 40 minutes and 240 kPa under 2 volts applied electric potential after 14 minutes. For test on silty clay (closed anode and opened cathode), a maximum pressure of about -180 kPa was measured after 10 minutes of treatment. The applied electric potential in the test on silty clay was not described in the report.

(c) Esrig (1968a)

Two reduced scale field tests were performed by Esrig (1968a). In one test, two 0.76 m (2.5 ft) long pipe electrodes were installed at 0.46 m (1.5 ft) apart and an electric potential of 250 volts at 3 to 5 A (amperes) was applied. The pore water pressure along the two electrodes was measured. The results are shown in Figure 4.2. A maximum pressure of -80 kPa was measured at anode after the electrical power was switched on for 2½ hours. Further development of negative pore water pressure was prevented due to the

formation of gas bubbles on the surface of the electrodes. In the other test, a 3.66 m (12 ft) square aluminium landing mat was used as anode placed horizontally to the ground with five 0.76 m (2.5 ft) long pipe electrodes spaced evenly and perpendicular to the mat as cathode. During the test, pore water pressure and voltage at selected locations between the electrodes were measured at depth 0.46 m (1.5 ft) and 0.76 m (2.5 ft). The results are shown in Figure 4.3 which shows that an almost linear relationship is obtained between the applied voltage and the induced pore water pressure. This proportionality leads to the hypothesis of Esrig that the voltage at each point determined the magnitude of the induced pore water pressure at that point.

(d) Johnston and Butterfield (1977)

Several laboratory tests on London clay with varying applied voltage (0.65 to 2.904 volts) at either opened anode-closed cathode or closed anode-opened cathode were performed by Johnston and Butterfield (1977). During the tests, induced pore water pressure, voltage distribution and current variation within the sample were measured. The pore water distribution for test with opened cathode-closed anode at 0.945 volts and test with opened anode-closed cathode at 2.904 volts are shown in Figure 4.4 and Figure 4.5 respectively. For the former case, negative pore water pressure was induced with maximum at anode. For the latter case, an almost linear positive pore water distribution was induced. The results indi ated that for test with closed anode and opened

cathode as boundary condition, negative pore water pressure will be induced with maximum at anode while for test with opened anode and closed cathode as boundary condition, positive pore water pressure will be induced with maximum at cathode as expected in the theory.

(e) Mitchell and Wan (1977)

The effect of induced negative pore water pressure on treated soil (kaolinite) was investigated by Mitchell and Wan (1977). In the investigation, pore water pressure distribution along the sample, volumetric strain, voltage distribution along the sample and current variation with time during the treatment were measured. The pore water pressure distribution for one of the tests is shown in Figure 4.6. An almost linear negative pore water pressure distribution was observed between anode and cathode at the end of the treatment. After the test, the water content and undrained shear strength of the treated sample were determined (Figure 4.7 and Figure 4.8). As expected, the higher the induced negative pore water pressure, the greater is the increase in shear strength and reduction in water content of the treated kaolinite. The results also illustrated that the effect of negative pore pressure is equivalent to direct mechanical loading to the soil. In this study, comparison of the experimentally measured and theoretically calculated pore water pressure (k_e and k_h measured independently) were also made. As indicated in one of the tests (Figure 4.9), the experimental measured value exceeded the predicted

value by about twice the amount. The writers explained that it was due to the continuous decrease in k_h during electro-osmotic consolidation (Figure 4.10) resulting in the development of greater negative pore water pressure.

4.2 Electric Potential Distribution Within Osmotic Cell

The osmotic cells used in the past were of different sizes and shapes. They ranged from a simple rectangular box to highly elaborated cylindrical cell. Each type of cell has its own boundary conditions. For the rectangular box, analysis of potential distribution within the box is complex in which the three dimensional boundary conditions have to be taken into consideration. For the cylindrical cell, a simple one-dimension solution as described in section 3.2 can be adopted and a linear potential distribution can be assumed.

A new solution was suggested by Banerjee and Vitayasupakorn (1984) for the development of potential distribution in a cylindrical cell. They emphasized that the electrode geometry and the boundary constraints should be taken into account when analyzing the electric potential distribution within the sample. They concluded that if these constraints were not included, there might be significant error in the theoretical solutions. After their study, the electric potential distribution $\phi(r,z)$ in a cylindrical space with two circular disc electrodes one at each end is given as:

$$\phi(r,z) = \phi_1 + \phi_2 + \phi_3 + \phi_4$$

where,

ϕ_1 = potential due to positive electrode

ϕ_2 = potential due to negative electrode

ϕ_3 = potential due to the charges along the side of cylinder arising from positive electrode

ϕ_4 = potential due to the charges along the side of cylinder arising from negative electrode

The details of the above relation is described in Banerjee and Vitayasupakorn (1984).

The study of potential distribution as given by the above equation with respect to various sample aspect ratios (length to diameter ratio) indicated that non-linearity in the potential distribution along the sample gradually diminished as the ratio becomes smaller. If the ratio equals to unity, a constant potential distribution can be assumed.

4.3 Electrodes

Besides the various shapes and sizes of electro-osmotic cells being used in the past, the electrodes used were also made of different materials and configurations. It is expected that different types of electrode material and their arrangement may affect the efficiency of the applied electric potential to the soil and the types of secondary effects which will accompany the process. In order to investigate the best material to be used as electrode and its arrangement to be incorporated with the osmotic cell, an in depth look into the

material, its arrangement used in the past and their efficiency were made. The characteristics are summarized in Table 4.1. There are enormous variations in the material types and electrode shapes being used. For example, in the tests of Johnston and Butterfield (1977), only 3 percent of the total applied voltage was recorded. It is suspected that there was a high resistance in the electrodes assemblies or in the soil-electrode interfaces where most of the applied electric potential were lost. It was reported that the high resistance at the boundary may be caused by the ionization of electrodes, the evolution of gas from electrolysis and deposition of compounds onto the electrodes. These factors may be responsible for the low efficiency.

4.4 Determination of Soil Parameter

The parameters needed for the mathematical equations described in section 3.2 are k_h (hydraulic permeability), k_e (electro-osmotic permeability) and c_v (coefficient of consolidation). The c_v and k_h can be deduced from the conventional consolidation tests and permeability tests and k_e can be measured in an osmotic cell. Banerjee and Mitchell (1980a,b) used a different technique and equipment set up in the determination of c_v, m_v, k_h and k_e. In the experiment, a large osmotic probe was used. The probe consisted of two ring electrodes fitted onto the insulated steel rod at a fixed distance. The probe was instrumented with pressure transducers, flow measuring device and volume change monitoring cell. The probe was inserted into a large test chamber, and

the surrounding soil was subjected to an applied electric potential. The induced pore water pressure, the flow rate and volume change were measured, and consequently the required parameters were deduced. Except for the test at lower stress range (0.5 kg/cm²), the comparison between the parameters obtained with the mechanical consolidation tests with those obtained using the probe showed a reasonable agreement between the two methods (Table 4.2). The discrepancy found in the lower stress range may be attributed to excessive variation of k_r with effective consolidation pressure. The finding supports the claim by many investigators (Johnston and Butterfield 1977, Esrig 1968a) that electro-osmotic consolidation is similar to the conventional consolidation.

4.5 Secondary Effects of Electro-Osmosis

Electro-osmotic process will inevitably be associated with secondary effects such as electrolysis, heat generation, ion-exchange, electrophoresis and variation in soil pH value. Some of these changes may be beneficial to the process and others may have adverse effect. A major problem during the electro-osmotic treatment is the generation of gas. If the generated gas cannot be removed, it will expand and tend to accommodate the developed pore water tension. As a result, the development of pore pressure will be affected and the resistance at the soil-electrode interface will be increased.

In order to prevent gas evolution, different measures were undertaken in the past such as the design of an escape duct, the isolation of electrodes from

soil sample, and the use of inert materials as electrodes. Geuze et al (1948) was the first to notice the seriousness of the problem and designed an escape duct made of piezometric tubing in an attempt to liberate gas. Suggestion such as the limitation of current through the test sample was frequently mentioned (Evans et al 1966, Mitchell 1967, Banerjee et al 1984) to minimize the generated gas. Johnston and Butterfield (1977) designed an elaborate electrode arrangement by separating the electrodes from the soil sample so that the evolved gas can be driven out. Wan and Mitchell (1975) suggested that by using silver chloride as electrode, generation of gas due to electrolysis can be prevented. However, all these methods have their limitations.

The experiment by Gray and Mitchell (1967) showed that by controlling the test conditions carefully, the secondary effects which accompanied the process can be greatly minimized. Measures such as,

(1) use of homogeneous and saturated soil sample

(2) proper choice of electrode material

(3) low applied electric potential and current density

(4) constant reversal of current direction

were shown to be able to suppress the adverse effects to a minimum level. Some measures did in fact reduce the secondary effects, but it may also reduce the effectiveness of the process. For instance, if too low an applied electric potential is used, the induced pore water pressure will not cause adequate consolidation for the process to be of any use in the treatment of soil. Some

electrode materials, such as silver chloride or platinum, may not be practical in engineering application.

4.6 Polarity Reversal

At the end of electro-osmotic treatment with anode sealed and cathode opened, the magnitude of the negative pore water pressure will be induced with maximum value at the anode and gradually decreased to zero at cathode. The shear strength and moisture content of the treated soil will correspondingly be different from one end to the other. The technique of electrode reversal, which is simply to reverse the electrical polarities and drainage directions at the end of a stage of treatment, can be applied to initiate further consolidation to the region where the consolidation was minimum. As a result, a more uniform water content and shear strength distribution within the sample can be obtained. This technique was first introduced by Titkov (1961). It was not studied until recently when Wan and Mitchell (1976) reported that with the reversal of electrode polarity after the first stage of treatment, significant amount of additional consolidation was obtained. In addition, more uniform increase in shear strength and reduction in water content along the length of the sample was detected. In the experiment, the polarity was reversed immediately after the first equilibrium (indicated by a little fluctuation of pore water pressure) was reached and the treatment was continued until no further settlement was detected. The power consumption for the second stage of

consolidation was reported to be only a fraction of that of the first stage (as low as about 20 percent). The time required to reach equilibrium was also shorter than in the normal polarity stage.

4.7 Review of Case Histories of Electro-Osmosis

Although the fundamental aspect of the complexities of soil-water-electricity interaction is not thoroughly known, electro-osmosis was applied to field problems since the process of treatment to soils was invented by L. Casagrande in 1939. In the field, electro-osmosis was proven to work very well in silt, sensitive silt and silty clay (Casagrande 1947, 1952a,b, 1953) as well as in the relatively soft clay by Fetzer (1967) and Chappell and Burton (1975). Bjerrum et al (1967) showed that the process worked equally well on soft sensitive clay. A selection of major case histories are discussed in this section from which the experience gained will be useful in the design of the proposed field test of this research project.

4.7.1 Sewage Treatment Plant, Ås, Norway (Bjerrum et al, 1967)

The plant is located about 30 km south of Oslo and is founded on an extremely sensitive marine clay deposit which has vane strength at the top 10 m of about 8 kPa, with moisture content, plastic limit and liquid limit of 31 %, 15 %, and 21 % respectively. During the construction of the treatment plant, it required an excavation of the site to a depth of 4.5 m. For a factor of safety

of 1.3 against base heave, the maximum depth of excavation was only 2.3 m.

The electrode installation for electro-osmosis covered an area of 200 m^2. The electrodes were arranged in 10 rows at 2 m spacing and at 0.6 - 0.65 m spacing along each row. The electrode was made of 19 mm diameter 10 m long reinforcement steel bars and were pushed 9.6 m into ground. Several piezometers and settlement gauges were installed at selected locations within the site. An average voltage of 40 volts at 250 amperes were applied for a total of 120 days.

During the treatment, average settlement of 8 mm/day was detected initially. The settlement gradually reduced and at the end of the treatment (day 120), only 4 mm/day was detected Through the course of the treatment, a total final settlement of 50 cm was observed representing a drop of 3.8 % in water content of the clay (from 31 % to 27.2 %). The pore water pressure of the soil during treatment was monitored by piezometers. The results for day 51 to day 120 at two locations, one at anode and the other at cathode are shown in Figure 4.11. In day 51, the polarity of the electrodes was reversed. During the reverse stage, the pore water pressure at the new anode was decreased to -50 kPa at day 54 and remain unchange until day 58 at which the polarity was reversed back again. Three days after the polarity was switched back to normal setting (day 60), the pore water pressure at anode was -50 kPa and remained relatively unchange throughout the treatment period. The constant pore water pressure may indicate that the process reached equilibrium

(the stage of small fluctuation in induced negative pore water pressure) at day 54 for the reverse stage and at day 60 for the normal stage. It may also represent the maximum pore water pressure that can be induced by the treatment for the given applied electric potential (40 volts) in the site.

After treatment, vane strengths and moisture contents were determined and the results are shown in Figure 4.12. The increased in strength is maximum at anode and no change in strength is detected at cathode. During the period of electrode reversal (day 51 to day 58), the pore water pressure at electrode (which was anode during the electrode reversal) was decreased to -50 kPa. It would be expected that a relatively uniform vane strength and moisture content between electrodes would be resulted if the technique of polarity reversal were applied appropriately. However, this drop in pore water pressure did not cause any change in strength of the soil near cathode. This nonuniform soil treatment may be due to the insufficient time of treatment in the stage of polarity reversal or the over-treatment of the soil at vicinity of anode (resulted in higher electrical resistance).

The vane strength with depth was also measured and the results for two locations which were at the mid-point between the electrodes are shown in Figure 4.13. For the variation of strength with depth, the maximum increase in strength after treatment is at the depth immediately below crust. The increase gradually reduces with depth. At depth 2 to 3 m above the base of the electrode, no change in strength was detected. It was also noticed that gas was

formed in some piezometers due to electrolysis causing some erroneous results After treatment, the excavation was successfully completed.

4.7.2 West Branch Dam, Warren, U.S.A. (Fetzer 1967)

The dam is approximately 3017 m (9900 ft) long with central 610 m (2000 ft) section at 24.4 m (80 ft) high (Figure 4.14b). The embankment consists of homogeneous impervious fill. The slope on both side of the embankment is at 3:1 from the top of the dam (elevation 307.8 m (1010 ft)) to elevation 299 m (981 ft) and 4.5:1 to elevation 295 m (968 ft). A 54.9 m (180 ft) wide berm located on the downstream and a 45.7 m (150 ft) wide berm on the upstream of the dam. The underlying deposit consists of 4.6 -7.6 m (15 - 25 ft) alluvial silty sand, 15.2 - 18.3 m (50 - 60 ft) soft to medium stiff clay, 3 - 6.1 m (10 - 20 ft) dense silt and 3 - 6.1 m (10 - 20 ft) very dense silty sand and very stiff clay to considerable depth. The medium to stiff clay stratum has moisture content ranging from 21 % to 40 %, liquid limit from 20 % to 49 % and plastic limit from 9 % to 25 %.

The construction of the dam was started in May 1963. Through several stages of construction, the fill was raised from elevation 285.9 m (938 ft) to elevation 304.5 m (999 ft) in October 22, 1964. At the last stage of construction which was to raise the fill to the final elevation at 307.8 m (1010 ft), measurement of conduits movement beneath the fill was made. On November 14, 1964, when the embankment elevation was 306.9 m (1007 ft),

the measurement indicated an acceleration in the rate of conduit movement. At that point, the placement of fill was stopped but the movement of the conduit continued. In addition, longitudinal cracks as wide as 25.4 mm (1") started to develop at elevation between 299 to 301.8 m (981 to 990 ft) from station 42+00 to station 49+00 at both upstream and downstream of the dam. The dam was found to be in the early stage of failure. When the top 3.7 m (12 ft) of fill was removed, the spreading stopped. Several piezometers were installed at the site and the piezometers detected very high pore water pressure of 443 kPa beneath the embankment in the soft to medium stiff clay stratum. Analysis indicated that the dissipation of pore water pressure in the stratum was extremely slow and considerable amount of time was required to raise the embankment to the designed level. After investigating all the possible alternatives of soil improvement, electro-osmosis was adopted in order to dissipate the excess pore water pressure.

The electro-osmotic installation consisted of 3 strips of electrodes of length 304.8 m (1000 ft). A 8 rows strip was provided along the crest of the dam and a 6 rows strip was provided at the outer edge of the berm at each side of the dam (Figure 4.14b). The electrode spacing was 6.1 m (20 ft). The anode was of 63.5 mm (2½") diameter extra-strength black steel pipe and the cathode was of 50.8 mm (2") diameter steel pipe placed inside a 355.6 mm (14") diameter sand filled hole together with an eductor well. Pumping of expelled water was required. Both the anodes and cathodes were installed to depth 41.2 m (135

ft) from the surface, as shown in Figure 4.14a. Several additional piezometers were also installed within the site.

Application of electricity at 150 volts was started on August 10, 1965 and continued until May 1966 during which the crest was constructed to the final elevation. The power was continued to applied to the outer 2 strips until August 1966.

Piezometer installed below the crest of the dam recorded a drop of water level by 19.8 m (65 ft) after the treatment (Figure 4.14c). Field shear strength tests indicated that the strength of clay at depth of 6.1 m (20 ft) below the alluvial silty sand interface was almost doubled as a result of the treatment. But the strength of the clay within the first 6.1 m (20 ft) below the silty sand stratum had little increase. As shown in Figure 4.14c, after the electro-osmotic treatment, the embankment was constructed to its final elevation without any significant increase in pore water pressure and movement.

4.7.3. Kooney Canal Hydroelectric Project, British Columbia (Wade 1976)

The project consists of excavating a trench through the forebay and penstock area. The underlying soil of the area is of glacio-lacustrine origin and has varying depth from 16 m in the forebay to 33 m in the penstock. The sensitive silt stratum located immediately above the bedrock caused instability of the slope during excavation. This layer has thickness varying from 2 m to 12 m with moisture content between 30 % to 40 %. The liquid limit is 26 -

35 % and the plastic limit varies from non-plastic to 7 %. The effective angle of internal friction is 27° to 32°. According to the analysis, the steepest slope that could be excavated was 3.5:1. Strengthening of the sensitive silt layer was therefore required to excavate a reasonably steep slope (2:1) for the trench. Preliminary laboratory tests on the sensitive silt by electro-osmosis revealed a convincing result that the shear strength increased from 50 kPa to 450 kPa in 14 days of treatment at 6.7 volts, indicating that the subsoil could be successfully strengthened by the process.

The electro-osmotic installation consisted of 5 double rows of electrodes along the penstock slope and two rows along the forebay slope. Each double row consisted of a single row of anodes and a single row of cathodes spaced at 3 m apart. The electrodes within each row were spaced at 6.5 m apart. The electrodes were made of 5 cm diameter steel pipes. At cathode, a 30 cm diameter hole was drilled first. Then a eductor pipe and a perforated plastic pipe together with electrode were positioned into the hole and backfilled with clean sand as shown in Figure 4.15. Pumping of expelled water was required. Both the anodes and cathodes were driven to the bedrock from the surface. Several piezometers were installed within the test site. An average of 120 volts at 600 amperes was applied for a period of 9 months.

All the piezometers detected a drop in water level within 3 days after the power was switched on. After 2 weeks of treatment, the water level dropped from 12 m to 3 m above bedrock and remain at that level throughout the

treatment. The rate of discharge was 270 l/min initially and decreased to 45 l/min towards the end of treatment. During the treatment, a total of 18000 cubic metres of water was removed.

After treatment, laboratory tests on the treated samples indicated that the effective friction angle of the silt increased from 27° to 35°. The trench was successfully excavated to the required steepness. The stability analysis indicated that the excavated slope had a factor of safety higher than unity under most severe conditions (earthquake with magnitude of 0.1 g and induced pore water pressure up to one-third of the overburden pressure). The nearby blasting for the excavation of powerhouse and penstock foundation did not cause any slumping or movement to the trench wall.

4.7.4 Big Pic River Bridge, Ontario, Canada (Soderman and Milligan 1961)

Electro-osmosis was first used to increase the bearing capacity of steel H-piles by Soderman and Milligan (1961) in the Big Pic River Bridge project which is part of the Trans-Canada Highway. The subsurface conditions consisted of 3 to 6.1 m (10 to 20 ft) of alluvial deposits, underlain by 12.2 to 18.3 m (40 to 60 ft) of soft to firm varved clay. The clay in turn was underlain by more than 76.2 m (250 ft) of silt and silty fine sand which was under artesian pressure. Test piles driven into this deposit had lower load capacities than piles extending only to the bottom of the varved clay deposit. Since the shorter piles could not provide the required design load of 36.3 metric

tons (40 tons), proposal was made to increase the capacity of the piles by electro-osmosis using the piles as anodes. Laboratory and field tests confirmed the validity of this suggestion.

After driving 17.1 m (56 ft) long H-piles for each pier, 21.3 m (70 ft) long cathodes were installed around the perimeter of the pile installation. The average distance between the piles and the cathodes was about 7 m (23 ft). Power was provided at 70 to 120 volts by a generator. The average current consumption per pile was about 15 A. After four weeks of treatment, the bearing capacity of the piles had typically increased to 63.5 to 90.7 metric tons (70 to 100 tons), which was approximately 2.5 to 3 times the capacity before treatment. A number of piles were blocked out of the pier footings for subsequent load testing to permit evaluation of the permanence of the treatment. Piles tested up to 10 years after treatment showed no significant loss in bearing capacity.

4.7.5 Highway at Berthierville, Quebec, Canada (Bozozuk and Labrecque 1969)

The autoroute along the North Shore of the St. Lawrence River between Montreal and Quebec City passes over deep beds of compressible marine clay. At Berthierville, 80 km east of Montreal, the autoroute crosses a railway spur line and Highway 41. At the crossing, a bridge over the highway supported by six 1 m diameter 82.3 m (270 ft) long piles seated 2.4 to 3 m into bedrock was constructed. The piles consist of a 13 mm thick steel tube filled with concrete.

In each pile, 20.4 tons (metric ton) of number 18-S deformed reinforcing bars were installed. This composite pile had a design capacity of 1814 tons of which 1090 tons was allowed for negative skin friction. The subsoils at the site are marine deposits of the ancient Champlain Sea. The upper 18 m consists of layers of sand, silty clay, stratified sand and silt, and stratified clayey silt. From 18 to 73 m the soil changes to gray silty clay and this zone is stronger than the material above. The gray silty clay formation is underlain with 9 m of fine sand which in turn rests upon shale bedrock. Consolidation tests indicate that the material is normally consolidated to a depth of 12 m, overconsolidated by 0.3 kg/cm^2 to a depth of 21 m and overconsolidated by 0.8 kg/cm^2 below 21 m. Considerable settlement was therefore expected mostly due to the consolidation of the upper 12 m of the soil.

Two piles (B-2 and B-3) had elongated after concreting due to the hydration of cement. This was quite surprising because the pile was expected to compress under the negative skin friction loads. This observation indicated that there existed relative movement between the fresh concrete and the steel tubular pile. This relative movement may reduce the bonding between concrete and the steel tube and consequently affect the resistance to lateral loading. Therefore, such movement should be avoided. An attempt was made to eliminate the skin friction loads with electro-osmosis by using the steel tube of the composite pile as cathode. The electric power was supplied by a 50 kVA gas driven generator. The power was applied until all measurable deformation

of the pile had ceased. For pile B-3, an average current of 475 A at 20.5 V was applied for 1.5 hours in which time the pile shortened about 0.25 mm. For pile B-2, a current of 475 A at 17.5 V was applied for 2.5 hours. The deformation gages installed inside the piles suggested that the electro-osmosis was at least partially effective to the bottom of the pile. However, there was no direct way of determining the effectiveness of electro-osmosis in eliminating the negative skin friction loads. Subsequent measurement of pile deformation indicated that the negative skin friction loads began to build up again soon after the experiment was finished.

4.7.6 Basse Chaine Bridge Abutment, Anger, France (Caron, 1971a,b)

The only unsuccessful case history on electro-osmosis reported is the treatment of the Base Chaine Bridge abutment at Anger, France. The excessive movement of the structure (90 mm over 8 years) after the completion of construction required strengthening of the foundation soil. The underlying soil profile is shown in Figure 4.16. Laboratory test showed a satisfactory strength increase on the soft clay stratum by injection of 35 % sodium silicate solution into the stratum. Based on the laboratory results, the field treatment was carried out with the electrode arrangement as shown in Figure 4.16. During test, significant amount of silicate were lost by gravity flow into the underlying sand stratum and the deposition of silica onto the anode was noted. The lost of silicate coupled with the deposition of silica resulted in the failure of the

treatment of the foundation soil.

This case history revealed the importance of identifying the presence of an unfavourable stratum which may lead to the failure of the process, since the existence of a sand or silt layer may prevent the generation of the negative pore water pressure.

4.7.7 Observations from Case Histories

Table 4.3 summarized the case histories discussed in the previous section. The case histories described previously indicate that electro-osmotic treatment in clays is as effective as in silts. This is in contrast to the common conception that silt is generally considered more susceptible to treatment. In the treatment of clays (Bjerrum et al 1967 and Fetzer 1967), there were about 200 to 400 percent increase in shear strength of the treated soil, indicating that the process is also effective in treating soft sensitive clay and silty clay. In the case reported by Wade (1976) in which the silt was treated, the shear strength increased was about 25 percent. The reason could be due to the difference in magnitude of the pore water pressure induced during treatment. Since the permeability of clay is lower than that of silt and as a result, the magnitude of negative pore water pressure induced will be higher in clays than in silts.

From the listed case histories, the applied electric potential used in the field varies from 40 volts to 160 volts. These values represent what would normally be the working potential for field application. For safety reason,

applied potential of higher value than indicated is generally not used.

In the past, very little attention was paid to the design of an efficient system. In most cases, there are reasons that may overshadow the design of a good system, such as in the case reported by Fetzer (1967). The attempt was to save the dam from failing and there was not so much concern on how expensive the treatment would be, but rather on how well and rapid the treatment could save the dam from failing. All these factors will inevitably cause the escalation of the cost. In essence, the cost justification must play an important role and should be kept to minimum if the process is to receive more general application, rather than as a last resort when field problem was encountered.

In most of the case histories, the materials used as anodes are steel pipe, steel reinforcement bar or steel rail. For the cathode, a big hole is usually drilled to install the electrode filled with filter sand and pumping of expelled water is required. The installation costs of such cathode system is expensive and the pumping costs may be as high as 25 % of the total costs of treatment (no exact figure can be obtained since the pumping costs were not reported). In addition, such electrode system may not be efficient since the sand filter at the cathode may dissipate quite significantly the applied electric potential and the gas evolution at anode may produce high electric resistance. As a result, long treatment time and higher power consumption are reported.

In most cases, such as the project reported by Bjerrum et al (1967), the

soils were not treated uniformly. Usually, the shear strength has better increase at the region near the anode and little to no increase near the cathode. The soil could be treated uniformly by reversing the polarity of electrodes and Bjerrum et at (1967) tried this technique in their project in Norway. However, this technique was not properly manipulated and he electrodes polarity was reversed for only three days out of 120 days of treatment.

From the experience learned in the case histories, it can be concluded that a detailed pre-treatment investigation of the subsoil conditions to avoid the adverse effects due to the sand or silt layer and a better electrode design together with the careful manipulation of electrode polarity reversal technique are the three most essential factors governing the effectiveness of the electro-osmotic treatment.

Table 4.1 Summary of Electrodes Used in Past Experiment

Type of Electrodes	Type of Power Supply	Applied Voltage/ Current	Voltage Across Sample
Platinum gauge backed by porous disc (Evans and Lewis 1966)	D.C. power pack with resistance of 100000 Ω	500 V 100 mA	0-2 V
Stainless steel wool electrode (anode) Galvanized wire mesh (cathode) (Morris et al 1985)	Continuous variable full-wave rectifier	not described	0.45 V/cm
Silver-silver chloride electrode with porous disc (Mitchell and Wan 1977)	Constant D.C.	10-1000 μA	-
Perforated plate connected to porous stone (Gray and Mitchell 1975)	Constant D.C.	not described	1.25 V/cm
Carbon rod (anode) steel mesh (cathode) (Esrig and Gemeinhardt 1967)	Transistorized power supply of D.C. current	50 mA maximum	1 V/cm
Stainless steel wire mesh connected to porous stone (Johnston and Butterfield 1977)	Millard Power pack Type L280, range 0-30 V, and Boulton-Paul power unit, type A322 range 0-600 V connected in series	100 V	3 V
Perforated steel anode and copper cathode (Wang & Vey 1953)	not described	112-116 V	-

Table 4.2 Comparison of Coefficient of Hydraulic Permeability, k_h, Values Obtained from Direct Loading Consolidation Tests and Electro-Osmotic Tests (after Banerjee and Mitchell 1980b)

Effective Consolidation Pressure kg/cm^2	From Log Fitting c_v and m_v 10^{-8} cm/s	From Square Root Fitting c_v and m_v 10^{-8} cm/s	From Electro-Osmosis 10^{-8} cm/s
0.5	18.93	16.848	4.14
1.0	7.018	5.49	26.63
2.0	8.1244	9.2125	4.16
4.0	3.72	3.28	1.42

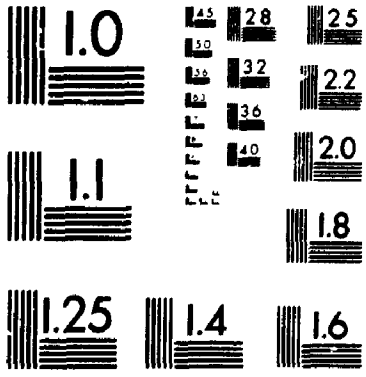

Table 4.3 Summary of Case Histories

Location and Reference	Factors Attributed to Instability	Soil Types	Geotechnical Properties							Treatment and Results
			ω (%)	ω_L (%)	ω_P (%)	S_t	Salinity (g/l)	k_h cm/s x 10^{-8}	k_e $cm^2/V\text{-}s$ x 10^{-5}	
As, Norway Bjerrum (1967)	low shear strength prevented excavation	sensitive clay of 12 m thick	31	21	15	100	0.9	2	2	* 40 V at 250 A for 4 months * ω dropped from 31 to 27 % * Cu increased from 1 to 4 t/m^2 * S_t decreased from 100 to 4 * P_I increased by 5 to 9 %
West Branch Dam Fetzer (1967)	rapid spreading and settlement of embankment	soft laminated clay of 18 m thick	30	36	19	4	N/A	3.8	4.6	* 75 V for 10 months * substantial decrease in piezometer level as much as 65 ft * adequate safety against steady seepage and drawdown conditions
Kooteney Canal British Columbia Wade (1976)	sensitive silt prevented excavation of steeper slope	sensitive silt of 4 to 40 ft	35	30	23	N/A	calcium carbonate 10 - 13 %	500	N/A	* 120 V at 600 A for 9 months * ϕ' increased from 27° to 35° * perched water table was removed * phreatic surface dropped by at least 30 ft
Big Pic River Bridge, Ontario Soderman and Milligan (1961)	insufficient bearing capacity of piles	12 to 18 m of soft to firm varved clay	20-50	30-60	20	N/A	N/A	N/A	N/A	* pile was used as anode * 70 to 120 V at 15 A per pile for 4 weeks * bearing capacity increased by 2.5 to 3 times the initial capacity of pile
Highway at Berthierville Quebec, Bozozuk and Labrecque (1969)	high negative skin friction	12 m Champlain Sea clay (soft sensitive clay)	28-60	28-60	20	30	N/A	N/A	N/A	* pile used as cathode * 17.5 to 20.5 V at 475 A for 2.5 to 1.5 hours * all measurable deformation of pile had ceased * negative sk . friction reduced but built up again soon after the power was switched off
Basse Chaine Bridge Abutment France Caron (1971)	excessive movement of abutment after completion of construction	soft clay stratum	N/A	N/A	N/A	N/A	N/A	N/A	N/A	* injection of 35 % sodium silicate solution * significant amount of the solution were lost to the underlying sand stratum * treatment not successful

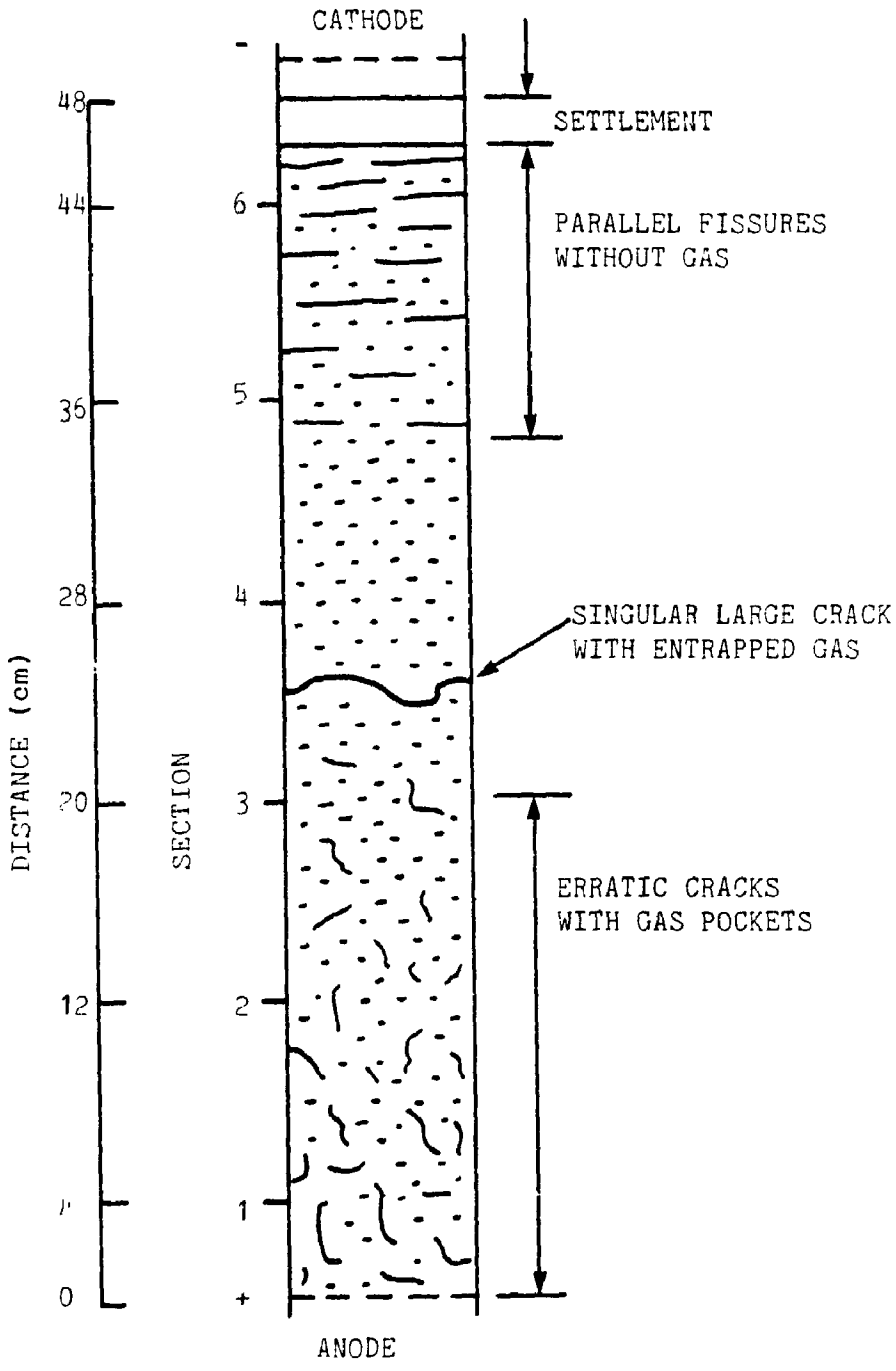

FIGURE 4.1 SOIL AFTER ELECTRO-OSMOTIC TREATMENT
(after Wang and Vey 1953)

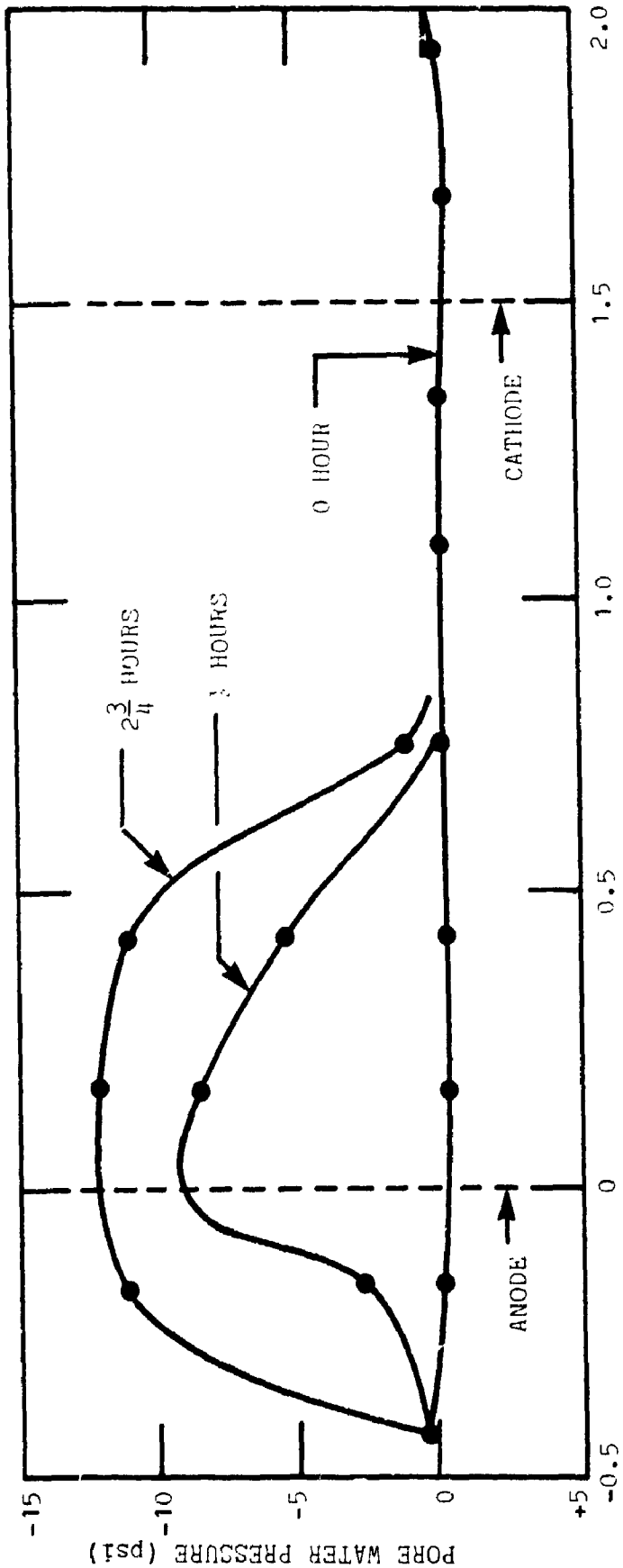

FIGURE 4.2 PORE WATER PRESSURE DISTRIBUTION WITH TIME (after Esrig 1968a)

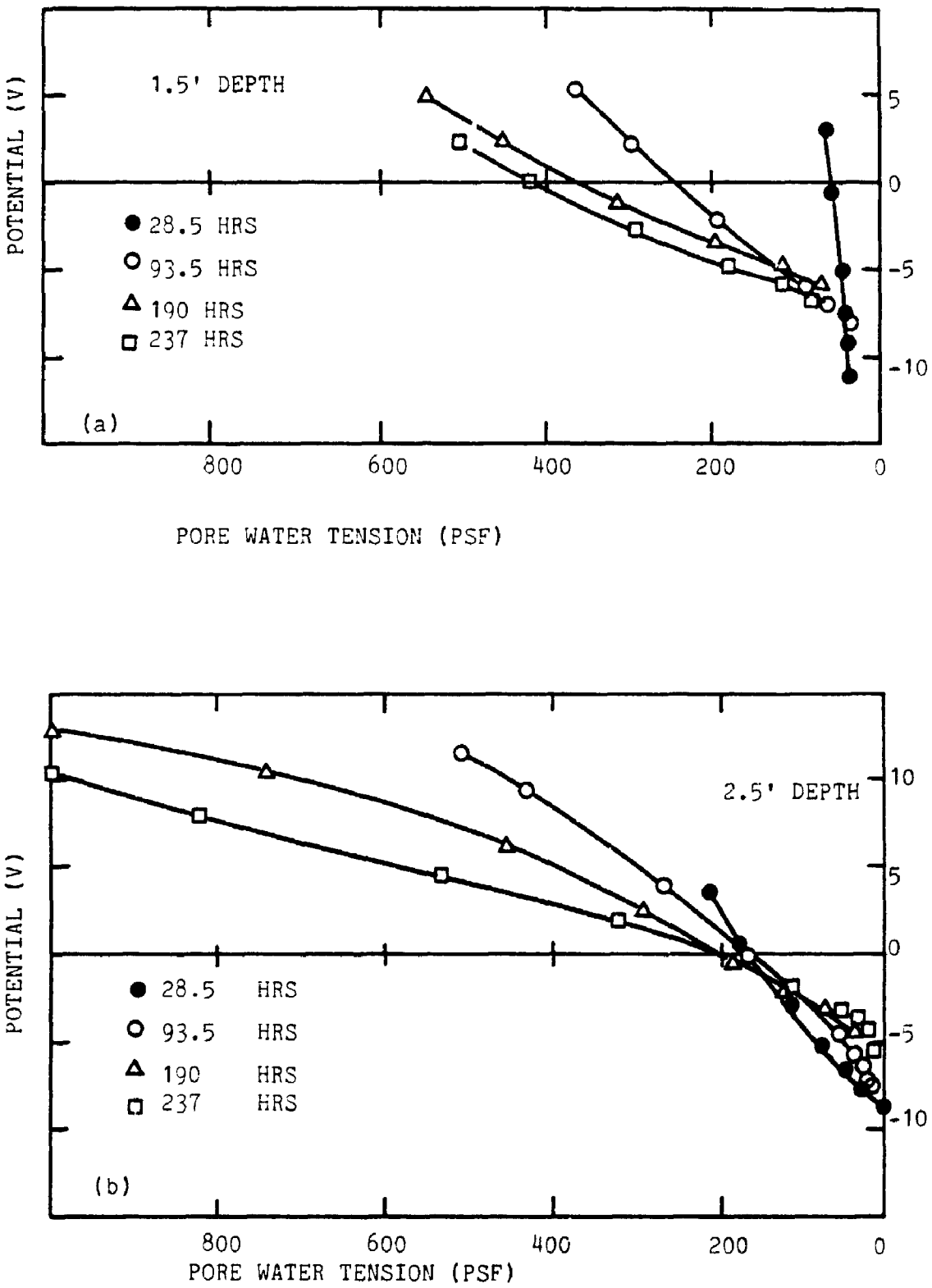

FIGURE 4.3 PORE WATER PRESSURE DEVELOPMENT WITH TIME AT DEPTH (a) 1.5 ft AND (b) 2.5 ft (after Esrig 1968 a)

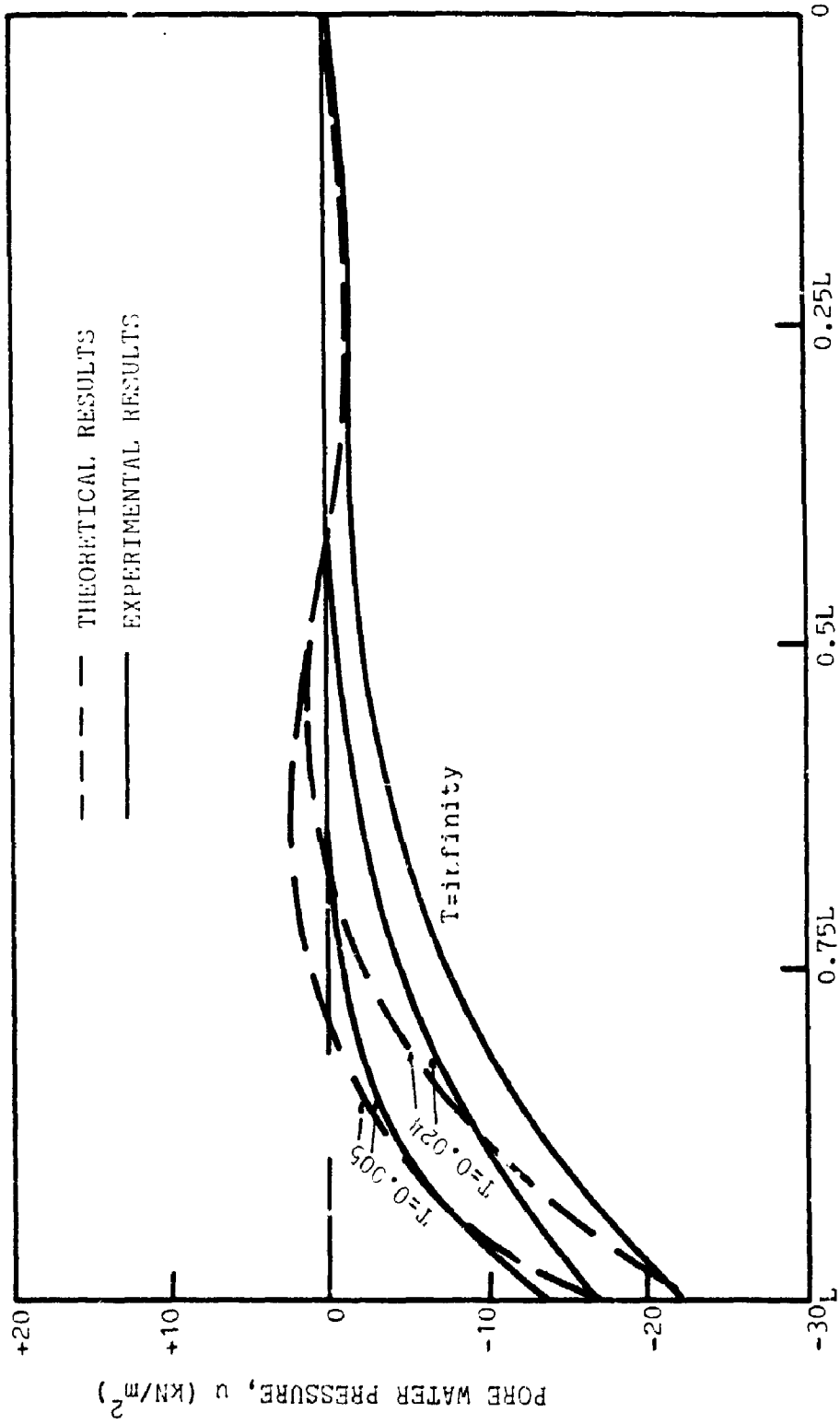

FIGURE 4.4 PORE WATER PRESSURE DEVELOPMENT WITH TIME AT APPLIED ELECTRIC POTENTIAL OF 0.945 V WITH CLOSED ANODE AND OPENED CATHODE (after Johnston and Butterfield 1977)

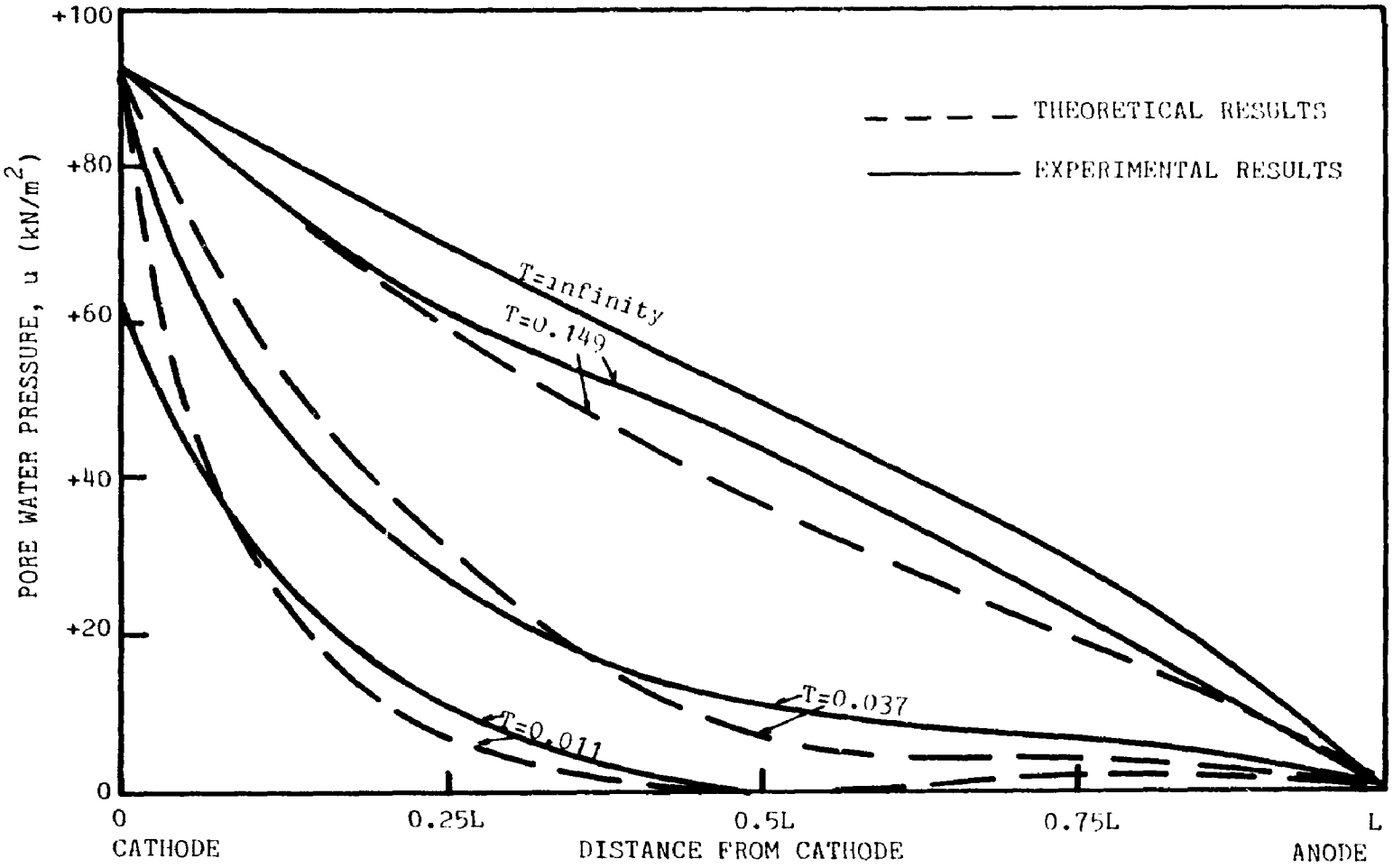

FIGURE 4.5 PORE WATER PRESSURE DEVELOPMENT WITH TIME AT APPLIED ELECTRICAL POTENTIAL OF 2.904 V WITH OPENED ANODE AND CLOSED CATHODE
(after Johnston and Butterfield 1977)

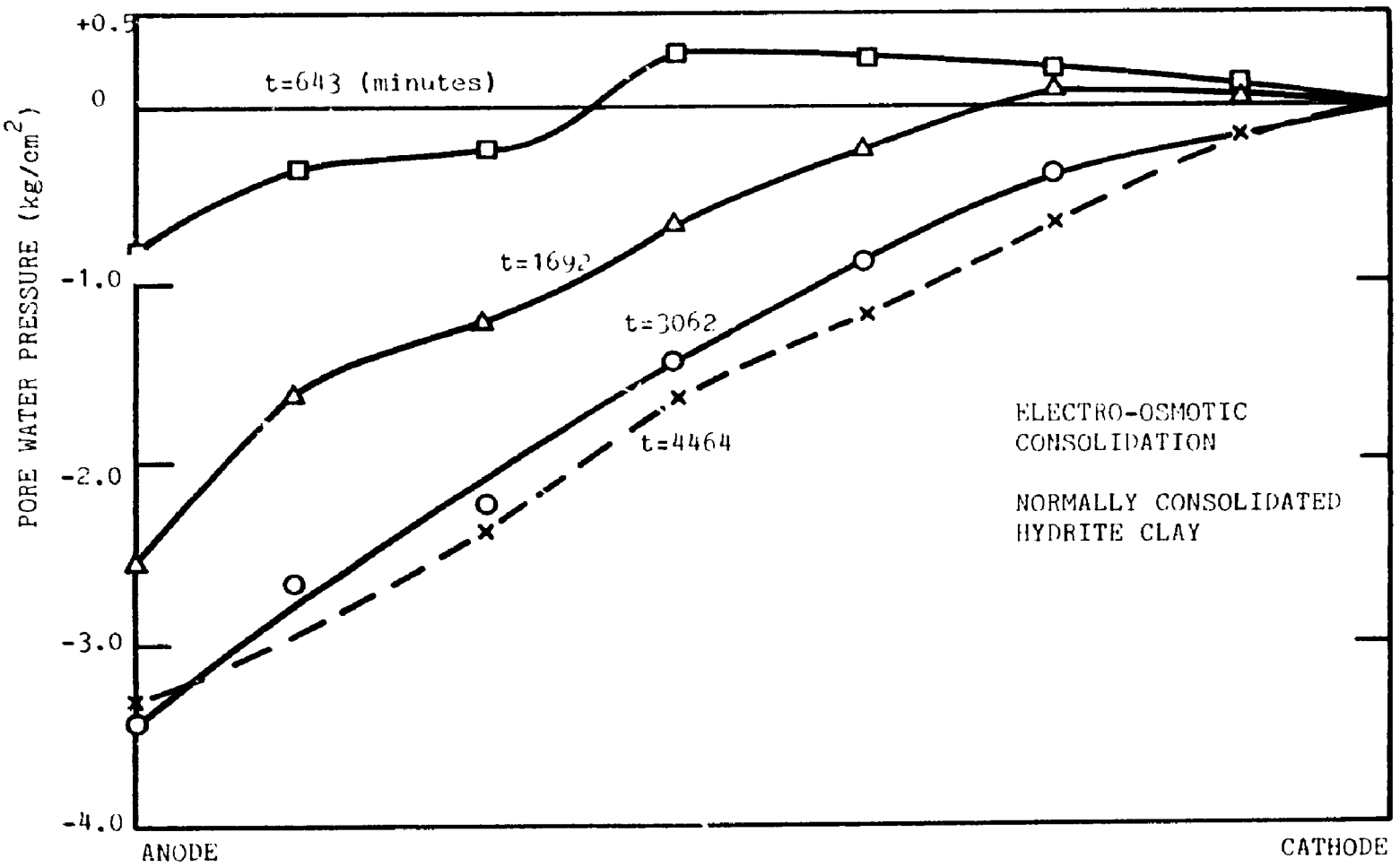

FIGURE 4.6 PORE WATER PRESSURE DISTRIBUTION WITH TIME (after Mitchell & Wan 1977)

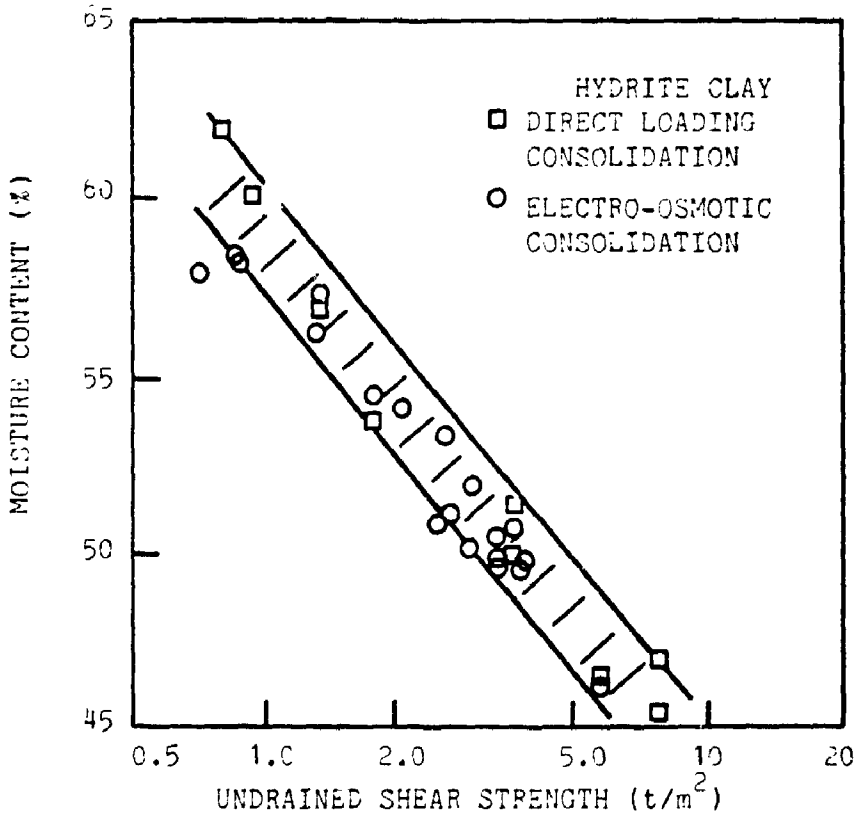

FIGURE 4.7 UNDRAINED SHEAR STRENGTH VS. MOISTURE CONTENT RELATIONSHIP FOR KAOLINITE CONSOLIDATED BY DIRECT LOADING AND BY ELECTRO-OSMOSIS (after Mitchell and Wan 1977)

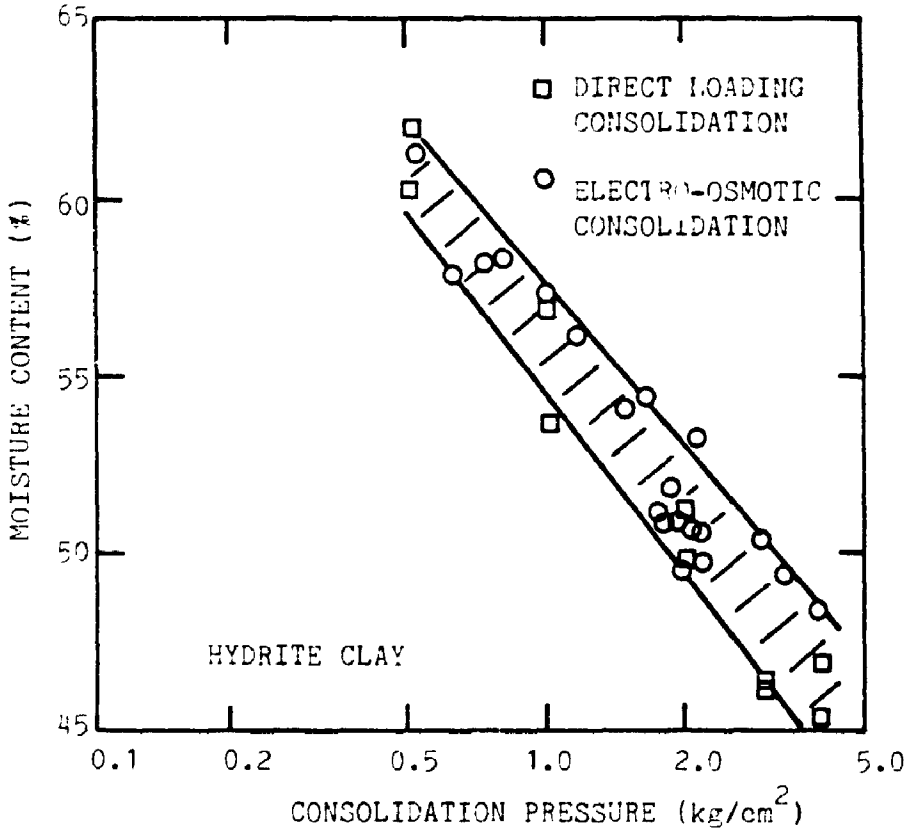

FIGURE 4.8 CONSOLIDATION PRESSURE AGAINST MOISTURE CONTENT FOR KAOLINITE CONSOLIDATED BY DIRECT LOADING (after Mitchell and Wan 1977)

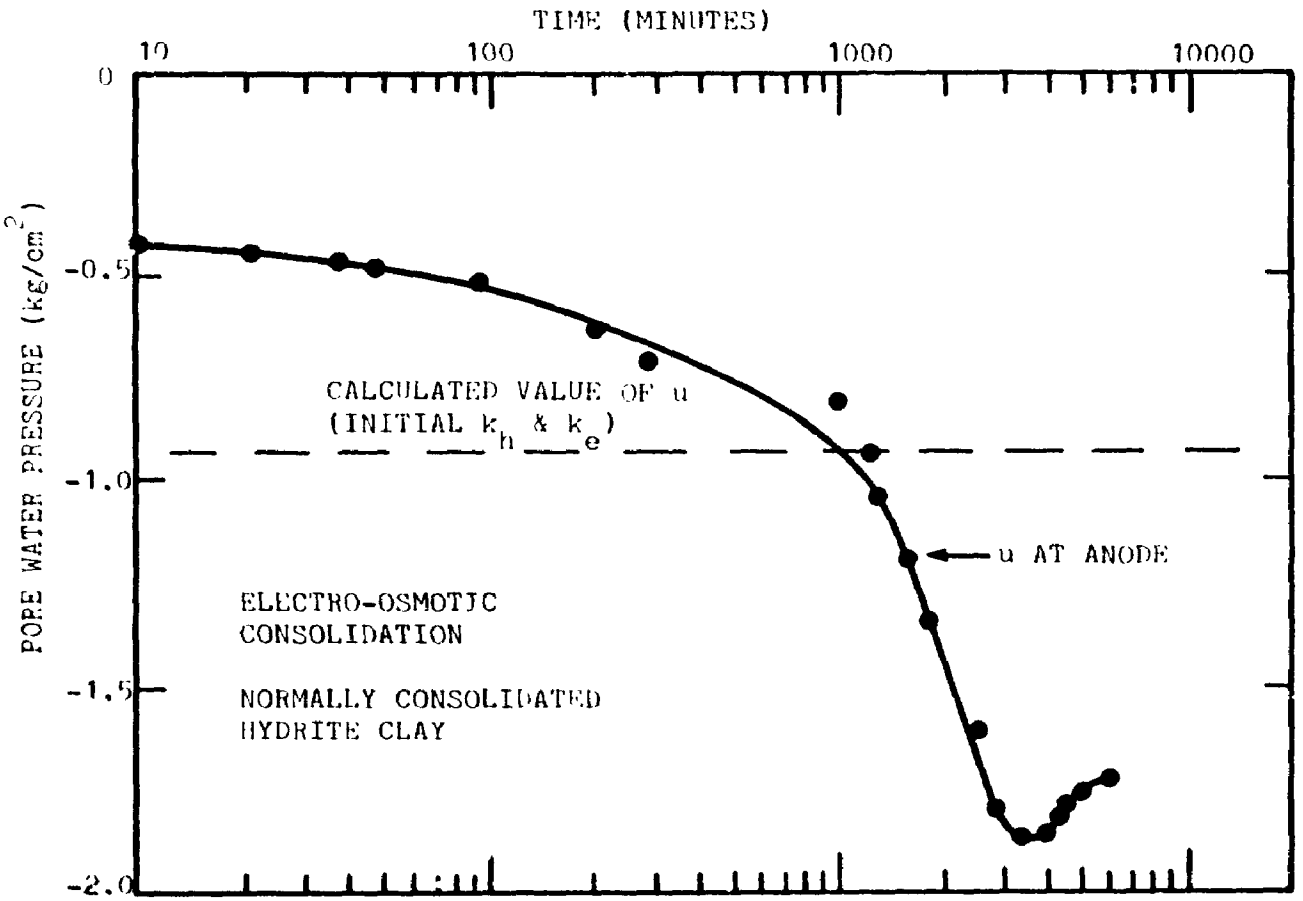

FIGURE 4.9 NEGATIVE PORE WATER PRESSURE MEASURED AT ANODE
(after Mitchell and Wan 1977)

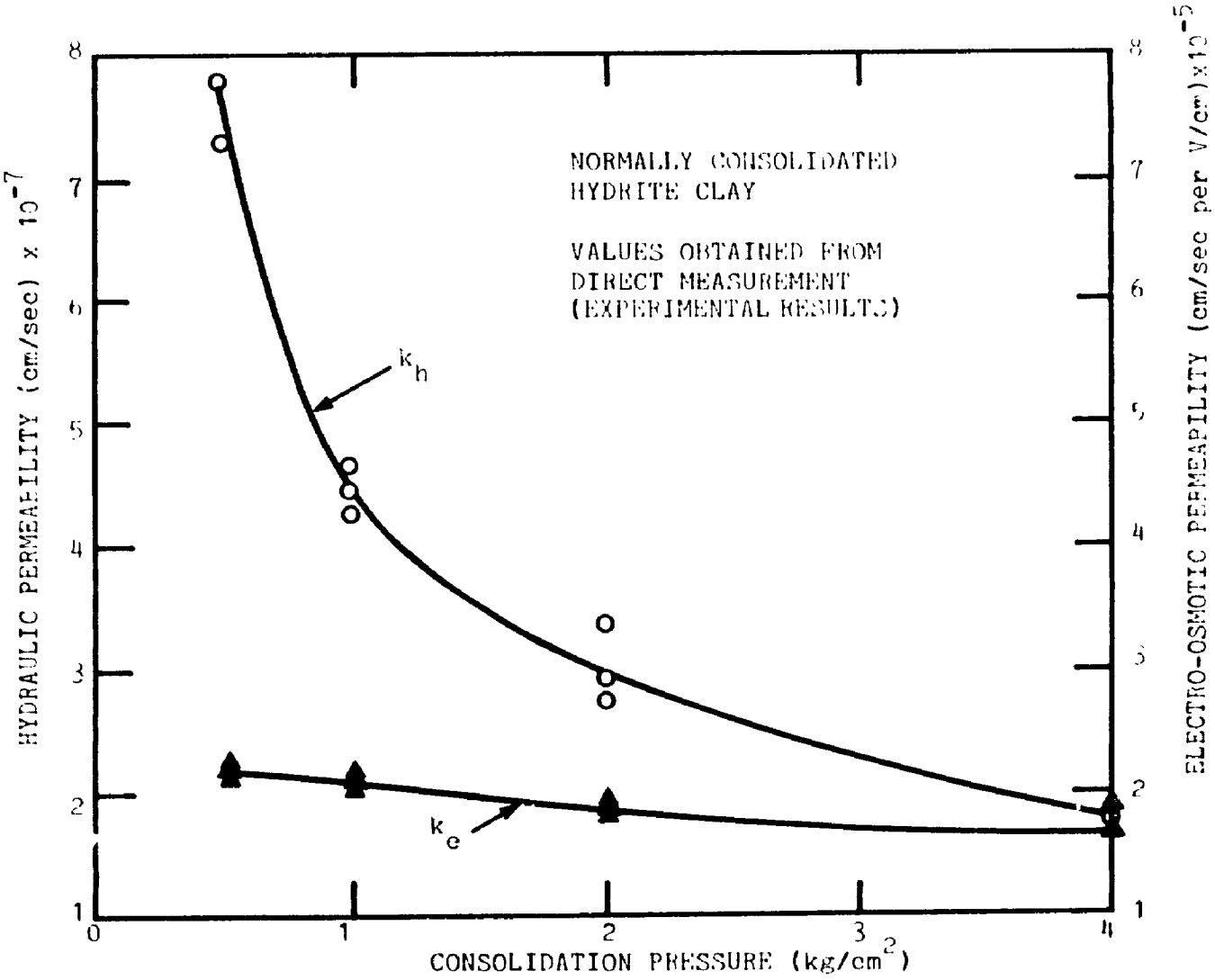

FIGURE 4.10 HYDRAULIC AND ELECTRO-OSMOTIC PERMEABILITY VALUES AS A FUNCTION OF CONSOLIDATION PRESSURE FOR KAOLINITE (after Mitchell and Wan 1977)

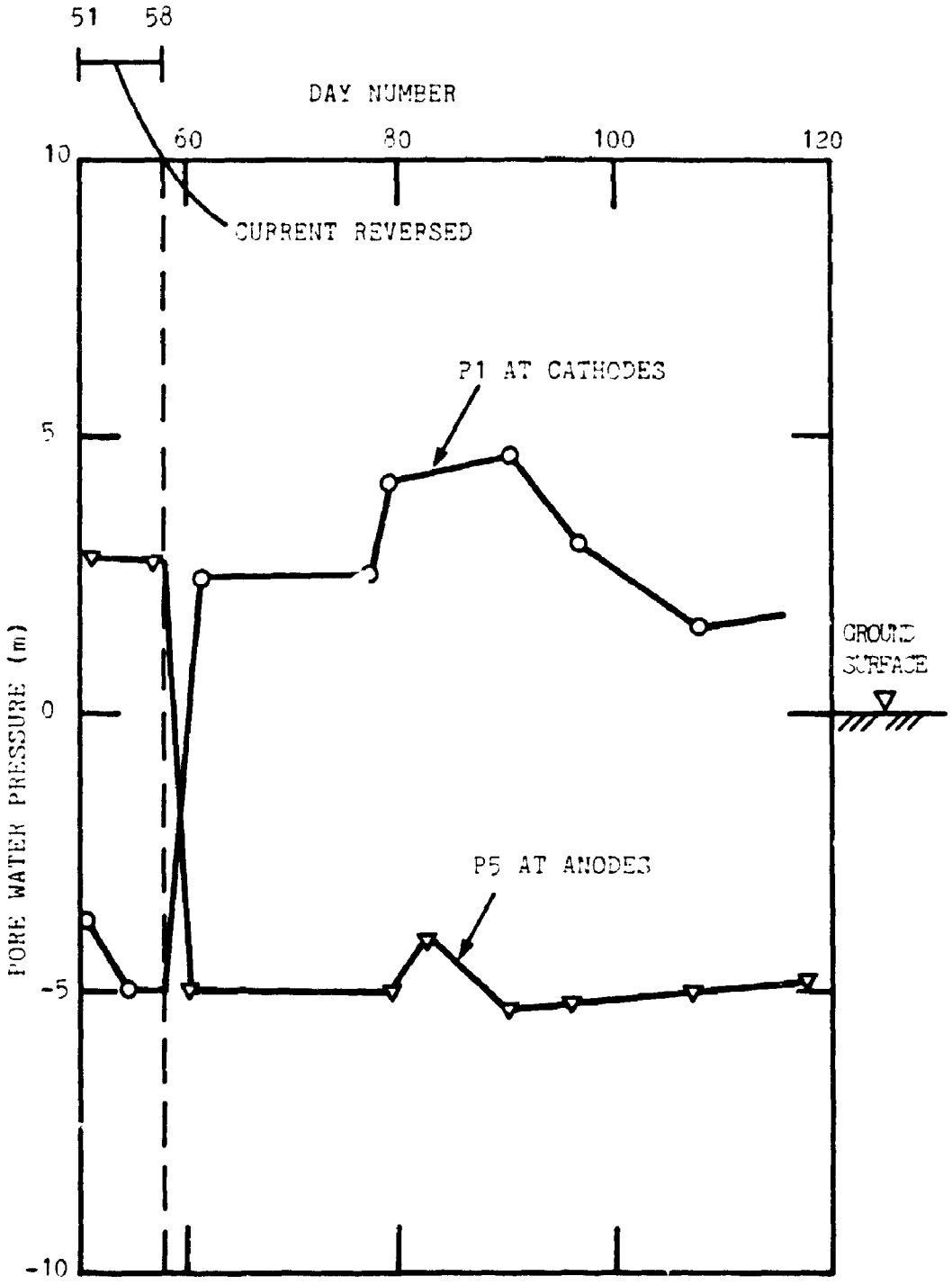

FIGURE 4.11 PORE WATER PRESSURE WITH TIME
(after Bjerrum et al 1967)

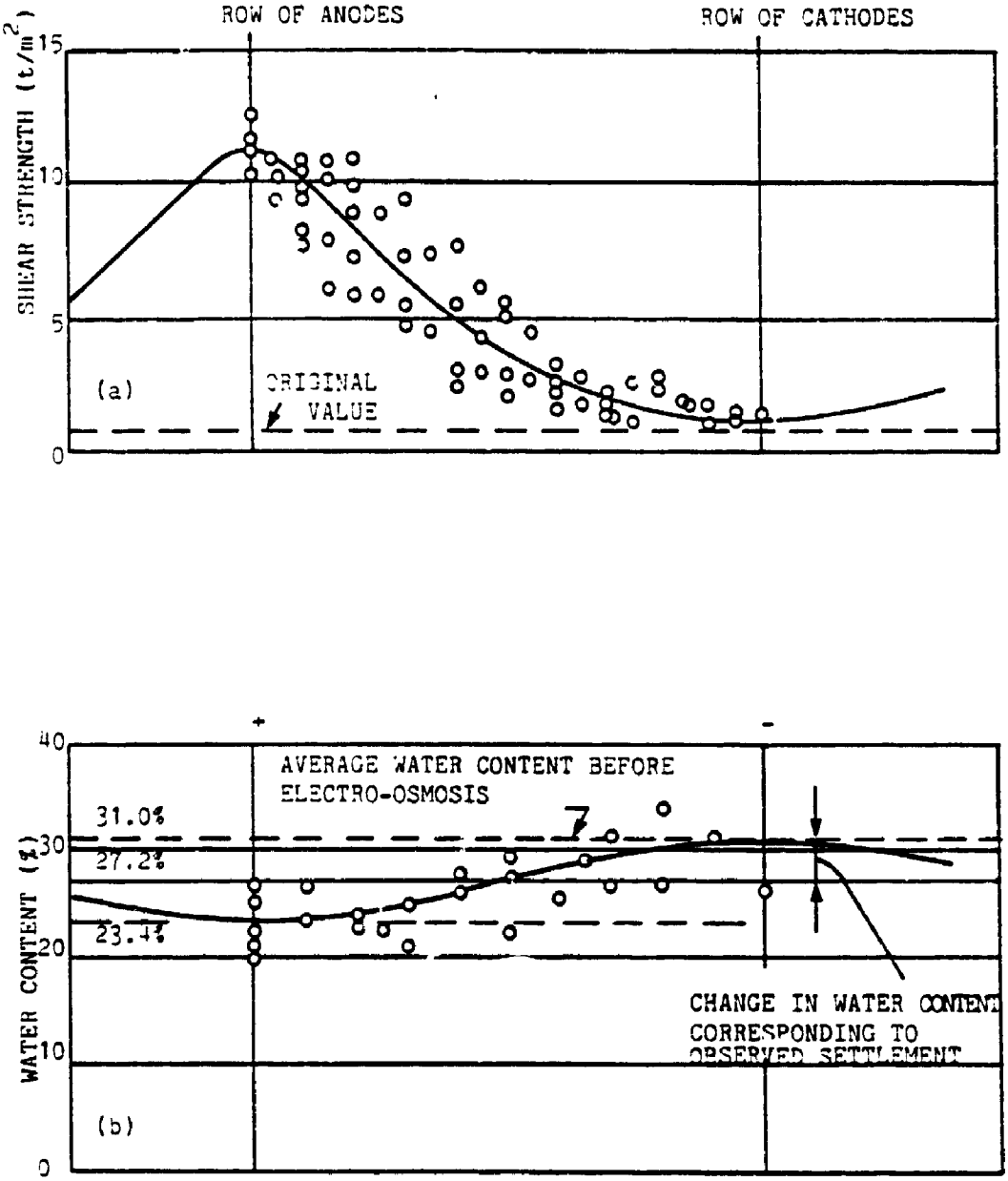

FIGURE 4.12 TEST RESULTS OF (a) UNDRAINED SHEAR STRENGTH AND (b) MOISTURE CONTENT OF CLAY BEFORE AND AFTER ELECTRO-OSMOTIC TREATMENT (after Bjerrum et al 1967)

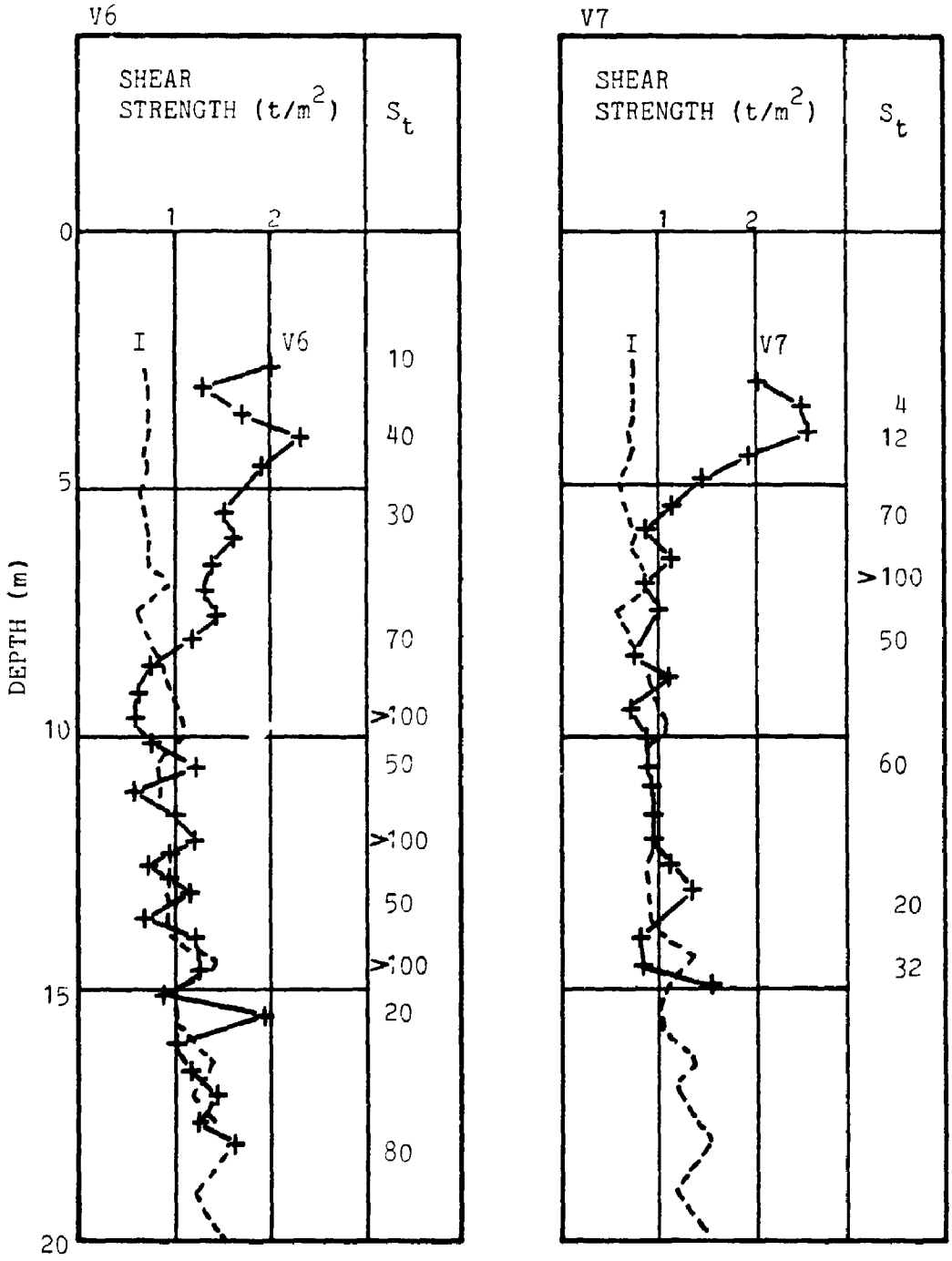

FIGURE 4.13 VARIATION OF VANE SHEAR STRENGTH WITH DEPTH AT LOCATIONS V6 AND V7 (after Bjerrum et al 1967)

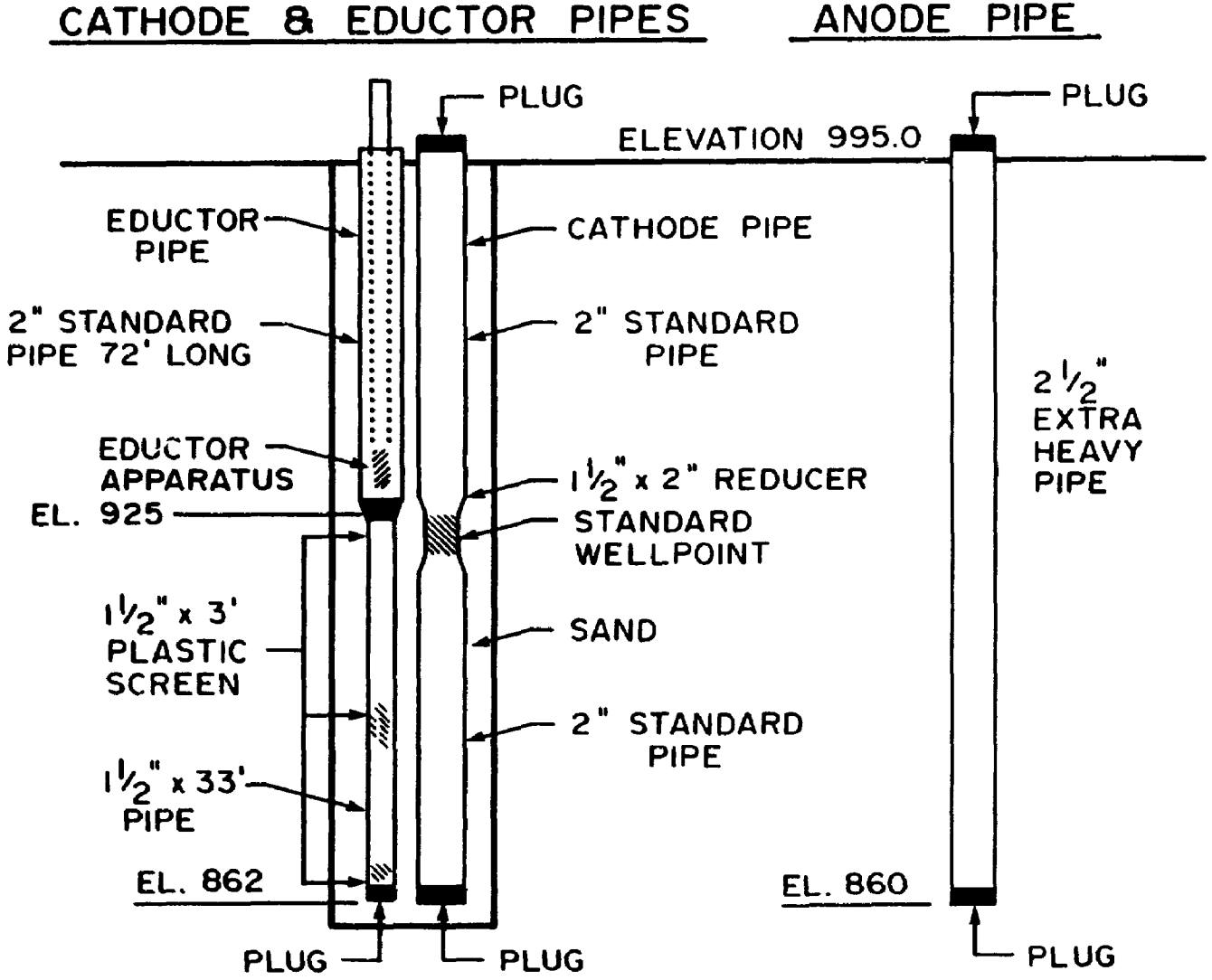

FIGURE 4.14a DETAILS OF ANODES AND CATHODES FOR WEST BRANCH DAM PROJECT (after Fet 1967)

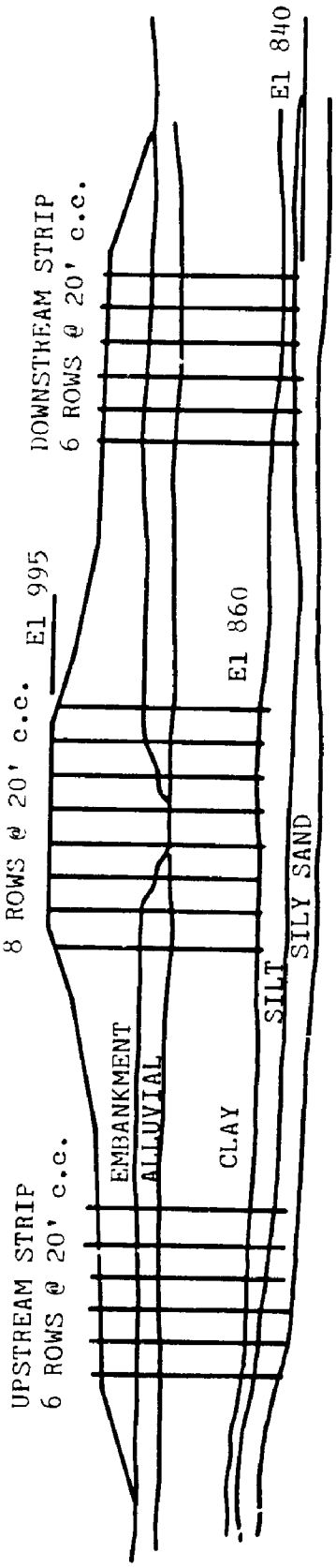

FIGURE 4.14b SECTION OF DAM SHOWING ELECTRO-OSMOTIC INSTALLATION, WEST BRANCH DAM PROJECT (after Fetzer 1967)

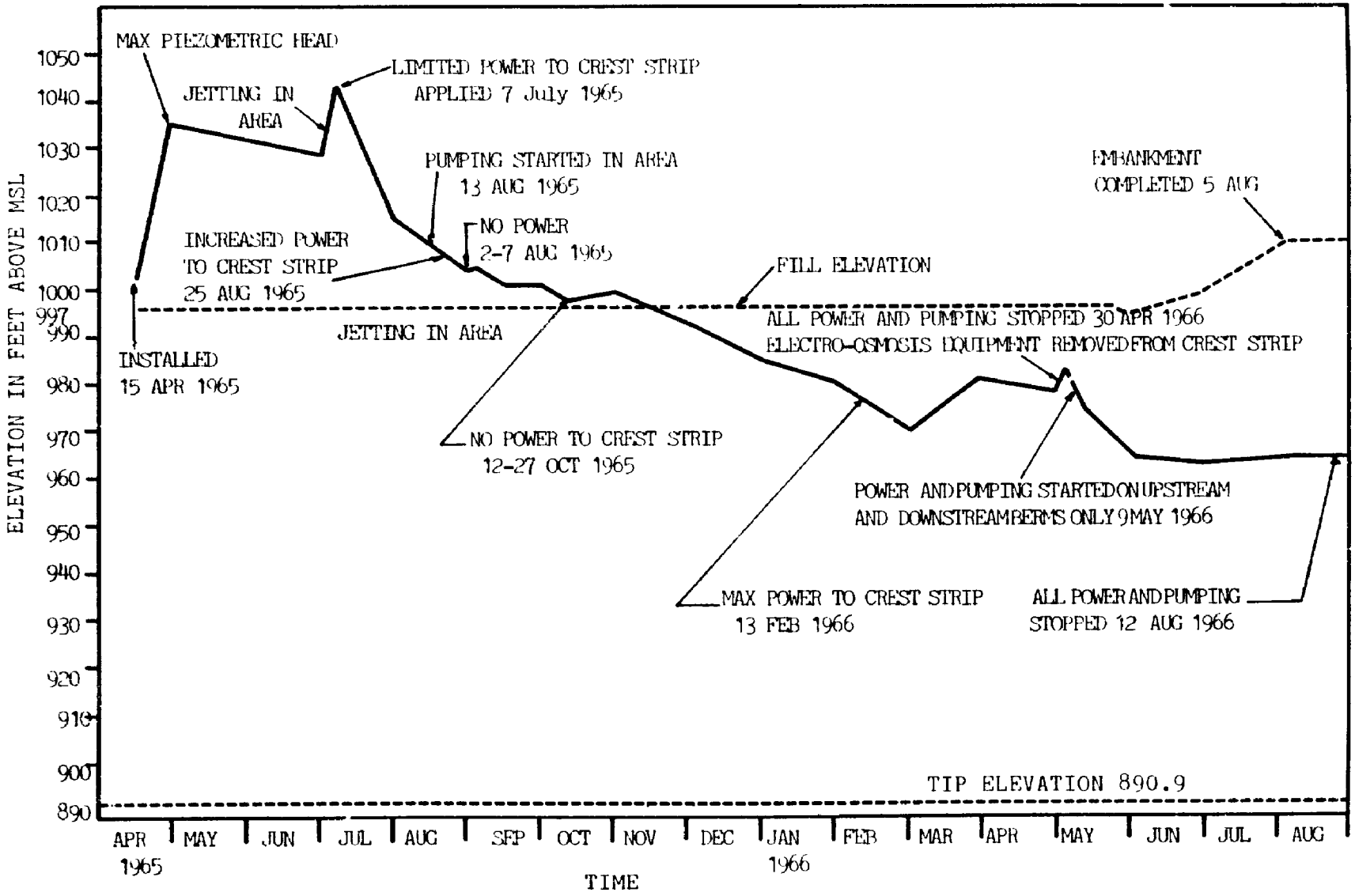

FIGURE 4.14c LOG OF PIEZOMETER NO. 3-DC, WEST BRANCH DAM PROJECT (after Fetzer 1967)

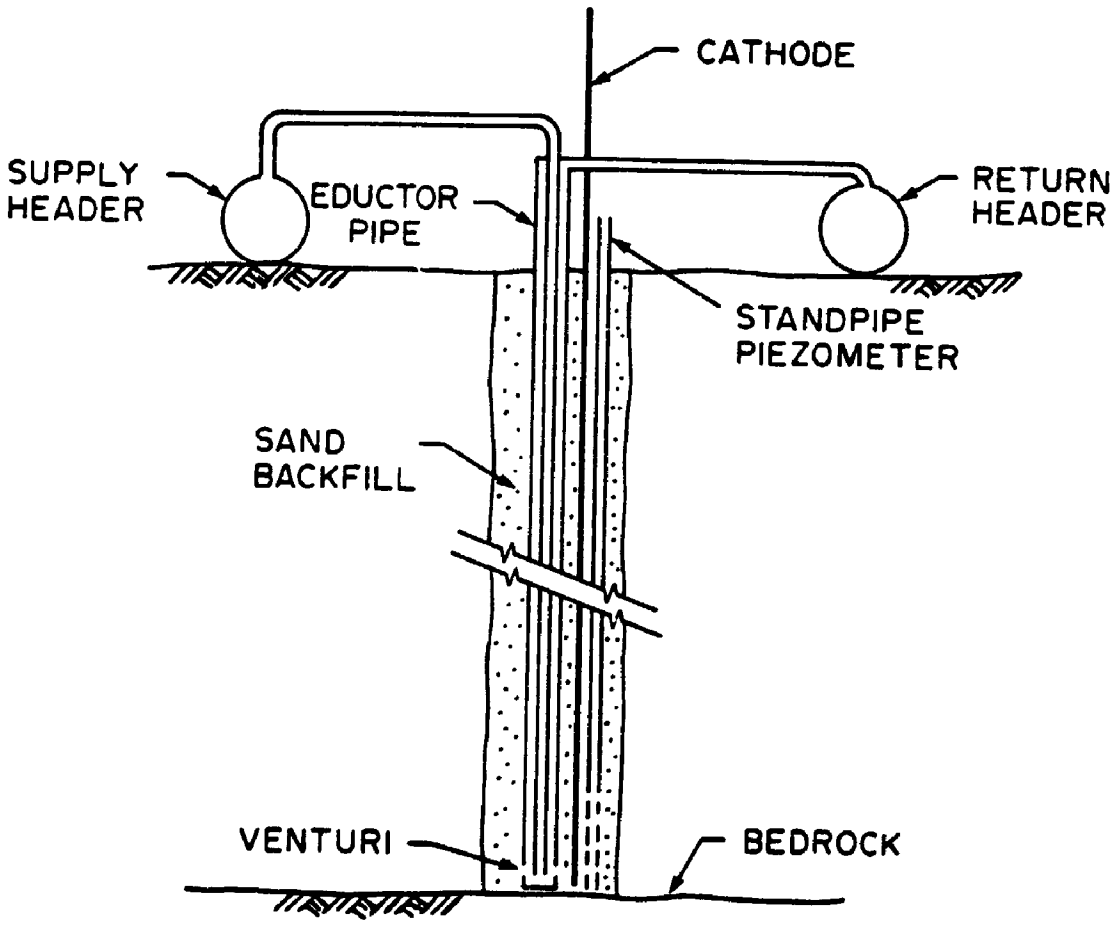

FIGURE 4.15 DIAGRAMATIC LAYOUT OF CATHODE INSTALLATION FOR KOONEY CANAL HYDROELECTRIC PROJECT (after Wade 1976)

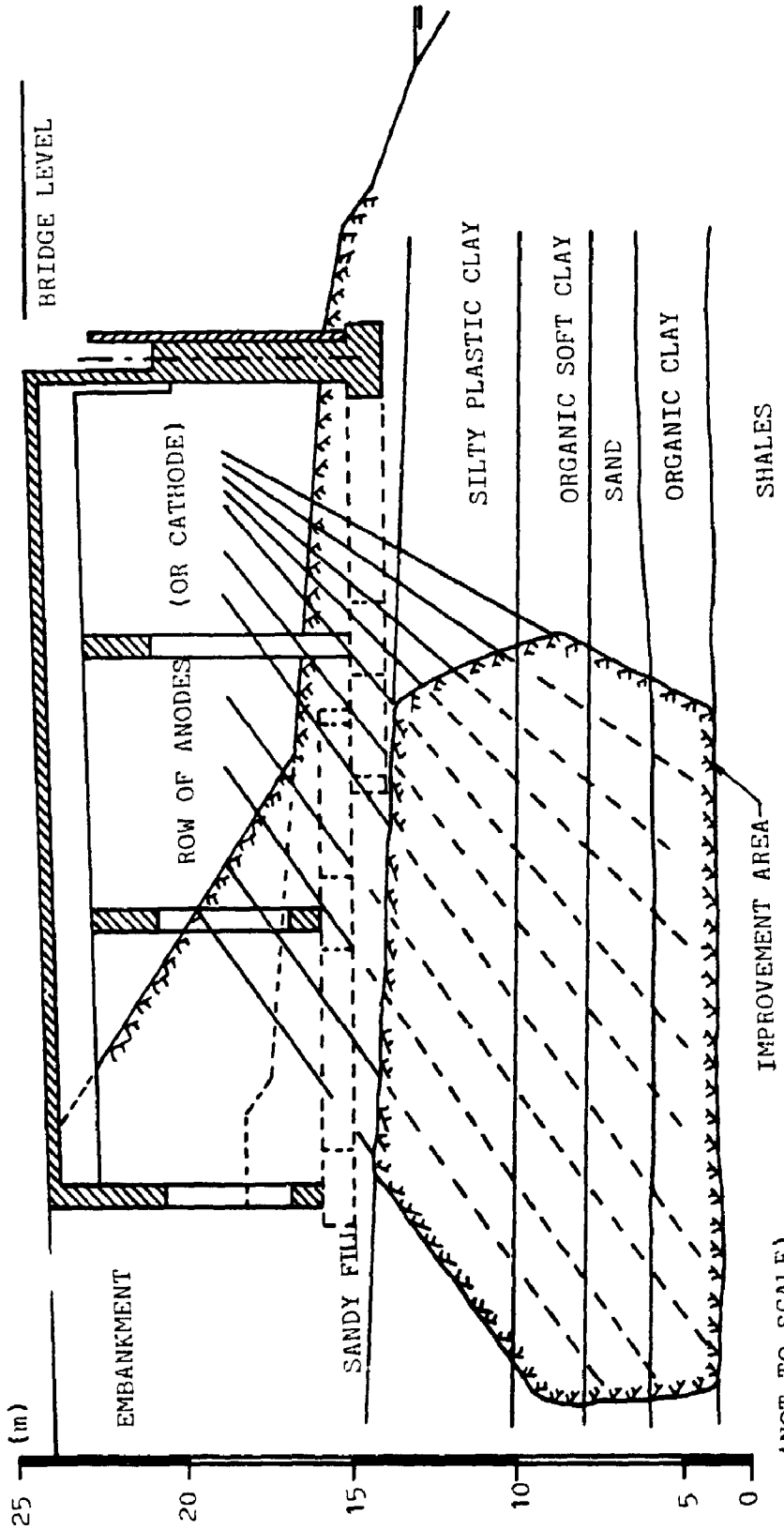

FIGURE 4.16 SOIL PROFILE UNDER THE BRIDGE ABUTMENT (after Caron 1971)

CHAPTER 5

ELECTRO-OSMOTIC CELL AND TEST PROCEDURES

5.1 Development of Electro-Osmotic Cell

Table 5.1 summarizes the features of previous experimental designs of electro-osmotic cell. In the development of osmotic cell, the following factors were taken into account:

(1) minimizing voltage loss between electrode and soil contact,

(2) removing the evolved gas during treatment,

(3) measuring the pore water pressure, potential difference within the sample and settlement of sample during treatment, and

(4) simulating the field stress and flow conditions in field application

One dimensional testing was adopted because of the ease of obtaining basic parameters. Determination of cell size was accomplished by taking the sample size and the sample aspect ratio into consideration. The sample should be of sufficient size to avoid the influence of local variation, and it should be small enough to avoid long consolidation time. The sample aspect ratio consideration is important in achieving uniform pc*ential distribution across the sample as mentioned in section 4.2.

An overview of the electro-osmotic test apparatus is shown in Figure 5.1 and the schematic diagram in Figure 5.2. Basically, the electro-osmotic cell (Figures 5.3 and 5.4) is made of 101.6 mm (4") plexiglas tubing of 304.8 mm (12") length

bounded by a top and a bottom plexiglas plates. The cell can accommodate soil sample of 101.6 mm (4") in diameter and various length up to 228.6 mm (9") long. Specially designed copper electrodes are placed at the top and the bottom of the soil sample. Lead wires are provided from both electrodes to the power supply device. A loading piston equipped with settlement dial gauge is provided at the top of the cell onto the top electrode. Drainage may be controlled at both ends of the cell. The apparatus is specially designed to dissipate the gas liberated at the electrodes by installing gas vents onto the drainage line at both ends. Several "o" ring fittings are fastened onto the side of the cell to house the voltage and pressure probes.

Special attention was focused onto the design of the electrode system. Several alternatives were investigated, among them was the use of coal as electrode material. The danger of using coal as electrode material is the generation of heat during electro-osmotic process together with the evolution of oxygen due to the electrolysis at the anode thus posing a possibility of catching fire. Other material such as steel and aluminium were also studied and corrosion at the anode was found. This results in the poor conductivity of electricity and hence reduces treatment efficiency. The use of silver chloride or platinum may be expensive and impractical. Copper was then chosen as the electrode material due to the good conductivity of copper oxide. The formation of copper oxide at the anode will also prevent the evolution of oxygen and hence the development of negative pore water pressure will not be affected. This can also be explained by the chemical reaction

as described in equations (3.16a) to (3.16e).

The soil-electrode interface is another potential area where energy loss might occur. A poor contact between the electrode and the soil will result in having a high resistance across the interface. It was found that a maximum contact between the soil and the electrode may be achieved if the electrode is made of two layers of copper rods welded together to form a circular disc. The first layer will enable the soil to fill in around each individual rod so that a maximum contact can be achieved. The second layer is to prevent any soil from squeezing past the disc. Copper rods of 4.8 mm (3/16") diameter were used in making up the disc electrodes. Each rod was cut to exact length and welded in place onto the prefabricated copper ring. Access for water and gas to escape through the disc was provided by filing off some of the material along each rod before it was welded together.

The seal at the top of the cell was maintained by placing a kapseal ring around the peripheral of the loading piston. The kapseal ring was used rather than the conventional type of seal such as the "o" ring because it is effective in making the seal between the cell and the piston and more importantly, it reduces friction at the contact area between the seal and the cylinder. The bottom of the cell was sealed by placing an "o" ring onto the bottom plate and the plate was pushed against the base of the cylinder and secured onto the top plate by means of the four threaded rods.

The potential difference across sample during test was measured by installing

the voltage probes at four intermediate points along the sample. The voltage probes are made of 1.6 mm (1/16") enamel wires and are fastened onto the side of the cell with an "o" ring fitting. One end of the probe was pushed about 50 mm into the sample and the other end is connected to a high impedance voltmeter for the measurement of potential difference from one probe to the other. A switch box was used so that the number of voltmeter required can be reduced to one. Enamel wire was used because of the coating on the wire will prevent any short circuiting to occur during treatment.

The pressure probe used to measure the negative pore water pressure is made of 1.6 mm stainless steel hypodermic tubing with one end plugged with a 1.6 mm porous tip and the other end connected to a pressure transducer and a readout device. The use of porous tip is to prevent the end of the probe from plugging up by soil when the probe is inserted into soil sample and serves as a sensing element for the pore water pressure. The connection for the pressure probes is the same as the voltage probes in that they are fastened onto the side of the cell with an "o" ring fitting. The readout device connecting to the pressure transducer consists of a switch box and a strain indicator. The detail of the pressure probe is shown in Figure 5.5.

A dial gauge is placed on top of the loading piston to monitor the settlement of sample.

The gas generated at the cathode was removed by the gas vent placed at the outlet of the drainage line. As shown in Figure 5.6, the gas vent consists of a gas

filter holder placed on top of a small cylinder. A filter membrane called "durapore filter" is placed inside the holder for filtering the evolved gas. The characteristic of the membrane is such that it will only filter gas and prevent water from passing through it. A differential pressure (70 kPa) as suggested by the filter manufacturer is provided between the inlet and the outlet of the filter. The outlet in this case is the atmospheric and the inlet is connected to the cell. The differential pressure was provided by applying back pressure to the cell. During treatment, whenever there is gas generated, it will find its way out to the atmosphere through the filter.

A potential area where problem might occur is at the interface between soil sample and the cylinder in that a film of water may be trapped at this boundary when the sample is pushed in place. This trapped water may cause electrical short circuiting and the treatment efficiency may be drastically reduced. The gap can be sealed off by applying a layer of high voltage grease around the interior of the cell. Other advantages of the grease are the reduction of the side friction between the soil sample and the cell during sample set-up and consolidation as well as reducing the friction between the loading piston and the cell.

5.2 Test Procedures

In this study, the samples tested were of 101.6 mm (4") diameter sample at various length trimmed from 304.8 mm (12") block samples of Wallaceburg clay and 152.4 mm (6") shelby tube samples of Gloucester clay. The exact dimension of each sample trimmed is important and care has to be taken that the sample fit

perfectly inside the osmotic cell. After the sample was trimmed, it was carefully pushed into place inside the osmotic cell. The loading piston together with one electrode fastened onto it was slowly lowered inside the cylinder until it touched the sample. The base plate with the other electrode fastened onto it was pushed in place. The top plate and the bottom plate were tightened onto the cell body by means of four threaded rods. The whole set up was placed on the loading table with hanger rested over the loading piston. The voltage and pressure probes were inserted 50 mm into the sample at intermediate location along the cylinder.

The test consists of two stages, the consolidation stage and the electro-osmotic treatment stage. The sample was consolidated to the effective overburden pressure by increments and a back pressure of 100 kPa was applied during the test. The electro-osmotic stage was started after the consolidation of the sample was virtually completed (pore pressure dissipated 95 %). During the application of electric potential, settlement of the sample, voltage distribution and pore water pressure at intermediate locations were monitored until the equilibrium (the stage of little fluctuation of pore water pressure) was reached. At equilibrium, the polarity of the electrode was reversed and the test was proceeded at the same applied electric potential as before. If required, the whole process could be repeated at higher applied electric potential. Immediately after the applied current was switched off, the pore water pressure and the settlement were continually monitored until the dissipation of the negative pore water pressure was completed. After the treatment, laboratory tests were carried out to determine the change of

the physical and mechanical properties of the soil.

5.3 Determination of Electro-Osmotic Permeability

A 38 mm (1.5") long sample was used to determine the electro-osmotic permeability k_e. A total of 3 tests were performed. One on the vertically trimmed Wallaceburg clay, one on the horizontally trimmed Wallaceburg clay and one on the vertically trimmed Gloucester clay. In each test, the sample was trimmed and placed inside a 76.2 mm (3") diameter osmotic cell. The drainage line at the top of the cell was opened to a reservoir of water and the bottom to the volume measuring device which consists of a 3.18 mm (1/8") nylon tubing connected to a 5 ml pipette. Voltage probes were inserted, one at each end of the sample to measure the effective voltage across the sample. After the initial consolidation, a pre-determined potential difference was applied to the sample with the top electrode as anode and bottom electrode as cathode. The discharge through the base of the osmotic cell was measured and the flow rate was determined. The electro-osmotic permeability k_e was then deduced by using equation (3.4a) with the measured flow rate and applied potential. The process was repeated for higher applied electric potential.

5.4 Model Test

In the past applications of electro-osmosis, the electrodes installation normally consisted of rows of metallic rods driven into ground. The spacings of electrodes,

between rows and within each row, as well as the sizes of electrodes used in each case history were different. Bjerrum et al (1967) used 10 m long, 19 mm diameter reinforcing iron bars at 2 m spacing between rows and 0.65 m spacing within the row. In Fetzer (1967), 41 m long of 63.5 mm steel rail at 6 m spacing between electrodes were used. In Wade (1976), 50 mm diameter steel pipe of 33.5 m length at 3 m spacing between rows and 6 m spacing within row were used. It is expected that each electrode layout may induce different potential distribution between anode and cathode. Hence, a different outcome of the results at the end of electro-osmotic treatment will be resulted.

An investigation into the effect of the different electrodes layout on the potential distribution was undertaken. Two tests were performed with the first test consists of equal electrode spacing and the second of variable spacing. Silver print was used as electrode material which was painted onto a conductive paper. The "fictitious electrodes" in each row were connected by small wire and lead to a power supply instrument and an electric potential was applied across each row of electrode. The equipotential lines within the row were determined with the aid of two sharp metallic probes, one placed onto the cathode (zero potential) and the other to locate the equipotential points. A network consisted of equipotential lines and current lines was then drawn.

The investigation was carried out further by including a simulated small scale test on remoulded and undisturbed Wallaceburg clay. The remoulded test (W-RM) was performed in a 101.6 mm width by 203.2 mm length by 76.2 mm height

(4" x 8" x 3") glass container. The tests on undisturbed sample of one 76.2 mm width by 127.0 mm length by 50.8 mm height (4" x 5" x 2") in size (W-UD1) and the other 76.2 mm width by 152.4 mm length by 50.8 mm height (3" x 6" x 2") in size (W-UD2) were performed inside a protective coat of wax. For the remoulded sample, three rows of 3.18 mm (1/8") copper tubing, three in each row were used. For the undisturbed sample, two rows of the same tubing with two tubings in each row were used. Along the side of each copper tubing, two rows of 1.6 mm diameter holes were drilled at 6.4 mm spacing. The purpose of these holes were to provide access for expelled water to flow into the tubing and out to the surface during treatment. In both tests, the tubing were pushed 50 mm into the soil.

The tests were not instrumented for measuring the induced pore water pressure and the volume of water discharged during treatment. For the remoulded sample, electric potential of 5 volts without electrode reversal was applied. At the end of the test, vane strengths and water contents were determined at intermediate locations between the electrodes. For the undisturbed samples, electric potential of 2.5 volts was first applied with polarity reversal. The process was repeated at applied electric potential of 4 volts with polarity reversal. After the tests, vane strengths and water contents were determined at the intermediate location between the electrodes. The results of these model tests will be described in Chapter 6.

Table 5.1 Some Previous Experimental Design of Electro-Osmotic Cells

Author	Principal Apparatus	Sample Size (mm)	Electrode Used	Parameters Measured During Test			
				PWP Distribution	Settlement	Voltage Distribution	Polarity Reversal
Casagrande (1952a)	standard oedometer	not described	platinum wire mesh	no	yes	no	no
Evans and Lewis (1966)	insulated cylinder	< 38 mm diameter	platinum gauge	at one electrode only	no	no	no
Esrig et al (1967)	lucite tubing	44 x 127	carbon rod and steel mesh	no	no	no	no
Johnston and Butterfield (1977)	triaxial cell	102 x 102	stainless steel mesh	yes	no	yes	no
Wan and Mitchell (1975)	consolidation flow box	60x200x200 (remoulded)	silver chloride	no	no	no	yes
Mitchell and Wan (1977)	standard oedometer	not described (remoulded)	silver chloride	yes	yes	yes	no
Casagrande (1983)	plexiglas tube	77 x 250	stainless steel wool and galvanized wire	no	no	no	no
Present Design	plexiglas tube	102 x 229	perforated copper disc	yes	yes	yes	yes

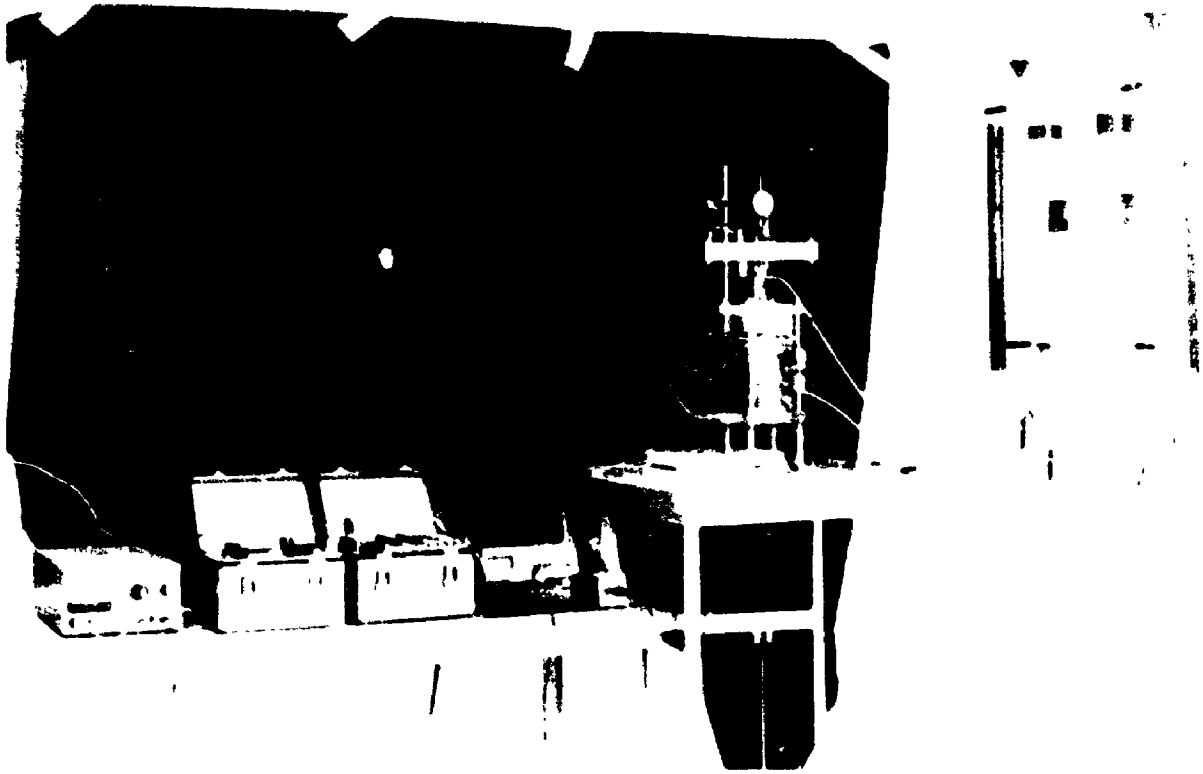

FIGURE 5.1 PHOTO OF ELECTRO-OSMOSIS TEST APPARATUS

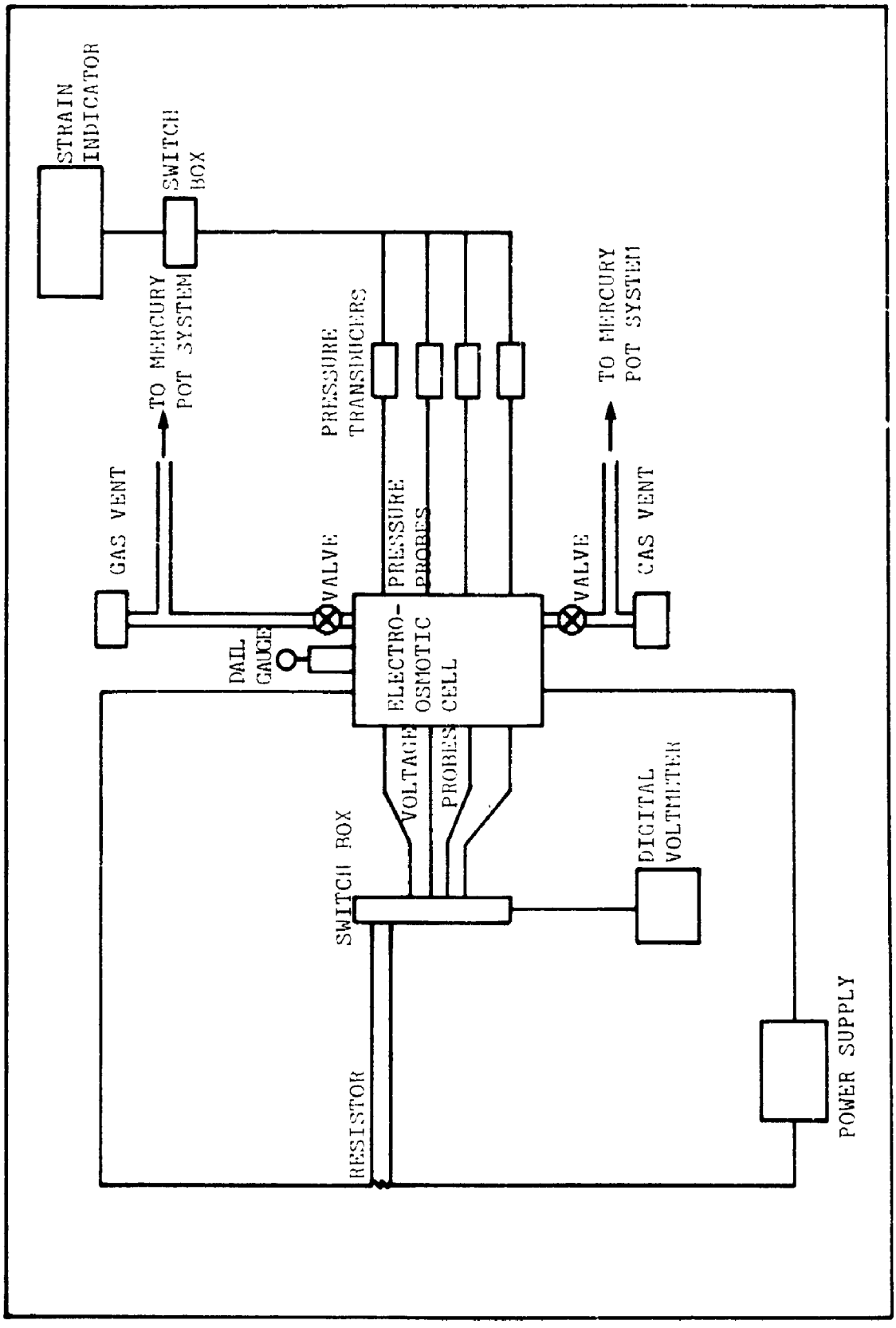

FIGURE 5.2 SCHEMATIC DIAGRAM FOR ELECTRO-OSMOSIS TEST APPARATUS

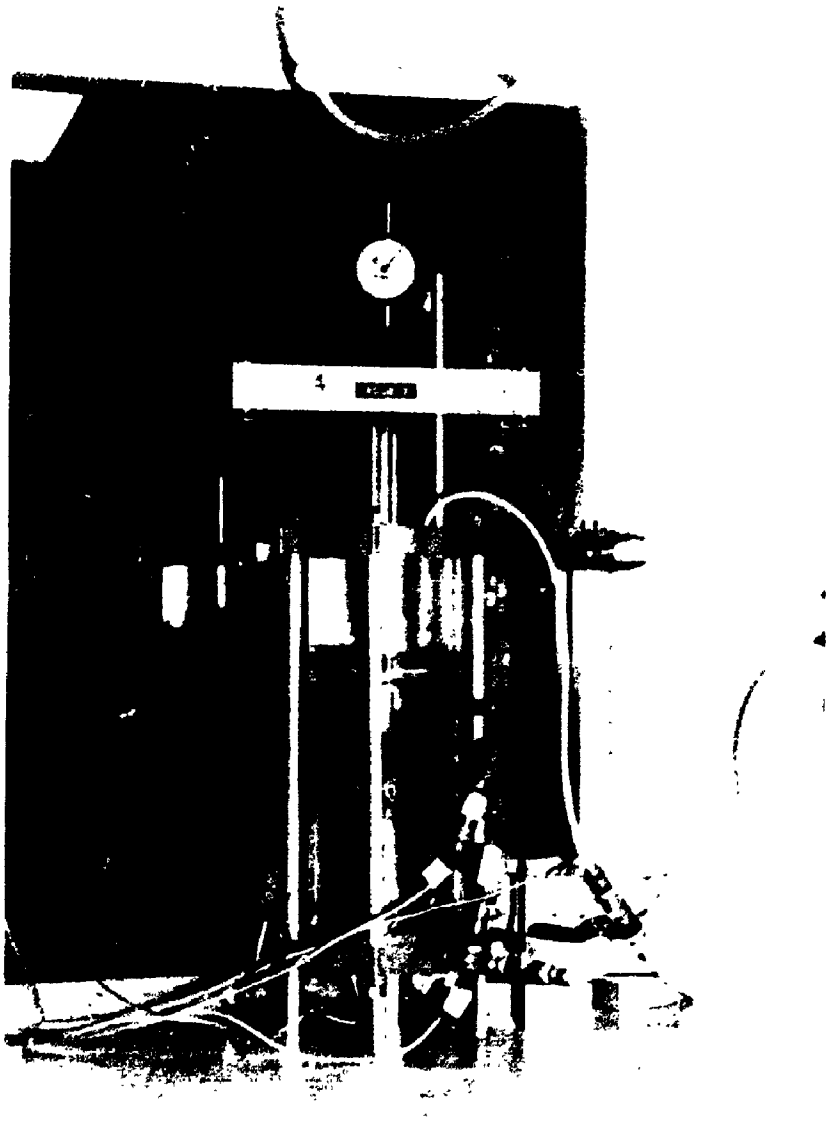

FIGURE 5.3 PHOTO OF ELECTRO-OSMOTIC CELL

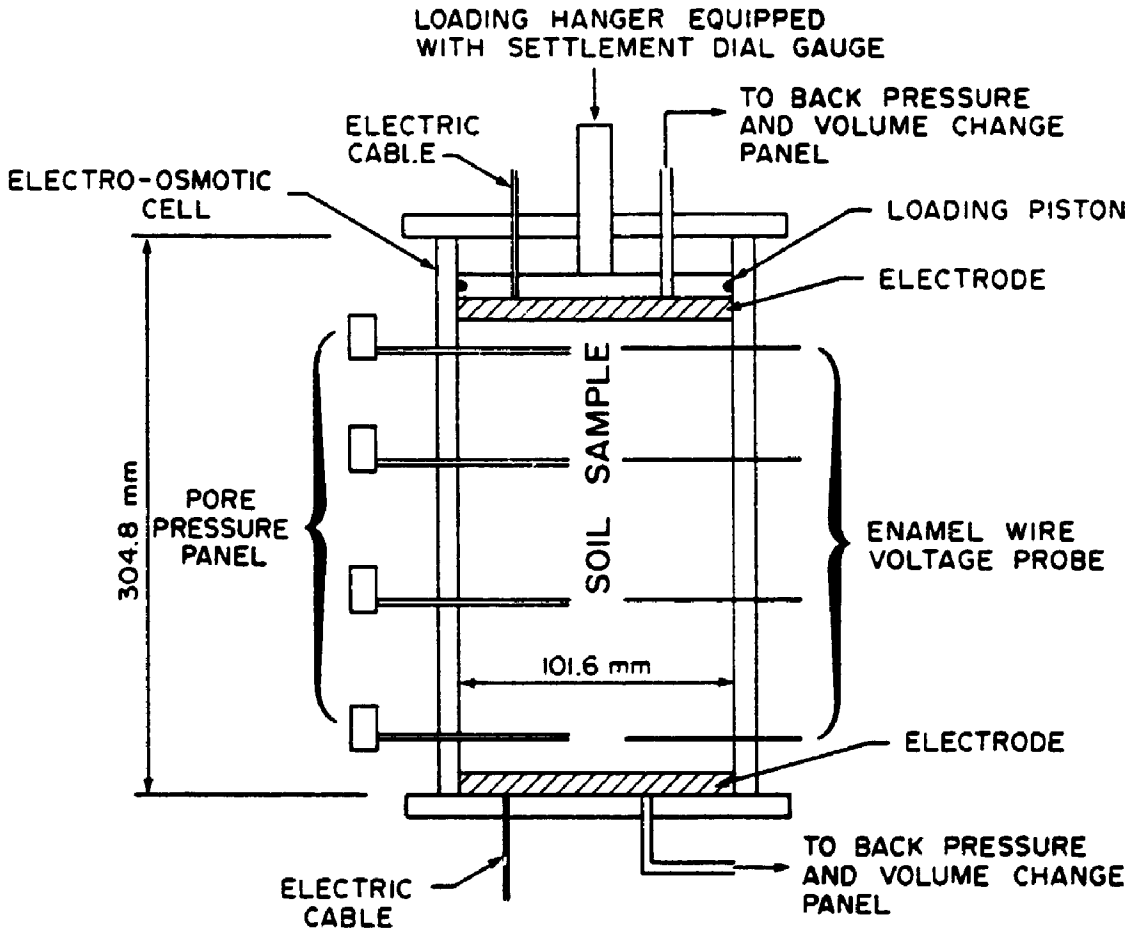

FIGURE 5.4 ELECTRO-OSMOTIC CELL

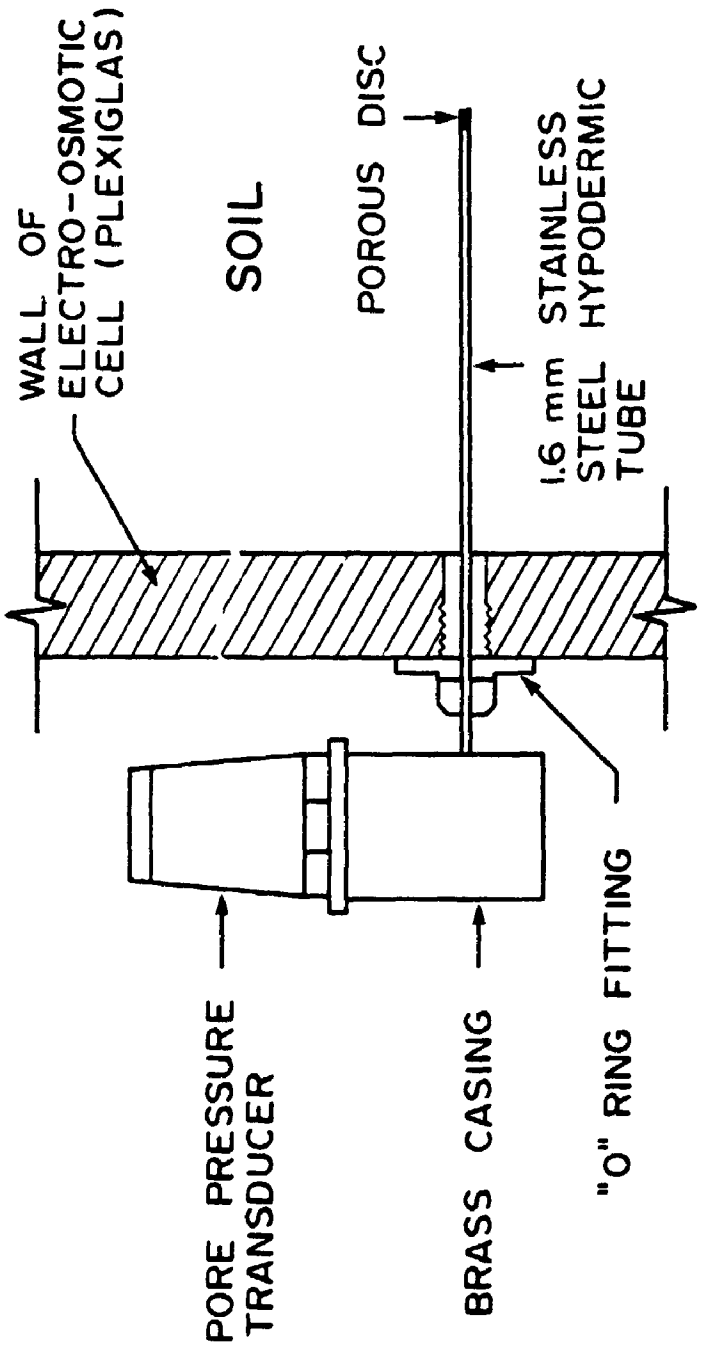

FIGURE 5.5 DETAILS OF PORE PRESSURE PROBE

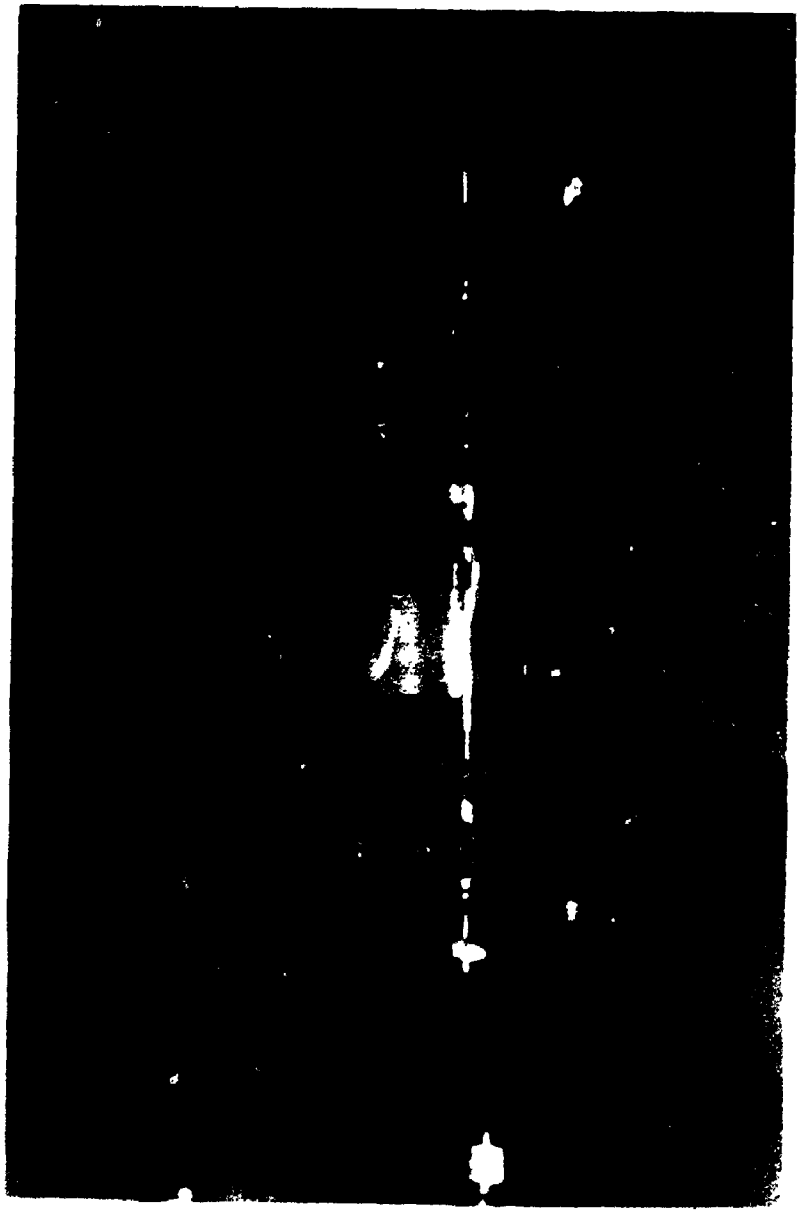

FIGURE 5.6 GAS VENT

CHAPTER 6

EXPERIMENTAL STUDY

6.1 Site Description and Location

Two clays of significantly different properties and extensive geotechnical data were investigated, the Wallaceburg clay and Gloucester clay. The location of the site for Wallaceburg clay sampling is shown in Figure 6.1. The site is located on Darcy Mckeough floodway, 640 m east of the Base Line and about 3 km west of the Highway 40. The location of the site within the floodway is shown in Figure 6.2. The physiographic region encompassed the site is known as the St. Clair Clays Plain. The region consists of a thick clay deposit overlying either limestone or black shale bedrock. The sedimentary deposits are generally classified as normally consolidated, water-lain tilts, products of the late Wisconsin Substage of Glaciation (Chapman and Putnam 1951, Quigley and Ogunbadejo 1976).

The site where the Gloucester clay samples were recovered is located at the Gloucester Test Fill area of the National Research Council, at about 20 km south-east of Ottawa. The location of the sampling site within the test fill area is shown in Figure 6.3. The sedimentary deposit encompassed the area is the marine deposit of Champlain Sea clay which covers the entire St. Lawrence lowland and Ottawa valley. The geological history of the deposit had been extensively investigated (Karrow 1961, Crawford 1961). Basically, the sediment

was formed during the retreat of the last ice sheet. The sediment now at that area was formed through various stages of deposition, erosion and redeposition.

6.2 Field Sampling

The Wallaceburg clay was recovered in the floor of the floodway where the top 4.6 m of the soil had been removed during the construction of the channel. The cross-section of the floodway is shown in Figure 6.4. A 2.5 m by 2.5 m pit was hand excavated to a depth of 1 m below the bottom of the channel. Inside the pit, several trenches of 0.6 m wide by 0.5 m deep were dug at 0.3 m interval. These trenches provided working space for trimming the sample. Block samples of 304.8 mm (12") cube were carefully trimmed and taken out of the pit. The sample were immediately wrapped with plastic bag to prevent any moisture ioss. A total of 8 samples were recovered. All of the samples were carefully transported back to the Soil Mechanics Laboratory of The University of Western Ontario where they were waxed and stored for future testing.

The Gloucester clay samples were recovered from the depth between 2 m to 6 m. They were of 152.4 mm (6") shelby tube samples.

6.3 Stratigraphy and Soils Properties

The subsoil condition at the Wallaceburg site consists of 0.15 m of topsoil, 2.9 m of stiff to very stiff brown silty clay crust, and 18 m of firm to soft grey

silty clay (Lo and Becker 1979). The grey silty clay stratum is comprised of the upper firm to soft silty clay stratum from depth 3.05 m to 12.2 m and the lower firm silty clay stratum below the 12.2 m. Block samples were obtained from the upper firm to soft silty clay stratum. Field vane strength of the clay measured was about 22 kPa with average moisture content of 38 percent. Average liquid and plastic limits are 44.7 and 20.9 % respectively. The sensitivity of the clay is about 5 with an overconsolidation ratio of 9.

The subsoil condition at the Gloucester test fill area consists of 20 m Champlain Sea Clay (Leda Clay) deposit. The deposit is classified into three basic layers according to index properties, undrained shear strength and preconsolidation pressure (Lo, Bozozuk and Law 1976). Layer 1 comprising of 2.3 m desiccated top crust overlies 4.7 m soft grey silty clay. Layer 2 is a 6.1 m thick grey clay and layer 3 is a 5.1 m thick grey silty clay. Tube sample of 152.4 mm (6") nominal diameter was obtained from the soft grey silty clay stratum of layer 1. Vane strength of the clay is about 12 kPa with moisture content varying from 60 to 80 percent. Average liquid and plastic limits are 48 and 24 % respectively. The sensitivity of the clay is about 100 with an overconsolidation ratio of 1.5. Details of the soil properties at the two sites may be found in the references cited.

6.4 Test Results

A total of ten electro-osmotic tests were performed on the Wallaceburg clay

and the Gloucester clay. Table 6.1 shows the sample depth, trimming orientation, sample length, applied electric potential and potential polarity for each test. Each test is completed by a cycle of normal and reversed polarity at a specific potential difference. All the tests were carried out with anode closed and cathode opened and the test results are summarized in Table 6.2. The description of the notations used for the tests is illustrated as follow:

WH-4 = horizontally trimmed Wallaceburg clay, 4" in length (101.6 mm)

WV-4 = vertically trimmed Wallaceburg clay, 6" in length (154.2 mm)

GV-8 = vertically trimmed Gloucester clay, 8" in length (203.2 mm)

For brevity and convenience of presentation, only typical results of each clay is presented and the complete record of results of all the tests performed is contained in Appendix A.

6.4.1 Results of Test on Wallaceburg Clay - Vertical Sample

In this section, test results of sample WV-8A are presented. The 101.6 mm (4") in diameter by 203.2 mm (8") in length sample was subjected to 3 volts and 4.5 volts applied electric potential with polarity reversal.

6.4.1.1 Pore Water Pressure

The generation of negative pore water pressure was initiated as soon as electric current was switched on. Its development with time are shown in Figure 6.5 for test at 3 volts and in Figure 6.6 for test at 4.5 volts. For normal

and reverse test at the given voltage, it was observed that the rate of pore water pressure development decreased with distance away from anode (the end with maximum induced pore water pressure) and at cathode, the pore water pressure remained unchanged with time. It was also noted that the rate of pore water pressure development varied with time. At early stage of treatment, the rate was greatest. As treatment continued, the rate decreased and eventually diminished as it approached equilibrium. At equilibrium, further treatment of the sample did not result in any further decrease in pore water pressure.

For 3 volts normal test, a nonlinear pressure distribution was developed at the early stage of development. The gradient gradually became more and more uniform as treatment progressed. At equilibrium, a constant gradient was developed with maximum negative pressure induced at anode and decreased linearly to zero at cathode. For 3 volts reverse test, the nonuniform pore water pressure gradient was also developed at intermediate stages of treatment. However, a constant gradient was not obtained at equilibrium. At higher voltage (4.5 volts), uniform gradient was obtained throughout the treatment with linear distribution at equilibrium for both normal and reverse tests.

The rate of pore water pressure development for the normal test was different from the reverse test. For 3 volts normal test, it took 1428 minutes to develop pressure of -42 kPa at anode. For 3 volts reverse test, a higher negative pressure was obtained in lesser time in which negative pressure of -69 kPa was obtained at anode in only 605 minutes. In the 4.5 volts normal

test, it took 1360 minutes to develop pressure of -150 kPa at anode. For the reverse test, it took only 735 minutes to develop the same pressure at anode.

In each applied electric potential, higher pore water pressure was induced at equilibrium in the reverse test than in the normal test. For 3 volts normal test, pressure of -75 kPa was induced at anode at equilibrium. For 3 volts reverse test, the maximum pressure of -102 kPa was induced at anode. For 4.5 volts normal test, maximum pressure at anode during treatment was -150 kPa. For 4.5 volts reverse test, the maximum pressure at anode was -178 kPa.

6.4.1.2 Settlement

Figure 6.7 shows settlement of the sample for treatment at 3 volts and Figure 6.8 shows additional sample settlements when applied voltage was increased to 4.5 volts. The figures indicate that the log-time plot of the electro-osmotically induced settlement curve is similar in shape to that of typical conventional consolidation curve.

During treatment at 3 volts, 3.62 mm (1.78 %) settlement was measured. At 4.5 volts, additional 3.50 mm (1.72 %) settlement was measured. A total of 7.11 mm (3.50 %) settlement was obtained for the test.

The settlement curves indicate that the sample during treatment continued to settle when equilibrium was reached. For 3 volts normal test, the induced pore water pressure at 2140 minutes and at 2955 minutes did not change much but an additional 0.52 mm (0.26 %) settlement was noticed during the period.

For 3 volts reverse test, an additional 0.45 mm (0.22 %) settlement was measured (between 1790 and 3170 minutes). For 4.5 volts normal and reverse tests, the amount of additional settlement at constant pore water pressure was not significant.

6.4.1.3 Voltage and Current

Figure 6.9 and Figure 6.10 show voltage distribution within sample with time during the tests. For 3 volts test, a greater variation in voltage with time was observed in the normal test than in the reverse test. For 4.5 volts test, the variation in voltage with time for both normal and reverse test during treatment was small. The smaller voltage variation for the 3 volts reverse test and for test at higher applied voltage indicate that homogeneity of sample increased with electrode reversal during treatment.

Figure 6.11 and Figure 6.12 show the current variation across the sample with time. The current through the sample followed a specific trend. At the start of the test, the current through the sample was maximum. The current continued to drop as treatment progressed until eventually a constant current was obtained. For 3 volts normal test, the current through the sample dropped from 15.2 mA (milliamperes) at the beginning of the test to a constant value of 12.6 mA at 1300 minutes. For 3 volts reverse test, an unusual trend in the current variation was obtained in which the current through the sample increased from 10.5 mA at the beginning of the test to 12.7 mA at 900 minutes

and then decreased to 12 mA at the end of the test. In the 4.5 volts test, the current dropped from 23.1 mA to a constant value of 19.6 mA for normal test and to 18 mA for reverse test.

6.4.1.4 Strength and Moisture Content

Vane strengths (by laboratory vane test device) and moisture contents of treated sample at different locations are shown in Figure 6.13 and Figure 6.14 respectively. The change in water content and strength of soil after treatment can be related to the induced pore water pressure during treatment. Figure 6.5 and Figure 6.6 show that the soil at vicinity to the electrodes were subjected to high negative pore water pressure during treatment. The shear strength increase and moisture content reduction at these regions were also maximum. In the middle of the sample, the induced pore water pressure was minimum during treatment and consequently the shear strength increase and moisture decrease were smallest. The treatment resulted in a strength increase from 23 kPa to an average of 40.5 kPa, representing a gain of 76.1 % in strength. The moisture content reduced from 38.5 % to 34.2 %.

6.4.2 Results of Test on Wallaceburg Clay - Horizontal Sample

Results for samples WH-6A and WH-6B are presented in this section. Both samples are 101.6 mm (4") in diameter and 152.4 mm (6") in length. Test WH-6A was subjected to 4 volts electric potential without electrode reversal.

Test WH-6B was subjected to 2 volts and 4 volts electric potential with electrode reversal.

6.4.2.1 Pore Water Pressure

The induced negative pore water pressure with time during treatment is shown in Figure 6.15 for sample WH-6A. It was observed that the initial rate of development of negative pore water pressure during each test was rapid and the rate reduced with time. At cathode, pore water pressure remained unchanged with time. The pore water pressure gradient along the sample during treatment was not uniform and the nonuniformity gradually diminished as treatment approached equilibrium. At equilibrium, a linear distribution was obtained with maximum induced negative pore water pressure at anode and zero pressure at cathode.

Similar to the test on vertically trimmed Wallaceburg clay, higher induced negative pressure for reverse test than for normal test was also observed in sample WH-6B at 2 volts test (Figure 6.21). At 2 volts, maximum pressure of -41 kPa was induced at anode for reverse test as compared to -33 kPa at anode for normal test. However, at 4 volts test (Figure 6.22), lower pressure was induced for reverse test (-100 kPa) than for normal test (-135 kPa).

Greater rate of pore water pressure development (as in the vertical samples) in the reverse test than in the normal test was also observed in sample WH-6B. At 2 volts normal test, it took 405 minutes for a pressure of -15 kPa

to develop at anode while at 2 volts reverse test, it took 355 minutes for a higher pressure of -24 kPa to develop at anode. At 4 volts normal test, it took 413 minutes for a pressure of -66 kPa to develop at anode while for reverse test, it took 283 minutes for the same pressure to develop at anode.

6.4.2.2 Settlement

Settlement of the samples during treatment is shown in Figure 6.16 for WH-6A and in Figures 6.23 and 6.24 for WH-6B. The similarity in the shape of the settlement curves in log-time plot to that of typical conventional consolidation curve of the same plot is again observed.

For test no. WH-6A, a total of 2.39 mm (1.57 %) settlement was obtained during treatment. For sample WH-6B at 2 volts, 1 mm (0.66 %) of sample settlement was measured. At 4 volts, an additional 2.72 mm (1.78 %) settlement was measured.

For sample WH-6A, during the period of small fluctuation in pore water pressure (between 1744 minutes and 2383 minutes), 0.43 mm (0.28 %) of sample settlement was measured. This amount represents quite a significant portion of the total settlement (2.39 mm). For sample WH-6B, at both 2 volts and 4 volts, no significant settlement was detected during the period of constant pressure.

6.4.2.3 Voltage and Current

Figures 6.17, 6.25 and 6.26 show the voltage distribution with time within sample during treatments. For sample WH-6A, initially an almost linear voltage distribution across the sample was obtained. As treatment continued, the variation in voltage with time increased in which most of the changes occurred at sections next to cathode. For sample WH-6B, at 2 volts on both normal and reverse test, the variation in voltage with time during treatment was small. But the distribution in voltage in the reverse test was again more uniform (as in vertical sample) than the distribution in the normal test. At 4 volts, small variation in voltage with time was obtained for both normal and reverse test. The voltage distribution in both normal and reverse test was quite uniform.

Flow of current through samples during treatment are shown in Figures 6.18, 6.27 and 6.28. The variation in current with time again followed the same trend as in the vertical sample. For WH-6A test, the current dropped from 22 mA to 19 mA at 1740 minutes. In the 2 volts normal test of sample WH-6B, the current dropped from 11 mA to a constant value of 7 mA at 1450 minutes. For 2 volts reverse test, except the initial unusual trend in which current through sample decreased from 11.1 mA to 9 mA at 200 minutes and increased to 11 mA at 360 minutes, the current through sample beyond 360 minutes again decreased to a constant value of 9.9 mA at 1075 minutes. At 4 volts normal test, the current dropped from 29 mA to constant value of 18.5 mA at 1180 minutes. For 4 volts reverse test, the current dropped from 21.5

mA to a constant value of 14.5 mA at 1450 minutes.

6.4.2.4 Strength and Moisture Content

Vane shear strength and moisture content at different locations within the sample are shown in Figure 6.19 and Figure 6.20 respectively for WH-6A test and Figure 6.29 and Figure 6.30 respectively for WH-6B test.

For sample WH-6A, both the induced pore water pressure and the increase in strength were maximum at anode and decreased in magnitude towards cathode with no change in strength at cathode. The change in moisture content along the sample exhibits similar trend as in the change in strength of the sample. The reduction in moisture content was maximum at anode and decreased magnitude towards cathode with no change in moisture content at cathode. The treatment caused strength to increase from 22.5 to 27 kPa and moisture content to decrease from 42.9 to 40.6 % at anode.

For sample WH-6B with polarity reversal (Figures 6.29 and 6.30), a more uniform increase in strength and decrease in moisture content were resulted along the sample after treatment as compared to that of WH-6A test. The strength increased from 23 kPa to an average of 37 kPa and moisture content decreased from 37.5 to an average of 33.7 %.

6.4.3 Results of Test on Gloucester Clay - Vertical Sample

Results of sample GV-8 are presented in this section. The 101.6 mm (4")

in diameter by 203.2 mm (8") in length sample was subjected to electric potential of 3 volts and 6 volts with electrode reversal.

6.4.3.1 Pore Water Pressure

The development of pore water pressure during treatment are shown in Figures 6.31 and 6.32 and similar observations as in the tests on Wallaceburg clay were made. At cathode, pore water pressure remained unchange with time. Pore water pressure gradient throughout the tests were fairly uniform.

In contrast to the tests on Wallaceburg clay, the rate of pore water pressure development in normal test and reverse test are almost identical. In addition, the maximum induced pressure in both normal and reverse tests are almost the same. At 3 volts, the maximum induced pressure measured at anode for the normal test was -26.5 kPa and for the reverse test was -27 kPa. At 6 volts, the maximum induced pressure measured at anode for the normal test was -75 kPa and for the reverse test was -67 kPa.

6.4.3.2 Settlement

Settlements of the sample are shown in Figure 6.33 for test at 3 volts and Figure 6.34 for test at 6 volts. The shape of the curves in log-time plot are again similar to that of the typical conventional consolidation curve.

At 3 volts, 5.42 mm (2.66 %) settlement was measured in the normal test and 2.09 mm (1.03 %) was measured in the reverse test. When the applied

voltage was doubled, quite a significant amount of additional settlement was induced. For the normal test, 5.71 mm (2.81 %) settlement was detected and for the reverse test, 6.76 mm (3.33 %) settlement was detected.

As for the tests on Wallaceburg clay, the samples continued to settle at equilibrium. For 3 volts normal test, an additional 0.25 mm (0.12 %) settlement was measured (between 680 and 1340 minutes). For 3 volts reverse test and 6 volts tests, the settlements at equilibrium were not significant.

6.4.3.3 Voltage and Current

Figures 6.35 and 6.36 show the voltage distribution at different times after the current was switched on. It may be seen that the distribution of voltage is continuous across the sample and there is no sudden decrease in voltage at electrode-soil interface. The trend in current variation during treatment is plotted in Figures 6.37 and 6.38. In the first 200 minutes of the test, the current through sample decreases rapidly then followed by a gradual drop to more steady current flow throughout the treatment. At 3 volts, the current through sample dropped from 9.5 mA to 7.5 mA for normal test and from 12.5 mA to 8.5 mA for reverse test. At 6 volts, the current dropped from 28.8 mA to 18 mA for normal test and to 27.6 mA to 23 mA for reverse test.

6.4.3.4 Strength and Moisture Content

Vane strengths and moisture contents of sample after treatment are shown

in Figures 6.39 and 6.40 respectively. The relation between the change in strength of the sample after treatment and the induced water pressure during treatment (as in the case of Wallaceburg clay) was again illustrated. At sections next to the electrodes, the induced pressure during treatment was the greatest and the resulted strength increase at these sections was the highest (from 11 kPa to 32 kPa). At the middle section, the induced pressure was the lowest and consequently the resulted strength increase at this section was the least (from 11 kPa to 27.5 kPa). Similarly, the reduction in moisture was the highest at both end sections (from 97.5 % to 60 %) and lowest at the middle section (from 97.5 % to 75 %).

6.5 Electro-osmotic Permeability

The electro-osmotic permeability tests were carried out in a 76.2 mm (3") diameter osmotic cell. The size of sample used in the tests was 76.2 mm (3") diameter by 38 mm (1.5") in length. A total of three tests were performed, one on a vertically trimmed Wallaceburg clay sample, one on a horizontally trimmed Wallaceburg clay sample and the other on a vertically trimmed Gloucester clay sample.

Figures 6.41 to 6.43 show the plots of electro-osmotic permeability with applied electric potential. For the vertically trimmed Wallaceburg clay, k_e varies from 7 to 15 x 10^{-6} $cm^2/v\text{-}s$ with applied voltage between 1 and 2.5 volts. For the horizontally trimmed Wallaceburg clay sample, it varies from 7 to 16 x

10^{-6} cm²/v-s with applied voltage between 1.5 and 3 volts. For the Gloucester clay sample, it ranges from 1.6 to 2 x 10^{-6} cm²/v-s with applied voltage between 1 and 4 volts.

These results revealed that there is a critical value of applied voltage below which the variation between k_e and the applied voltage is significant. Beyond the critical voltage, k_e is constant. The critical applied voltage for the vertically trimmed Wallaceburg clay, horizontally trimmed Wallaceburg clay and the vertically trimmed Gloucester clay samples are 2.5, 3 and 3 volts respectively.

6.6 Model Test

Equipotential lines and current flow lines between rows of anodes and cathodes on a simulated electrodes layout were determined by using the procedures described in section 5.4. Silver print was used as electrodes painted into rows at selected locations on a conductive paper. An electric potential of 10 volts was applied across the rows of anodes and cathodes. With metallic probes one being placed at cathode and the other to locate the potential difference between two points, equipotential lines and current flow lines were drawn. Two tests were performed with one at equal electrode spacing within the row and the other with variable electrode spacing within the row. The test results are shown in Figures 6.44 and 6.45.

A total of three electro-osmotic model tests were performed, one test on remoulded Wallaceburg clay and two tests on undisturbed Wallaceburg clay.

The remoulded sample (W-RM) was of 101.6 mm width by 203.2 mm length by 75.2 mm height (4" x 8" x 3") in size. Two sizes of undisturbed sample (W-UD1 AND W-UD2) were used, one of 75.2 mm width by 127 mm length by 50.8 mm height (3" x 5" x 2") and the other of 75.2 mm width by 177.8 mm length by 50.8 mm height (3" x 7" x 2") in size.

For the test on remoulded clay (sample W-RM), water and gas were observed to flow out through the cathode at about 5 minutes after electric potential was switched on. The rate of discharge reduced with time. No water was detected at the beginning of the third day of treatment. At the anodes, soil around each electrode settled. The settlement created a noticeable region of depression surrounding the anodes. Blue substance which is believed to be copper oxide was deposited onto the anodes. The deposit accumulated as the time of treatment progressed. After two days of treatment, vertical cracks of soil were started to develop around the anode. The cracks are 25 mm in length and extended all the way down to the bottom of the container.

Vane tests and moisture content tests were performed at different locations between the rows of electrodes after the treatment. The vane device penetrated 25.4 mm (1") from the surface. The results are shown in Figure 6.46. Moisture content tests were carried out along two sections on the block, one between the electrodes and the other across the electrodes and the results are shown in Figure 6.47.

From the figures, the increase in vane strength after treatment is maximum

at the vicinity around the anode but no change in strength at cathode. The vane strength of the remoulded clay before treatment was 8 kPa. After treatment, the measured vane strength at anode is 32 kPa which represented a four fold increase. The moisture content reduction after treatment showed a similar trend as in strength increase. After treatment, the reduction in water content is the maximum at the region where the increase in strength is greatest. At cathode, where there is no change in vane strength after treatment, the water content remained unchange. Lines of equal undrained shear strength within the treated area were drawn (Figure 6.46). When compared with the sketch of equipotential lines drawn on the conductive paper (Figures 6.44 and 6.45), similarity in the pattern between the two sketches is clearly shown. It suggests that effective electric potential at any one location will determine the magnitude of strength increase at that location.

For the tests on undisturbed sample (W-UD1 and W-UD2), as soon as electric power was switched on, water was observed to flow out from the cathodes. The W-UD1 test, in which the sample is 50 mm smaller in length than sample W-UD2, reached equilibrium after 2 days of treatment while the W-UD2 test required 3 days to attain the equilibrium at 2.5 volts applied electric potential. When polarities were reversed, there was no detectable immediate changes. After 2 hours, water and gas started to flow out from the new cathodes. Water ceased to flow at the end of the second day after reversal for W-UD1 test and at the end of third day after reversal for W-UD2 test. At

higher voltage (5 volts), the time to reach equilibrium was faster on both normal and reverse test. It required 2 days for W-UD2 and 1 day for W-UD1 to reach equilibrium. Since the samples were enclosed in wax to prevent it from drying out, phenomenon such as cracks and deposition of blue compound were unable to be detected during the treatment. After the test, when the enclosed wax was removed, no evidence of crack was found. Blue coloured compounds were deposited onto all the electrodes.

Vane strength was determined on the treated samples at different locations. The vane device was penetrated into the soil 25.4 mm (1") from the surface of the sample. The results are shown in Figures 6.48 and 6.50 for W-UD1 and W-UD2 respectively. Moisture content tests were performed along two sections of the blocks, one across the electrodes (section 1) and the other along the electrodes (section 2). The results are shown in Figures 6.49 and 6.51 for W-UD1 and W-UD2 respectively. When compared to the results of remoulded test, a more uniform increase in vane strength resulted after treatment for the undistributed tests because of polarity reversal. The region around the electrodes again showed a higher increase in vane strength. The average vane strength after treatment was increased from 22 kPa to 33 kPa (50 % increase) for both tests. As for the change in moisture content, a more uniform decrease in water content resulted. After treatment, the electrodes adhered tightly to the soil. Electrodes after treatment were found to be severely oxidised.

The test results described will be further discussed in Chapter 7.

Table 6.1 Summary of Test Program for Laboratory Investigation of Electro-Osmosis

Soil Type	Orientation	Test No.	Sample Length (mm)	Applied Voltage (V)	Polarity[1]
Wallaceburg Clay	Vertical Sample	WV-4	101.6	2.5	N,R
				4.0	N
		WV-8A	203.2	3.0	N,R
				4.5	N,R
		WV-8B	101.6	5.0	N
Wallaceburg Clay	Horizontal Sample	WH-3	76.2	2.0	N,R
				4.0	N,R
		WH-6A	152.4	4.0	N
		WH-6B	152.4	2.0	N,R
				4.0	N,R
		WH-9	228.6	2.0	N,R
				4.0	N,R
				6.0	N,R
Gloucester Clay	Vertical Sample	GV-4A	101.6	3.0	N,R
		GV-4B	101.6	1.5	N,R
				2.4	N,R
				4.0	N,R
		GV-8B	203.2	3.0	N,R
				6.0	N,R

! N = normal polarity, R = reversed polarity

Table 6.2 Summary of Test Results of Laboratory Investigation of Electro-Osmosis

Test No.	Sample Length mm	Voltage Polarity[i] V	Δu[ii] kPa	Settlement δ/L %	Average Shear Strength[iii] Initial kPa	After Treatment kPa	Increase %	Average Moisture Content Initial %	After Treatment %	Decrease %
GV-4A	101 6	3 N,R	-28	3.35	11.0	18.0	63.6	97.5	82.7	15.2
GV-4B	101.6	1.5 N,R	-15	2.75						
		2.4 N,R	-36	3.74						
		4.0 N,R	-53	6 60	11.0	23.5	113.6	69.0	57.1	17.2
GV-8	203.2	3.0 N,R	-27	3.69						
		6.0 N,R	-75	9.83	11.0	30.0	172.7	97.5	67.8	30.5
WV-4	101.6	2.5 N,R	-68	0.77						
		4.0 N	-136	1.25	22.5	36.5	62.2	38.5	35.6	7.5
WV-8A	203.2	3.0 N,R	-102	1.78						
		4.5 N,R	-178	3.50	23.0	40.5	76.1	38.5	34.2	11.2
WV-8B[iv]	203.2	5.0 N,R	-120	1.91	22.0	42.0	90.9	38 5	33.8	12.2
WH-3	76.2	2.0 N,R	-52	1.20						
		4.0 N,R	-105	2.49	23.0	32.5	41 3	37.5	34.5	8.0
WH-6A	152.4	4.0 N	-100	1.57	22 5	27.0	20.0	42.9	40.6	5.4
WH-6B	152.4	2.0 N,R	-41	0.66						
		4.0 N,R	-135	2.44	23.0	37.0	60.9	37.5	33.7	10.1
WH-9	228.6	2.0 N,R	-46	0.47						
		4.0 N,R	-104	2.24						
		6.0 N,R	-180	3.22	22.0	39.0	77.3	37.5	32.8	12.5

Notes: (i) N,R = normal and reversed polarity respectively
(ii) Δu = maximum induced negative pore water pressure measured near anode
(iii) Undrained shear strength obtained by laboratory vane test
(iv) Sample cracked during treatment and pore pressure estimated by extrapolation
G = Gloucester Clay, W = Wallaceburg Clay, H = horizontal trimming, V = vertical trimming

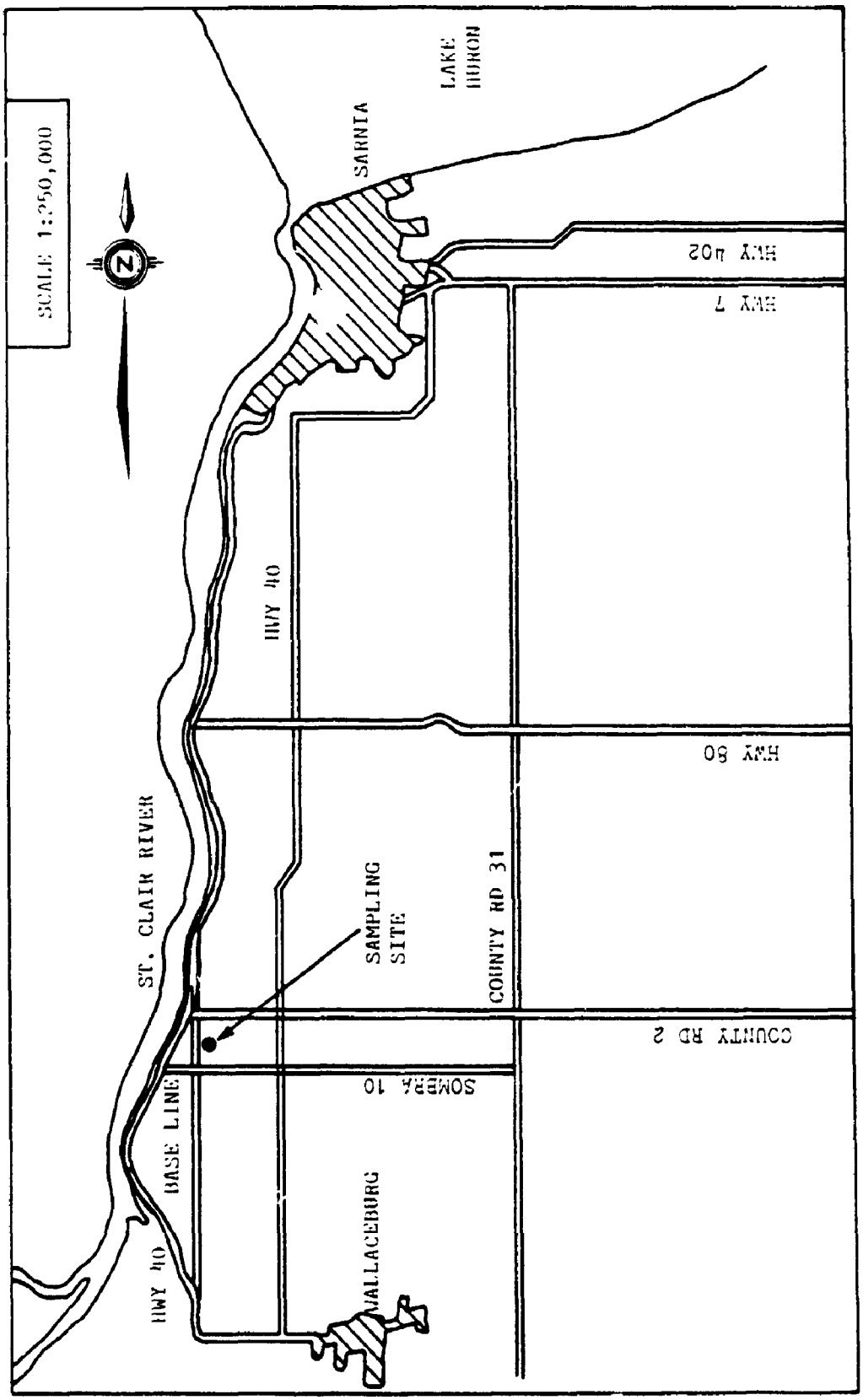

FIGURE 6.1 SAMPLING SITE OF WALLACEBURG CLAY

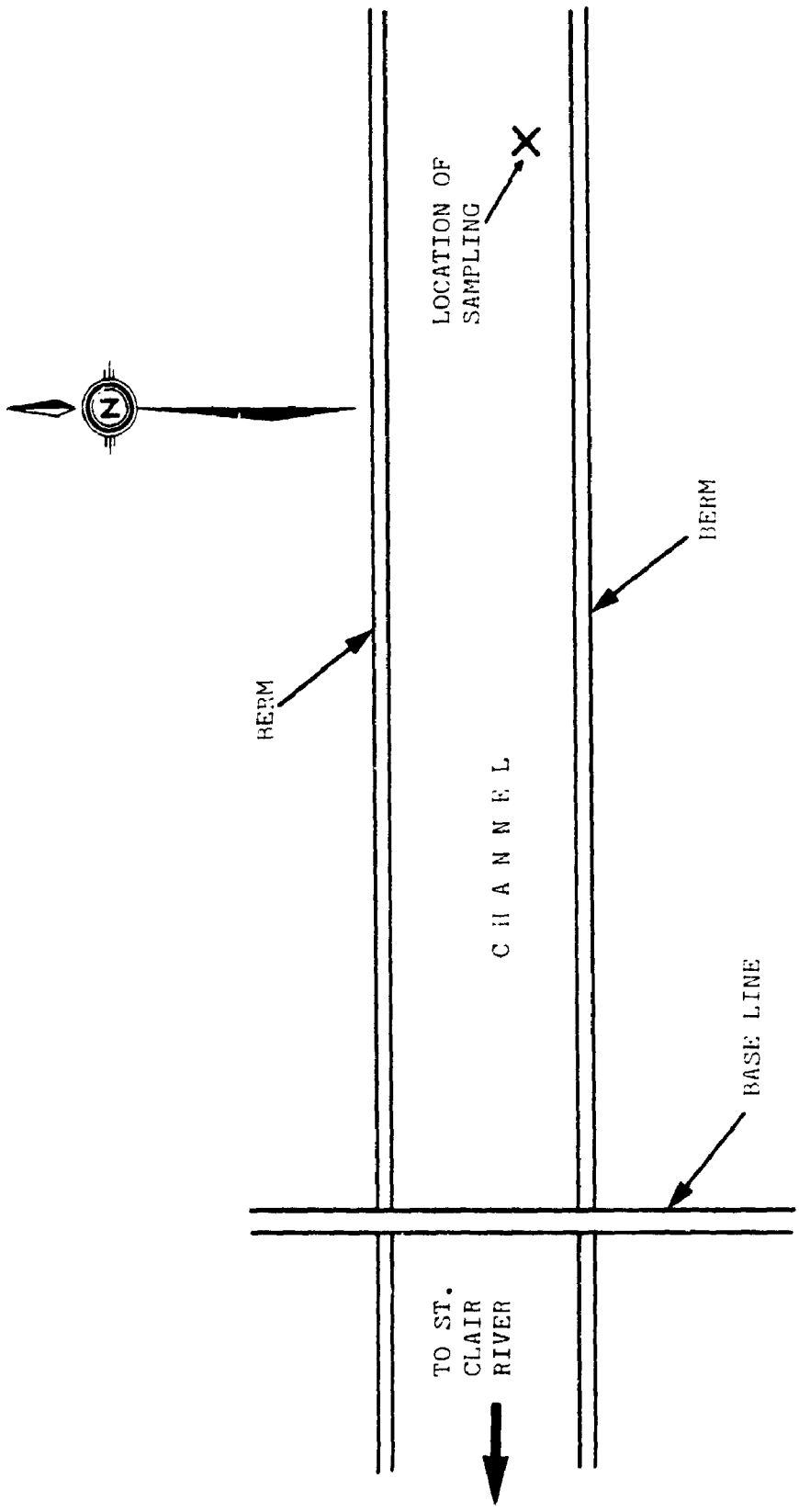

FIGURE 6.2 SAMPLING SITE IN THE FLOODWAY

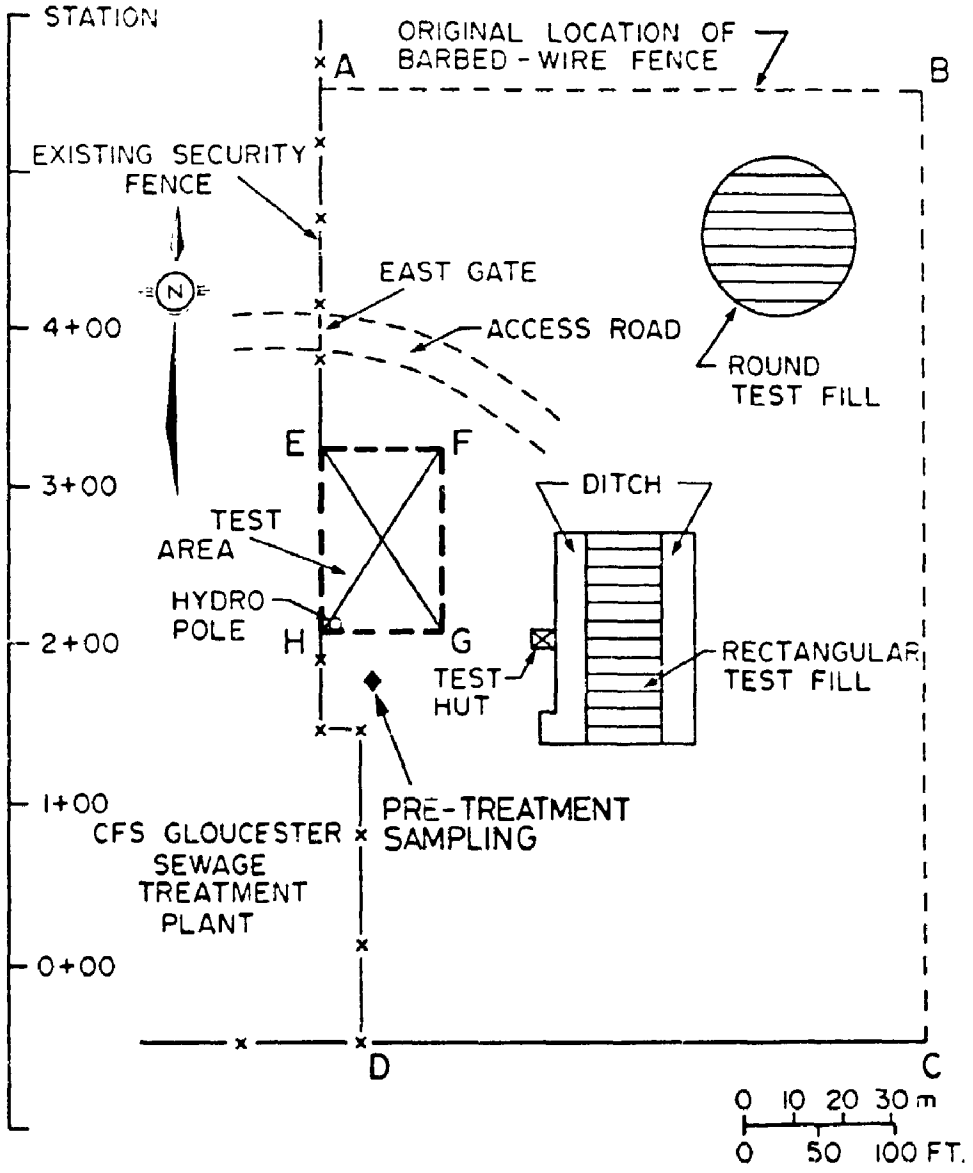

FIGURE 6.3 SAMPLING LOCATION OF GLOUCESTER CLAY IN GLOUCESTER TEST FILL SITE

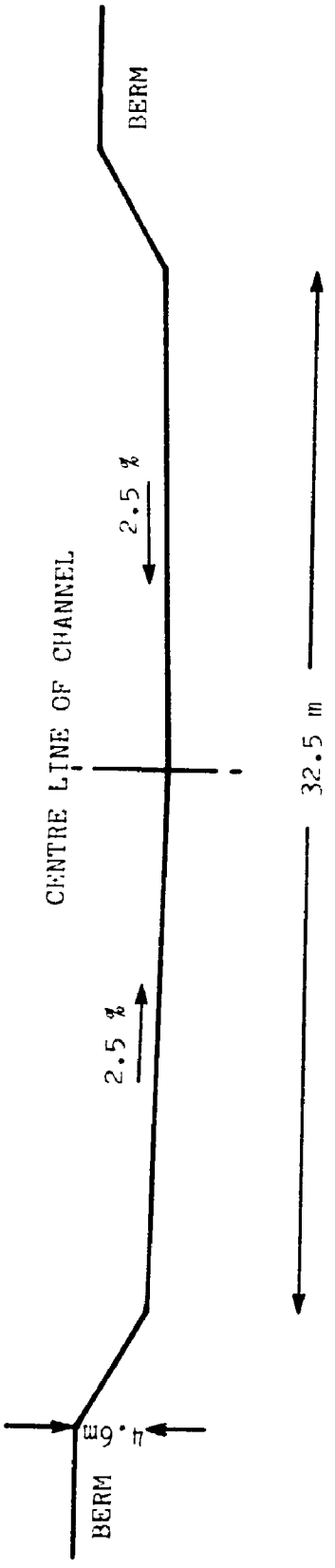

FIGURE 6.4 CROSS-SECTION OF DARCY MCKEOUGH FLOODWAY CHANNEL

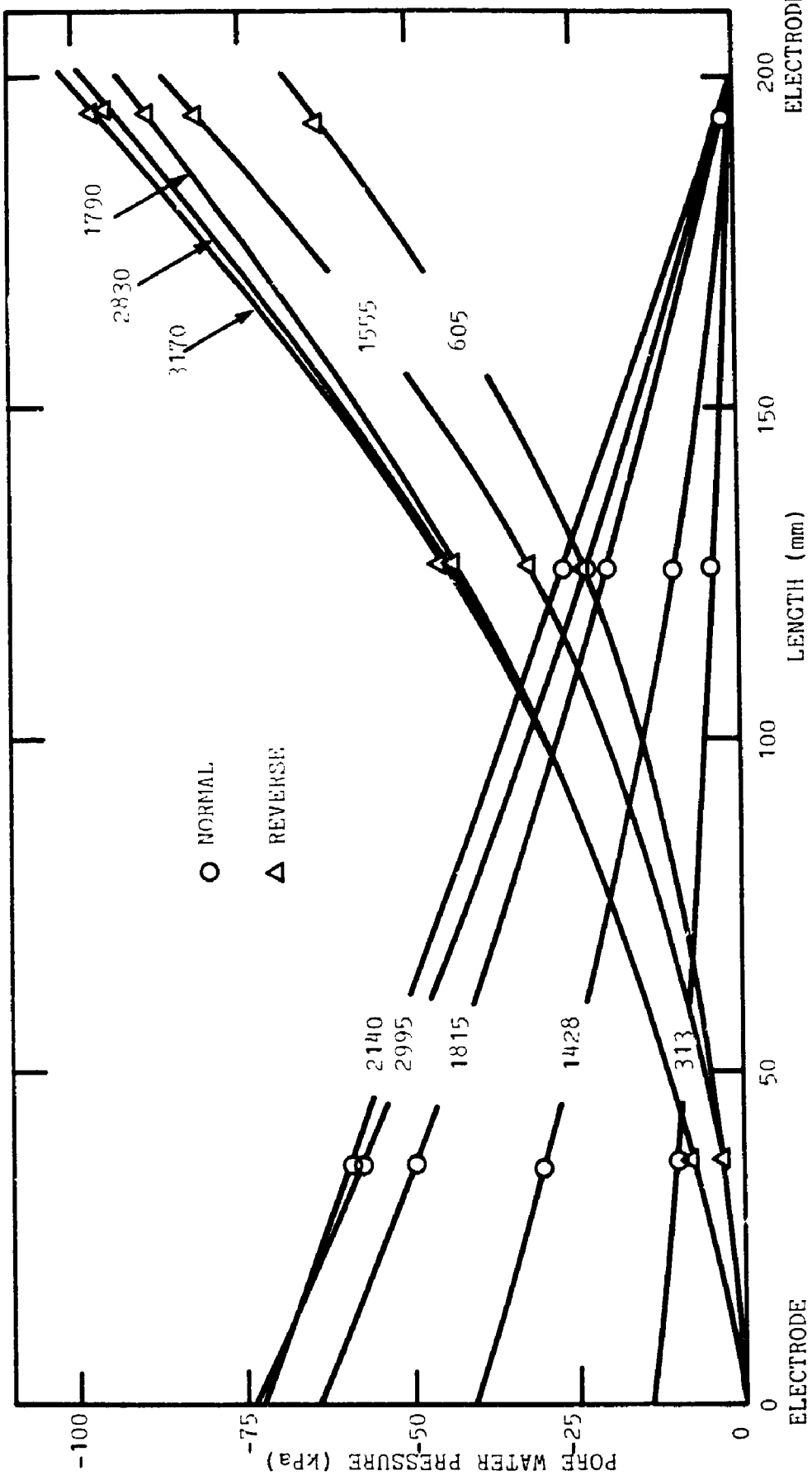

FIGURE 6.5 PORE WATER PRESSURE DISTRIBUTION WITH TIME (MINUTES), TEST WV-8A, 3 V

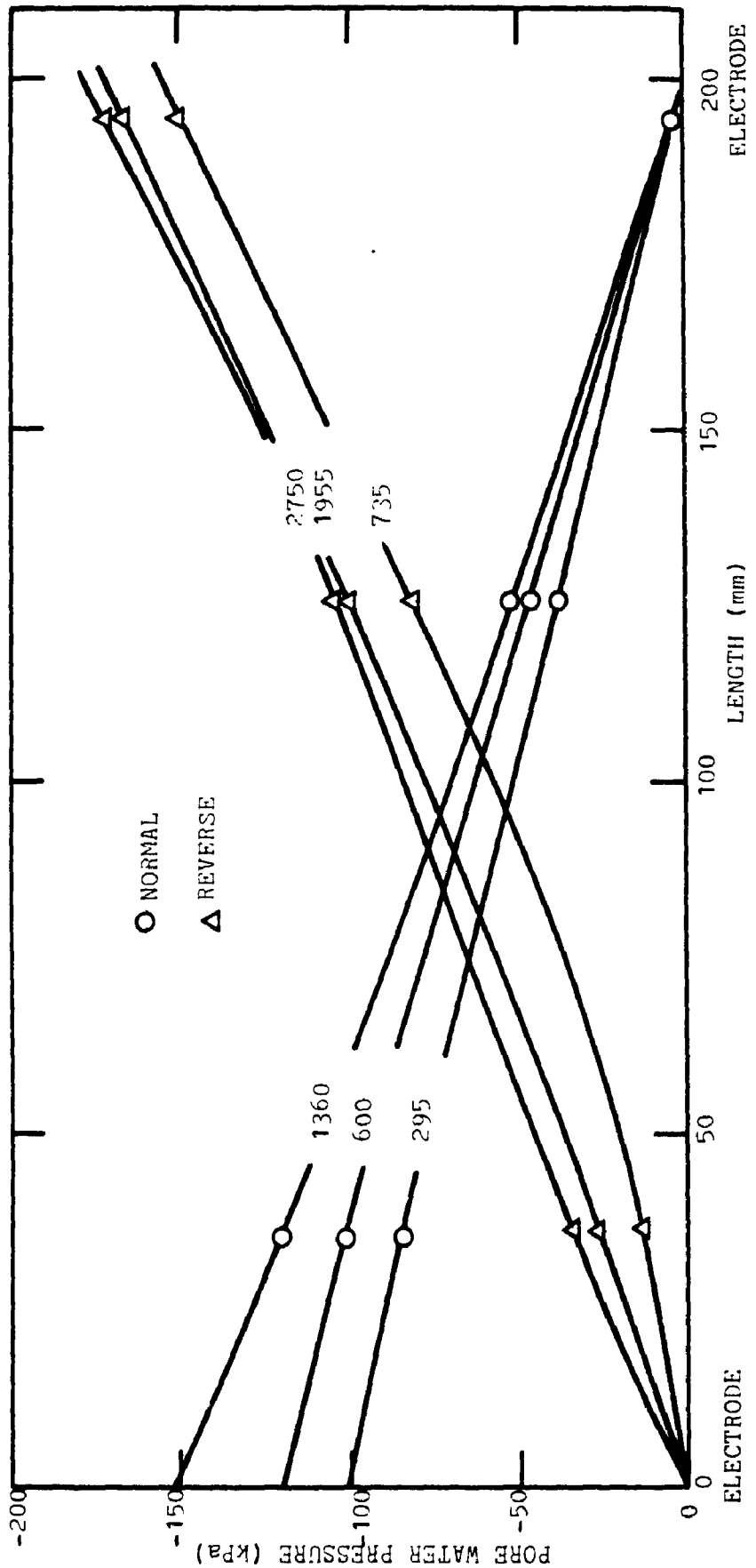

FIGURE 6.6 PORE WATER PRESSURE DISTRIBUTION WITH TIME (MINUTES), TEST WV-8A. 4.5 V

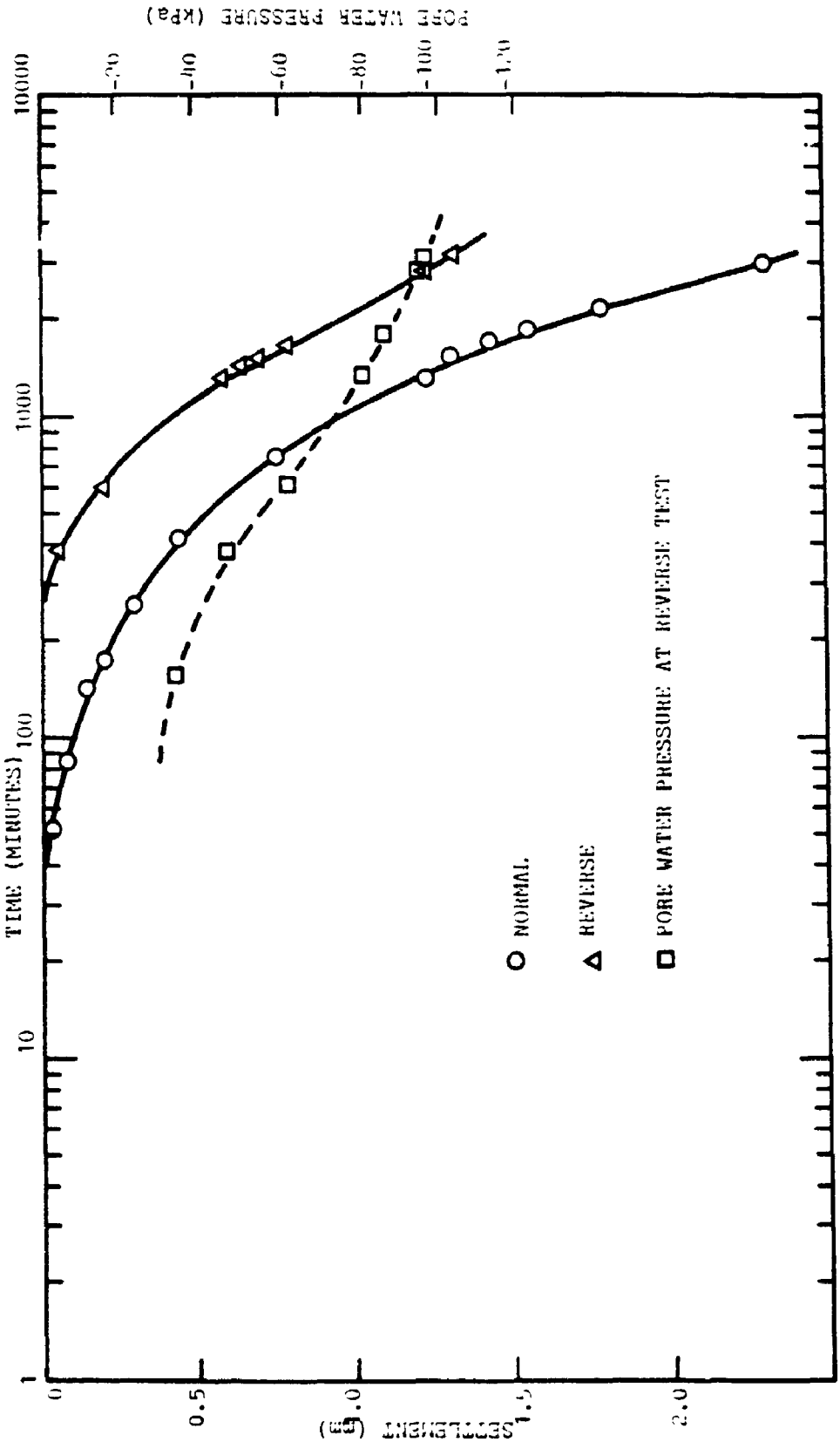

FIGURE 6.7 SETTLEMENT AND PORE WATER PRESSURE AT ANODE WITH TIME, TEST WV-2A, 3 V

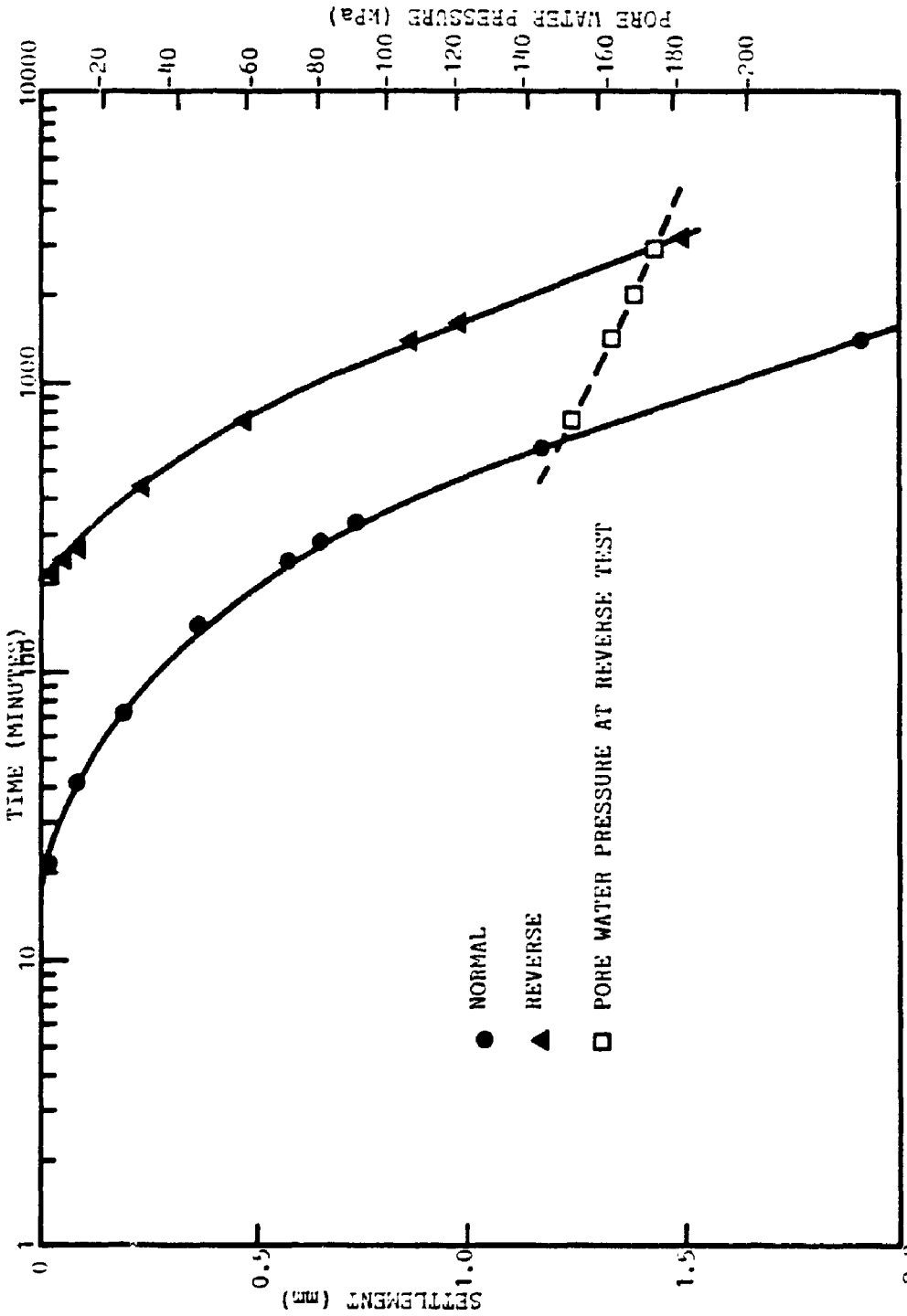

FIGURE 6.8 SETTLEMENT AND PORE WATER PRESSURE AT ANODE WITH TIME, TEST WV-8A, 4.5 V

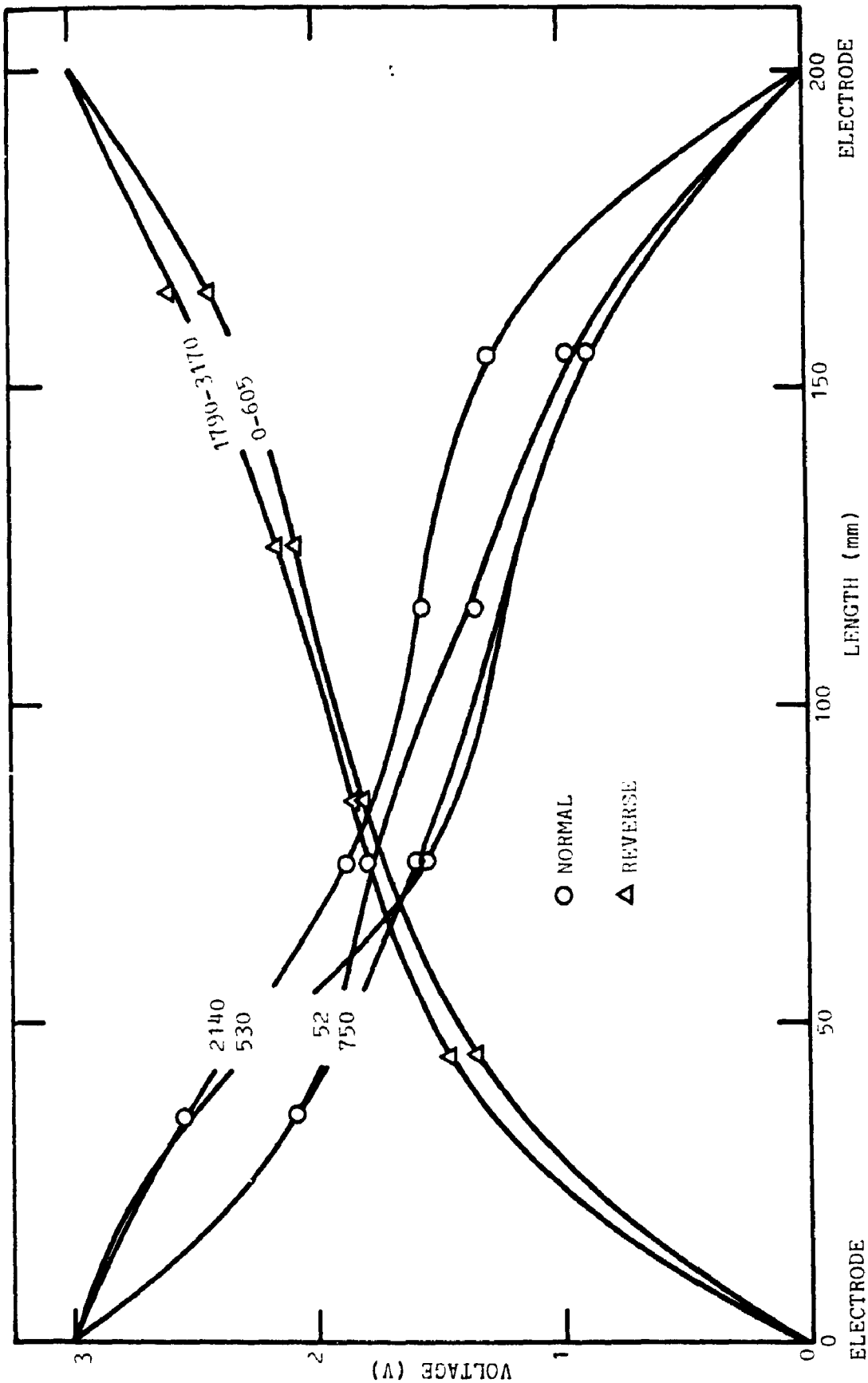

FIGURE 6.9 VOLTAGE DISTRIBUTION WITHIN SAMPLE WITH TIME (MINUTES), TEST WV-8A, 3 V

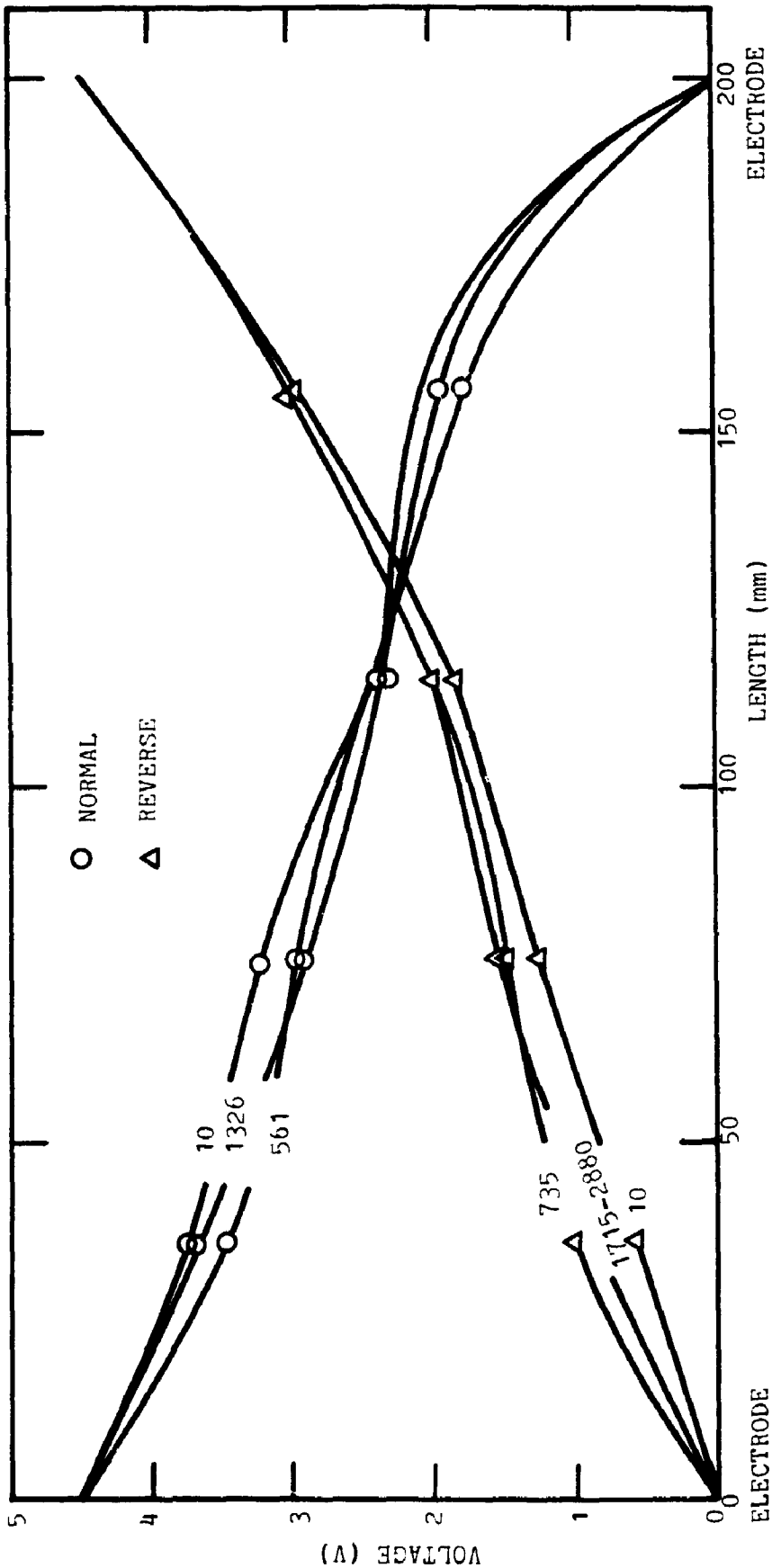

FIGURE 6.10 VOLTAGE DISTRIBUTION WITHIN SAMPLE WITH TIME (MINUTES), TEST WV-8A, 4.5 V

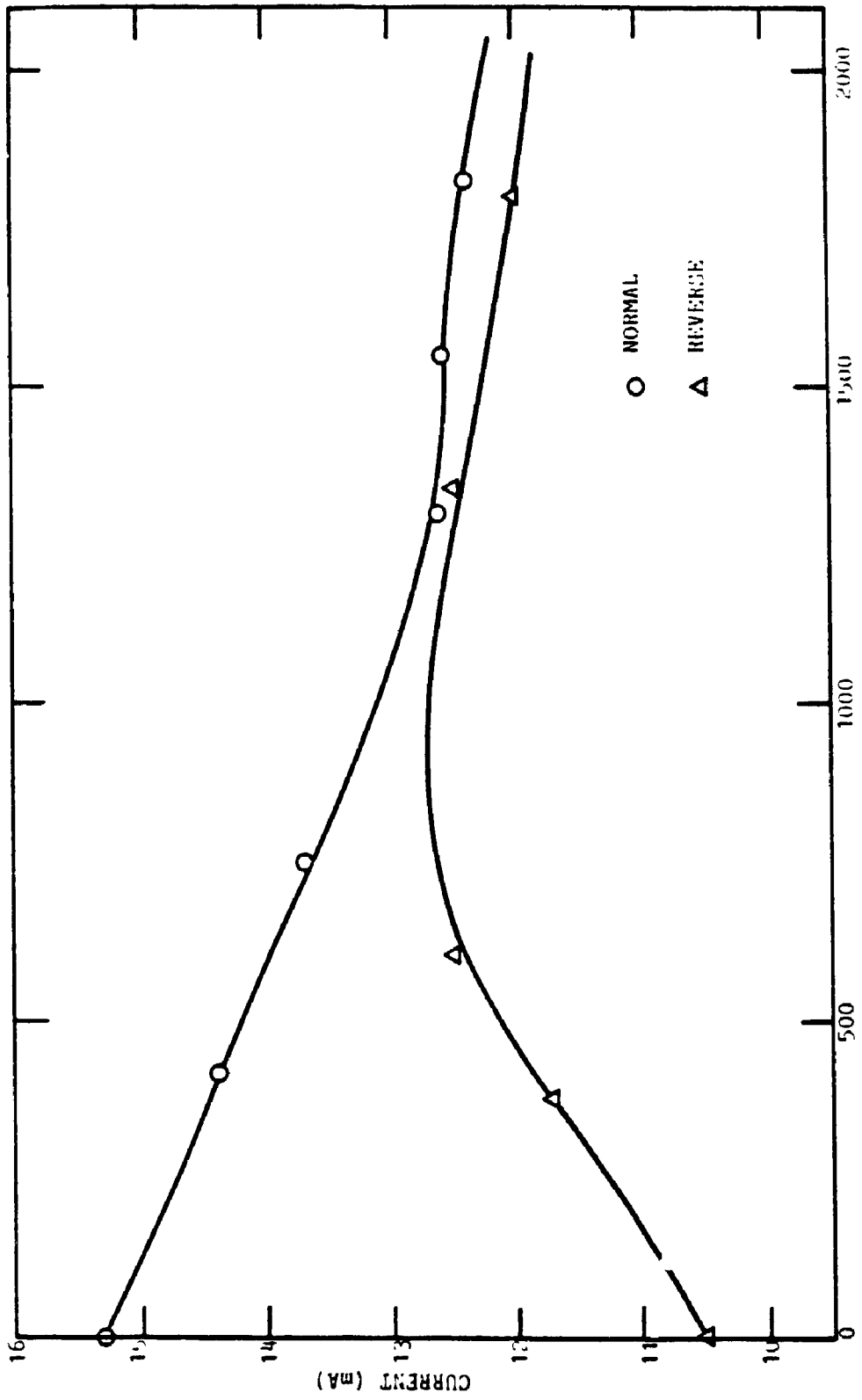

FIGURE 6.11 CURRENT VARIATION WITH TIME, TEST WV-8A, 3 V

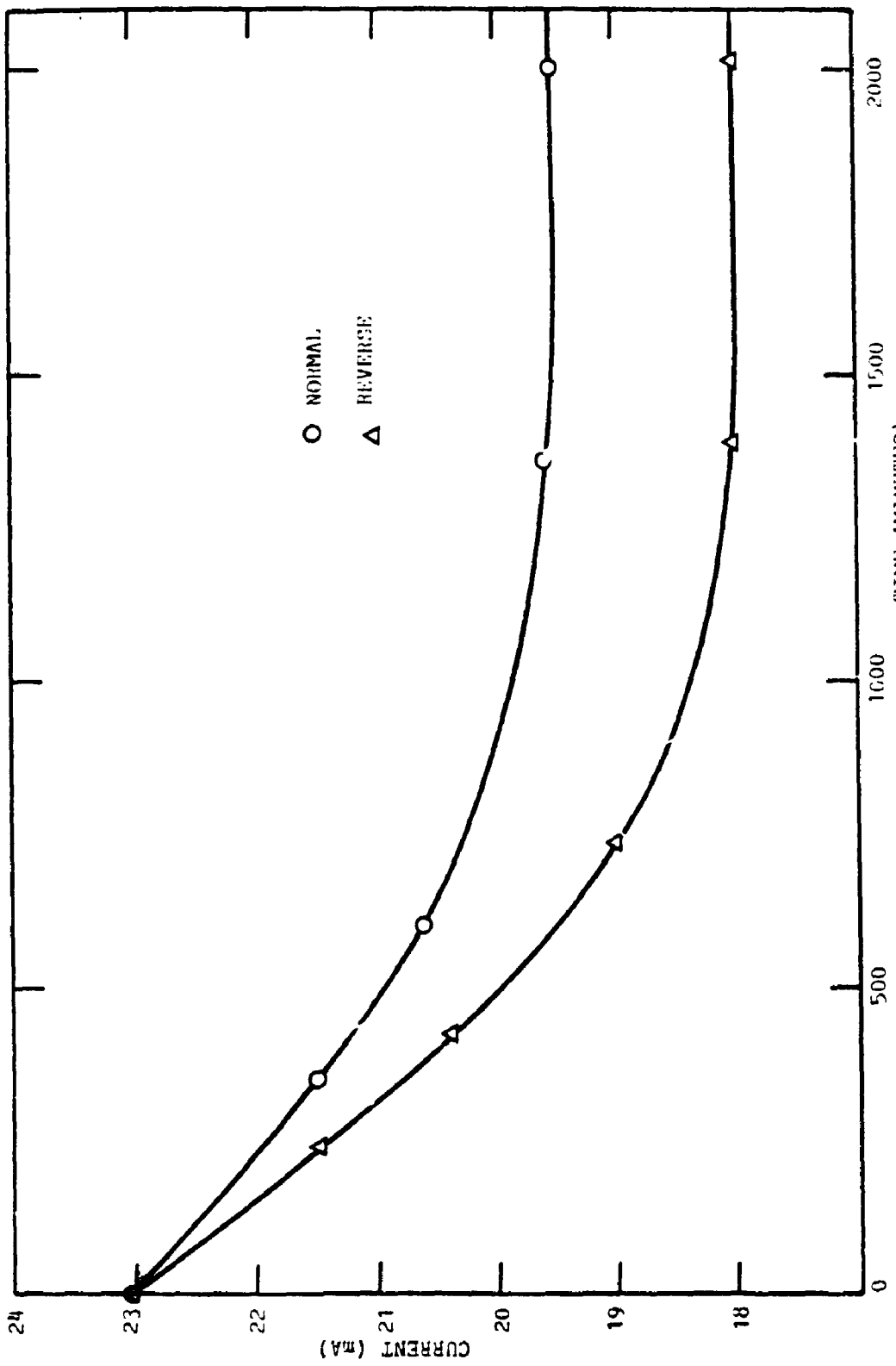

FIGURE 6.12 CURRENT VARIATION WITH TIME, TEST WV-8A, 4.5 V

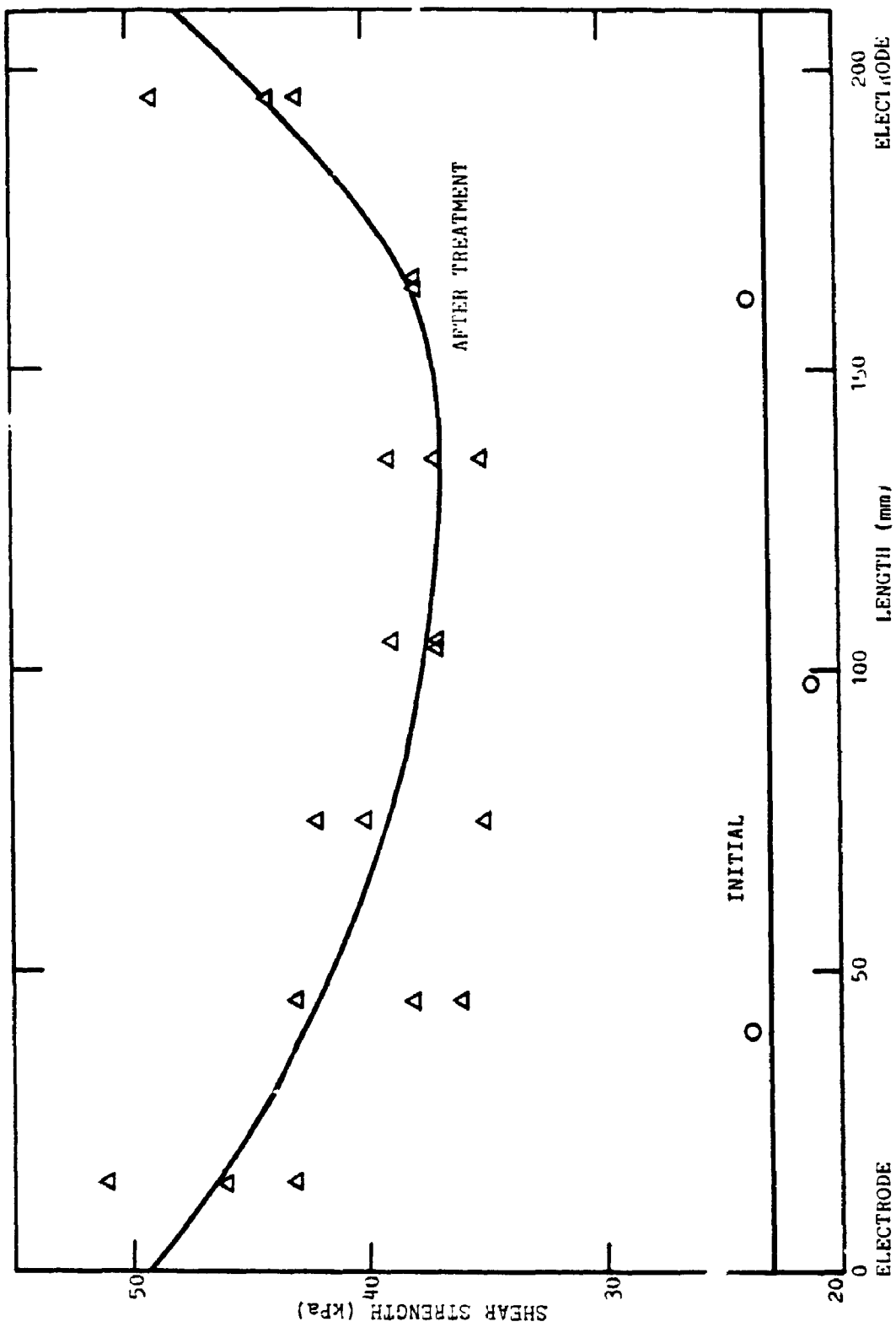

FIGURE 6.13 SHEAR STRENGTH BEFORE AND AFTER TREATMENT, TEST W-8A, 3 AND 4.5 V WITH POLARITY REVERSAL

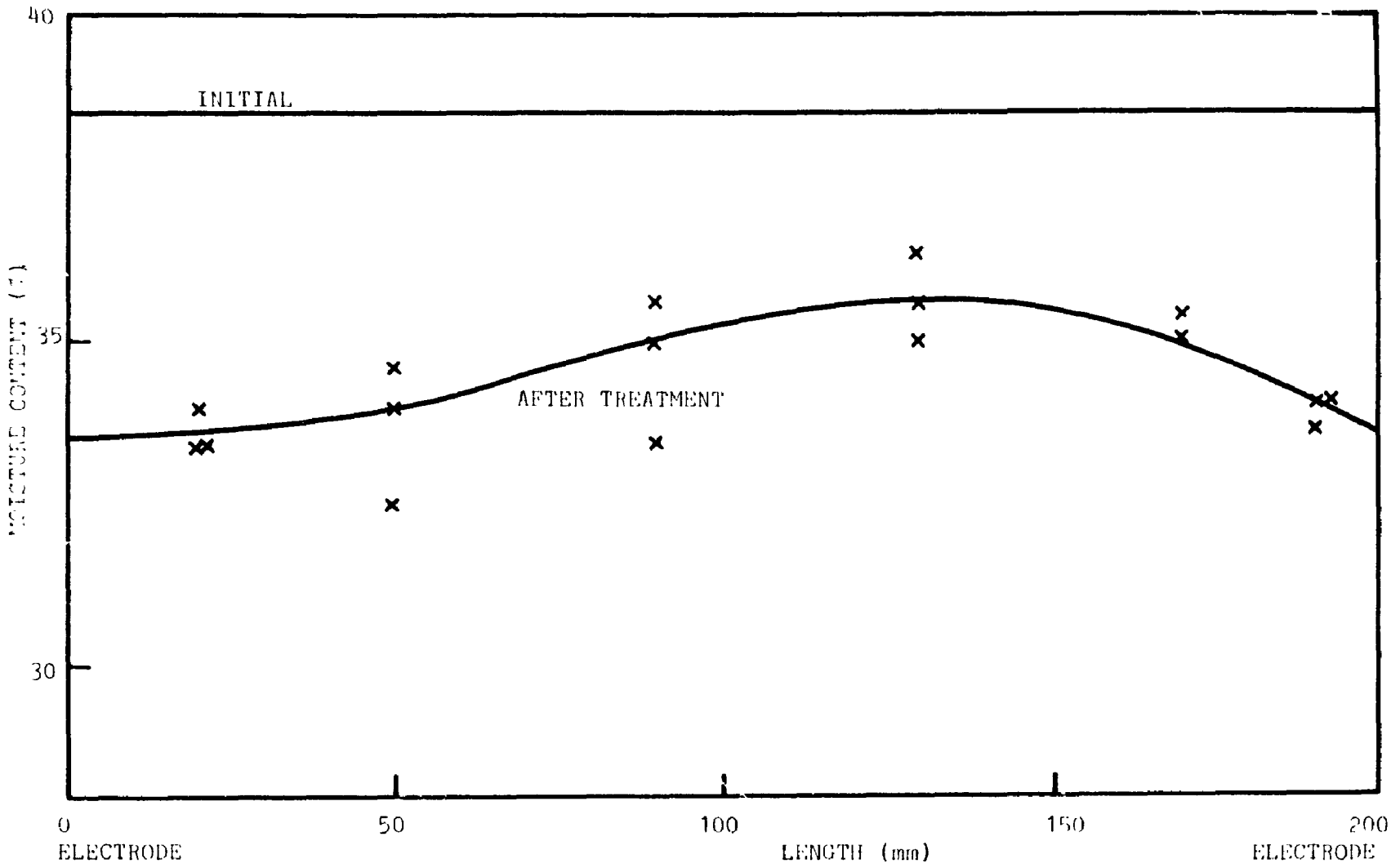

FIGURE 6.14 MOISTURE CONTENT BEFORE AND AFTER TREATMENT, TEST WV-8A, 3 AND 4.5 V WITH POLARITY REVERSAL

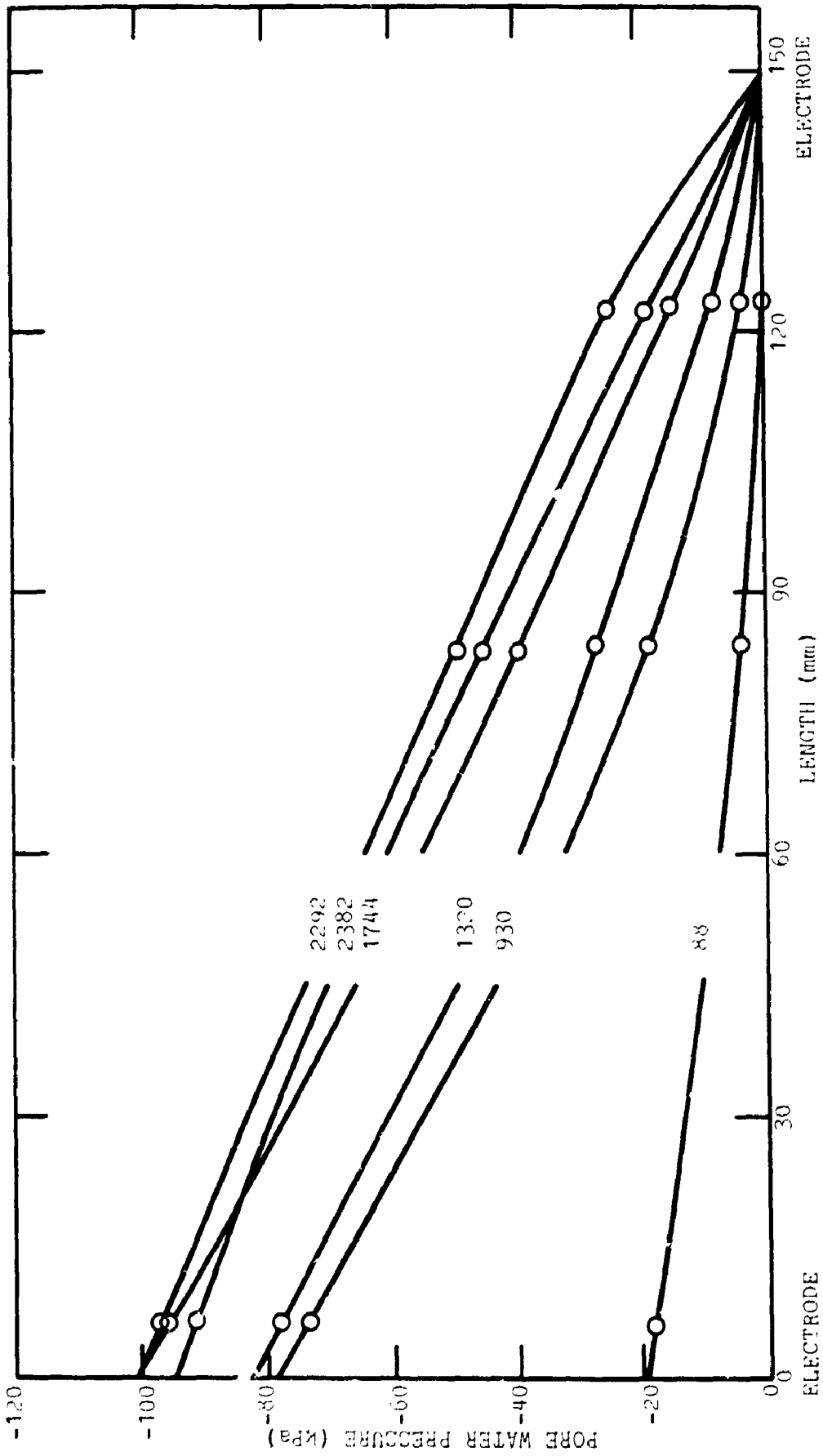

FIGURE 6.15 PORE WATER PRESSURE DISTRIBUTION WITHIN SAMPLE WITH TIME (MINUTES)
TEST WH-6A, 4 V WITHOUT POLARITY REVERSAL

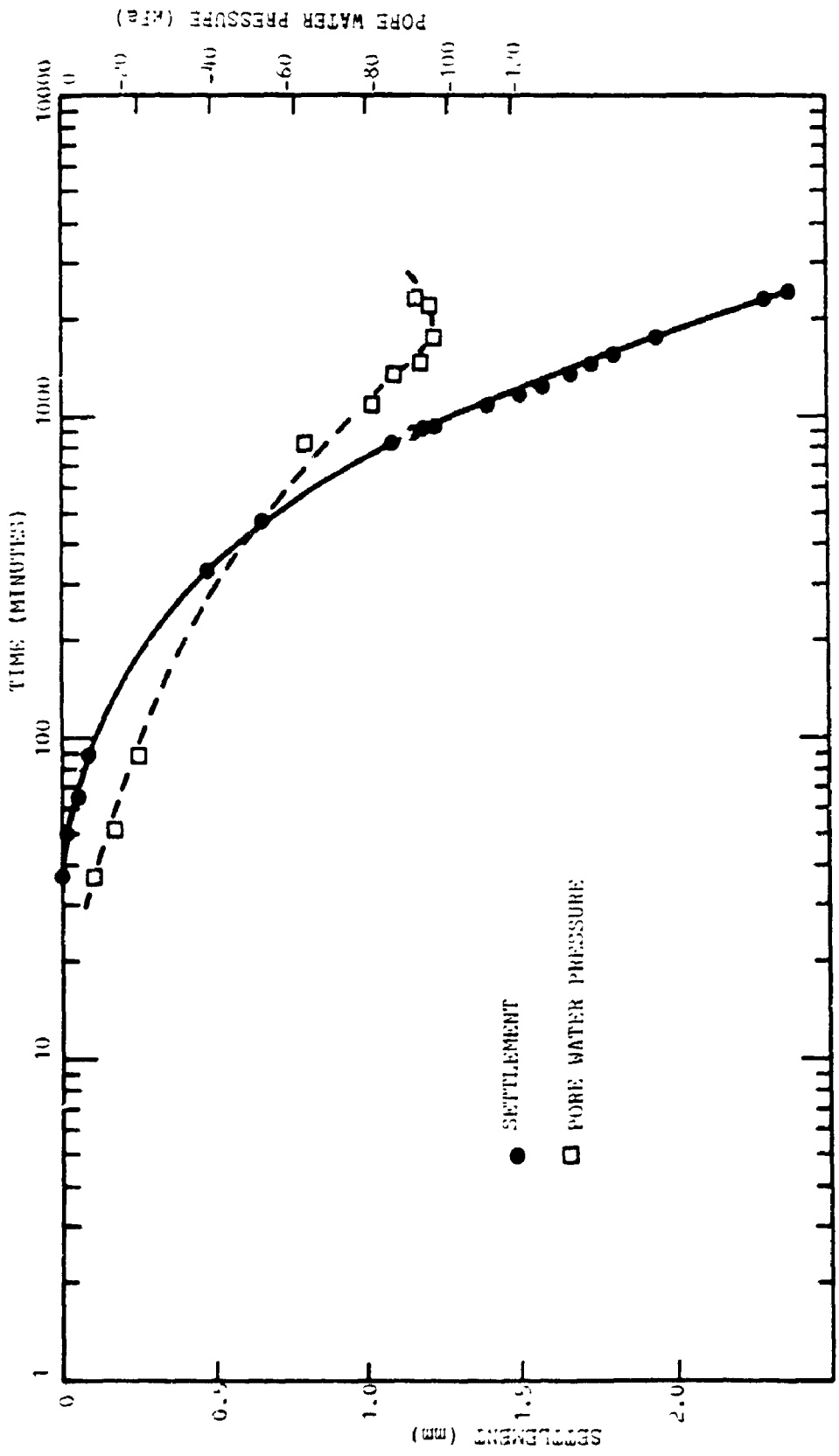

FIGURE 6.16 SETTLEMENT AND PORE WATER PRESSURE AT ANODE WITH TIME, TEST WH-6A, 4 V

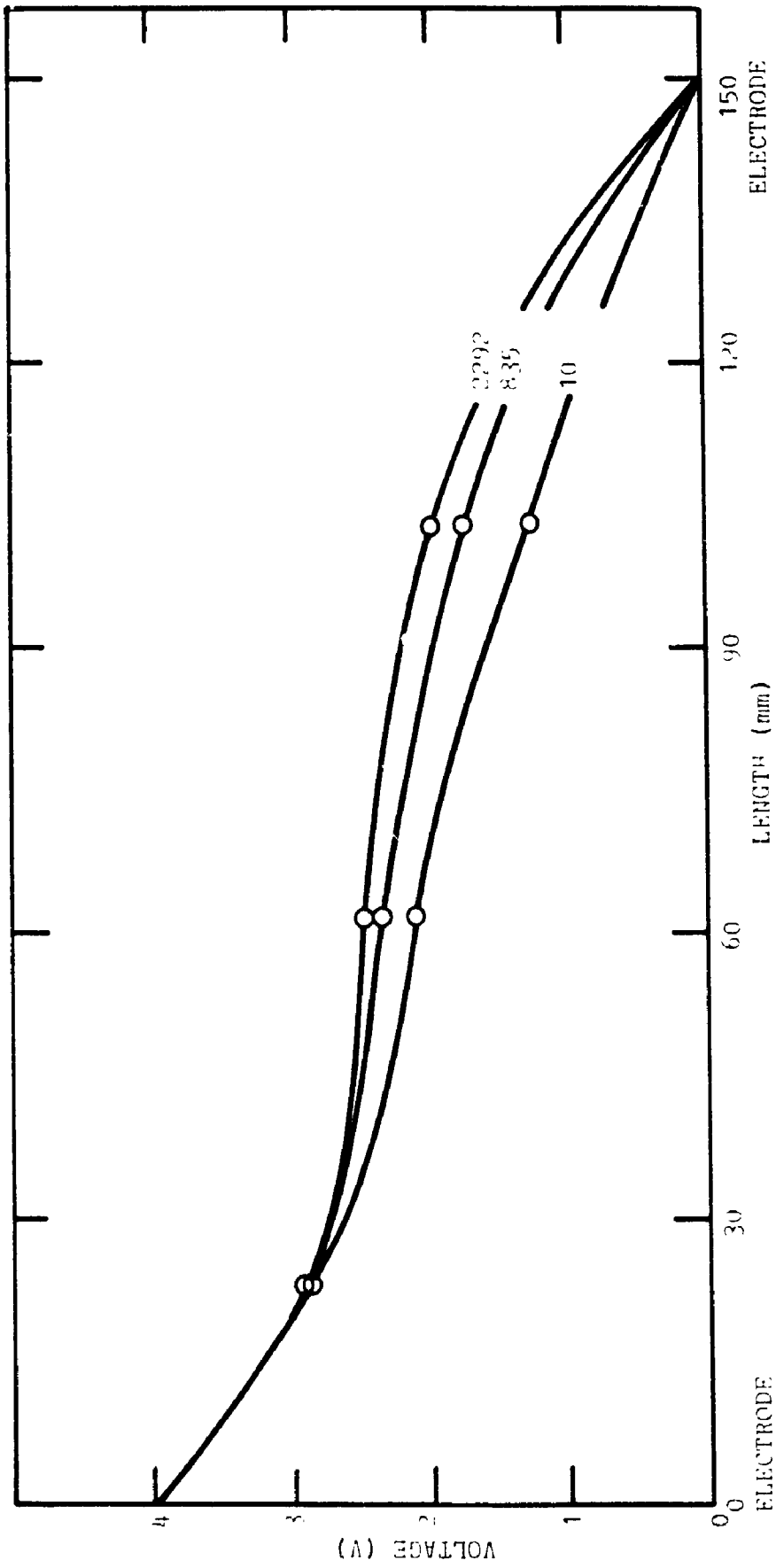

FIGURE 6.17 VOLTAGE DISTRIBUTION WITHIN SAMPLE WITH TIME (MINUTES), TEST WH-6A 4 V

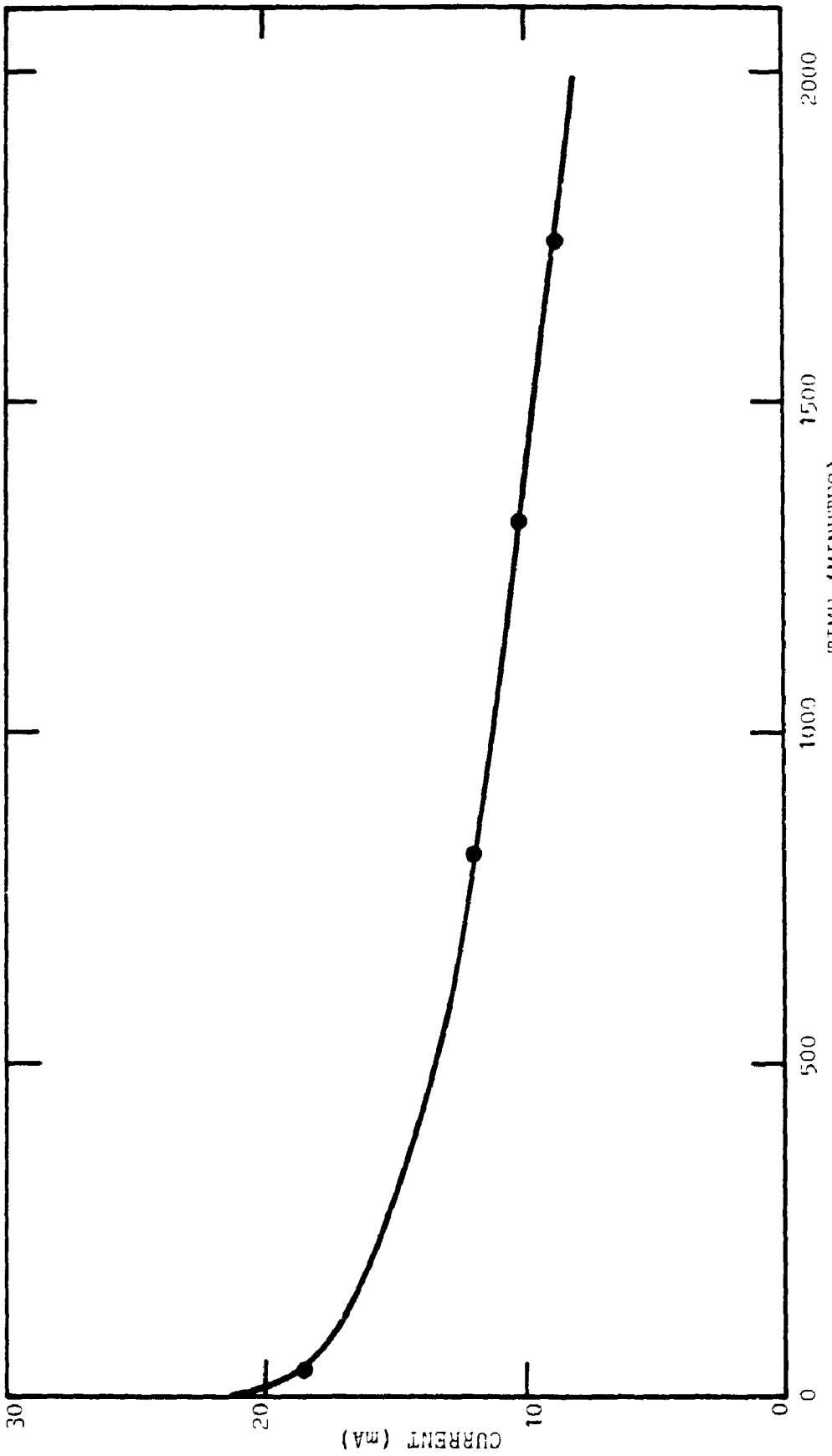

FIGURE 5.18 CURRENT VARIATION WITH TIME, TEST WH-6A, 4 V

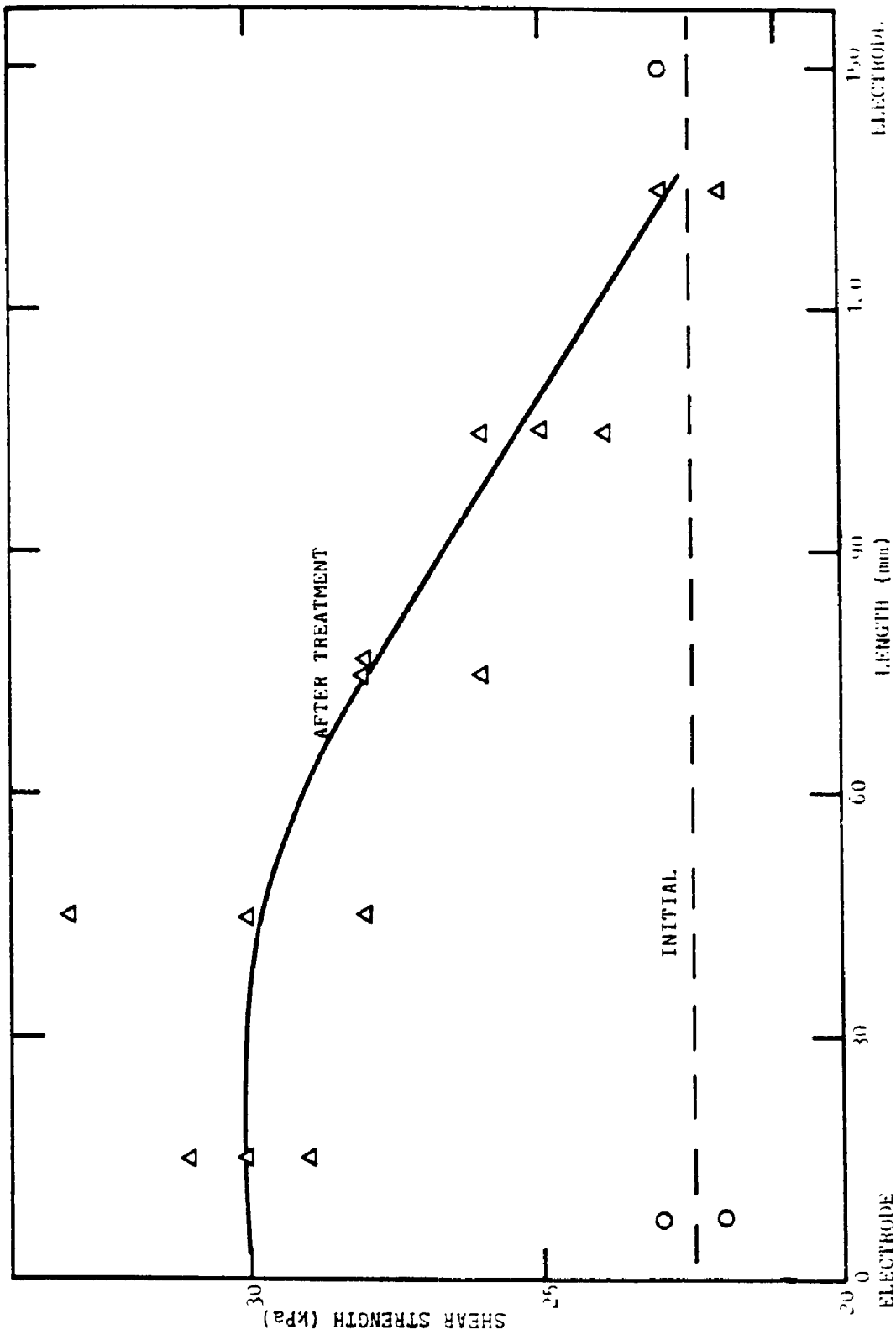

FIGURE 6.19 SHEAR STRENGTH BEFORE AND AFTER TREATMENT, TEST WH-6A, 4 V WITHOUT POLARITY REVERSAL

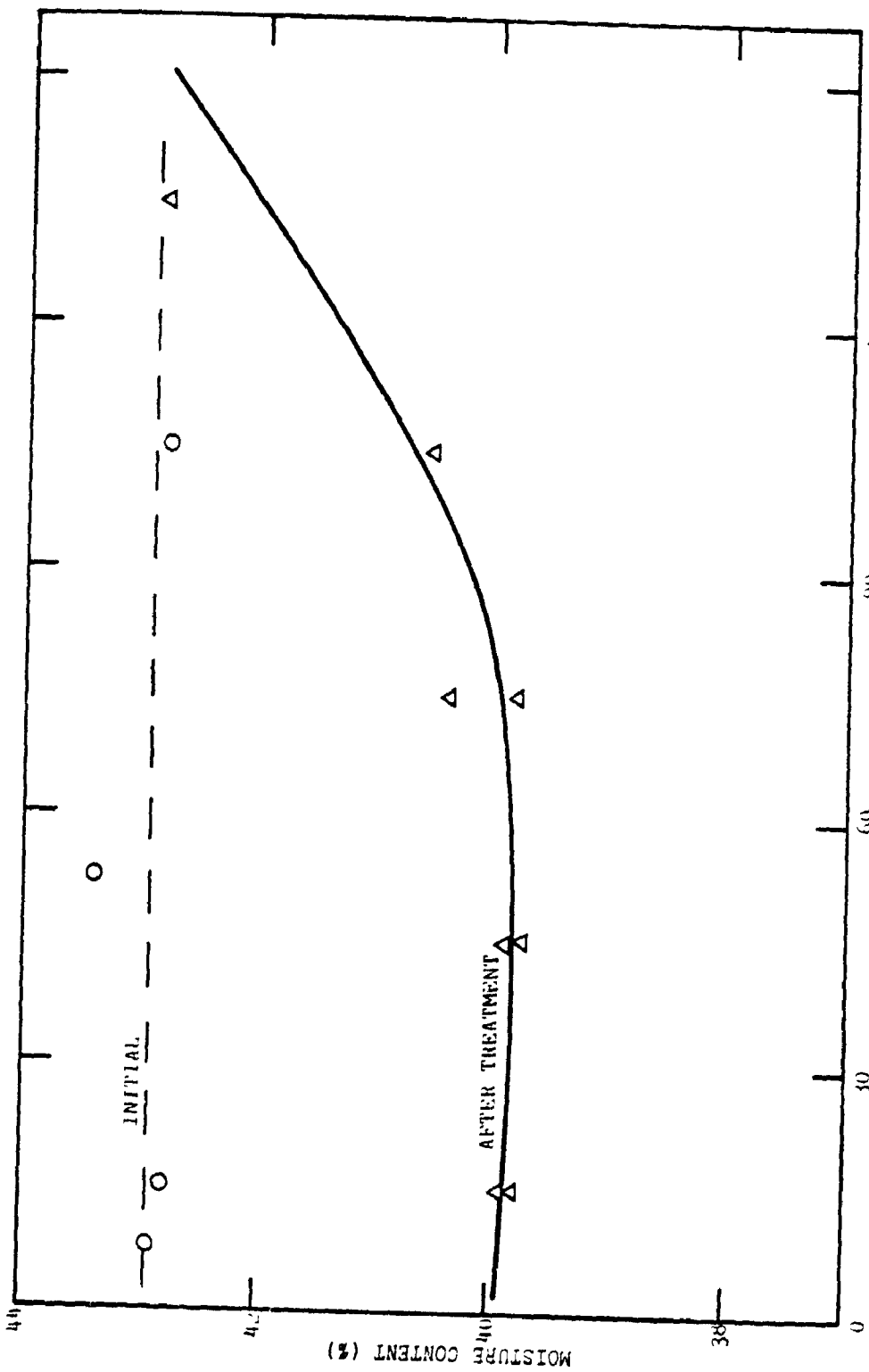

FIGURE 6.20 MOISTURE CONTENT BEFORE AND AFTER TREATMENT, TEST WH-6A, 4 V WITHOUT POLARITY REVERSAL

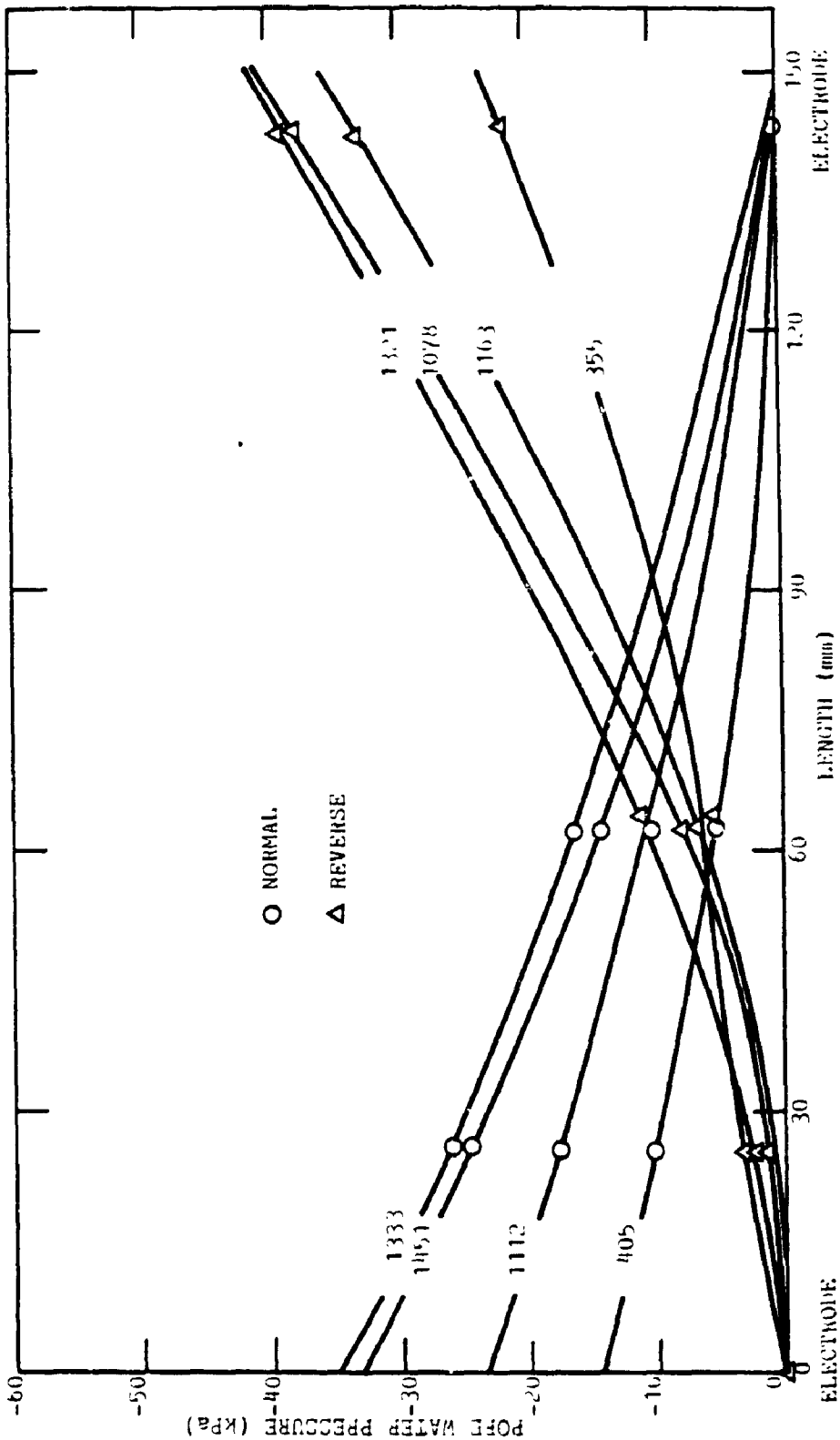

FIGURE 6.21 PORE WATER PRESSURE DISTRIBUTION WITH TIME (MINUTES), TEST WH-6B, 2 V

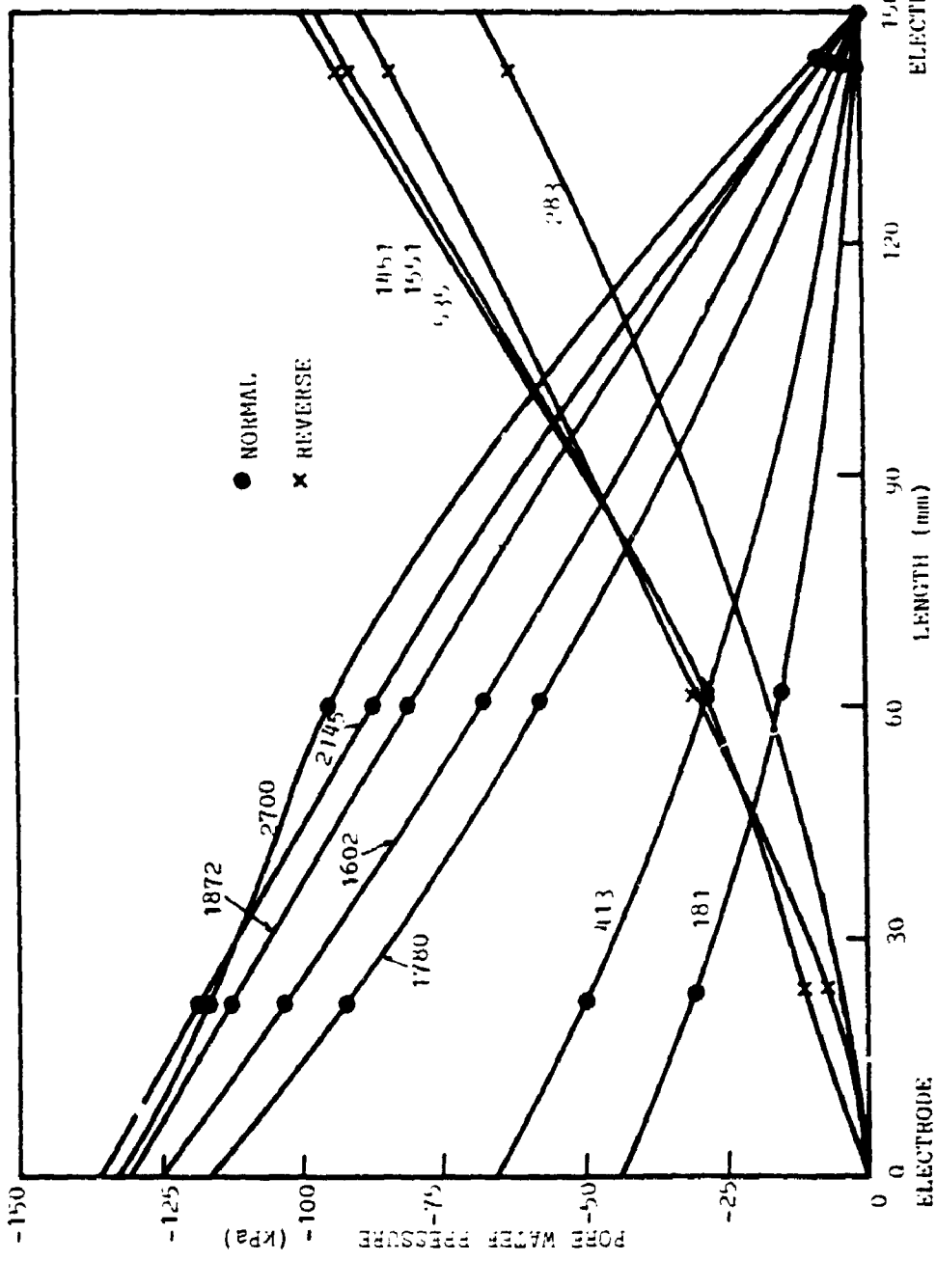

FIGURE 6.22 PORE WATER PRESSURE DISTRIBUTION WITH TIME (MINUTES), TEST WH-68, 4 V

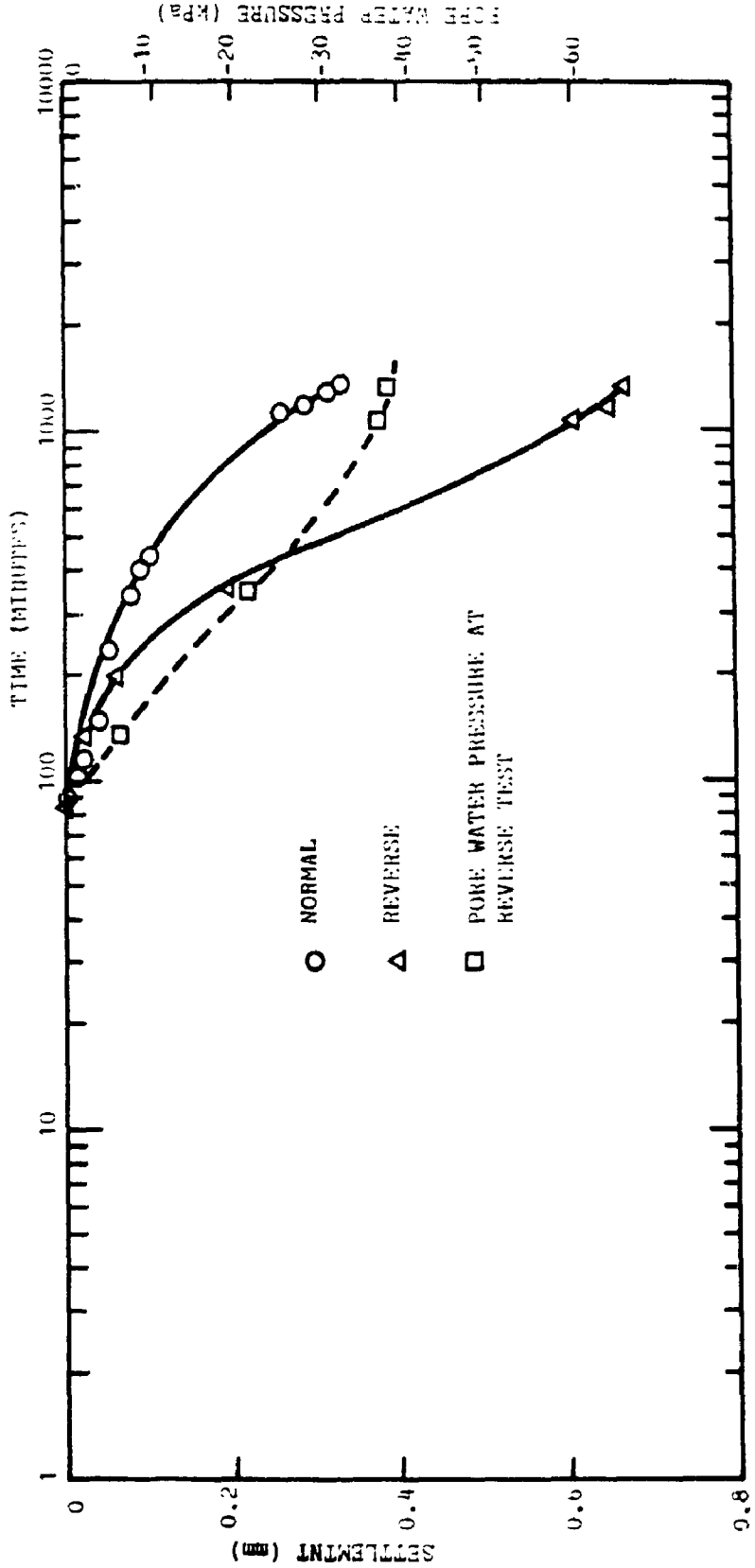

FIGURE 6.23 SETTLEMENT AND PORE WATER PRESSURE AT ANODE, TEST WH-6B, 2 V

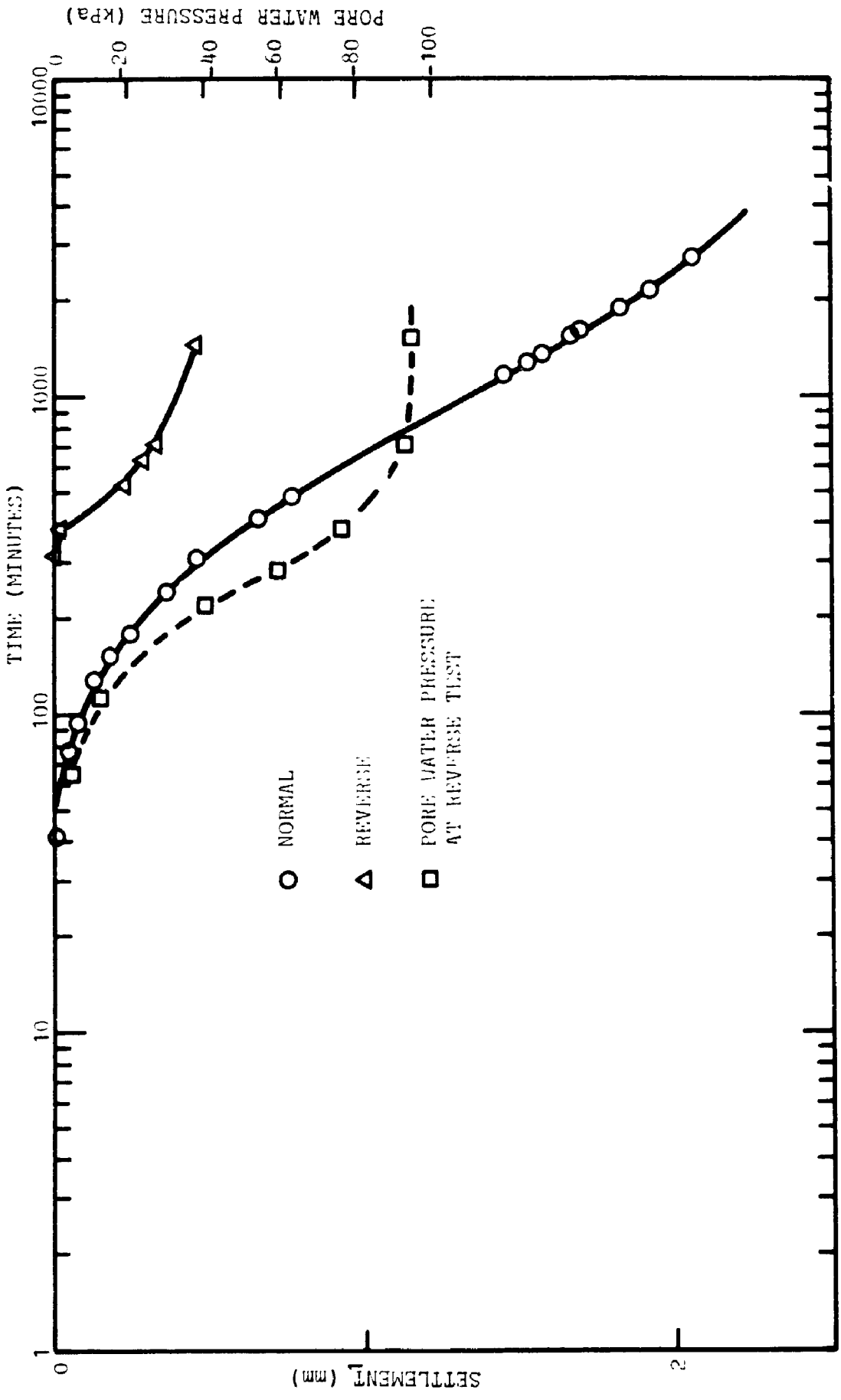

FIGURE 6.24 SETTLEMENT AND PORE WATER PRESSURE AT ANODE WITH TIME, TEST WH-6B, 4 V

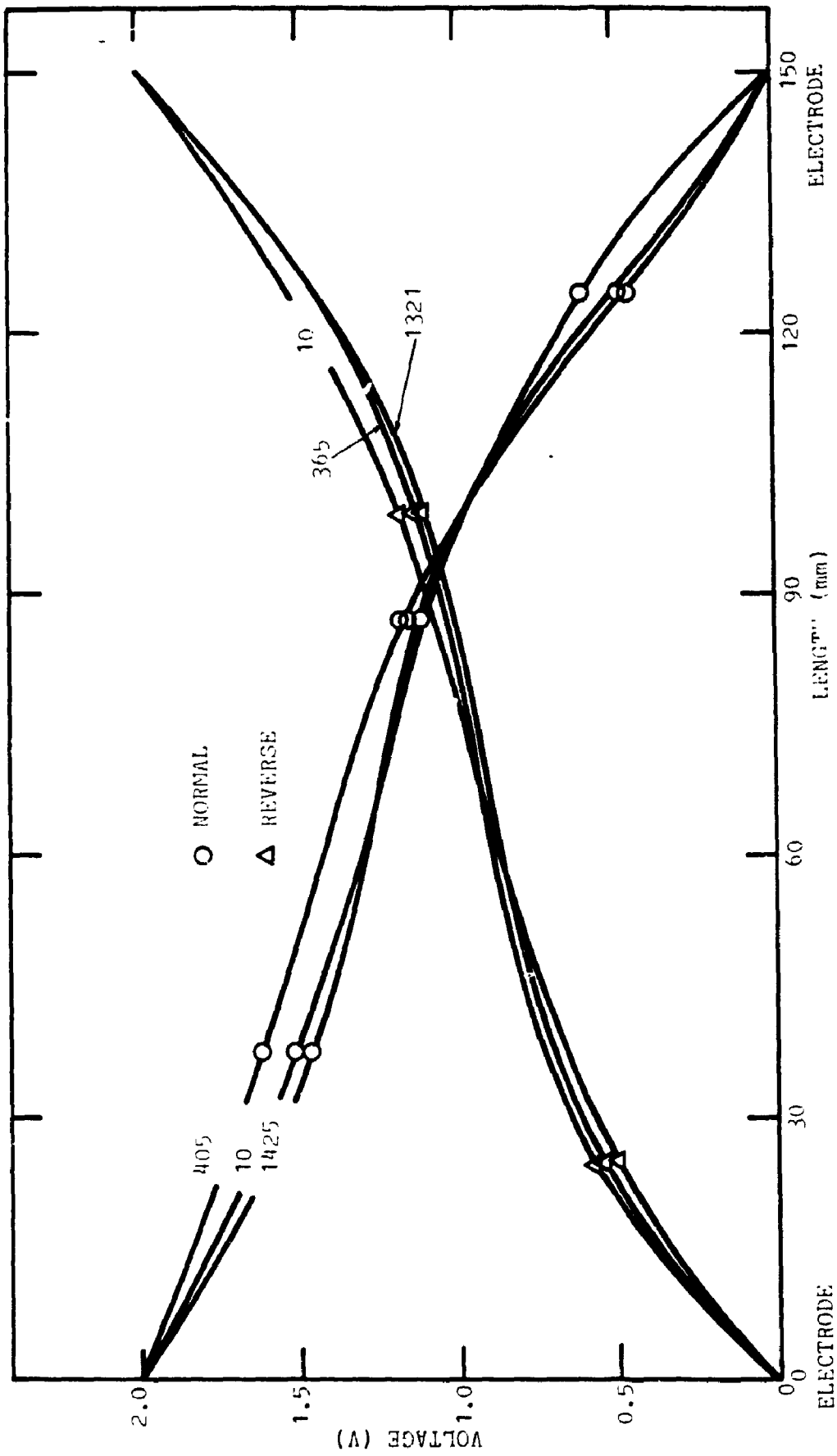

FIGURE 6.25 VOLTAGE DISTRIBUTION WITHIN SAMPLE WITH TIME (MINUTES), TEST WH-61, 2 V

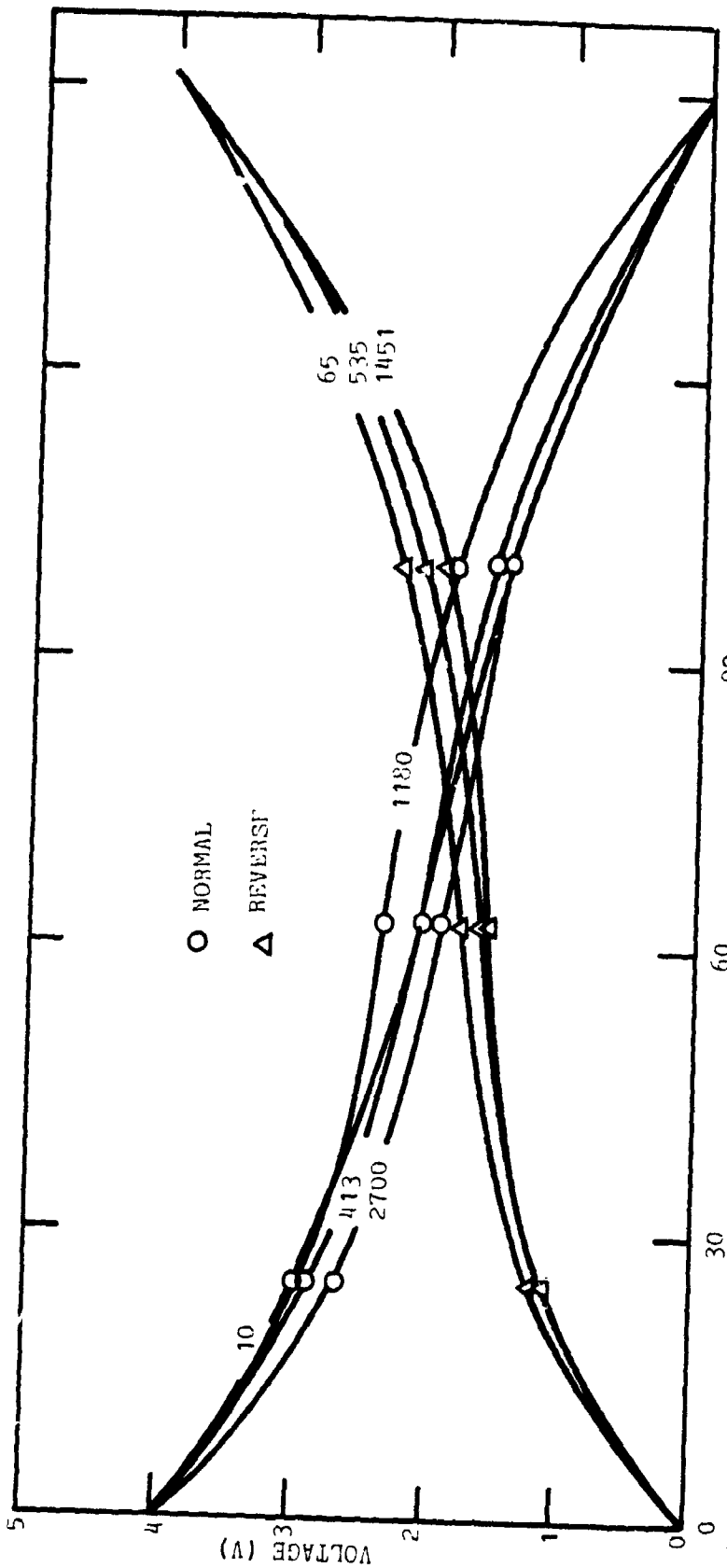

FIGURE 6.26 VOLTAGE DISTRIBUTION WITHIN SAMPLE WITH TIME (MINUTES), TEST WH-6B, 4 V

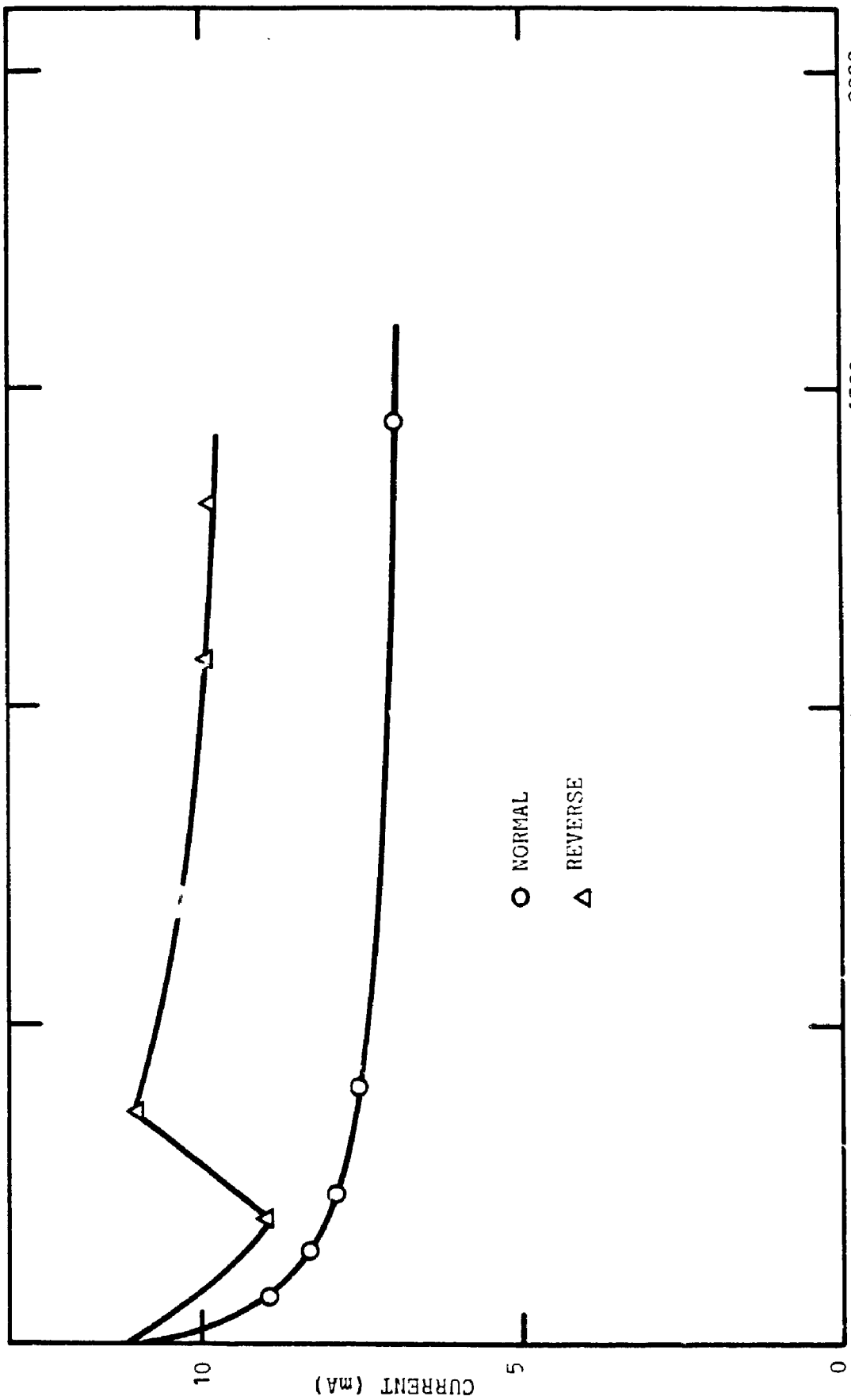

FIGURE 6.27 CURRENT VARIATION WITH TIME, TEST WH-6B, 2 V

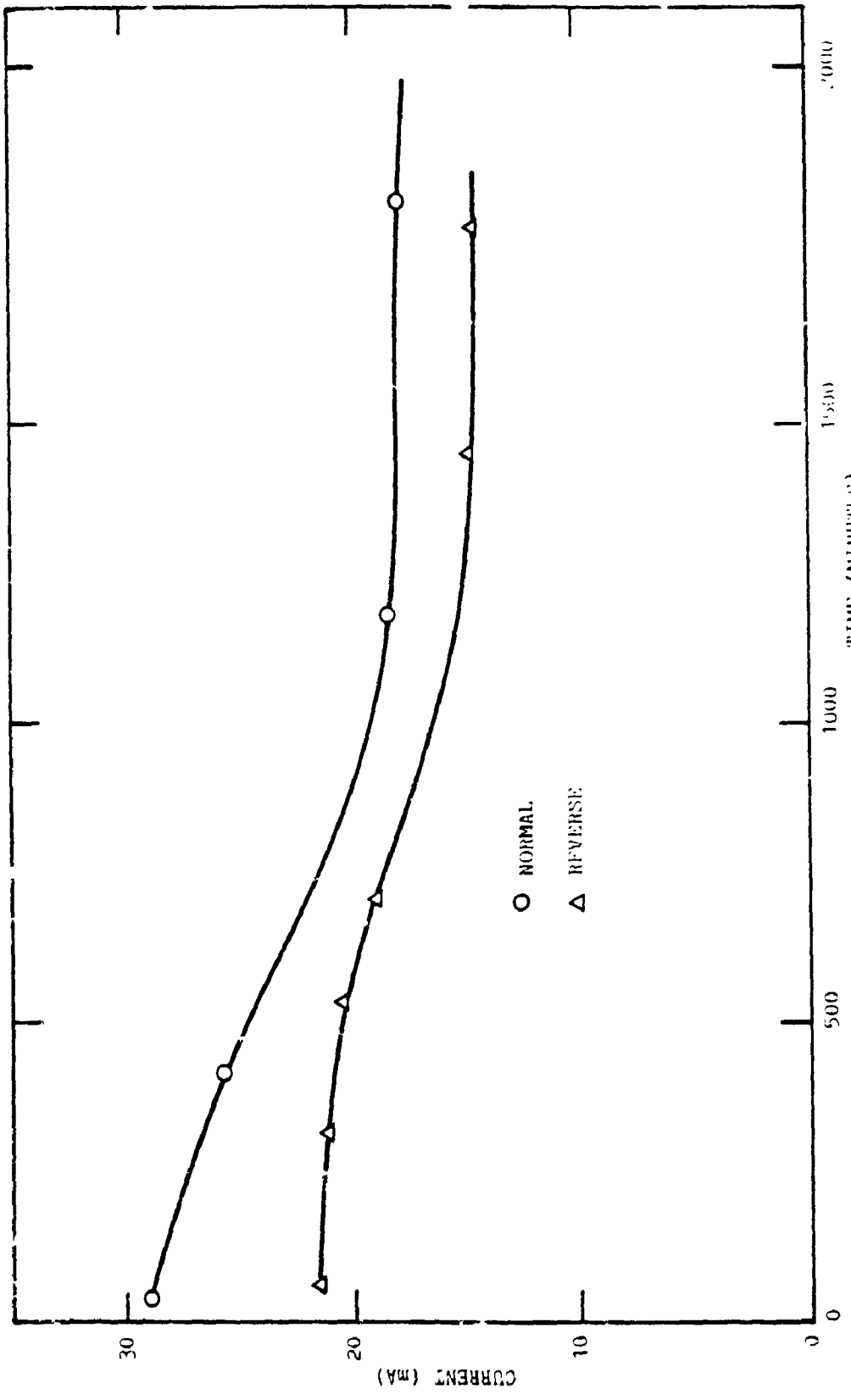

FIGURE 6.28 CURRENT VARIATION WITH TIME, TEST WH-6V, 4 V

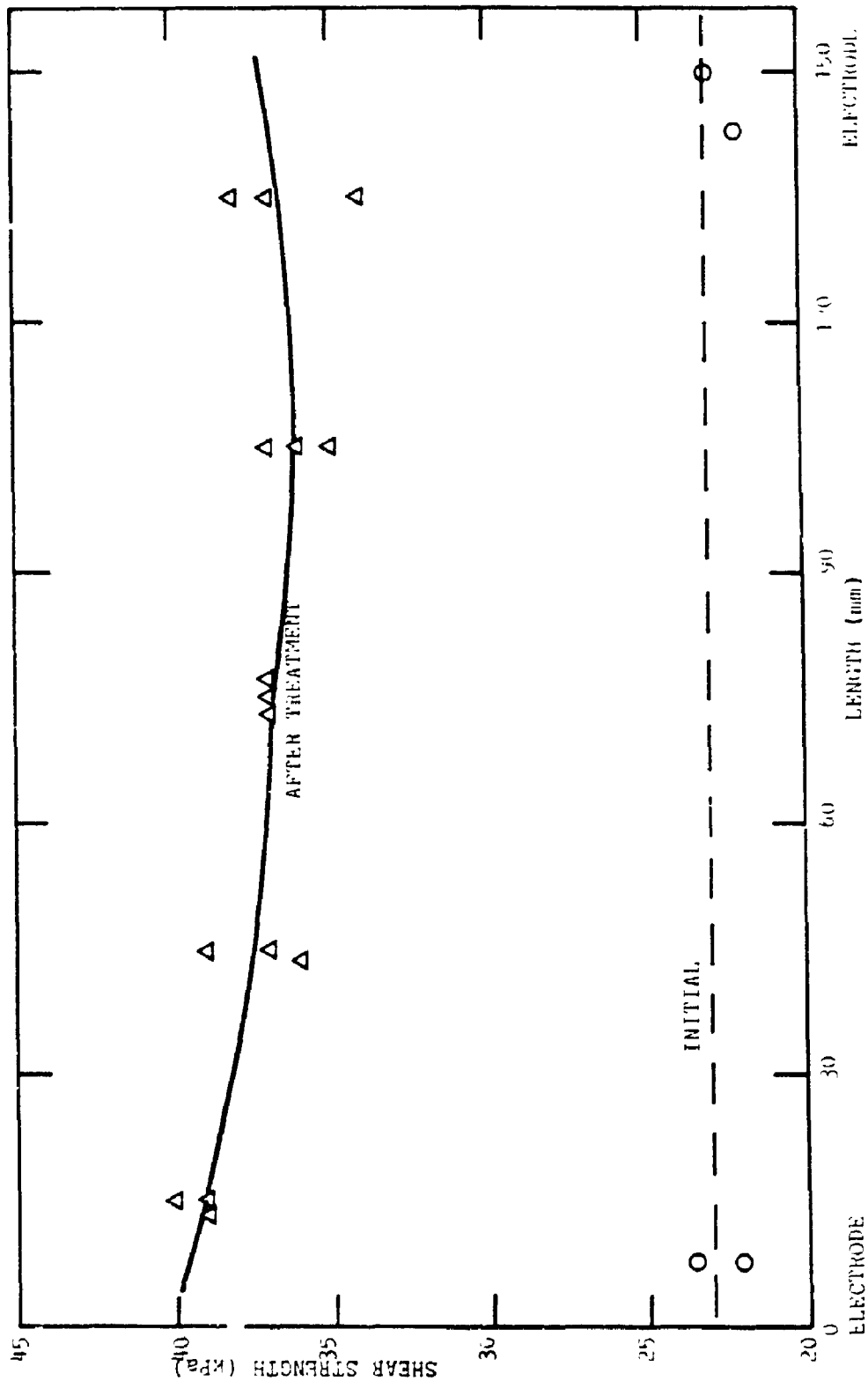

FIGURE 6.29 SHEAR STRENGTH BEFORE AND AFTER TREATMENT, TEST WH-6P, [illegible] AND 4 V WITH POLARITY REVERSAL

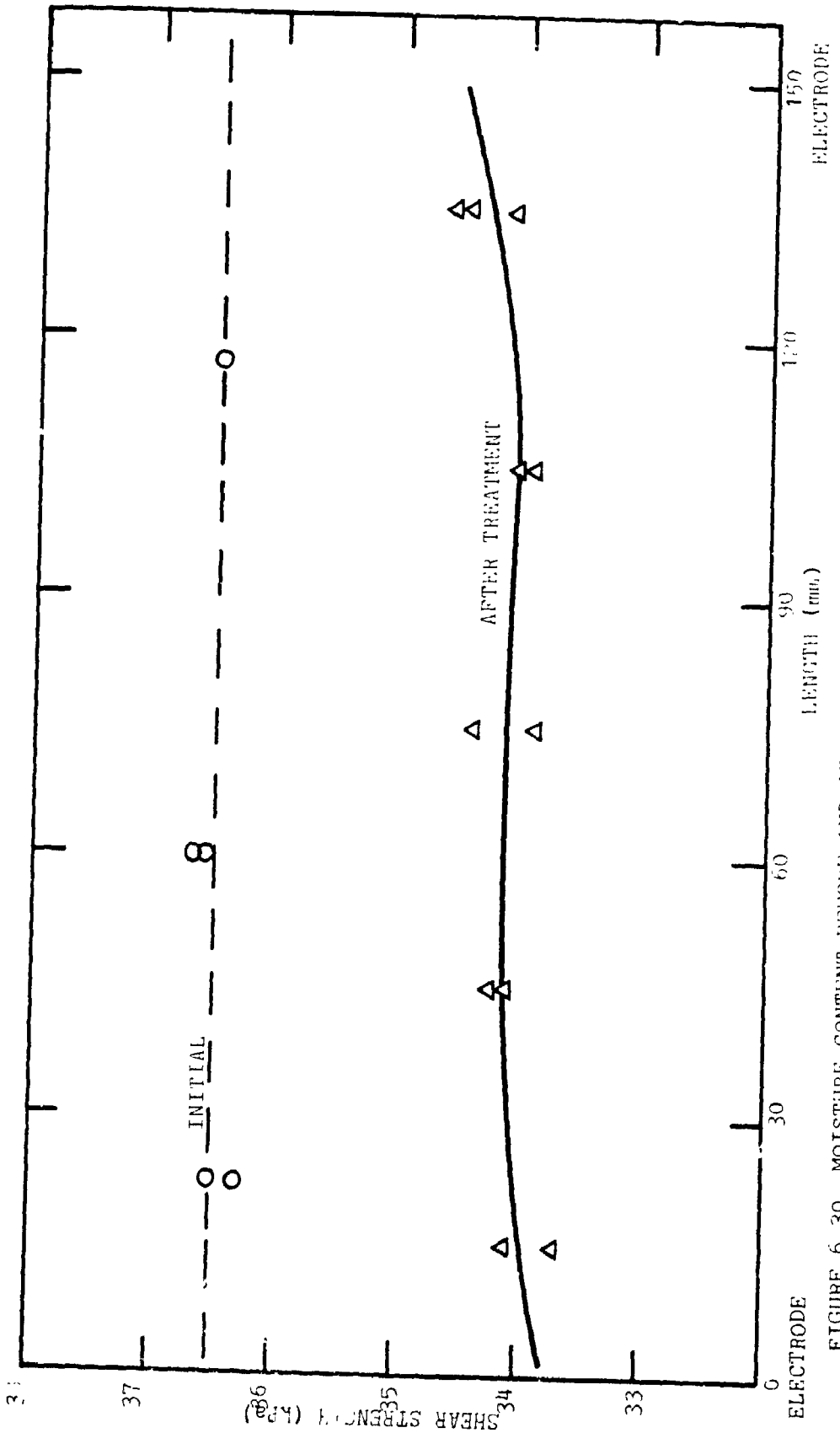

FIGURE 6.30 MOISTURE CONTENT BEFORE AND AFTER TREATMENT, TEST WH-6B
2 AND 4 V WITH POLARITY REVERSAL

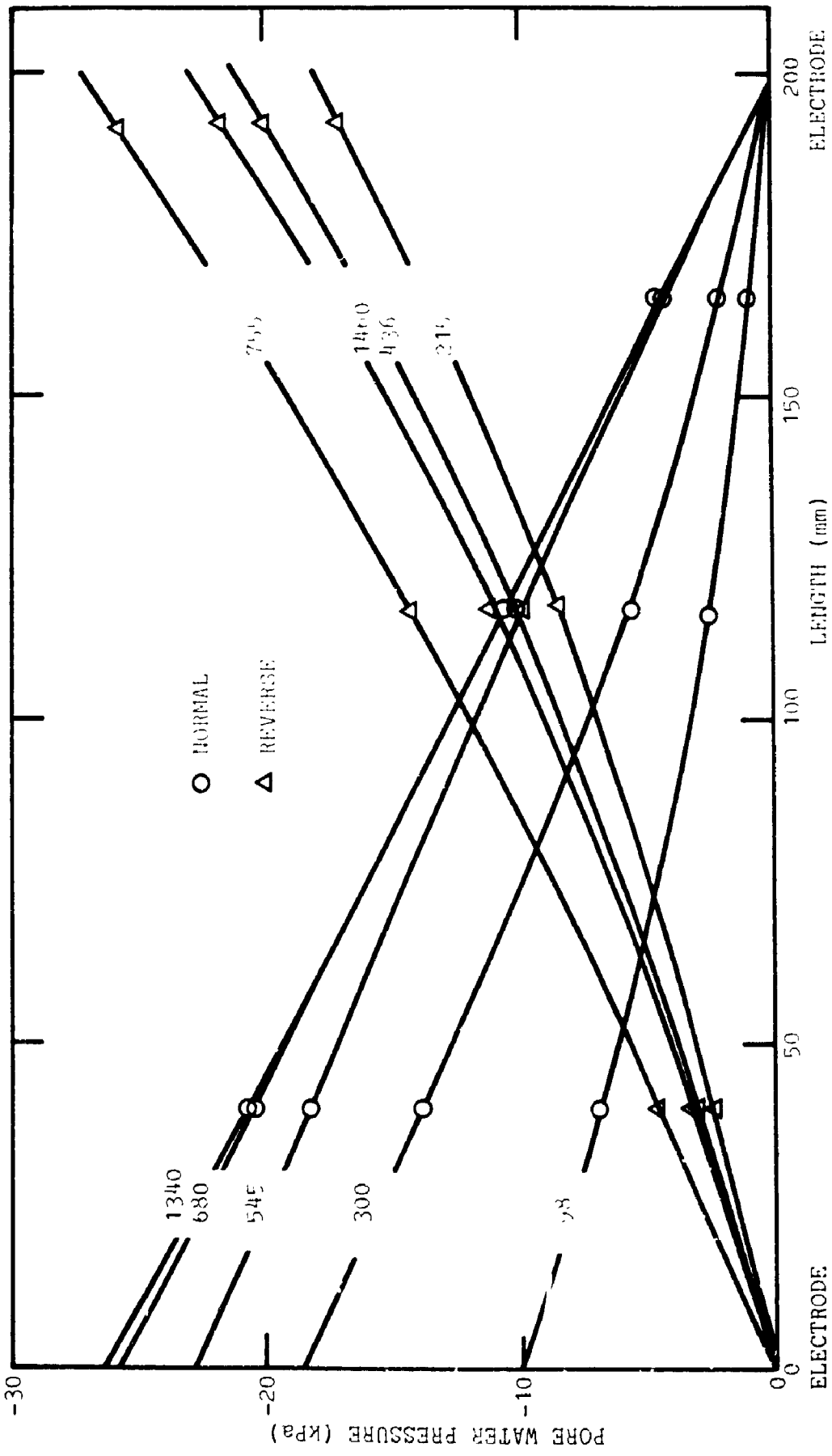

FIGURE 6.31 PORE WATER PRESSURE DISTRIBUTION WITH TIME (MINUTES), TEST GW-8, 3 V

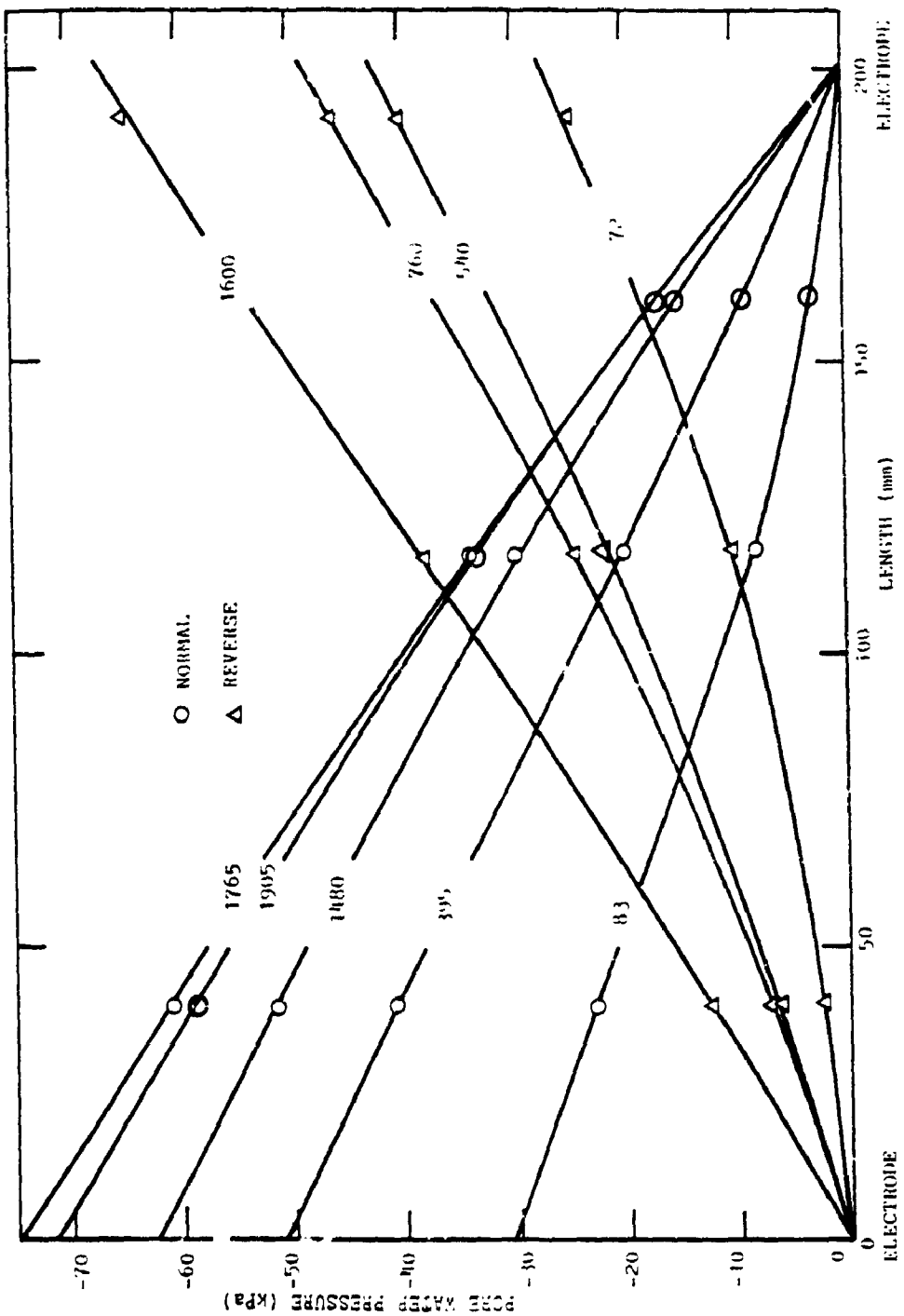

FIGURE 6.32 PORE WATER PRESSURE DISTRIBUTION WITH TIME (MINUTES), TEST GV-8, 6 V

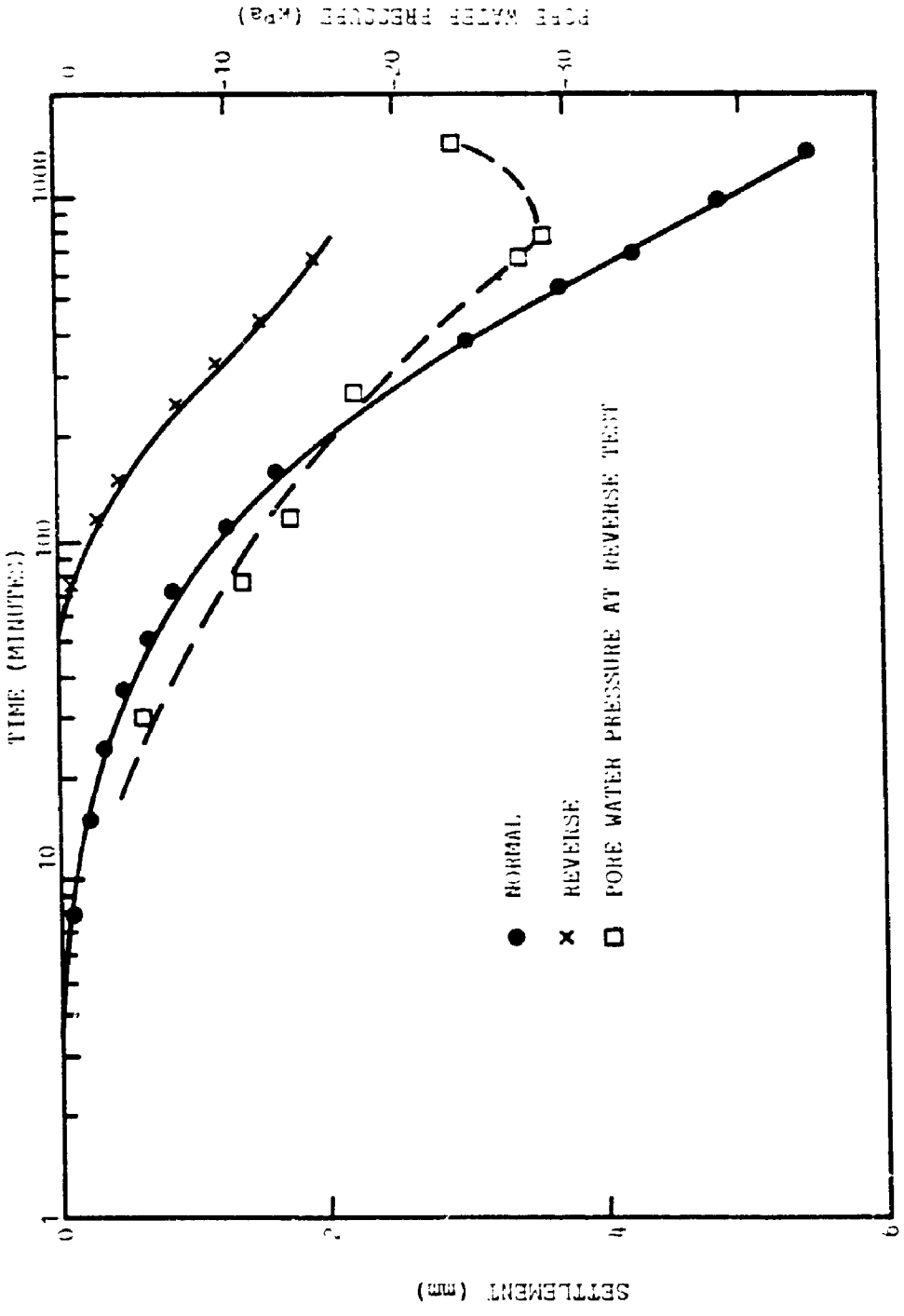

FIGURE 6.3 SETTLEMENT AND PORE WATER PRESSURE AT ANODE WITH TIME, TEST GV-8, 3 V

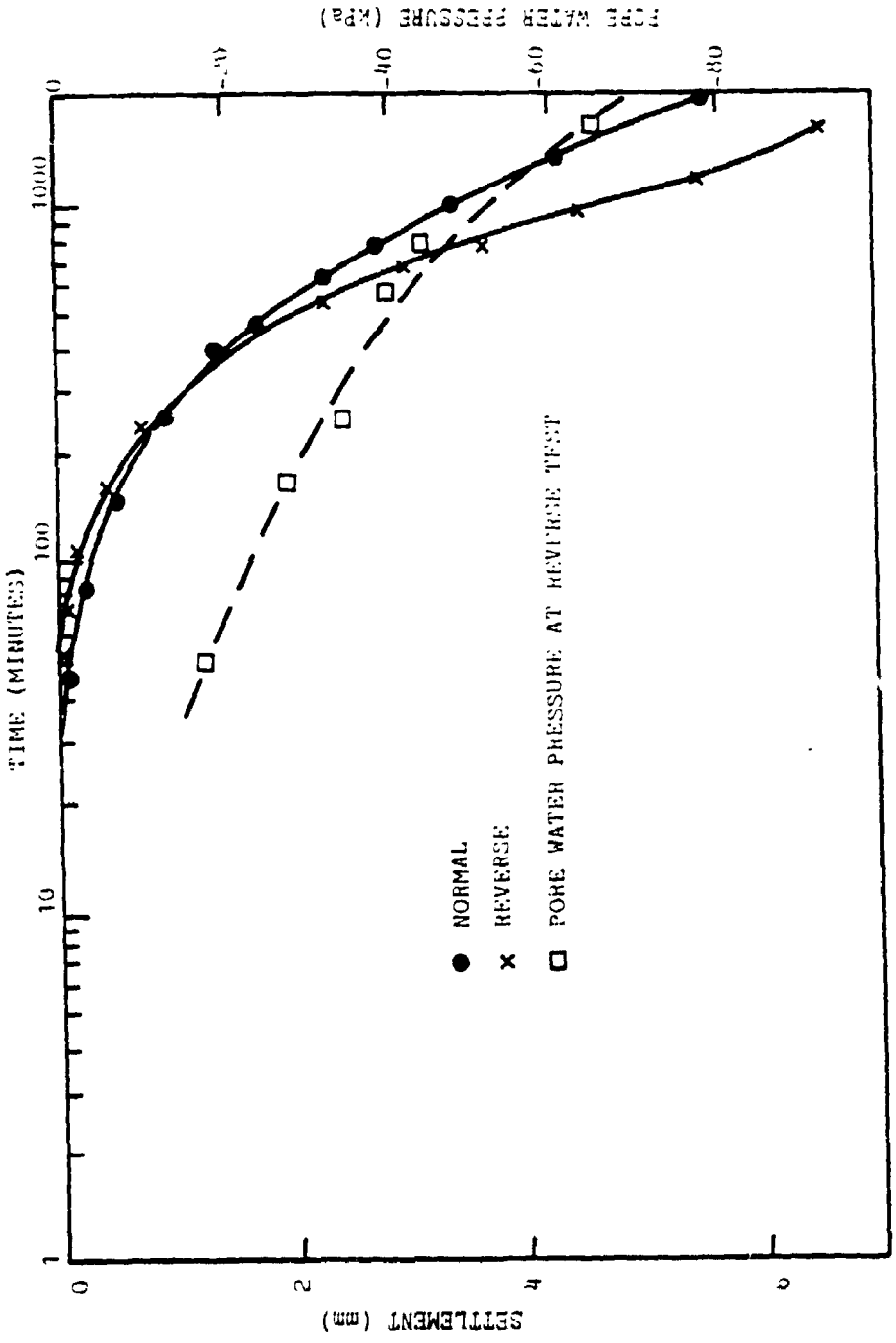

FIGURE 6.34 SETTLEMENT AND PORE WATER PRESSURE AT ANODE WITH TIME, TEST GV-8, 6 V

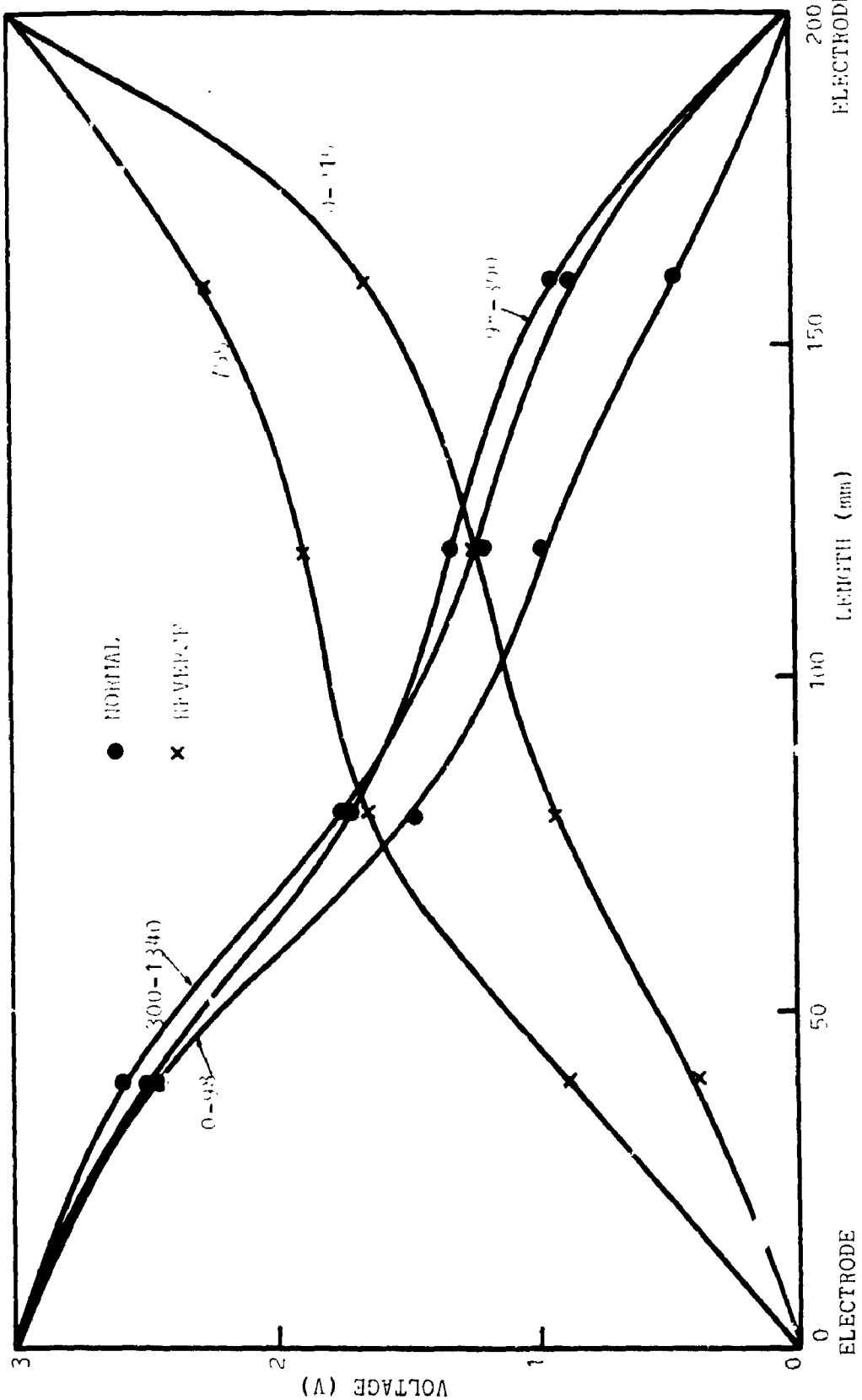

FIGURE 6.35 VOLTAGE DISTRIBUTION WITHIN SAMPLE WITH TIME (MINUTES), TEST GV-2, 3 V

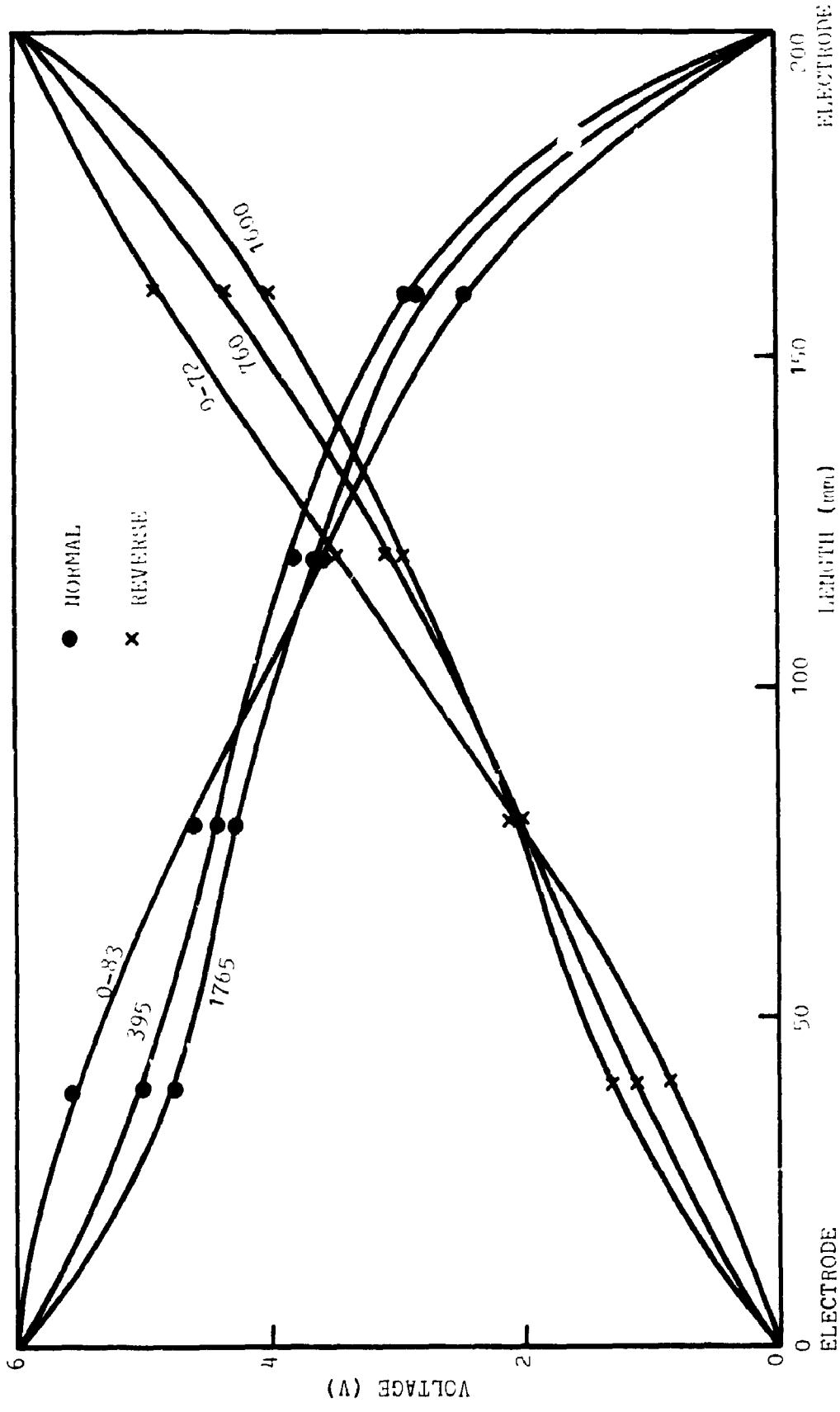

FIGURE 6.36 VOLTAGE DISTRIBUTION WITHIN SAMPLE WITH TIME (MINUTES), TEST GV-3, 6 V

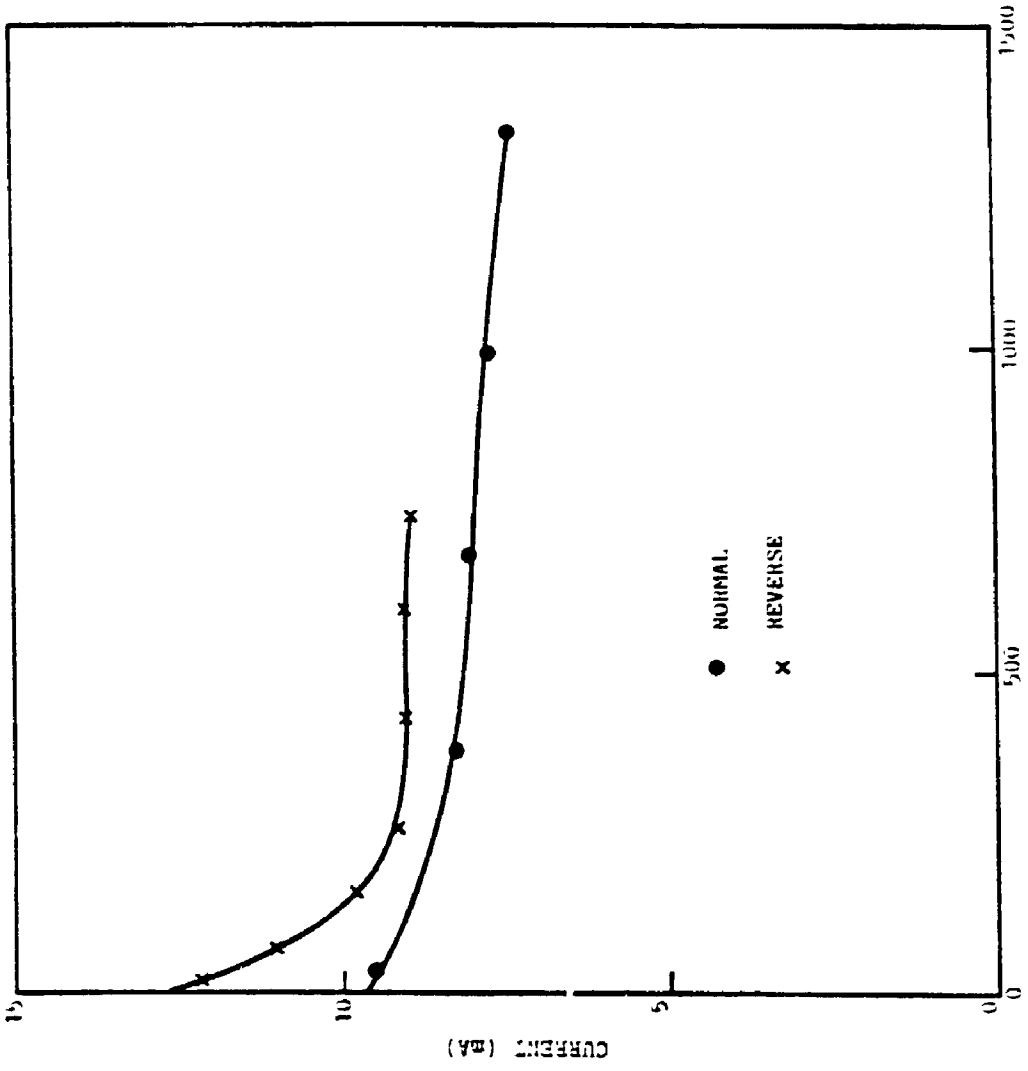

FIGURE 6.37 CURRENT VARIATION WITH TIME, TEST GV-8, 1 V

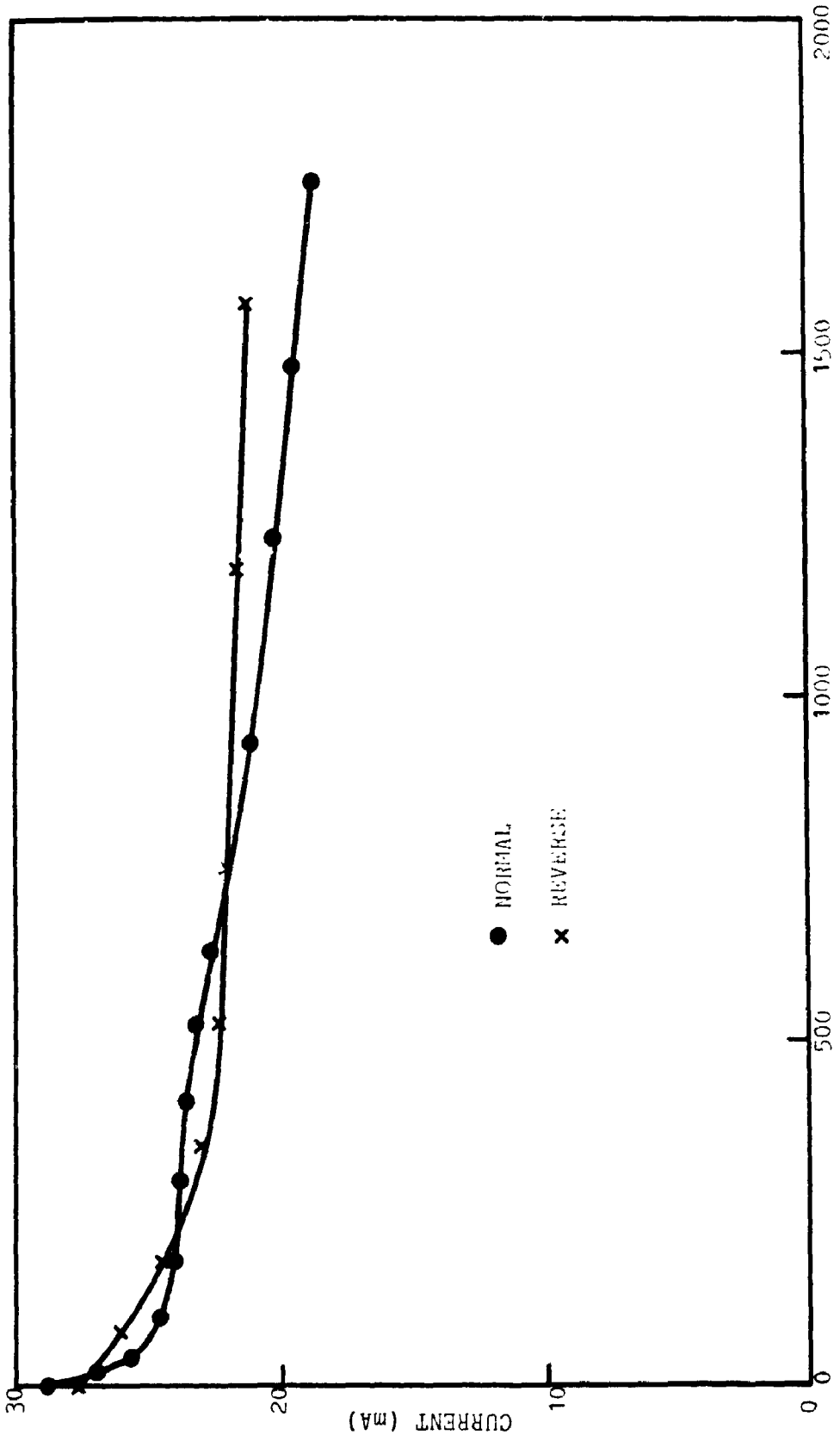

FIGURE 6.38 CURRENT VARIATION WITH TIME. TEST GV-8, 6 V

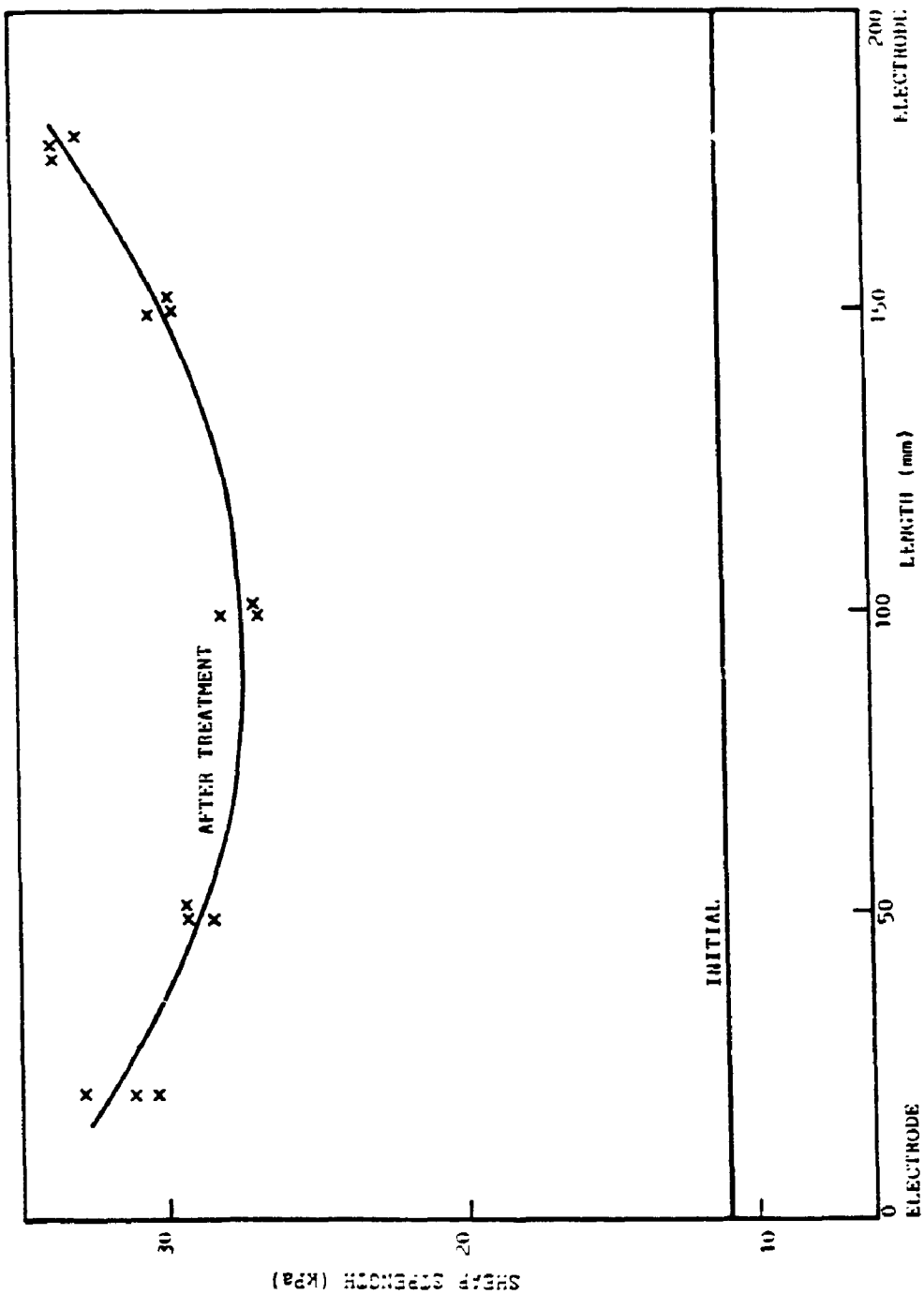

FIGURE 6.39 SHEAR STRENGTH BEFORE AND AFTER TREATMENT, TEST GV-8, 3 AND 6 V WITH POLARITY REVERSAL.

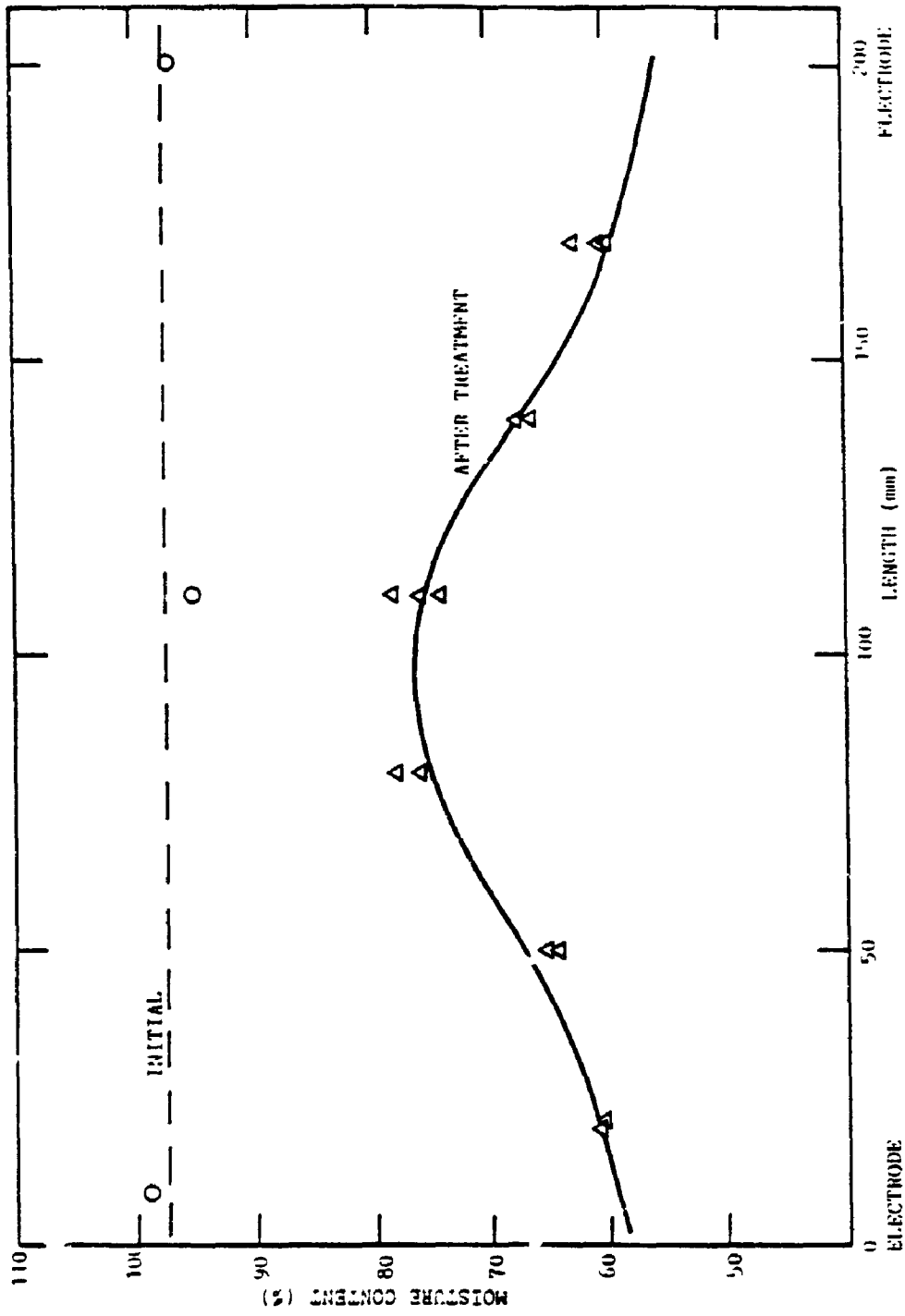

FIGURE 6.40 MOISTURE CONTENT BEFORE AND AFTER TREATMENT, TEST GV-8
5 AND 6 V WITH POLARITY REVERSAL

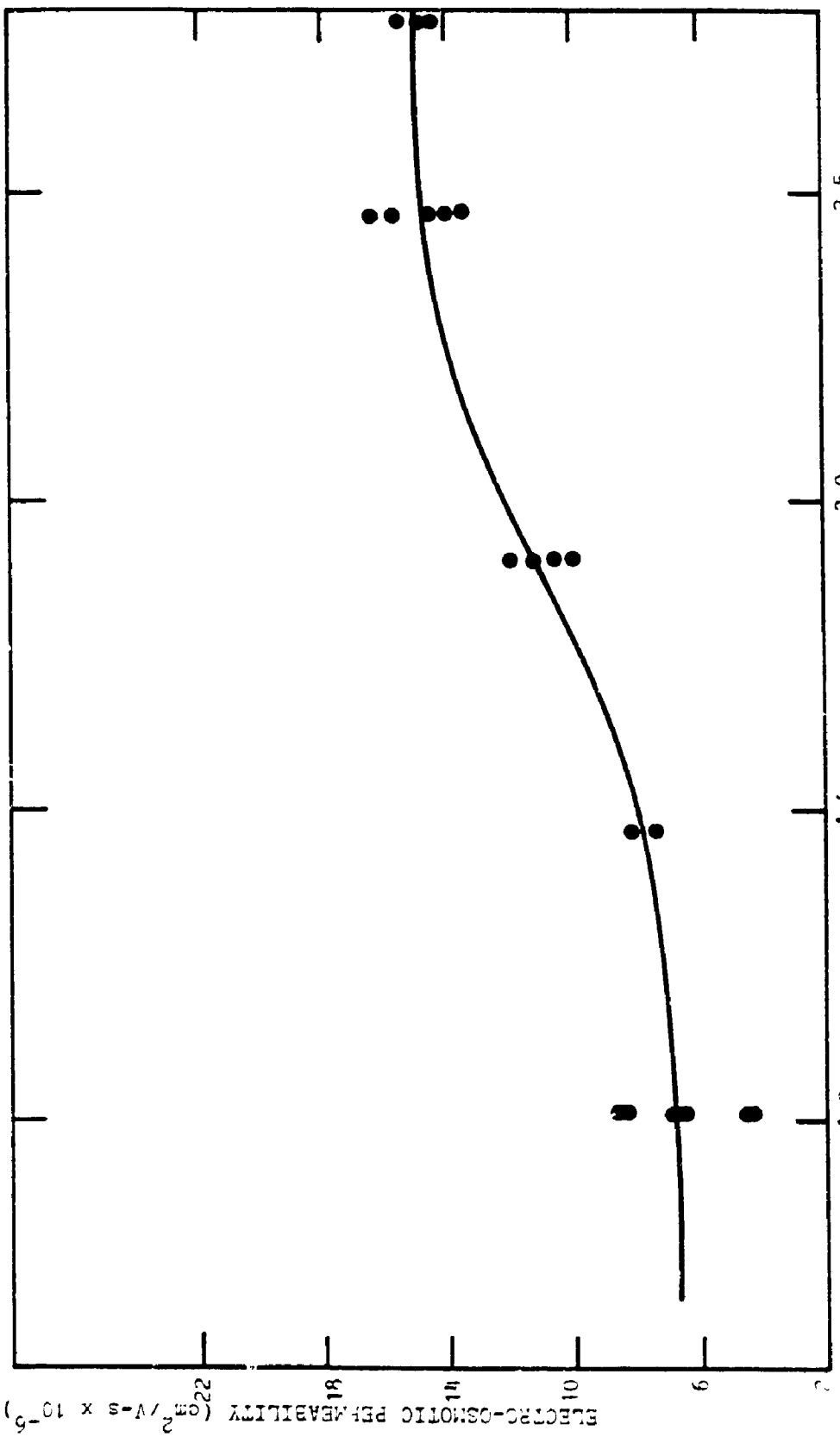

FIGURE 6.4.1 VARIATION OF ELECTRO-OSMOTIC PERMEABILITY WITH APPLIED VOLTAGE FOR VERTICALLY TRIMMED WALLACEBURG CLAY

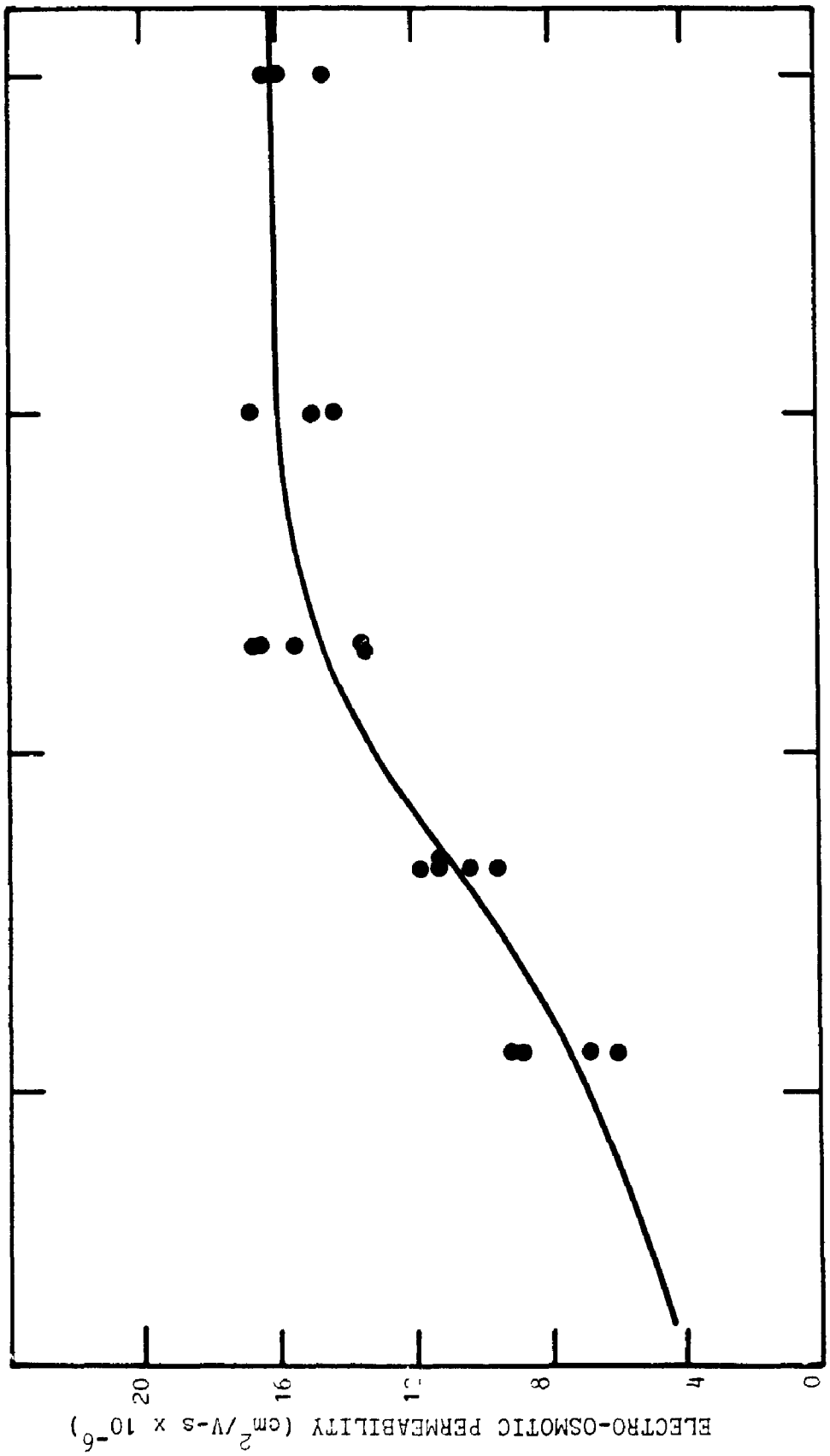

FIGURE 6.42 VARIATION OF ELECTRO-OSMOTIC PERMEABILITY WITH APPLIED VOLTAGE FOR HORIZONTALLY TRIMMED WALLACEBURG CLAY

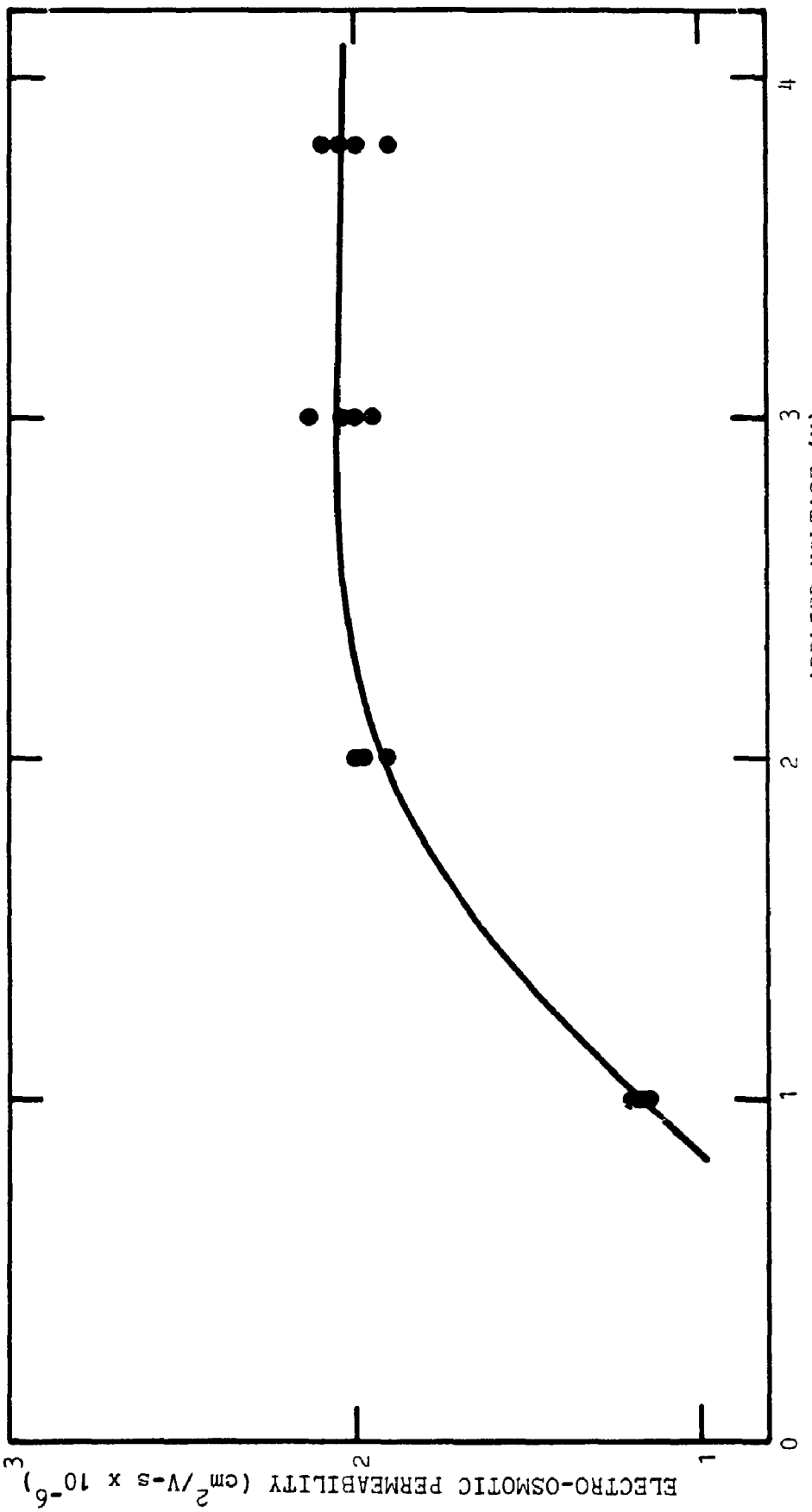

FIGURE 6.43 VARIATION OF ELECTRO-OSMOTIC PERMEABILITY WITH APPLIED VOLTAGE FOR VERTICALLY TRIMMED GLOUCESTER CLAY

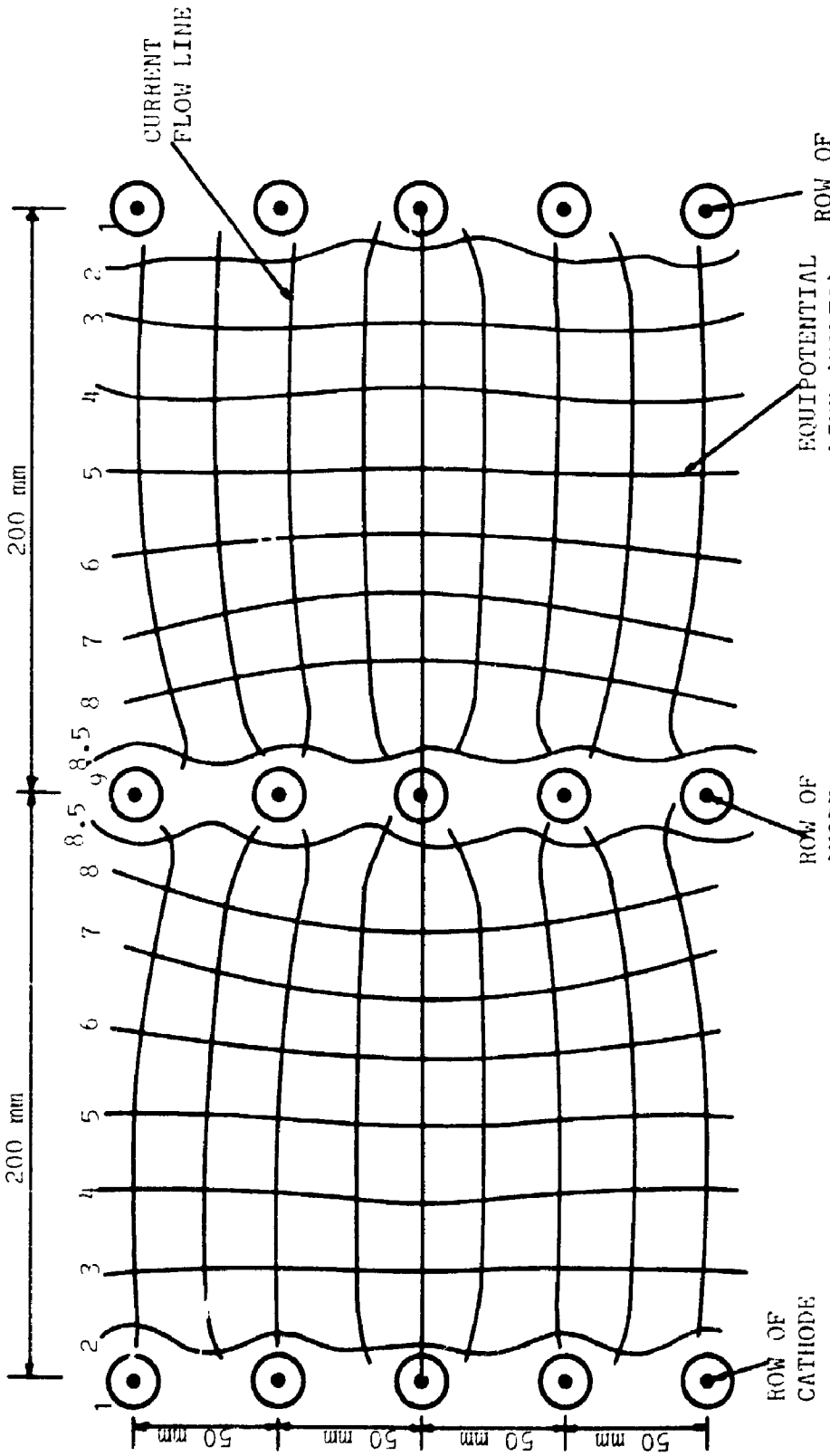

NOTE: THE VALUES REPRESENT THE POTENTIAL DIFFERENCE OF THE CORRESPONDING EQUIPOTENTIAL LINE

FIGURE 6.44 SKETCH OF EQUIPOTENTIAL LINES (VOLTS) AND CURRENT FLOW LINES MEASURED FOR EQUAL ELECTRODE SPACING (APPLIED VOLTAGE = 10 V)

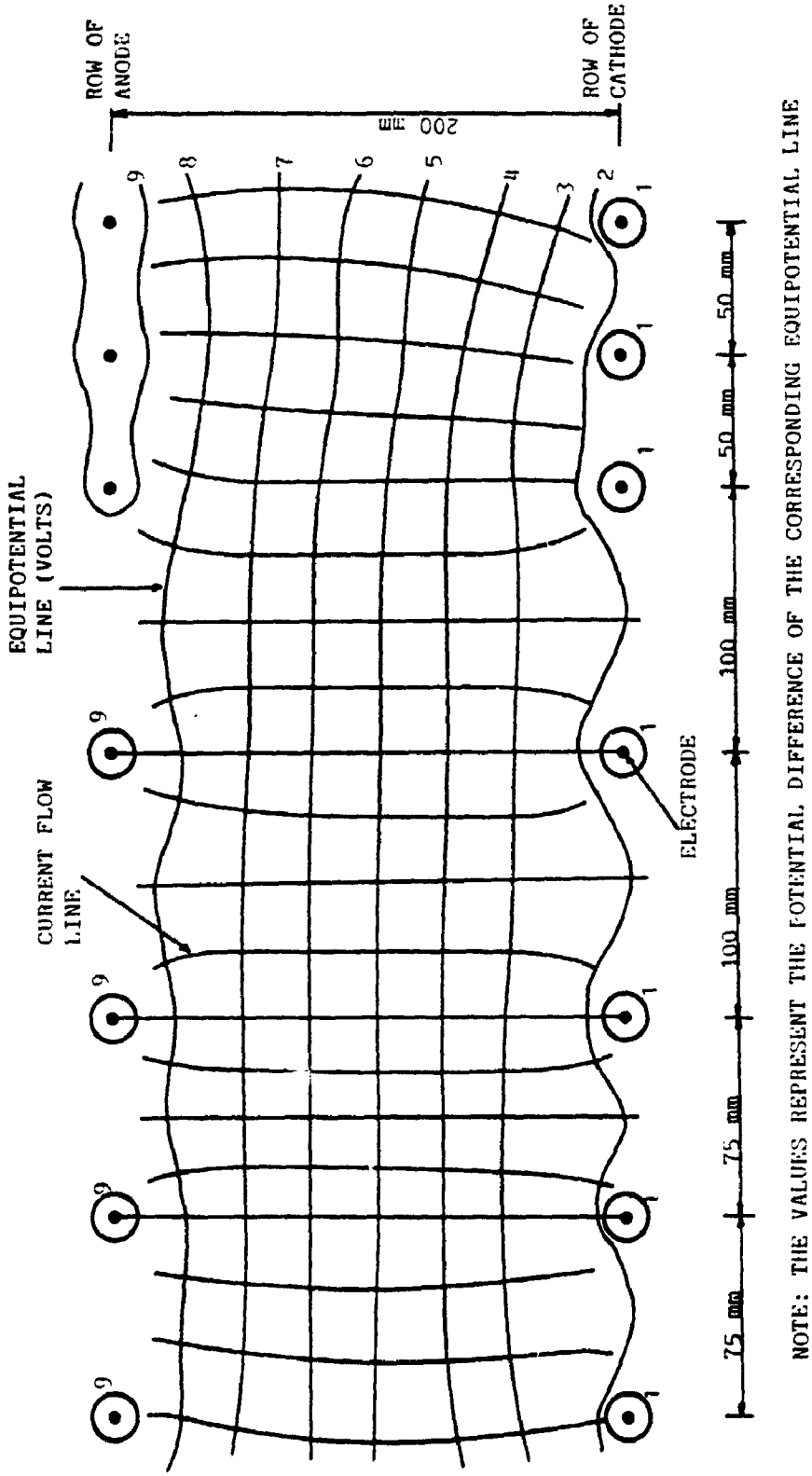

NOTE: THE VALUES REPRESENT THE POTENTIAL DIFFERENCE OF THE CORRESPONDING EQUIPOTENTIAL LINE

FIGURE 6.45 SKETCH OF EQUIPOTENTIAL LINES (VOLTS) AND CURRENT FLOW LINES MEASURED FOR VARIABLE ELECTRODE SPACINGS (APPLIED VOLTAGE = 10 V)

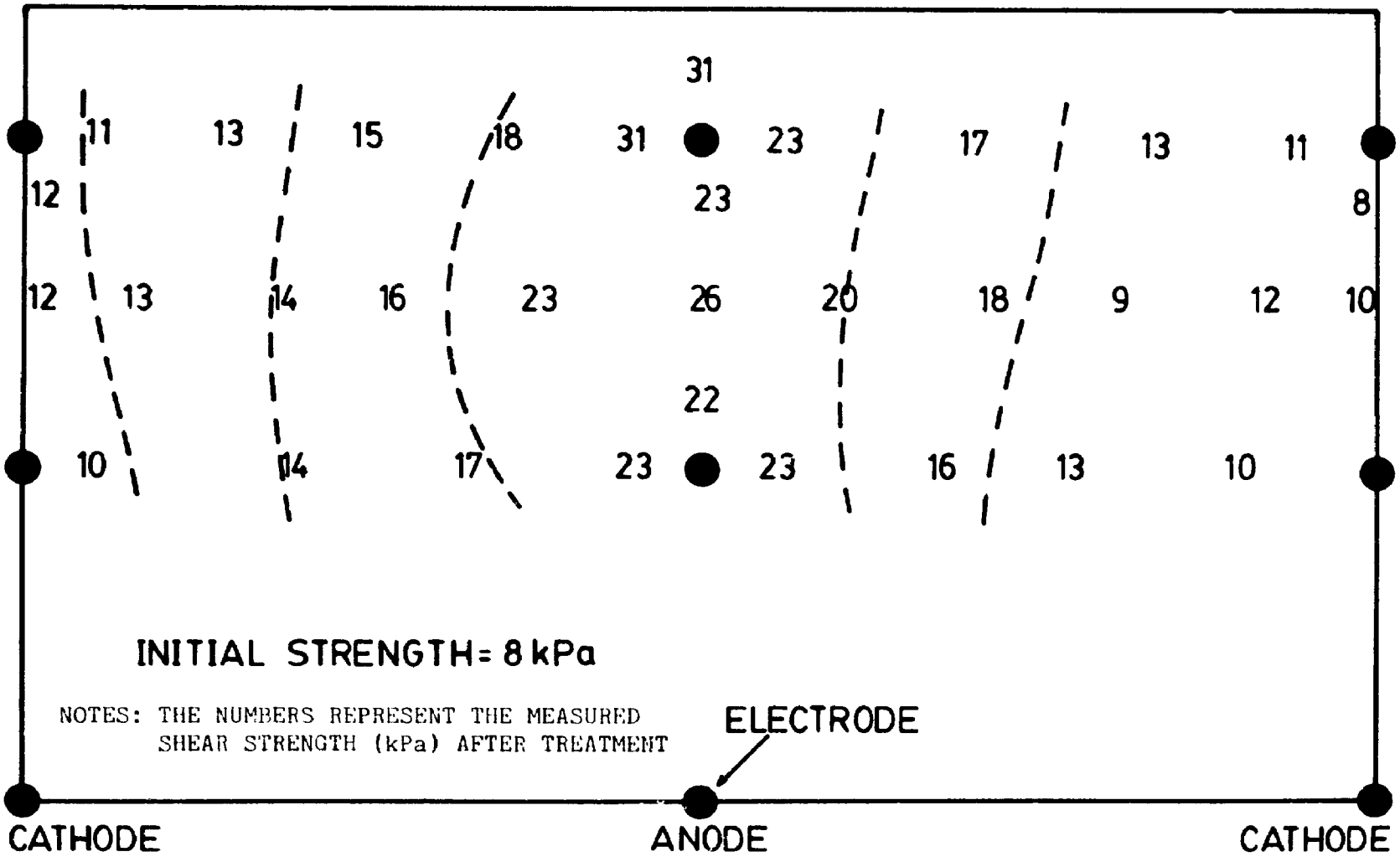

FIGURE 6.46 SHEAR STRENGTH (kPa) RESULTS AFTER ELECTRO-OSMOTIC TREATMENT, TEST W-RM APPLIED VOLTAGE 5 VOLTS WITHOUT POLARITY REVERSAL

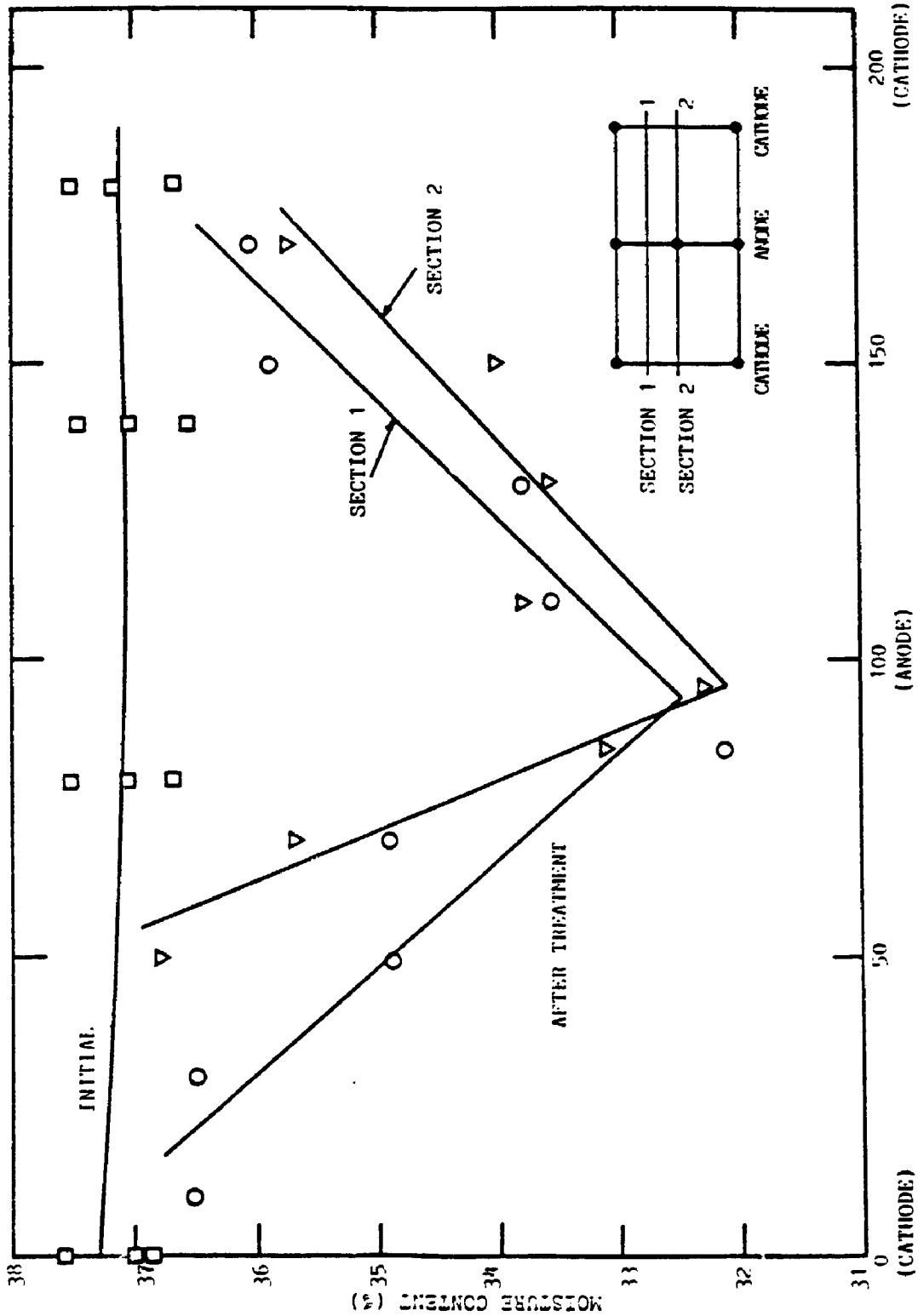

FIGURE 6.47 MOISTURE CONTENT RESULTS AFTER ELECTRO-OSMOTIC TREATMENT, TEST W-RM
APPLIED VOLTAGE 5 VOLTS WITHOUT POLARITY REVERSAL

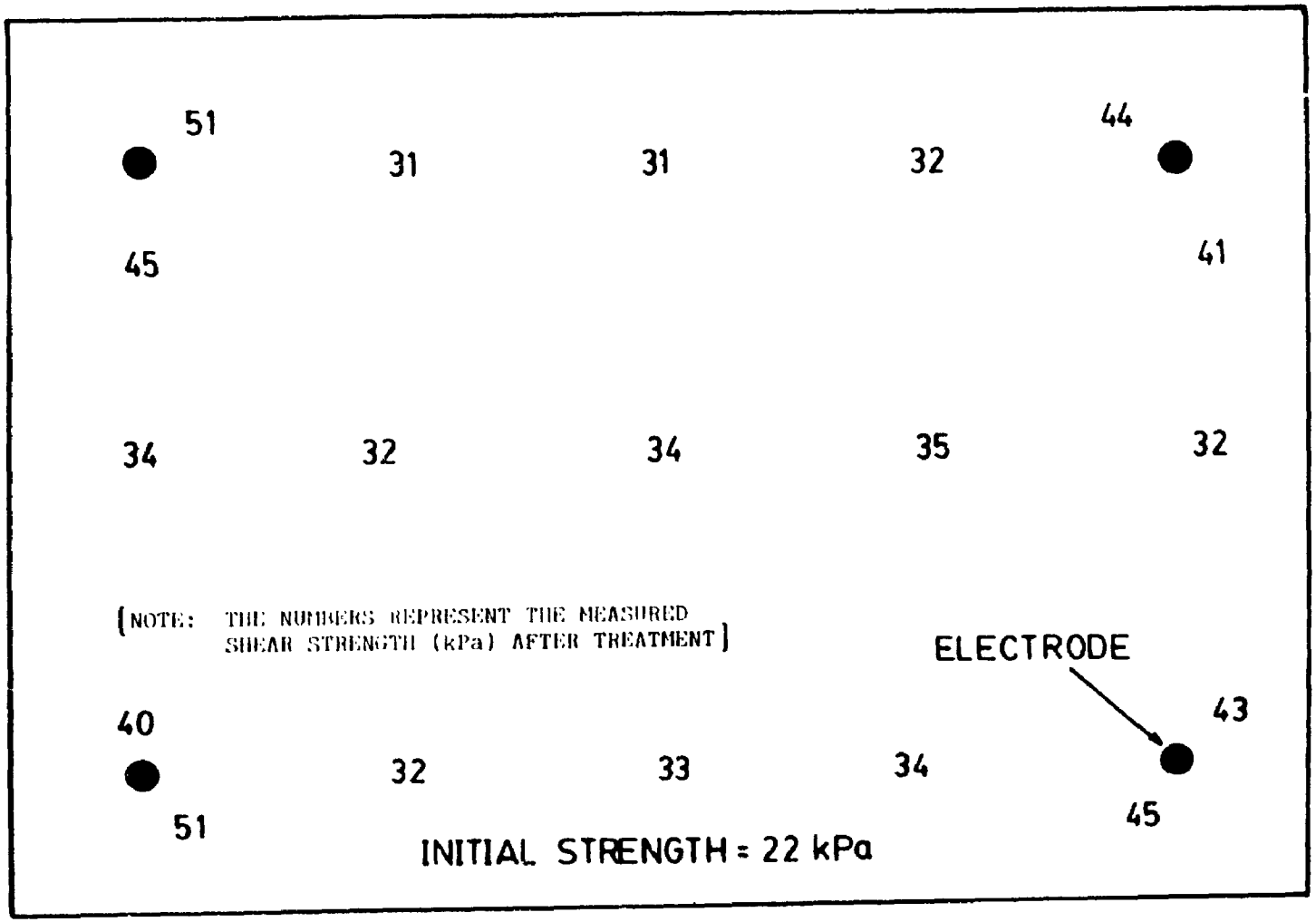

FIGURE 6.48 SHEAR STRENGTH (kPa) RESULTS AFTER ELECTRO-OSMOTIC TREATMENT, TEST W-UD1, APPLIED VOLTAGE 2.5 VOLTS AND 4 VOLTS WITH POLARITY REVERSAL

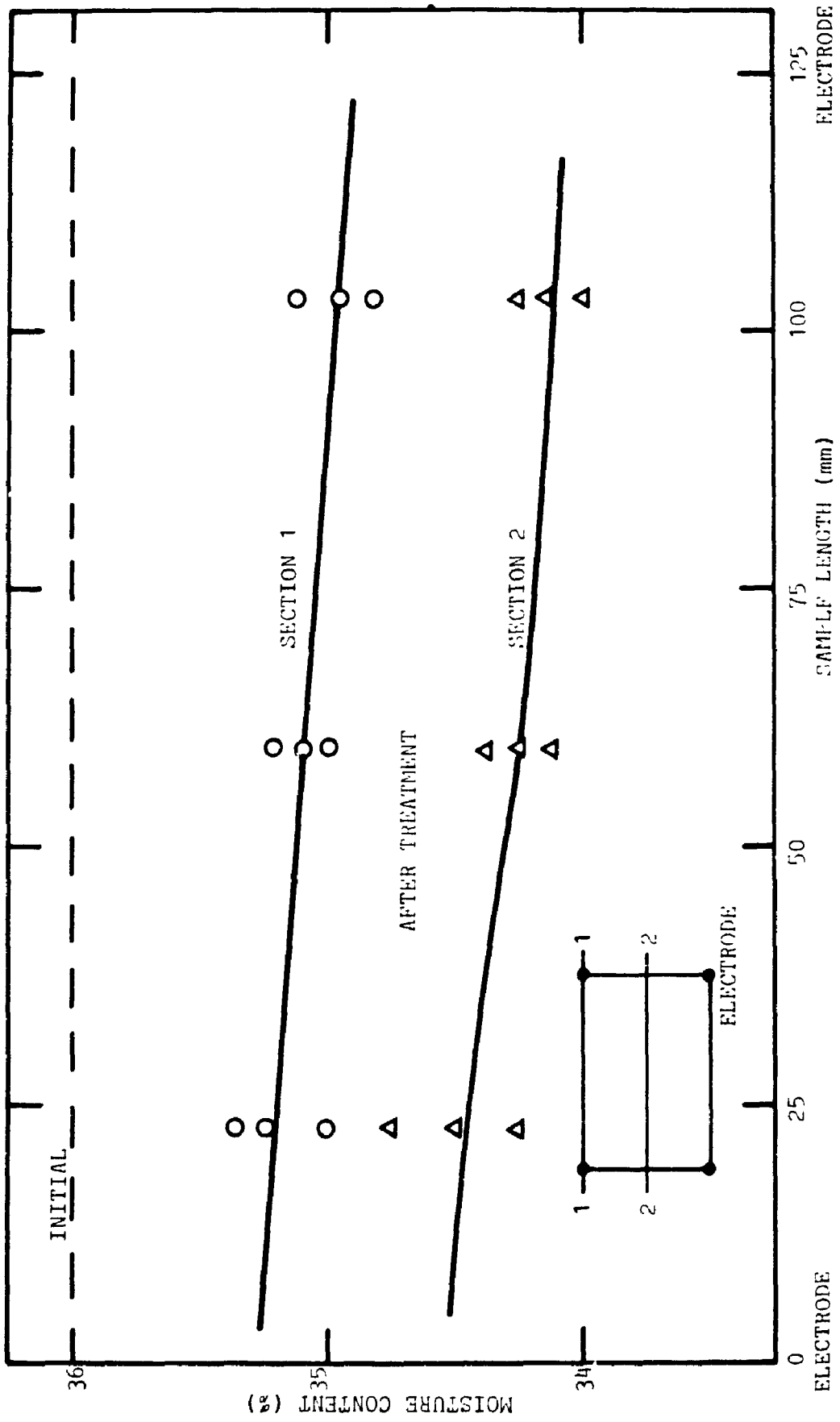

FIGURE 6.49 MOISTURE CONTENT RESULTS AFTER ELECTRO-OSMOTIC TREATMENT, TEST W-UD1, APPLIED VOLTAGE 2.5 VOLTS AND 4 VOLTS WITH POLARITY REVERSAL

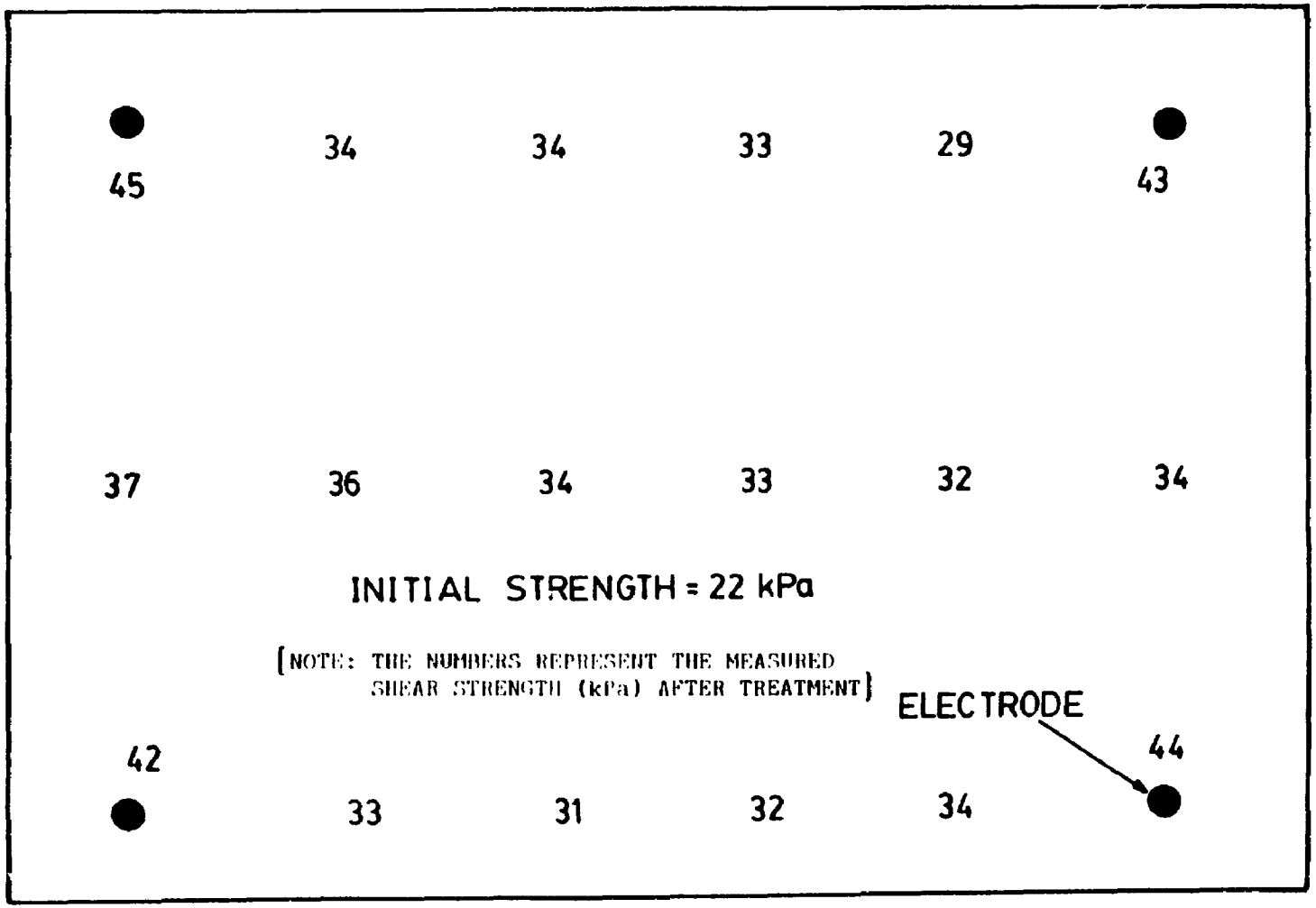

FIGURE 6.50 SHEAR STRENGTH (kPa) RESULTS AFTER ELECTRO-OSMOTIC TREATMENT, TEST W-UD2, APPLIED VOLTAGE 2.5 VOLTS AND 4 VOLTS WITH POLARITY REVERSAL

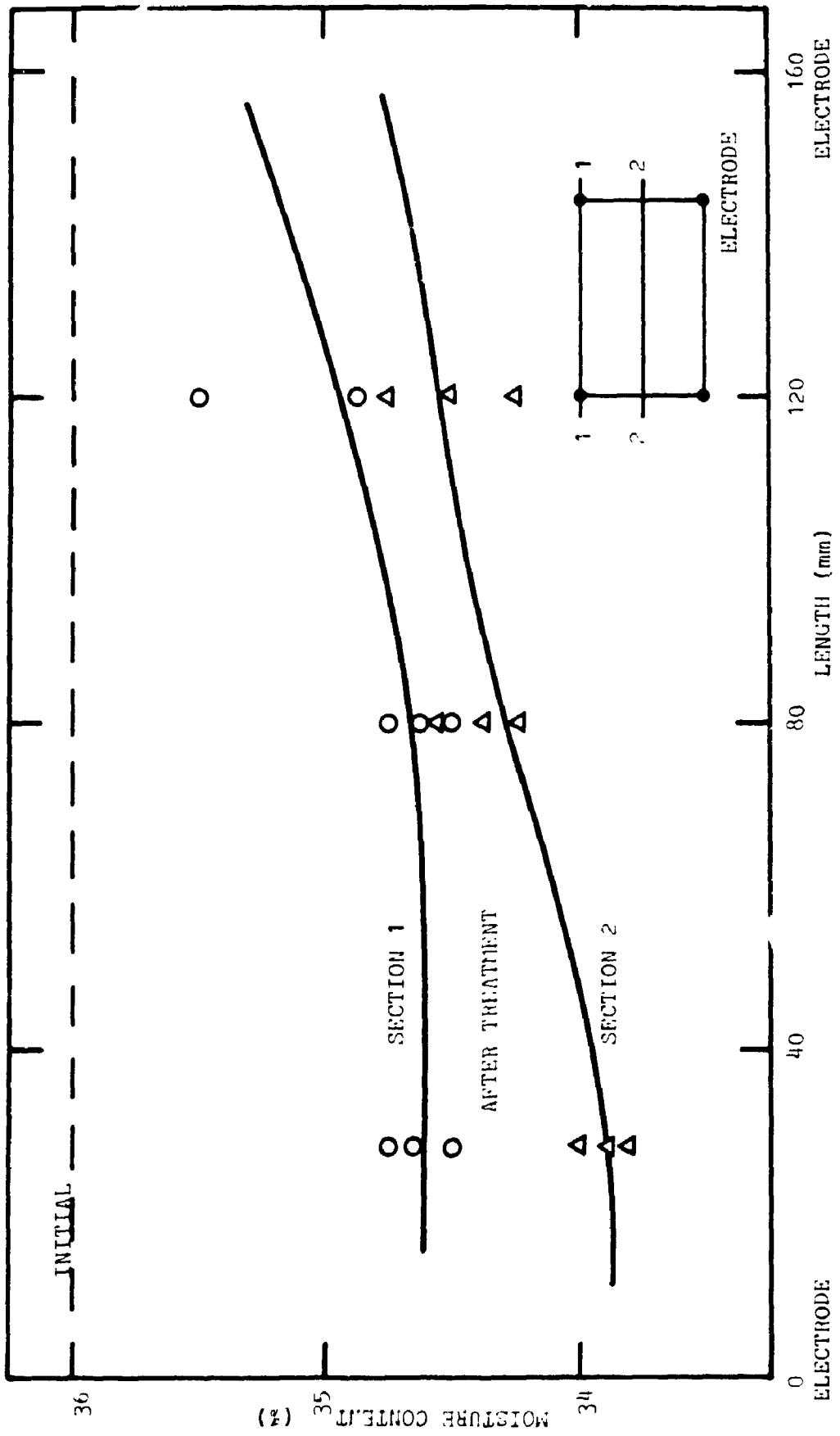

FIGURE 6.51 MOISTURE CONTENT RESULTS AFTER ELECTRO-OSMOTIC TREATMENT, TEST W-UD2, APPLIED VOLTAGE 2.5 VOLTS AND 4 VOLTS WITH ELECTRODE REVERSAL

CHAPTER 7

FURTHER DISCUSSION OF TEST RESULTS

In the previous chapter, the results of tests have been described and general observations made. Further analysis of the results are presented in this chapter.

7.1 Observations at Electrodes

During treatment, the evolution of gas was seen to escape through the drainage line at cathode. In one test (GV-8), as much as 100 ml of gas was collected. It suggested that there is quite a severe chemical reaction taking place at the cathode. It was also noticed that there was no gas accumulate at the cathode and the gas escaped from the specially designed cathode disc through the gas vent to the atmosphere. This was further confirmed by the pattern of pore water pressure distribution, voltage distribution and current flow trend as described earlier.

At anode, the development of pore water pressure indicates that no significant evolution of gas is taken place during treatment. The formation of blue compound around anode agrees with the initial assumption that copper will be oxidized at anode to form the blue colour copper oxide rather than the reduction of water to oxygen. The likelihood of gas evolution at anode was also investigated during the electro-osmotic permeability test. During the

process, the anode was opened to a reservoir of water. Any evolved gas at anode can be seen bubbled out to the surface of the reservoir. A careful surveillance for several hours concluded that no gas was liberated.

7.2 Prediction of Induced Negative Pore Water Pressure

Prediction of negative pore water pressure development was made by using the soil parameter (hydraulic permeability) obtained by Law (1974) for Gloucester clay, Lo and Becker (1979, 1980) for Wallaceburg clay and independently measured electro-osmotic permeability (section 6.5). The values of hydraulic permeability are shown in Table 7.1. The comparison of the experimental with theoretical results are made with tests not affected by cracking. The theoretical maximum negative pore water pressure induced at equilibrium is calculated by equation (3.10) and the comparison with experimental values are listed in Table 7.2.

Table 7.2 indicates that, for vertically trimmed Gloucester clay and vertically trimmed Wallaceburg clay, the calculated maximum negative pore water pressure at equilibrium during the first stage of voltage application are very close to the experimental values. While at the second or third stage of voltage application, the calculated values are usually lower than the experimental values. This is due to the fact that, after the first stage of voltage application, the soil was consolidated due to the generated negative pore water pressure and hence the hydraulic permeability k_h decreased. On inspecting

equation (3.10), the lower the k_h value, the higher will be the induced negative pore water pressure. However, the calculation, in which the hydraulic permeability was assumed constant, cannot reflect the real experimental changes. As a result, a lower negative pore water pressure is predicted. If a new k_h value (i.e., a lower hydraulic permeability) is used in the prediction, a higher negative pore water pressure will be obtained and this value may be close to the experimental value.

For the horizontally trimmed Wallaceburg clay, the predicted negative pore water pressure are in general around 2.8 times lower than the experimental values. This discrepancy of results is due to the way how the horizontal hydraulic permeability was determined. As report by Lo and Becker (1979, 1980), the horizontal hydraulic permeability (17×10^{-8} cm/s) was an average value obtained from field test result. As described earlier in section 6.3, the subsoil contains a layer of silt which is quite permeable. This relatively high permeability will dominate the average permeability value obtained from the field test. The soil treated by electro-osmosis was recovered from a lower permeability layer without any silt layer, and therefore a lower permeability should be assumed in the prediction. This results in under-estimating the experimental negative pore water pressure.

The theory and experiment are further compared by using equation (3.9) and the appropriate values of k_e, k_h and c_v. The electro-osmotic permeability was determined by conducting the electro-osmotic permeability test as described

in section 6.5 and the coefficient of consolidation was estimated from the electro-osmotic settlement curve and the corresponding values were 2 x 10^{-} cm^2 /V-s and 18.1 m^2 /year respectively. The average hydraulic permeability was taken to be 2.16 x 10^{-8} cm/s (Law 1974). The calculated induced negative pore water pressure was then determined at different time of treatment (98, 300 and 1340 minutes) for 3 volts normal test. The calculated and measured negative pore water pressure distribution for sample GV-8 are plotted in Figure 7.1. It can be seen that the theory under-predicts the measured values but the difference is relatively small. However, the theoretical prediction of pore water pressure at 3 volts reverse test and 6 volts test were not performed here due to the significant decrease of hydraulic permeability after the 3 volts normal treatment and this could not be measured during the experiment.

The effect of sample length to the generation of negative pore water pressure for the soils treated is also investigated. Tables 7.3 and 7.4 summarize the investigation results for Gloucester clay and horizontally trimmed Wallaceburg clay. Tables 7.3 and 7.4 indicate that the induced maximum negative pore water pressure is similar for different tests at the same voltage and is independent of sample length. Tests GV-4A and GV-8 have the similar pore water pressure of -28 kPa and -27 kPa respectively in the 3 volts test. The same is observed for the horizontally trimmed Wallaceburg clay (Table 7.4). This effect cannot be compared in the vertically trimmed Wallaceburg due to the different voltages used in the test. The observation that the induced maximum

negative pore water pressure is independent of the sample length is consistent with the theory. In equation (3.10), the induced maximum negative pore water pressure at equilibrium is independent of sample length. According to the theory, the induced pore pressure is proportional to the applied voltage (effective voltage), with the assumption that the soil parameters (k_h and k_e) are constants throughout the test. The direct proportionality of the pore pressure and applied voltage will be discussed later in section 7.7.

7.3 Shear Strength and Moisture Content

Undrained shear strength (determined by laboratory vane test) and moisture content tests were carried out on each sample along the sample length after treatment. Test results for samples GV-8, WV-8A, WH-6A and WH-6B are plotted in Figures 7.2b and 7.3 for comparison. The figures illustrate that there are substantial increase in shear strength and decrease in moisture content after treatment. The average undrained shear strength increased by 172.7 %, 76.1 % and 60.9 % for samples GV-8, WV-8A and WH-6B respectively for a treatment time of less than 2000 minutes (1.5 days). In addition, by using the electrode reversal technique, the shear strength distribution along the sample is fairly uniform. On the contrary, sample WH-6A treated at 4 volts without electrode reversal has only slight shear strength increase near the anode while the shear strength remains unchanged near the cathode. The average shear strength increase for this sample is only 20.0 % which is very low compared

with the other samples. This indicates that the polarity reversal plays an important role to achieve uniformity of treatment.

It is observed that the increase in undrained shear strength of Gloucester clay is about 2.5 times higher than that of Wallaceburg clay. This may be due to the fact that the Gloucester clay has low initial shear strength (11 kPa) and high initial moisture content (80 %) which are favourable for the electro-osmotic process.

For the Wallaceburg clay, the vertically trimmed sample has higher increase in undrained shear strength than that of the horizontally trimmed sample. This may be due to the slightly higher hydraulic permeability of the horizontally trimmed sample resulting in the lower induced negative pore water pressure as indicated by equation (3.10) that the higher the hydraulic permeability k_h, the smaller the induced negative pore water pressure at equilibrium. The explanation is consistent with the experimental results shown in Table 6.2 in that the horizontally trimmed samples have in general lower induced negative pore water pressure when compared with the vertically trimmed samples. The anisotropic soil property has therefore some effect to the electro-osmotic process and care has to be taken in selecting the appropriate parameter for analysis. In fact, the electro-osmosis test of the horizontally trimmed sample simulates the field condition in which the electrodes are installed vertically to the ground and the electric current flows horizontally.

The average percentage decrease in moisture content for samples GV-8, WV-

8A, WH-6B and WH-6A are 30.5 %, 11.2 %, 10.1 % and 5.4 % respectively. The trend of moisture content decrease is similar to that of undrained shear strength increase.

By using equation (3.13) and Figures 6.35 and 6.36, the resistivity of soil at any point along the sample can be determined. A plot of parameter PJ/L against sample length is shown in Figure 7.2a. Since the current flow is uniform across the sample by condition of continuity, the figure shows that the resistivity of the soil after treatment is higher near the two electrodes and minimum at the middle of the sample.

Comparing curve 1 in Figure 7.2a and curve 1 in Figure 7.2b, it is noted that the resistivity and shear strength increase variations along the sample length have the same pattern, indicating that the soil resistivity plays a significant role in affecting the shear strength increase.

7.4 Stress-Strain Behaviour and Sensitivity

Unconfined compression tests were conducted on the Gloucester clay samples after treatment. Due to the limitation that quite a number of different tests have to be performed, only small cylindrical samples of 25 mm in diameter and 50 mm in length can be recovered along the sample length after treatment for unconfined compression test. Since the sample size is smaller than the standard size (50 mm diameter by 100 mm length) for triaxial test, no attempt has been made to carry out triaxial test in terms of effective stresses. The

purpose of conducting the unconfined compression test here, in spite of its limitations, is to obtain some idea on the change of the stress-strain behaviour before and after treatment for comparison purpose. However, comprehensive series of consolidated undrained triaxial test on standard size sample have been performed on the samples recovered from the field after the field test by electro-osmosis in Gloucester Test Fill area. These results will be discussed in Chapter 17.

Representative stress-strain curves for samples GV-4A, GV-4B, GV-8 and a pre-treatment sample are plotted in Figure 7.4. The corresponding test results are summarized in Table 7.5. The peak strength of each sample increases in the same trend as in the laboratory vane strength test described earlier. It can be seen from Figure 7.4 that both the pre-peak deformation modulus and the post-peak strength increased. It may be seen from Table 7.5 that the undrained modulus of the Champlain Sea clay increases with applied voltage to approximately 8 times the initial value at a voltage of 6 volts. The behaviour of post-peak decrease in strength, a feature commonly observed in sensitive clay, as measured by the brittleness index I_B (Bishop 1967) also shows improvement. The value of I_B reduces from the initial value of 0.39 to 0.20. It may be seen from Table 7.6 that the sensitivity of the soil also decreased. The sensitivity decreases from a nominal value of 100 for the pre-treated sample to 76, 51 and 38 for samples GV-4A, GV-4B and GV-8 respectively, resulting in the percentage decrease in about 24 to 62 %.

From the above test results it is evident that the electro-osmosis method not only reduces the moisture content and increases the shear strength, but also improves the stress-strain characteristics and lower the sensitivity of the soil. This improvement of stress-strain property may play a significant role in the design considerations of earth structures.

7.5 Consolidation

A series of conventional consolidation test was performed on the Gloucester clay before and after treatment. The results are plotted in the form of the change of void ratio versus the applied pressure in Figure 7.5. It may be observed that there is a general trend of decreasing compressibility consistent with the increase in undrained modulus discussed previously. The preconsolidation pressure increases from 53 kPa for the pre-treatment sample to 74, 83, and 92 kPa for samples GV-4A, GV-4B and GV-8 respectively resulting in the increase of 51 to 88 % of preconsolidation pressure (Table 7.7). The increase in preconsolidation pressure is a result of the negative pore pressure generated which is equivalent to internal effective stress under which the soil consolidates. The samples are therefore virtually "overconsolidated" by the electro-osmosis process. This pseudo-overconsolidation may explain why the effects of treatment are permanent.

From the settlement-time curves of the electro-osmotic treatment, the coefficient of electro-osmotic consolidation can be determined by the same

procedure as outlined for the conventional consolidation test. As shown in Table 7.8, for the Gloucester clay, the coefficient of consolidation increased from the pre-treated value of 0.45 m^2/year to the maximum of 18.1 m^2/year for sample GV-8 after 3 volts test. This shows that the soft sensitive clay can be consolidated and strengthened by electro-osmosis in a quicker rate than conventional mechanical loading.

For the vertically trimmed Wallaceburg clay, the two coefficients of consolidation are quite similar in value. The electrical coefficient is higher at higher applied voltage. This implies that higher "electrical loading" is required to consolidate this type of soil (over-consolidated clay). No attempt has been made here to compare the coefficients for the horizontally trimmed Wallaceburg clay due to the insufficient data of the conventional coefficient.

7.6 Effect of Applied Voltage on Pore Pressure, Shear Strength Increase and Settlement

To investigate the relationship between the applied potential and the maximum induced negative pore water pressure, the results of all the tests performed are plotted in Figure 7.6. It can be seen that the magnitude of pore water pressure generated is dependent on the applied electric potential. In general, the higher the applied voltage, the greater is the induced negative pore water pressure. Furthermore, within the range of voltage used, there appears to be a linear relationship between the applied electric potential and the

maximum induced pore water pressure for each soil type in a given direction of electro-osmotic treatment. The exception is the test at 5 volts of specimen WV-8B which cracked during treatment and thus releasing the negative pressure. The size of the sample are noted in brackets in Figure 7.6. There is evidence that the relationship is independent of sample size. This linear relationship is consistent with the prediction of equation (3.10) which shows that the induced pore water pressure is proportional to the effective voltage at a particular section of the sample assuming that the values of the electro-osmotic and hydraulic permeability are constant throughout the test. This relationship will be useful in the design of electro-osmosis treatment for a required amount of increase in strength.

Similar plots are shown in Figures 7.7 and 7.8 with the percentage increase in shear strength against the applied voltage and the settlement against the applied voltage respectively.

7.7 Physical and Chemical Changes

Table 7.9 summarizes the average values of liquid limit, plastic limit, pH value, carbonate content and salinity of the Gloucester clay and Wallaceburg clay before and after treatment. For Gloucester clay, the liquid limit increased slightly from 48.4 % to 52.8 %, while the plastic limit increased slightly from 29.5 % to 31.2 %. The pH value of soil and expelled water collected from cathode increases from 8.2 to 10.3 and to 11.5 respectively. The carbonate

content of soil increases from 2.8 % to 3.6 %. In addition, the salinity of soil increases from 1.7 g/l to 2.5 g/l after treatment. The increase in carbonate content of the soil after treatment provides a better bonding of the soil particles and consequently contribute to the increase in shear strength while the increase in salt content increases the remoulded strength and thus contributing to the decrease in sensitivity. For the Wallaceburg clay, there is practically no change in the liquid limit, plastic limit and pH value of the soil. Similar to the Gloucester clay, the carbonate content and salinity increase from 5.3 % to 7.8 % and 2.5 g/l to 7.2 g/l respectively.

From the test results obtained, these simple physical chemical tests provide a possible explanation of the electro-osmotic process chemically. A more detailed analysis has been performed on the Gloucester clay samples recovered from full scale field test and the results will be discussed in Chapter 17.

7.8 Tension Cracks and Radial Shrinkage

One of the most noticeable electro-osmotically induced irregularity during treatment is the tension crack which can prevent development of negative pore water pressure. Some slight tension cracks were noted on test WV-8B at the beginning of reverse test at 5 volts. The cracks were vertical and were located throughout the perimeter at vicinity to the anode. The cracks extended up to about half the sample length as time of treatment progressed, as shown in Figure 7.9. There was only small additional settlement as a result of the cracks.

The causes of the formation of cracks may be due to the treatment time and the magnitude of the applied electric potential. This observation suggests that the occurrence of the cracks can be prevented if the soil homogeneity can be maintained at reasonable level. This can be achieved by applying a small voltage at the beginning of the treatment and increasing the applied voltage gradually with electrode polarity reversal. For the rest of the tests in which these procedures were followed, no cracks was observed throughout the treatment.

Another effect accompanying the process is radial shrinkage. The shrinkage started at anode, progressed towards cathode. There is no definite pattern of when shrinkage will occur with respect to the drop in pore water pressure or applied electric potential. If shrinkage is extensive, the effect on negative pore water pressure development during treatment will be unavoidable. Figures A.11 (WV-8B, 5 volts), A.18 (WH-3, 4 volts) and A.29 (WH-9, 6 volts) show the slightly distorted pore water pressure development resulted from the presence of extensive shrinkage. However, this type of shrinkage would only occur in the laboratory test due to the limited sample size. In the field, the volume of soil is unlimited and settlement of the ground rather than radial shrinkage will result.

7.9 Implication of Model Tests

As described in section 6.6, the similarity between the vane strength profile

and the potential distribution revealed that the magnitude of voltage at one location will determine the amount of strength increase at that location after electro-osmotic treatment. This result is consistent with the electro-osmotic test that the induced negative pore water pressure at any point is directly proportional to the effective voltage of that point and consequently, the shear strength will increase in the same manner.

The fact that cracks were found on test W-RM (which was treated with 5 volts without reversal for 3 days) and not on tests W-UD1 AND W-UD2 (which were treated with 2 volts and 4 volts with electrodes reversal) suggests that the formation of the cracks may be due to long treatment time at high applied voltage. Therefore, the procedures of the gradual increase in the applied voltage and regular reversal of electrode polarity during treatment may avoid the formation of crack in the tests W-UD1 and W-UD2.

The flowing of water out of cathode during treatment gives an indication that the same design of the electrode may perform well in the field. In the field, an increase in pore water pressure at the region may force the expelled water into the perforated pipes and out to the surface. Water and gas were shown to seep out at cathode-soil interface on the solid electrode in the field work by Bjerrum et al (1967). It was reported that the increase in positive pore water pressure around the cathode region was quite significant during the treatment in which as much as 20 kPa above normal was measured. This increase in positive pore water pressure may cause the temporary reduction in

strength during treatment. This type of electrode design is very similar to the closed cathode system in which high positive pore water pressure will be resulted (Johnston and Butterfield 1977). The holes drilled along the tubing will help to release the pore pressure and increase the rate of water discharge. Furthermore, gas produced due to chemical reaction can be escaped through these holes and as a result, a better contact between soil and electrode can be maintained.

Table 7.1 Summary of Hydraulic Permeability for Wallaceburg and Gloucester Clay

Soil Type	Direction	Hydraulic Permeability 10^{-8} cm/s
Wallaceburg!	vertical	4
Wallaceburg!	horizontal	17*
Gloucester+	vertical	2.16

Notes:

! from Lo and Becker (1979, 1980)

* average value from field test result (Lo and Becker 1980)

+ pre-treatment test result

Table 7.2 Comparison of Experimental and Predicted Maximum Negative Pore Water Pressure at Equilibrium

Test No.	Voltage V	Pore Water Pressure (kPa)	
		Experimental	Predicted
GV-4A	3.0 N,R	-28	-27.3
GV-4B	1.5 N,R	-15	-13.6
	2.4 N,R	-36	-21.8
	4.0 N,R	-53	-36.3
GV-8	3.0 N,R	-27	-27.3
	6.0 N,R	-75	-54.5
WV-4	2.5 N,R	-60	-92.0
	4.0 N	-136	-147.2
WV-8A	3.0 N,R	-102	-110.4
	4.5 N,R	-178	-165.5
WH-3	2.0 N,R	-52	-18.5
	4.0 N,R	-105	-36.9
WH-6A	4.0 N	-100	-36.9
WH-6B	2.0 N,R	-41	-18.5
	4.0 N,R	-135	-36.9
WH-9	2.0 N,R	-46	-18.5
	4.0 N,R	-104	-36.9
	6.0 N,R	-180	-55.4

Notes: Cracks observed in Test WV-8B and the result is not compared here
N,R = normal and reversed polarity respectively

Table 7.3 Effect of Sample Length to the Generation of Negative Pore Water Pressure for Gloucester Clay Samples

Test No.	Sample Length mm	Voltage V	Maximum Pore Pressure Measured kPa
GV-4A	101.6	3	-28
GV-8	203.2	3	-27

Note: The applied voltage of GV-4B is different from GV-4A and GV-8 and the result is not compared here

Table 7.4 Effect of Sample Length to the Generation of Negative Pore Water Pressure for Horizontally Trimmed Wallaceburg Clay

Test No.	Sample Length	Maximum Pore Pressure Measured (kPa)	
	mm	Applied Voltage=2 V	Applied Voltage=4 V
WH-3	76.2	-52	-105
WH-6A	152.4	---	-100
WH-6B	152.4	-41	-135
WH-9	228.6	-46	-104

Table 7.5 Summary of Unconfined Compression Test Results of Gloucester Clay Samples Before and After Treatment

Test No.	Peak Shear Strength kPa	Failure Strain %	Brittleness Index, I_B	Undrained Modulus kPa
Pre-Treatment	17.2	1.6	0.39	1720
GV-4A	26.5	2.0	0.25	5300
GV-4B	35.4	1.9	0.22	8850
GV-8	43.7	1.4	0.20	14560

Note: undrained modulus obtained at half peak strength

Table 7.6 Comparison of Sensitivity of Gloucester Clay Samples Before and After Treatment

Test No.	Sensitivity	Percentage Decrease %
Pre-Treatment	100	--
GV-4A	76	24
GV-4B	51	49
GV-8	38	62

Table 7.7 Comparison of Pre-Consolidation Pressure of Gloucester Clay Sample Before and After Treatment

Test No.	Pre-Consolidation Pressure kPa	Percentage Increase %
Pre-Treatment	49	--
GV-4A	74	51.0
GV-4B	83	69.4
GV-8	92	87.8

Table 7.8 Comparison of Coefficients of Consolidation*

Test No.	Voltage	Coefficient of Consolidation (m^2/year)	
	V	Conventional+	Electro-Osmosis
WV-4	2.5 N,R	5	2.8
	4.0 N		1.3
WV-8A	3.0 N,R	5	3.3
	4.5 N,R		7.9
WH-3	2.0 N,R	N/A	3.6
	4.0 N,R		3.1
WH-6A	4.0 N	N/A	2.4
WH-6B	2.0 N,R	N/A	4.4
	4.0 N,R		3.8
WH-9	2.0 N,R	N/A	4.1
	4.0 N,R		5.0
	6.0 N,R		5.3
GV-4A	3.0 N,R	0.45	8.9
GV-4B	1.5 N,R	0.45	3.6
	2.4 N,R		3.9
	4.0 N,R		3.8
GV-8	3.0 N,R	0.45	18.1
	6.0 N,R		6.5

* Cracks observed ¬ Tests WV-8B and the result is not compared here

+ Average values from Lo and Becker (1979) for Wallaceburg clay and pre-treatment test result for Gloucester Clay

Table 7.9 Physical and Chemical Properties of Wallaceburg and Gloucester Clays After Treatment

	Gloucester Clay		Wallaceburg Clay	
	Initial	After Treatment	Initial	After Treatment
Liquid Limit (%)	48.4	52.8	43.7	44.6
Plastic Limit (%)	29.5	31.2	20.8	20.9
Soil pH Value	8.2	10.3	7.2	7.3
pH of expelled water	8.2	11.5	---	---
Carbonate Content (%)	2.8	3.6	5.3	7.8
Soil Salinity (g/l)	1.7	2.5	2.5	7.2

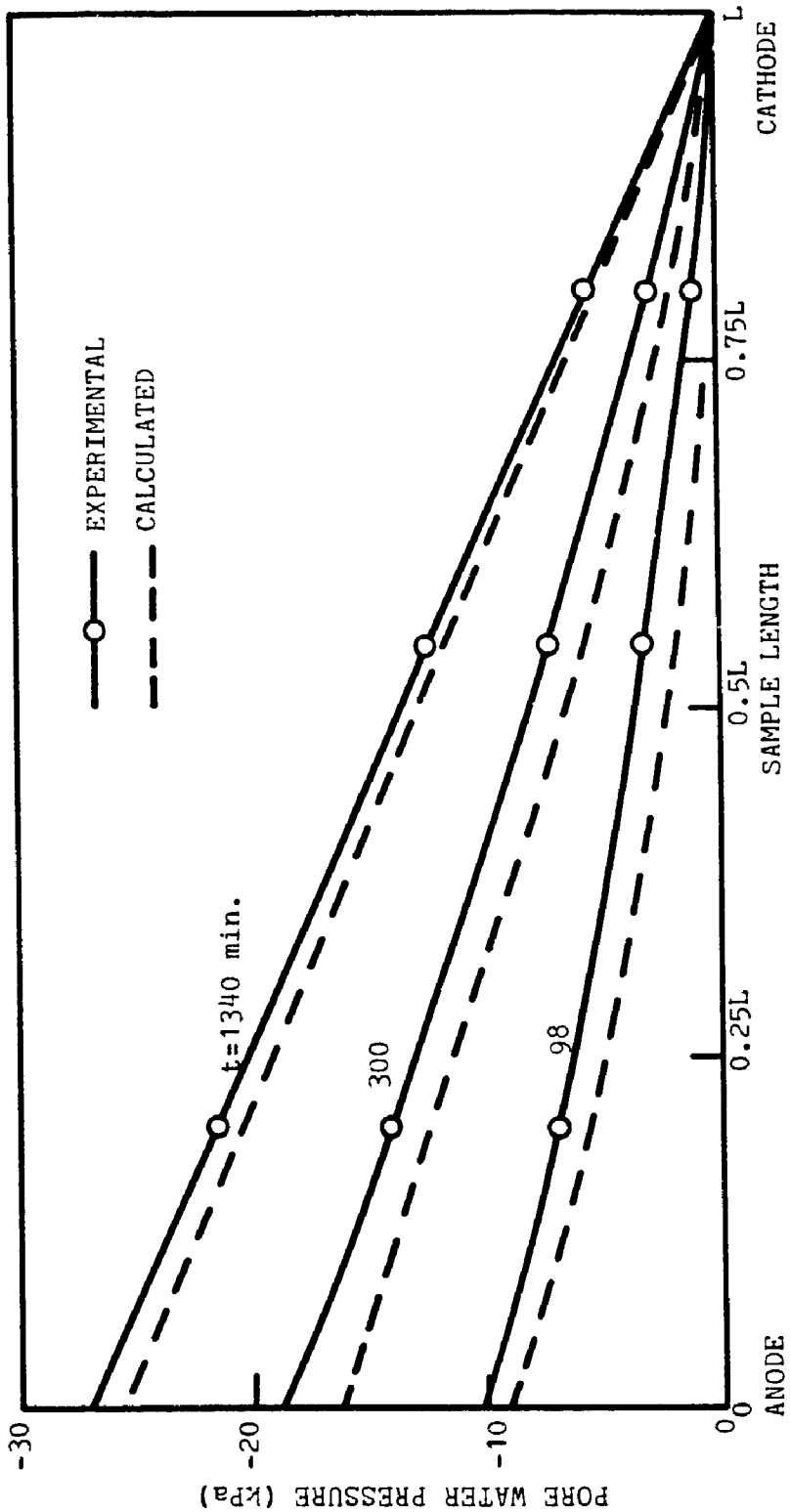

FIGURE 7.1 COMPARISON OF EXPERIMENTAL AND CALCULATED NEGATIVE PORE WATER PRESSURE DISTRIBTUIONS FOR SAMPLE GV-8

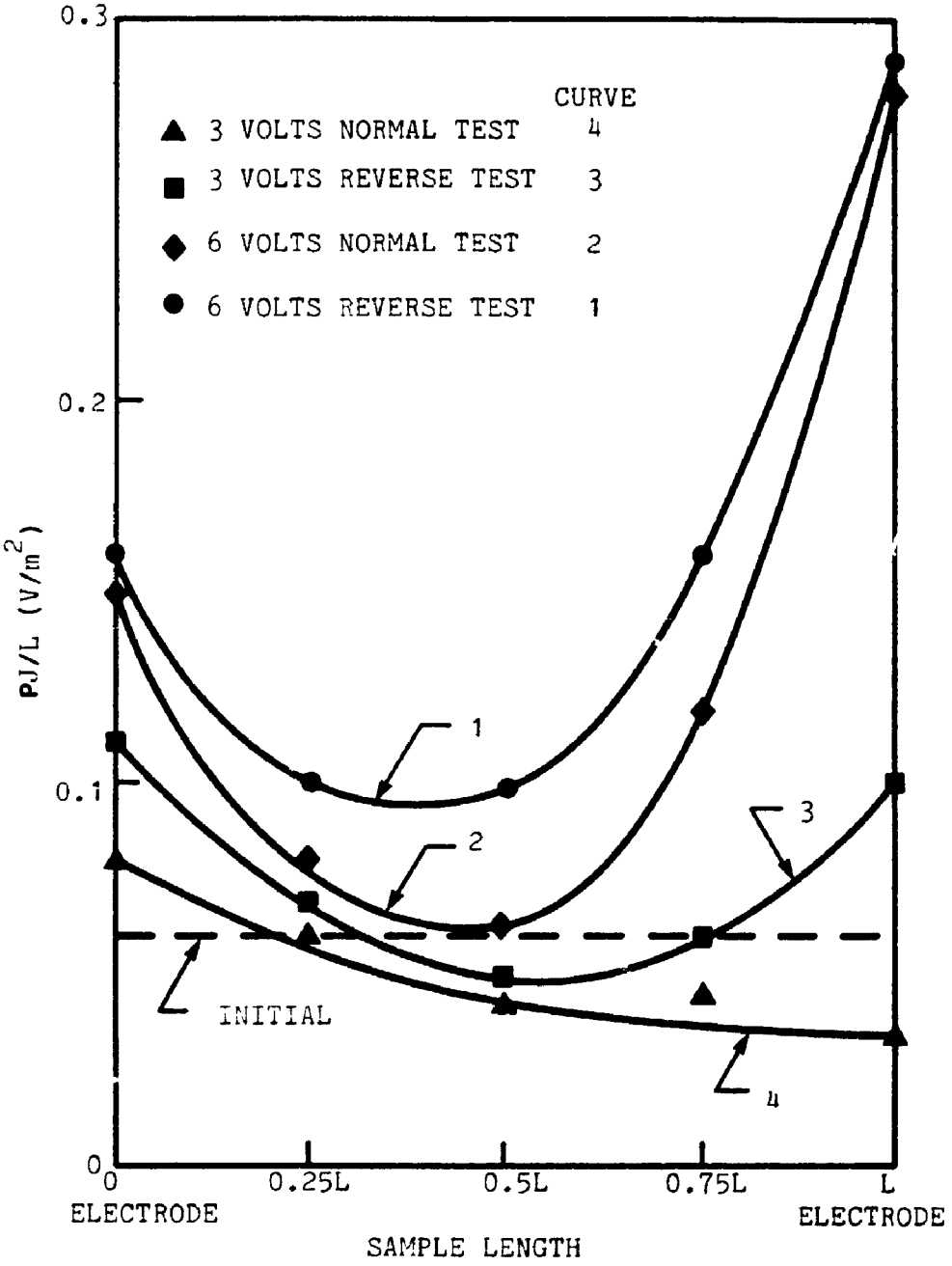

FIGURE 7.2a PLOT OF PJ/L AGAINST SAMPLE LENGTH FOR SAMPLE GV-8

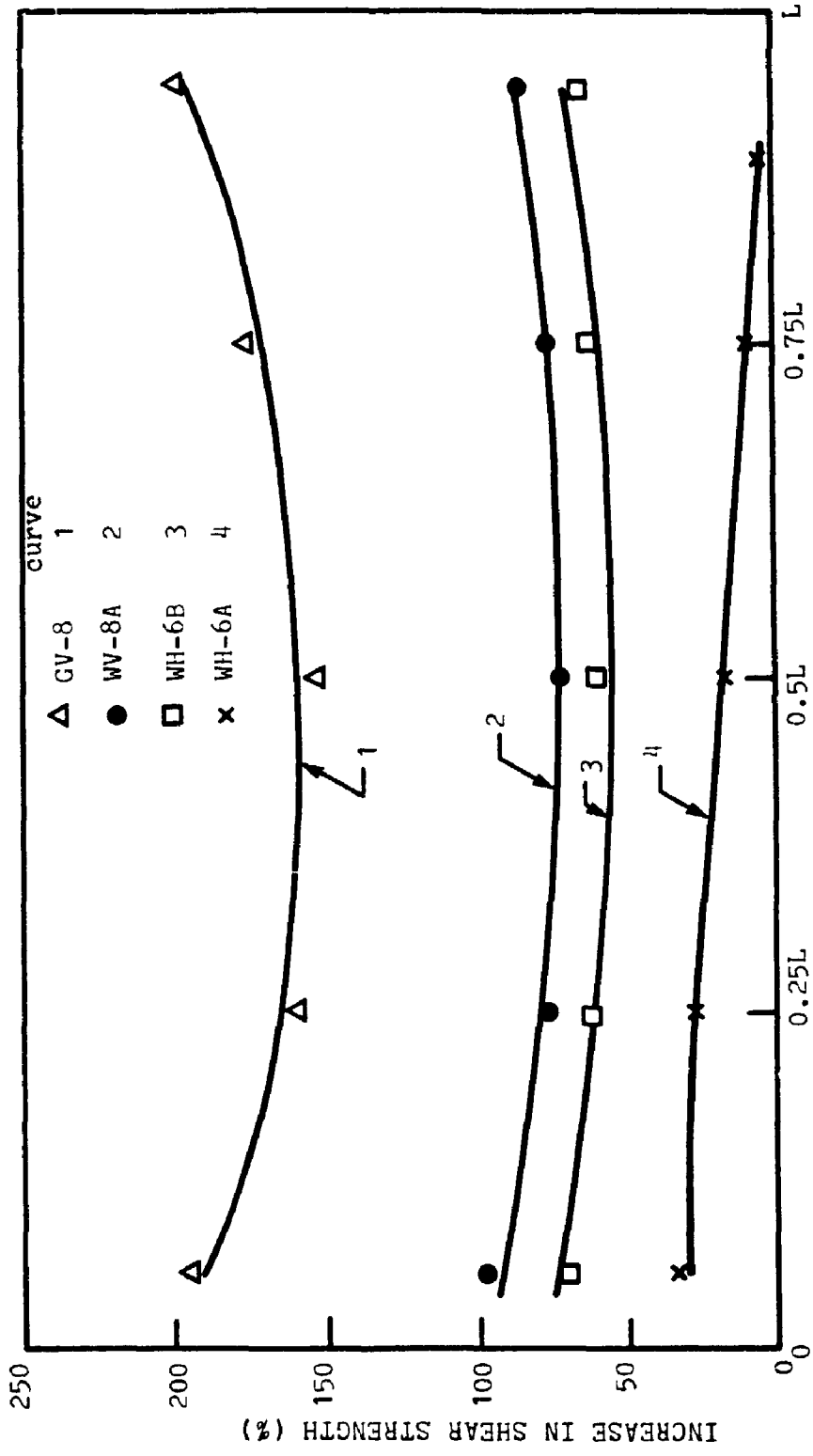

FIGURE 7.2b DISTRIBUTION OF SHEAR STRENGTH INCREASE OF VARIOUS SAMPLES AFTER TREATMENT

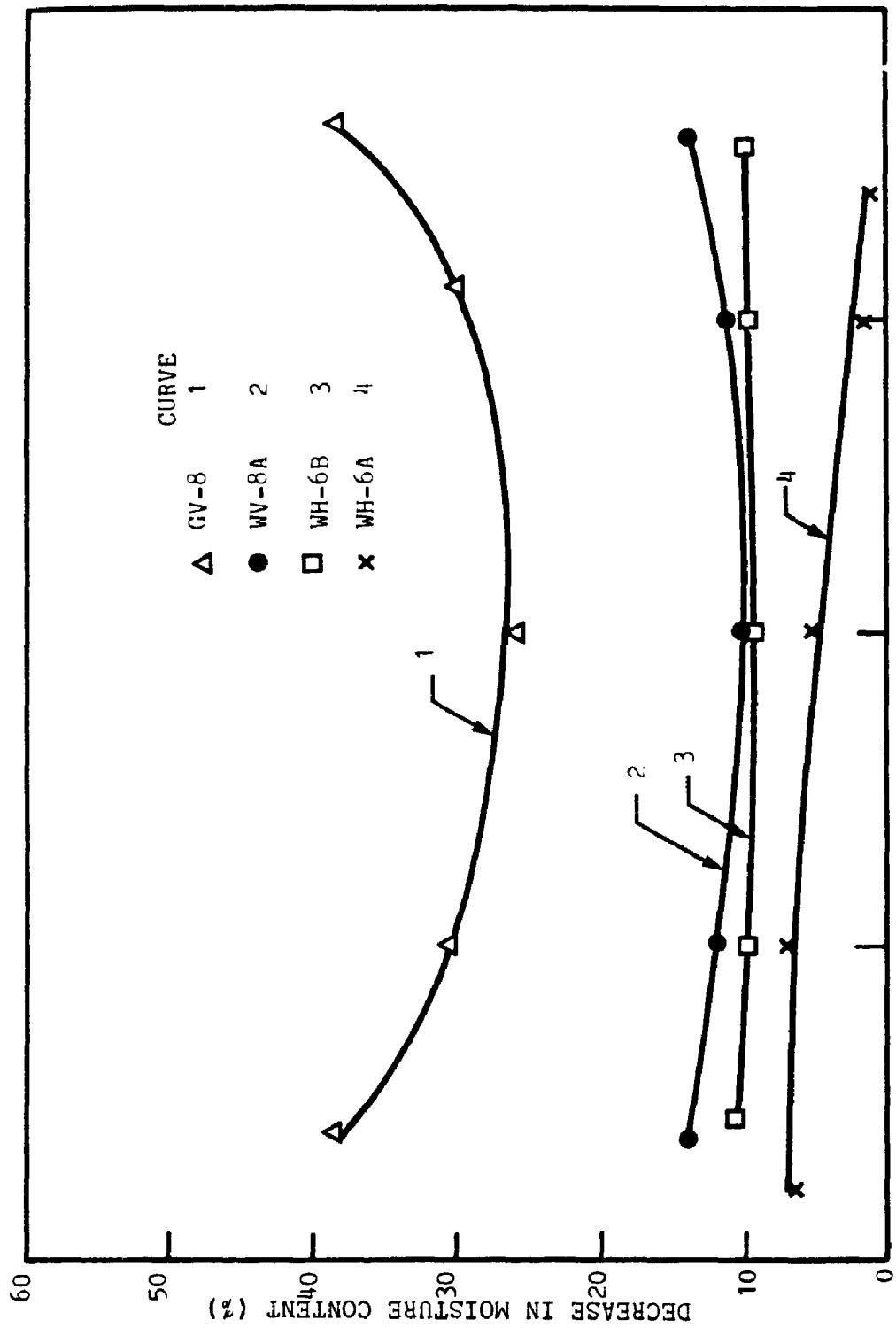

FIGURE 7.3 DISTRIBUTION OF MOISTURE CONTENT DECREASE OF VARIOUS SAMPLES AFTER TREATMENT

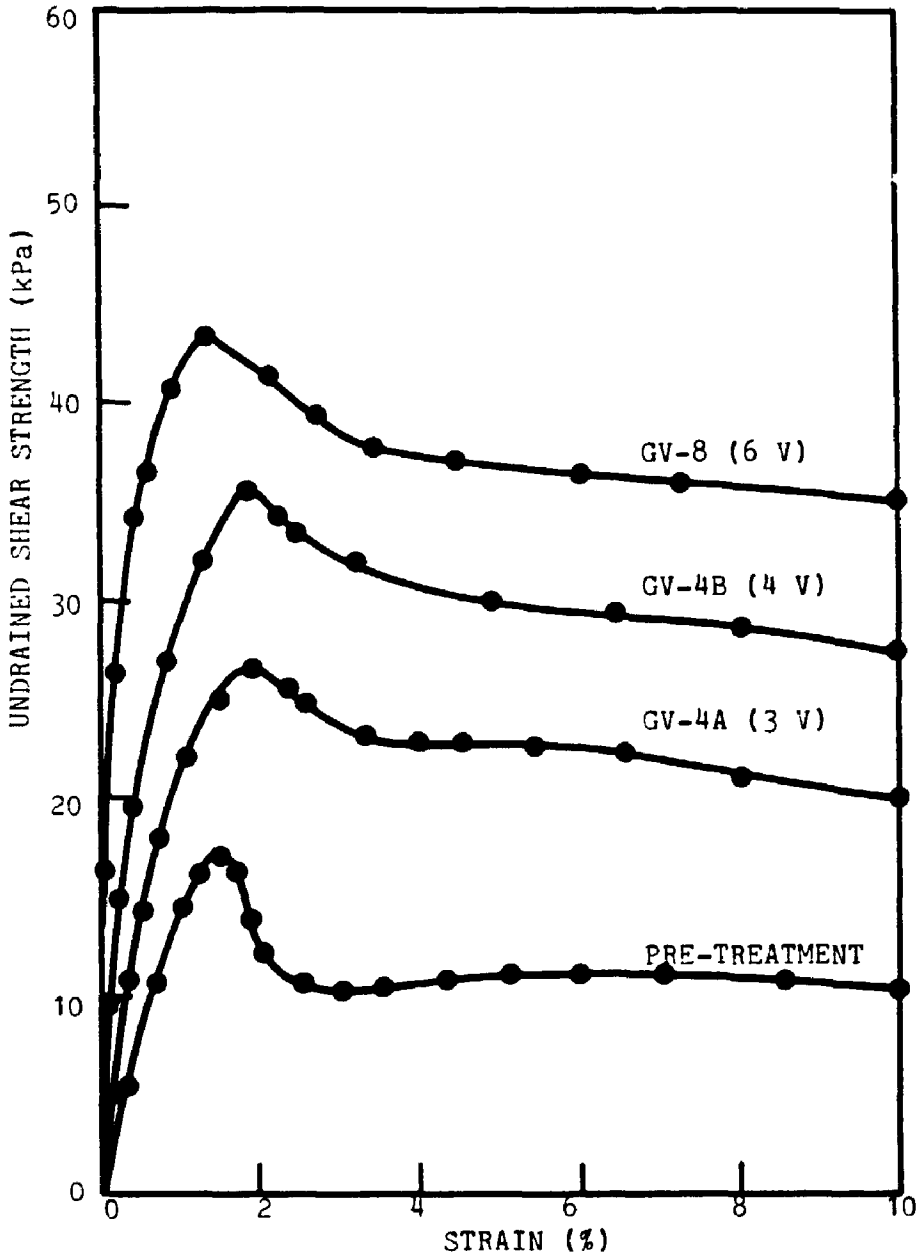

FIGURE 7.4 UNCONFINED COMPRESSION TEST OF GLOUCESTER CLAY SAMPLES BEFORE AND AFTER TREATMENT

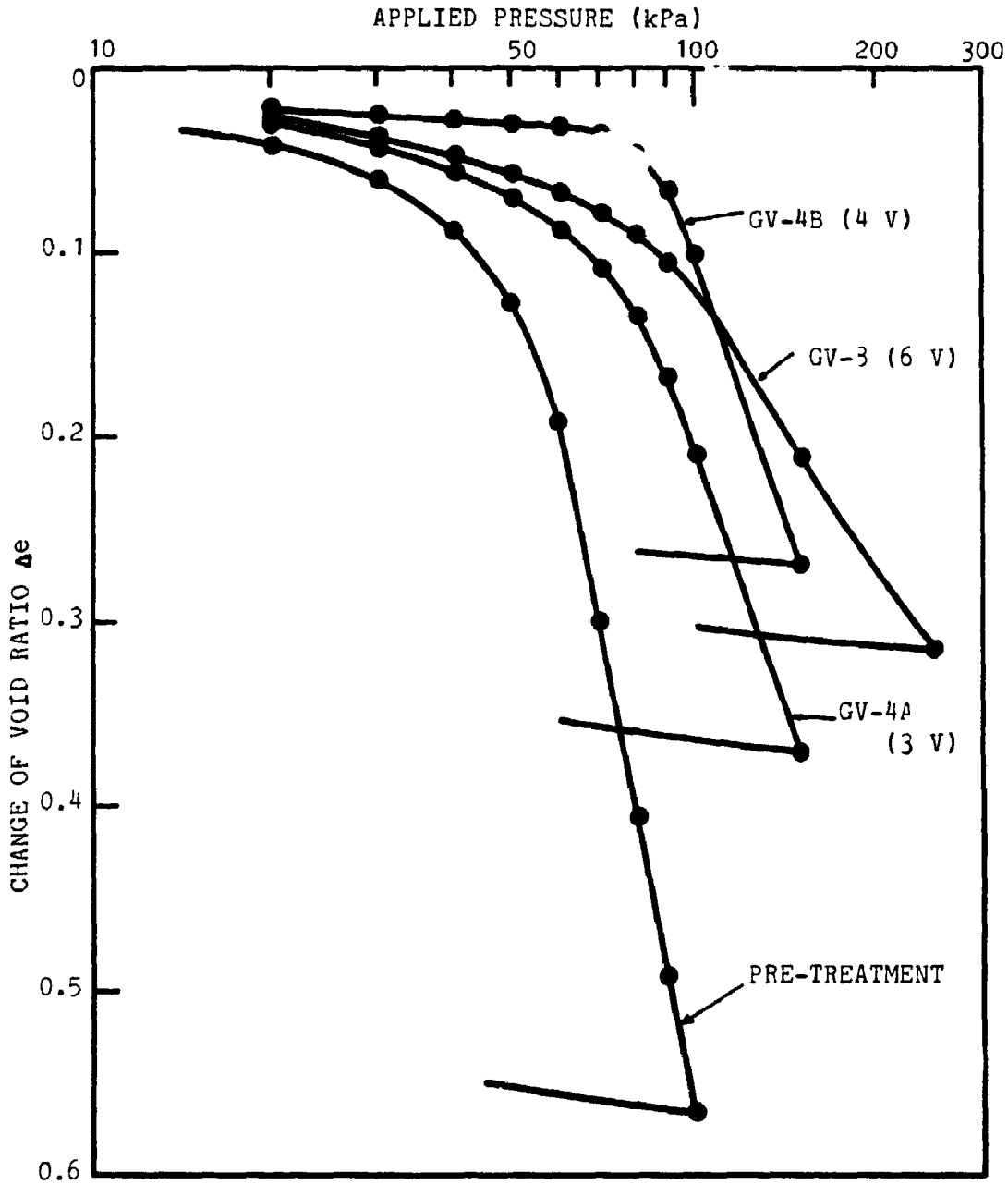

FIGURE 7.5 CONSOLIDATION CURVES FOR GLOUCESTER CLAY SAMPLES BEFORE AND AFTER TREATMENT

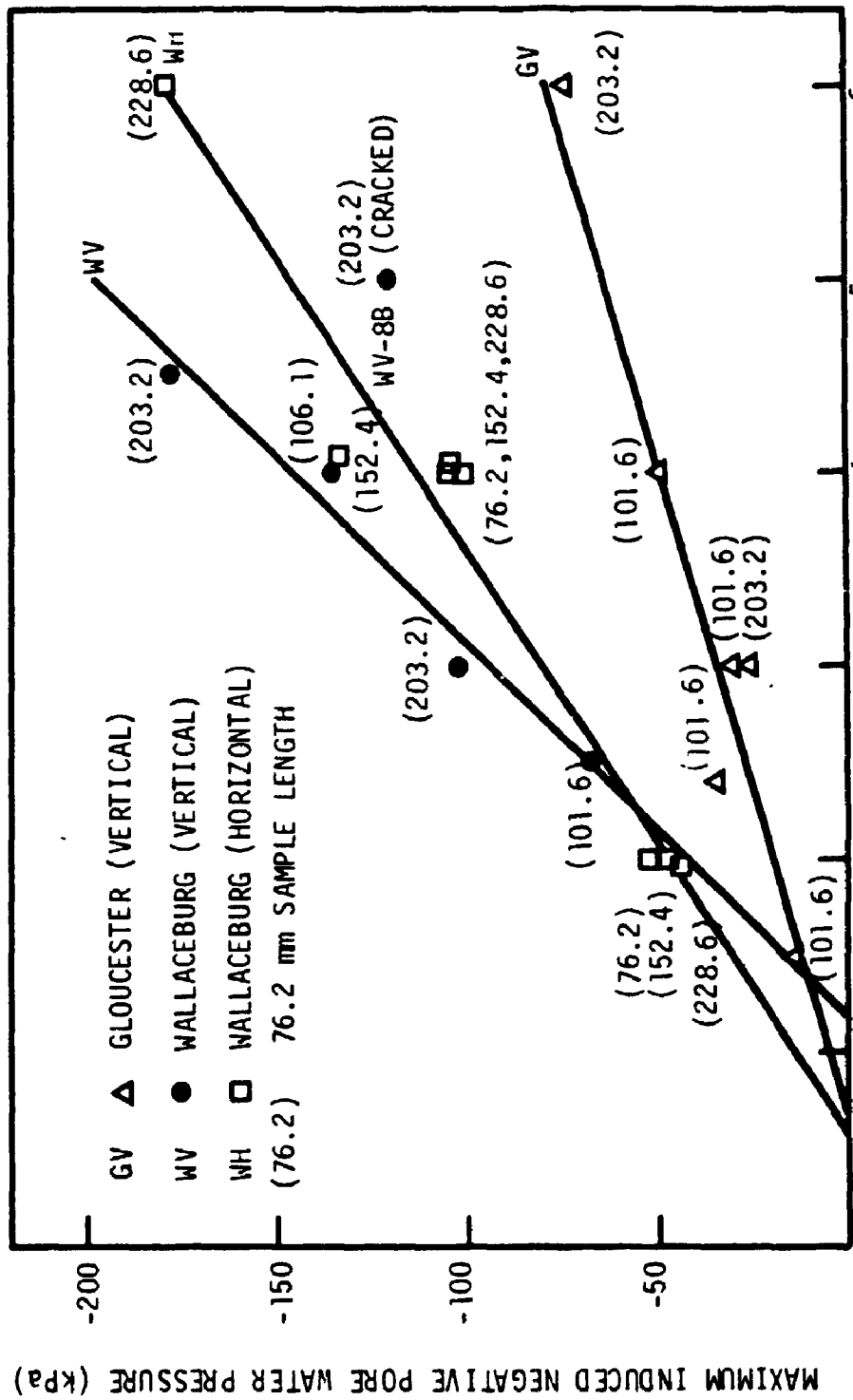

FIGURE 7.6 RELATION BETWEEN THE MAXIMUM INDUCED NEGATIVE PORE WATER PRESSURE WITH APPLIED VOLTAGE FOR DIFFERENT SOIL TYPES

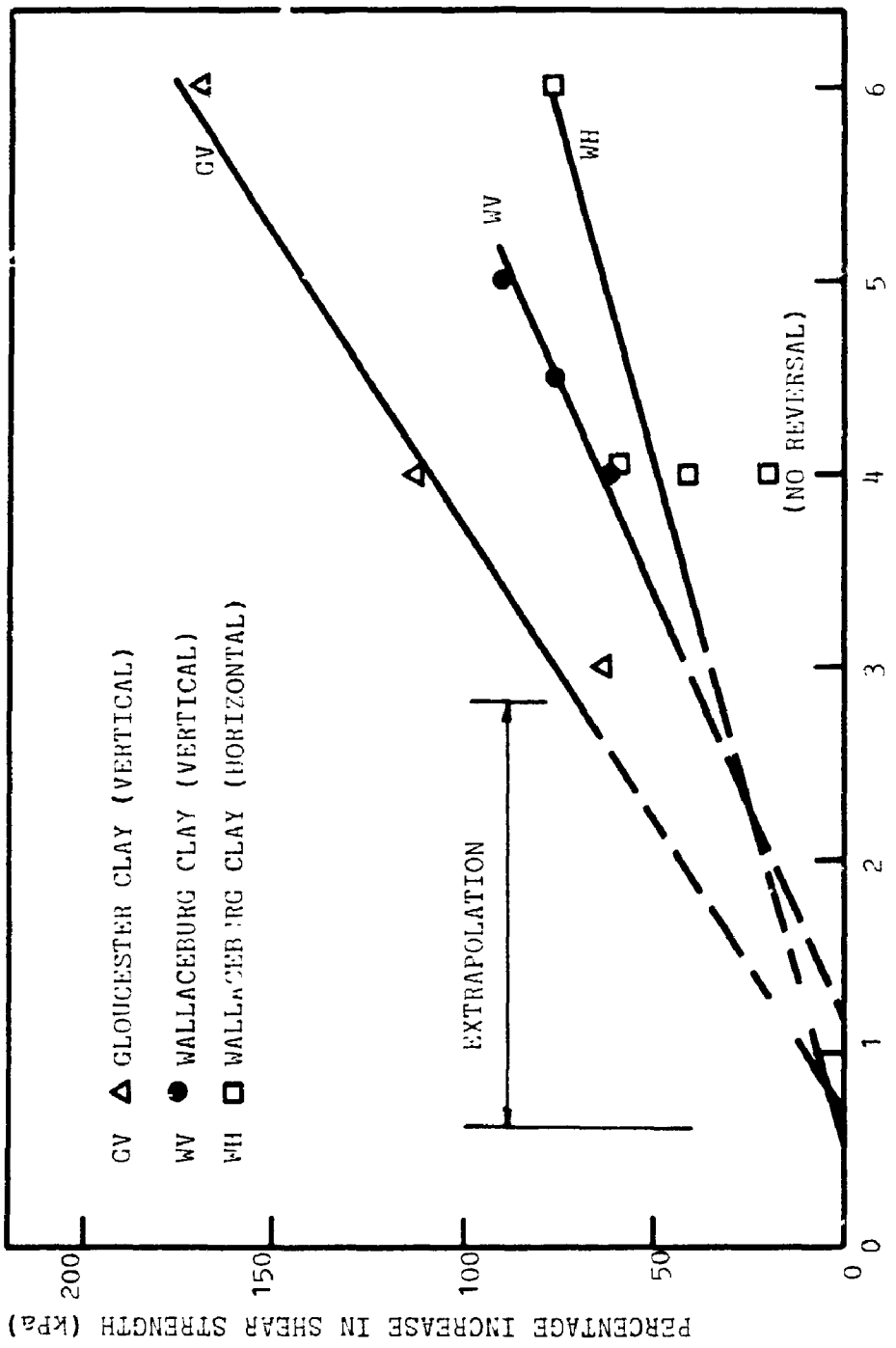

FIGURE 7.7 RELATION BETWEEN THE INCREASE IN SHEAR STRENGTH WITH APPLIED VOLTAGE FOR DIFFERENT TYPES OF SOIL

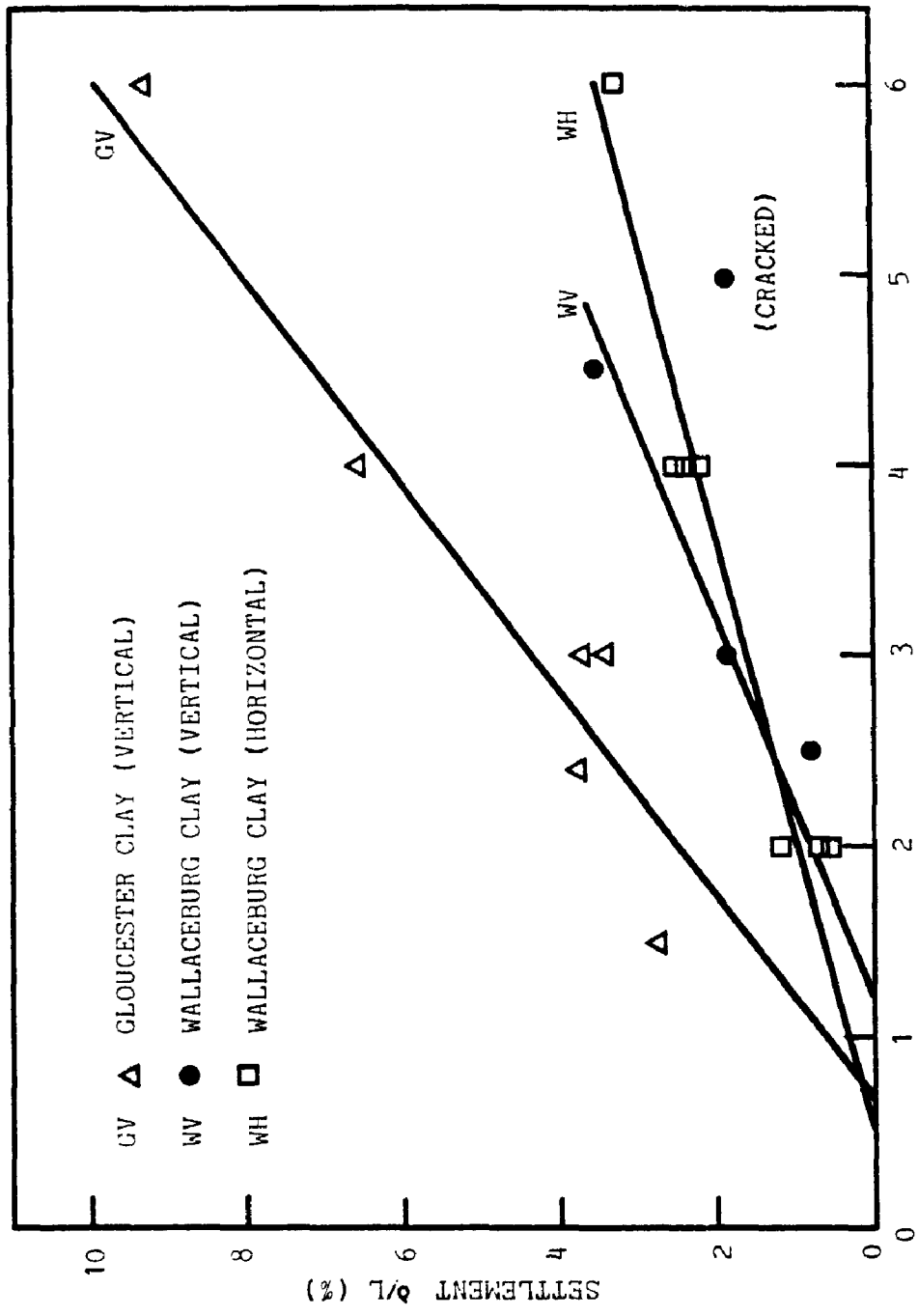

FIGURE 7.8 RELATION BETWEEN SETTLEMENT WITH APPLIED VOLTAGE FOR DIFFERENT TYPES OF SOIL

FIGURE 7.9 CRACKS IN TEST WV-8B

CHAPTER 8

CONCLUSIONS ON ELECTRO-OSMOSIS LABORATORY INVESTIGATION

An experimental investigation on the electro-osmotic strengthening of vertically trimmed Gloucester clay, vertically and horizontal trimmed Wallaceburg clay was performed by applying relatively small potentials (up to 6 volts) to different sample lengths. Laboratory tests were carried out on the sample before and after treatment to study the changes of strength and deformation properties and the effectiveness of the electro-osmotic process. Based on the results of this study, the following conclusions may be drawn.

(a) The electro-osmotic cell developed, with the specially designed electrodes, is efficient in that it can prevent the gas accumulation near the electrodes and improve the electrode-soil contact. There is no abrupt loss of electric potential at the electrode-soil interface. As a result, an approximately linear voltage distribution along the sample length is obtained and the current flow is fairly steady at the later stage of the treatment. The applied electric potential can be considered as the effective voltage for the treatment.

(b) The induced negative pore water pressure at equilibrium along the sample length is also a linear distribution with maximum negative pressure induced at anode and decreased to zero at cathode. This result indicates that the induced negative pore water pressure is directly related to the

effective voltage at that location. This observation is consistent with the one-dimensional electro-osmotic consolidation theory as described by equations(1) and (2) developed by Esrig (1968a).

(c) Substantial increase in undrained shear strength and decrease in moisture content were obtained for treatment of less than 2000 minutes (1.5 days). The increase in shear strength is as high as 172 % with moisture content reduced by 30 % for Gloucester clay at a potential difference of 6 volts. The technique of electrode reversal enables more uniform treatment of the soil and this technique can be applied in the field to minimize nonuniformity of change in soil properties.

(d) With regard to the stress-strain behaviour of the soft sensitive clay, the electro-osmosis increases the undrained modulus and reduces the brittleness index and sensitivity. This shows that the electrical treatment not only improves the soil properties but also changes the soil behaviour.

(e) A comparison of the consolidation curves of the Gloucester clay before and after treatment revealed that the treated clay is less compressible and the preconsolidation pressure increased from 49 kPa to the maximum of 92 kPa, an increase of 88 %. The clay is virtually "overconsolidated" by the electro-osmosis process, indicating that the effect of treatment is permanent.

(f) The maximum induced negative pore water pressure is in linear relation with the applied voltage.

(g) Both clays showed increase in carbonate content and salinity after treatment. This indicates a better cementation bonding of the soil particles and consequently increases the shear strength and reduces the sensitivity of the clays.

It follows from the above conclusions that the electro-osmotic treatment of soft sensitive clays is efficient in the laboratory and its effects to the strength and deformation parameters are beneficial in all aspects by conventional geotechnical measures. It was considered in the past that this process required high electrical power consumption and caused non-uniform strength increase. From the results of this investigation, it is expected that, with specially designed field electrodes and applying judiciously the technique of electrode reversal, the treatment will receive wider application in engineering practice.

PART II

LABORATORY INVESTIGATION OF DIELECTROPHORESIS

CHAPTER 9

INTRODUCTION

Electrostatics is a class of phenomenon recognized as the interaction of electrical charges which are either stationary or moving. This interaction is solely due to the charges themselves and their position but is not due to their motion.

The motion of matter in nonuniform electric fields was first noted by Gilbert (1600) that a water droplet changed in shape as electrified amber was brought near. Wincker (1748) and Priestley (1769) observed the attractive forces on organic liquids. Recently, Pohl (1951) advanced the theory of dielectrophoresis related to the motion of a neutral particle in a nonuniform field. Since then, much experimental work was performed to find its possible applications. The applications include the pumping of liquids and powders, classification and separation of minerals, cooling of surfaces, imaging in Xerography, removal of particle from suspension in liquids or gases, classification of microorganisms, separation of living cells from dead cells, separation of normal from abnormal cells, treatment of fresh water for bacterial and algal removal, precipitation of smoke particles of gas exhausted from diesel

engine and so on.

However, most of the applications of dielectrophoresis have only been involved in physical, chemical and biological areas. Nothing has been done for the application in geotechnical engineering. In view of the situation, a preliminary laboratory test was carried out to explore the prospect of this process in engineering practice. It was found that after applying a nonuniform field to a soil mass for 28 days, the moisture content of the treated soil decreased and the shear strength increased drastically. Following these tests, a systematic investigation was then established to study the mechanism of this process and its potential applications in soil strengthening.

The investigation involved a review of the theory of dielectrophoresis and a series of laboratory experiments on two different types of soils (Wallaceburg and Gloucester clays). The objectives of the study are:

(a) to explore the technology of dielectrophoresis for the possible applications in soil strengthening, especially in soft sensitive clay,

(b) to study the mechanism of the process, and

(c) to study the correlation of parameters such as settlement, moisture content, shear strength, applied electric potential and electrode depth.

CHAPTER 10

DIELECTROPHORESIS THEORY AND ITS APPLICATION

10.1 General Concepts

In order to investigate dielectrophoresis, the basic laws of electrostatics and the field concept of electrical phenomena have to be studied first. Since most civil and geotechnical engineers are not familiar with electrostatics, the following general concepts are discussed to enable a better understanding of the theory of dielectrophoresis.

10.1.1 The Electric Field

If a quantity is associated with every point of a region and if the time and space variation of this quantity are subject to definite laws expressed as a function of the space coordinates and time, then it can be considered that a field is associated with that region. In a similar manner, a force field known as the electric field is associated with bodies that are charged. The electric field intensity E, is defined as the force F per unit charge q experienced by a small test charge placed in an electric field. It can be written as,

$$E = \frac{F}{q} \qquad (10.1)$$

where both **E** and **F** are vector quantities. The bold typed letters are used here for vector notations.

Experiments conducted by Coulomb showed that the following holds for two charged bodies that are very small in size compared to their separation d, so that they can be considered as point charges:

(1) the magnitude of the force is proportional to the product of the magnitudes of the charges,

(2) the magnitude of the force is inversely proportional to the square of the distance between the charges,

(3) the magnitude of the force depends on the medium,

(4) the direction of the force is along the line joining the charges,

(5) like charges repel; unlike charges attract,

Therefore, for two point charges q_1 and q_2, the force F experienced by the charges is given as (Coulomb 1785),

$$F = \frac{q_1 q_2}{4\pi\epsilon_o d^2} \qquad (10.2)$$

where,

ϵ_o = permittivity of free space = 8.854×10^{12}

d = distance between two charges

Equation (10.2) is known as the Coulomb's Law.

10.1.2 Dielectrics

In electricity, conductors are characterized by abundance of free electrons that give rise to conduction current under the influence of an applied electric field. In dielectric materials, the bound electrons are predominant. Under the application of an external electric field, the bound electrons of an atom are displaced such that the centroid of the electron cloud is separated from the centroid of the nucleus. The atom is then said to be polarized, thereby creating an electric dipole, as shown in Figure 10.1a. This kind of polarization is called electronic polarization. The schematic representation of an electric dipole is shown in Figure 10.1b. The strength of the dipole is defined by the electric dipole moment **p** given as,

$$\mathbf{p} = q\mathbf{d} \tag{10.3}$$

where **d** is the vector displacement between the centroid of the positive and negative charges, each of magnitude q coulombs.

In certain dielectric materials, polarization may exist in the molecular structure of the material even under the application of no external electric field. The polarization of individual atoms and molecules, however, is randomly oriented, and hence the net polarization on a macroscopic scale is zero. The application of an external field results in torques acting on the microscopic dipoles, as shown in Figure 10.1c, to convert the initially random polarization into a partially coherent one along the field, on a macroscopic scale. This kind of polarization is known as orientational polarization. A third kind of

polarization known as ionic polarization results from the separation of positive and negative ions in molecules formed by the transfer of electrons from one atom to another in the molecule. When a dielectric material is placed in an electric field, the induced dipoles produce a secondary electric field and this effect will be discussed later in this chapter.

It is also defined as,

$$\epsilon = \epsilon_o K \qquad (10.4)$$

where the quantity K is known as the relative permittivity or dielectric constant of the dielectric, and ϵ is the permittivity of the dielectric. The permittivity ϵ takes into account that the effects of polarization and the dielectric constant K is an experimentally measurable parameter and its values for several dielectric materials are listed in Table 10.1.

10.1.3 Description of Dielectrophoresis

Dielectrophoresis is defined as the motion of neutral particle as induced by its polarization in a nonuniform electric field (Pohl 1951). This is analogous to the effect of a magnet attracting a piece of soft iron. The movement of the iron towards one of the magnetic poles is a response to the nonuniform magnetic field. If the magnetic field is uniform, no net force will be resulted.

In a uniform electric field, a charged particle is drawn along the field lines towards the electrode of opposite charge while a neutral particle, even though it is polarized, remains stationary, as shown in Figure 10.2a. The polarization

of the neutral particle may result in a torque if the particle is elongated or anisotropic and the resultant dipole tends to align the particle to achieve minimum energy in the field.

When a nonuniform field is applied to the same particles as shown in Figure 10.2b, the charged particle behaves as before and it moves toward the electrode of opposite charge. A neutral particle is polarized by the nonuniform field such that a negative charge appears on the side nearest the positive electrode and a positive charge on the other side. Since the body is overall neutral, the two effective charges are equal. But the fields acting on the two sides are unequal and this results in a net translational force. This force generally results in the neutral body being impelled into the region of stronger field. As shown in Figure 10.2b, the field on the negatively charged side is stronger than the other side and hence a net force pulling the particle towards the positive electrode is produced.

An important observation is that the force on the neutral body by the nonuniform field is in the same direction no matter which electrode is positive or negative. This is due to the fact that the polarization of the particle reverses in the same frequency as the field, as shown in Figures 10.3a and 10.3b. In Figure 10.3a, the neutral body is polarized and is attracted towards the positive electrode where the field is stronger. When the polarity of the electrodes is reversed, the polarization of the particle reverses in the same time in response to the change of direction of electric field. As a result, the particle is attracted

towards the new negative electrode where the field is stronger. In other words, the neutral particle only responds to the intensity of the field but not to the polarity of electrodes. This implies that in dielectrophoresis, the applied electric field can be generated by an alternating potential. If the particle is charged, the alternating electric field tends to make it vibrate about its original position with the same frequency as the switching of electrode polarity, and no net translational movement is resulted.

10.2 The Dipole Moment

The effect of polarized atom in an electric field can be represented by two equal and opposite charges (+q and -q) separated by a distance d, of the order of atomic dimensions (Figure 10.4). This type of distribution of charges is referred to as a point dipole, because of the very tiny atomic size. As shown in Figure 10.4, if the line connecting the charges +q and -q is along the z-axis and the mid-point of the line is coincident with the origin, then the moment of this pair of charges with respect to an arbitrary point **r** is,

$$\mathbf{p} = \mathbf{p}(\mathbf{r}) = \sum_{i=1}^{2} q_i(\mathbf{r}_i - \mathbf{r})$$

$$= \mathbf{a}_z qd \qquad (10.5)$$

where $\mathbf{r}$, $\mathbf{r}_1$, $\mathbf{r}_2$ are defined in Figure 10.4, and $\mathbf{a}_z$ is the unit vector in the z-direction and $\mathbf{p}$ is the dipole vector.

Equation (10.5) shows that the dipole moment is independent of $\mathbf{r}$. It also

suggests that the dipole moment of an atomic dipole is a macroscopically infinitesimal vector quantity, since q is finite and d is macroscopically infinitesimal. Referring to Figure 10.4, the potential V(r) of the point dipole is,

$$V(r) = V^{+}(r) + V^{-}(r)$$

$$= \frac{q}{4\pi\epsilon_o}\left(\frac{1}{r_1} - \frac{1}{r_2}\right) \qquad (10.6)$$

Since,

$$\frac{1}{r_1} - \frac{1}{r_2} = \frac{r_2 - r_1}{r_1 r_2}$$

As d is very small, from Figure 10.4,

$$r_2 - r_1 \approx d\cos\theta$$

and, $r_1 r_2 \approx (r + \frac{d}{2}\cos\theta)(r - \frac{d}{2}\cos\theta) \approx r^2$

Therefore,

$$\frac{1}{r_1} - \frac{1}{r_2} \approx \frac{d\cos\theta}{r^2}$$

and equation (10.6) becomes,

$$V(r) \approx \frac{qd}{4\pi\epsilon_o}\frac{\cos\theta}{r^2} \qquad (10.7)$$

From equation (10.5) and Figure 10.4,

$$\mathbf{p}\cdot\mathbf{r} = \mathbf{a}_z qd\cdot\mathbf{r} = rqd\cos\theta$$

Equation (10.7) becomes,

$$V(r) = \frac{1}{4\pi\epsilon_o} \frac{\mathbf{p}\cdot\mathbf{r}}{r^3}$$

or,

$$V(r) = -\frac{1}{4\pi\epsilon_o} \mathbf{p}\cdot\nabla\frac{1}{r} \qquad (10.8)$$

From the potential function equation for the static electric field (Hippel 1954), the corresponding electric field is,

$$E(r) = -\nabla V(r)$$

Therefore,

$$E(r) = \frac{1}{4\pi\epsilon_o} \nabla[\mathbf{p}\cdot\nabla\frac{1}{r}] \qquad (10.9)$$

Equations (10.8) and (10.9) are plotted in Figure 10.5 which shows the trace of electric field E and equipotential V. It is observed that the electric field lines are similar to the lines of magnetic field of a bar magnet.

10.3 The Dielectrophoretic Force

For an uncharged dielectric sphere of radius R placed in a homogeneous external field E_e pointing in the positive z-direction, as shown in Figure 10.6, the field distribution produced by the polarization of the sphere is obviously symmetrical around the z-axis. Let V_e and V_i be the potentials outside and inside of the sphere respectively and consider the following boundary conditions:

(1) $V_e = V_i$ at the surface of the sphere,

(2) the normal component of electric flux density is continuous as no surface charge exists,

(3) at a very great distance from the sphere, the external field will remain undisturbed, and

(4) in the centre of the sphere, the potential stay finite.

The solution to the Laplace Equation, which governs the behaviour of the potential in a charge-free region characterized by uniform permittivity, as given by Hippel (1954) is,

$$V_e = \left(\frac{K_1 - K_2}{K_2+2K_1}\frac{R^3}{r^3} - 1\right)E_e z$$

$$V_1 = -\frac{3K_1}{K_2+2K_1}E_e z$$

where K_1 and K_2 are the dielectric constants of the sphere and the medium. Consequently, the field strength, in the interior of the sphere is (in terms of vector quantity),

$$E_{in} = -\nabla V_1 = \frac{3K_1}{K_2+2K_1}E_e \qquad (10.10)$$

Equation (10.10) indicates that the field strength inside the sphere is constant and parallel to the original external field.

From equation (10.1), the force acting on a positive charge at a distance $\mathbf{r}^+$ is:

$$\mathbf{F}^+ = q\mathbf{E}_e(\mathbf{r}^+)$$

and the force acting on negative charge at $\mathbf{r}^-$ is,

$$\mathbf{F}^- = q\mathbf{E}_e(\mathbf{r}^-)$$

The resultant force is therefore,

$$\mathbf{F}_e = \mathbf{F}^+ + \mathbf{F}^-$$

$$= q(\mathbf{E}_e(\mathbf{r}^+) - \mathbf{E}_e(\mathbf{r}^-)) \qquad (10.11)$$

As defined by Taylor series expansion and neglecting the higher order terms, the field for the dipole moment taken in the positive z-direction is,

$$\mathbf{E}_e(\mathbf{r}^+) = \mathbf{E}_e(\mathbf{r}^-) + d\frac{\partial \mathbf{E}_e}{\partial z} \qquad (10.12)$$

Combining equations (10.5), (10.11) and (10.12),

$$\mathbf{F}_e = qd\frac{\partial \mathbf{E}_e}{\partial z} = (p_z\frac{\partial}{\partial z})\mathbf{E}_e \qquad (10.13)$$

For the dipole oriented in an arbitrary direction, the force is,

$$\mathbf{F}_e = (p_x\frac{\partial}{\partial x} + p_y\frac{\partial}{\partial y} + p_z\frac{\partial}{\partial z})\mathbf{E}_e = (\mathbf{p}\cdot\nabla)\mathbf{E}_e \qquad (10.14)$$

For the simple case where the dielectric body is isotropically, linearly and homogeneously polarizable, Pohl and Pickard (1969) suggested that,

$$\mathbf{p} = \alpha v\mathbf{E}_e \qquad (10.15)$$

where α is the polarizability or the dipole moment per unit volume and v is the volume of the particle. From equations (10.14) and (10.15),

$$\mathbf{F}_e = \alpha v(\mathbf{E}_e \cdot \nabla)\mathbf{E}_e$$

$$= \tfrac{1}{2}\alpha v \nabla(E_e^2) \qquad (10.16)$$

By definition (Hippel 1954),

$$\alpha = (K_2 - K_1)\epsilon_o E_\alpha \qquad (10.17)$$

and $$v = \frac{4\pi}{3} R^3 \qquad (10.18)$$

and combing equations (10.10), (10.16), (10.17) and (10.18), in a nonuniform external field $\mathbf{E}_e$, a net translational force acting on the sphere (particle) is,

$$\mathbf{F}_e = 2\pi R^3 \epsilon_o K_1 \frac{K_2 - K_1}{K_2 + 2K_1} \nabla(E_e^2) \qquad (10.19)$$

Equation (10.19) describes the net force $\mathbf{F}_e$ due to the replacement of the dielectric of the medium (K_1) by that of the sphere (K_2) and the term (K_2-K_1) represents such replacement. This force results in the translational movement of the particle (sphere) inside a nonuniform electric field. This equation suggests that the magnitude of the force is dependent on the dielectric constants of the medium and particle, and the size of the particle as well.

10.4 Effect of Field Geometry

One commonly used electrode design has a cylindrical symmetry, and is consisted of a central wire electrode running axial in a conducting outer cylinder. In this case, with the inner electrode of radius r_1 at potential V_1 and the outer cylinder of radius r_2 at ground potential, the electric field intensity E at any radial distance r can be shown (Boast 1948) to be,

$$E = \frac{q}{2\pi\epsilon r} \tag{10.20}$$

where ϵ is the permittivity of the medium. Since $E = -\partial V/\partial r$ and by integrating equation (10.20), the electrical potential across the cylindrical system is,

$$V_1 = \frac{q}{2\pi\epsilon} \ln\frac{r_1}{r_2} \tag{10.21}$$

Similarly, from equation (10.21), the electrical potential V_{cyl} at any point at radial distance r from the centre electrode is ($r_1 < r < r_2$),

$$V_{cyl} = \frac{q}{2\pi\epsilon} \ln\frac{r}{r_2} \tag{10.22}$$

Combing the two equations,

$$V_{cyl} = V_1\left(\frac{\ln(r/r_2)}{\ln(r_1/r_2)}\right) \tag{10.23}$$

Since $\mathbf{E} = -\nabla V$, therefore (Pohl and Pickard 1969),

$$\nabla(E_{cyl}^2) = -\frac{2V_1^2}{r^3(\ln(r_1/r_2))^2}\,\mathbf{r}_o \tag{10.24}$$

where $\mathbf{r}_o$ is the unit radial vector. On substituting equation (10.24) into

equation (10.19), the dielectrophoretic force on a particle in a cylindrical field can then be determined. The negative sign of the above equation indicates that the particle will move in the same direction as the converging field towards the centre electrode, under the condition that K_2 is greater than K_1.

10.5 Possible Application of Dielectrophoresis in Geotechnical Engineering

As described in Chapter 9, the major applications of dielectrophoresis are in the physical and biological areas. Since the development of the theory of dielectrophoresis by Pohl in 1951, there has been no application of this theory in geotechnical engineering. As discussed in section 10.3, equation (10.19) suggests that there is a net translational force to pull a neutral polarizable particle towards the stronger field when a nonuniform field is applied.

In the soil-water system, the dielectric constant of clay (medium) is around 4 to 10 and that of water (particle) is 80 (Table 10.1). It can be hypothesized that, when a nonuniform field is applied to a soil mass, the water particle may move towards the direction of converging field. In other words, the moisture content in the soil mass may be decreased and hence it may increase the shear strength of the treated soil. Based on this hypothesis, a series of laboratory tests were designed and performed to explore the possibility of applying dielectrophoresis in soil strengthening.

Table 10.1 Approximate Dielectric Constants of Various Materials (after Foecke 1961)

Material	Dielectric Constant
Air	1.0
Bakelite	5.0
Barium strontium titanate	10000
Barium titanate	1200
Glass	6.0
Mica	5.8
Paraffin	2.2
Polystyrene	2.6
Porcelain	6.0
Quartz (fused)	5.0
Rubber (hard)	3.1
Shellac	3.0
Titanium dioxide	110
Water (distilled)	81
Water (sea)	80

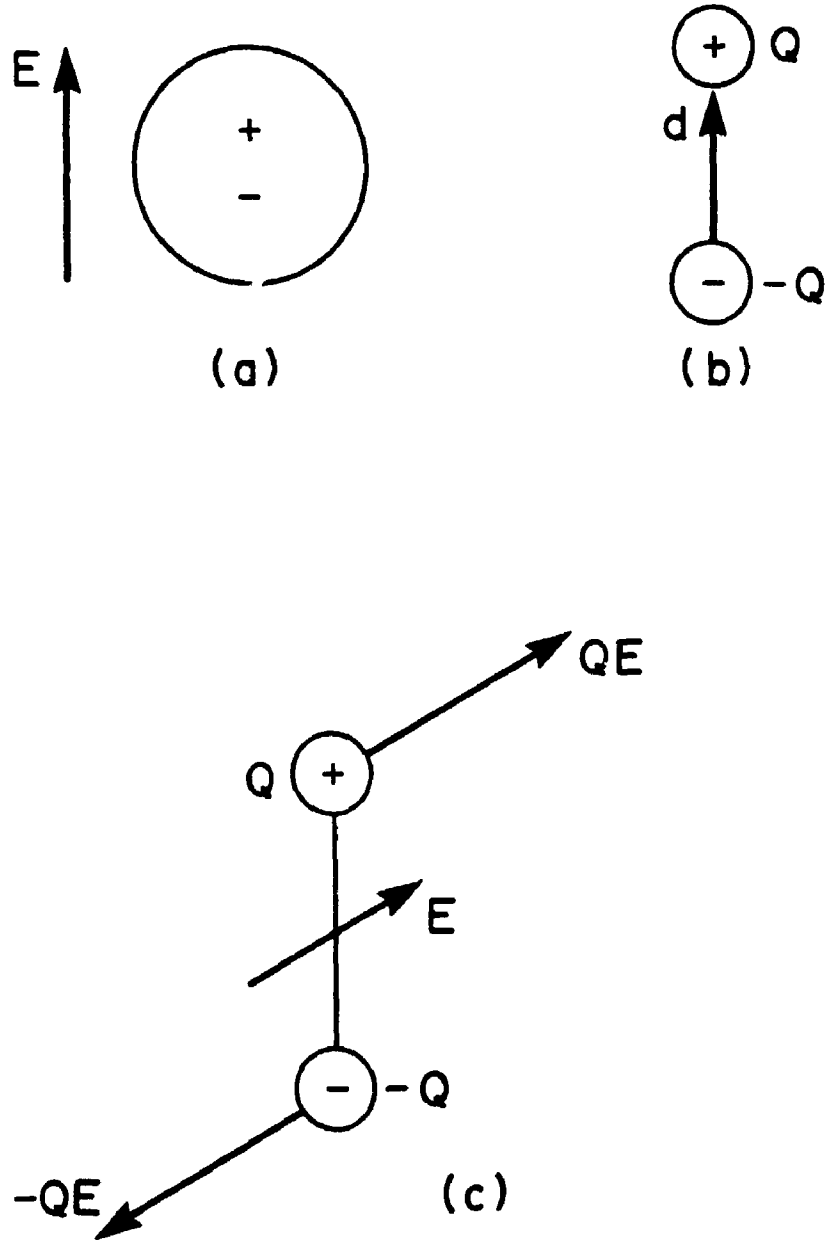

FIGURE 10.1 (a) AN ELECTRIC DIPOLE (b) SCHEMATIC REPRESENTATION OF AN ELECTRIC DIPOLE (c) TORQUE ACTING ON AN ELECTRIC DIPOLE IN AN EXTERNAL ELECTRIC FIELD

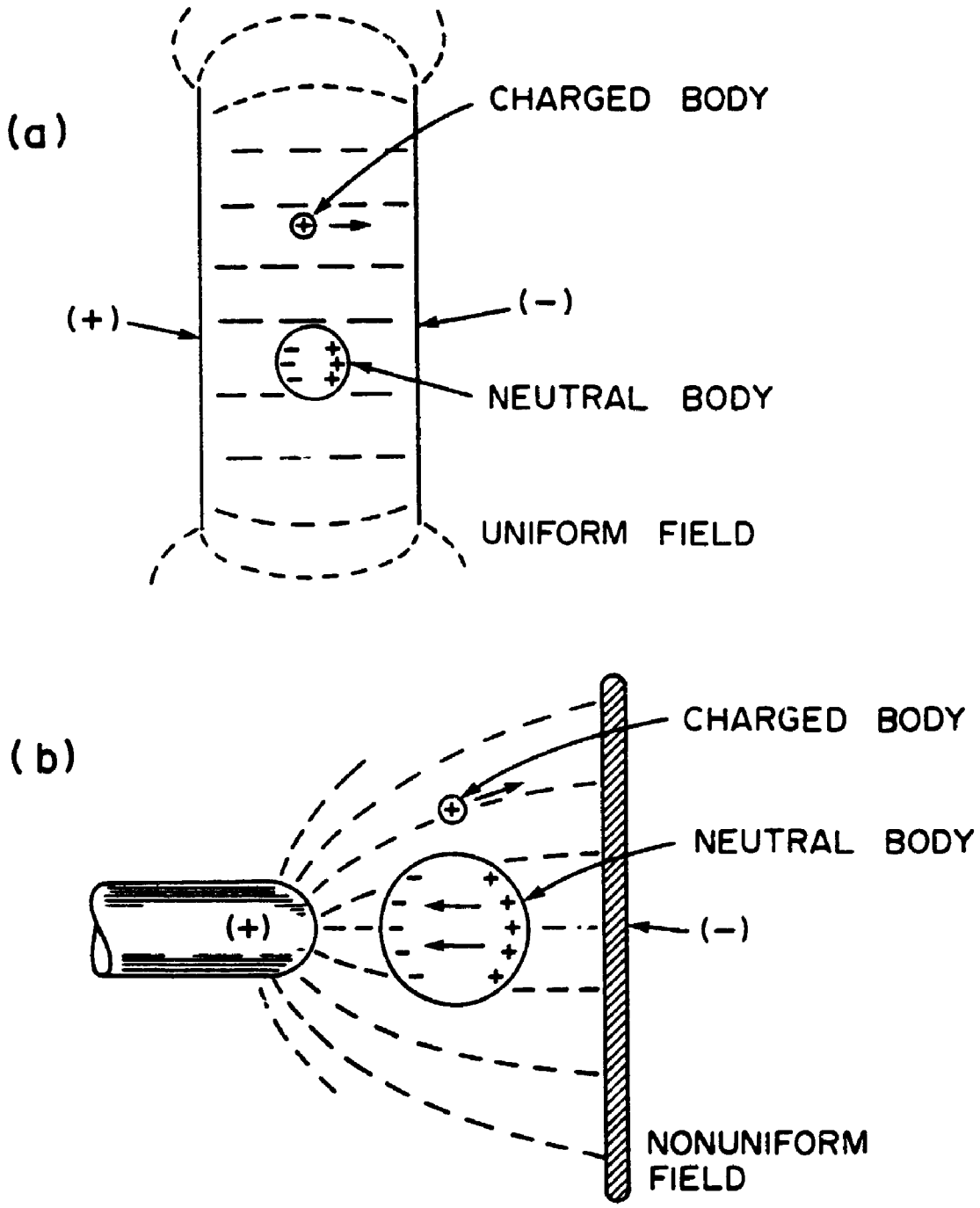

FIGURE 10.2 COMPARISON OF BEHAVIORS OF NEUTRAL AND CHARGED BODIES IN (a) A UNIFORM ELECTRIC FIELD (b) A NON-UNIFORM FIELD (after Pohl 1978)

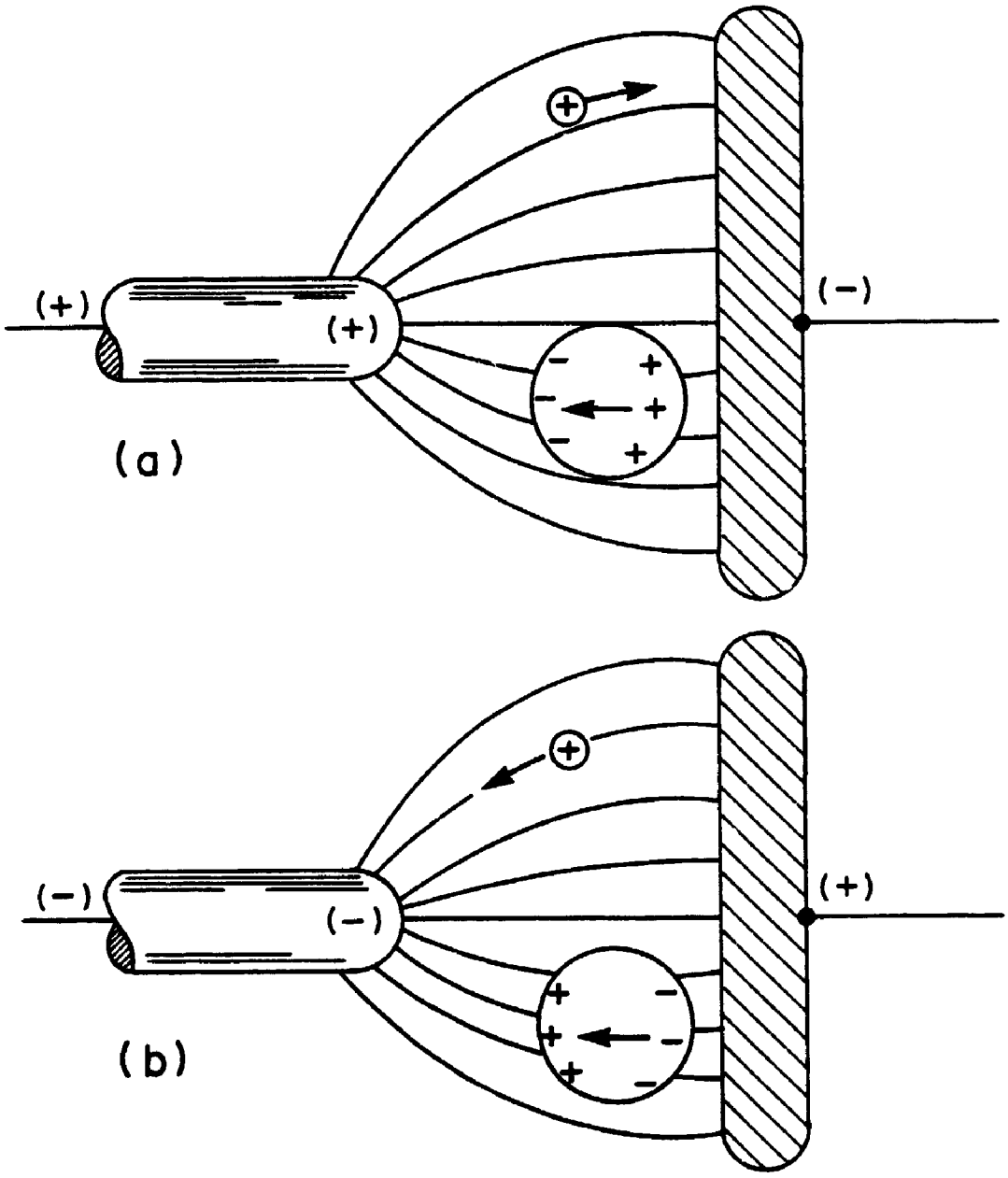

FIGURE 10.3 COMPARISON OF BEHAVIORS OF NEUTRAL AND CHARGED BODIES IN AN ALTERNATING NONUNIFORM ELECTRIC FIELD (after Pohl 1978)

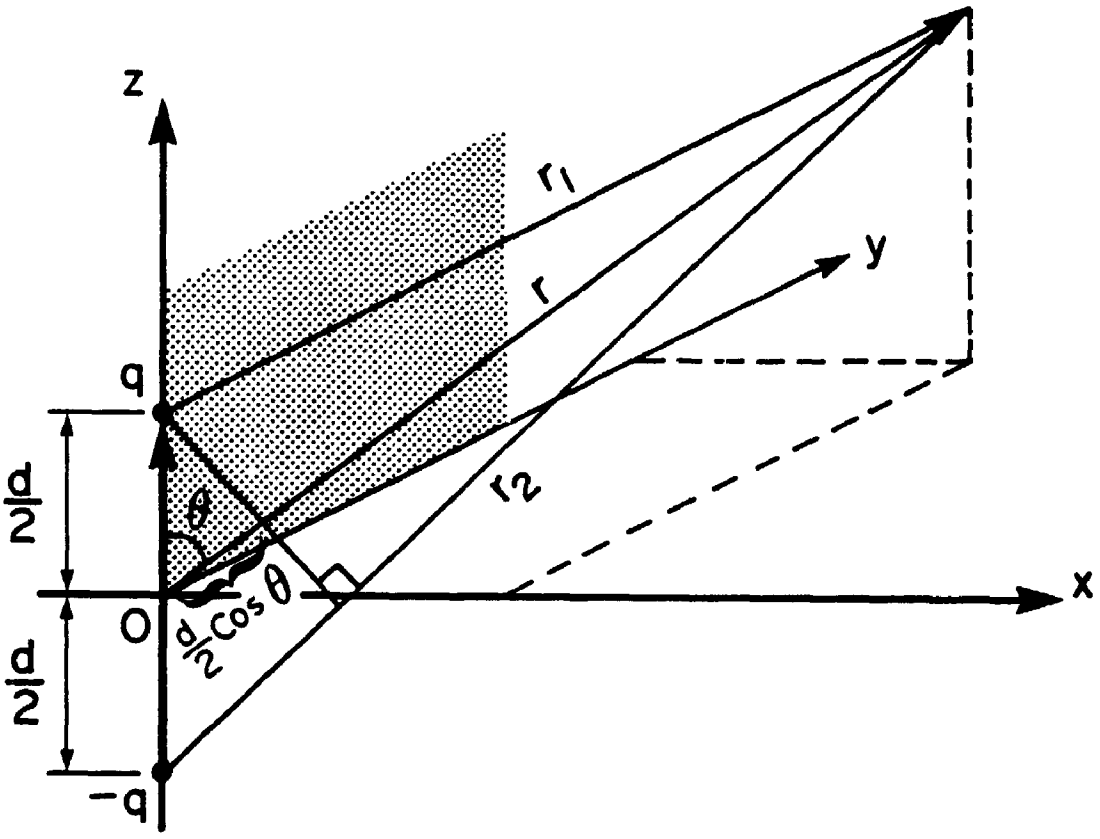

FIGURE 10.4 A DIPOLE AT THE ORIGIN AND A POINT OF OBSERVATION AT **r** (after Javid and Brown 1963)

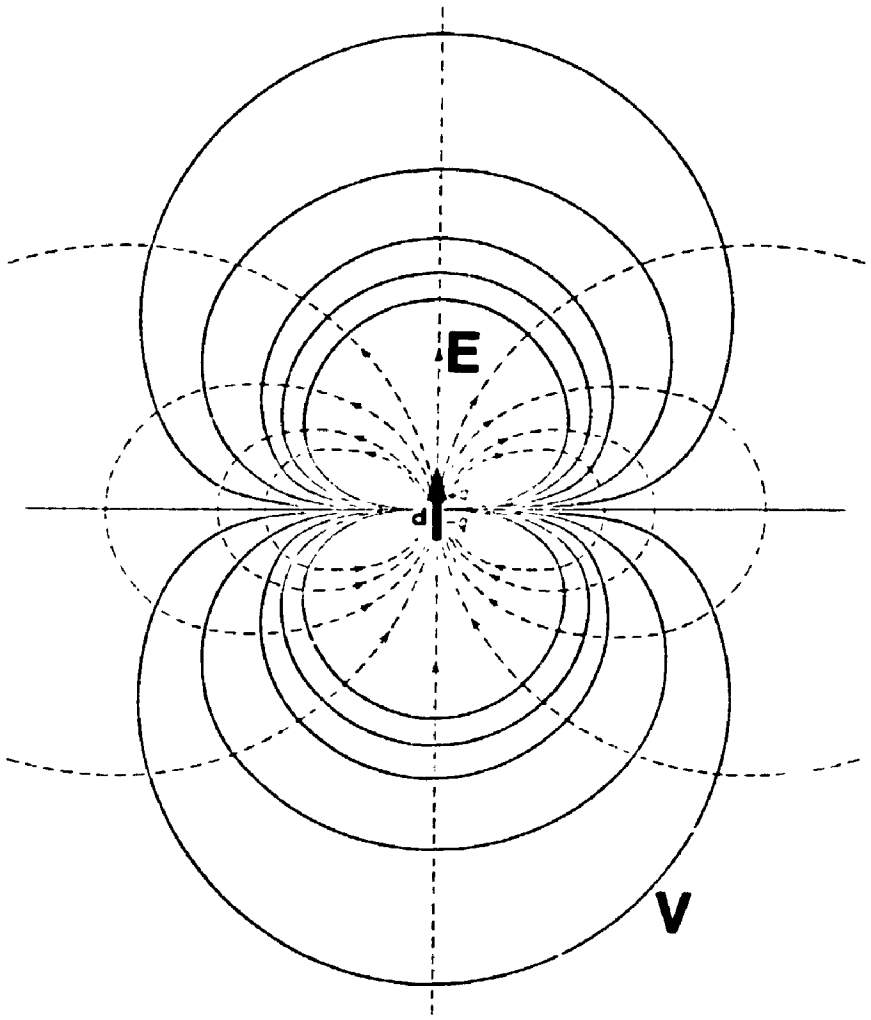

FIGURE 10.5 ELECTRIC FIELD LINES **E** (DASHED LINES) AND EQUIPOTENTIALS **V** (SOLID LINES) OF AN ELECTRIC POINT DIPOLE (after Javid and Brown 1963)

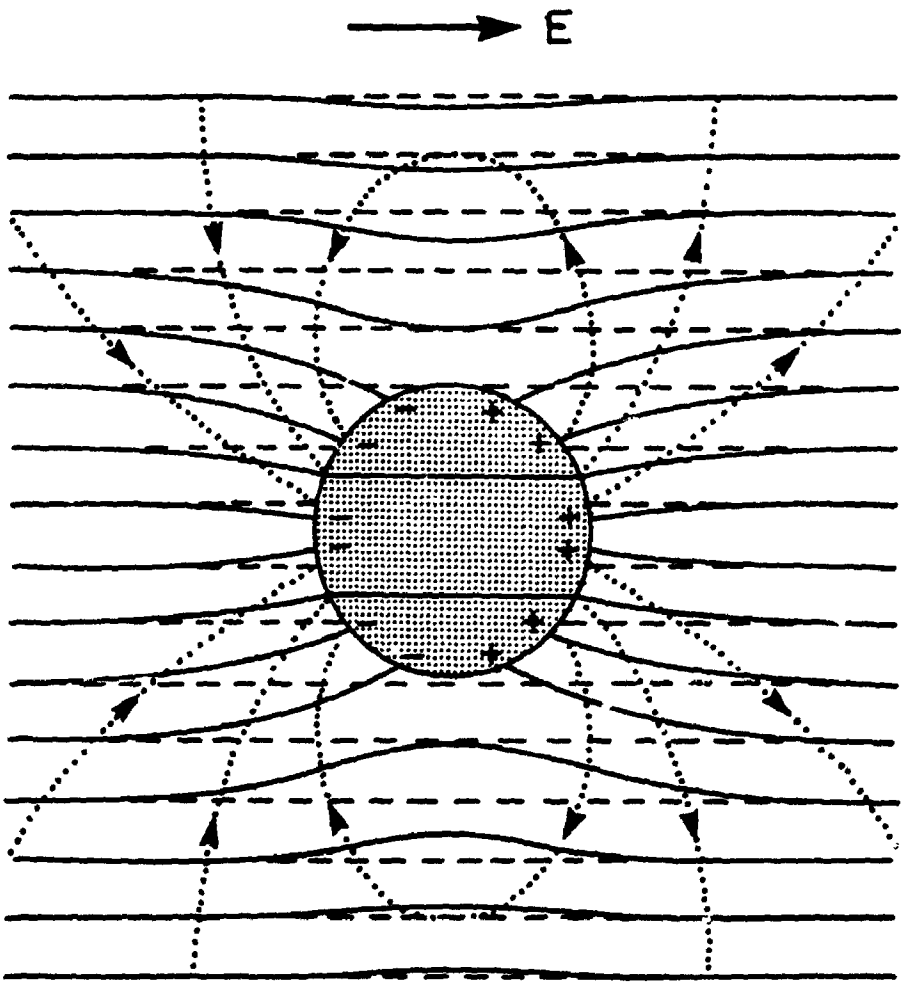

FIGURE 10.6 DIELECTRIC SPHERE IN HOMOGENEOUS FIELD
(after Von Hippel 1954)

CHAPTER 11

EXPERIMENTAL STUDY

11.1 General

The soils used for the laboratory investigation for dielectrophoresis were the Wallaceburg and Gloucester clays (same as those used in the electro-osmosis tests). The sample size for Wallaceburg clay was the 254 mm (10") cubic block sample whereas the Gloucester clay was the 152.4 mm (6") diameter shelby tube sample of 203.2 mm (8") in length. The soils properties are already discussed in sections 6.1 to 6.3.

The test program in this experimental study consists of four phases. Phase 1 is the preliminary study of dielectrophoresis. The purposes were to study the possibility of using dielectrophoresis to strengthen the soil sample and to observe its effects on the changes of soil properties. After obtaining some test results from the first phase, a systematic study was performed in the second phase in which the effects of varying the applied voltage and electrode depth to the change in soil properties were investigated. The possibility of applying the dielectrophoresis in the field was studied by a reduced scale model test and the effect of electrode spacing was also investigated. The high voltage electrode for the field was then designed after the third phase and a high voltage of 60 kilovolts (kV) was applied to test its lifetime performance in the last phase of the study. Gloucester tube samples were used in the phase 2 study while

Wallaceburg block samples were used in the rest of the tests. The test program is summarized in Table 11.1 and the explanation of the notations used are,

W20KV3 = Wallaceburg block sample, 20 kV applied voltage with 3" (76.2 mm) electrode depth,

G10KV2 = Gloucester tube sample, 10 kV applied voltage with 2" (50.8 mm) electrode depth.

11.2 Test Apparatus and Procedures

Two different apparatus were designed for the first and second phases of study to accommodate the differences in sample shapes and sizes.

11.2.1 Apparatus and Procedures for Preliminary Study

The Wallaceburg block samples were used in the preliminary study. The apparatus is shown in the photo of Figure 11.1 and in a schematic diagram of Figure 11.2. It consists of six insulated electrodes inserted through six 25.4 mm diameter holes pre-drilled into a 254 mm (10") cubic block sample. The grounded steel body acts as a rigid frame to support the plastic cover and the electrodes. The upper plexiglas plate can be adjusted up and down by means of a nylon screw and hence the electrode depth embedded in the soil mass can be regulated. As shown in Figures 11.1 and 11.2, the distributed array of electrodes consists of two central electrodes as ground electrode and four surrounding electrodes maintained at an alternating potential of 20 kV relative

to the ground electrode. Due to the high voltage in the electrode, a special design is required to avoid any corona effect (the effect of ionization of air in a high electric field intensity region). As shown in Figure 11.3, the electrode consists of a long copper rod with 4.8 mm in diameter and 300 mm in length. The copper rod is inserted in an acrylic tube of 13 mm in diameter filled with silicone oil of high dielectric constant. The choice of an ac voltage source rather than dc (direct current) voltage source is to avoid any charge concentration around the electrode of constant polarity. According to Gauss theorem, the charge concentration will cancel the electric field.

The four sides and the bottom of the clay mass were maintained at ground potential by means of four copper sheets held tightly against the four sides of the soil mass by springs and wires and a steel plate at the bottom. With the described arrangement, the electric field lines converge towards all six holes, and diverge towards the rest of the clay mass.

Eight settlement pins were installed on the top surface of the sample to monitor the settlement of the sample during treatment (by means of a travelling telescope). Metallic dial gauge and pore water pressure transducer were not installed due to the effect of high voltage. In fact, a pore water pressure transducer was damaged during the first trial test.

The potential was applied by a high voltage transformer connected by high voltage cable to the sample. In the first phase of the study, 20 kV ac potential was applied to three samples for a period of 26 to 28 days with three different

electrode depths of 76.2 mm (3"), 127 mm (5") and 190.5 mm (7.5"). The test program is summarized in Table 11.1. During the treatment, the settlement of the sample was monitored. Moisture content tests and undrained shear strength tests (by laboratory vane device) were carried out before and after treatment to determine the changes in soil properties. Since the sample was not protected during the experiment, some natural drying of the test specimens may have occurred during treatment. Therefore correction factors were developed by performing a control test (for settlements, shear strengths and moisture contents) on a sample with the same test environment except the application of voltage.

11.2.2 Apparatus and Procedures for Phase 2 Study

The Gloucester tube samples were used in this study. The apparatus is basically similar to that described in section 11.2.1, and the general arrangement of the test apparatus is shown in Figure 11.4. The only difference here is the supporting frame used and the electrode configuration. As shown in Figure 11.5, the high voltage electrode at the centre of the tube sample is supported by a simple four-leg stand made of plexiglas strip. The electrode depth embedded in the soil can be adjusted by using the nylon screw. The circumferential surface of the soil sample was maintained at ground potential by means of twenty copper rods (4.8 mm diameter) with the same embedded depth as the high voltage electrode. With such arrangement, an axis-symmetric

field geometry can be generated with the electric field lines converge towards the centre high voltage electrode and diverge towards the cylindrical surface.

All the eight samples were treated for 21 days by applying three different potentials of 10 kV, 18 kV and 25 kV with three different electrode depths of 50.8 mm (2"), 101.6 mm (4") and 152.4 mm (6"). The test program is summarized in Table 11.1. Due to the limited availability of Gloucester clay samples, the test of 10 kV applied voltage with 101.6 mm (4") electrode depth was not performed. In order to eliminate the effect of natural drying, the samples were still covered by their original wax, as shown in Figure 11.5. During the treatment, the settlement of the sample was monitored by the six settlement pins installed. Moisture content tests and undrained shear strength tests were performed before and after treatment to determine the changes of soil properties.

11.3 Test Results

A total of three Wallaceburg block samples were tested in the preliminary study and eight Gloucester tube samples were treated in the phase 2 study. The test results of average settlements, change of moisture contents and change of undrained shear strengths of the samples are summarized in Table 11.2. The results of preliminary study have been presented by Inculet and Lo (1988).

11.3.1 Results of Preliminary Study

The surface settlement of the sample was monitored by eight settlement pins installed. Individual measurement showed that the variation of surface settlement was small (±3 % variation). The relationships between settlement (average of 8 pins) with time and with different electrode depths are shown in Figure 11.6. It can be seen that the settlements began to occur soon after the application of voltage. After about 10 days of treatment, the settlements increased to a higher rate. It is also noticed that with an increase in depth of the electrode, both the magnitude and the rate of settlement increased. The average settlements after treatment were 2.88 mm, 5.47 mm and 8.80 mm for tests W20KV3, W20KV5 and W20KV7.5 respectively.

The moisture contents and shear strengths within the specimens were measured at various depths of 64 mm, 127 mm and 190 mm evenly distributed before and after the tests. In general, six to eight measurements of shear strength and water content were made at each depth. The average test results are summarized in Table 11.2 which indicates that there was a considerable decrease in moisture content and increase in shear strength. The reduction in moisture contents were 11.2 %, 18.8 % and 24.9 % and the gain in shear strengths were 28.5 %, 125 % and 966 % for the tests of W20KV3, W20KV5 and W20KV7.5. These changes are consistent with the occurrence of settlement, since settlement is caused by the expulsion of pore water in the clay mass. It may be observed from this experiment that the application of dielectrophoresis

in soil strengthening was in principle demonstrated.

11.3.2 Results of Phase 2 Study

In the Phase 2 study, the effects of applied potential and electrode depth are investigated. The settlement curves for the tests with different applied potentials and different electrode depths are plotted in Figure 11.7. Similar to the preliminary study, the settlement began to occur soon after the application of voltage. Figure 11.7 also indicates that the higher the applied potential, the higher the settlement for constant electrode depth. Similarly, the deeper the electrode penetrated into the sample, the higher the settlement was observed for a given potential. The settlements ranged from 1.22 mm to 2.96 mm for the two extreme cases in the tests G10KV2 and G25KV6 respectively.

The decrease in moisture content and increase in shear strength of each sample treated are summarized in Table 11.2. After the application of electricity for 21 days, the moisture contents reduced by 4.2 % and 15.5 % and the shear strengths increased by 5.0 % and 150 % for samples G10KV2 and G25KV6 respectively.

In order to investigate the mechanism of dielectrophoretic treatment of soil, further tests such as unconfined compression tests, consolidation tests, limits tests and chemical tests were performed and the analysis will be discussed in Chapter 12.

11.4 Model Test

As discussed in the previous sections, it was demonstrated that the clays could be strengthened by dielectrophoresis. Model test was then designed to explore the possible electrode configuration for the field application. Two high voltage electrodes (A1 and A2) and two ground electrodes (G1 and G2) were installed in a Wallaceburg block sample with the electrode configuration and electrode spacings as shown in Figures 11.8 and 11.9. For each electrode, clearance was maintained between the electrodes (high voltage and ground electrodes) and the cylindrical surface of the hole so that water could escape from the hole. The electrode depth of all the electrodes was 180 mm (7") deep with four different electrode spacings of 100 mm, 140 mm, 180 mm and 200 mm. It gave a ratio of the electrode spacing to electrode depth of around 0.55, 0.8, 1.0 and 1.1 respectively. An electric potential of 15 kV was applied for 28 days. The sample was covered by its original wax to minimize any natural drying effect.

The settlement-time curve is plotted in Figure 11.10. The average settlement after treatment was 4.25 mm. The settlement curve is similar to the curves obtained in the preliminary and phase 2 studies. After treatment, the moisture contents and undrained shear strengths at four different levels of depth were measured at the following locations:

(i) mid-point between any two pairs of electrodes,

(ii) at the centre of the grid.

The average post-treatment values compared with the average pre-treatment values are summarized in Table 11.3. The average reduction of moisture contents were 15.4 %, 10.4 %, 8.7 % and 6.1 % and the average increase in shear strengths were 59.9 %, 45 %, 37.6 % and 30.2 % for the electrode spacings of 100 mm, 140 mm, 180 mm and 200 mm respectively. At the centre of the grid, the moisture content reduced by 3.8 % and the shear strength increased by 22.8 %. This result reflects that the closer the electrode spacing, the higher the moisture content reduction, and concurrently the higher the shear strength increase. Furthermore, this treatment effect can be extended to the centre of the grid, which is considered as the inactive zone with the weakest electric field intensity.

11.5 Lifetime Test of Field Electrode

With the test results obtained from the above three phases of studies, it was proposed to carry out a field test to explore the possibility of incorporating the technique into practice. The major factor affecting the success of the treatment would be the electrode design. As shown in sections 11.3 and 11.4, the concept of electrode design would be appropriate for the dielectrophoretic treatment, except that the material used, such as the acrylic tube, may be too fragile. Therefore a similar concept of electrode design was developed by using the heavy duty materials. As illustrated in Figure 11.11, the electrode consists of a 12.7 mm (½") diameter copper pipe inserted in a 38.1 mm (1.5") heavy

duty PVC pipe (Schedule 80 with 300 psi compressive strength) filled with silicone oil. The copper pipe is held in place at the centre of the PVC pipe by means of PVC spacers. The choice of the materials for electrode is to consider the availability of the materials. The 12.7 mm (½") copper pipe and 38.1 mm (1.5") PVC pipe are easily available in most hardware stores. It can also be ordered in large quantity from the manufacturer at lower costs with short delivery time.

The lifetime performance, or the durability of the new electrode was then tested with the arrangement as shown in Figure 11.12. A high potential of 60 kV ac was applied by a high voltage transformer (to be used in the field test) to the field electrode which was placed 177.8 mm (7") inside a block sample (Wallaceburg clay) for a period of 49 days (7 weeks). A gap of 12 mm in the hole between electrode and soil was maintained. The electrode was inspected (with power off) daily to check for any damage or irregularity. After the seven weeks of treatment, the electrode was found to be intact without any trace of irregularity. This result demonstrates that the new electrode can carry high alternating potential for a long period of treatment.

Table 11.1 Summary of Dielectrophoretic Test Program

Soil Type	Test No.	Applied Voltage (kV)	Electrode Depth (inch)	Electrode Depth (mm)	Treatment Time (day)	Phase
Wallaceburg Clay	W20KV3	20	3.0	76.2	27	1
	W20KV5	20	5.0	127.0	28	
	W20KV7.5	20	7.5	190.5	26	
Gloucester Clay	G10KV2	10	2.0	50.8	21	2
	G10KV6	10	6.0	152.4	21	
	G18KV2	18	2.0	50.8	21	
	G18KV4	18	4.0	101.6	21	
	G18KV6	18	6.0	152.4	21	
	G25KV2	25	2.0	50.8	21	
	G25KV4	25	4.0	101.6	21	
	G25KV6	25	6.0	152.4	21	
Wallaceburg Clay	Model Test	15	7.0	177.8	28	3
Wallaceburg Clay	Lifetime Test	60	7.0	177.8	49	4

Table 11.2 Summary of Test Results for Wallaceburg and Gloucester Clay Samples

Test No.	Average* Settlement (mm)	Average Moisture Content (%)			Average Shear Strength (kPa)!		
		Initial	After	Decrease (%)	Initial	After	Increase (%)
W20KV3	2.88	31.3	27.8	11.2	24.9	32.0	28.5
W20KV5	5.47	30.9	25.7	16.8	20.8	46.8	125.0
W20KV7.5	8.80	40.9	30.7	24.9	22.5	240.0	966.7
G10KV2	1.22	84.9	81.3	4.2	10.0	10.5	5.0
G10KV6	1.55	86.2	80.8	6.3	11.0	11.9	8.2
G18KV2	1.82	63.5	58.3	8.2	12.0	15.2	26.7
G18KV4	2.01	65.1	59.1	9.2	12.0	15.8	31.7
G18KV6	2.36	59.8	53.9	9.9	9.0	12.2	35.6
G25KV2	2.49	69.5	61.4	11.7	12.0	26.2	118.3
G25KV4	2.58	61.4	52.8	14.0	9.3	21.7	133.3
G25KV6	2.96	62.1	52.5	15.5	14.6	36.5	150.0

* the average settlements as shown are the corrected values from the measured settlement due to natural drying effect
! shear strength obtained by laboratory vane test

Table 11.3 Summary of Test Results for Model Test

Measurement Between Electrodes	Electrode Spacing mm	Average Moisture Content (%)			Average Shear Strength (kPa)		
		Initial	fter	Decrease (%)	Initial	After	Increase (%)
G2 - A2	100	34.5	29.2	15.4	20.2	32.3	59.9
A2 - G1	140	34.5	30.9	10.4	20.2	29.3	45.0
G1 - A1	180	34.5	31.5	8.7	20.2	27.8	37.6
A1 - G2	200	34.5	32.4	6.1	20.2	26.3	30.2
Centre of Grid	---	34.5	33.2	3.8	20.2	24.8	22.8

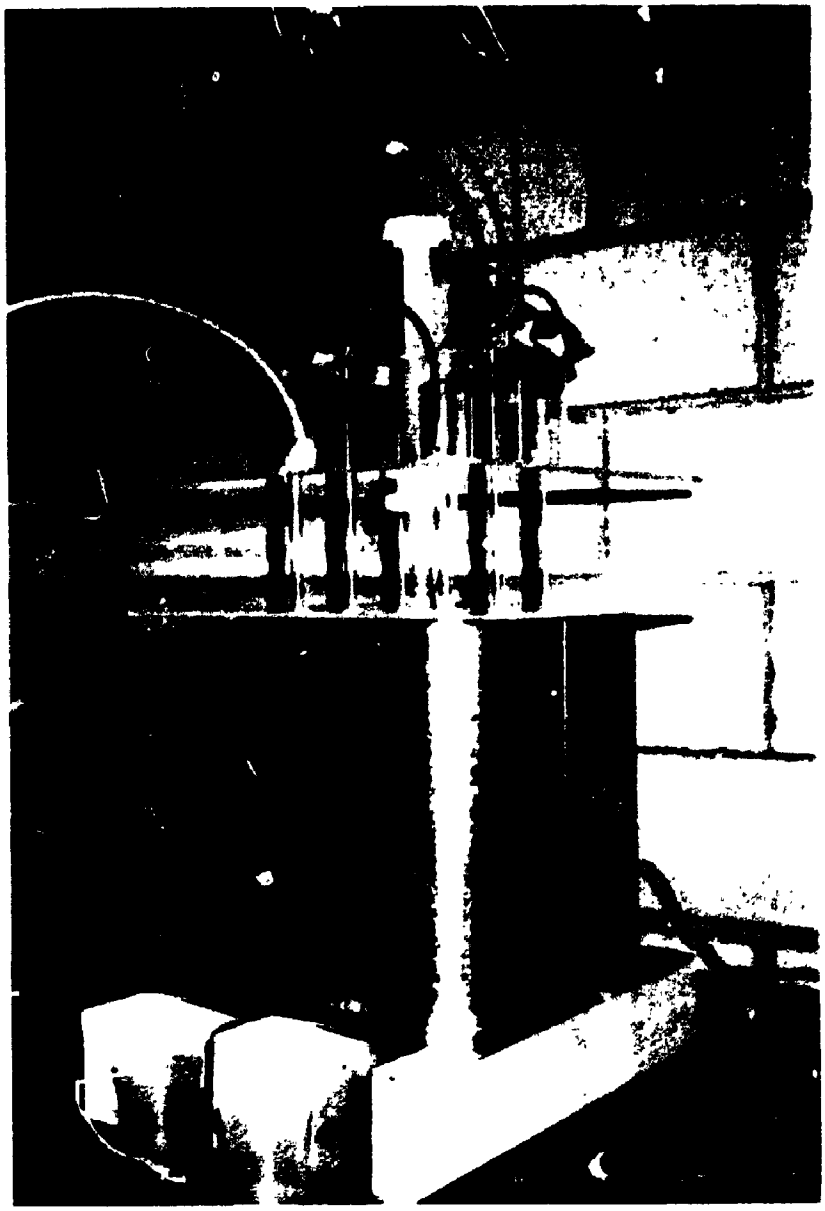

FIGURE 11.1 PHOTO OF APPARATUS FOR DIELECTROPHORETIC TEST OF WALLACEBURG CLAY

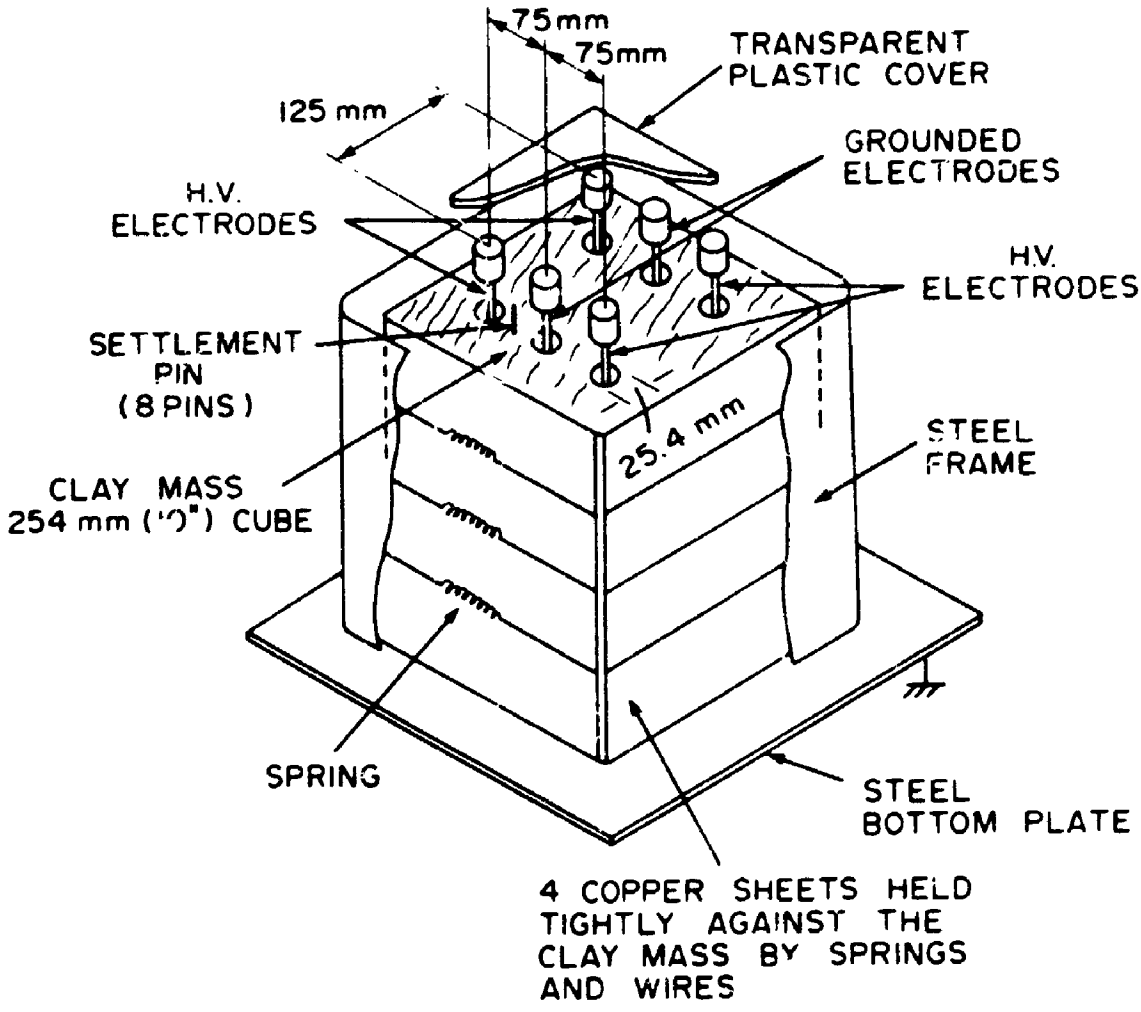

FIGURE 11.2 APPARATUS FOR DIELECTROPHORETIC TEST OF WALLACEBURG CLAY

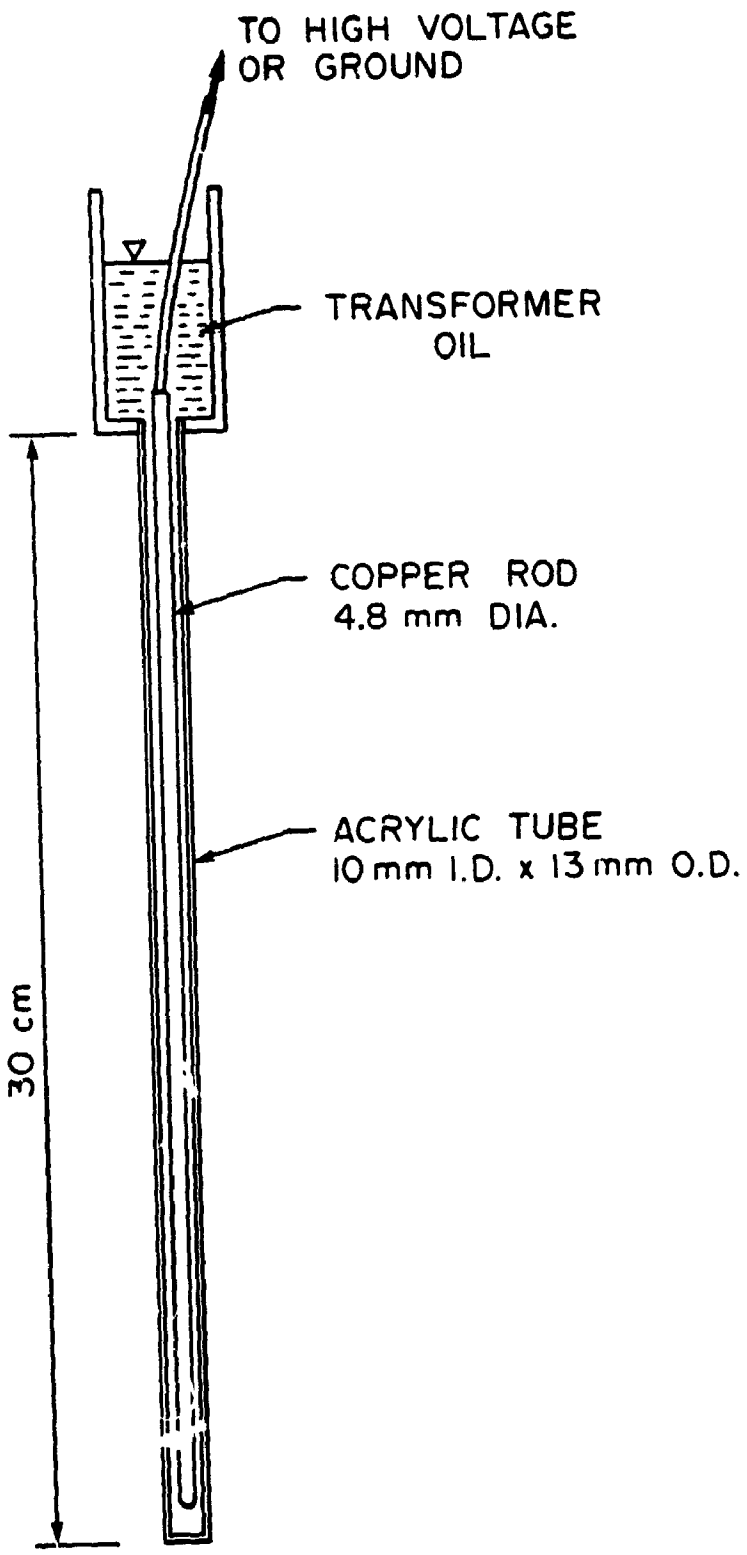

FIGURE 11.3 DESIGN DETAILS OF THE HIGH VOLTAGE ELECTRODE FOR LABORATORY TEST

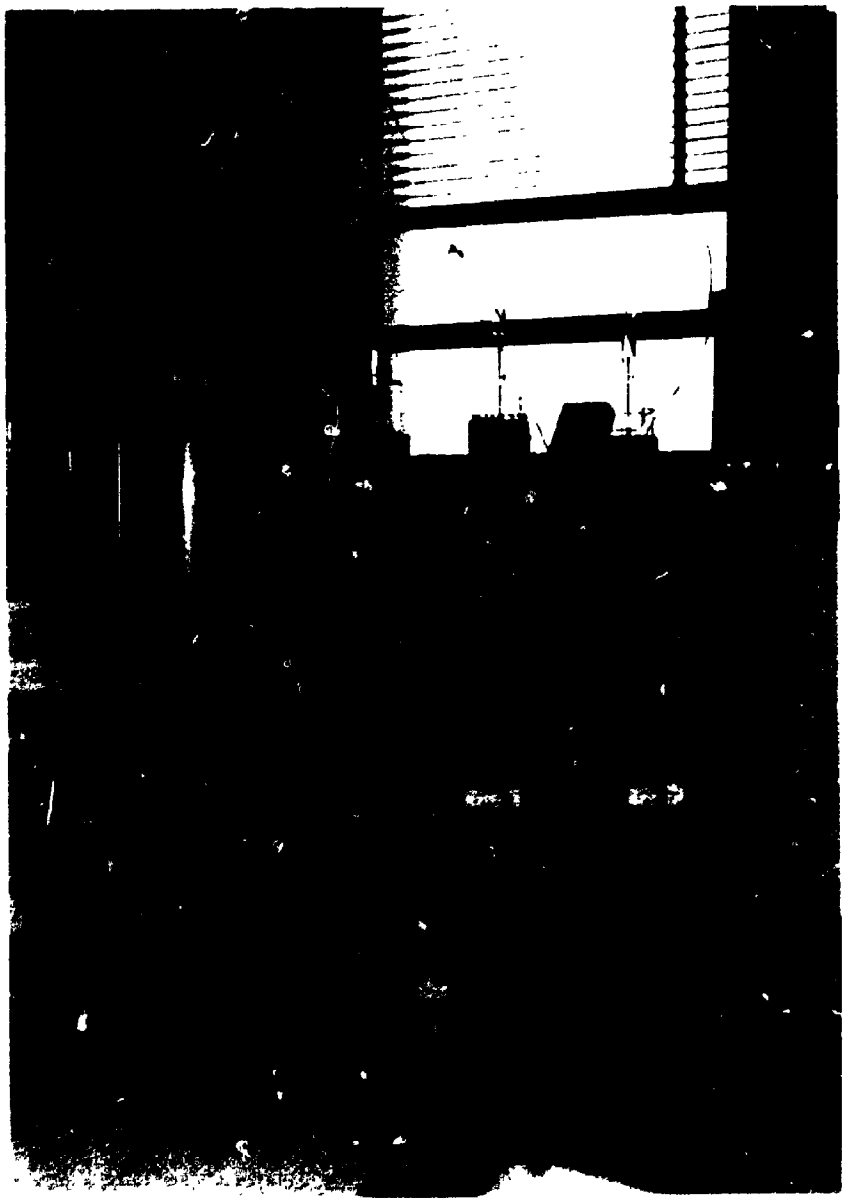

FIGURE 11.4 GENERAL ARRANGEMENT OF DIELECTROPHORETIC TEST OF GLOUCESTER CLAY

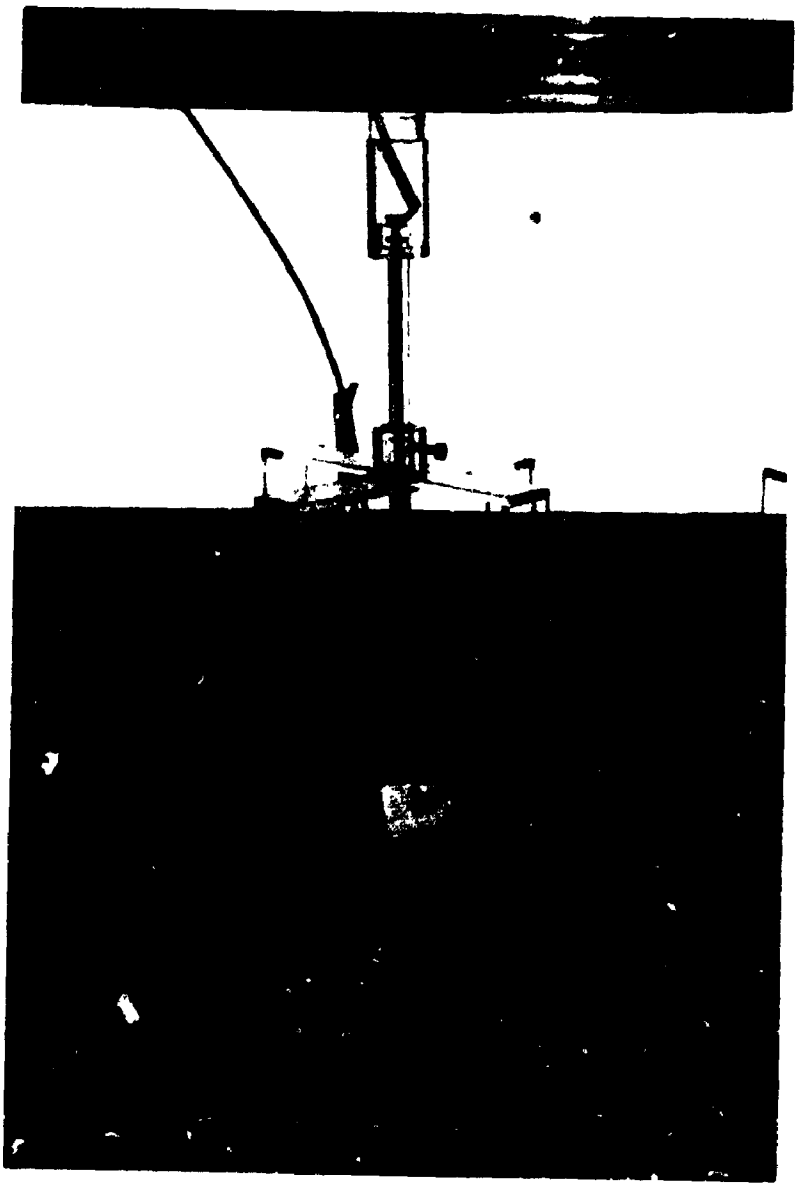

FIGURE 11.5 DIELECTROPHORETIC TEST OF GLOUCESTER CLAY BY APPLYING HIGH VOLTAGE CYLINDRICAL FIELD

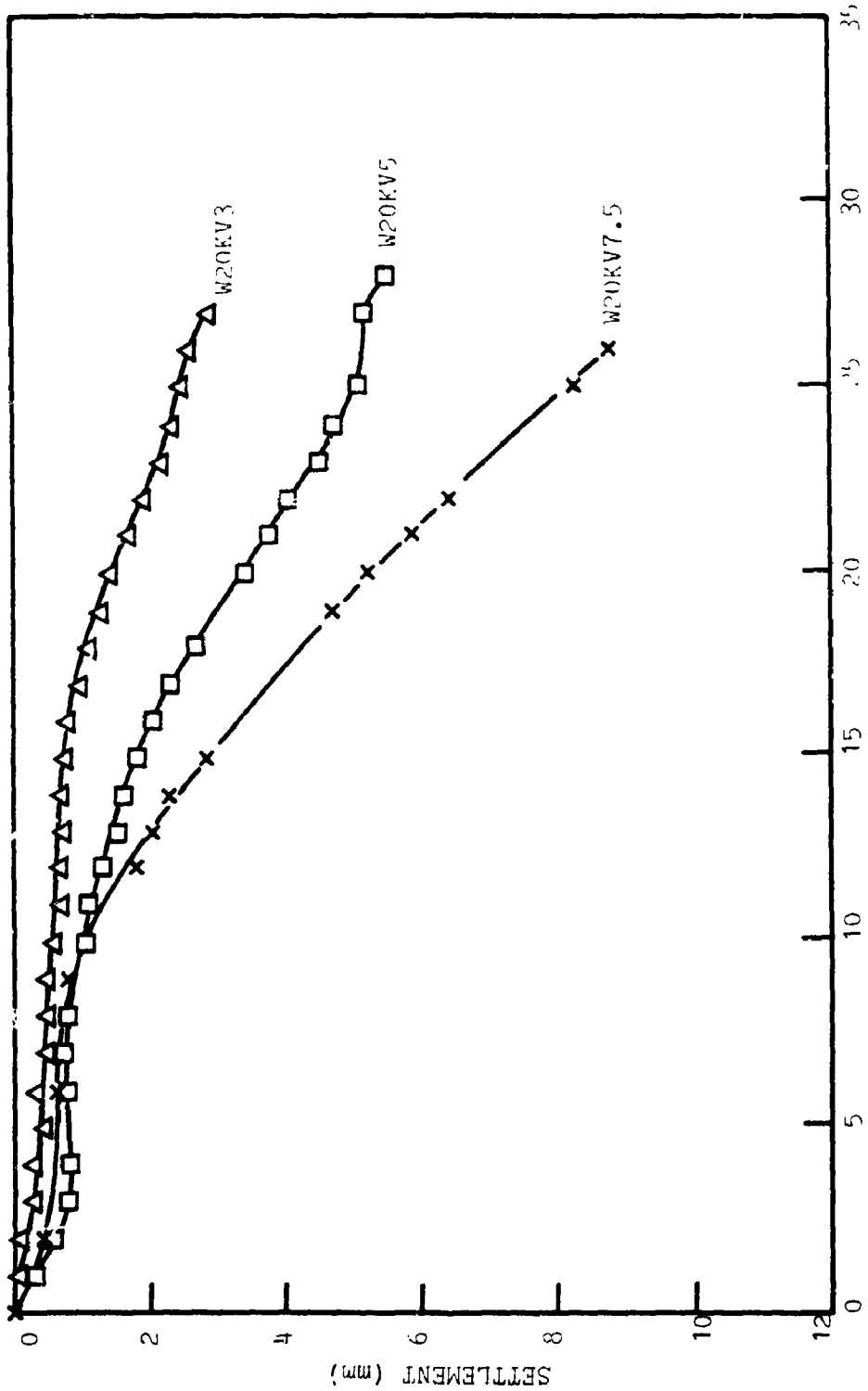

FIGURE 11.6 SETTLEMENT-TIME CURVES FOR WALLACEBURG CLAY FOR DIFFERENT ELECTRODE DEPTHS

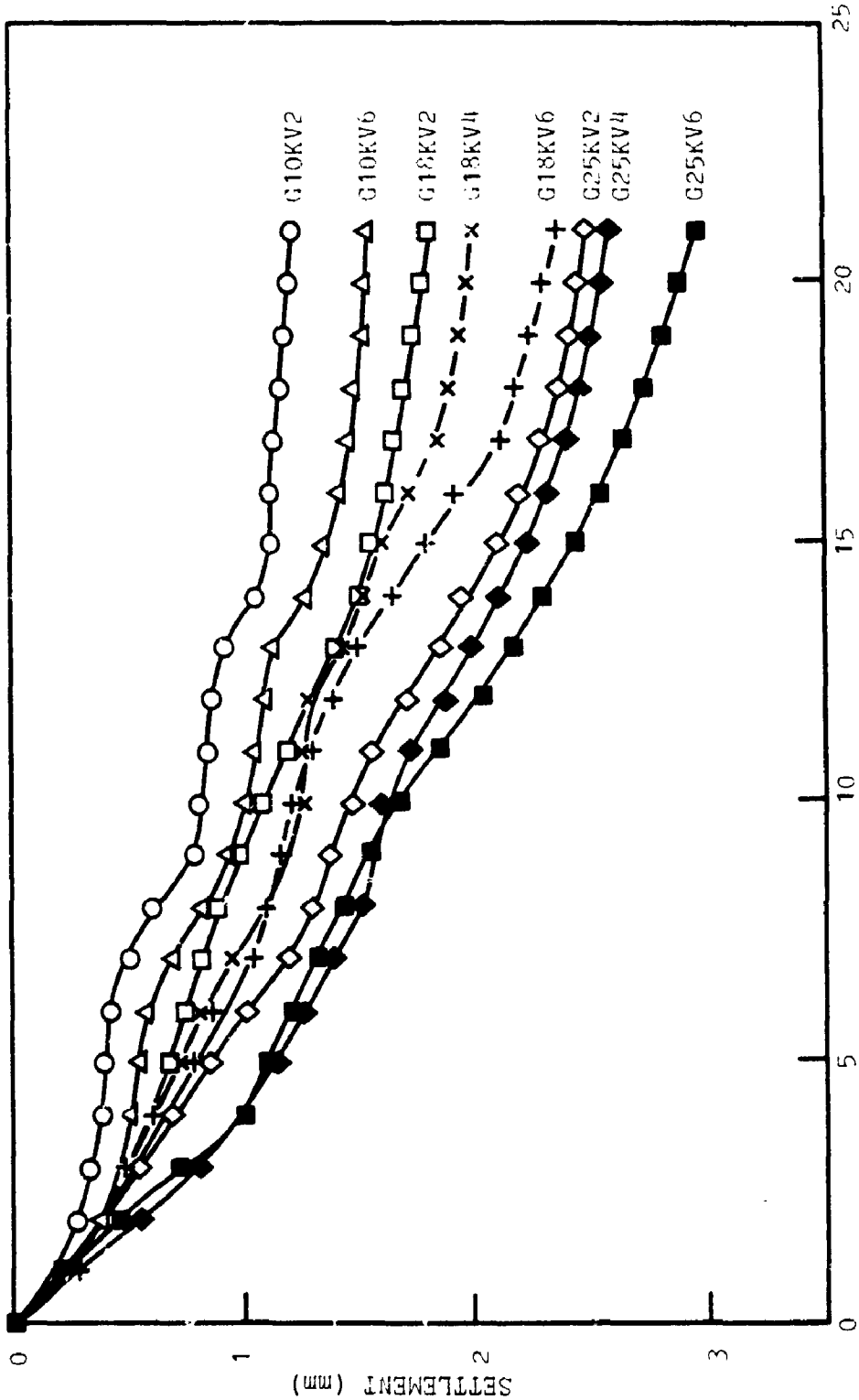

FIGURE 11.7 SETTLEMENT-TIME CURVES FOR GLOUCESTER CLAY

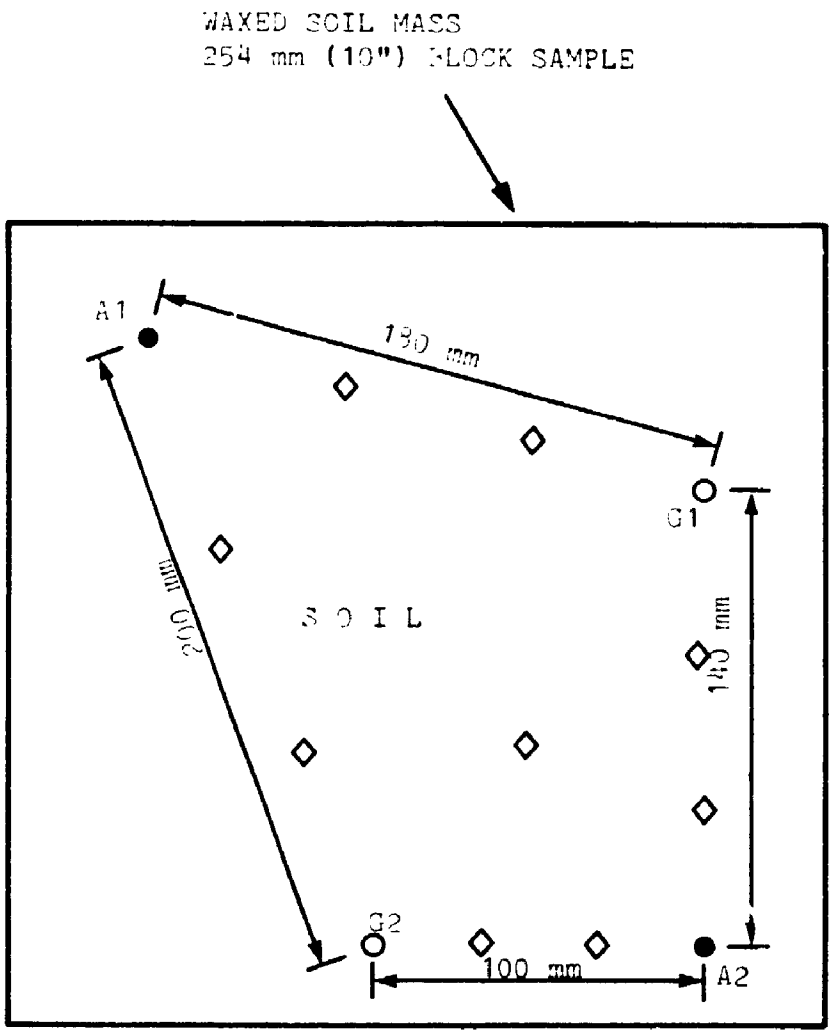

NOTES: A1 AND A2 ARE HIGH VOLTAGE ELECTRODES
G1 AND G2 ARE GROUND ELECTRODES
ELECTRODE DEPTH = 177.8 mm (7")
APPLIED VOLTAGE = 15 kV
◇ SETTLEMENT PINS

FIGURE 11.8 PLAN VIEW OF ELECTRODE CONFIGURATION OF MODEL TEST USING WALLACEBURG CLAY BLOCK SAMPLE

FIGURE 11.9 PHOTO OF GENERAL ARRANGEMENT OF MODEL TEST

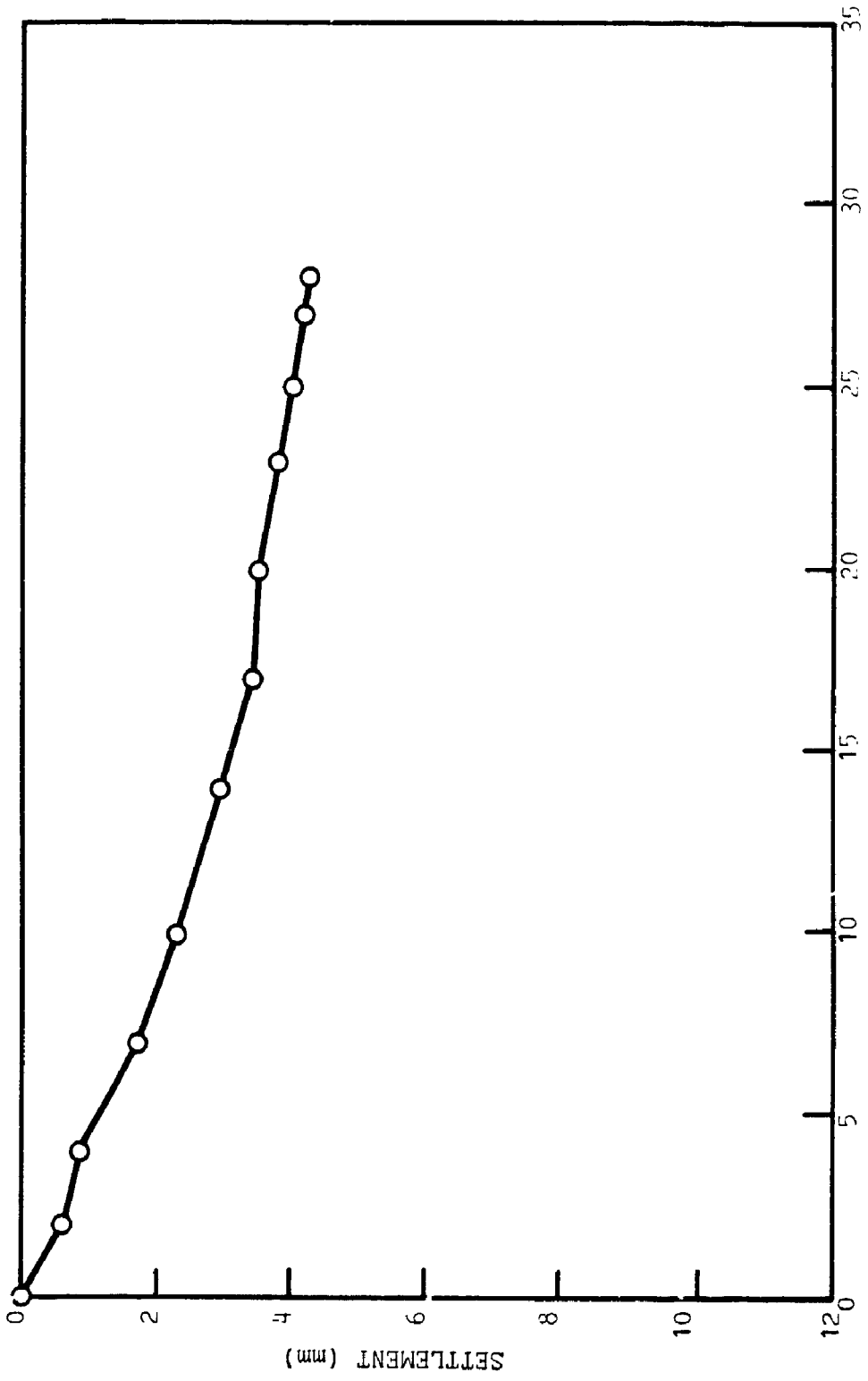

FIGURE 11.10 SETTLEMENT-TIME CURVE FOR MODEL TEST (WALLACEBURG CLAY)

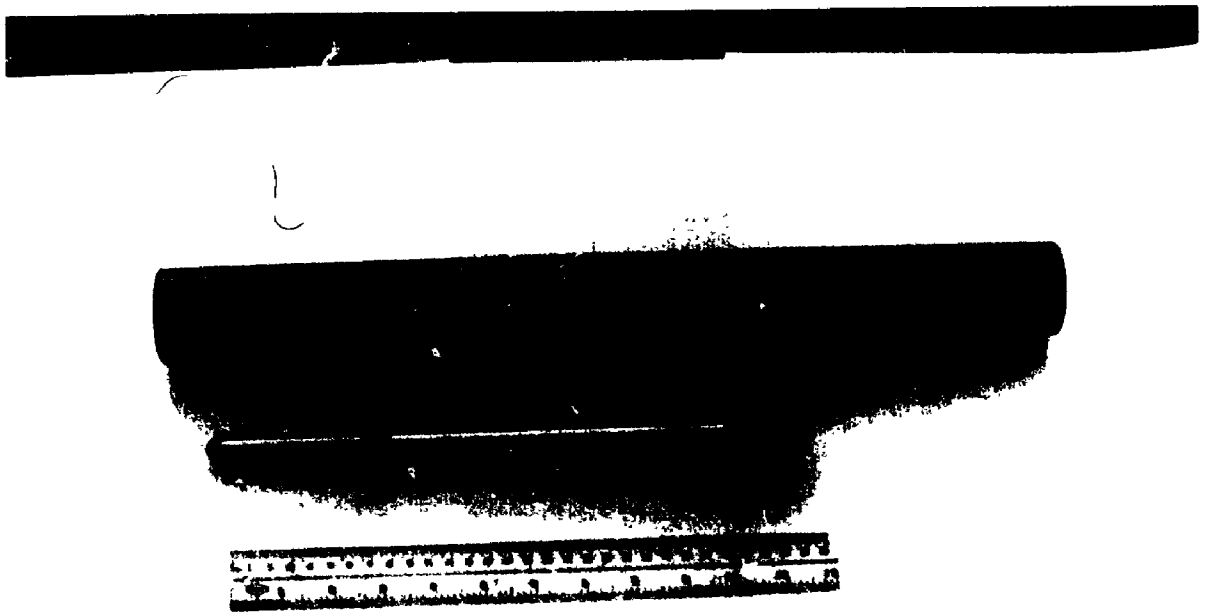

FIGURE 11.11 DESIGN OF HIGH VOLTAGE ELECTRODE FOR FIELD TEST

FIGURE 11.12 GENERAL ARRANGEMENT OF LIFETIME TEST OF HIGH VOLTAGE ELECTRODE FOR FIELD TEST

CHAPTER 12

ANALYSIS OF TEST RESULTS OF DIELECTROPHORESIS

An experimental study of dielectrophoresis was performed and the test results were described in the previous chapter. A series of conventional soil laboratory tests were carried out on the samples before and after treatment in order to study the change in soil properties and explore the mechanism of the process. Further analysis of the test results performed are described in this chapter.

12.1 Observations at Electrodes

In electro-osmosis, water moves towards cathode and can be collected by means of an appropriate drainage system, while in dielectrophoresis, no water can be collected at the electrodes. During the preliminary study on Wallaceburg clay, water condensation was observed on the lower plexiglas plate, as shown in Figure 12.1. However, such water condensation was not observed in the control test. Therefore, it is unlikely that the water was formed by natural drying of the soil mass. This observation indicates that water molecules migrated to the electrodes along the converging electric field and then evaporated at the region between clay surface and electrodes. The phenomenon of water condensation reflects the water movement in the soil mass towards the electrodes. It can be hypothesized that such water movement may induce

negative pore water pressure in the soil mass and in effect causes settlement of the sample. However, no pore water pressure transducer can be installed in this experiment due to the high electric potential. Thus the hypothesis cannot be proved in this experiment. Nevertheless, this hypothesis can be supported by the settlement behaviour and the conventional consolidation test results in the latter part of this chapter.

12.2 Settlement

As shown in Figures 11.6, 11.7 and 11.10 of Chapter 11, the shapes of the settlement curves are different from that of the conventional consolidation test. Unlike the case in electro-osmosis, the settlement value in the dielectrophoretic treatment tended to increase at a constant rate over time: the longer the treatment time, the higher the settlement value. This observation indicates that the efficiency of dielectrophoretic treatment in soil is better than the electro-osmotic treatment. The soil properties may be improved to a greater extent by dielectrophoresis.

The result also suggested that, the higher the applied electric potential and the deeper the electrode depth, the higher the settlement. This observation tends to correlate with equation (10.19), in which the dielectrophoretic force increases with the applied electric potential. For the effect of electrode depth, the higher settlement corresponding to the deeper electrode depth is due to the large volume of the soil mass treated. Since the soil mass used in the

experiment is limited in size, more water particles can be extracted from the soil mass in the same period of treatment time. Consequently, higher settlement is resulted.

The effect of electrode depth to settlement is further analyzed by plotting the percentage settlement (δ/h, where δ is the settlement and h is the sample height) against the electrode depth to sample height ratio (d/h, where d is the electrode depth), as shown in Figures 12.2 and 12.3 for Wallaceburg clay and Gloucester clay respectively. The figures indicate that there is a linear relationship between the normalized settlement and the normalized electrode depth. Such relationship is also noticed when the percentage settlement is plotted against the applied voltage for the case of Gloucester clay, as shown in Figure 12.4. Furthermore, this relationship provides an approximate method to estimate settlement of a soil sample treated under an applied electric potential within the range of the voltage used in this experiment. When compared with Figure 7.8 of the electro-osmotic tests, both processes have the similar trend of linear relationship between settlement and applied electric potential. As explained in section 7.2, the induced negative pore water pressure at equilibrium in electro-osmosis varies linearly with the applied voltage. If the same concept can be applied in dielectrophoresis, it may be hypothesized that the settlement of the treated sample would be due to the generation of negative pore water pressure. However, more experimental and theoretical analysis are required to support this hypothesis.

In addition to the linear relationship, it was also observed that the measured settlement of each settlement pin was approximately the same during the treatment, indicating that the soil was treated uniformly.

12.3 Shear Strength and Moisture Content

The changes of shear strength and moisture content are the most important consideration in this experimental study. As shown in Table 11.2, the increase in shear strength was as high as 966 % for the treatment on Wallaceburg clay under 20 kV (28 days of treatment) and 150 % for Gloucester clay under 25 kV (21 days of treatment). This result indicates that the effectiveness of the dielectrophoresis treatment may be better than that of the electro-osmotic treatment.

After the treatment, the shear strengths and moisture contents were measured at various depths and at various locations within the soil sample to examine the uniformity of treatment. In general, several measurements of shear strength and moisture content were made at each level of depth. It was observed that the measurements showed only ± 3 % of variation, indicating that the soil was treated uniformly. The average values are presented in Table 11.2

The increase in shear strength and decrease in moisture content for the Wallaceburg clay samples are further plotted as function of electrode depth to sample height ratio, as shown in Figures 12.5 and 12.8 respectively. Similar plots for Gloucester clay samples are also illustrated in Figures 12.6 and 12.9.

As in the case of settlement, a linear relationship is again obtained: the deeper the electrode, the larger volume of the soil can be treated and the better is the improvement of the soil properties (increase in shear strength and reduction in moisture content). In Figures 12.7 and 12.10, the relationship between the shear strength increase and moisture content reduction with the applied voltage are plotted respectively for the Gloucester clay. The figures indicate that the improvement of the soil properties is a linear function with the applied electric potential. In combining the Figures 12.6, 12.7, 12.9 and 12.10, a linear relationship between the shear strength increase (in log scale) and moisture content decrease can also be established, as shown in Figure 12.11. Such relationship follows very well the principle of classical soil mechanics, implying that the dielectrophoretic strengthening of clay is mainly due to the extraction of pore water from the soil mass. The pore water extraction may lead to the generation of negative pore water pressure resulting in the consolidation of the soil. The effect of dielectrophoresis to the consolidation of soil, especially to the preconsolidation pressure, will be investigated by performing one-dimensional consolidation tests and the test results will be discussed in section 12.5.

12.4 Stress-Strain Behaviour and Sensitivity

Unconfined compression tests were conducted on the Gloucester clay samples after treatment to study the changes in the stress-strain behaviour. Due to the limitation of the sample size, only a small cylindrical sample of 25 mm

in diameter and 50 mm in length can be recovered for the test. Since the volume of the treated soil for test G10KV2, G18KV2 and G25KV2 is too small (only 50 mm or 2" of the soil was treated), the unconfined compression test could not be performed for these samples. The stress-strain curves before and after treatment for samples G10KV6, G18KV4, G18KV6, G25KV4 and G25KV6 are plotted consecutively in Figures 12.12 to 12.16 and the corresponding test results are summarized in Table 12.1. The test results indicate that the post-peak strength increased substantially. For example, in test G25KV6, the brittleness index (I_B) decreased from a value of 0.41 before treatment to a post-treatment value of 0.07. The undrained moduli were also increased by about 3 times the initial value. Furthermore, the sensitivity of the soil also decreased, as shown in Table 12.2. The sensitivity decreased by around 25 to 87 % for the Gloucester clay samples. The dielectrophoretic treatment is therefore useful in improving the overall soil properties of the soft sensitive clay.

12.5 Consolidation

Conventional consolidation tests were performed on the Gloucester clay samples before and after treatment. The test results are summarized in Table 12.3. The preconsolidation pressure of the clay increased by 6 kPa for sample G10KV2 to a maximum of 51 kPa for sample G25KV6, corresponding to the increase of 10.5 % and 58.6 % respectively. With the exception of sample G25KV4, the increase in preconsolidation pressure after treatment is higher for

deeper electrode and higher electric potential. This result is consistent with the settlement, shear strength, moisture content and unconfined compression test results. For the ease of comparison, the consolidation curves are plotted as the change of void ratio (Δe) against the applied pressure (log scale) for the eight Gloucester clay samples after treatment in Figure 12.17. It can be seen from the figure that the soil is less compressible for the more intensive treatment. In addition, it also indicates that the soil is "over-consolidated" by the electric field, which is analogous to the mechanical dead load acting onto the soil. The mechanism of dielectrophoresis is therefore due to the removal of moisture in the pore volume of the soil mass and consequently the soil consolidates.

12.6 Physical and Chemical Changes

Table 12.4 summarizes the test results of plastic limits and liquid limits of the Wallaceburg and Gloucester clay samples before and after treatment. Similar to the electro-osmosis test, there were practically no change in plastic and liquid limits for the Wallaceburg clay. There was a slight increase in liquid limits for the Gloucester clay samples but the plastic limits remained unchange.

Chemical tests such as carbonate content, salinity and pH value tests were also performed to study the chemical changes (Table 12.5). The carbonate content of the Wallaceburg clay increased drastically from an average of around 7 % to around 22 %, resulting in an increase of approximately 3 fold. For the Gloucester clay, the carbonate content increased from an average of 2.5 % to

7 % with an increase of approximately two fold. The higher carbonate content in the soil contributes to a better cementation bonding of the soil particles. As a result, the soil has higher shear strength and lower sensitivity.

The salinity of the Wallaceburg clay also increased two times from an average of 3.2 g/l to 6.5 g/l. For the Gloucester clay, the salinity increased from an average of 1.35 g/l to 2.15 g/l. The increase in salinity was mainly due to the reduction of moisture content and consequently increased the electrolyte concentration. Unlike the electro-osmotic treatment, the pH values of the soil after treatment were practically unchanged.

It should be noted that, in dielectrophoresis, the high voltage electrodes are not in contact with the soil. Therefore, the electro-chemical reaction such as electrolysis is unlikely to take place. Furthermore, the unchanged pH value of the soil after treatment provides an indication that there is no decomposition of the water molecule into hydrogen ion and hydroxide ion. However, there may exist other of electro-chemical reactions in the sample during the process due to the presence of the electric field. A detailed electro-chemical analysis should be carried to investigate the mechanism chemically but this study is outside the scope of the present research.

12.7 Crack and Shrinkage

Cracks were observed in the Gloucester clay samples a few days after the treatment. A typical pattern of crack is shown in Figure 12.18. At this early

stage of treatment, it is possible that the crack formation may be due to the decrease in moisture content of the centre part of the soil near the high voltage electrode, while the moisture content of the soil near the ground electrodes at the cylinder surface remained the same. This results in the differential radial shrinkage at the centre of the cylinder and hence creates the tensile force which cracked the soil mass. This explanation is further supported by the slightly wider crack width at the part near the centre (Figure 12.18), indicating that the crack propagated in the direction from the ce .ire outward. Furthermore, all the cracks were vertical down to the same level as the high voltage electrode. However, no crack was observed in the Wallaceburg clay.

Unlike the electro-osmosis, the formation of crack may not affect the dielectrophoretic process. This is due to the fact that water is removed by the electric field rather than by electric current. Nevertheless, the effect of crack formation will be less serious in the field due to the infinite soil mass and the larger volume of water in the soil.

12.8 Implication of Model Test

It was demonstrated that the electrical configuration of the model test (Wallaceburg clay) described in section 11.4 is possible for field application. The electrodes can be installed by drilling a hole in the soil and leaving a gap between the electrode and the soil. The ground electrode is simply a copper pipe which reduces the costs for the electrode.

The test results of the decrease in moisture content and increase in shear strength are further plotted with the electrode spacing, as illustrated in Figures 12.19 and 12.20. The linear relationship of these figures are also obtained. The figures indicate that the closer the electrode spacing, the higher be the moisture content reduction and higher the shear strength increase. The test results obtained in this model test indicate that the same design of electrode configuration may function satisfactory in the field. As shown in the lifetime test in section 11.5, the heavy duty high voltage electrode may be suitable for the long term field treatment under high electric potential.

Table 12.1 Summary of Unconfined Compression Test Results of Gloucester Clay Samples Before and After Treatment

Test No.		Peak Shear Strength (kPa)	Failure Strain (%)	Brittleness Index, I_B	Undrained Modulus (kPa)
G10KV6	initial	17.9	2.2	0.55	1250
	after	20.8	2.6	0.25	2330
G18KV4	initial	19.8	1.2	0.47	2450
	after	26.3	2.2	0.24	3690
G18KV6	initial	15.9	2.2	0.36	1660
	after	21.0	2.4	0.21	2550
G25KV4	initial	15.2	2.2	0.33	1250
	after	36.8	2.8	0.11	5630
G25KV6	initial	25.2	2.3	0.41	2540
	after	60.2	4.8	0.07	6250

Note: undrained modulus obtained at half peak strength

Table 12.2 Comparison of Sensitivity of Gloucester Clay Samples Before and After Treatment

Test No.	Initial Sensitivity	Post-Treatment Sensitivity	Percentage Decrease (%)
G10KV2	100	70	30
G10KV6	100	70	30
G18KV2	20	6	70
G18KV4	20	15	25
G18KV6	20	10	50
G25KV2	90	21	77
G25KV4	60	15	75
G25KV6	60	8	87

Table 12.3 Comparison of Pre-Consolidation Pressure of Gloucester Clay Sample Before and After Treatment

Test No.	Pre-Treatment kPa	Post-Treatment kPa	Net Increase kPa	Percentage Increase %
G10KV2	57	63	6	10.5
G10KV4	44	53	9	20.5
G18KV2	35	47	12	34.3
G18KV4	38	52	14	36.8
G18KV6	43	62	19	44.2
G25KV2	65	97	32	49.2
G25KV4	49	94	45	91.8
G25KV6	87	138	51	58.6

Table 12.4 Comparison of Plastic and Liquid Limits of Samples Before and After Treatment

Test No.	Pre-Treatment		Post-Treatment	
	PL (%)	LL (%)	PL (%)	LL(%)
W20KV3	20.0	46.6	22.2	42.4
W20KV5	20.8	43.7	18.1	45.1
W20KV7.5	22.4	39.2	20.2	41.2
G10KV2	22.7	42.9	24.0	47.2
G10KV6	25.3	56.5	21.7	58.4
G18KV2	21.1	44.3	23.8	46.2
G18KV4	21.1	44.3	22.6	45.0
G18KV6	21.1	44.3	24.4	49.8
G25KV2	25.7	46.3	26.0	50.3
G25KV4	21.1	45.6	24.7	48.7
G25KV6	25.7	46.3	23.3	51.7

Table 12.5 Summary of Chemical Test Results of Samples Before and After Treatment

Test No.	Carbonate Content (%)		Salinity (g/l)		Soil pH Value	
	Initial	After	Initial	After	Initial	After
W20KV3	7.3	20.7	3.21	5.66	7.6	7.9
W20KV5	5.8	22.8	3.21	6.41	7.4	7.7
W20KV7.5	7.7	23.0	3.14	7.32	7.2	7.7
G10KV2	2.3	3.4	1.36	1.53	8.8	8.9
G10KV6	2.4	3.8	1.33	1.59	8.7	8.9
G18KV2	5.8	6.8	1.38	1.74	8.8	8.8
G18KV4	5.8	6.1	1.41	2.47	8.9	8.6
G18KV6	6.1	7.4	1.37	2.25	8.9	8.0
G25KV2	2.6	4.8	1.31	1.92	8.6	8.9
G25KV4	2.6	6.8	1.34	2.13	8.7	8.6
G25KV6	2.4	7.9	1.31	3.59	8.8	8.9

FIGURE 12.1 PHOTO SHOWING WATER CONDENSATION ON SUPPORTING PLEXIGLAS PLATE

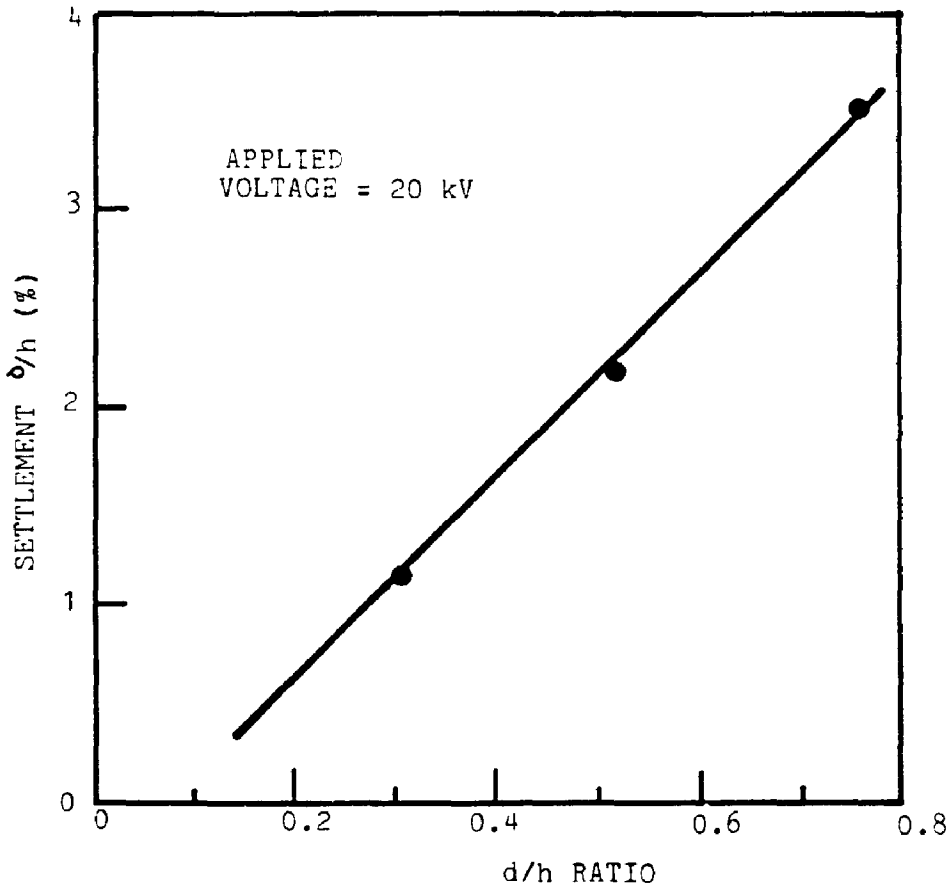

FIGURE 12.2 PLOT OF SETTLEMENT AND ELECTRODE DEPTH TO SAMPLE HEIGHT RATIO FOR WALLACEBURG CLAY

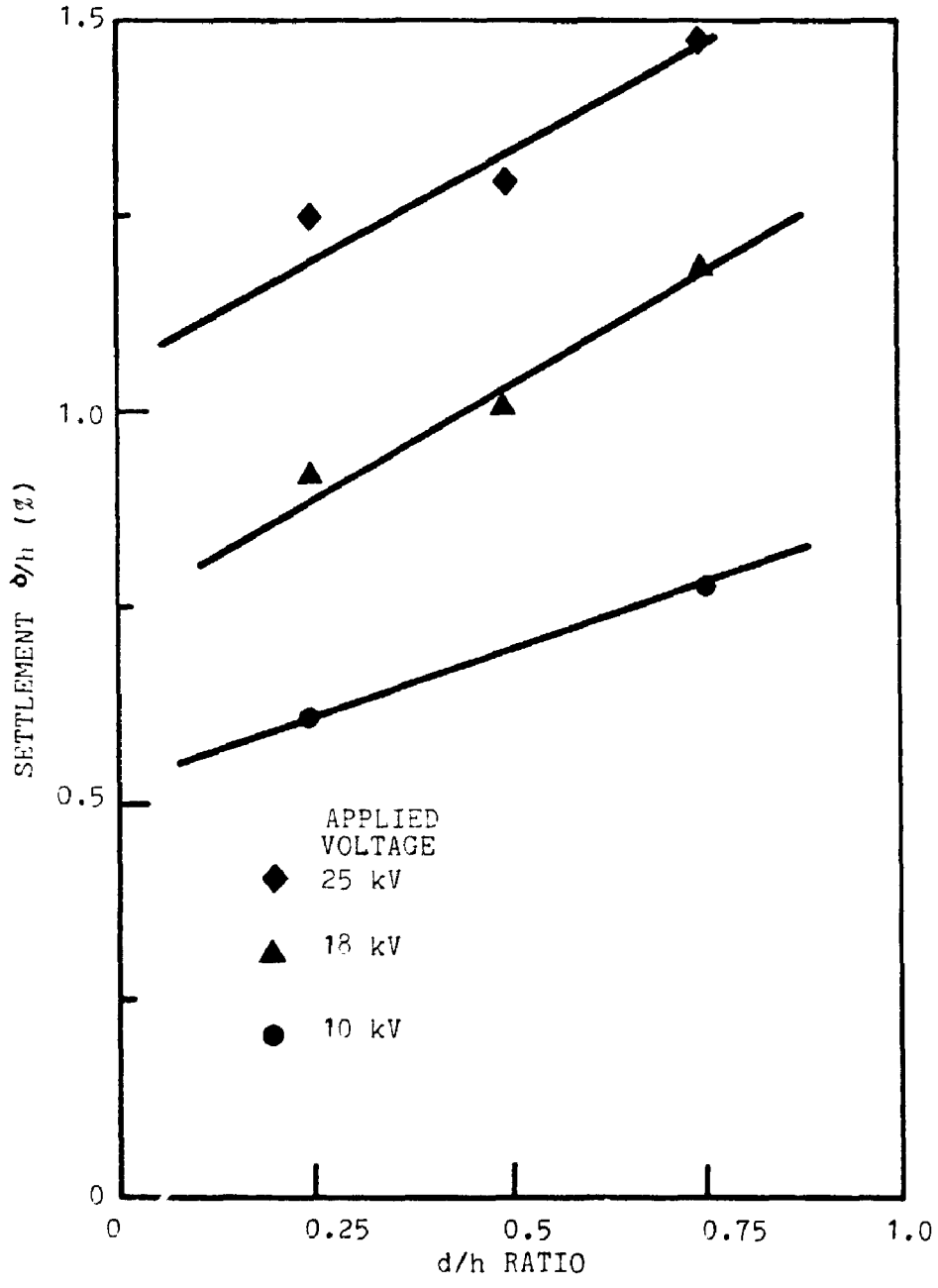

FIGURE 12.3 PLOT OF SETTLEMENT AND ELECTRODE DEPTH TO SAMPLE HEIGHT RATIO FOR GLOUCESTER CLAY

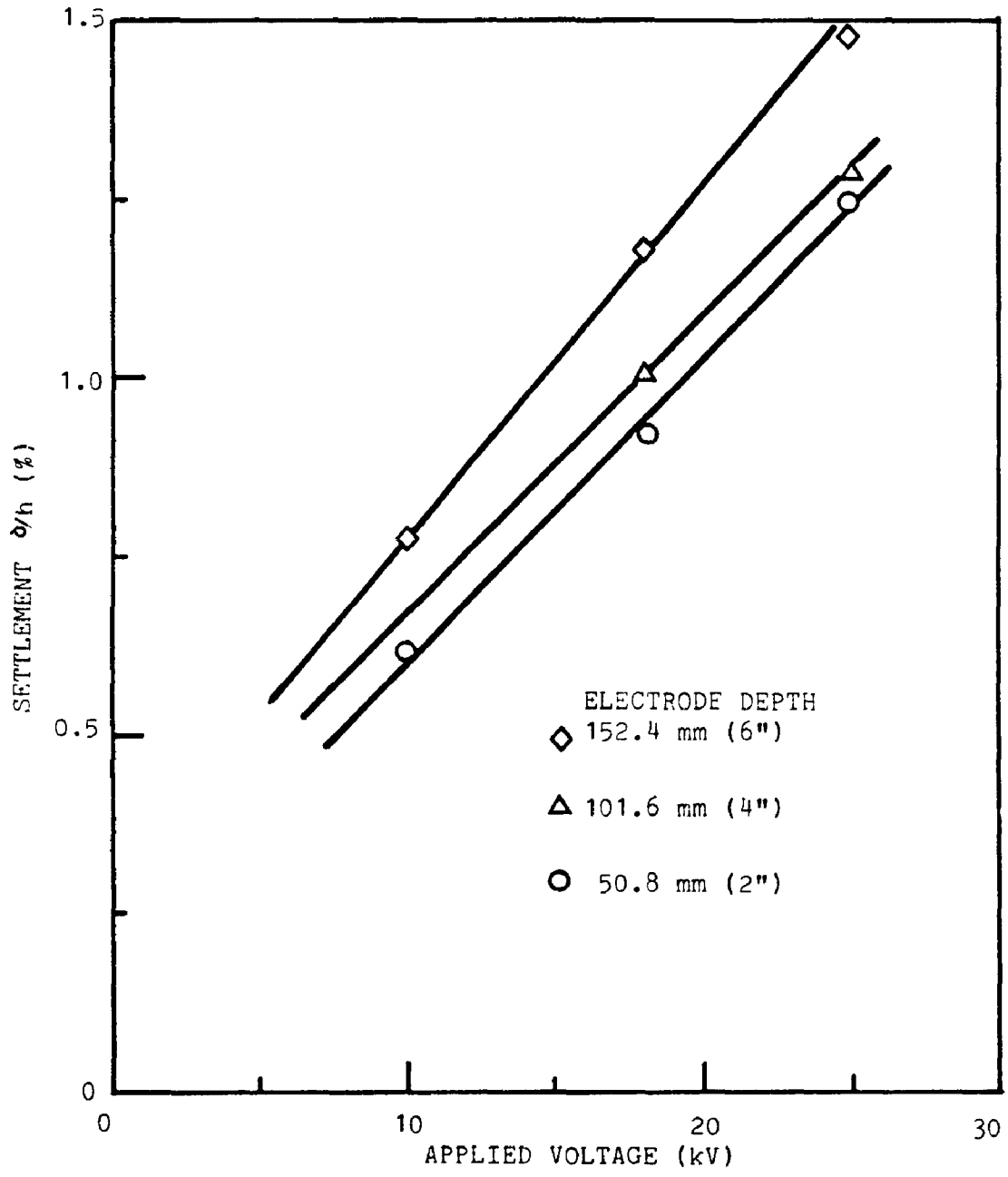

FIGURE 12.4 PLOT OF SETTLEMENT AND APPLIED VOLTAGE FOR GLOUCESTER CLAY

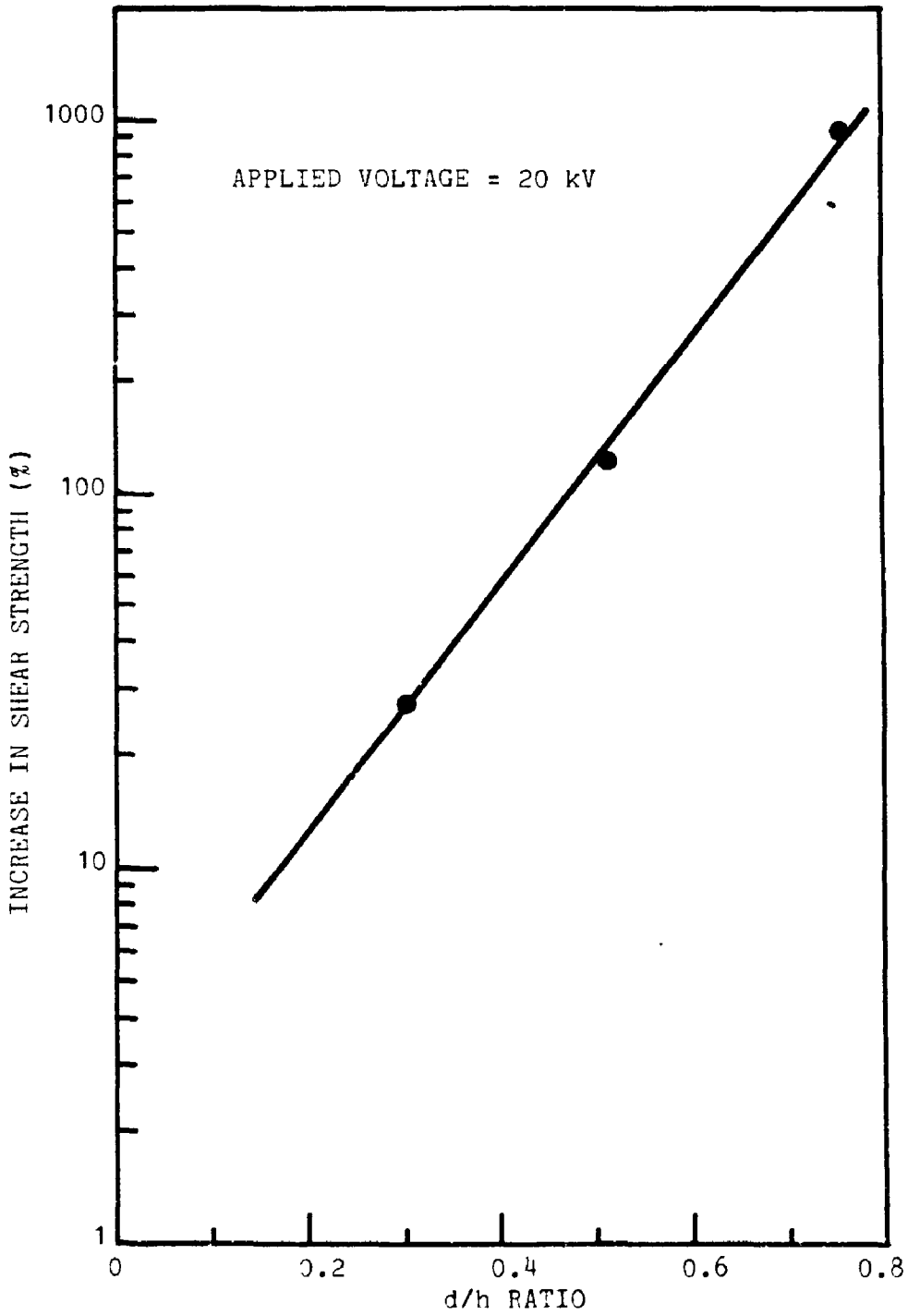

FIGURE 12.5 PLOT OF SHEAR STRENGTH INCREASE AND ELECTRODE DEPTH TO SAMPLE HEIGHT RATIO FOR WALLACEBURG CLAY

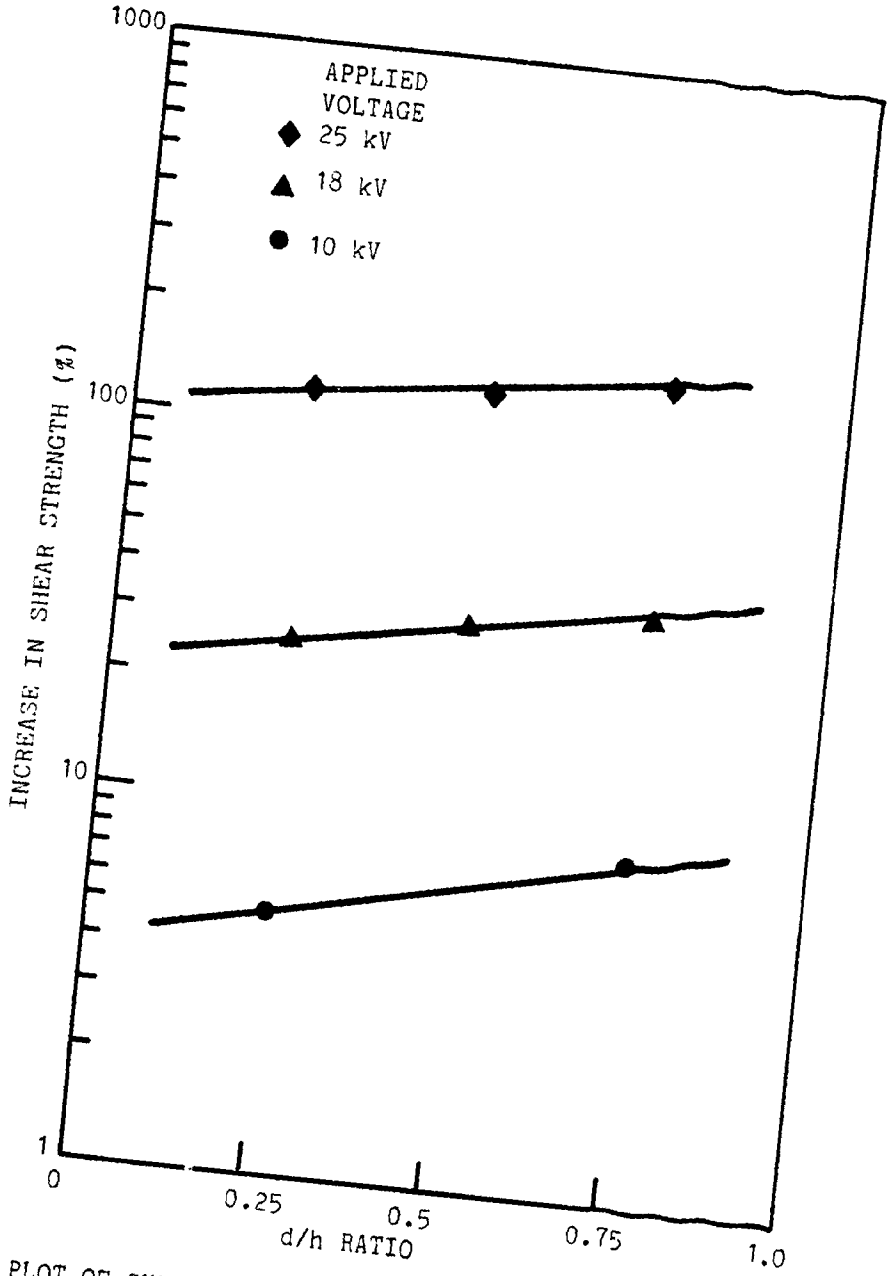

FIGURE 12.6 PLOT OF SHEAR STRENGTH INCREASE AND ELECTRODE DEPTH TO SAMPLE HEIGHT RATIO FOR GLOUCESTER CLAY

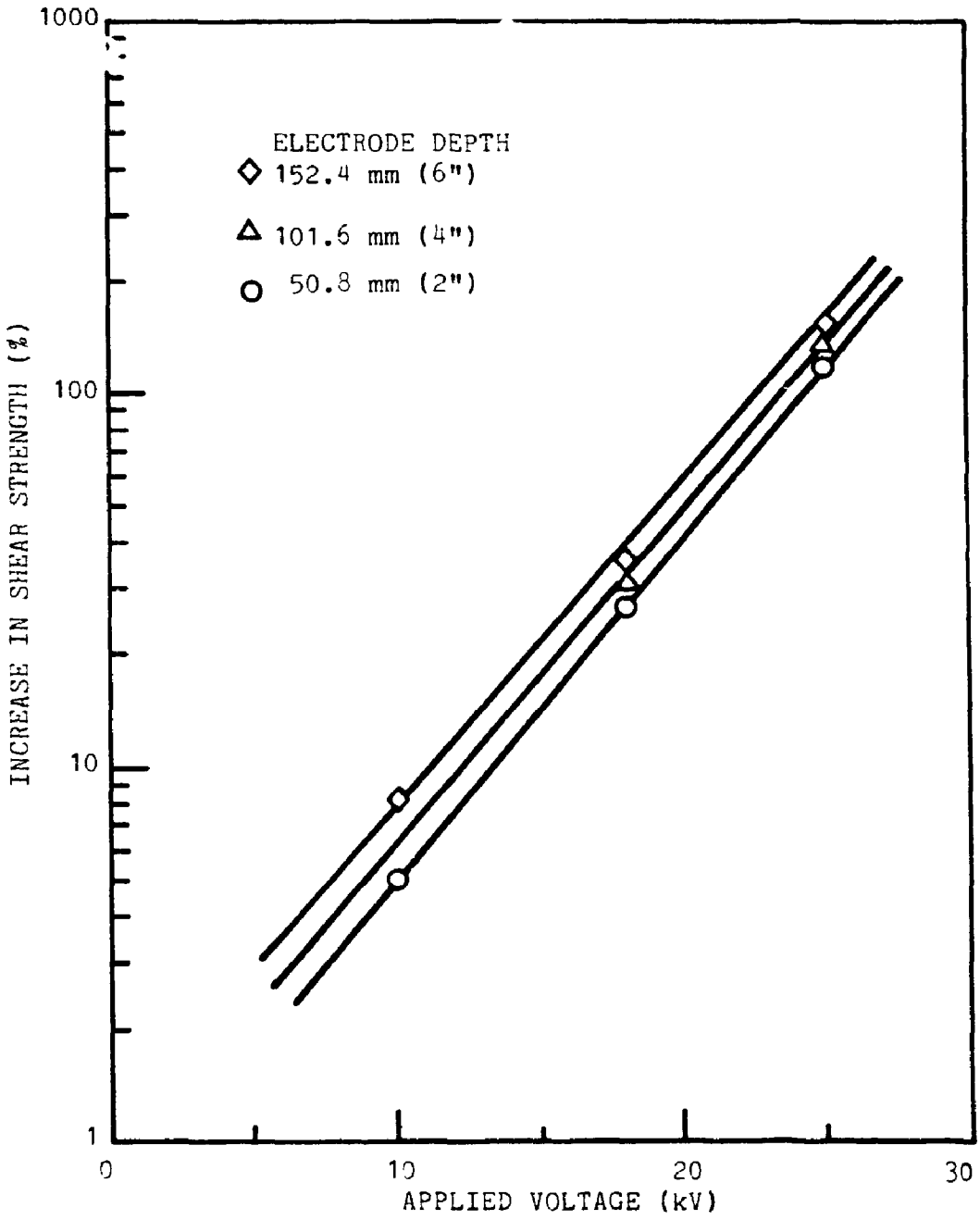

FIGURE 12.7 PLOT OF SHEAR STRENGTH INCREASE AND APPLIED VOLTAGE FOR GLOUCESTER CLAY

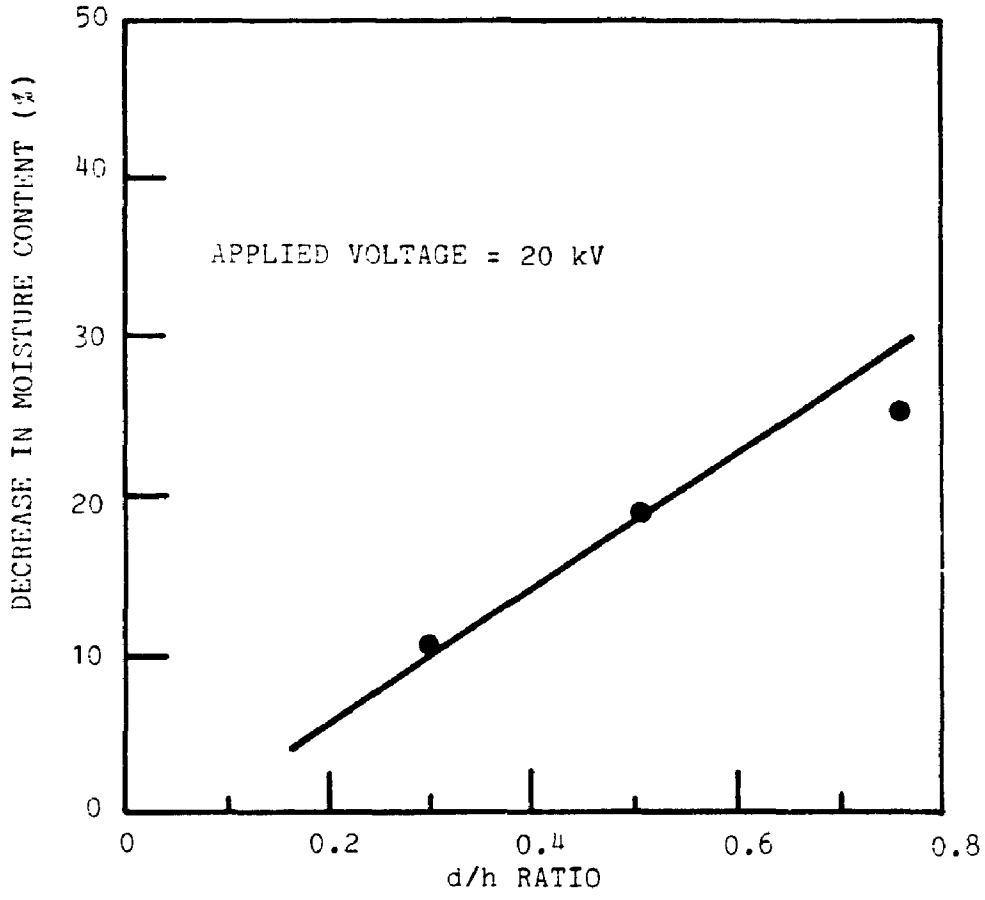

FIGURE 12.8 PLOT OF MOISTURE CONTENT DECREASE AND ELECTRODE DEPTH TO SAMPLE HEIGHT RATIO FOR WALLACEBURG CLAY

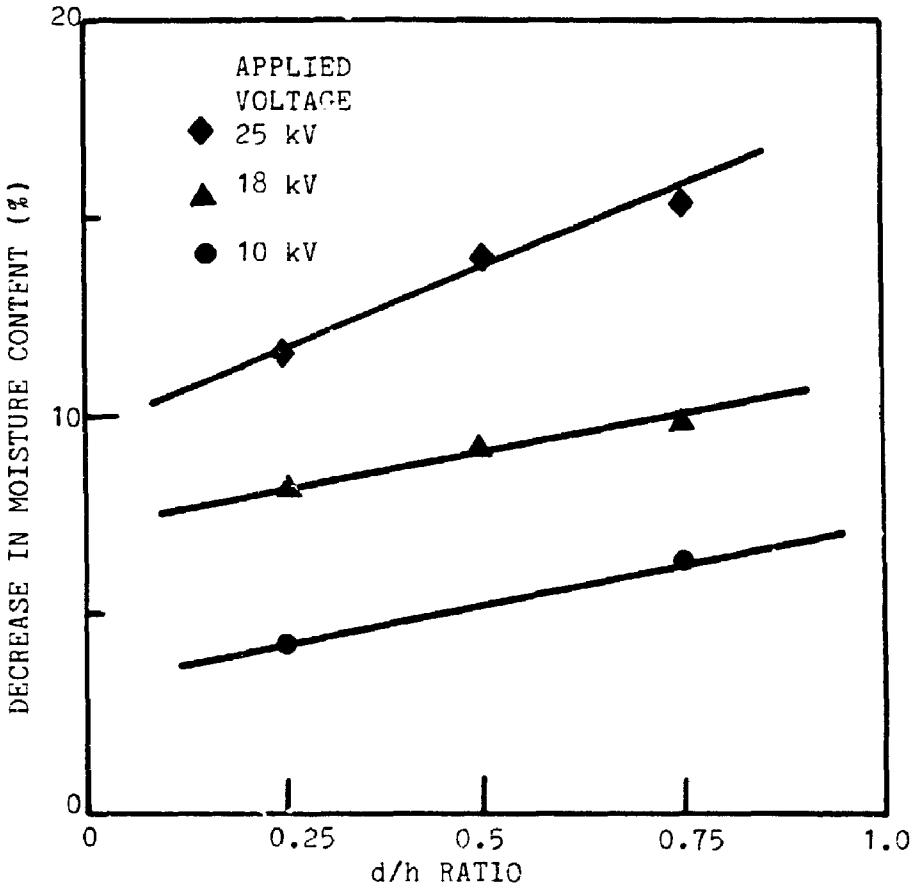

FIGURE 12.9 PLOT OF MOISTURE CONTENT DECREASE AND ELECTRODE DEPTH TO SAMPLE HEIGHT RATIO FOR GLOUCESTER CLAY

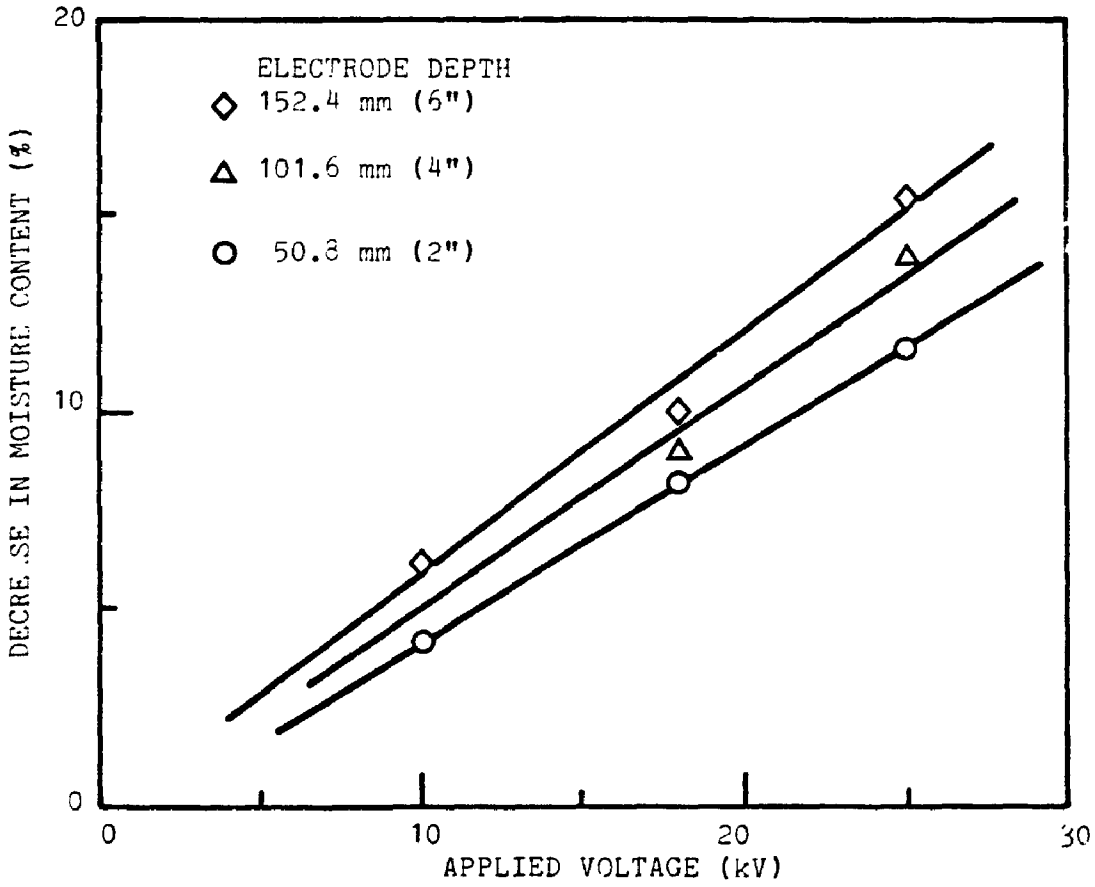

FIGURE 12.10 PLOT OF MOISTURE CONTENT DECREASE AND APPLIED VOLTAGE FOR GLOUCESTER CLAY

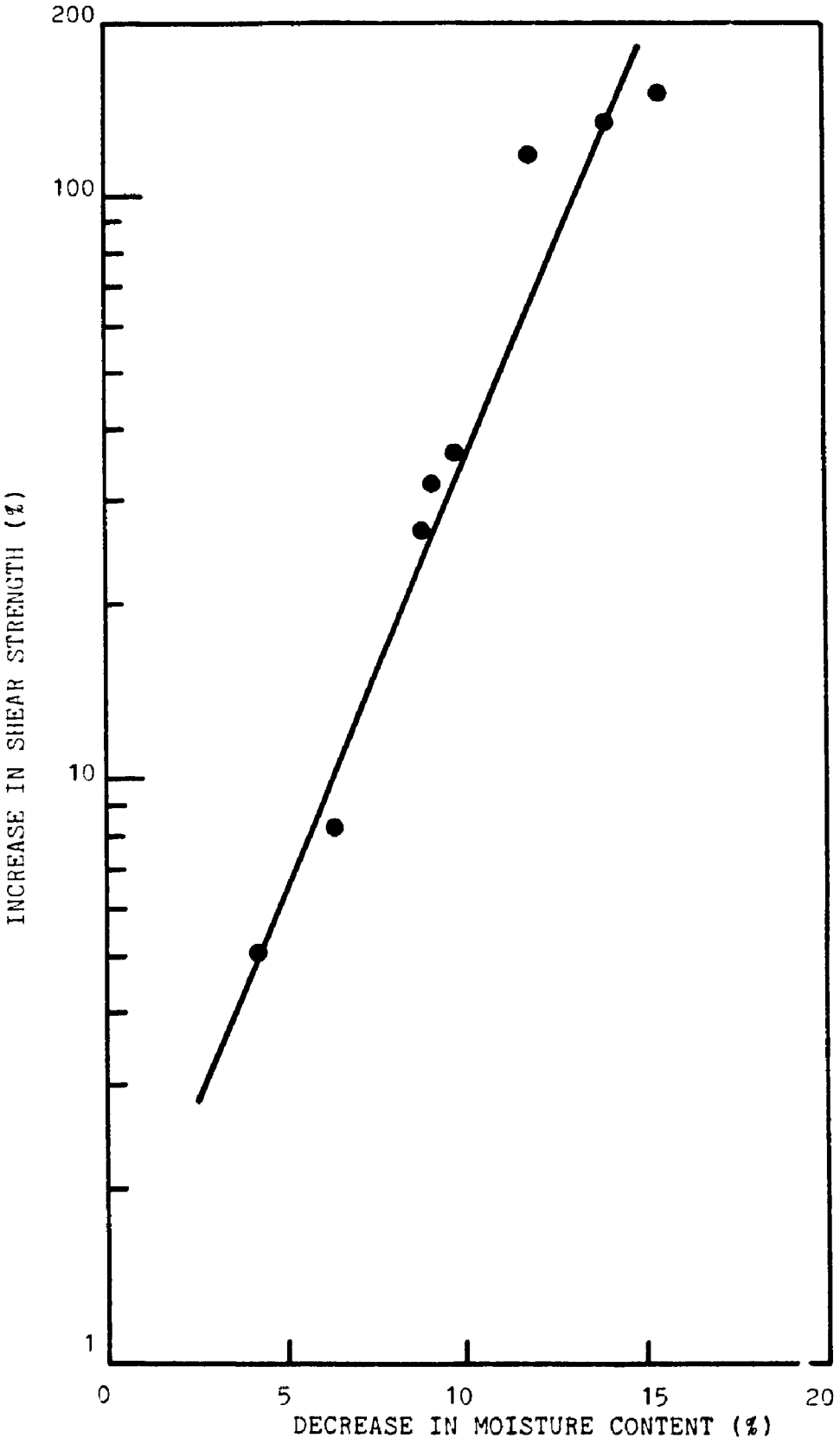

FIGURE 12.11 PLOT OF SHEAR STRENGTH INCREASE WITH MOISTURE CONTENT REDUCTION FOR GLOUCESTER CLAY SAMPLES AFTER TREATMENT

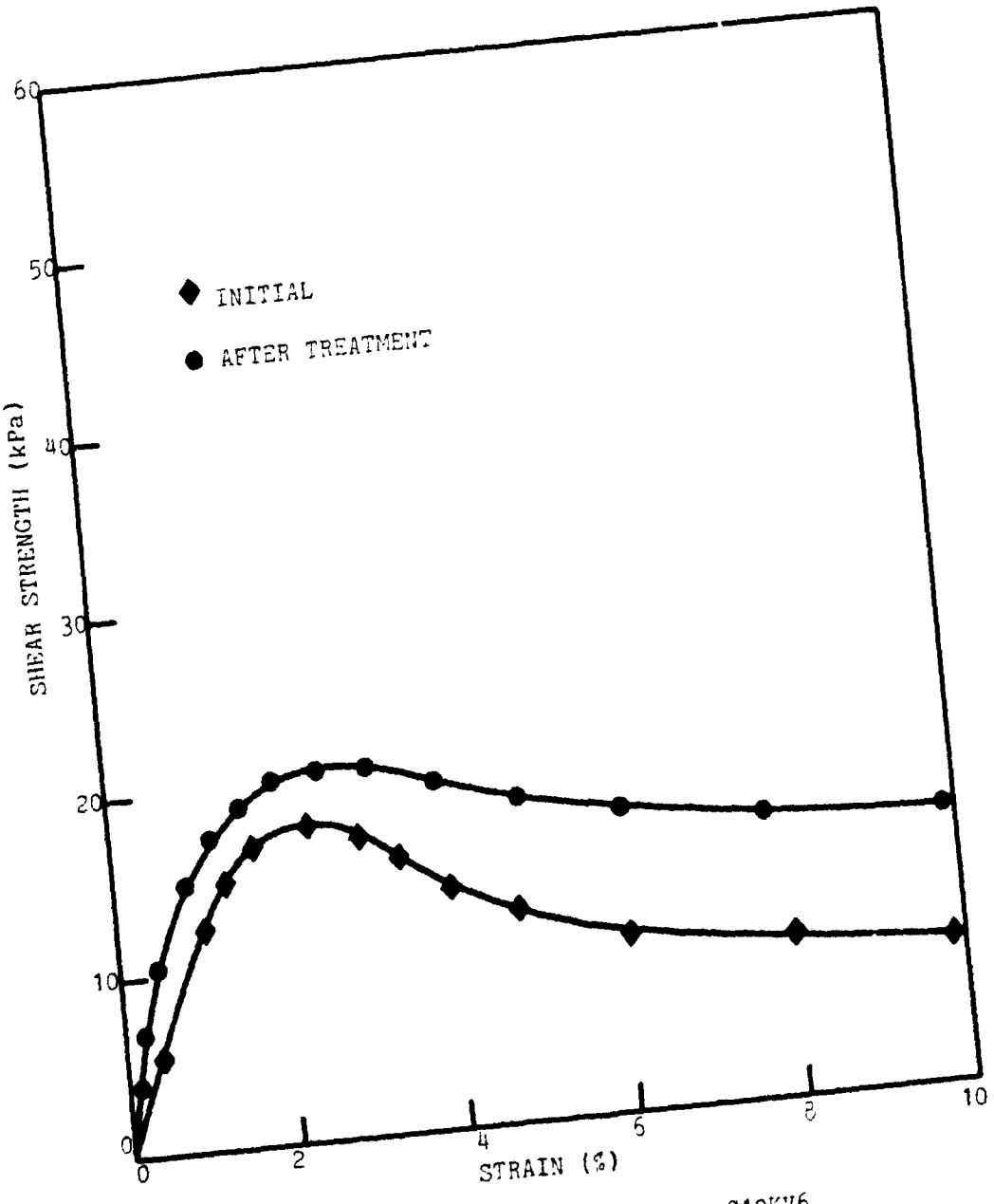

FIGURE 12.12 UNCONFINED COMPRESSION TEST OF G10KV6

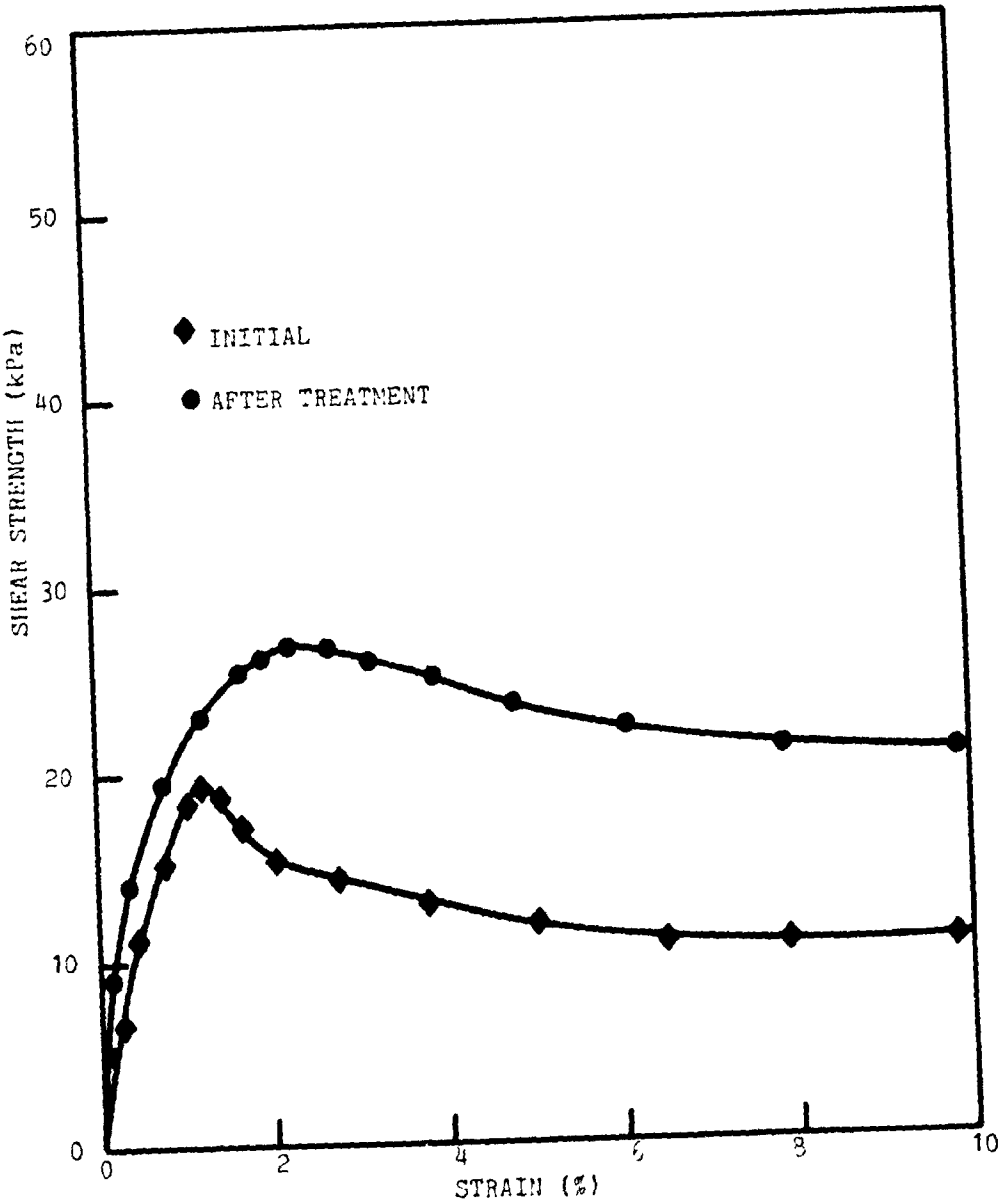

FIGURE 12.13 UNCONFINED COMPRESSION TEST OF G18KV4

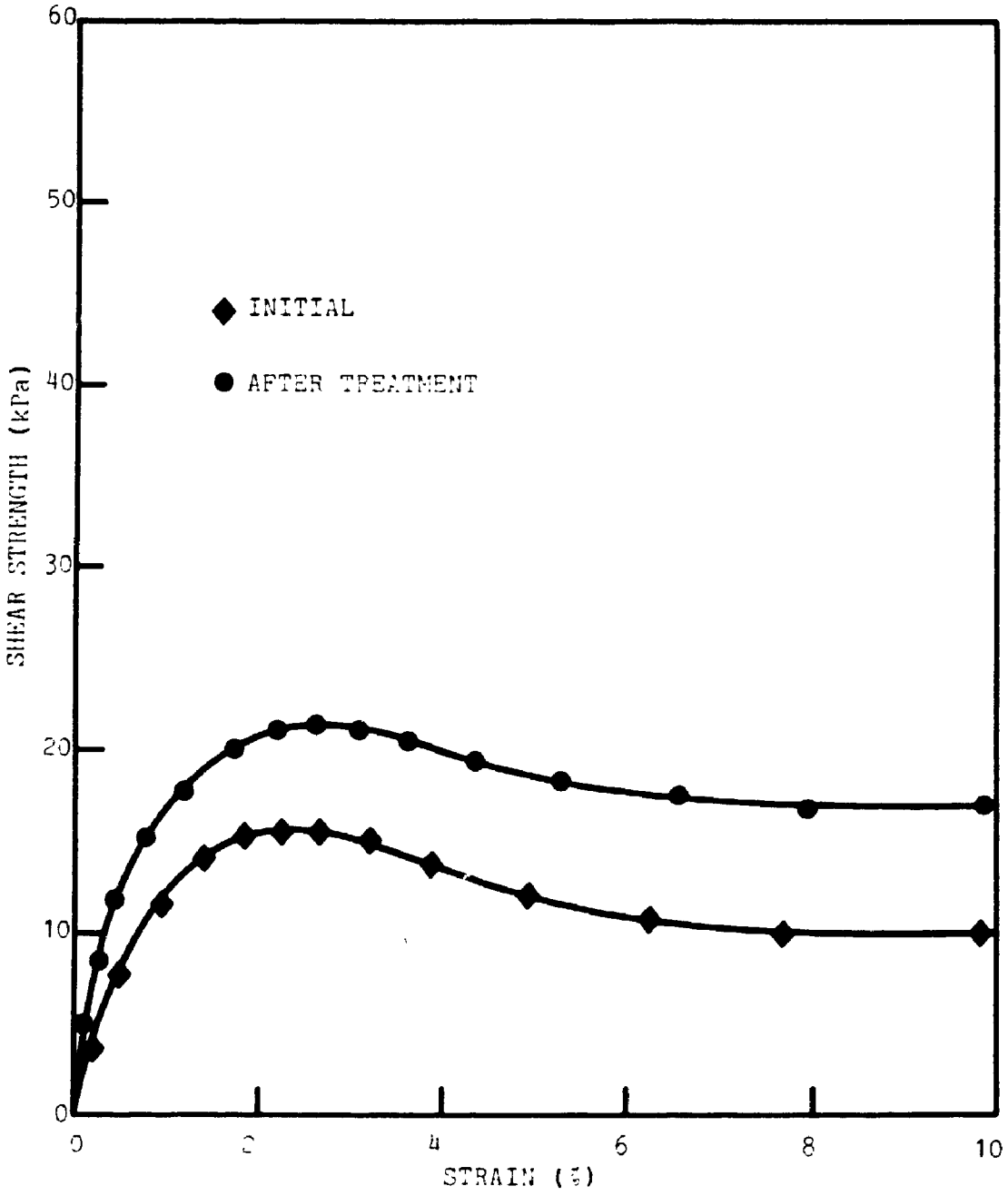

FIGURE 12.14 UNCONFINED COMPRESSION TEST OF G18KV6

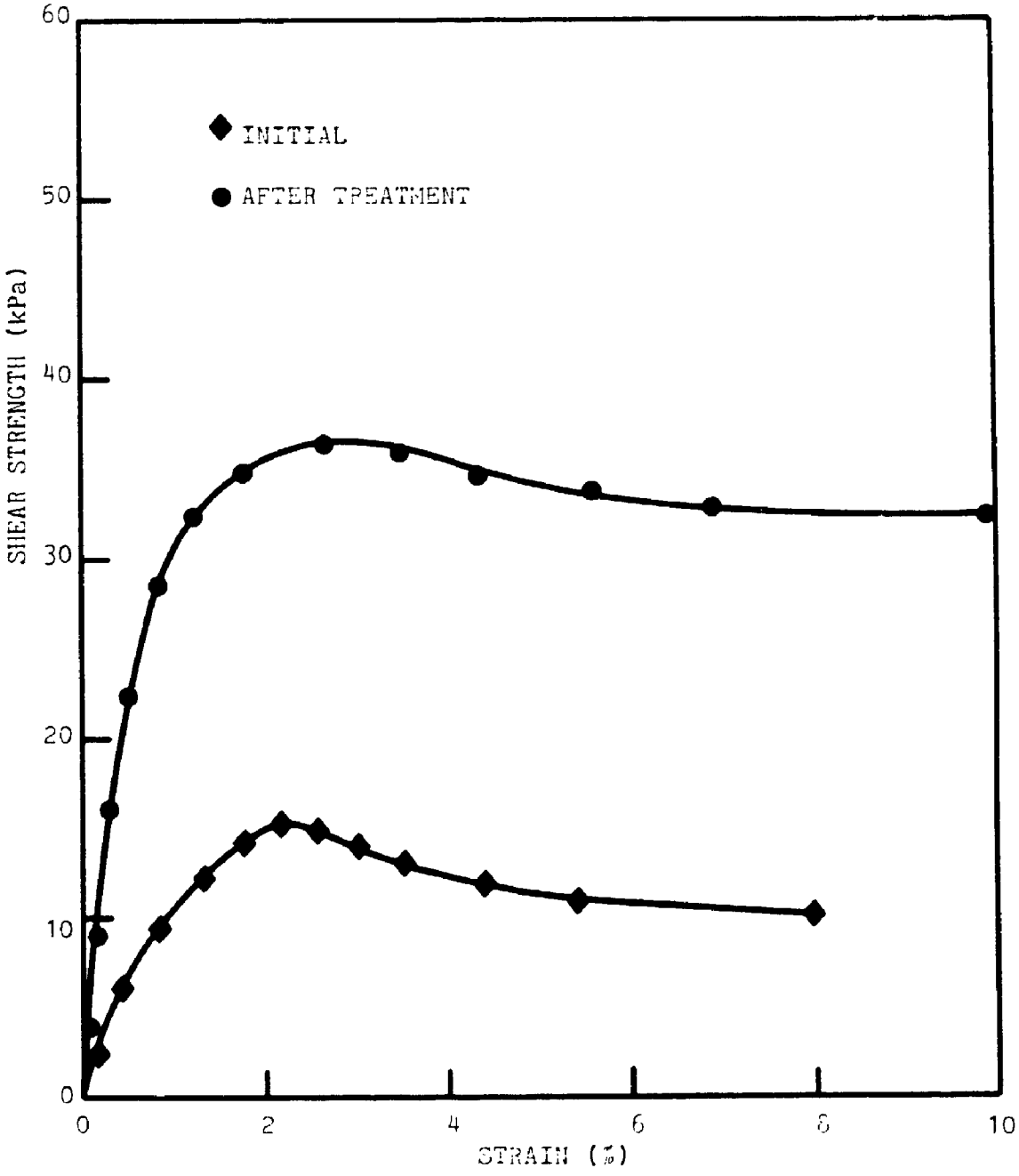

FIGURE 12.15 UNCONFINED COMPRESSION TEST OF GV25KV4

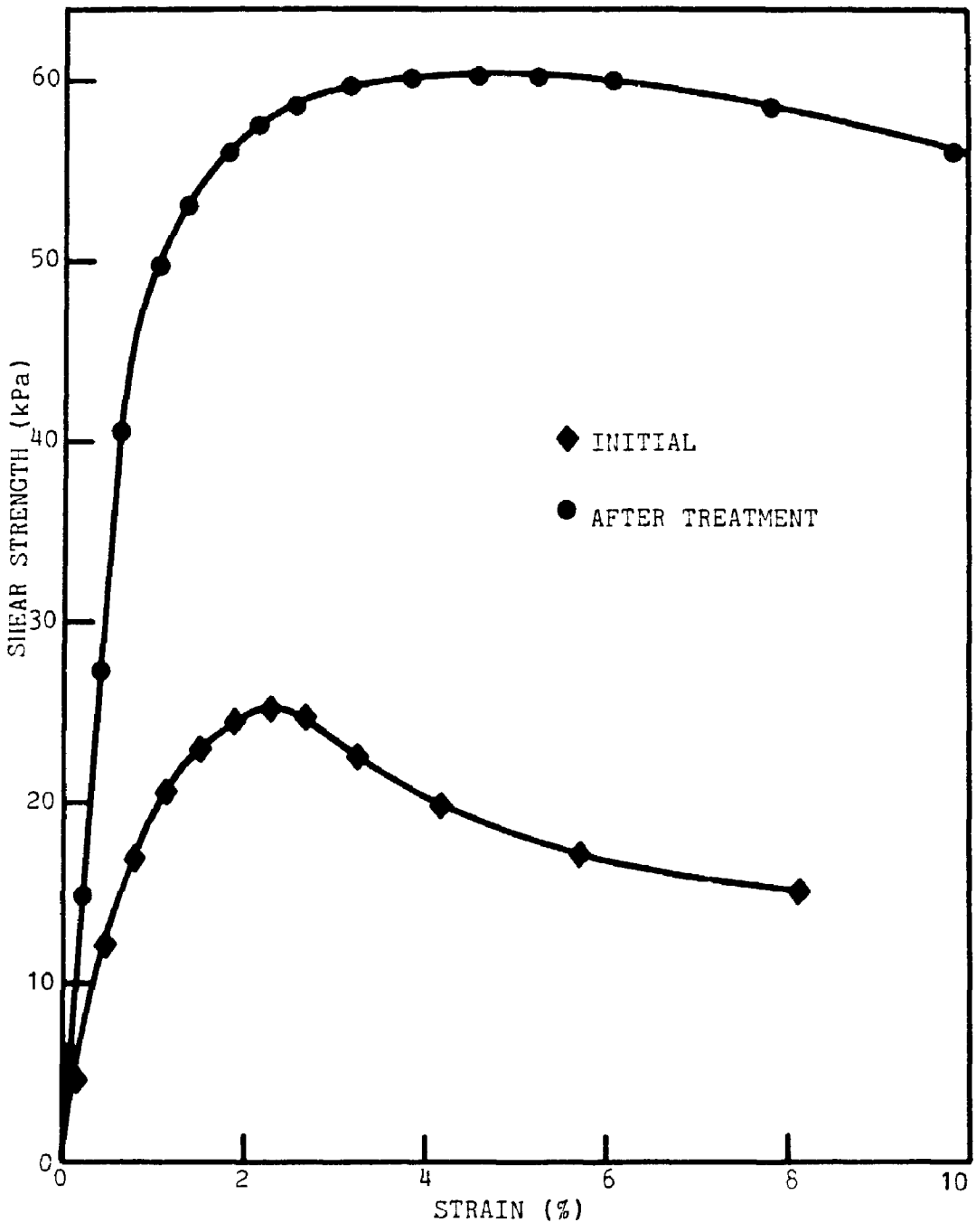

FIGURE 12.16 UNCONFINED COMPRESSION TEST OF G25KV6

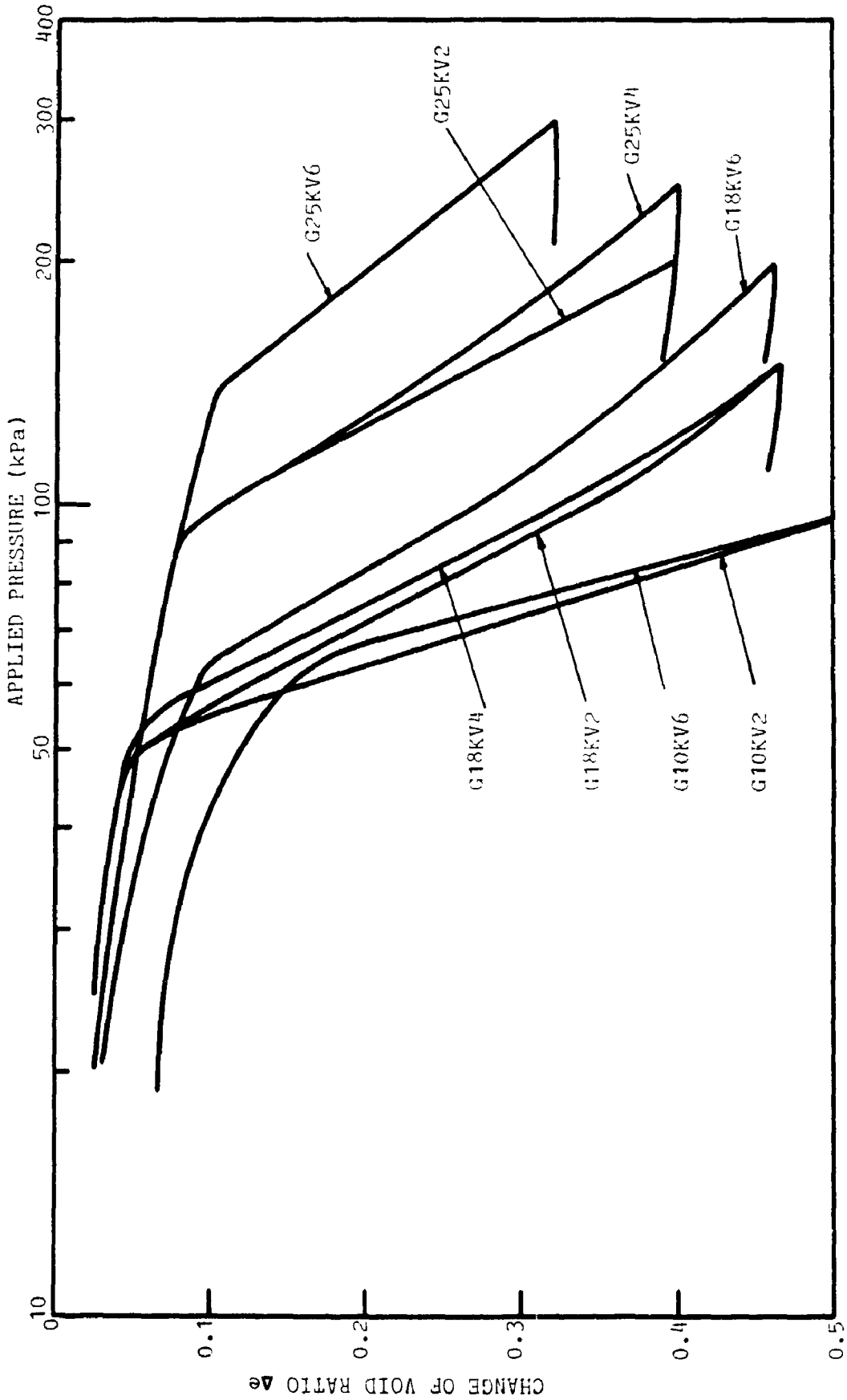

FIGURE 12.17 CONSOLIDATION CURVES FOR GLOUCESTER CLAY SAMPLES BEFORE AND AFTER TREATMENT

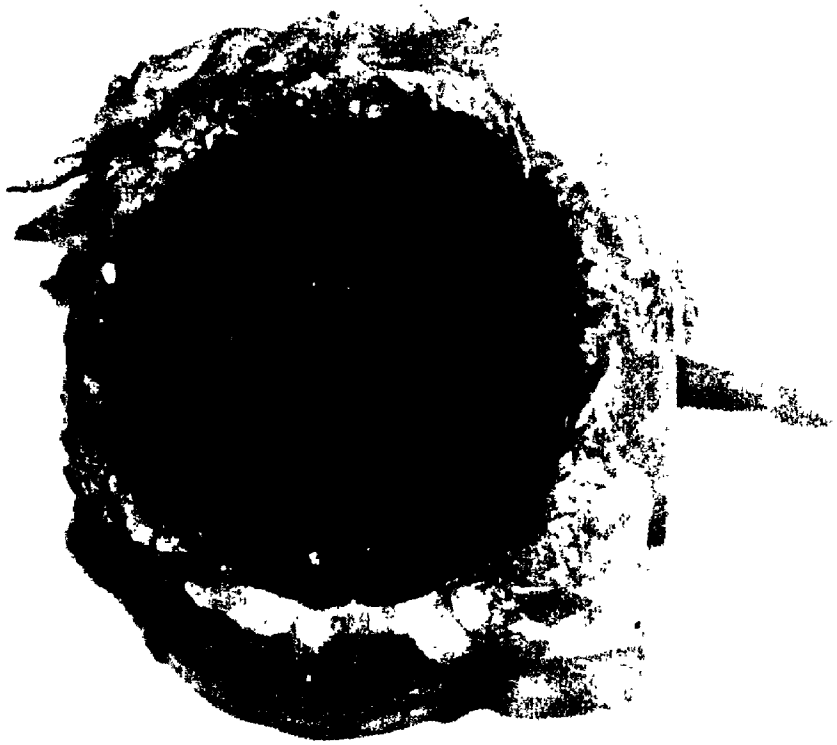

FIGURE 12.18 TYPICAL EXAMPLE OF CRACK PATTERN OF A GLOUCESTER CLAY SAMPLE AFTER DIELECTROPHORETIC TREATMENT

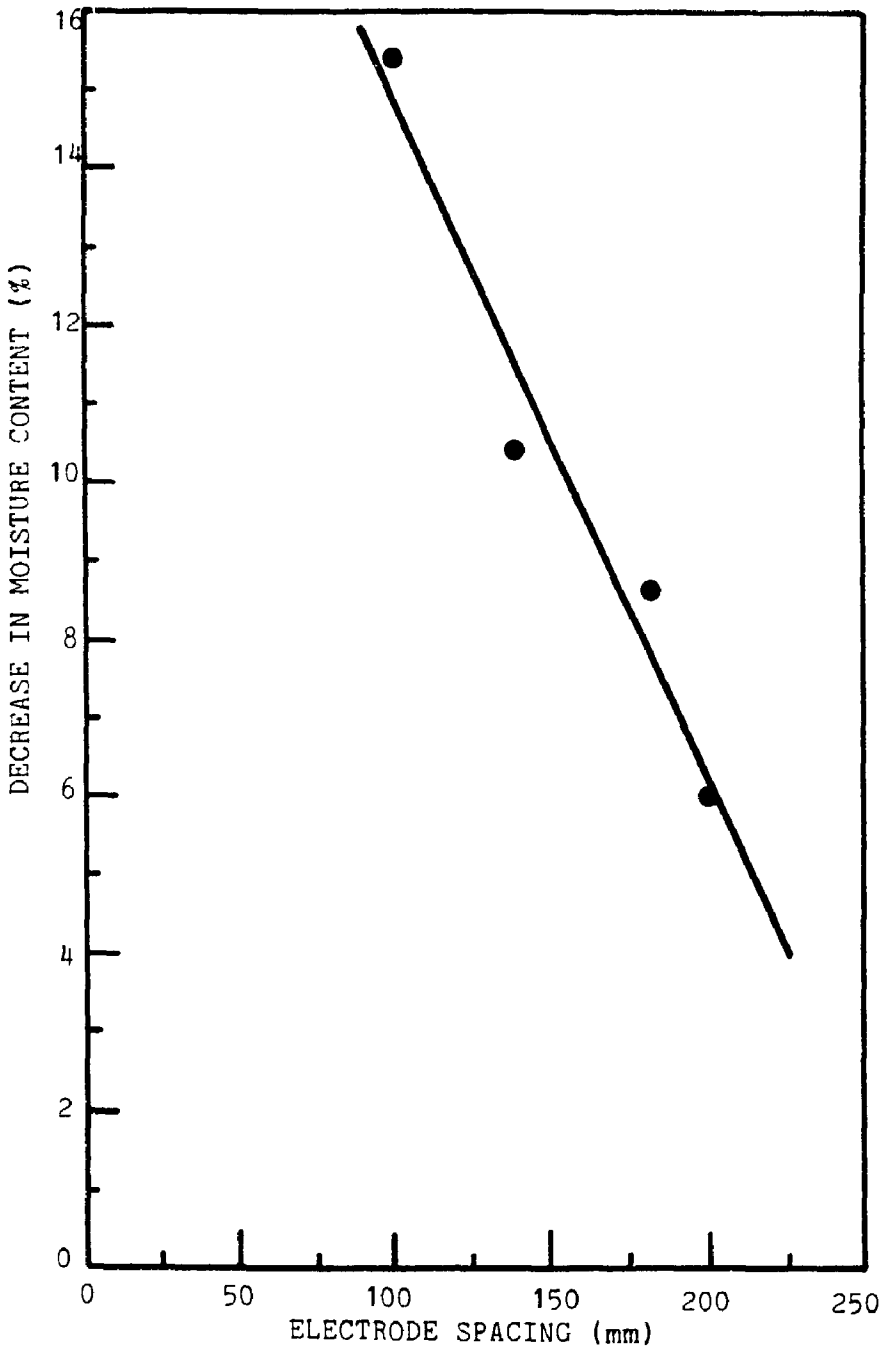

FIGURE 12.19 PLOT OF MOISTURE CONTENT DECREASE AND ELECTRODE SPACING FOR MODEL TEST (WALLACEBURG CLAY)

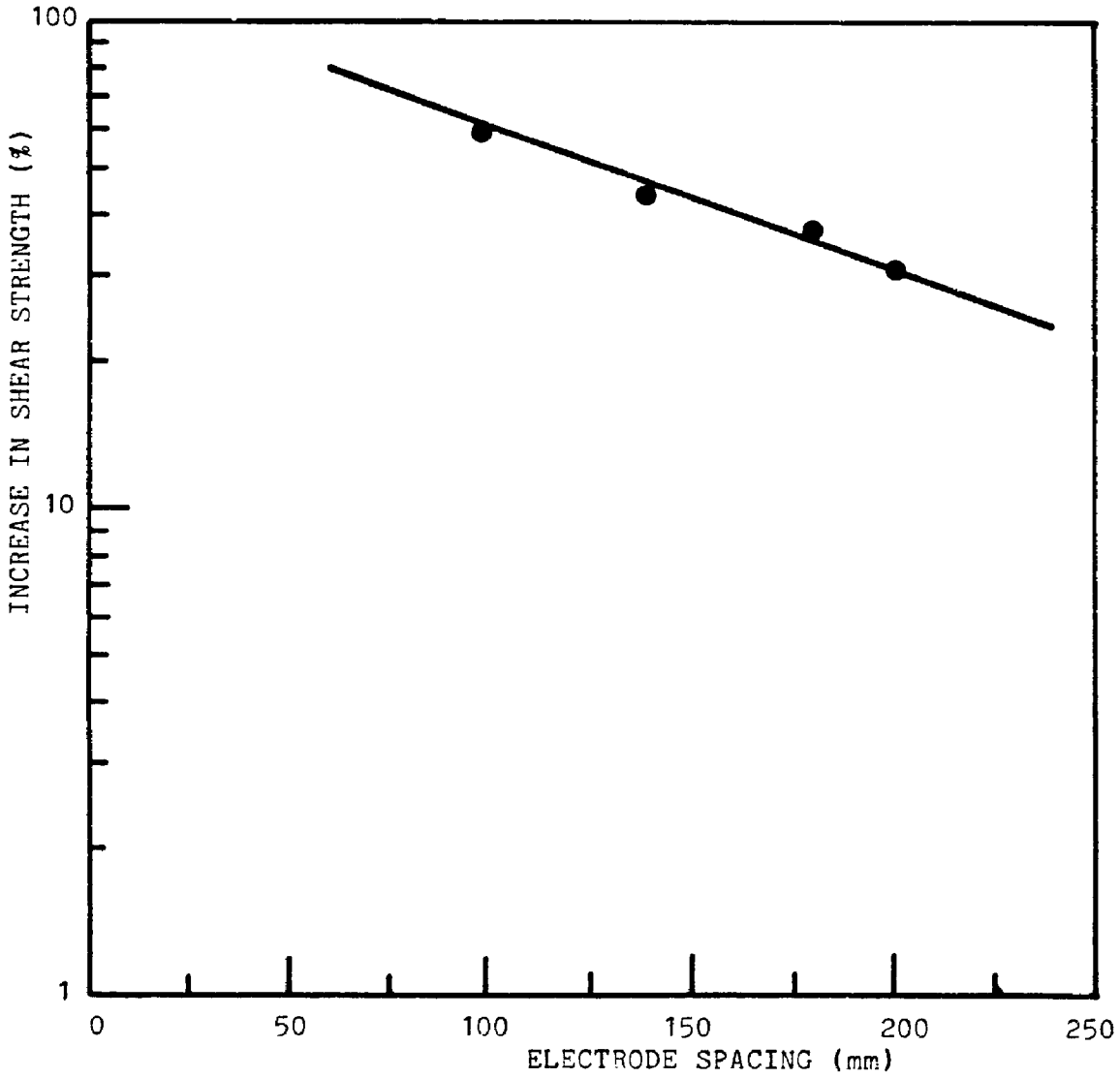

FIGURE 12.20 PLOT OF SHEAR STRENGTH INCREASE AND ELECTRODE SPACING FOR MODEL TEST (WALLACEBURG CLAY)

CHAPTER 13

CONCLUSIONS ON DIELECTROPHORESIS LABORATORY INVESTIGATION

An experimental study on the dielectrophoretic strengthening of Wallaceburg and Gloucester clays was performed by applying different voltages with different electrode depths. Laboratory tests were carried out on the samples before and after treatment to study the change of soil properties as a results of the dielectrophoretic process. From the test results, the following conclusions may be drawn.

(a) It was observed that water droplets condensed on the plexiglas plate and the ground electrode (copper rod) surface. This observation may be due to the migration of water molecules towards the converging field.

(b) Significant increase in undrained shear strength and decrease in moisture content were obtained for the soil after treatment. The shear strengths increased by 966 % for Wallaceburg clay (under 20 kV) and 150 % for Gloucester clay (under 25 kV). Concurrently, the moisture contents reduced by 24.9 % and 15.5 % for Wallaceburg clay and Gloucester clay respectively. Furthermore, the soil was treated uniformly. By comparing this improvement of soil properties with electro-osmosis, the effectiveness of dielectrophoresis is therefore evident.

(c) The results of settlement, shear strength and moisture content tests indicated that the efficiency of treatment will not drop with treatment

time (unlike in the case of electro-osmosis). There is a tendency that the clay mass, which is soft in its natural state, can be turned into a hard clay.

(d) The settlement, shear strength increase and moisture content decrease are linear function of electrode depth to sample height ratio and the applied voltage, within the test conditions employed.

(e) The overall stress-strain behaviour (brittleness index, undrained modulus and sensitivity) of the soft sensitive clay (Gloucester clay) is improved by the process.

(f) The preconsolidation pressure of the Gloucester clay (phase 2 study) after treatment has a maximum increase of 58.6 %. The increase in preconsolidation pressure due to the treatment suggests that the soil is "over-consolidated" by the alternating electric field which is analogous to the mechanical dead load acting onto the soil.

(g) The Gloucester clay has a slight increase in liquid limit after treatment but no change in plastic limit. However, there is no appreciable change in the plastic and liquid limits for the test on Wallaceburg clay.

(h) Both clays have increase in carbonate contents and salinity after treatment but no change in pH values. The bonding between soil particles is therefore improved. The unchanged pH value indicates that there is no decomposition of water molecule and the adverse effect due to electrolysis is not evident.

(i) With regard to the model test and lifetime test, it was demonstrated that the electrode configuration and the design of field electrode are possible for the field test.

Through this experimental study, it is evident that the electrical strengthening of clays by dielectrophoresis is effective and there is a considerable improvement of soil properties. Although dielectrophoresis is a new form of technology particularly in geotechnical engineering, it is definitely a powerful process for soil improvement. As one may realize in the present experimental study, most of the result cannot be explained quantitatively by the existing theory in dielectrophoresis due to the fact that the knowledge of dielectrophoresis are based on dilute solutions. Therefore, further study is necessary to develop an adequate theory for this topic. At the present moment, due to the limited data available, experiment is usually simpler to carry out to explore the process than theoretical development for the analysis of test results. This experimental investigation should therefore be considered as a front-line research to explore the potential applications of this new technique. With the experience gained here, a systematic research program with the development of suitable laboratory test apparatus may be established for further investigation. Recommendations for future research will be discussed later in chapter 19.

ELECTRICAL STRENGTHENING OF SOFT SENSITIVE CLAYS

Volume II

by

Kai Sing Ho

Faculty of Engineering Science

Submitted in partial fulfilment

of the requirements for the degree of

Doctor of Philosophy

Faculty of Graduate Studies

The University of Western Ontario

London, Ontario

September 1990

TABLE OF CONTENTS

VOLUME II

PART III : ENGINEERING APPLICATION OF ELECTRO-OSMOSIS AND DIELECTROPHORESIS - FIELD TEST

Page

LIST OF TABLES

LIST OF FIGURES

APPENDIX

NOMENCLATURE

A	area (m^2)
A_o	concentration of wall charge of clay (ionic equivalents/unit volume of pore fluid)
C	constant
CIU	isotropically consolidated undrained triaxial test
c_v	coefficient of consolidation (m^2/year)
DP	dielectrophoresis
E	electric field (V/m)
E(x)	electric field at position x (V/m)
EO	electro-osmosis
F	force (N)
F_e	dielectrophoretic force (N)
F_o	Faraday constant (9.648456×10^4 C-mol^{-1})
h	hydraulic head (m)
i_e	electrical potential gradient (V/m)
i_h	hydraulic gradient
J	current density (A/m^2)
K	dielectric constant
k_e	electro-osmotic permeability (m^2/s-V)

k_h	hydraulic permeability (m/s)
L	sample length (m)
n	porosity
N	number of capillaries
p	dipole moment (coulomb-m)
pwp	pore water pressure (kPa)
q, q_1, q_2	charges (coulomb)
q_e	flow rate due to applied electric potential (m^3/s)
q_h	flow rate due to hydraulic gradient(m^3/s)
r	radius (m)
t	time (second)
T_v	time factor in one dimensional consolidation theory
u	pore water pressure (kPa)
u_o	constant
U(t)	degree of consolidation
V	electric potential (V)
V(x)	electric potential at position x (V)
V_e	velocity of water induced by applied electric potential gradient (m/s)
V_h	velocity of water induced by hydraulic gradient (m/s)
V_t	total velocity of water induced by electric potential and hydraulic gradients (m/s)

x	distance (m)
α	polarizability, constant
ß	constant
γ_w	unit weight of water (kN/m^3)
ϵ	permittivity of the dielectric (Farad/m)
ϵ_o	permittivity of free space = $1/36\pi \times 10^{-9}$ (Farad/m)
ζ	zeta potential (V)
η	fluid viscosity (kg/m-s)
ν	pore radius (m)
$P(x)$	resistivity at position x (ohm-m)
σ_c	preconsolidation pressure (kPa)

PART III

ENGINEERING APPLICATION OF

ELECTRO-OSMOSIS AND DIELECTROPHORESIS - FIELD TEST

CHAPTER 14

INTRODUCTION

As discussed in Parts I and II of the thesis, it was shown by the laboratory investigation that the electro-osmosis and dielectrophoresis methods were effective in strengthening and consolidating the soft sensitive clay. A field test was therefore proposed and undertaken in July-August 1989 to assess the effectiveness of the two treatment techniques in strengthening the soft sensitive clay (Champlain Sea clay) in Gloucester Test Fill site. The objectives of the field tests are,

(a) to verify the applicability of the two processes for strengthening of the soft sensitive clay in the field,

(b) to develop an efficient and economical version of electro-osmosis method for engineering practice,

(c) to compare the electro-osmotic with the dielectrophoretic treatments, and

(d) to study the limitations of the two processes.

In the electro-osmotic treatment, as discussed in section 4.7.7 on the case histories, the efficiency of most of the previous treatments were quite low and

consequently resulted in long treatment time and high costs. Unsuccessful treatment was also reported. It was found from past experience that the effects of the subsoil conditions (sand and silt layers), the electrode design and the proper application of the electrode polarity reversal are the factors controlling the success of the electro-osmosis method. These factors are taken into consideration in the design of field tests. A special electrode was designed based on the model test results described in sections 6.6 and 7.10 to prevent gas accumulation around the electrode and to allow pore water in the soil to flow out from the cathode without pumping. The variations of settlement, vane shear strength and voltage distribution during treatment were monitored and tube samples were recovered before and after treatment for laboratory tests.

The dielectrophoretic treatment in this field test is a pioneer research since there is no such test performed (both in the laboratory or in the field) in the area of geotechnical engineering in the past. It is to explore from the field test, the possible field application of this technique and to accumulate experience on any problems that may be encountered. It is therefore expected that several iterations and modifications of the dielectrophoretic method may be required before it can be applied to engineering practice. Based on the results of the model test and lifetime test (sections 11.4, 11.5 and 12.8), an electrode deemed suitable for carrying high electric potential was designed for the field test. The variation of settlement and vane shear strength were also monitored during treatment.

Since 1967, a test embankment had been constructed by the National Research Council of Canada (Bozozuk and Leonards 1972, Lo, Bozozuk and Law 1976) to study the field behaviour of soft sensitive clay. The laboratory investigations of electro-osmosis and dielectrophoresis of this research project were performed on the same soft sensitive clay recovered from the same test area in Gloucester. It is therefore proposed to perform the field test in the Gloucester Test Fill site due to the existence of an extensive data base so that the experimental results of the electro-osmotic and dielectrophoretic treatments can be critically compared. It is also of both engineering and economic importance to study the soft sensitive clay of the Champlain Sea deposit which underlies a wide area in Eastern Canada.

CHAPTER 15

THE FIELD TEST - ELECTRO-OSMOSIS

The field test consists of two test areas, the electro-osmosis and dielectrophoresis test areas. The electro-osmotic treatment will be discussed in this chapter followed by the dielectrophoretic treatment in Chapter 16.

15.1 Description of the Test Area

The field test was performed in the Gloucester test fill site at Canada Forces Station (C.F.S.) in which a test embankment was constructed in 1967 by the Division of Building Research, National Research Council of Canada, at a location of 21 km south-east of Ottawa. The purpose of this test embankment was to study the field performance of the soft sensitive clay. The initial performance of the embankment was described and analyzed by Bozozuk and Leonards (1972). Subsequent study was carried out by Lo, Bozozuk and Law (1976) to analyze the long-term settlement of the embankment. The test fill site (which has been designated as "National Test Site") is surrounded by security fence with a locked entrance, providing an enclosed area for security. The field test area was approximately 15 m west of the test embankment located at the west end of the Gloucester test fill site as shown in Figure 15.1 (area enclosed by EFGH). The dimensions of the field test area was 40.25 m by 29.87 m (132 ft by 98 ft) with the south and west sides surrounded by

security fence and the other two sides by snow fence, as illustrated in Figures 15.2 and 15.3. The field test area was sub-divided into two test areas, the electro-osmotic test area in the north end and the dielectrophoretic test area in the south end.

The electric potential for electro-osmosis was supplied by the direct current rectifier with power rating of 120 V and 60 A, housed inside a ventilated metallic transport container of size 3 m by 6 m located at the centre of the test area, as shown in Figures 15.2 to 15.4. Inside the container, a high voltage transformer of 60 kV and 10 kVA power rating was installed for the dielectrophoretic treatment, as shown in Figure 15.4. A main power supply of two phases, 220 V, 60 A were obtained from the nearby office of the Royal Canadian Legion, Branch 627. The high voltage transformer inside the container was separated from the direct current rectifier by two steel gates. The metallic container, rectifier, transformer and steel gates were electrically grounded to the adjacent grounding rods to avoid electrical hazard. The grounding of the high voltage area was ensured every time after turning off the power by touching the steel gate, transformer, high voltage cable and container with a specially designed grounding stick. A security guard was employed during the treatment period to look after the field test area at night and in the weekends.

The subsoil conditions of this site have been described in sections 6.1 and 6.3. A detailed geotechnical profile is shown in Figure 15.5 (Bozozuk and

Leonards 1972). For the present investigation (July-August 1989) field vane tests and moisture content tests were carried out inside the test area before treatment and the test results are plotted in the same figure for comparison. It may be seen that the field vane strengths were approximately similar. The average moisture content of the pre-treatment test is about 80 % compared to an average of 60 % by Bozozuk and Leonards (1972). However, the trends of moisture content variation in both cases are similar.

As can be seen from the soil profile in Figure 15.5, the average vane shear strength of the soil above 5.5 m (18 ft) was lower than 20 kPa while that below this level was higher than 30 kPa. It was therefore decided to treat the soft soil between 1.5 m and 5.5 m level. The total length of the electrode was 6.1 m (20 ft) and the length of the electrode embedded into the soil was 5.5 m (18 ft).

15.2 Electrode Design and Installation

As discussed in section 4.7.7 on the experience obtained from the case histories, the design of the electro-osmosis electrode played an important role in the effectiveness of the treatment. In past applications (with the exception of Bjerrum et al 1967), as shown in Figures 4.14 and 4.15, the design of cathode usually consisted of iron pipe and eductor pipe installed in a pre-drilled hole of substantial size (about 400 mm diameter) and filled up with clean filter sand. The installation and material costs of electrodes are therefore quite high

and particularly, pumping of expelled water is usually required. The anode is usually made of iron pipe, rail or steel bar and as explained in section 3.3 and equation 3.19, the product of the electro-chemical reaction is the formation of iron oxide and hydroxide of high electrical resistance which decrease the efficiency of the treatment. Furthermore, such design of cathode and anode prohibited the application of electrode polarity reversal.

From laboratory and model tests (sections 6.6 and 7.10), it was shown that the use of perforated copper pipe was more effective. It provided passage for expelled water and gas to flow into the cathode and out to the surface during treatment and no pumping of water was required. The undesirable effect of high resistance metallic oxide and hydroxide was also eliminated due to replacement by copper oxide and hydroxide of high conductivity. With this electrode design, both the anode and cathode are identical and the manufacturing and installation costs of the electrodes are therefore reduced. The detail of the electrode designed for the field test is shown in Figure 15.8. A 50.8 mm (2") nominal diameter copper pipe (O.D. 60.3 mm, I.D. 52.4 mm and wall thickness 3.97 mm) was used as electrode with 9.5 mm holes drilled at 50.8 (2") spacing along the pipe. For the ease of pushing the electrode into the ground, a cone-shaped steel shoe was installed at the tip of electrode.

From the unsuccessful application reported by Caron (1971a,b), it is deduced that continuous sand and silt layers in the subsoil are not favourable for the treatment. Due to the relatively high conductivity of such layers, it

would cause short circuiting of the system. If the groundwater table is higher than these layers, water from these layer will flow into the perforated electrode and affect the efficiency of the treatment. In view of this observation, the subsoil condition of the field test area was carefully studied and it was found that the top 1.22 m (4 ft) of crust (top soil, fine sand and silt) would have adverse effect to the treatment. It was therefore necessary to insulate that part of electrode by putting several layers of varnish coating onto the pipe surface, as shown in Figure 15.6. To avoid short circuiting of the system due to heavy rainfall and flooding of the ground surface, the top 0.3 m (1 ft) of the electrode was also insulated. Furthermore, no hole was drilled along the insulated portion of the electrode to avoid any groundwater and rain water from flowing into the electrode. The total length of the electrode was 6.1 m (20 ft) with an embedded length of 5.5 m (18 ft) to treat the top 5.5 m of soft soil excluding the crust. Four weep-holes were drilled at 0.3 m (1 ft) below the top of electrode to allow water flowing out from the pipe and to avoid corrosion of the contact of the electric cable and copper pipe. Several trenches were dug to divert the expelled water from the treatment area.

The electrode was then pushed into the soil by a drilling rig and care was taken to install the electrode vertically, as shown in the photo in Figure 15.7. Due to disturbance of the highly sensitive clay during installation, the electrodes were filled with slurry (remoulded clay) during pushing. The interior of the electrodes were cleaned by flushing water into the copper pipes.

15.3 Electrode Layout

In the electro-osmotic test area, nine electrodes were installed in a 9.15 m (30 ft) square grid configuration, as shown in Figure 15.2. Two square grids of 3.05 m and 6.1 m were formed by electrodes EO1-EO2-EO5-EO4 and electrodes EO5-EO6-EO9-EO8 respectively so that the effect of spacing on the treatment could be studied. The electrical circuiting was arranged so that the Row A electrodes (EO1-EO4-EO7) were of the same polarity (positive) while the Row B electrodes (EO2-EO5-EO8) were of opposite polarity (negative). The Row C electrodes (EO3-EO6-EO9) were of the same polarity (positive) as Row A. The polarity of the electrodes was then reversed midway in the treatment period. It is therefore expected from this electrode configuration that water will flow out from the centre row of electrode during treatment with normal polarity and from the two outer row of electrode when the polarity is reversed. The layout of the electrodes after installation is shown in the photo in Figure 15.8.

15.4 Instrumentation and Monitoring

During the electro-osmotic treatment, the variations of ground settlement, vane shear strength and voltage distribution with treatment time were monitored. The settlement was monitored by means of steel settlement auger of 0.61 m (2 ft) length with 0.15 m (6") embedded in the soil and the settlement was measured by means of surveying instruments. The layout of the settlement augers is shown in Figure 15.9.

The variation of field vane shear strength with treatment time was measured by means of the Norwegian field vane apparatus with vane size of 55 mm by 110 mm. Tests were carried out before, during and after treatment. The vane was pushed manually to the required depths for testing.

Fourteen voltage probes were installed to measure the voltage distribution and variation of soil, as shown in Figure 15.10. The voltage probe was made of 12.7 mm diameter copper pipe with 1.33 m (5 ft) embedded in the soil. The surface of the copper pipe was covered by a layer of insulation coating with only the bottom 0.3 m uncoated. The purpose was to limit the measurement of the voltage distribution in the soft clay but not in the crust layer.

No piezometer was installed in the test areas due to the fact that the piezometer tubing would disturb considerably the electric field of the test area. As reported by Bjerrum et al (1967), gas was formed inside the piezometer tubing due to electrolysis of the groundwater resulting in some erroneous measurement of pore water pressure. Furthermore, the piezometers are usually designed to measure positive pore pressures while negative pore water pressure is expected to occur during the process. In view of the possible errors of measurement and complications to the process that may arise, it was decided to omit the installation of piezometer.

15.5 Test Procedures as Performed

At the beginning of treatment, Row A and Row C electrodes were

connected to the positive terminal of the rectifier and the Row B electrodes were connected to the negative terminal. On day 1 (July 24, 1989), a direct voltage of 25 volts was applied. As water was expelled from the soil, the electrical resistance of the soil increased and consequently decreased the current flow. The applied electric potential was therefore regulated periodically in order to maintain a relatively constant level of current flow of approximately 40 A (ampere). The variations of applied voltage and current with time can be seen in Table 15.1 and Figure 15.11. Due to the thunderstorm in day 4 and for safety reason, the power was switched off and re-started on day 5 morning. On day 18 (August 10, 1989), based on the field vane test results (to be discussed later), it was decided to reverse the current flow. In this treatment, the polarities of Row A and Row C electrodes were negative and Row B were positive. The maximum applied voltage was 120 V.

During the treatment, the following quantities were measured daily except in weekends:

(a) settlement of soil surface

(b) field vane strength at different locations, tests performed as required

(c) voltage distribution in the soil between electrodes

(d) current and voltage variation of power supply

(e) pH values of water collected from cathode

(f) collection of water samples for laboratory analysis.

After the treatment, nine field vane test profiles were performed at different locations to determine the post-treatment shear strength increase and to investigate the uniformity of treatment. Two boreholes to recover 127 mm (5") diameter samples were drilled, halfway between two 3.05 m electrodes and two 6.1 m electrodes for detailed laboratory tests.

15.6 Test Results

The installation was completed in two weeks and the voltage was applied on July 24, 1989 (day 1). The electrode polarity was reversed on August 10, 1989 (day 18) and the treatment was completed on August 25, 1989 (day 33), resulting in 32 days of treatment with 17 days of normal polarity and 15 days of reversed polarity. The variations of settlement, field vane strength, voltage distribution and power consumption are discussed in this chapter. The results of pH values measurement and chemical tests of water samples will be reported in Chapter 17.

15.6.1 Observations at Electrodes

On day 1 of treatment, a direct voltage of 25 volts was applied and the effect of electro-osmosis was observed immediately. About 50 minutes after the application of electric potential, water started to flow out from the cathodes, as shown in the photo in Figure 15.12. Gas bubbles were also observed in the expelled water and they were expected to be hydrogen due to electrolysis of

water. At anode, the copper pipe electrode was initially filled with water up to the level of groundwater table. When the electric power was on, no water was found inside the pipe.

15.6.2 Settlement Measurement

The results of settlement measurement are summarized in Table 15.2 and plotted in Figures 15.13 to 15.16. For clarity of presentation, only the settlement with treatment time curves of augers S2, S4, S6 and S8 are shown in Figure 15.13. The settlement curves S2, S6 and S8 in Figure 15.13 indicate that during the treatment with normal polarity, the average settlement rate was about 3.3 mm/day. The maximum settlement up to day 18 was 62 mm. For settlement curve S4, since the auger was installed near to electrode EO5 which was a cathode during normal polarity, it recorded the upward movement of the ground surface between day 1 and day 8 to a maximum value of 50 mm. From day 9 onward, the soil commenced to settle and up to day 18 the soil settled by 32 mm, resulting in a net heave of 18 mm. When the electrode polarity was reversed on day 18, the augers S2, S6 and S8 showed no appreciable further settlement while auger S4 recorded a constant rate of settlement of about 1.6 mm/day, with a further settlement of 24 mm. At the end of treatment, with the exception of auger S4, the settlement of the treated area was 38 to 68 mm, with an average settlement of 51 mm. Figures 15.14 to 15.16 show the settlement-time profiles recorded by the three rows of

settlement augers.

15.6.3 Field Vane Test

A total of 28 vane test profiles[1] were performed during and after treatment, with the test locations as shown in Figure 15.17. The tests were carried out between 2 m and 6 m depth to investigate the shear strength changes in the soft clay layer and the effects of treatment on the clay below electrode tips, if any. Four strength profiles were carried out at 43 days (two strength profiles, EOV24 and EOV25) and at 10 months (two strength profiles, EOV27 and EOV28) after treatment in order to check the long term effect of the treatment. Tests were also carried out in the "inactive zone" where the electric field intensity was expected to be minimal. Table 15.3 summarizes the test results. Typical profiles of vane shear strength and the corresponding percentage of shear strength increase with depth at different times of treatment are shown in Figures 15.18 to 15.35. The average final shear strength between the electrodes and average shear strength variation with time are plotted in Figures 15.36 and 15.37 respectively.

From all the vane shear strength profiles obtained, it was observed that the shear strength increase at 2 m depth was relatively higher than those measured

---

[1] Remoulded shear strength test was not performed due to the slight deformation of the vane test equipment but this deformation has no adverse effect to the measurement of undisturbed strength. The remoulded shear strength was measured in the laboratory on the tube samples (see Chapter 17).

at different levels. This observation may be due to the variation of soil properties. From Figure 15.5, the soil at 2 m depth is the soft grey-brown silty silt with relatively lower moisture content and lower sensitivity (Layer B of Layer 1) while the soil below that is the soft grey silty clay with relatively higher moisture content and higher sensitivity (Layer C of Layer 1). Due to the difference in soil properties, the degree of shear strength increase would be different. The field test results show that the soil in Layer B is relatively easier to be strengthened than the soil in Layer C. Due to this variation, the shear strength measured at 2 m depth was not included in the calculation of average shear strength of the profile.

The average vane shear strength before treatment of the upper layer of soft clay between 2 m and 5.5 m is 18.2 kPa. From Table 15.3, the maximum average shear strength increase is 62 % (day 29) in test EOV13. The average shear strength increase of the soil after treatment halfway between a pair of electrodes of 3.05 m spacing is 50.8 % (day 29) and that of 6.1 m spacing is 36 % (day 32), as shown in Figures 15.18 to 15.21. In the centres of 3.05 m and 6.1 m square grids, which are considered to be the inactive zone of the treatment area, the average shear strength increase is 27 % and 23 % respectively (Figures 15.22 to 15.25), amounting to more than half of the shear strength increase of the corresponding increase in the middle of two electrodes. Another inactive zones of the test area are in the tests EOV22, EOV23 and EOV26 where the shear strengths increase are 11 %, 7.6 % and 8.3 %

respectively (Figure 15.32 and 15.33). The uniformity of electro-osmotic treatment to the shear strength increase was also investigated by performing vane tests at different locations between two pair of electrodes. Vane tests EOV13, EOV14 and EOV15 were carried out after treatment between electrodes EO7 and EO8 (3.05 m spacing), and tests EOV16, EOV17 and EOV18 between electrodes EO8 and EO9 (6.1 m spacing), with the test holes located evenly between two electrodes. The shear strength profiles are plotted in Figures 15.26 to 15.29 and the average shear strength increase between electrodes is presented in Figure 15.36. The results show that the shear strength increased rather uniformly, to a value of 50 % for 3.05 m electrode spacing and 36 % for 6.1 m electrode spacing.

The increase of shear strength with treatment time is presented in Figure 15.37. It may be seen that for the 3.05 m electrode spacing, a rapid increase in shear strength occurred in the first few days of treatment, with 16 % increase on day 3. The rate of strength increase gradually diminished with time up to day 18. When the electrode polarity was reversed, the rate of strength increase picked up again and showed a trend of further strength increase beyond day 33, if the treatment had been continued. The curves for the other three regions (6.1 m electrode spacing, centre of 3.05 m square grid and centre of 6.1 m square grid) show the steady increase in shear strengths with relatively constant rates and there are trends of further shear strength increase beyond day 33 as well. The long term effect of the process was also investigated by

carrying out two vane test profiles (EOV24 and EOV25) on day 76 (43 days after treatment) and two vane profiles (EOV27 and EOV28) at 10 months after power shut off. For the test profiles performed at 43 days after treatment (EOV24 and EOV25), the shear strengths measured at halfway of two electrodes of 6.1 m spacing were increased by 37.5 % to 38.8 % (Figures 15.30 and 15.31). For the test profiles performed at 10 months after treatment, the shear strengths measured at halfway of two electrodes of 3.05 m and 6.1 m spacings (EOV27 and EOV28) were 58.3 % and 37.9 % respectively (Figures 15.30, 15.31 15.31a and 15.31b). As shown in Figure 15.37, there is no appreciable change in shear strength in the long run.

During the treatment with normal polarity, it was observed that water seeped into electrode EO4 (anode in this case) and maintained an average water level of 4 m inside the electrode (1.5 m above electrode tip). The seepage may be due to the localized pervious layer in the test area. Due to this effect, vane test profile EOV4 showed a lower shear strength increase of only 16.1 % on day 11 and exhibited a trend of shear strength decrease with depth, as shown in Figures 15.34 and 15.35. When the electrode polarity was reversed, electrode EO4 became cathode and there was no water observed in the new anode (electrode EO5). Further vane test (EOV21) on day 31 showed a uniform increase in shear strength of 1.6 % with depth.

15.6.4 Voltage Distribution and Power Consumption

As a result of pore water being extracted from the soil. the eiectrical resistance of the soil increased and the current density would vary at an applied potential difference. As shown in Table 15.1 and Figure 15.11, there was a variation in applied voltage and current during the period of treatment. During the first 3 days the applied voltage was set at 25 V in order to examine how the current dropped due to the increase in resistance. The current dropped from 31.9 A to 28 A. From then on the current was kept to a level of around 35 to 40 A and the applied voltage was regulated periodically. The maximum voltage applied in normal treatment was 65 V with a current flow of 44.8 A. On day 18, the electrode polarity was reversed and the applied voltage was set to -40 V with a current flow of -53.9 A. The magnitude of current dropped to -19.6 on day 19 and the applied voltage was adjusted to -100 V in order to maintain a current flow of -44.4 A. The magnitude of current dropped again on day 22 to -19.8 A. The applied voltage was then set to the maximum capacity of the rectifier of 120 V and the magnitude of current increased to -26.1 A. From then on the applied voltage was constant while the magnitude of current flow increased gradually to a maximum of -43.4 A. On day 33, the current was -39.6 A just before power shut off.

Sixteen voltage probes were installed with the locations as shown in Figure 15.10 to measure the voltage distribution in the test area. Table 15.4 summarizes the test results. The voltage variations in soil between electrodes

EO4-EO5-EO6 and electrodes EO7-EO8-EO9 are plotted in Figures 15.38 and 15.39 respectively. It may be seen that the potential drop between the anode and the nearest voltage probe at 0.76 m was high while that at halfway between electrodes is low. This indicates that the power consumption at vicinity to anode is quite high.

15.7 Advantages of the Improved Version for Electro-Osmosis

As discussed in the preceding sections, several modifications have been made in the design of electrodes and techniques of treatment. From the test results presented, it appears that these modifications improved the effectiveness of the electro-osmosis process. The advantages of the improved version are discussed in this section.

15.7.1 Effects of New Electrode Design

One of the reasons of the slow development of the electro-osmotic strengthening method is due to the high electricity consumption for the process and for water pumping. In the field test, the effect of electro-osmosis was so obvious that water flowed out from the cathodes 50 minutes after the power was switched on. This shows an improvement of the electrode design that water can flow out from the cathode without pumping and as a result, the installation and electricity costs can be reduced drastically. Another advantage of the new electrode design is the release of water around cathode that reduces

the development of excess pore water pressure in the soil at the vicinity of the cathode and therefore reduces the risk of shear strength decrease, as reported in Bjerrum et at (1967).

The electrodes developed also eliminates the problem of gas accumulation around electrodes. Due to electrolysis of water, hydrogen and oxygen are produced at cathode and anode respectively and the gas formation increases the electrical resistance of the system and decreases the efficiency of electro-osmotic treatment. In the present field test, the holes in the electrodes provide the passage for the gas generated into the electrode, together with the flow of expelled water. This results in the better soil conductivity and the reduction of gas pressure development in the soil. The electrode-soil contact and consequently treatment efficiency are improved.

As a result of the electrical insulation of part of the electrode in the pervious crust, no short circuiting problem occurred during treatment. It is therefore demonstrated by the field test that the adverse effects of any undesirable soil layer can be avoided by insulation. It also emphasizes the need to investigate and interpret the subsoil conditions carefully to ensure the success of the process.

15.7.2 Heave at Cathode

As described in section 15.6.2, the settlement auger S4 near the cathode shows upward and then downward ground movement and the heave was

reduced to settlement after polarity reversal. This shows an improvement in the effectiveness of treatment compared with the problem reported by Casagrande (1952a,b) that the soil near to cathode had considerable upward movement. This observation also suggests that the soil could be treated relatively uniformly by using the technique of polarity reversal. The problem of differential settlement may be reduced, particularly if the reversal of polarity had been undertaken earlier than day 18. The uniformity of treatment as obtained may be assessed in Figures 15.14 to 15.16 in which the profile of ground settlement of three sections of the test area are plotted. With the exception of auger S4 which is close to the cathode, the three settlement profiles at the end of treatment show maximum differential settlement approximately ±20 % of the average final settlement. In future applications, this amount may be reduced by a judicious usage of the technique of polarity reversal.

Another implication of ground settlement is the consolidation of the soft clay. Since the pore water was extracted by the process, the volume of the pore space was decreased leading to the settlement and consolidation of the clay. As will be discussed in Chapter 17, consolidation of clay is the major mechanism of the electro-osmotic process.

15.7.3 Undrained Shear Strength

From the test results described in section 15.6.3, the field test showed that the shear strength increased substantially in a relatively short period of 32

days. The results also indicate that the 6.1 m electrode spacing can also increase significantly by 40 %, implying that a wider electrode spacing may be used. The increase in shear strengths in the inactive zones was not expected in the past applications and as discussed in section 4.7, very close electrode spacing was used in order to improve the shear strength in these areas. In this field test, the shear strengths in these zones are increased significantly, especially in the centre of the square grids. This further shows the effectiveness of the process with the special electrode design.

With regarding to achieving uniformity of shear strength increase, the electrode polarity reversal appears to be an useful technique. As reported previously (Bjerrum et al 1967), the treatment of soil was nonuniform in that the shear strength decreased from anode to cathode with no strength increase at the cathode. The field test shows that the soil can be treated more uniformly by reversing the electrode polarity as shown in Figure 15.36.

From the plot of shear strength increase with treatment time in Figure 15.37, it appears that the soil between 3.05 m electrode spacing was slightly over-treated. The resistance of the over-treated soil increased significantly and hence decrease the efficiency of the process at the later stage of treatment with normal polarity. However, this situation was improved when the electrode polarity was reversed. For the curve corresponding to 6.1 m electrode spacing, due to a wider spacing, the soil was treated slowly and no sign of over-treatment was detected. This result indicates an advantage of using wider

electrode spacing, and is further supported by the results plotted in Figure 15.36. For long term effects, two vane test profiles (EOV27 and EOV28) were performed 10 months after electric power shut off and no further change in shear strength was found indicating the shear strength improvement due to the electro-osmotic treatment is permanent. This behaviour can be explained by the results of laboratory consolidation test (section 7.6) that the soil is over-consolidated by the electric potential and the preconsolidation pressure increased after treatment. The situation of switching off the electric power is similar to the unloading stage of the consolidation test and by the principle of classical soil mechanics, the change in void ratio in the rebound of soil due to unloading is small. Hence the electro-osmotic treatment is proved to be permanent. More consolidation tests on the undisturbed tube samples recovered from the test area after treatment will be carried out and the test results will be discussed later in Chapter 17.

In the case record reported by Bjerrum et al (1967), the embedded depth of the electrodes was 9.6 m. It was observed, however, that the shear strength increased to a depth of about 6 m, and no effect was detected below this depth. A possible reason for this "depth effect" is that gas was formed at the electrodes during treatment and due to the soil over-burden pressure, it was difficult for the gas to escape to the atmosphere and eventually accumulated at the lower part of the electrode. This results in the increase of resistance of the system and decrease in efficiency of the process. The electrode used in the field test

are of different design and, as can be seen from the shear strength profiles, no such phenomenon of "depth effect" of electrode was observed and the strength increased throughout the depths of the electrodes. Furthermore, from all the vane test results, there is no appreciable change in shear strength of soil below the tips of electrodes.

A problem was encountered at electrode EO4 that water was observed inside the electrode due to water seepage from the crust at the top 1.22 m and the shear strength increase was affected as shown by test profile EOV4. In this case, water inside anode was injected by the generated negative pore water pressure into the soil, resulting in lower extent of moisture content reduction of soil. As a result, the shear strength increase was affected. However, when the electrode polarity was reversed, electrode EO4 became cathode and since there was no water observed in the new cathode (electrode EO5), no "depth effect" was observed in the field vane test profile EOV21. This observation demonstrates another advantage of applying the procedure of electrode polarity reversal.

15.7.4 Power Consumption

The total power consumption in the field test was 2136 kWh, approximately 1 % of the total project cost. This may be compared with the case reported by Bjerrum et at (1967) in which the cost of electricity was as high as 25 % of the total project cost. The present version of electro-osmotic

treatment in this test may therefore be considered to be relatively efficient and economical. It is expected that the electricity cost of a project of similar size to that in Norway would be slightly higher due to a higher resistance and power loss in a larger treatment area. Unfortunately, comparison with other reported cases in clays could not be made because the costs and power consumption were seldom reported.

Two undisturbed tube samples were recovered in the electro-osmotic treatment area for laboratory analysis and the test results will be discussed in Chapter 17.

Table 15.1 Summary of Power Supply for Electro-Osmosis Treatment

Date	Day No.	D.C. Rectifier Output		Remarks
		Voltage (V)	Current (A)	
July 24	1	25	31.9	power on
25	2	25	31.2	
26	3	25	28.0	
		29	32.2	
27	4	29	26.9	
		35	30.8	
		0	0.0	thunderstorm, power off
28	5	25	34.7	
31	8	25	30.6	
		30	36.5	
Aug. 1	9	30	34.6	
		40	39.5	
2	10	40	34.7	
		65	42.3	
3	11	65	40.8	
4	12	65	40.6	
8	16	65	44.8	
9	17	65	44.8	
10	18	65	43.6	
		-40	-53.9	polarity reversal
11	19	-40	-19.6	
		-100	-44.4	
14	22	-100	-19.8	
		-120	-26.1	
15	23	-120	-27.3	
16	24	-120	-28.2	
17	25	-120	-29.8	
18	26	-120	-28.9	
21	29	-120	-33.6	
23	31	-120	-43.4	
24	32	-120	-40.5	
25	33	-120	-39.6	
		0	0.0	power off

Table 15.2 Settlement Measurement in Electro-Osmosis Test Area

Date	Day No.	Settlement of Each Settlement Auger (mm)														Remarks
		S1	S2	S3	S4	S5	S6	S7	S8	S9	S10	S11	S12	S13	S14	
July 24	1	0	0	0	0	0	0	0	0	0	0	0	0	0	0	power on
27	4	2	6	-5	-21	4	3	1	8	2	1	1	1	1	1	
31	8	4	15	-3	-50	4	4	7	23	2	4	1	1	3	1	
Aug. 2	10	8	18	6	-40	12	12	18	36	5	7	10	8	6	6	
4	12	17	30	14	-35	29	31	34	40	11	14	26	13	20	18	
8	16	39	49	36	-16	49	55	55	57	33	38	53	33	42	38	
10	18	44	59	41	-18	64	58	58	62	38	43	53	26	37	33	polarity reversal
11	19	40	54	41	-13	54	58	58	67	38	43	53	40	44	45	
14	22	39	51	36	-13	54	53	54	62	33	38	48	18	27	20	
15	23	41	52	36	-13	54	55	54	62	36	38	53	38	45	42	
16	24	44	57	41	-8	59	58	59	67	39	43	55	40	48	45	
17	25	44	57	41	-7	56	58	61	67	38	42	53	38	47	45	
18	26	46	59	46	-2	59	63	64	69	41	48	58	41	52	47	
21	29	49	60	46	1	61	62	64	68	44	48	60	43	53	50	
23	32	44	57	41	3	59	63	64	67	41	48	58	43	47	47	
25	33	44	57	40	6	57	58	64	68	38	46	57	43	47	45	

Notes: positive values for settlement, negative for heave

Table 15.3 Summary of Field Vane Test Results

Location	Day No.	Average Shear Strength (kPa)	Average Shear Strength Increase (%)
EOV1[a]	---	18.2	0
EOV2	3	21.1	16.2
EOV3	9	24.3	33.7
EOV4	11	21.2	16.1
EOV5	11	20.1	10.7
EOV6	11	24.9	36.6
EOV7	17	22.2	22.0
EOV8	17	22.0	20.8
EOV9	17	24.7	35.5
EOV10	18	21.5	18.4
EOV11	18	23.2	27.7
EOV12	24	23.8	30.5
EOV13	29	29.5	62.2
EOV14	29	27.4	50.8
EOV15	29	26.1	43.6
EOV16	32	23.5	29.2
EOV17	32	24.8	36.5
EOV18	32	25.5	40.1
EOV19	33	23.2	27.5
EOV20	33	22.4	23.1
EOV21	31	26.3	44.6
EOV22[b]	76	20.2	11.1
EOV23	77	19.6	7.6
EOV24	76	25.3	38.8
EOV25	76	25.0	37.5
EOV26	77	19.7	8.3
EOV27[c]	335	28.0	58.3
EOV28[c]	335	25.1	37.9

Notes:-
(a) pre-treatment test
(b) 43 days after treatment
(c) 10 months (302 days) after treatment

Table 15.4 Summary of Voltage Distribution in Electro-Osmosis Test Area

Date	Day	Voltage in Voltage Probes and Electrodes (V)																				
	No.	EO4	V1	V2	V3	EO5	V4	V5	V6	V7	EO6	EO7	V8	V9	V10	EO8	V11	V12	V13	V14	EO9	V15	V16
July 24	1	25	17.0	15.1	12.7	0	13.1	15.2	16.8	18.3	25	25	17.6	15.8	13.1	0	13.9	15.7	16.8	17.9	25	12.6	15.0
25	2	25	16.7	14.8	12.5	0	13.0	15.1	16.8	18.3	25	25	17.1	15.4	12.7	0	13.7	15.6	16.8	18.1	25	12.3	14.8
26	3	29	16.6	14.6	12.2	0	13.0	15.6	17.8	19.8	29	29	17.0	15.3	12.5	0	13.8	16.1	17.5	19.2	29	12.1	14.8
27	4	35	16.1	14.1	11.3	0	12.5	15.0	17.2	19.4	35	35	16.7	14.9	12.1	0	13.3	15.6	17.25	19.2	35	11.5	14.3
28	5	25	17.3	15.3	12.7	0	13.1	15.5	17.3	19.0	25	25	18.1	16.0	13.1	0	14.0	16.1	17.4	18.7	25	12.4	15.3
31	8	30	17.5	15.5	12.8	0	13.5	16.2	18.5	20.6	30	30	17.8	15.8	12.9	0	14.3	16.7	18.2	19.9	30	12.5	15.5
Aug. 1	9	30	16.5	14.6	12.0	0	12.7	15.3	17.4	19.4	30	30	16.6	14.8	12.1	0	13.3	15.6	17.1	18.8	30	11.7	14.5
		40	18.1	16.0	13.1	0	14.0	16.9	19.3	21.6	40	40	19.3	17.0	13.8	0	15.2	18.0	19.8	22.2	40	13.0	16.4
2	10	40	16.3	14.4	11.8	0	12.6	15.2	17.4	19.5	40	40	16.9	14.9	12.1	0	13.4	15.8	17.3	19.3	40	11.6	14.5
		65	19.1	16.9	13.8	0	14.7	17.8	20.4	22.9	65	65	20.3	17.7	14.3	0	15.7	18.5	20.4	22.8	65	13.5	17.0
3	11	65	18.3	16.2	13.2	0	14.1	17.1	19.6	21.8	65	65	19.8	17.2	13.8	0	15.2	18.0	19.8	22.2	65	12.6	16.2
4	12	65	17.8	15.7	12.8	0	13.7	16.6	19.0	21.2	65	65	20.0	17.2	13.8	0	15.0	17.7	19.6	22.0	65	12.6	16.2
8	16	65	19.0	16.8	13.5	0	14.4	17.5	20.1	22.4	65	65	21.1	18.1	14.5	0	16.0	19.0	21.2	24.2	65	13.1	17.1
9	17	65	18.9	16.7	13.4	0	14.2	17.3	19.9	22.2	65	65	21.3	18.2	14.5	0	15.8	18.7	20.8	23.6	65	13.0	17.0
10	18	65	18.7	16.5	13.3	0	14.1	17.1	19.7	21.9	65	65	20.9	17.9	14.2	0	15.5	18.4	20.5	23.2	65	12.9	16.8
10	18	0	9.8	12.7	16.2	40	15.1	11.2	8.0	4.9	0	0	7.5	10.7	15.1	40	13.4	9.9	7.7	4.9	0	16.6	12.0
11	19	0	5.7	7.8	10.7	100	9.3	6.2	3.1	1.3	0	0	2.3	4.9	8.6	100	7.1	4.6	3.2	1.5	0	11.0	6.3
14	22	0	4.2	6.1	8.9	120	7.5	4.8	2.9	1.5	0	0	1.1	2.6	4.4	120	4.0	2.9	2.2	1.5	0	8.5	4.2
15	23	0	4.4	6.3	9.6	120	7.9	5.0	3.1	1.6	0	0	1.3	3.1	5.4	120	4.7	3.2	2.5	1.6	0	9.4	4.4
16	24	0	4.5	6.5	9.8	120	8.0	5.1	3.2	1.7	0	0	1.5	3.4	6.1	120	5.1	3.5	2.6	1.7	0	9.6	4.7
17	25	0	4.7	6.7	10.1	120	8.3	5.4	3.4	1.9	0	0	2.3	4.4	7.8	120	6.3	4.1	3.1	2.0	0	9.6	5.2
18	26	0	4.8	6.7	9.8	120	8.2	5.4	3.5	2.1	0	0	2.8	5.1	8.6	120	7.0	4.6	3.4	2.3	0	9.5	5.6
21	29	0	6.2	8.5	12.2	120	10.3	6.9	4.6	2.8	0	0	3.3	5.7	9.2	120	7.8	5.4	4.2	3.0	0	11.6	6.7
23	31	0	8.2	11.2	16.3	120	13.5	9.1	6.2	3.8	0	0	5.2	8.5	13.0	120	11.3	8.0	6.4	4.7	0	15.1	9.7
24	32	0	7.7	10.5	15.0	120	12.6	8.7	6.0	3.8	0	0	4.8	7.8	11.5	120	10.0	7.2	5.8	4.4	0	14.0	8.8
25	33	0	7.9	10.9	16.0	120	13.1	8.8	6.0	3.8	0	0	4.7	7.5	11.1	120	9.8	7.2	5.8	4.4	0	14.0	8.9

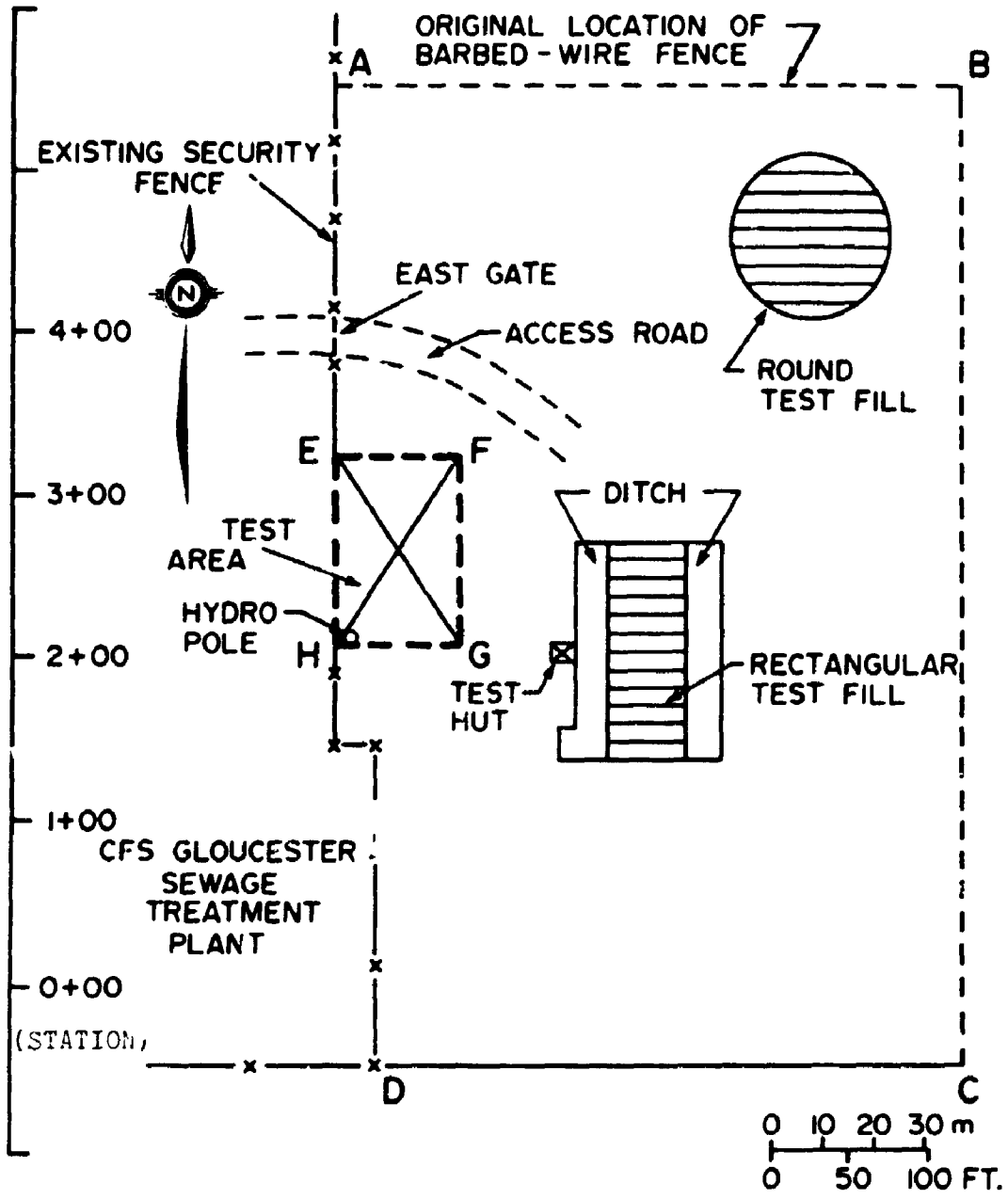

FIGURE 15.1 GENERAL LAYOUT OF THE GLOUCESTER TEST FILL SITE

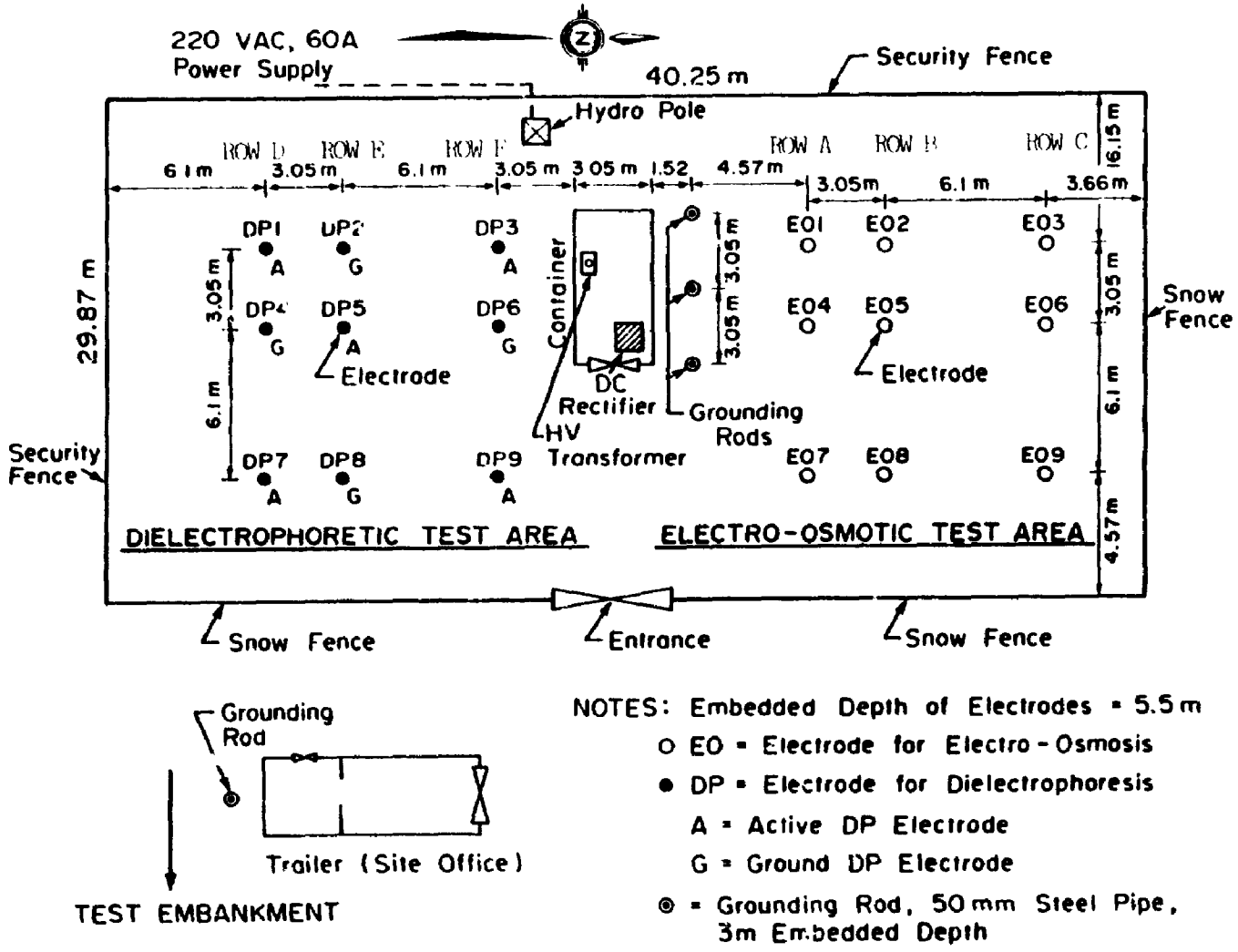

FIGURE 15.2 GENERAL LAYOUT OF TEST AREAS AND ELECTRODE CONFIGURATION

FIGURE 15.3 PHOTO SHOWING THE GENERAL LAYOUT OF THE TEST AREA

FIGURE 15.4 DC RECTIFIER AND HIGH VOLTAGE TRANSFORMER INSIDE THE TRANSPORT CONTAINER

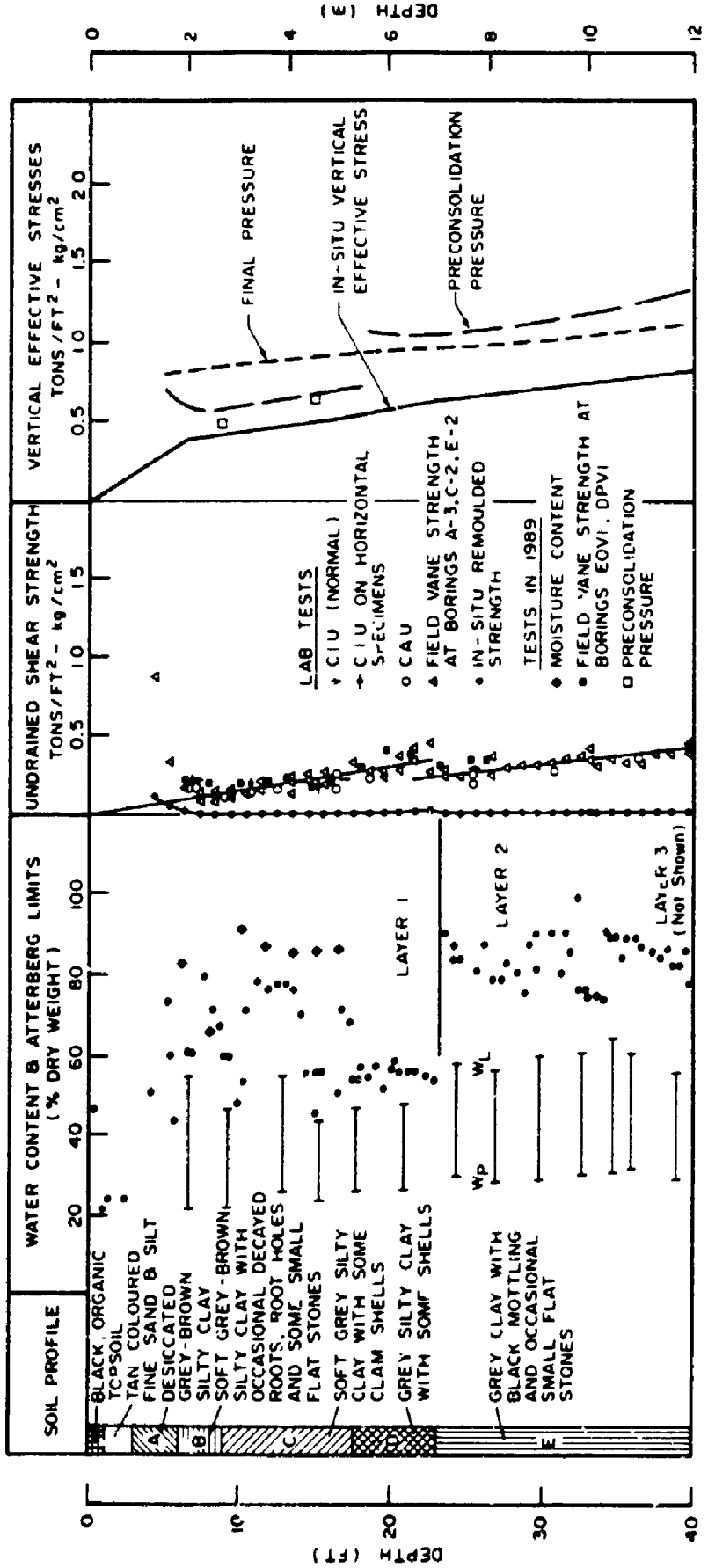

FIGURE 15.5 GEOTECHNICAL PROFILE OF SUBSOIL CONDITION IN GLOUCESTER TEST FILL SITE BEFORE TREATMENT. PROFILE UP-DATED DURING FIELD TEST (after Kozoŭk and Leonards 1972, part of profile not shown)

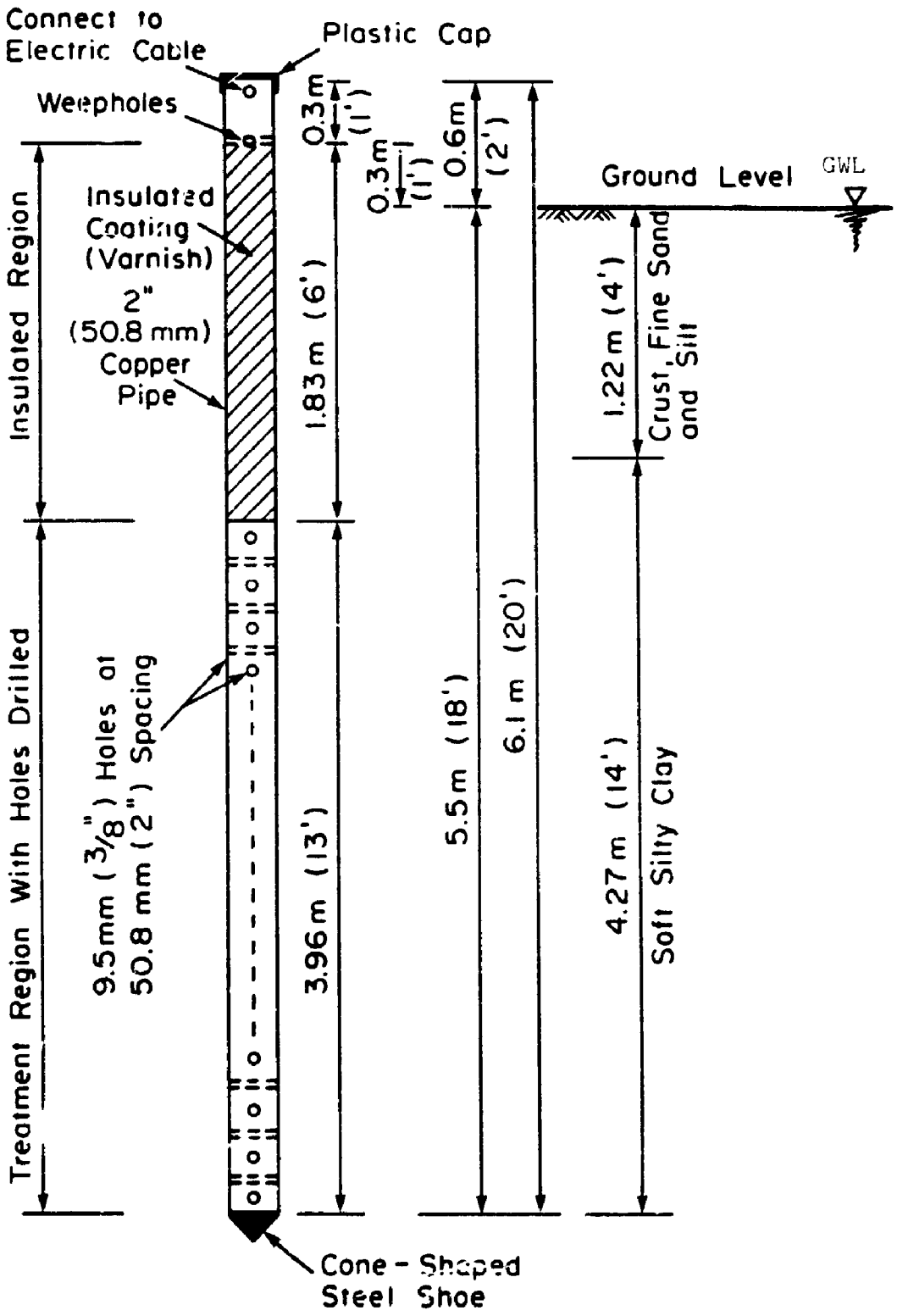

FIGURE 15.6 DETAILS OF ELECTRODE FOR ELECTRO-OSMOSIS

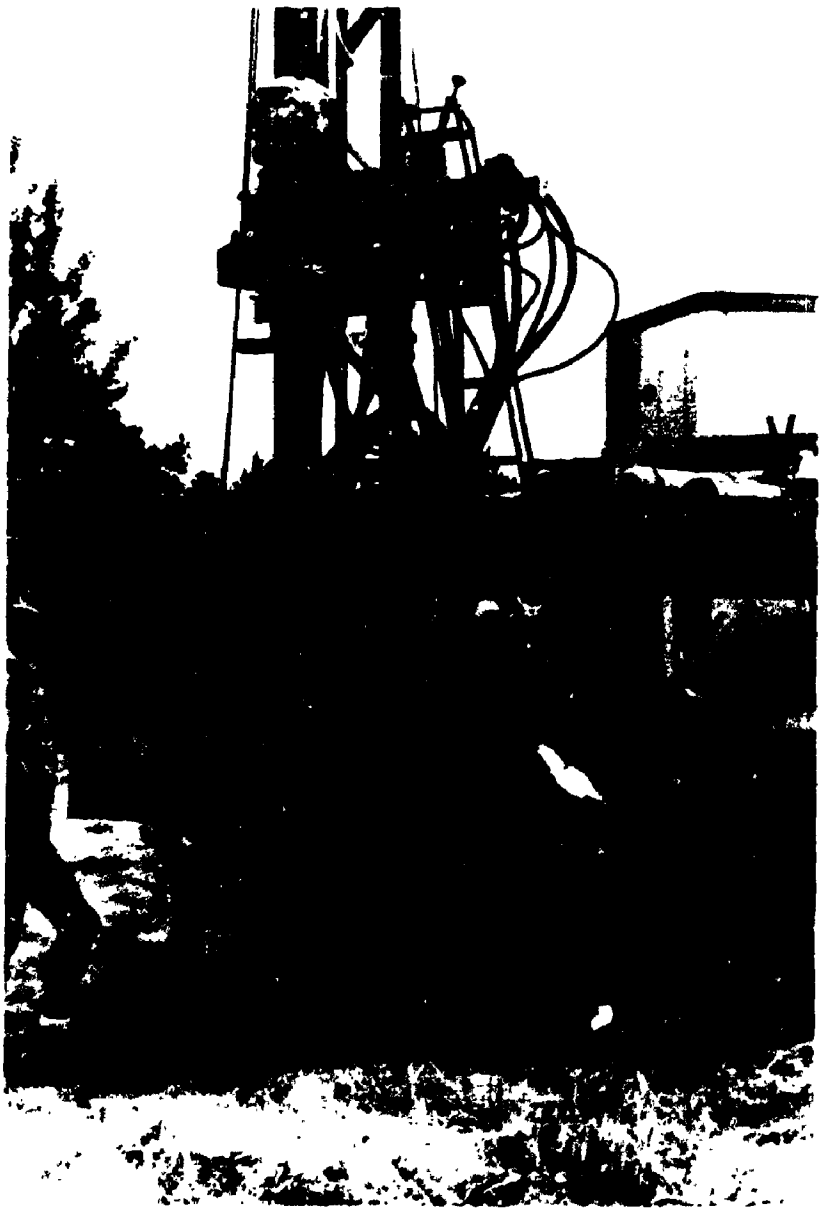

FIGURE 15.7 ELECTRO-OSMOSIS ELECTRODE AND INSTALLATION

FIGURE 15.8 TEST AREA FOR ELECTRO-OSMOTIC TREATMENT

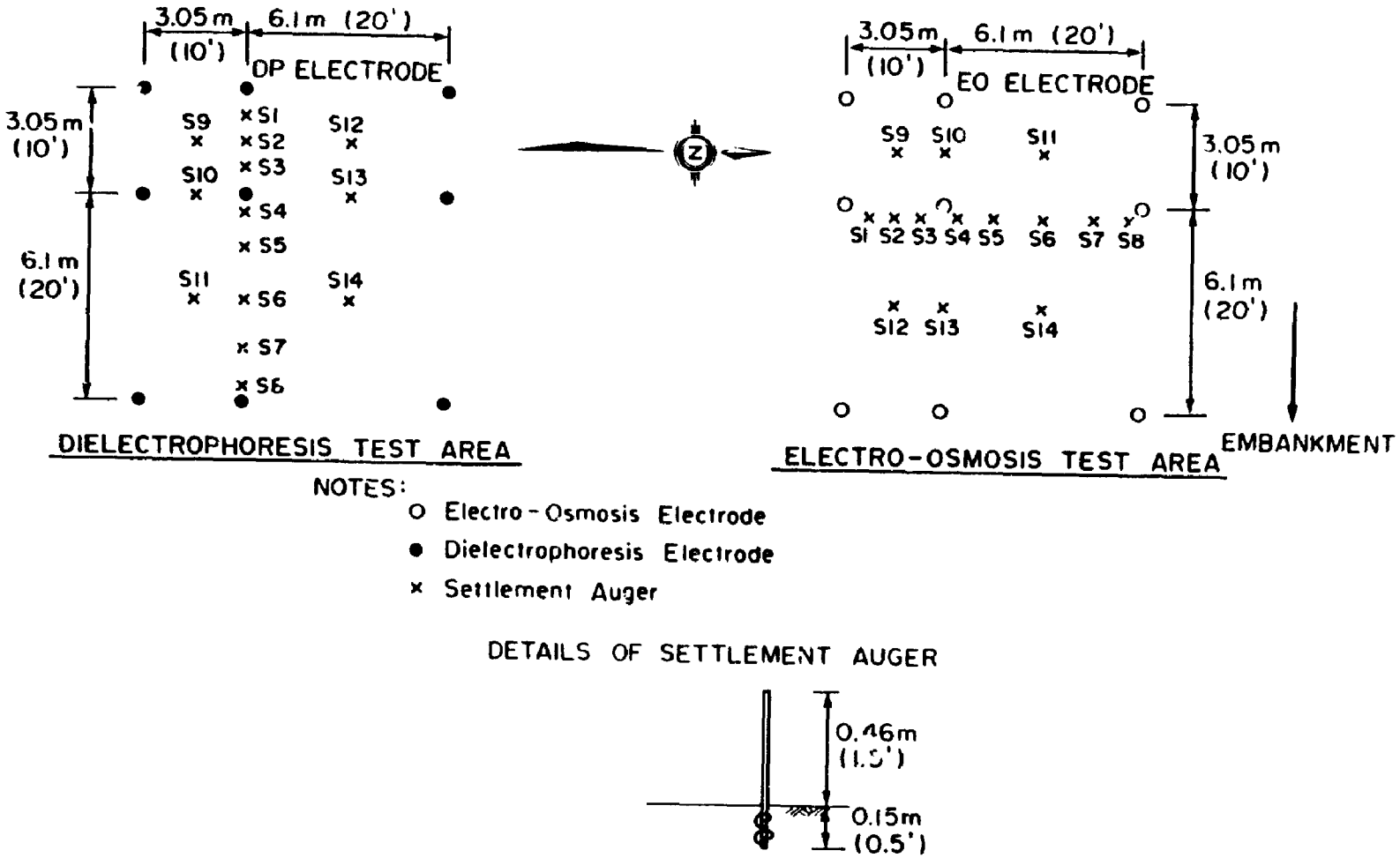

FIGURE 15.9 LAYOUT OF SETTLEMENT AUGERS

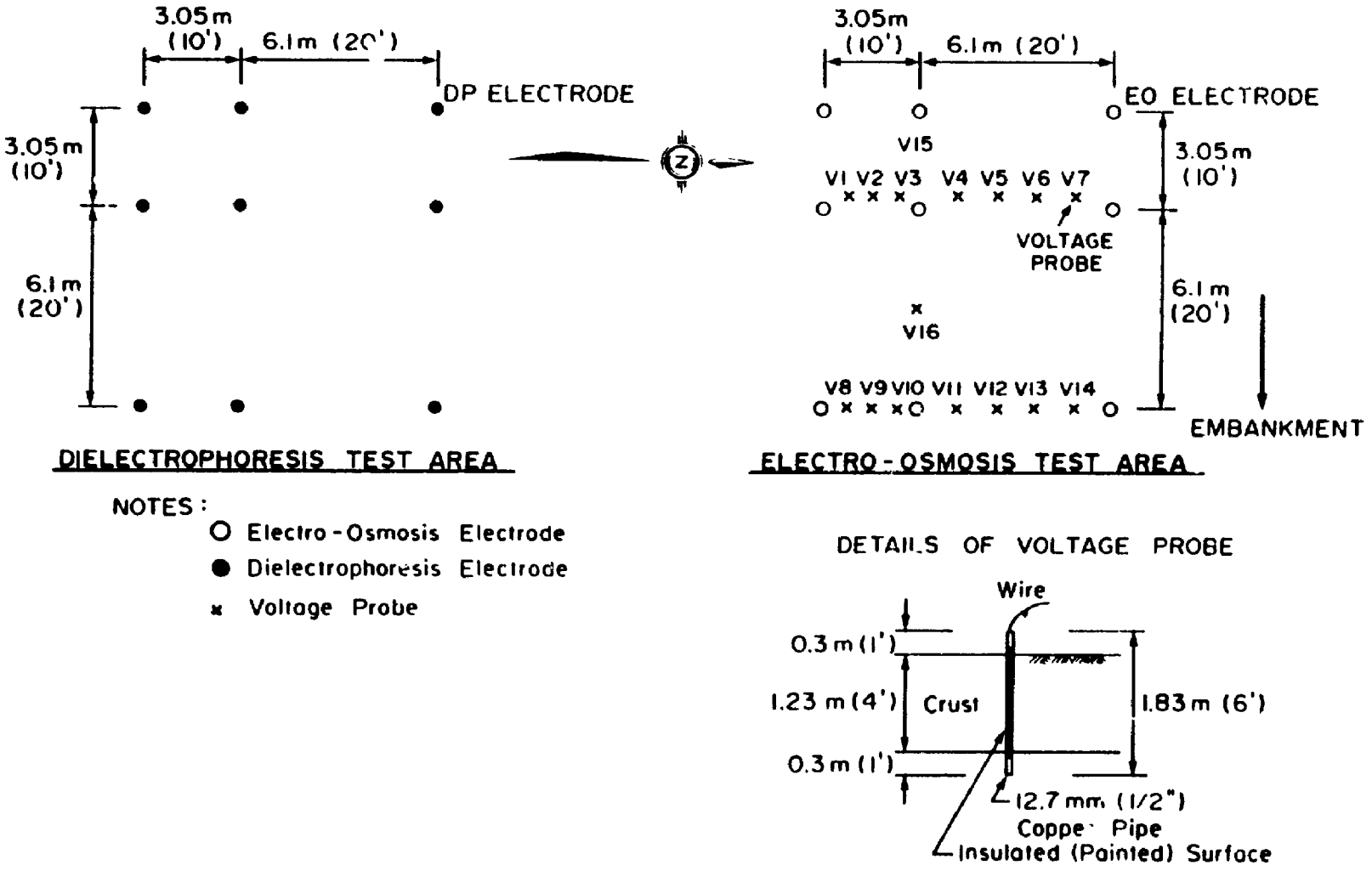

FIGURE 15.10 LAYOUT OF VOLTAGE PROBES

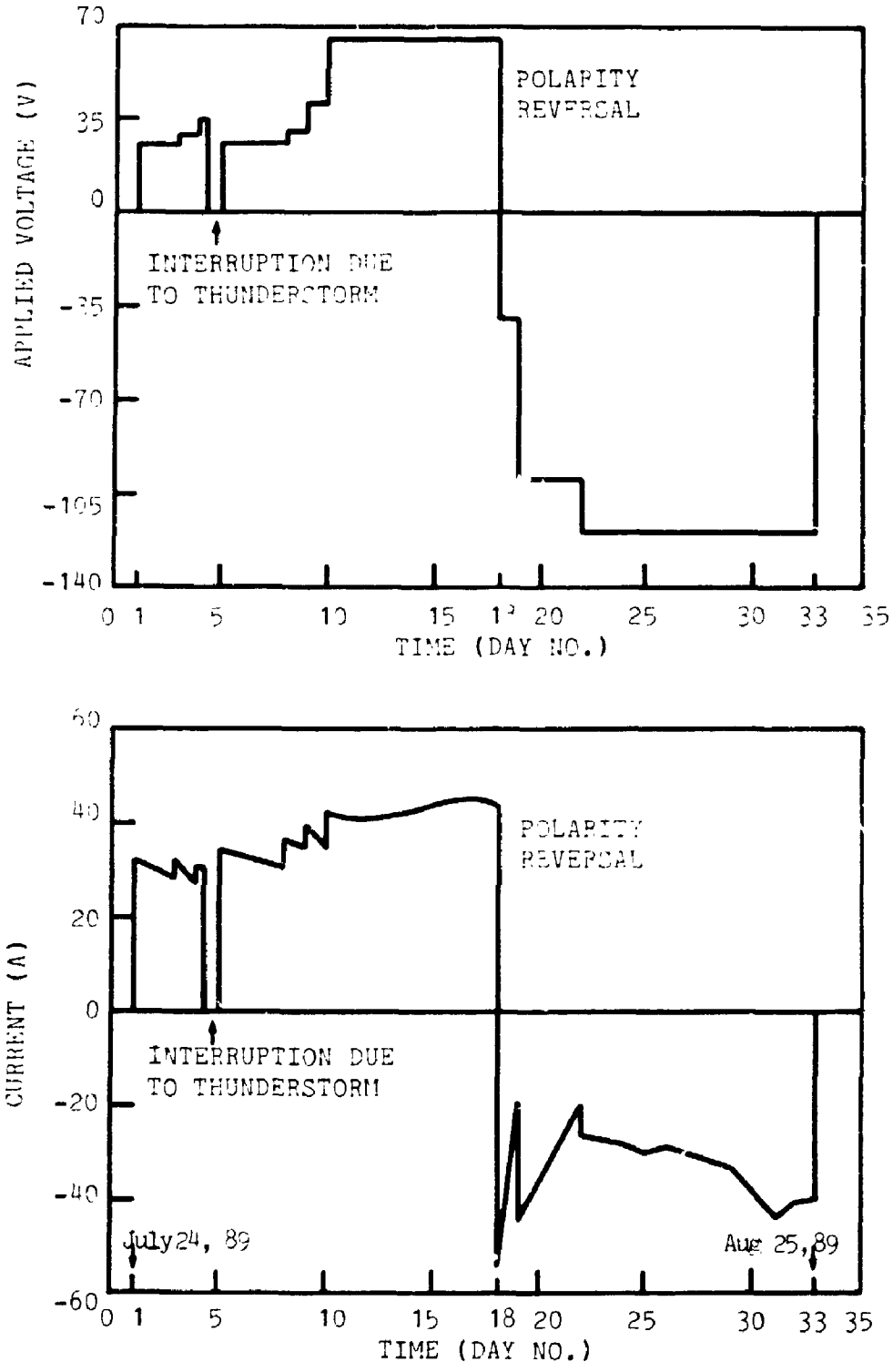

FIGURE 15.11 APPLIED VOLTAGE AND CURRENT VARIATIONS WITH TREATMENT TIME

FIGURE 15.12 PHOTO SHOWING WATER FLOWING OUT FROM THE CATHODE DURING TREATMENT AND NO PUMPING IS REQUIRED

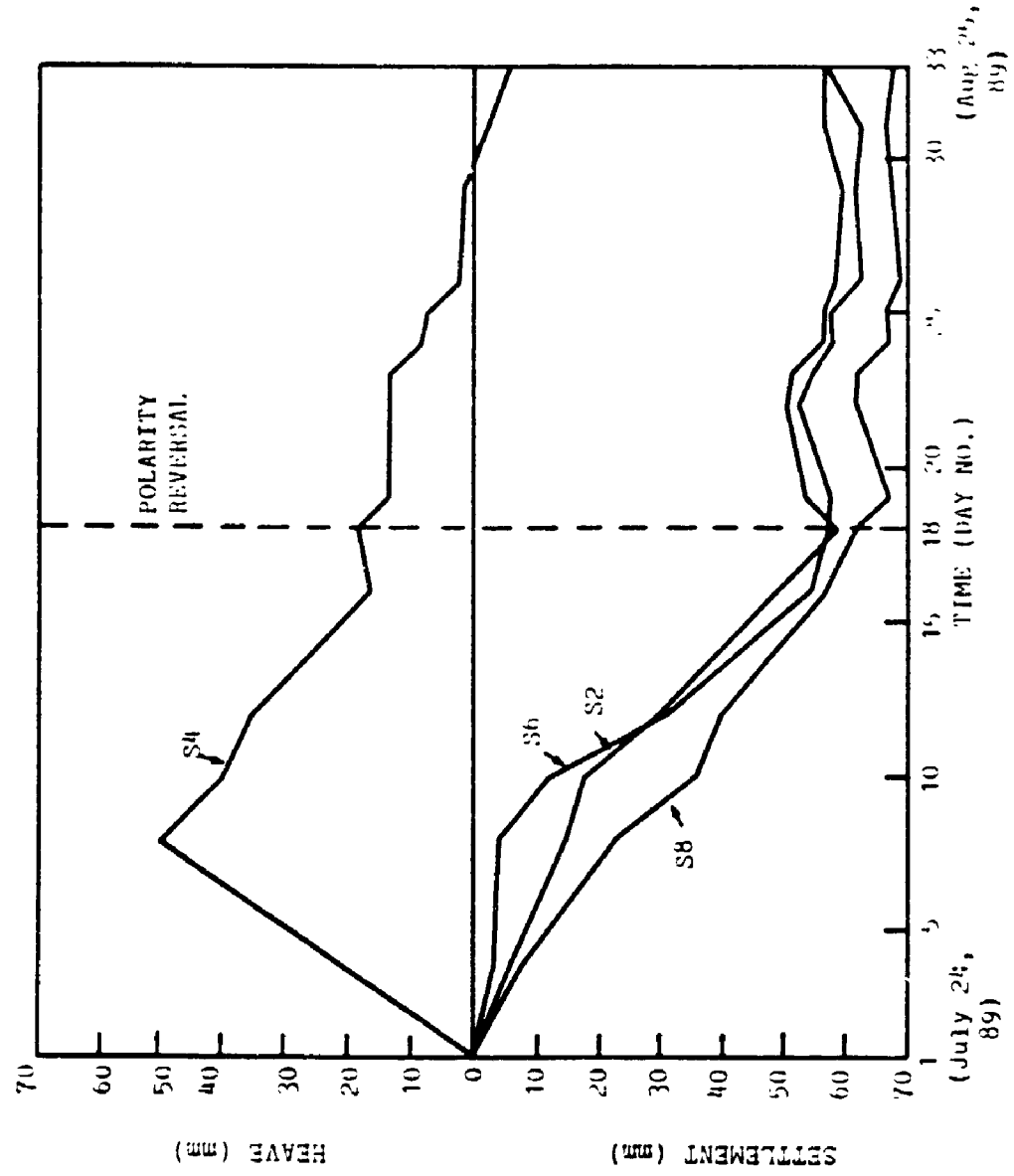

FIGURE 15.13 MEASURED SETTLEMENTS WITH TIME

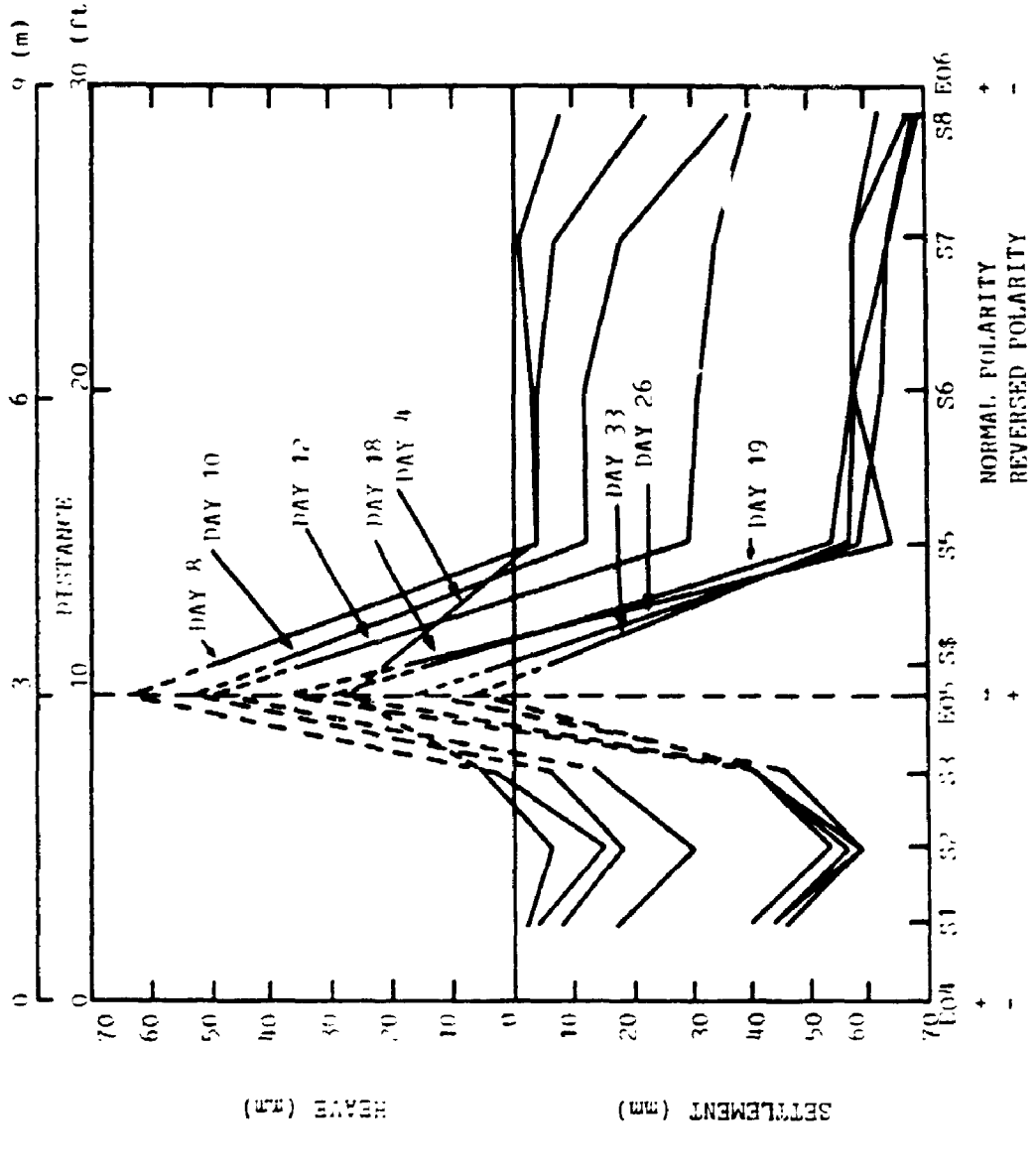

FIGURE 15.14 SETTLEMENT PROFILES ALONG ELECTRODES E04-E05-E06 (AUGERS S1-S8)

POSITIONS OF SETTLEMENT AUGERS AND ELECTRODES

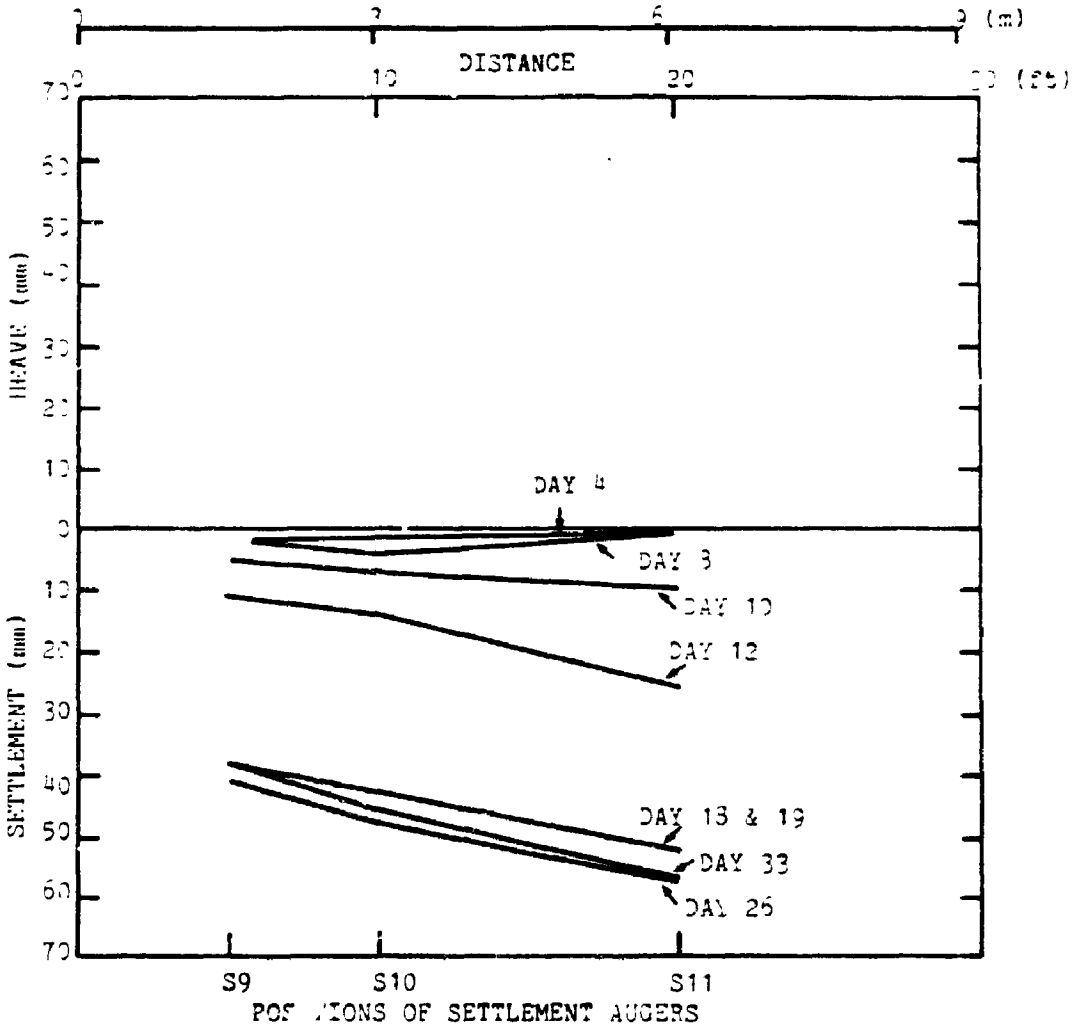

FIGURE 15.15 SETTLEMENT PROFILES FOR AUGERS S9-S10-S11

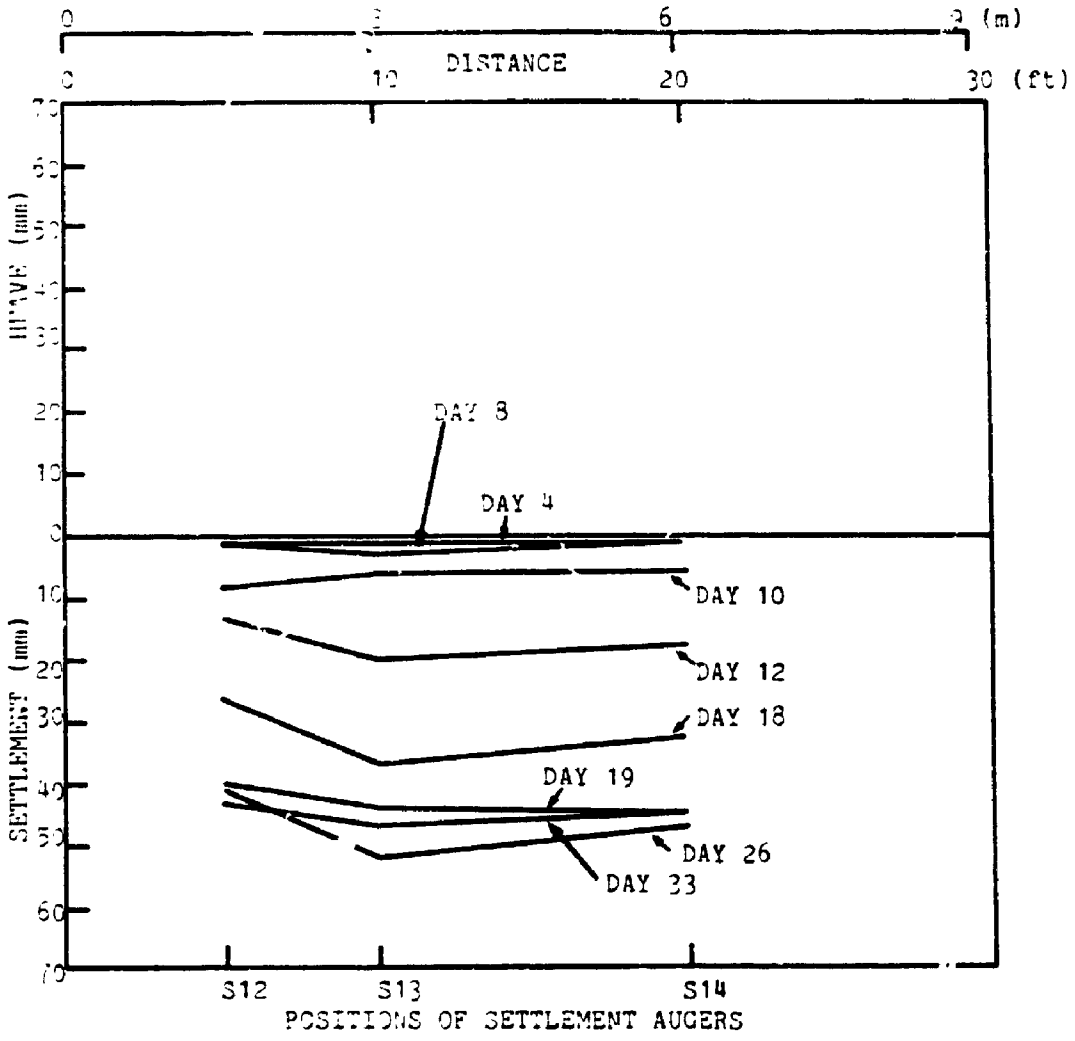

FIGURE 15.16 SETTLEMENT PROFILES FOR AUGERS S12-S13-S14

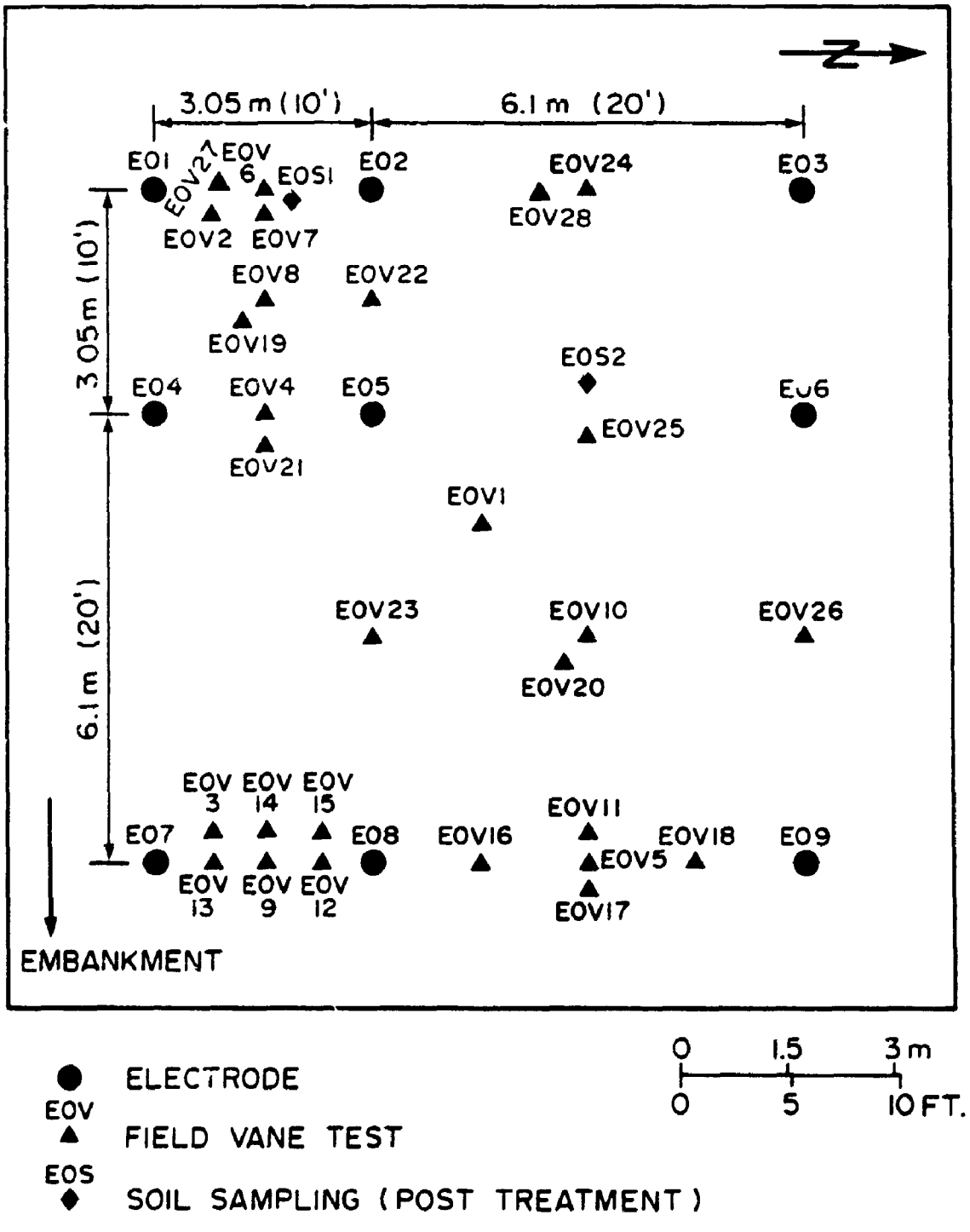

FIGURE 15.17 LAYOUT OF FIELD VANE TEST AND SAMPLING

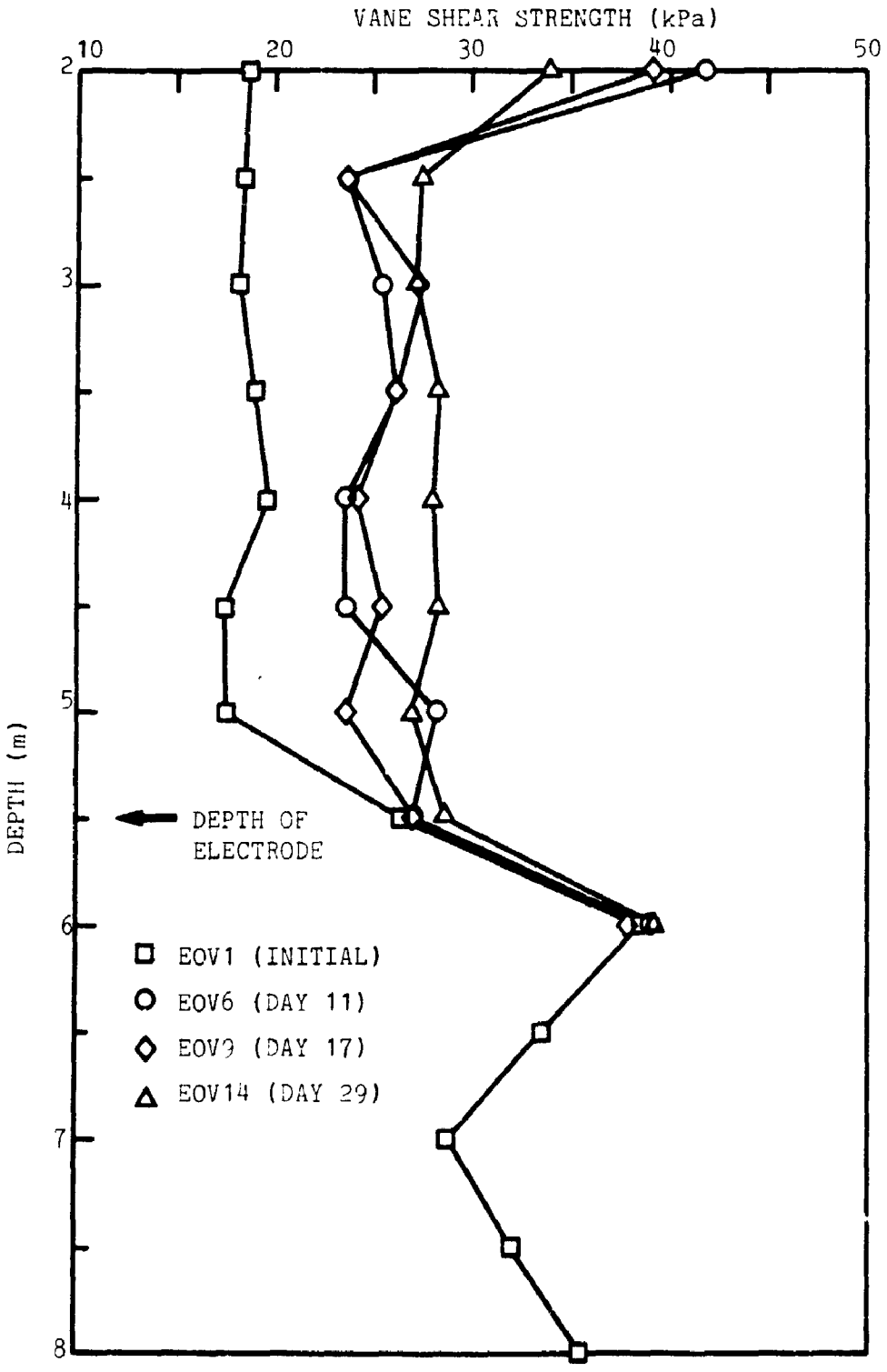

FIGURE 15.18 VARIATION OF VANE SHEAR STRENGTH PROFILES WITH TIME AT HALF-WAY OF ELECTRODES OF 3.05 m (10') SPACING

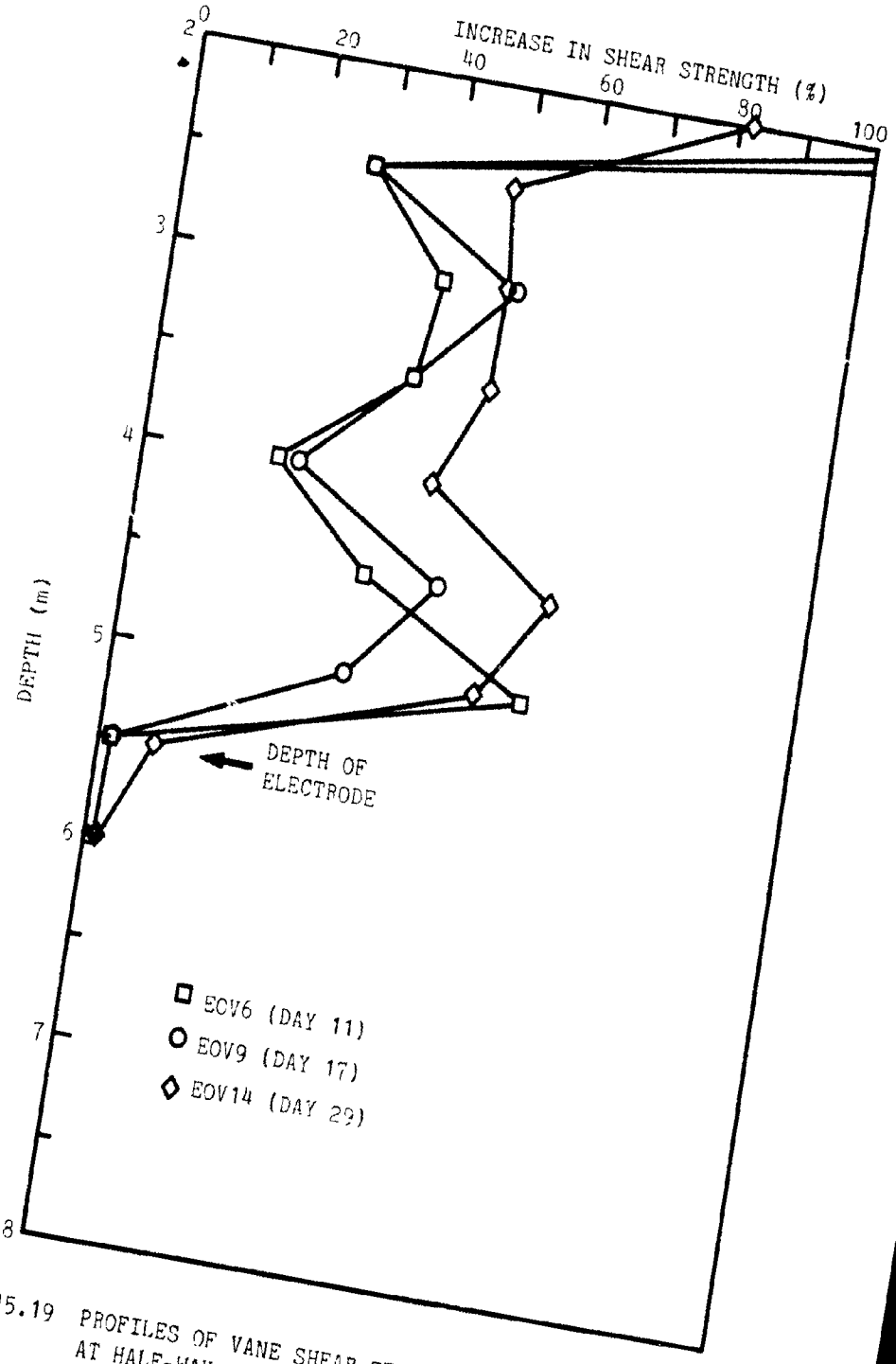

FIGURE 15.19 PROFILES OF VANE SHEAR STRENGTH INCREASE WITH TIME AT HALF-WAY OF 2 ELECTRODES OF 3.05 m (10') SPACING

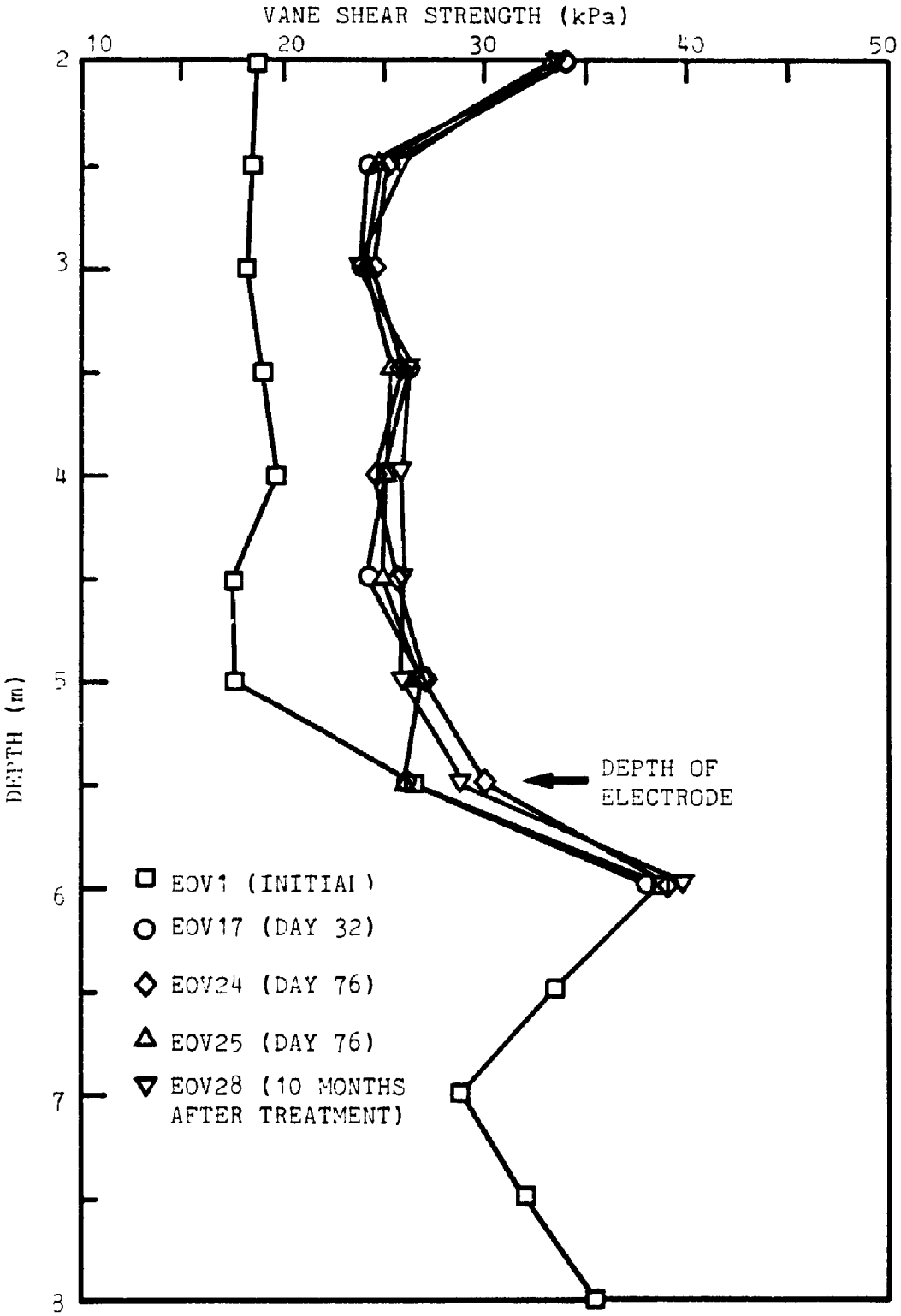

FIGURE 15.30 VARIATION OF VANE SHEAR STRENGTH PROFILES AT 43 DAYS AND AT 10 MONTHS AFTER TREATMENT AT HALFWAY OF ELECTRODES 6.1 m (20') SPACING

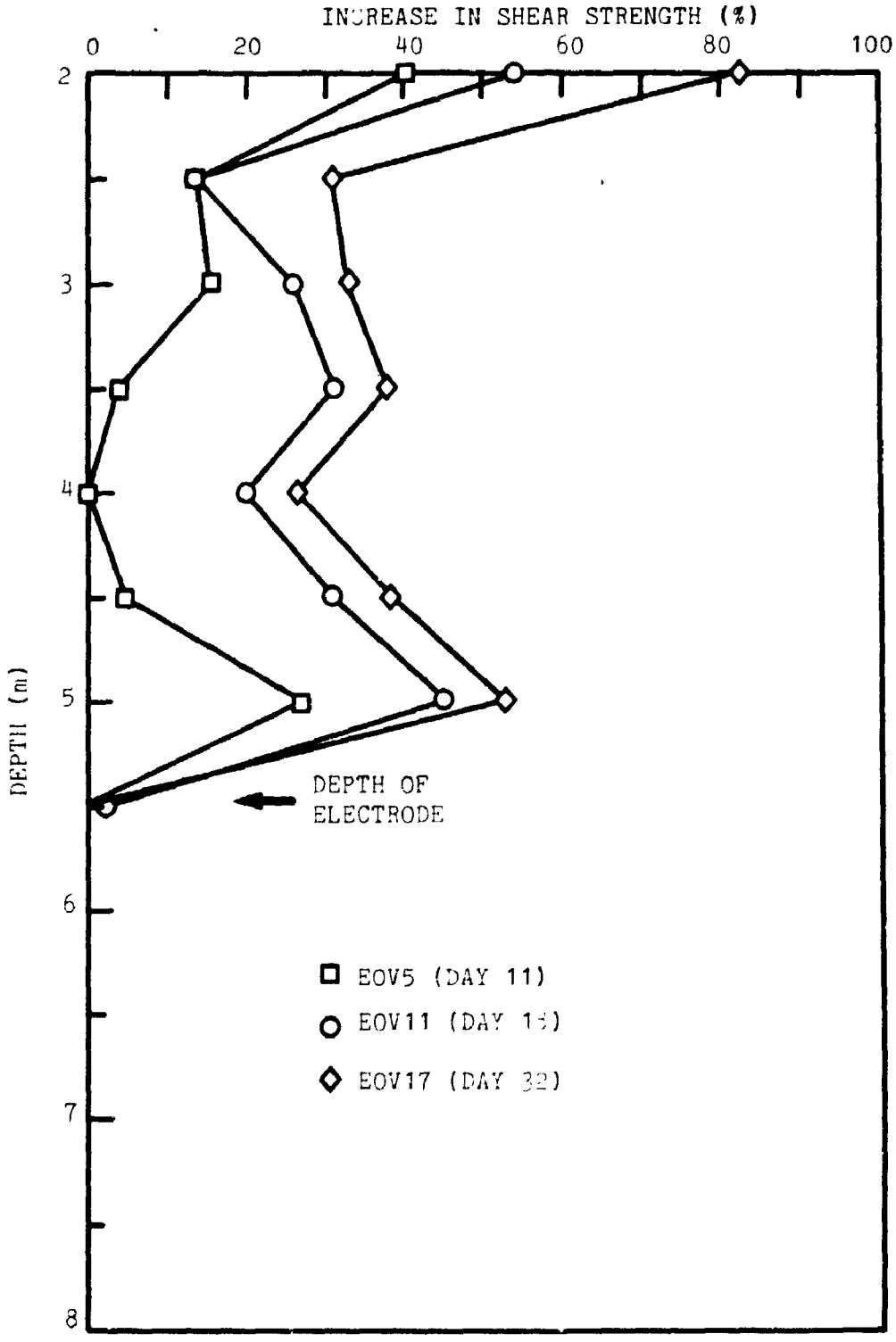

FIGURE 15.21 PROFILES OF VANE SHEAR STRENGTH INCREASE WITH TIME AT HALF-WAY OF 2 ELECTRODES OF 6.1 m (20') SPACING

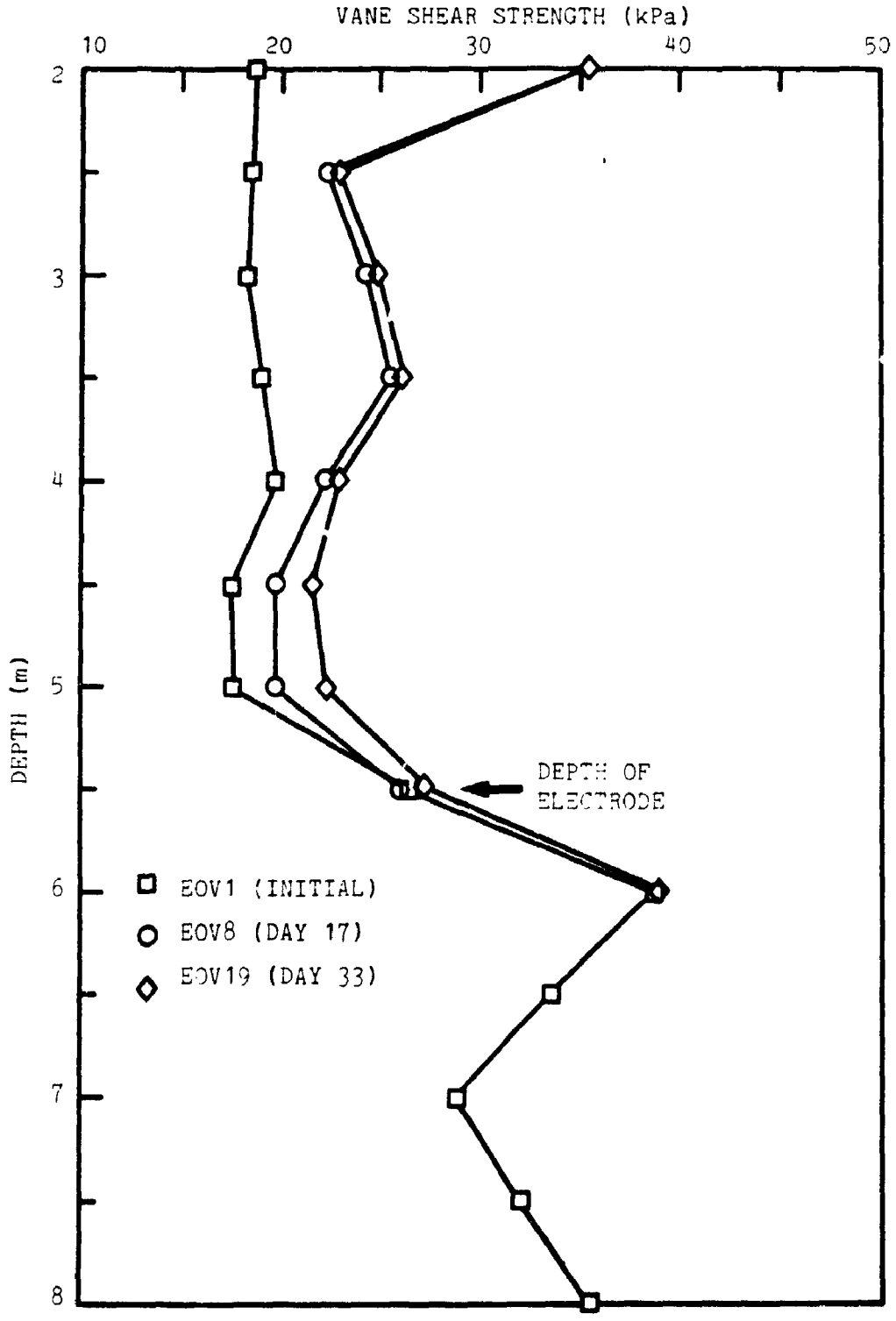

FIGURE 15.22 VARIATION OF VANE SHEAR STRENGTH PROFILES WITH TIME AT CENTRE OF 4 ELECTRODES OF 3.05 m (10') SQUARE GRID

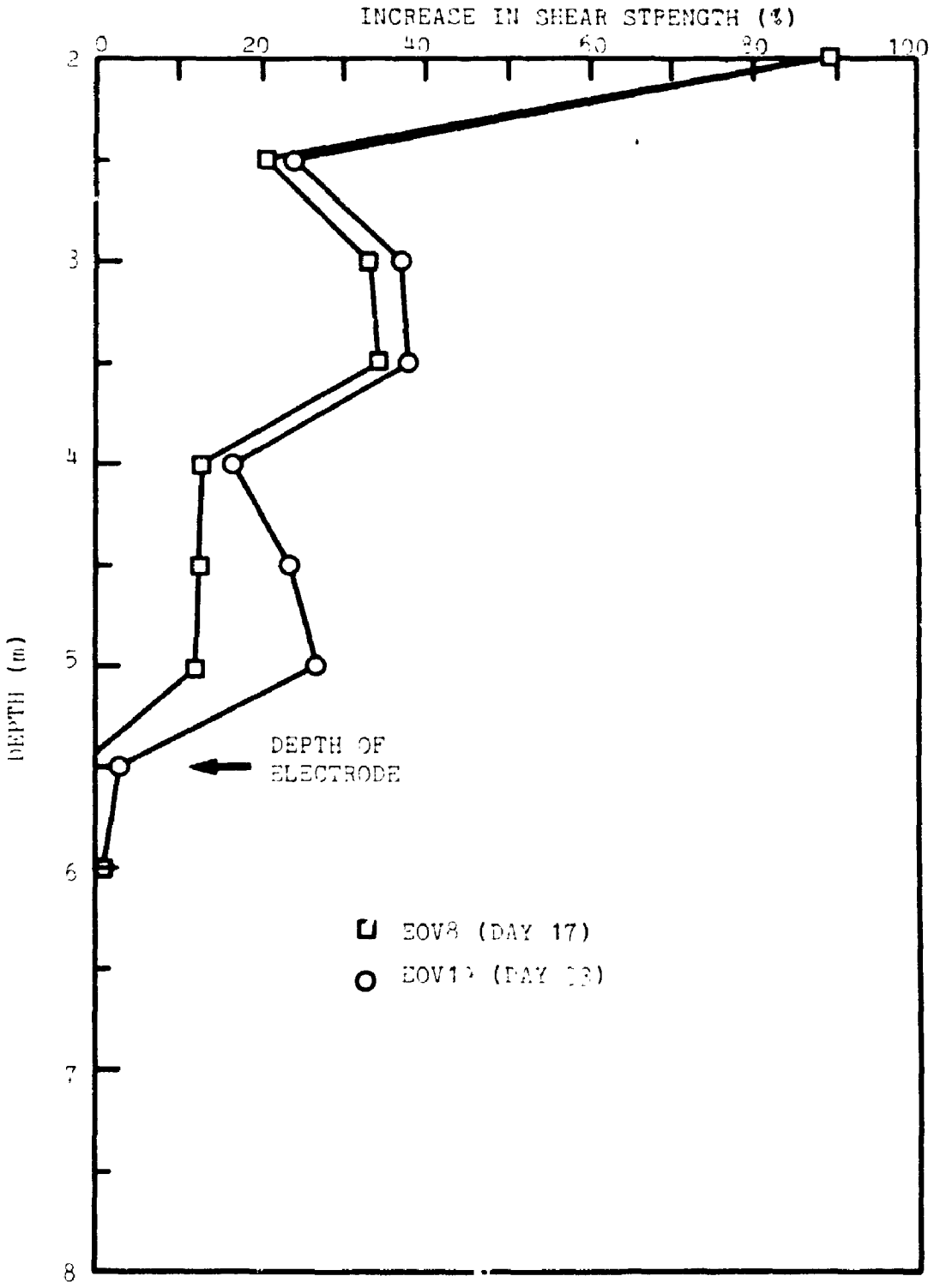

FIGURE 15.23 PROFILES OF VANE SHEAR STRENGTH INCREASE WITH TIME AT CENTRE OF 4 ELECTRODES OF 3.05 m (10') SQUARE GRID

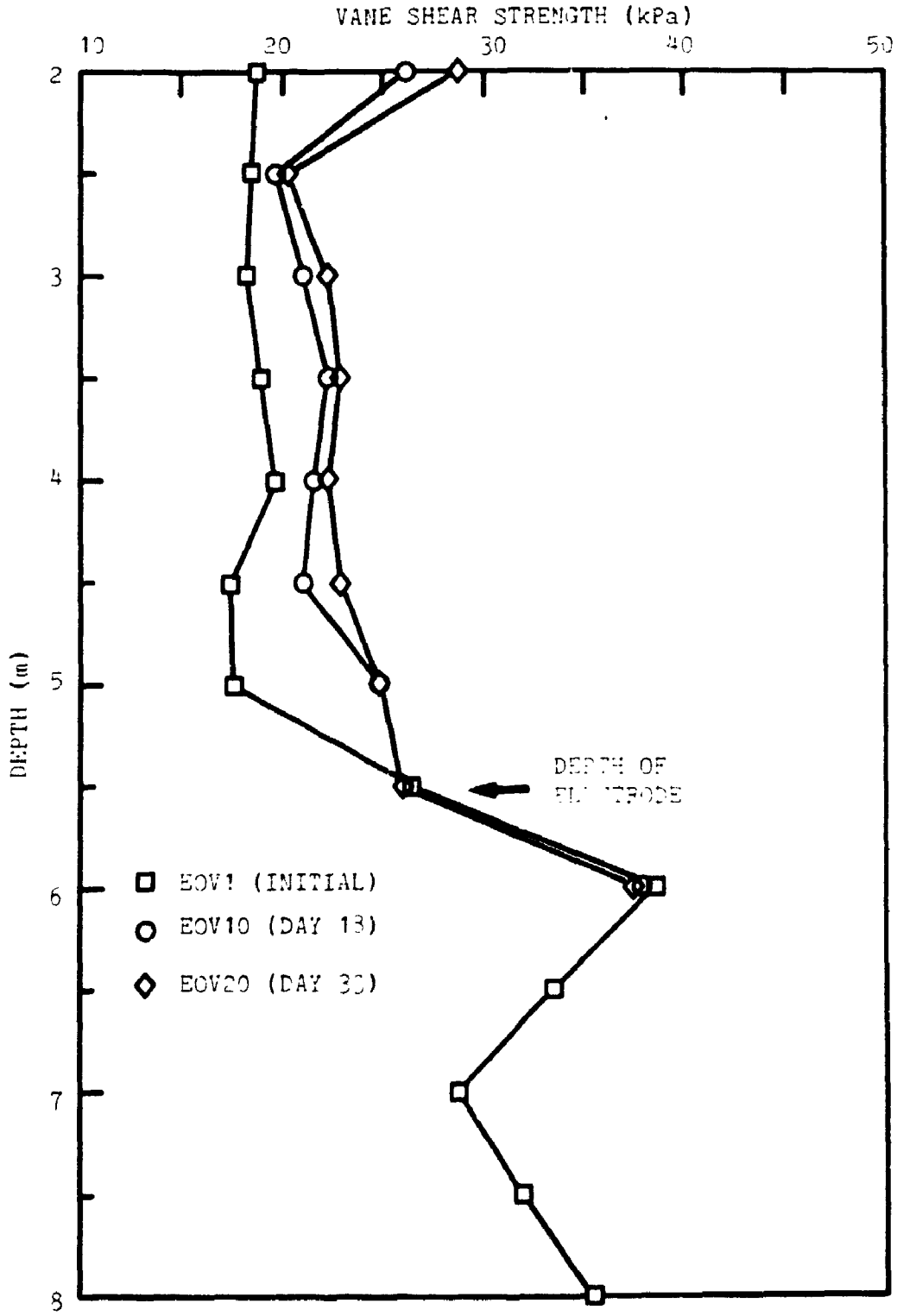

FIGURE 15.24 VARIATION OF VANE SHEAR STRENGTH PROFILES WITH TIME AT CENTRE OF 4 ELECTRODES OF 6.1 m (20') SQUARE GRID

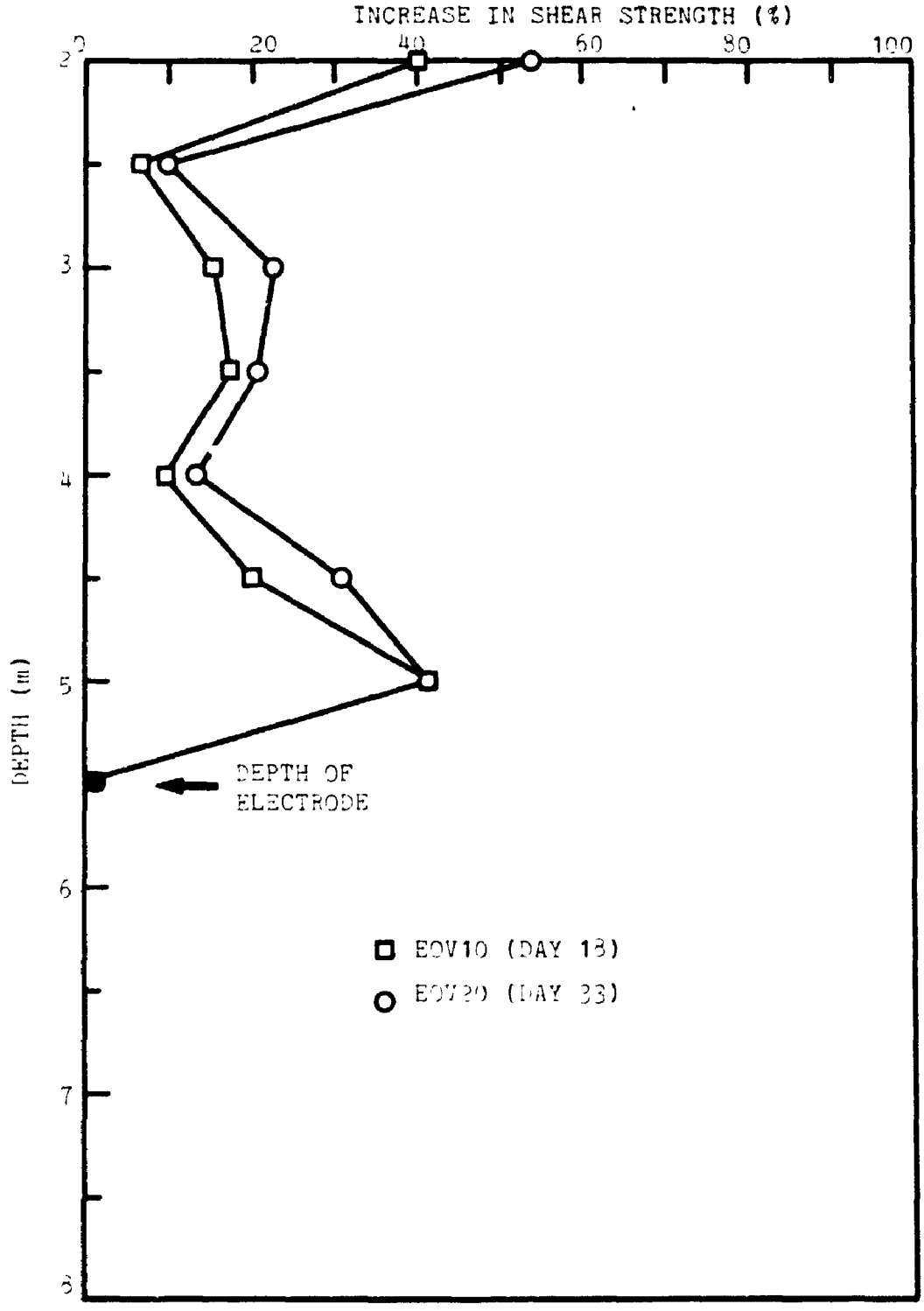

FIGURE 15.25 PROFILES OF VANE SHEAR STRENGTH INCREASE WITH TIME AT CENTRE OF 4 ELECTRODES OF 6.1 m (20') SQUARE GRID

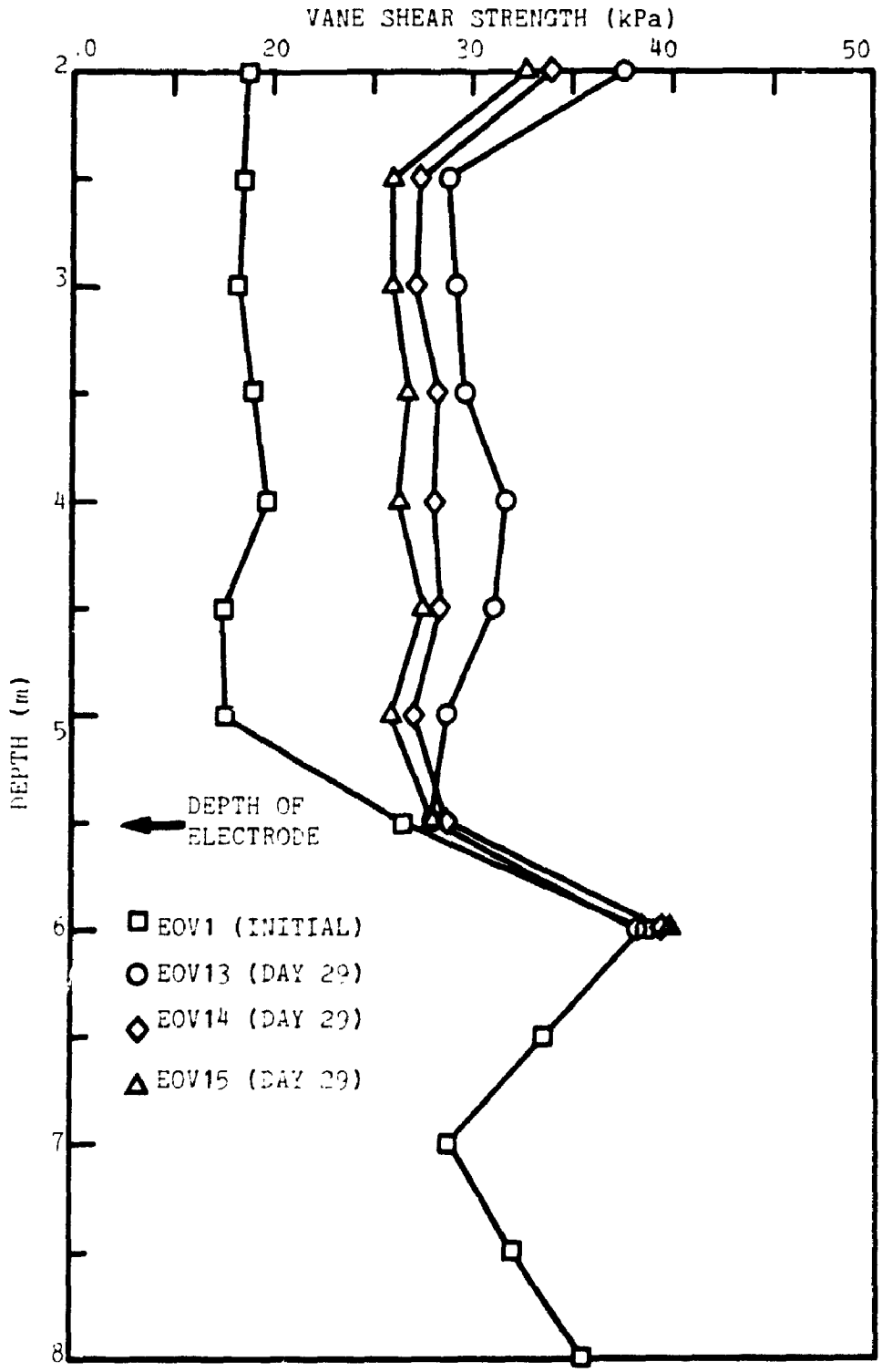

FIGURE 15.26 VARIATION OF VANE SHEAR STRENGTH PROFILES AT DIFFERENT LOCATIONS BETWEEN 2 ELECTRODES OF 3.05 m (10') SPACING SHOWING TH UNIFORMITY OF TREATMENT

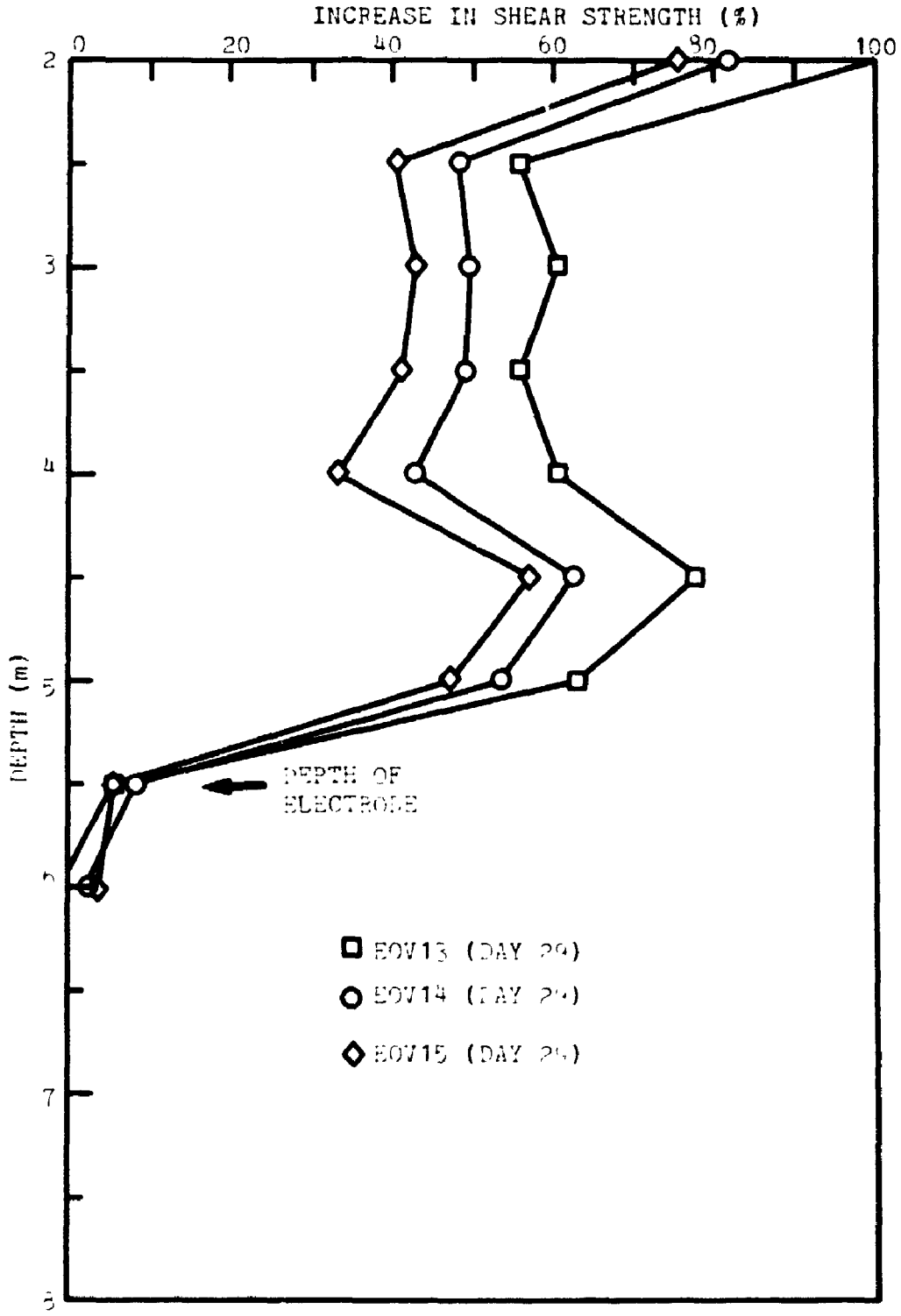

FIGURE 15.27 PROFILES OF VANE SHEAR STRENGTH INCREASE AT DIFFERENT LOCATIONS BETWEEN 2 ELECTRODES OF 3.05 m (10') SPACING SHOWING THE UNIFORMITY OF TREATMENT

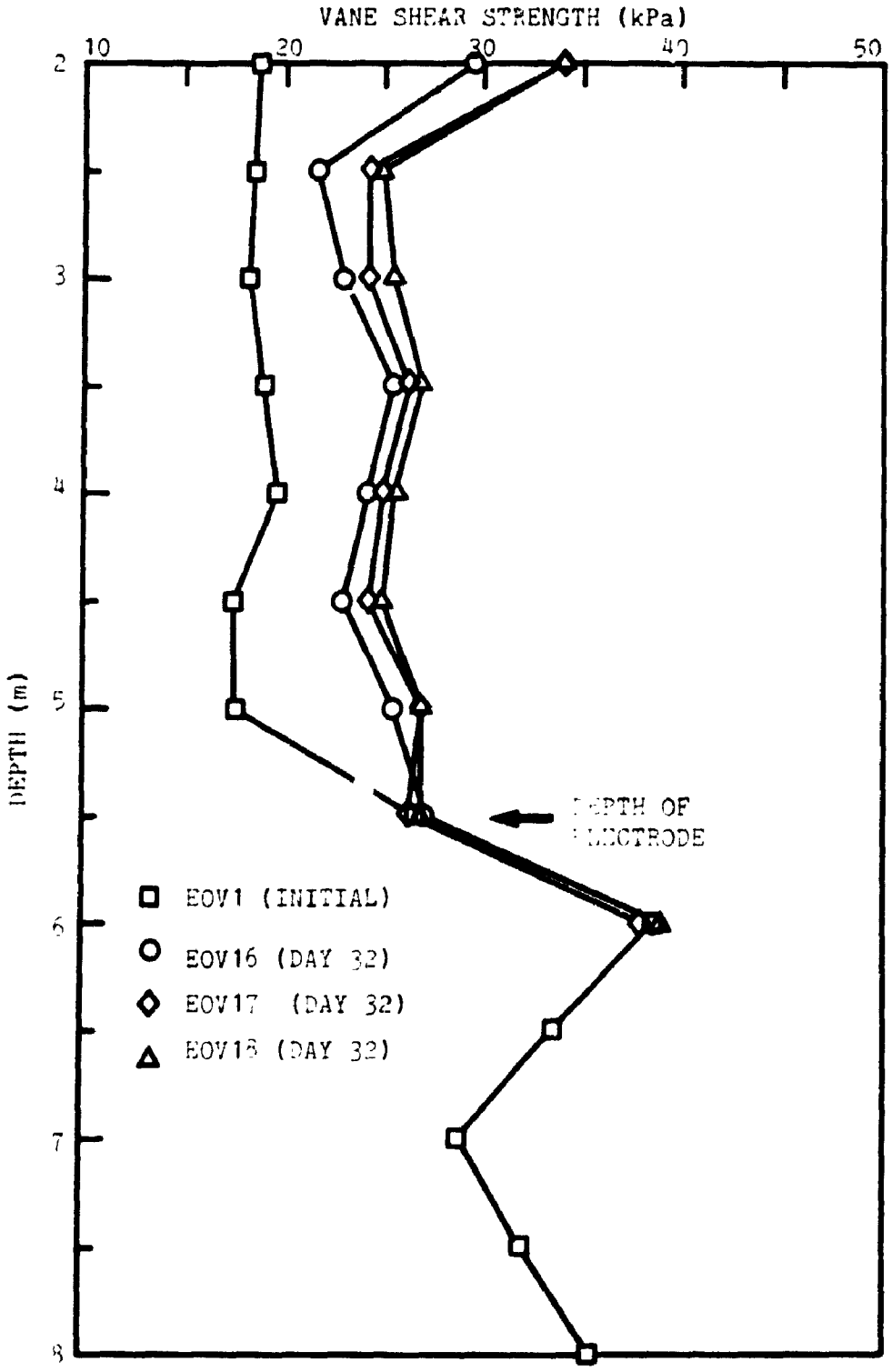

FIGURE 15.28 VARIATION OF VANE SHEAR STRENGTH PROFILES AT DIFFERENT LOCATIONS BETWEEN 2 ELECTRODES OF 6.1 m (20') SPACING SHOWING THE UNIFORMITY OF TREATMENT

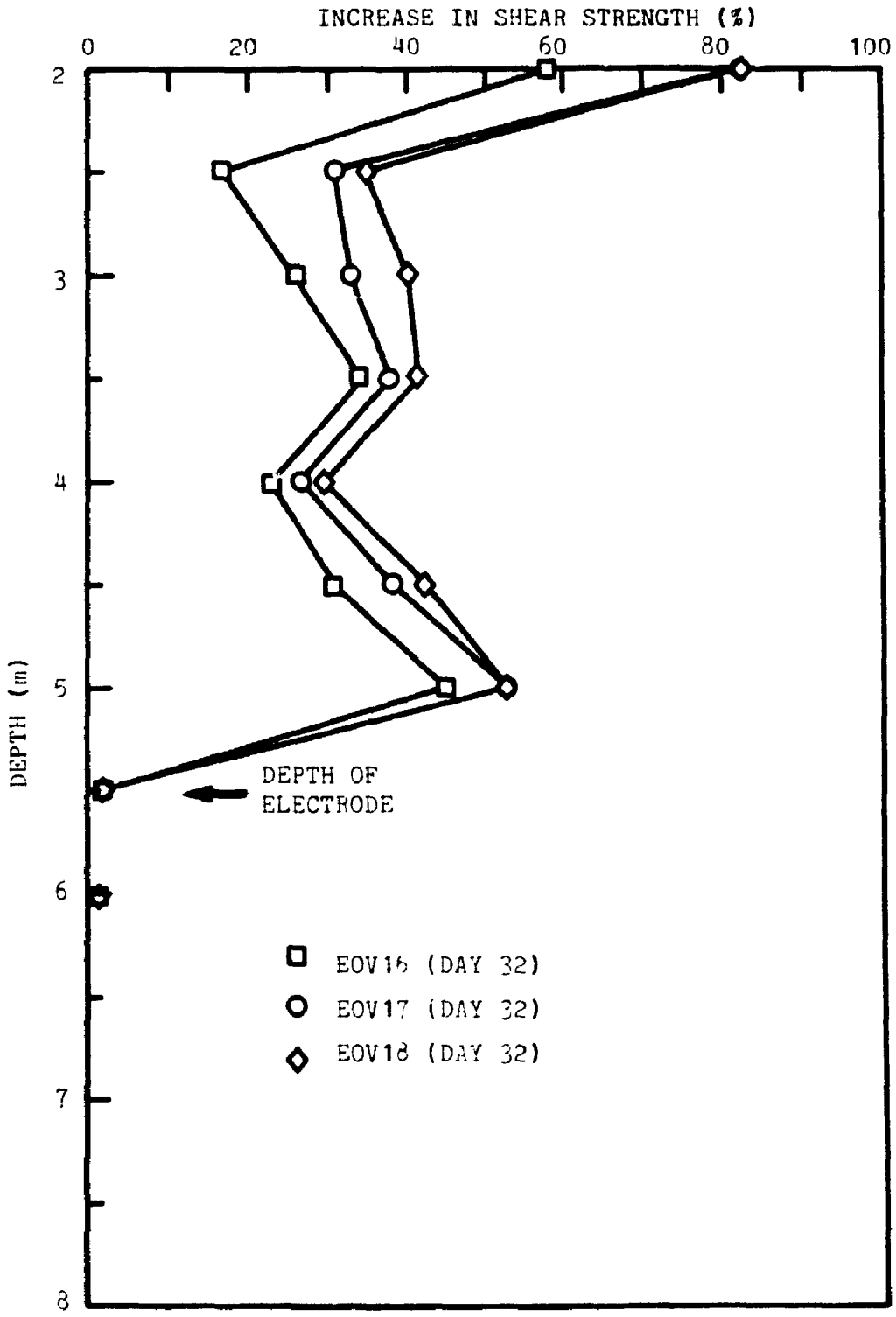

FIGURE 15.29 PROFILES OF VANE SHEAR STRENGTH INCREASE AT DIFFERENT LOCATIONS BETWEEN 2 ELECTRODES OF 6.1 m (20') SPACING SHOWING THE UNIFORMITY OF TREATMENT

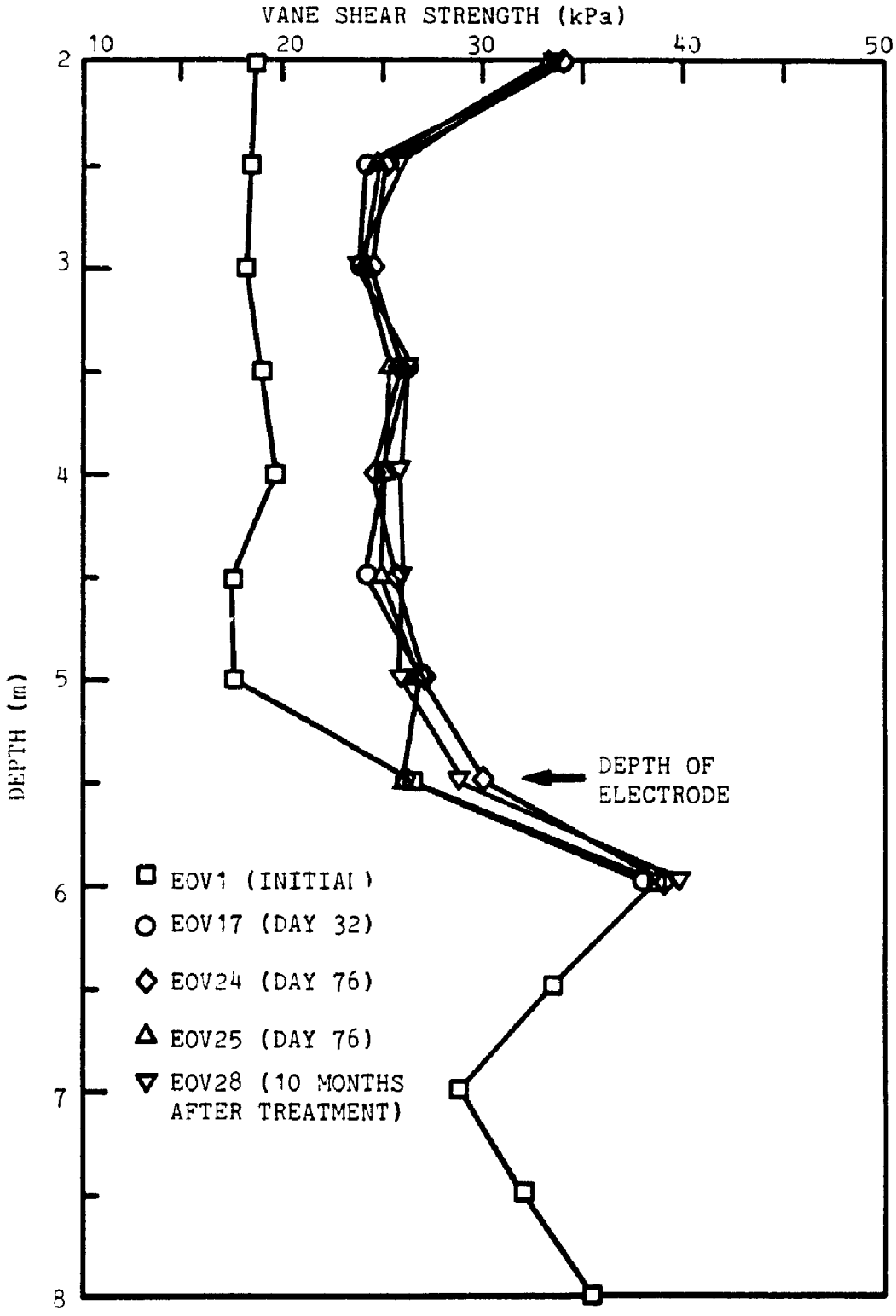

FIGURE 15.30 VARIATION OF VANE SHEAR STRENGTH PROFILES AT 43 DAYS AND AT 10 MONTHS AFTER TREATMENT AT HALFWAY OF ELECTRODES 6.1 m (20') SPACING

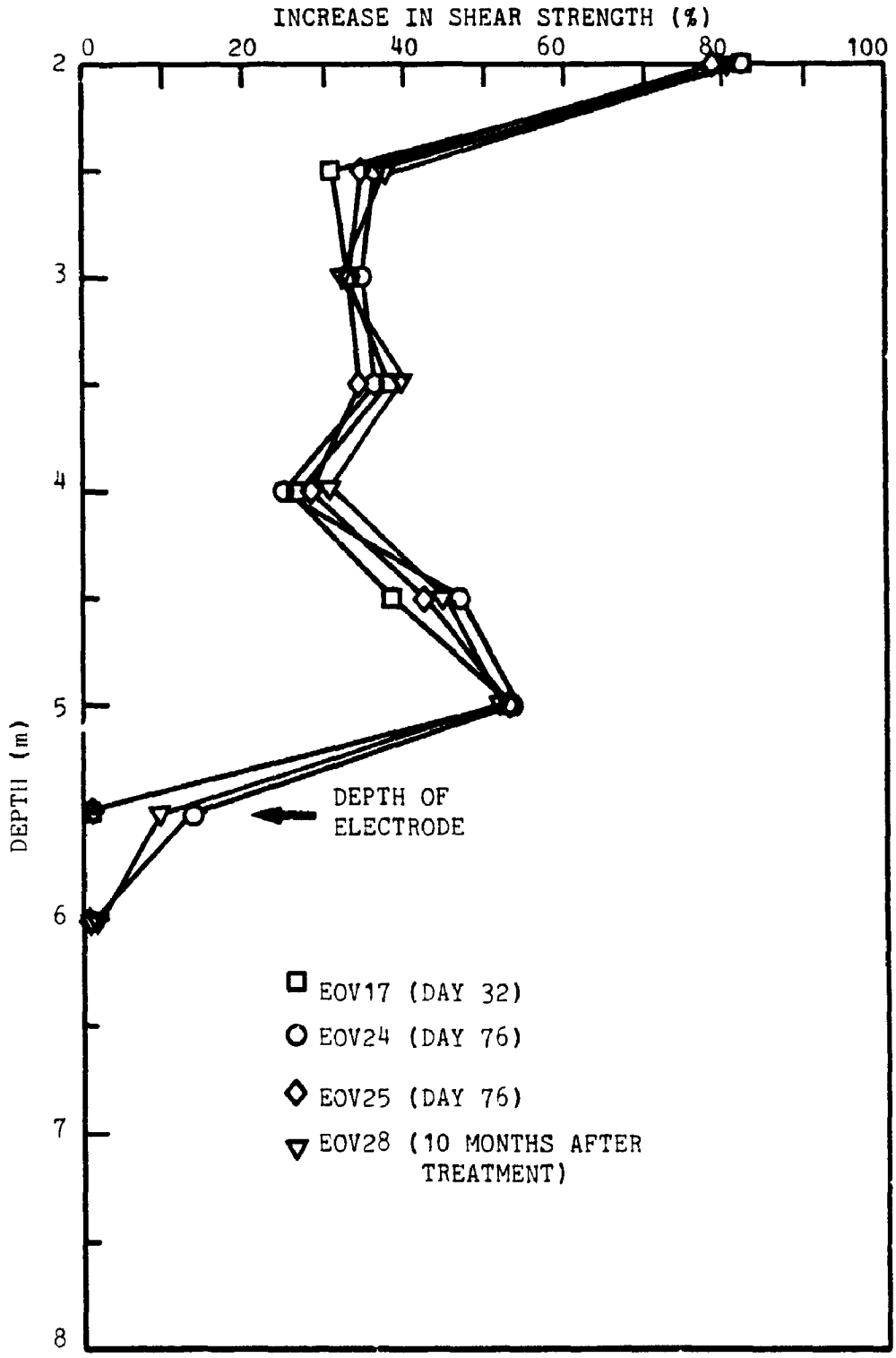

FIGURE 15.31 PROFILES OF VANE SHEAR STRENGTH INCREASE AT 43 DAYS AND AT 10 MONTHS AFTER TREATMENT AT HALFWAY OF ELECTRODE OF 6.1 m (20') SPACING

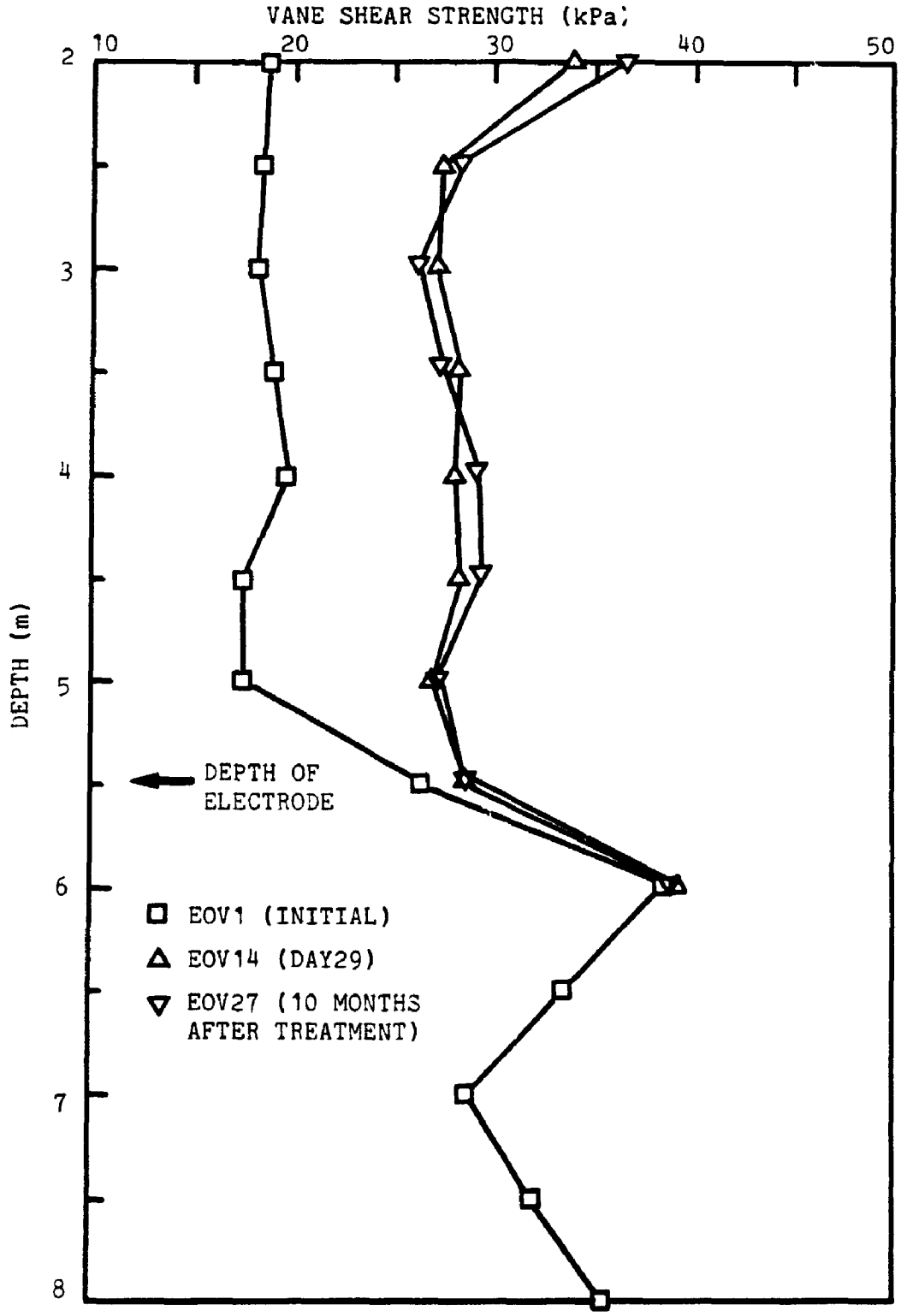

FIGURE 15.31a VARIATION OF VANE SHEAR STRENGTH PROFILES AT 10 MONTHS AFTER TREATMENT AT HALFWAY OF ELECTRODES OF 3.05 m SPACING

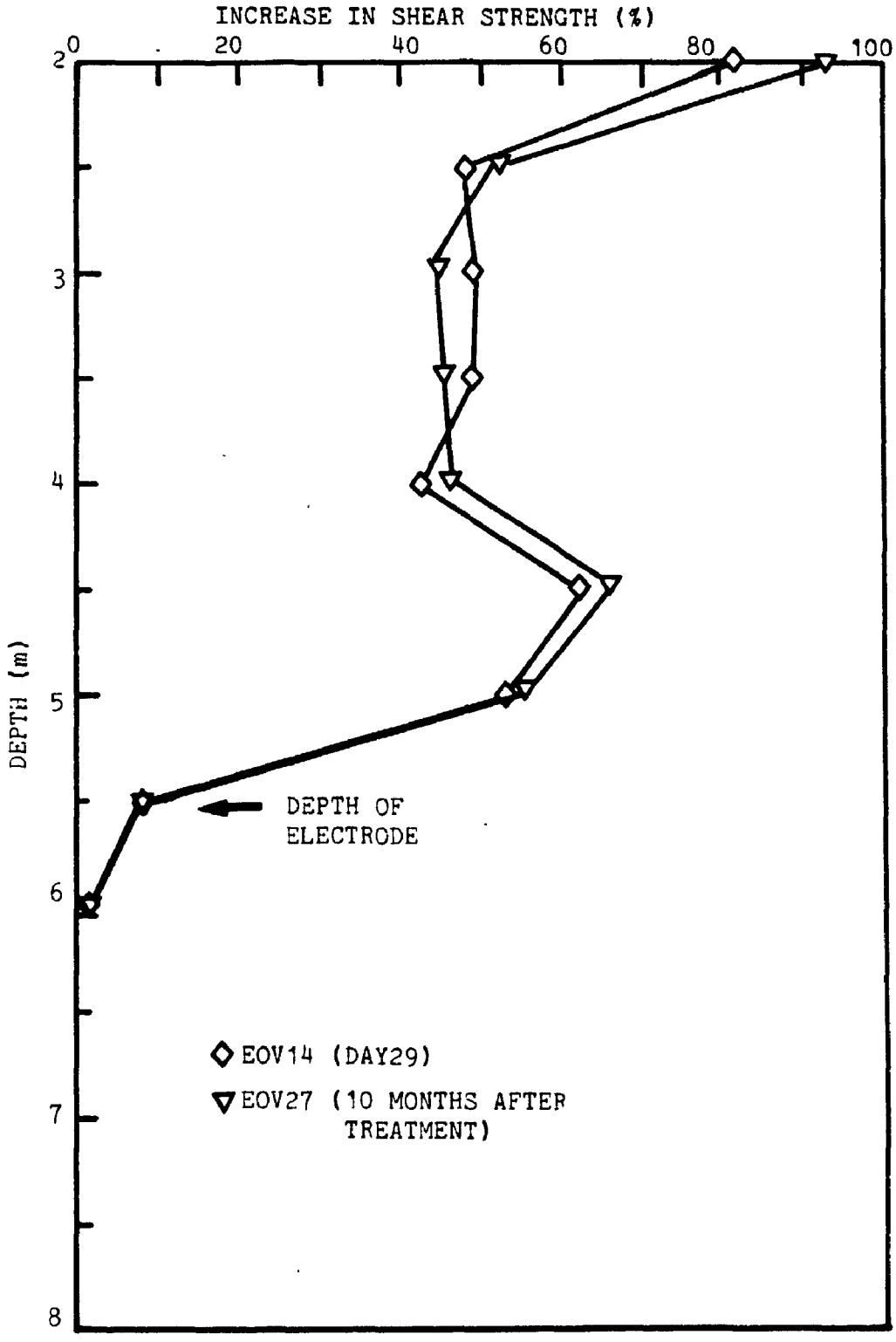

FIGURE 15.31b PROFILES OF VANE SHEAR STRENGTH INCREASE AT 10 MONTHS AFTER TREATMENT AT HALFWAY OF ELECTRODE OF 3.05 m SPACING

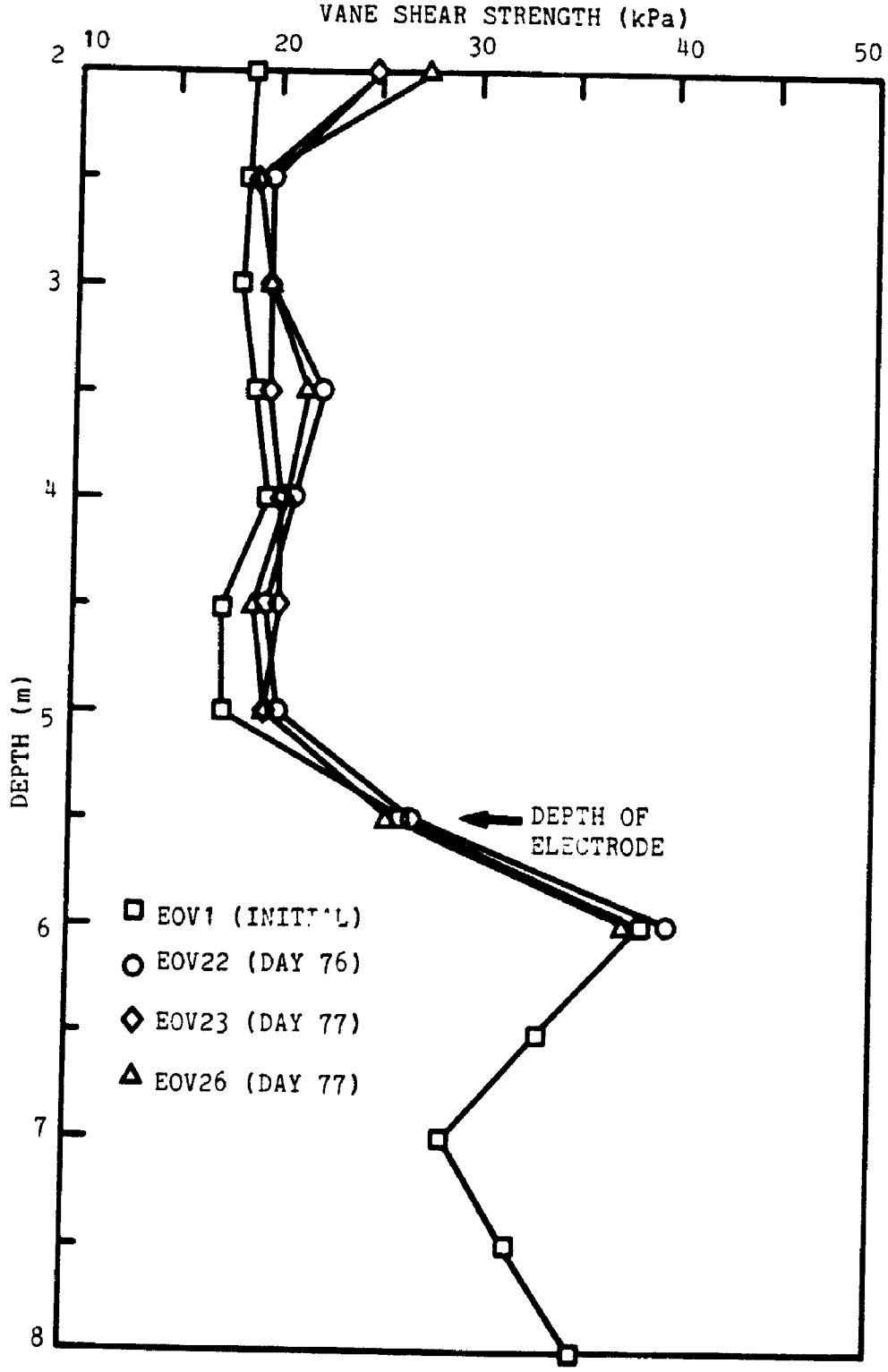

FIGURE 15.32 VARIATION OF VANE SHEAR STRENGTH PROFILES AT INACTIVE ZONES

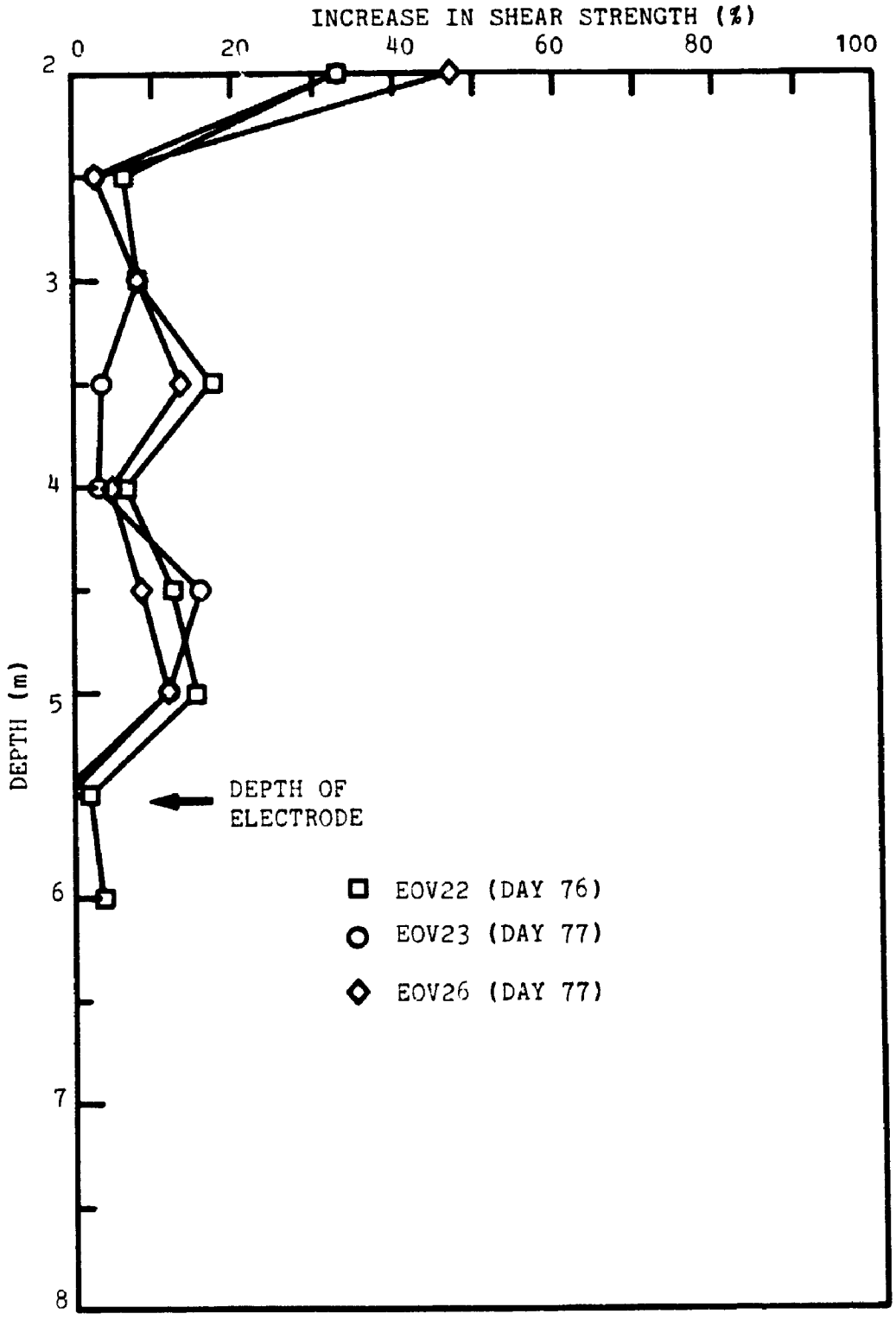

FIGURE 15.33 PROFILES OF VANE SHEAR STRENGTH INCREASE AT INACTIVE ZONES

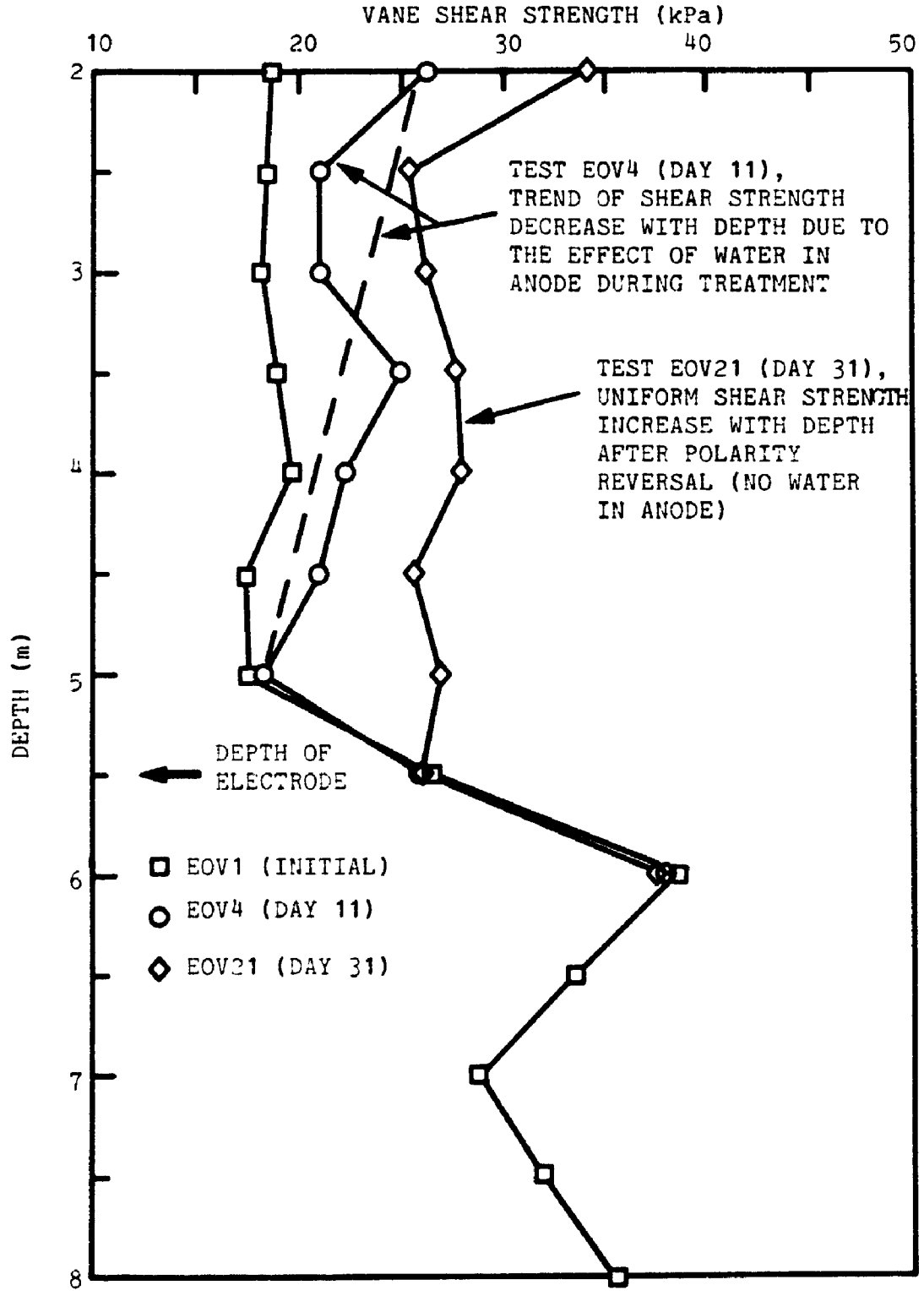

FIGURE 15.34 VARIATION OF VANE SHEAR STRENGTH PROFILES DUE TO THE EFFECT OF WATER IN ANODE DURING TREATMENT

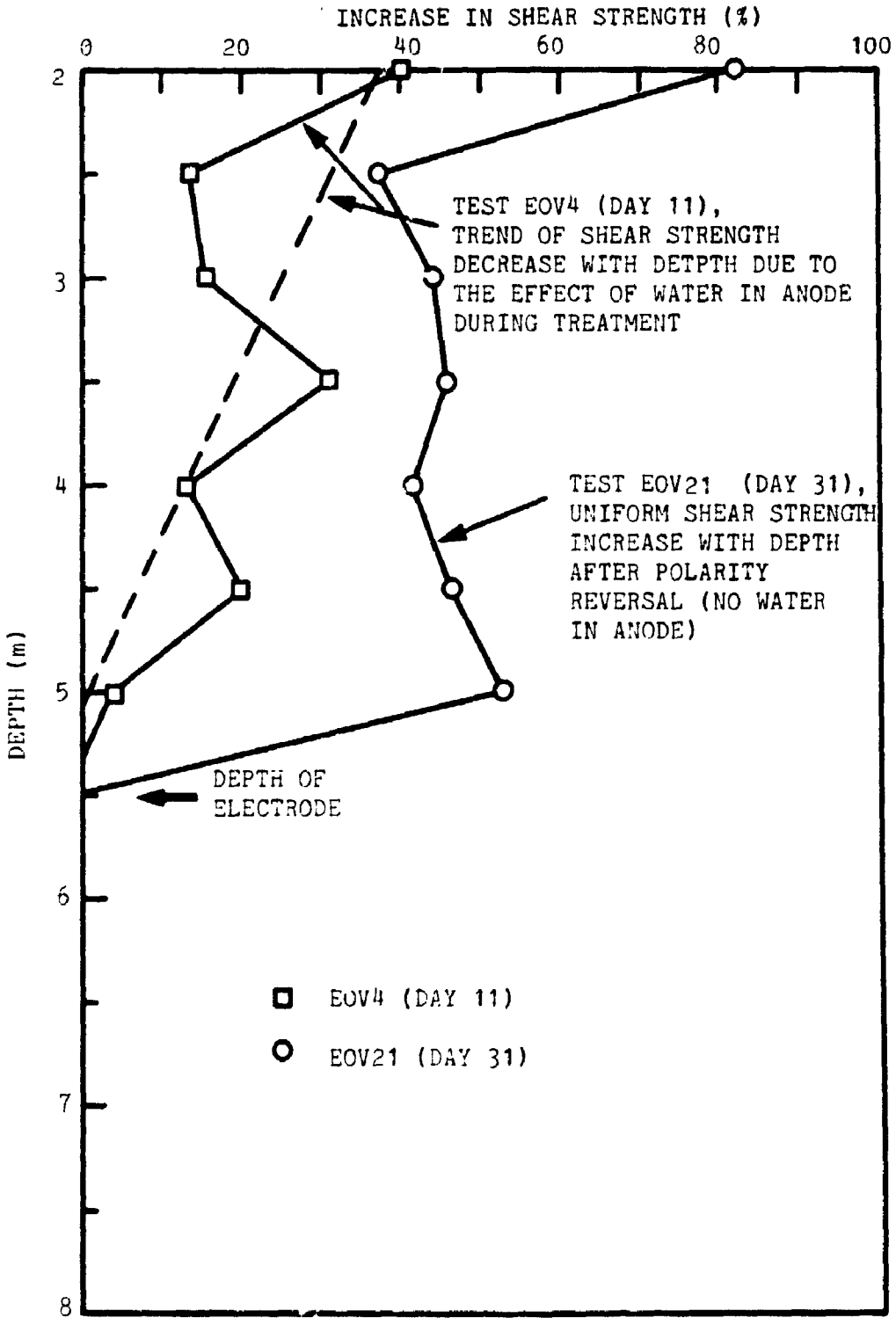

FIGURE 15.35 PROFILES OF VANE SHEAR STRENGTH INCREASE DUE TO THE EFFECT OF WATER IN ANODE DURING TREATMENT

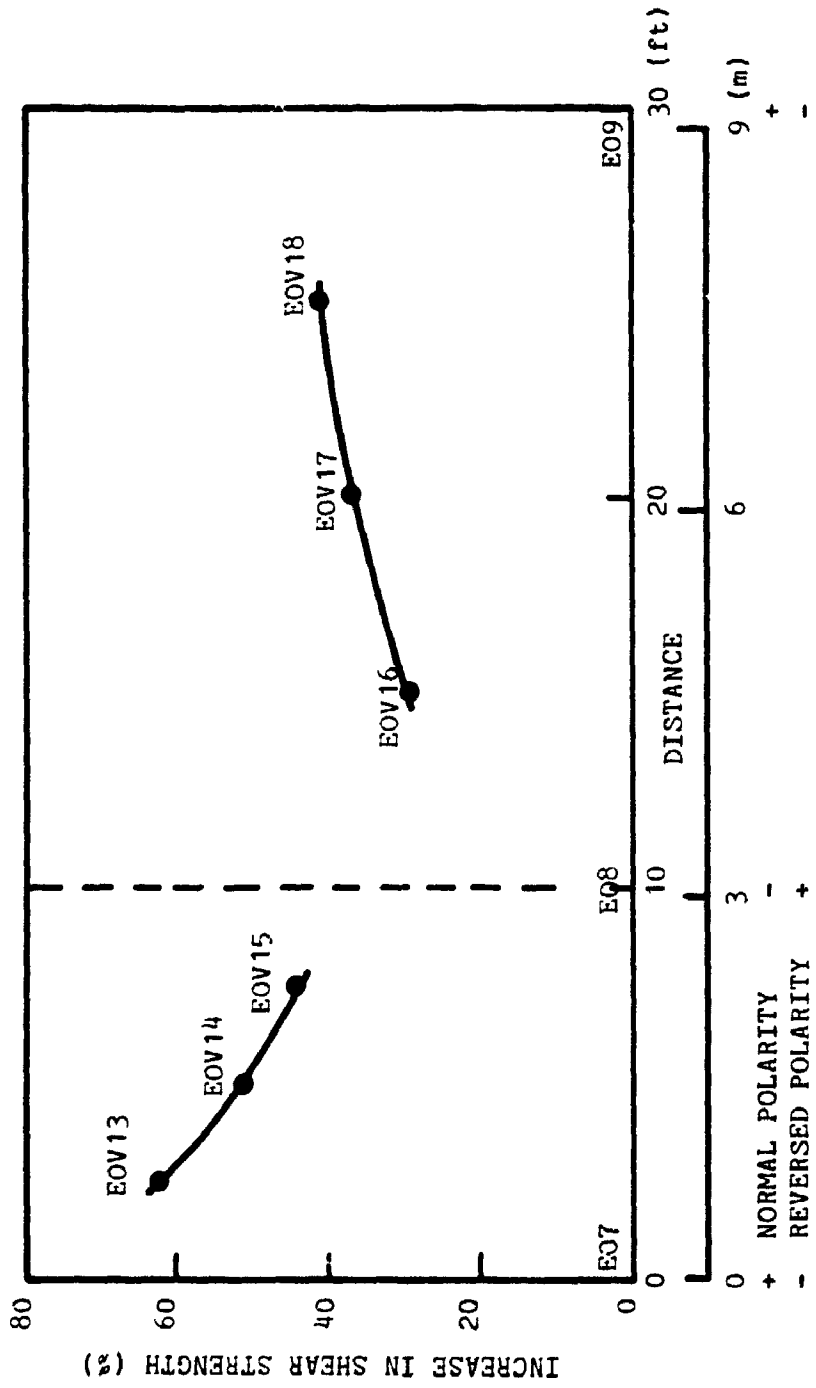

FIGURE 15.36 VARIATION OF SHEAR STRENGTH BETWEEN ELECTRODES E07-E08-E09 AFTER TREATMENT

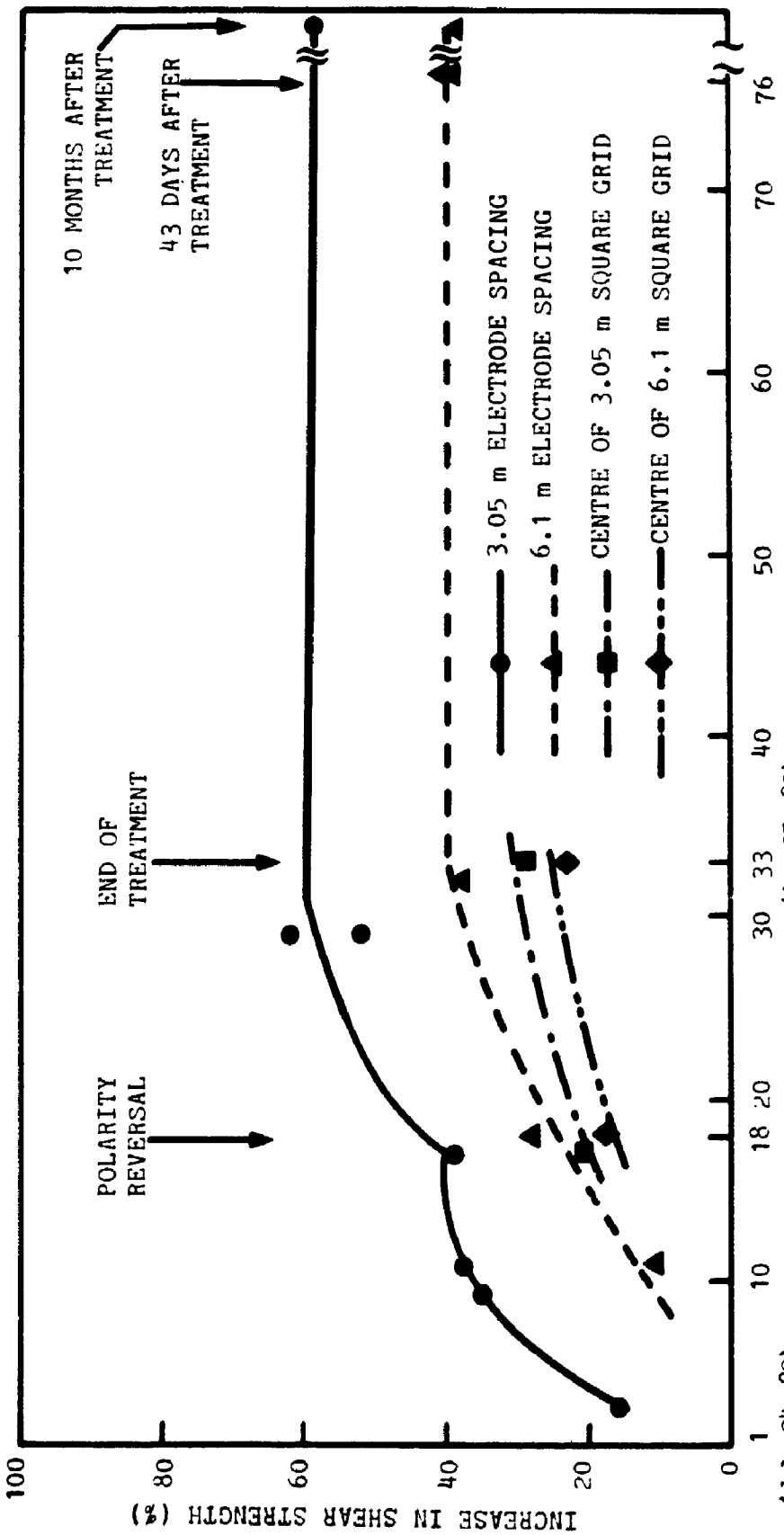

FIGURE 15.37 PERCENTAGE INCREASE IN SHEAR STRENGTH WITH TREATMENT TIME

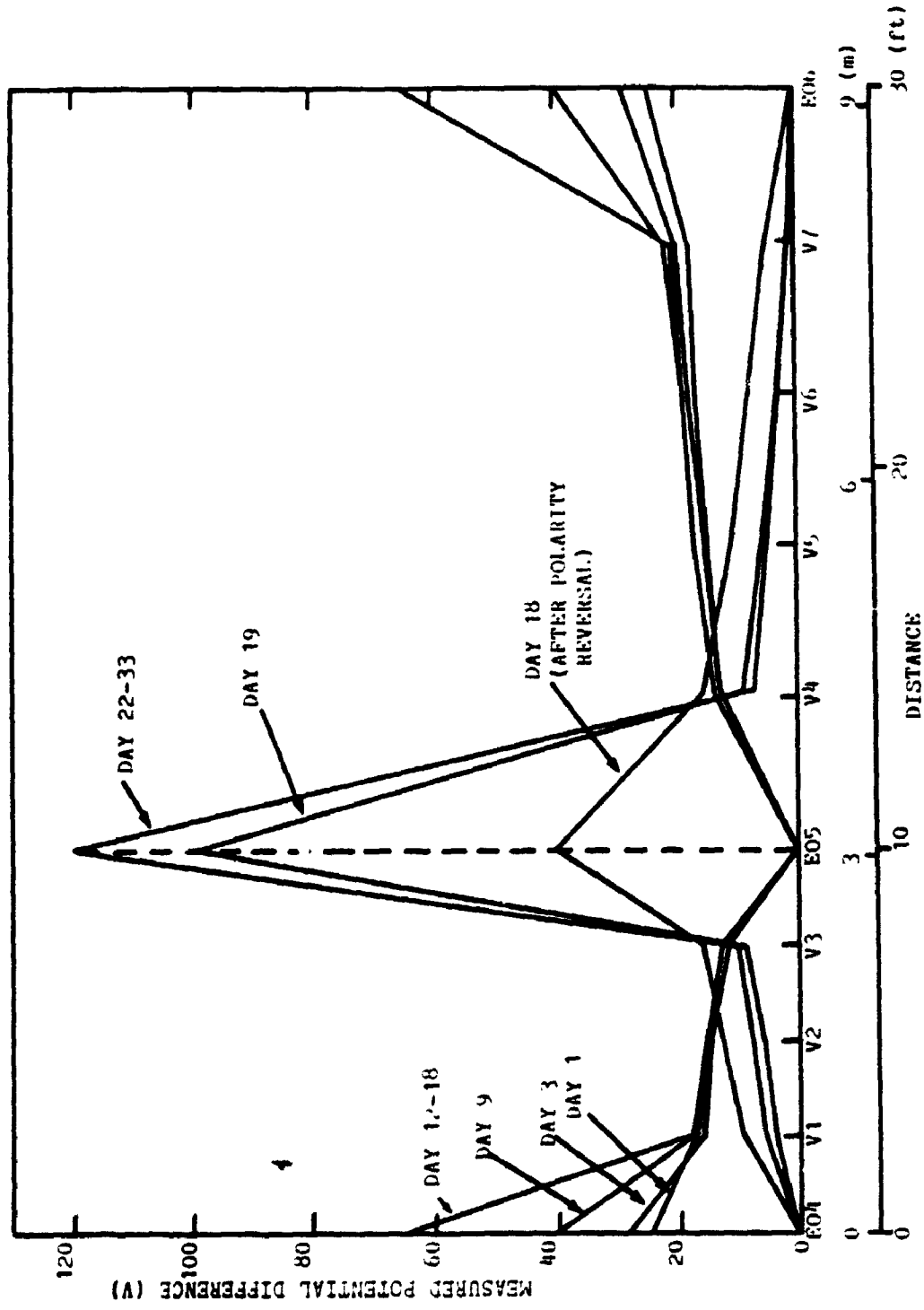

FIGURE 15.38 VOLTAGE VARIATION IN SOIL BETWEEN ELECTRODES EO4-EO5-EO6

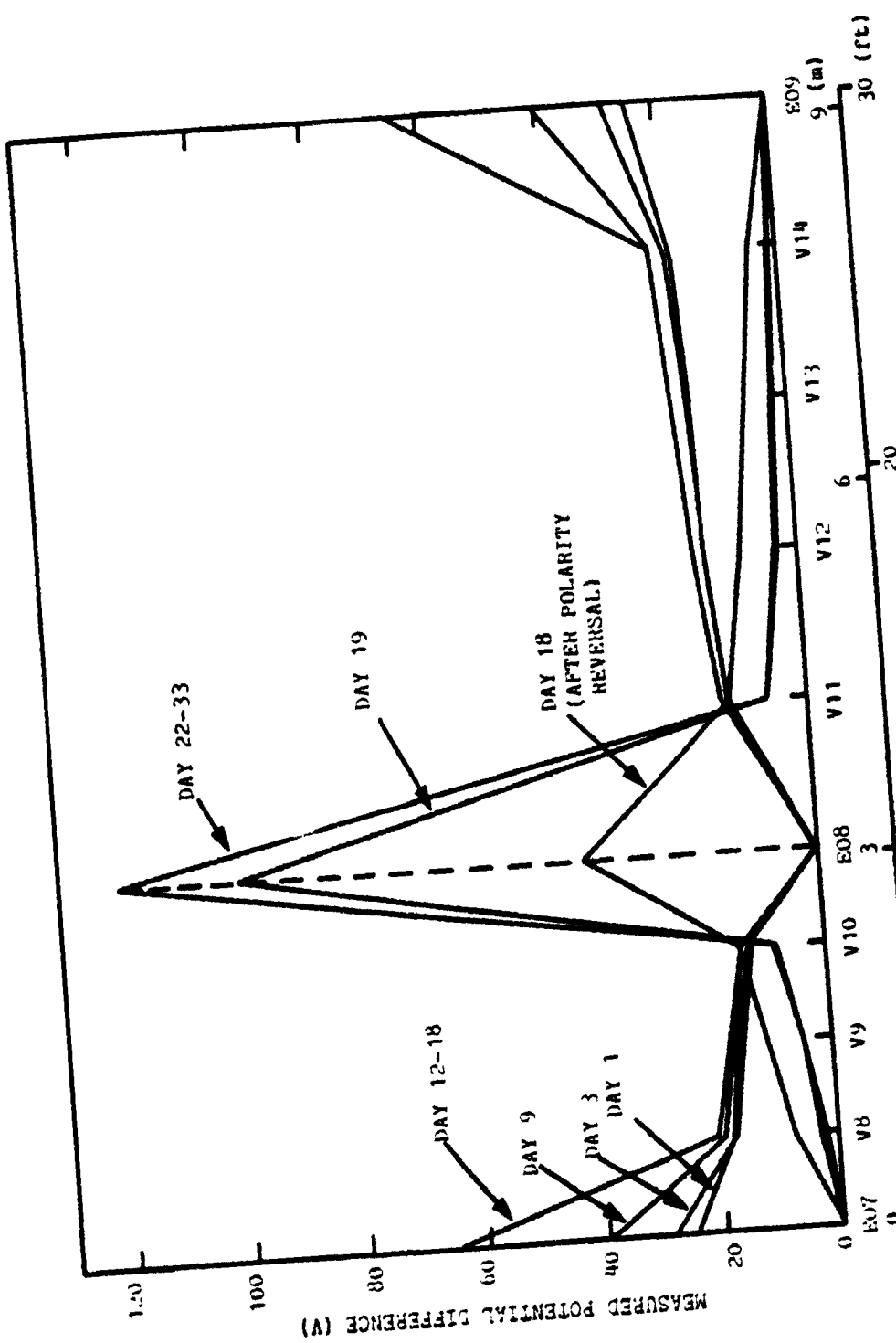

FIGURE 15.39 VOLTAGE VARIATION IN SOIL BETWEEN ELECTRODES E07-E08-E09

CHAPTER 16

THE FIELD TEST - DIELECTROPHORESIS

This chapter will focus on the dielectrophoretic field treatment of soft sensitive clay in the Gloucester test fill site. The site location, general layout of field test area, method of power supply and soil conditions were already discussed in section 15.1.

16.1 Design of Electrodes for Dielectrophoresis and Installation

The design of the electrode for dielectrophoretic field treatment was based on the test results obtained from the model test and lifetime test discussed in Chapters 11 and 12. The field electrode identical to the high voltage electrode for the lifetime test (Figure 11.11) was then manufactured with the details as shown in Figure 16.1. It consisted of a 12.7 mm (½") diameter thin wall copper plumbing pipe inserted into a 38.1 mm (1½") high strength pvc pipe filled up with silicone oil. The copper pipe was fixed at the centre of the pvc pipe by means of pvc spacers. The copper pipe was supported by a pvc electrode holder such that the tip of the copper pipe was 152.4 mm (6") above the tip of the pvc pipe. Such arrangement is to avoid any corona effect (ionization due to high charge concentration) at the tip of the copper pipe. The top and bottom of the pvc pipe were sealed by pvc caps. The electrode top was covered by a steel shield and copper ring to avoid any corona effect and short circuiting of

due to rainfall. The design of ground electrode was similar to that of the high voltage electrode except that no pvc pipe was used due to the fact that the ground electrode had zero potential and no insulation was therefore required.

As explained in the model test (section 11.4), a gap has to be maintained between the electrode and the cylindrical surface of the hole. A 76.2 mm (3") diameter pvc slotted pipe was installed in a pre-drilled hole to avoid soil collapse inside the hole and to allow water migrate into the hole. The electrode (high voltage electrode or ground electrode) was then sunk into the slotted pipe and held into position by means of pvc spacers, as shown in Figures 16.2 and 16.3. The total length of the electrode was 6.1 m (20 ft) with 5.5 m (18 ft) embedded length to treat the top 5.5 m of soil, with the same reason as described in section 15.1.

The applied potential to the system was about 45 kV which was so high that the cost of an insulated electric cable would be expensive. Especially, under the severe field conditions (heavy rainfall, hot sunshine, wet and dry effects), the insulation of the high voltage cable will deteriorate. It was therefore decided to use flexible copper tubing without any insulation as high voltage cable. The flexible copper tubing was suspended 1 m above ground by a specially designed cable hanger which was made of 50 mm diameter ABS pipe. The standard grounding cable was used to connect the ground electrodes, grounding rods and the grounding terminal of the high voltage transformer.

16.2 Electrode Configuration

In the dielectrophoretic test area, a similar electrode configuration to the electro-osmotic test area was arranged, with the same initial electrode length. Out of the nine electrodes installed, five of them were high voltage electrodes and the other four were ground electrode. Electrodes DP1, DP3, DP5, DP7 and DP9 were high voltage electrodes whereas electrodes DP2, DP4, DP6 and DP8 were of ground (zero) potential. With this arrangement, any one electrode will be surrounded by adjacent electrodes of different type so that the soil between any two electrodes can be treated. The electrode configuration after installation is shown in the photo in Figure 16.4.

16.3 Instrumentation and Monitoring

During the dielectrophoretic treatment, the variation of ground settlement and vane shear strength with treatment time were monitored. Similar to the electro-osmotic treatment, the settlement was monitored by means of steel settlement auger of 0.61 m (2 ft) length with 0.15 m (½") embedded in the soil and the settlement was measured by means of surveying instruments. The layout of the settlement augers in the two test areas is shown in Figure 15.9. The variation of field vane shear strength with treatment time was measured by means of the Norwegian field vane test equipment with vane size of 55 mm by 110 mm. The tests were carried out before, during and after treatment and in different locations.

Due to the high electric potential applied in the dielectrophoretic test area, no voltage probe and piezometer were installed to avoid any electric hazard.

16.4 Description of Field Treatment and Test Procedures

The installation of electrodes was completed in the same time as for electro-osmosis. Electrodes DP1, DP3, DP5, DP7 and DP9 are high voltage electrodes and electrodes DP2, DP4, DP6 and DP8 are ground electrodes. Figure 16.6a shows a circuit diagram for the dielectrophoretic field treatment. After the installation, it was found that the holes were filled up with water due to water seepage. Pumping was tried but the hole filled up with water again within one hour. Continuous pumping to dry the hole was found to be impractical. It was decided to try to run a test with water inside the holes. An alternating potential of 45 kV was gradually applied but after 15 minutes of treatment, electrical short circuiting occurred. All the high voltage electrodes were then pulled out and inspected. Several cracks on the pvc pipes were found in electrodes DP3, DP7 and DP9, as shown in Figure 16.5. The electrical short circuiting of the system was therefore due to the broken insulation of the high voltage electrodes. The test was re-started again on August 8, 1989 (day 1) with two high voltage electrodes and two ground electrodes forming a 3.05 m square grid (electrodes DP1, DP2, DP4 and DP5). The electrode length was reduced to 4.5 m to reduce the current flow and the risk of electrical hazard. The applied potential was 30 kV on day 1 and increased to 35 kV on day 2.

No electrical short circuiting was observed. On August 11, 1989 (day 4), three new high voltage electrodes were built in the field to replace the defective electrodes. A potential of 30 kV was applied again. But after 30 minutes of running, the system broke down again due to the damage of high voltage electrode DP9. In view of the limited supply of material and time, it was decided to run the test with only eight electrodes and a potential of 30 kV was re-applied. No electrical problem was then observed and on August 15, 1989 (day 8) the voltage was increased to 35 kV. The electric potential was then increased periodically to a maximum of 44.3 kV and the electrodes still functioned properly. The treatment was stopped on August 28, 1989 (day 21). The electrodes were then pulled out after treatment and all of them were in good condition. The power supply record is summarized in Table 16.1. The results are plotted in Figure 16.6b.

During the period of field treatment, the following are monitored daily except in the weekends, with the power shut off during measurement:

(a) ground settlement

(b) variation of primary current and voltage[1] supply

(c) variation of secondary voltage[2] output

(d) field vane tests as required

---

[1] Primary current and voltage are the electrical input to the high voltage transformer. The main power supply of two phases, 220 V, 60 A ac were obtained from the nearby office of the Royal Canadian Legion.

[2] Secondary voltage is the electric potential output from the high voltage transformer, after stepping up the primary voltage. In this field test, the secondary voltage can be as high as 60 kV.

After the treatment, four field vane test profiles were carried out to investigate the post-treatment shear strength increase.

16.5 Test Results

The dielectrophoretic treatment started on August 8, 1989 (day 1) and completed on August 28, 1989 (day 21) resulting in a total of 20 days of treatment.

16.5.1 Settlement Measurement

Sixteen settlement augers were installed as shown in Figure 15 Table 16.2 summarizes the record of settlement measurement. The ground settlement with treatment time is plotted in Figure 16.7 which indicates a settlement at an approximate rate of 0.5 mm/day. From Table 16.2, the average settlement of the test area was 11 mm. Furthermore, no evidence of upward ground movement was detected. The settlement profiles along augers S1 to S8 and along augers S9 to S11 are plotted in Figures 16.8 and 16.9 respectively. It can be seen from the Figures that the ground settlement is quite uniform.

16.5.2 Results of Field Vane Tests

A total of nine field vane test profiles between 2 m and 4.5 m depth were performed during and after treatment with the test locations as shown in Figure 16.10. The test results are summarized in Table 16.3. The shear strength

profiles are plotted in Figures 16.11 to 16.18. The maximum shear strength increase was 13.7 % at a location of 0.3 m from the high voltage electrode DP5 and the average shear strength increase of the test area was about 10 %. The increase in shear strength at halfway of 3.05 m electrode spacing and 6.1 m electrode spacing were 11.5 % and 4.6 % respectively. At the centres of the 3.05 m and 6.1 m square grids, the shear strengths increased by 4.7 % and 4.6 % respectively. The test results indicate that the inactive zone can also be treated to certain extent by dielectrophoresis.

The variation of shear strength increase with treatment time is plotted in Figure 16.19. It can be seen that the shear strength increases with time though at a small rate. It appears that if longer treatment time was allowed, the improvement of shear strength might have been greater.

16.6 Discussion of Test Results

16.6.1 Settlement

From the test results obtained, the average settlement of the ground surface was 11 mm after 20 days of treatment. When compared with the average settlement of about 35 mm on day 21 in the electro-osmotic test area, the settlement recorded in the dielectrophoretic test area is only one-third of the other treatment. As settlement is an indication of soil consolidation, it is therefore expected that the degree of consolidation of the soft clay in the dielectrophoretic treatment area is lower than that in the electro-osmotic

treatment area.

16.6.2 Undrained Shear Strength

Due to the effect of water in the holes, the rate of shear strength increase was affected. The presence of water in the hole will ground the electric field and reduce significantly the field intensity. As described by equation 10.19, the dielectrophoretic force is proportional to the square of electric field intensity. The reduction of the field intensity leads to the smaller translational force to move the water molecules. Consequently, the field shear strength increase did not occur to the extent, as expected from the laboratory tests as discussed in Chapters 11 and 12. With the experience gained in the field test, the method of electrode installation should be modified such that the electric field intensity will not be weakened by the inclusion of groundwater. Nevertheless, it is important to note that the design of high voltage electrode is still suitable for the field test, especially if the water could be removed from the hole.

The uniformity of treatment was also investigated by plotting the average shear strength results at different locations between electrodes, as shown in Figure 16.20. This figure indicates that the shear strength increase is maximum at the location nearest the electrode and minimum at halfway between electrodes of 6.1 m spacing. This observation can be explained by the theory of dielectrophoresis that the field strength decreased with distance and concurrently the dielectrophoretic force reduced.

Due to the effect of water inside the holes, the effectiveness of dielectrophoretic treatment is not as good as expected by the laboratory test results. Nevertheless, the process can still be considered to be successful as the treatment demonstrated some degree of soil improvement. Since the dielectrophoretic field treatment is a pioneer research and it was the first time to apply this technique in engineering practice, it is expected to encounter some difficulties. However, this first field test provides a good opportunity to accumulate experience for the future field tests or applications. The recommendations for future research will be discussed in Chapter 19.

Table 16.1 Summary of Power Supply for Dielectrophoresis

Date	Day No.	Primary Supply		Secondary Output		Remarks
		Voltage V	Current A	Voltage kV	Current mA	
Aug 8	1	210	2.6	30.0	18.2	2 active and 2 ground electrodes
9	2	210	3.4	35.0	20.4	
10	3	210	3.4	35.0	20.4	
11	4	210	5.1	30.0	35.7	4 active and 4 ground electrodes
14	7	210	4.5	30.0	31.5	
15	8	210	6.4	35.0	38.4	
16	9	210	8.0	40.0	42.0	
17	10	210	8.0	40.0	42.0	
18	11	210	8.2	41.0	42.0	
21	14	210	9.3	43.5	44.9	
23	16	210	9.6	42.5	47.4	
24	17	210	9.1	42.3	45.2	
25	18	210	9.6	44.3	45.5	
28	21	210	10.0	44.3	47.4	treatment completed

Table 16.2 Settlement Measurement in Dielectrophoresis Test Area

Date	Day No.	Settlement of Each Settlement Auger (mm)													
		S1	S2	S3	S4	S5	S6	S7	S8	S9	S10	S	S12	S13	S14
Aug 8	1	0	0	0	0	0	0	0	0	0	0	0	0	0	0
11	4	3	3	4	4	4	4	3	4	2	4	1	1	1	1
15	8	5	5	5	8	8	8	5	8	5	10	7	5	4	2
17	10	10	10	12	13	13	13	13	10	10	11	9	8	9	2
18	11	10	10	13	12	13	13	10	9	10	12	9	8	9	2
21	14	10	7	15	13	13	13	12	14	12	15	11	9	10	3
25	18	10	7	15	14	13	14	13	13	13	15	11	9	11	3
28	21	11	8	16	14	14	14	15	15	12	14	10	9	10	3

Notes: positive values for settlement, negative for heave

Table 16.3 Summary of Field Vane Test Results

Location	Day No.	Average Shear Strength (kPa)	Average Increase in Shear Strength (%)	Remarks
DPV1	--	18.2	0.0	pre-treatment
DPV2	7	18.9	4.0	
DPV3	7	18.7	2.5	
DPV4	10	20.0	9.9	
DPV5	17	19.8	9.0	
DPV6	21	20.3	11.5	treatment completed
DPV7	21	20.7	13.7	
DPV8	22	19.0	4.6	
DPV9	22	19.1	4.7	

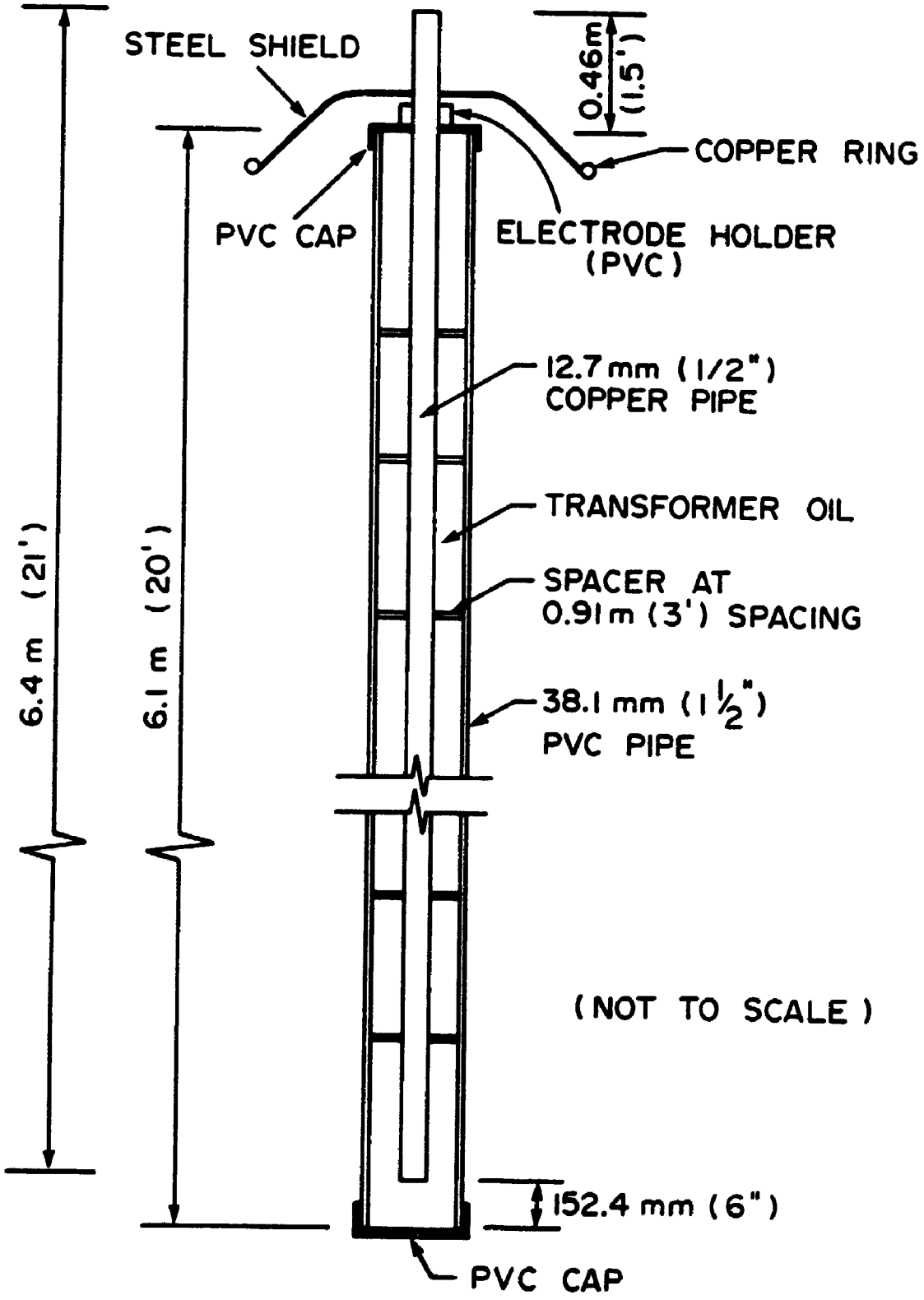

FIGURE 16.1 DETAILS OF HIGH VOLTAGE ELECTRODE FOR DIELECTROPHORESIS

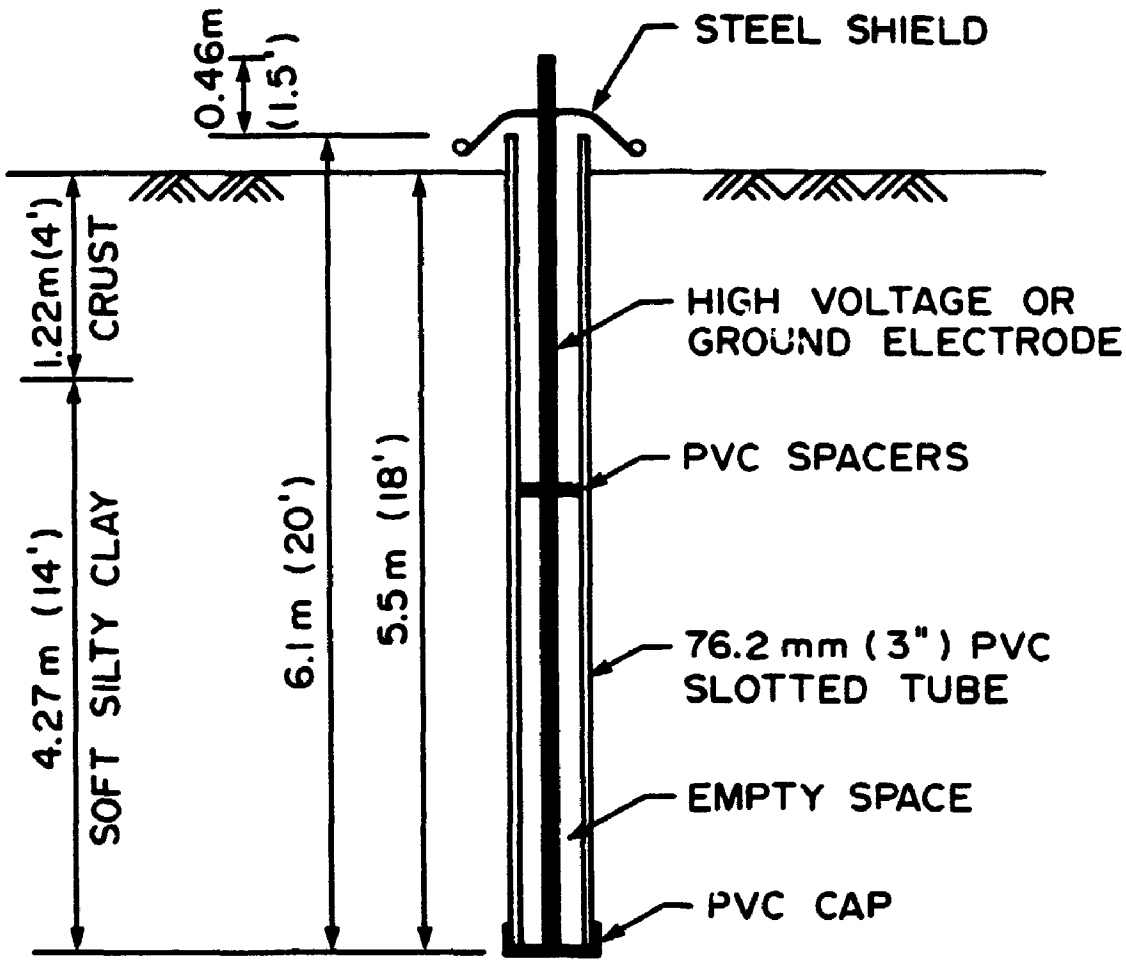

FIGURE 16.2 INSTALLATION OF ELECTRODE FOR DIELECTROPHORESIS

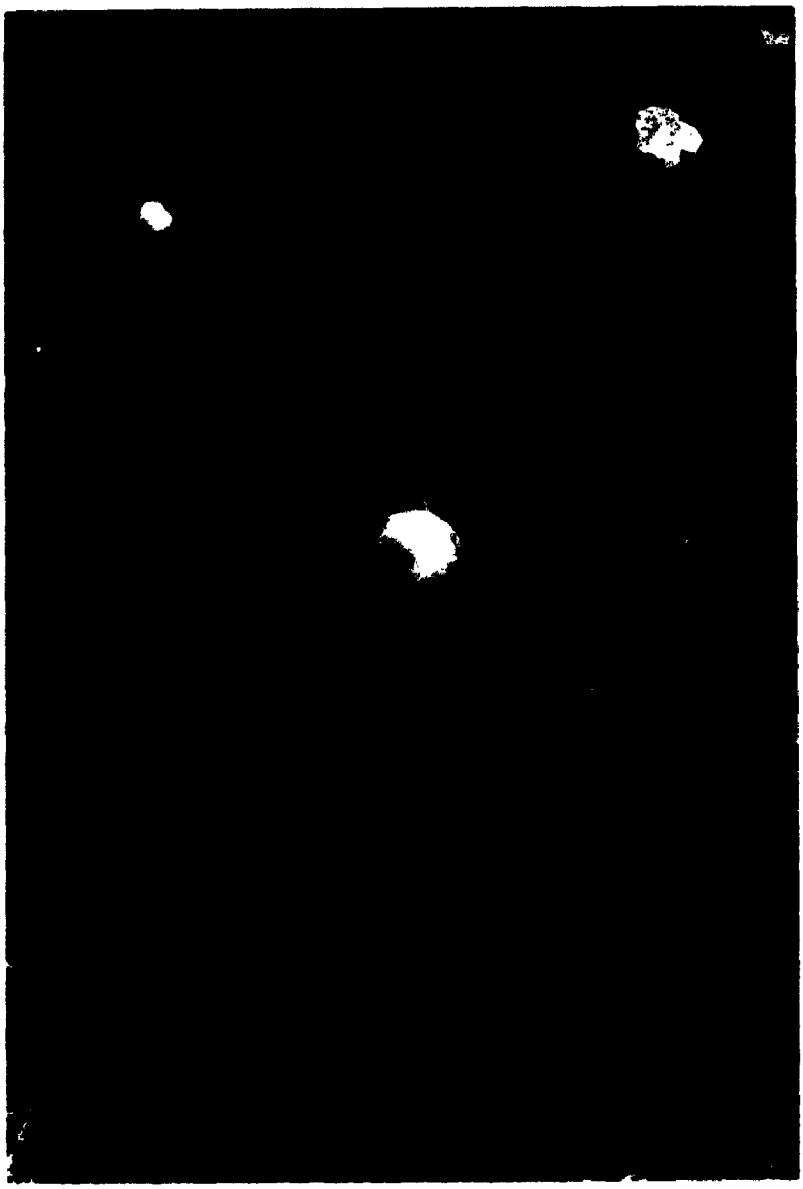

FIGURE 16.3 DIELECTROPHORESIS ELECTRODES

FIGURE 16.4 TEST AREA FOR DIELECTROPHORETIC TREATMENT

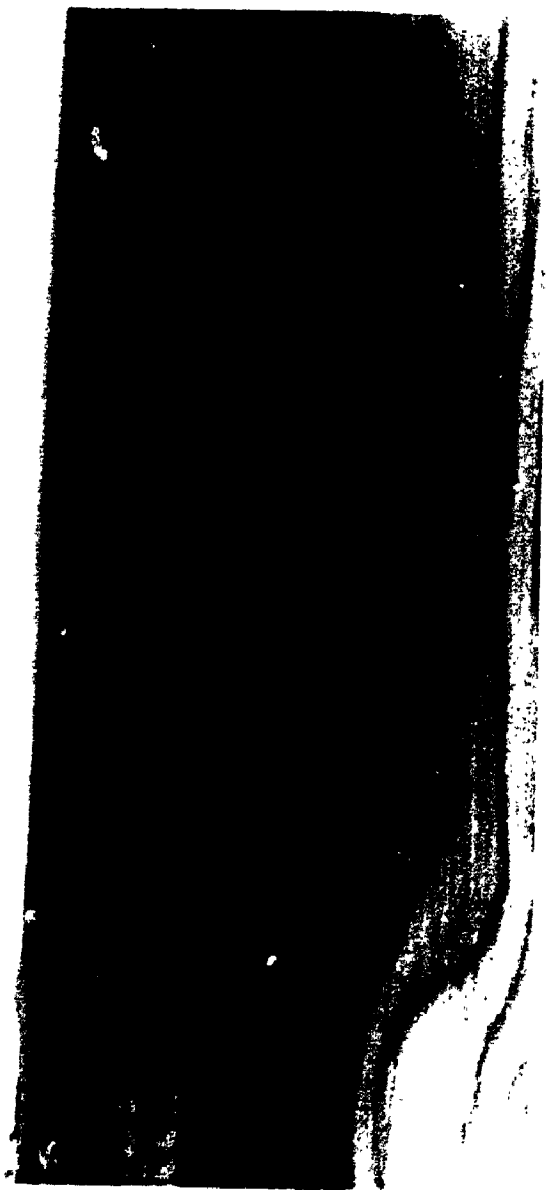

FIGURE 16.5 TYPICAL CRACK PATTERN OBSERVED ON ELECTRODE

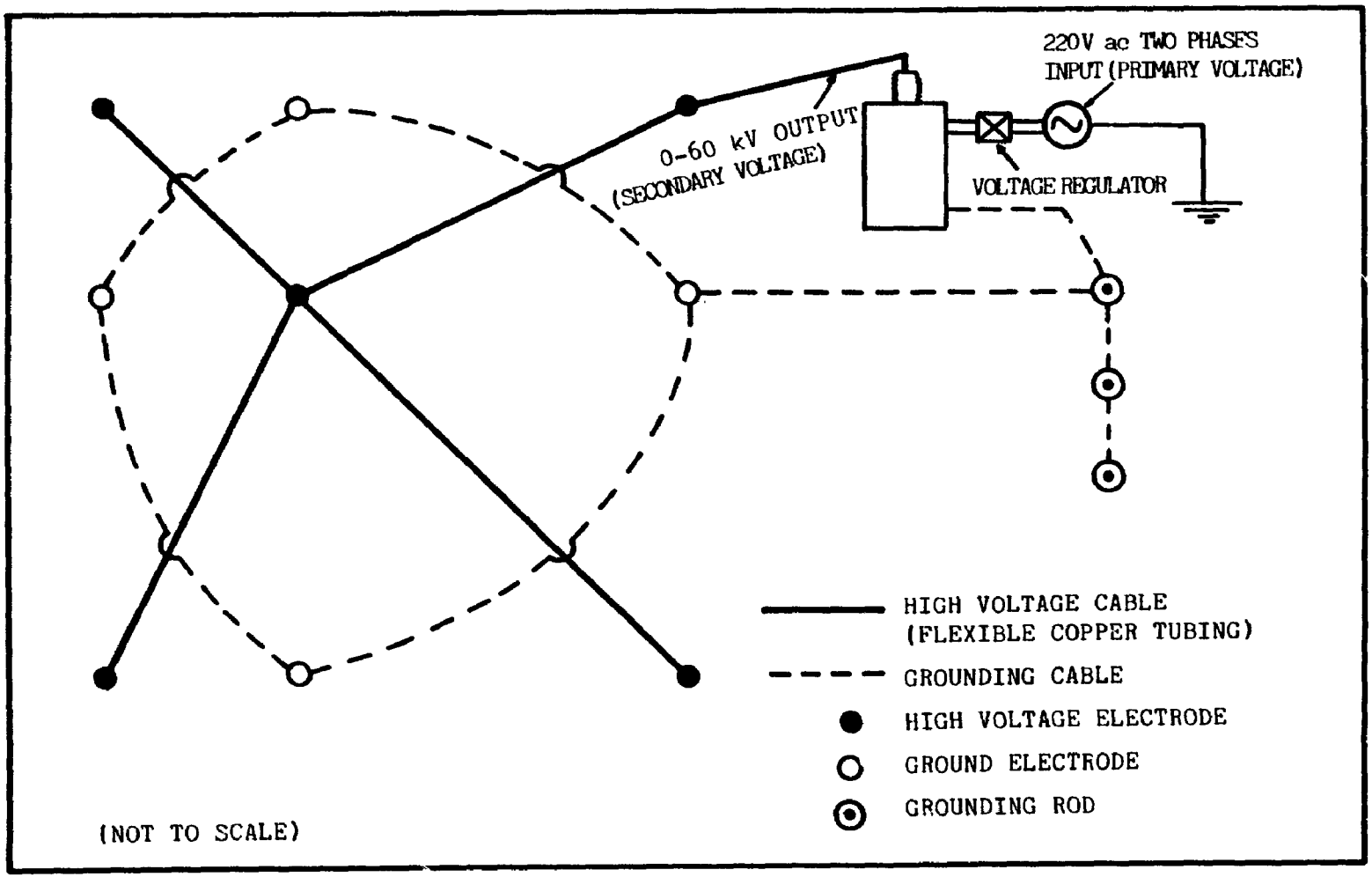

FIGURE 16.6a CIRCUIT DIAGRAM FOR DIELECTROPHORETIC FIELD TREATMENT

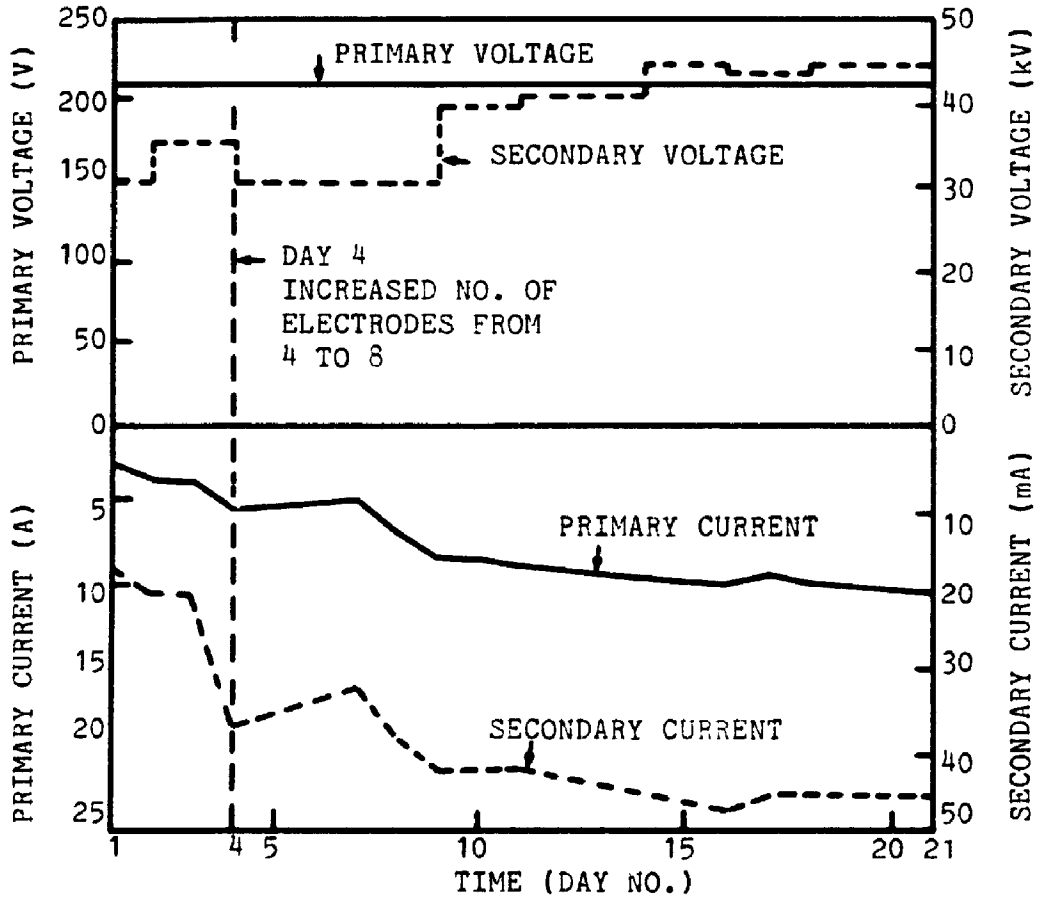

FIGURE 16.6b VARIATION OF POWER SUPPLY OF HIGH VOLTAGE TRANSFORMER WITH TREATMENT TIME

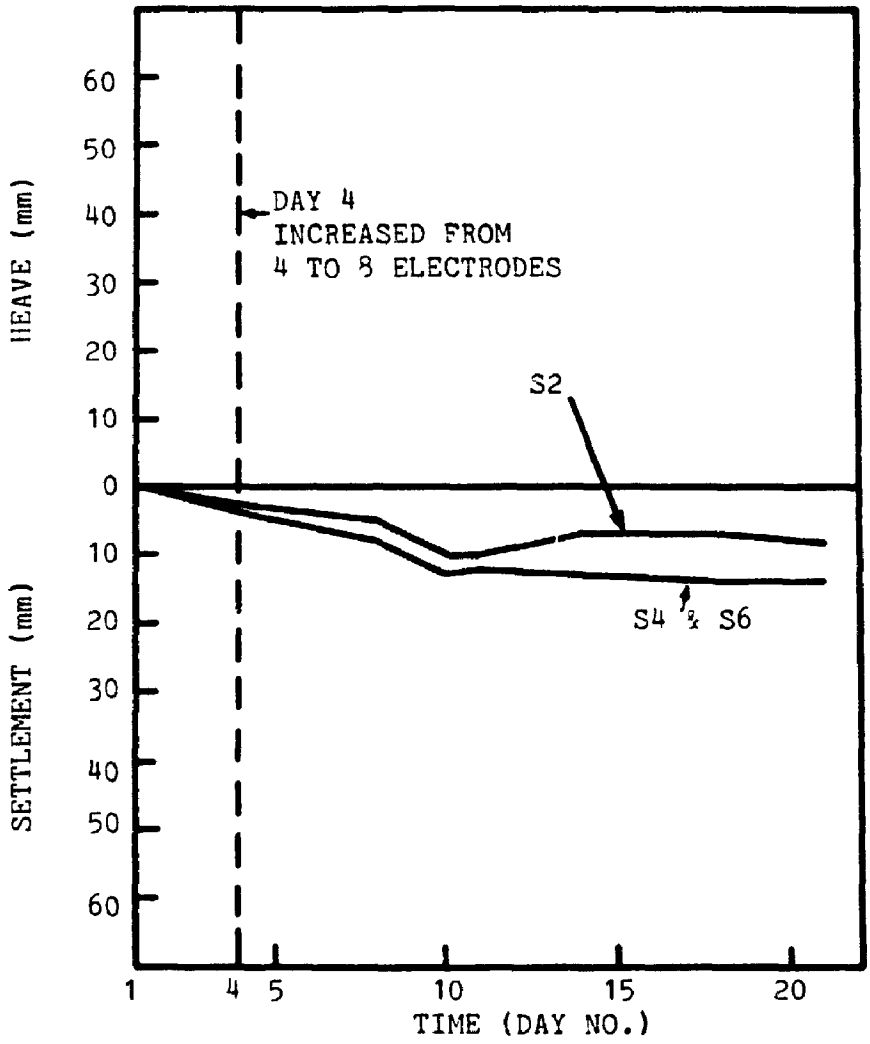

FIGURE 16.7 MEASURED SETTLEMENT WITH TIME

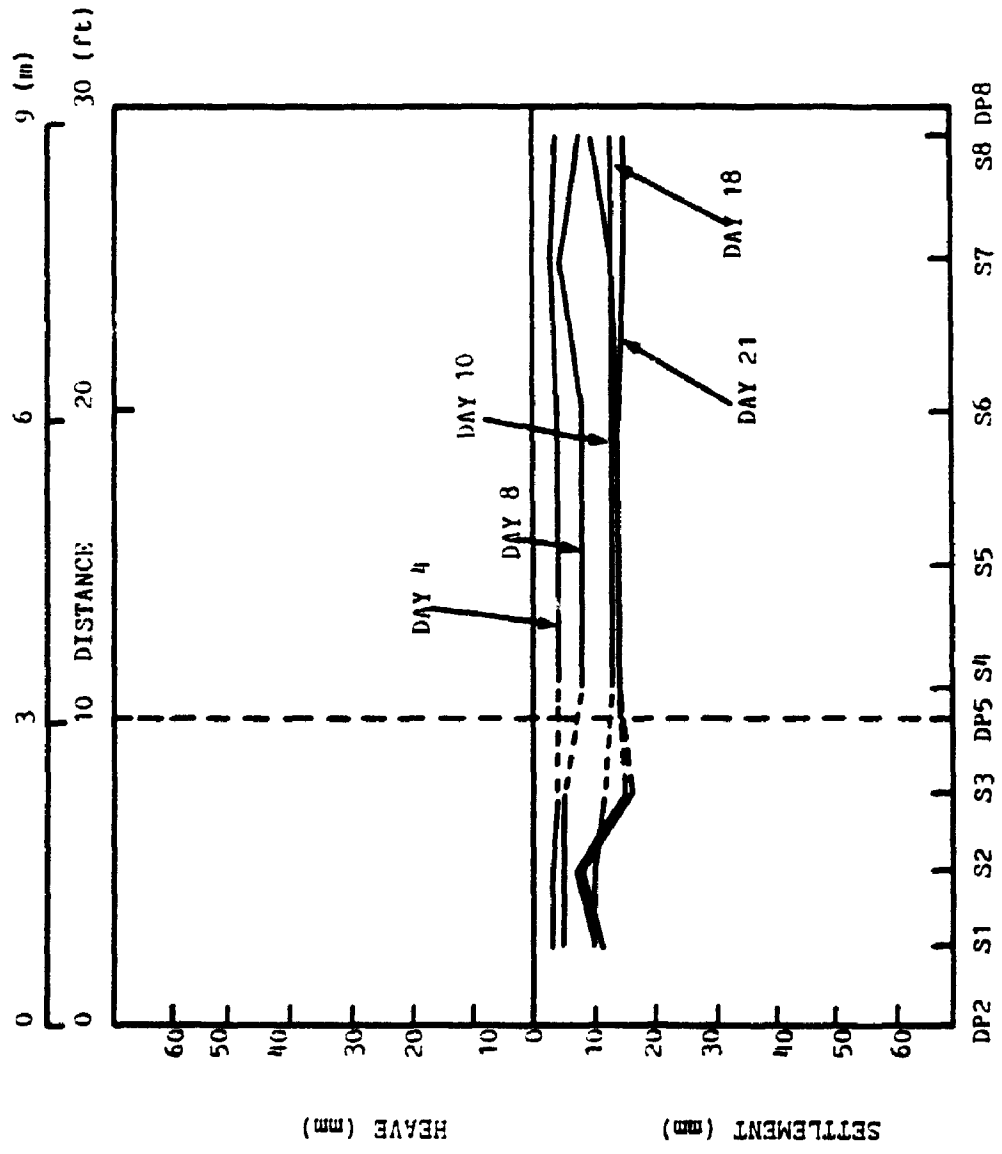

FIGURE 16.8 SETTLEMENT PROFILES BETWEEN ELECTRODES DP2-DP5-DP8 (SETTLEMENT AUGERS S1-S8)

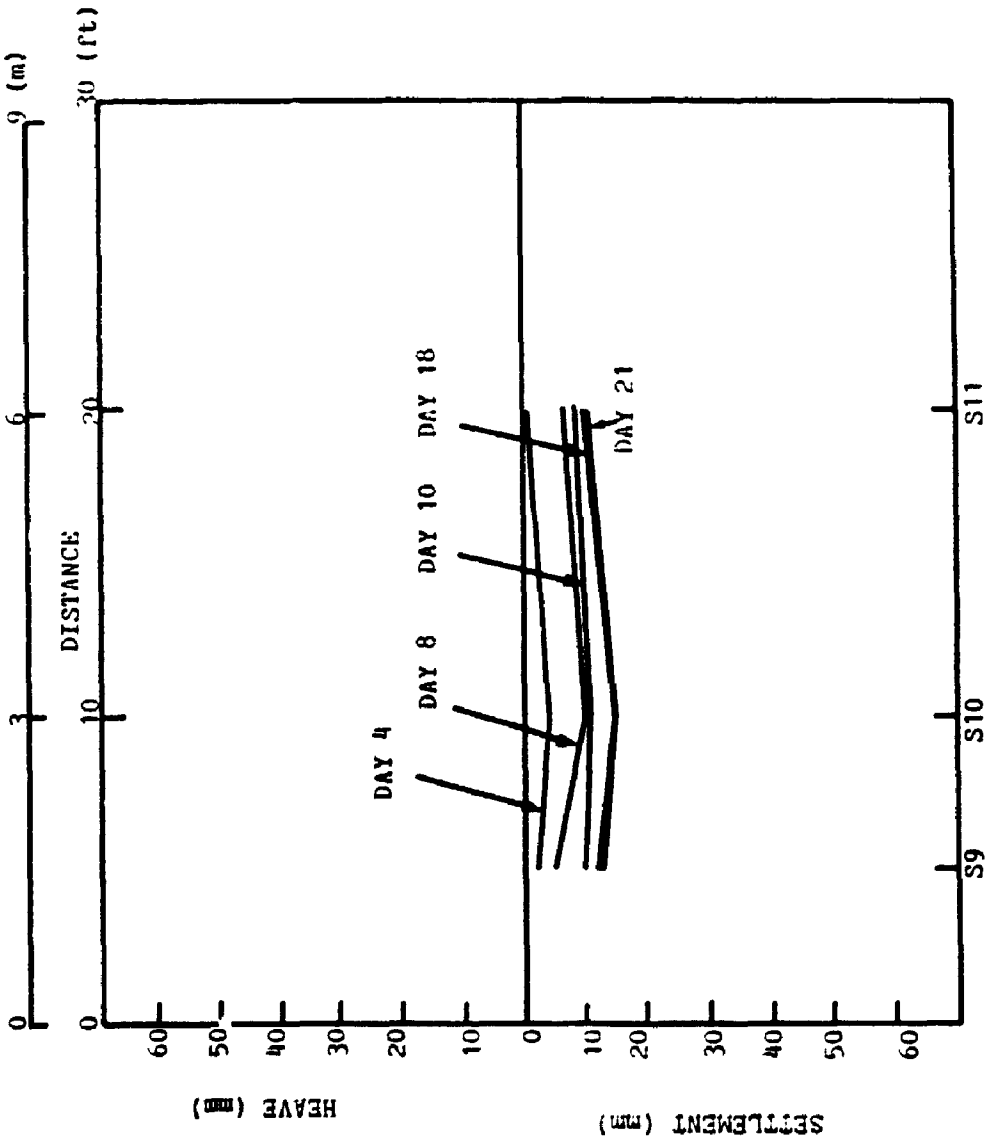

FIGURE 16.9 SETTLEMENT PROFILES BETWEEN AUGERS S9-S10-S11

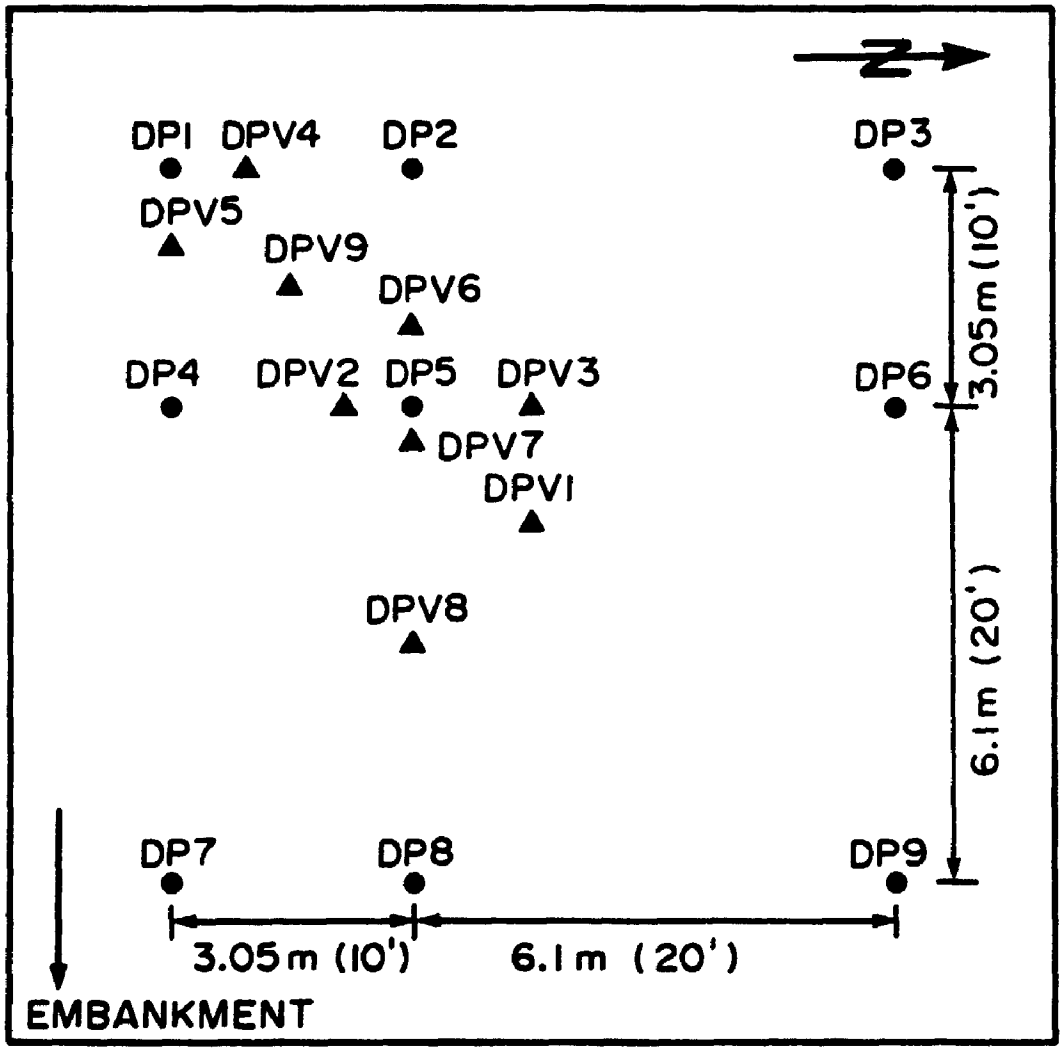

FIGURE 16.10 LOCATIONS OF FIELD VANE TEST

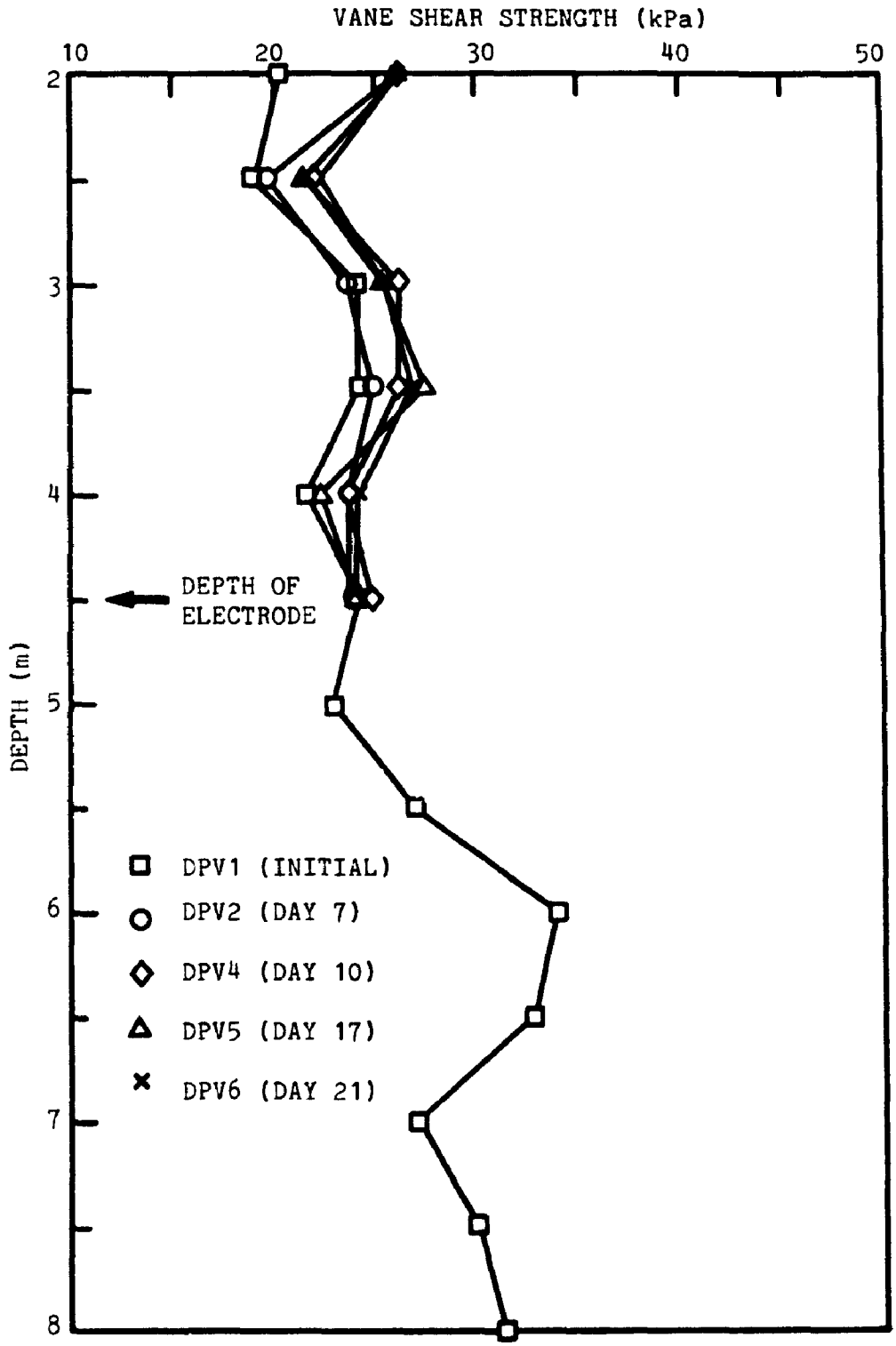

FIGURE 16.11 VARIATION OF VANE SHEAR STRENGTH PROFILES WITH TIME AT 0.91 m (3') FROM HIGH VOLTAGE ELECTRODE

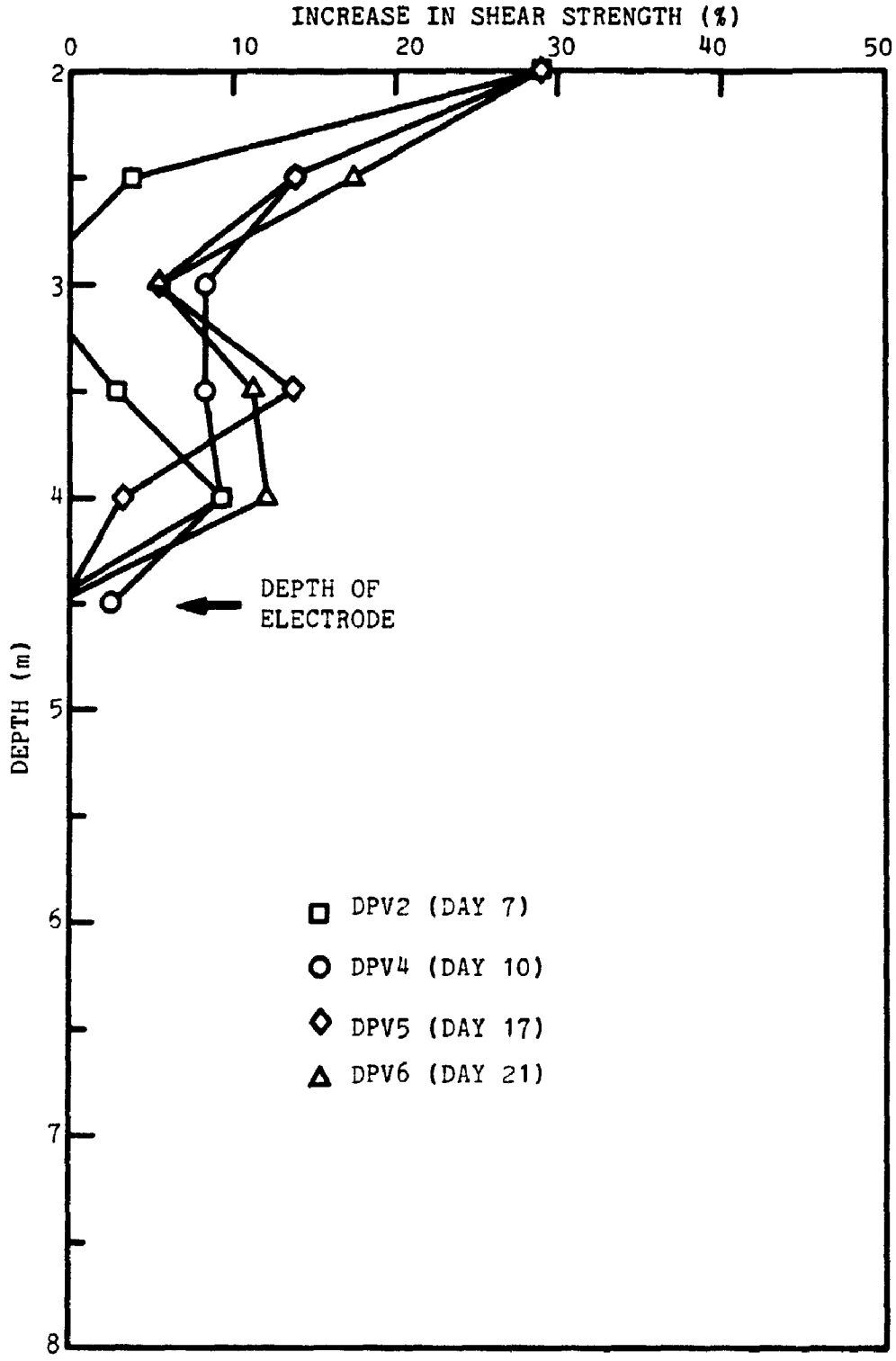

FIGURE 16.12 PROFILES OF VANE SHEAR STRENGTH INCREASE WITH TIME AT 0.91 m (3') FROM HIGH VOLTAGE ELECTRODE

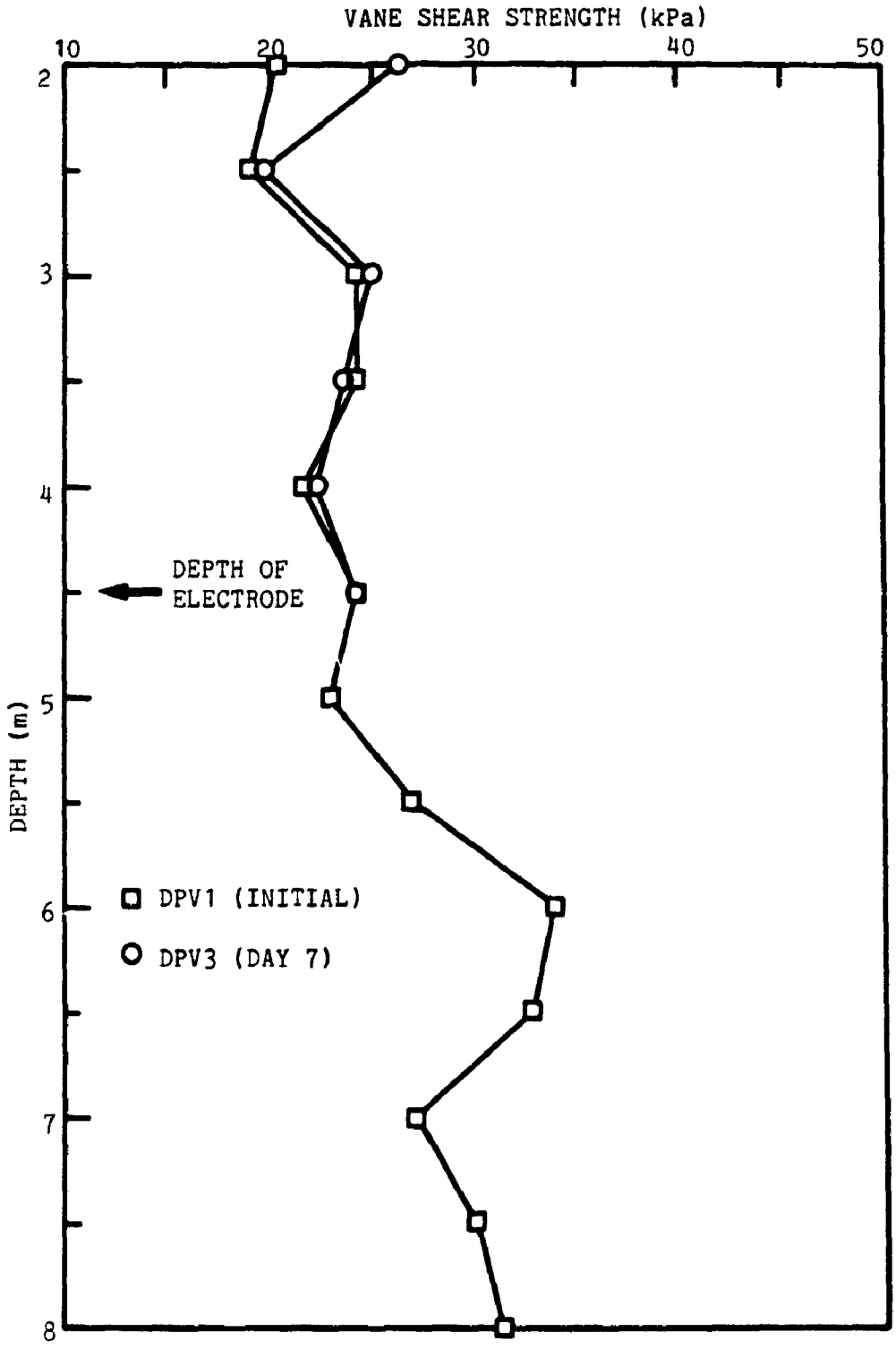

FIGURE 16.13 VARIATION OF VANE SHEAR STRENGTH PROFILES AT 1.52 m (5') FROM HIGH VOLTAGE ELECTRODE

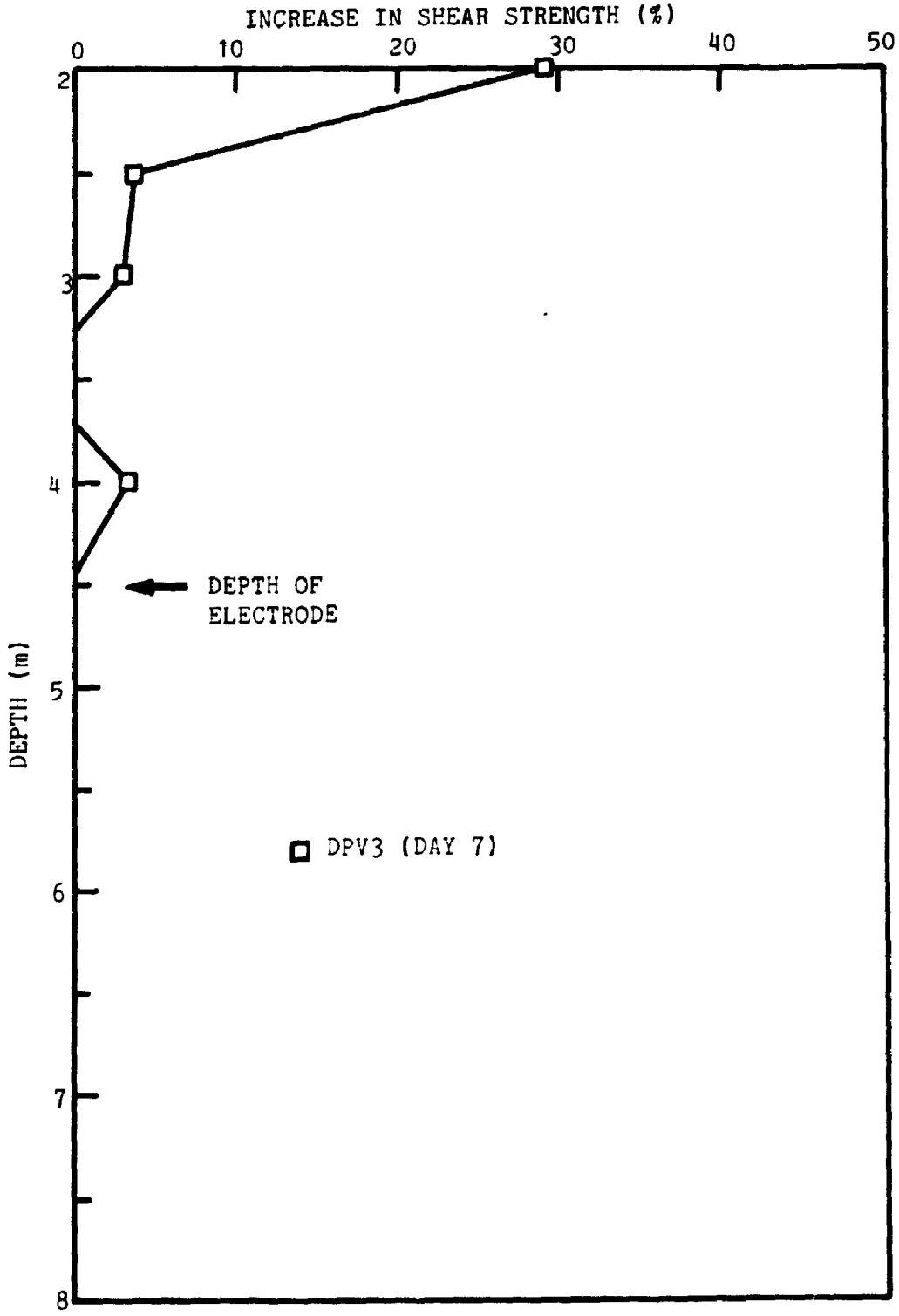

FIGURE 16.14 PROFILE OF VANE SHEAR STRENGTH INCREASE AT 1.52 m (5') FROM HIGH VOLTAGE ELECTRODE

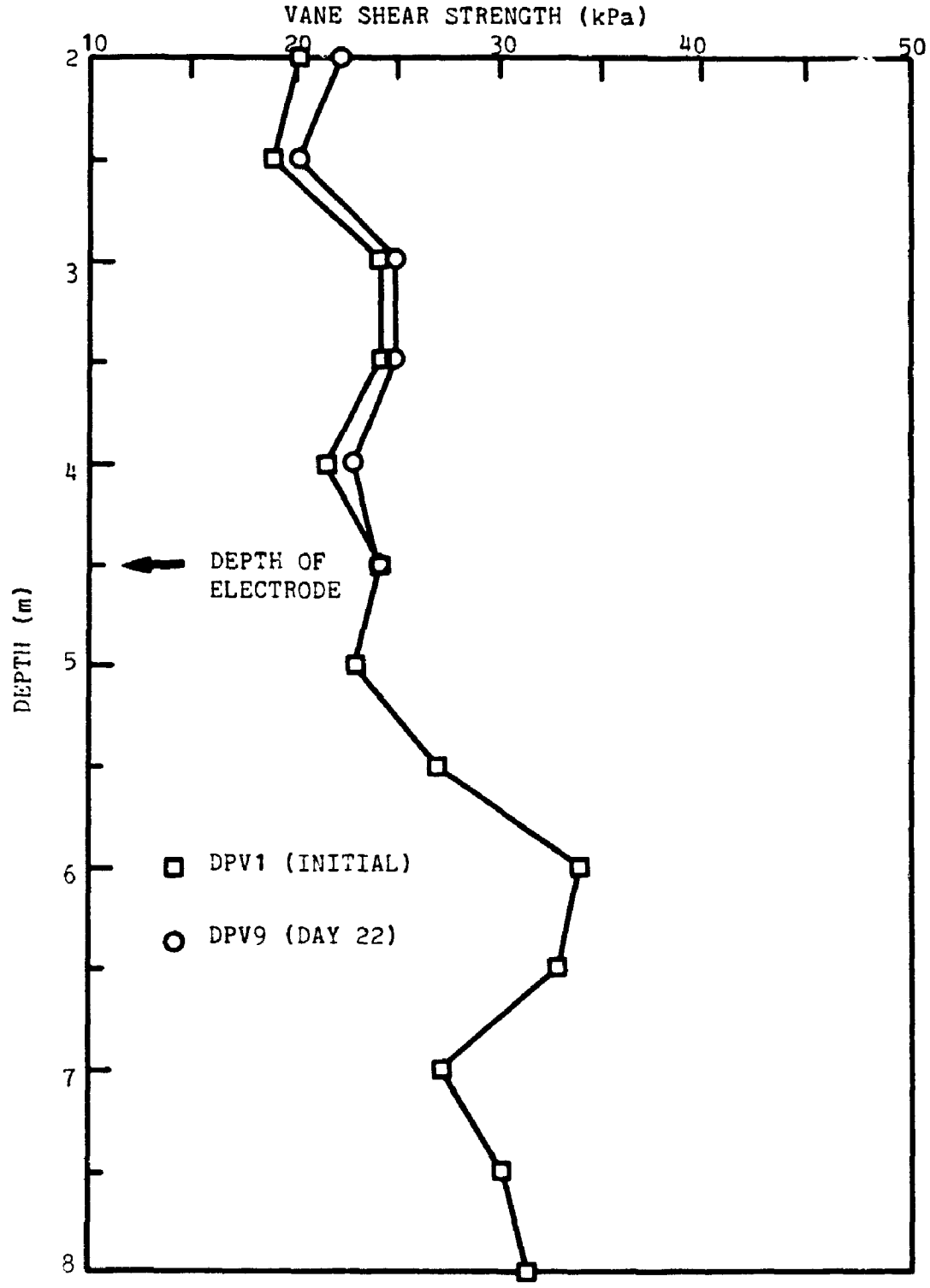

FIGURE 16.15 VARIATION OF VANE SHEAR STRENGTH PROFILES WITH TIME AT CENTRE OF 4 ELECTRODES OF 3.01 m (10') SQUARE GRID

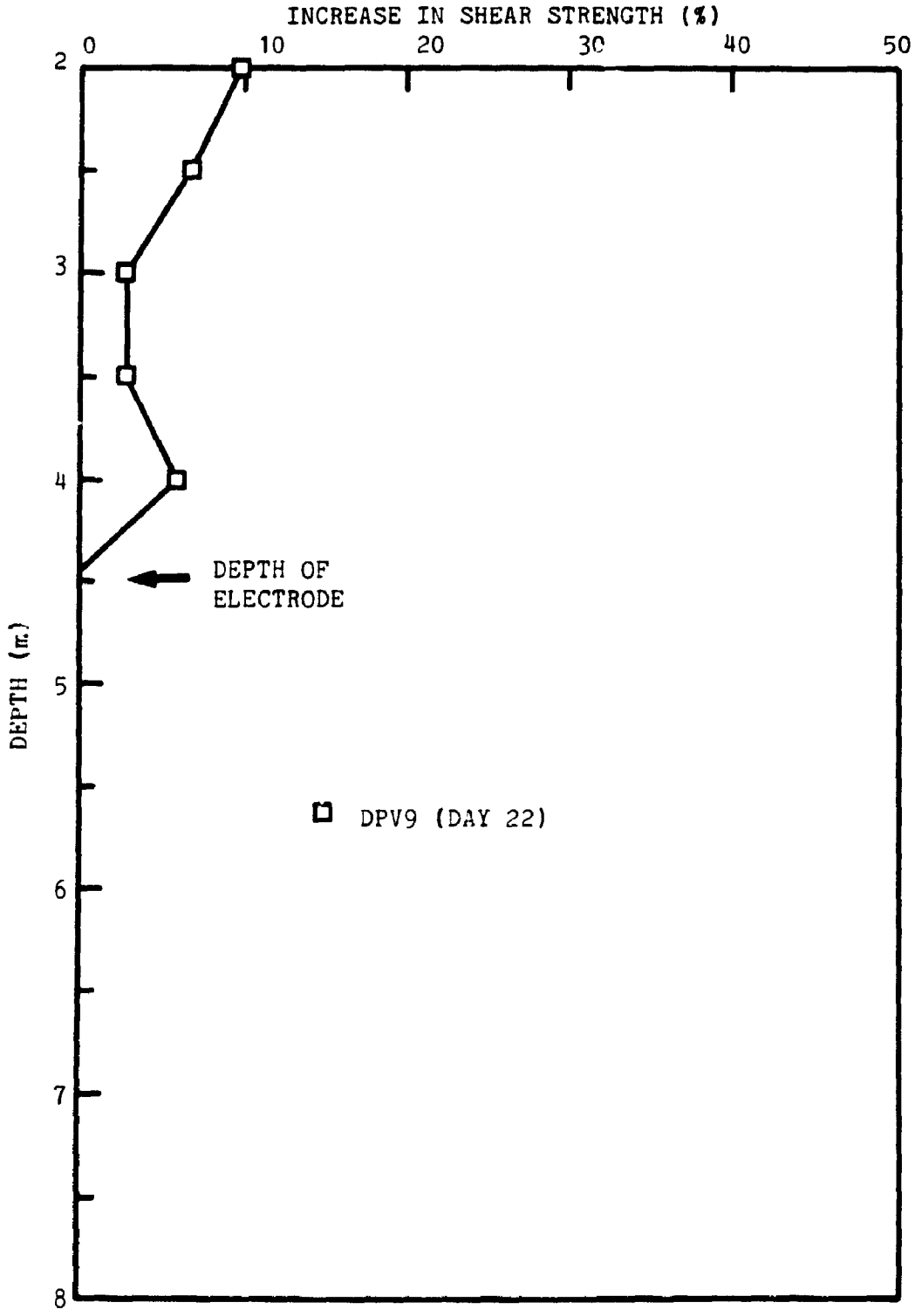

FIGURE 16.16 PROFILES OF VANE SHEAR STRENGTH INCREASE WITH TIME AT CENTRE OF 4 ELECTRODES OF 3.01 m (10') SQUARE GRID

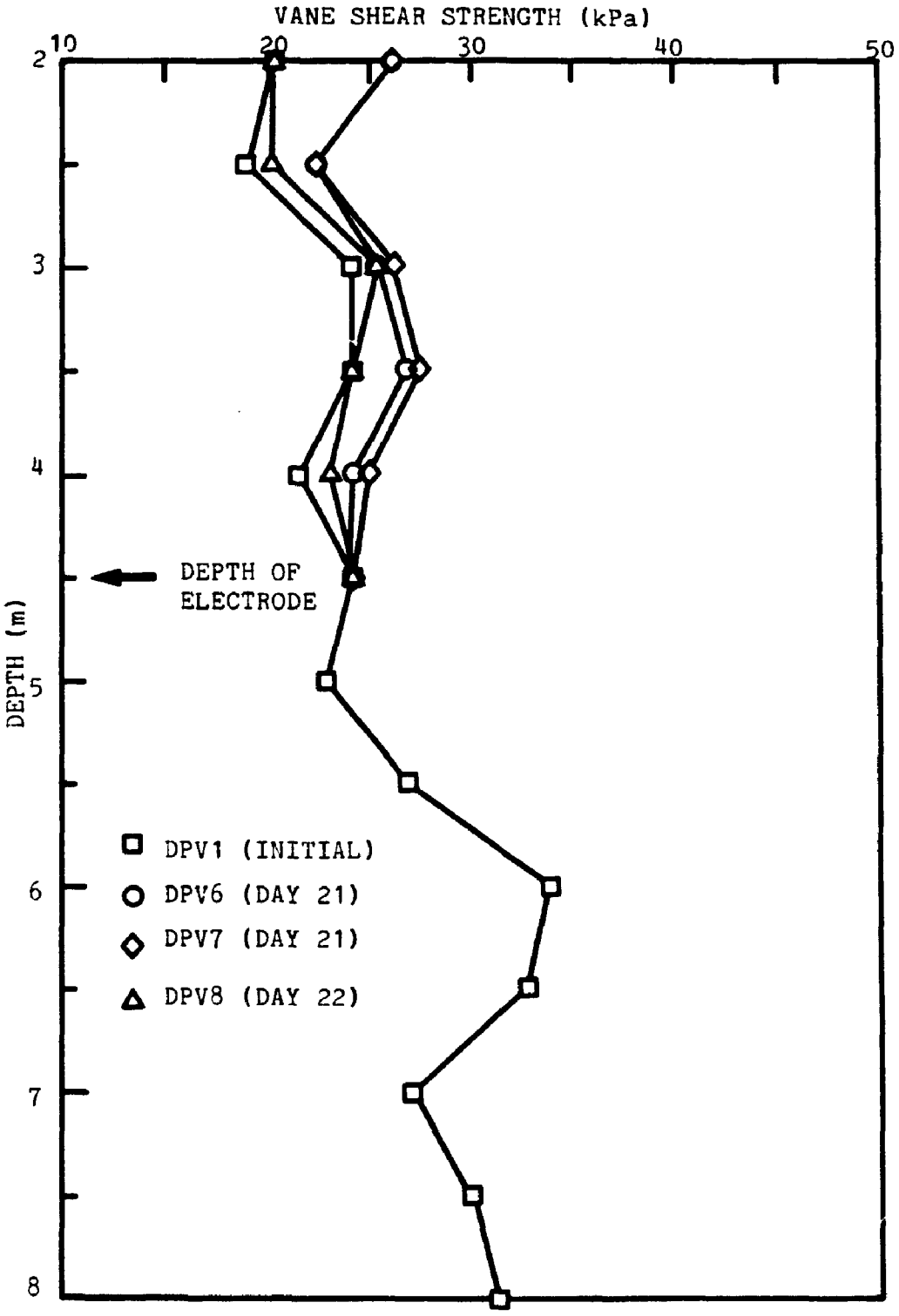

FIGURE 16.17 VARIATION OF VANE SHEAR STRENGTH PROFILES AT DIFFERENT LOCATIONS BETWEEN ELECTRODES DP2-DP5-DP8 AFTER TREATMENT

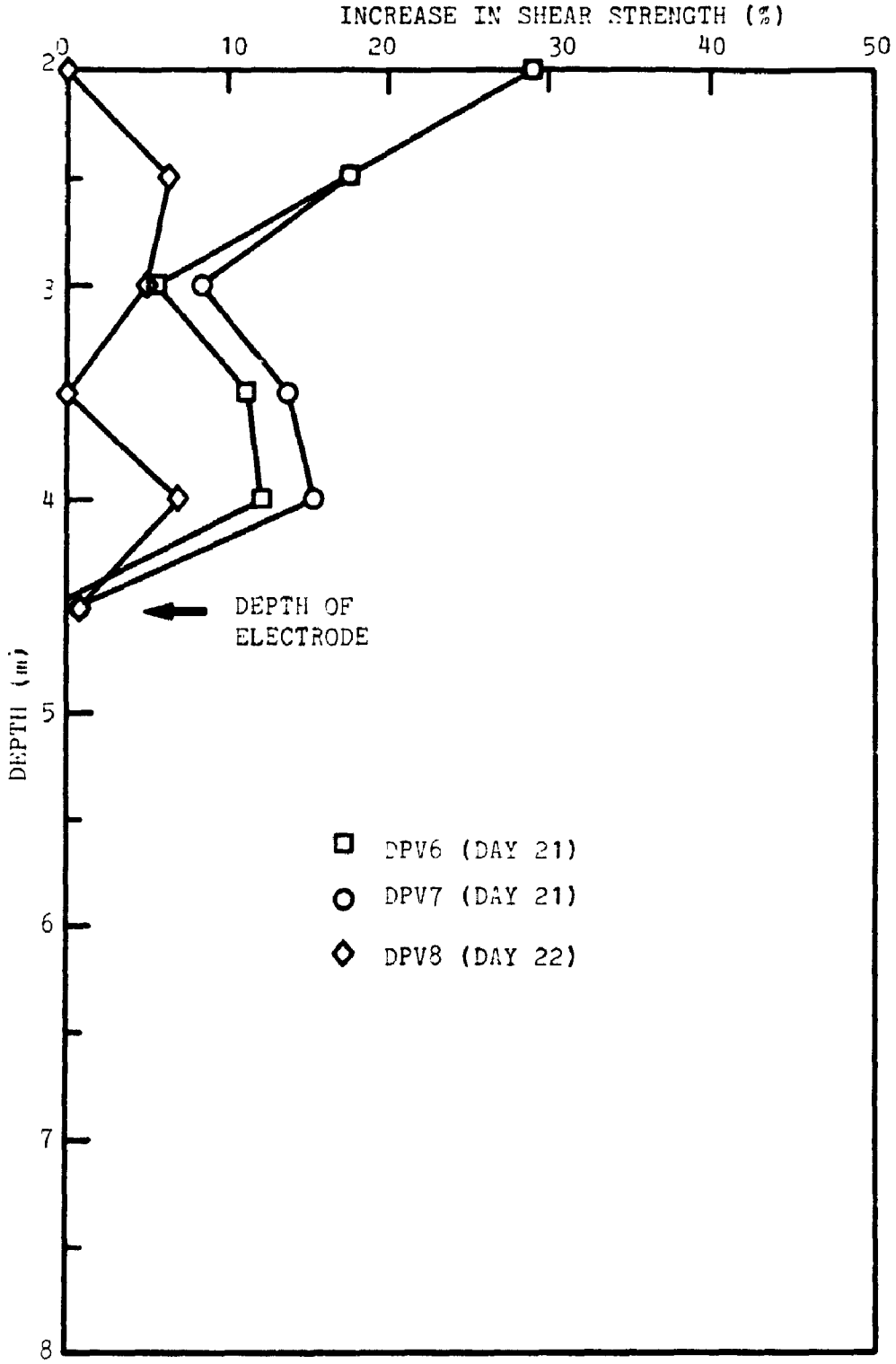

FIGURE 16.18 PROFILES OF VANE SHEAR STRENGTH INCREASE AT DIFFERENT LOCATIONS BETWEEN ELECTRODES DP2-DP5-DP8 AFTER TREATMENT

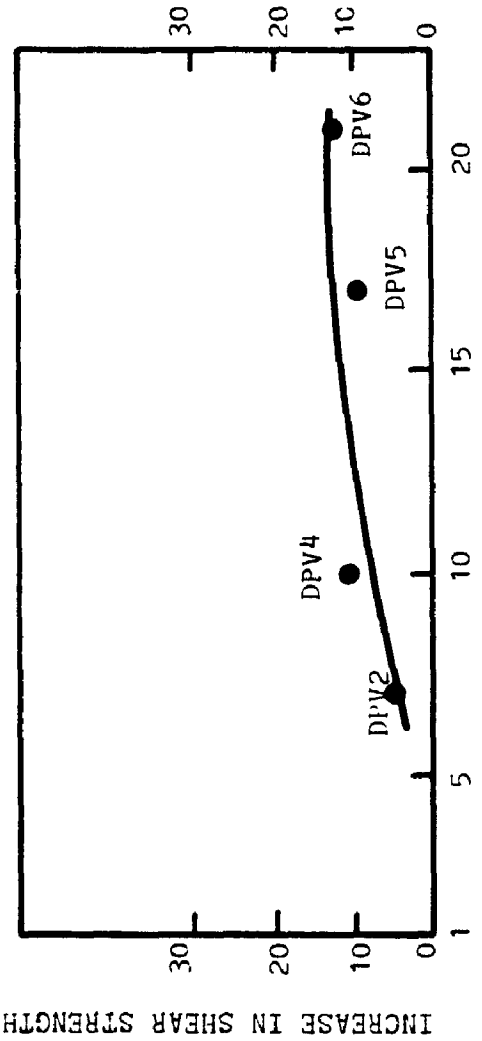

FIGURE 16.19 INCREASE OF VANE SHEAR STRENGTH WITH TREATMENT TIME AT LOCATION 0.91 m (3') FROM HIGH VOLTAGE ELECTRODE

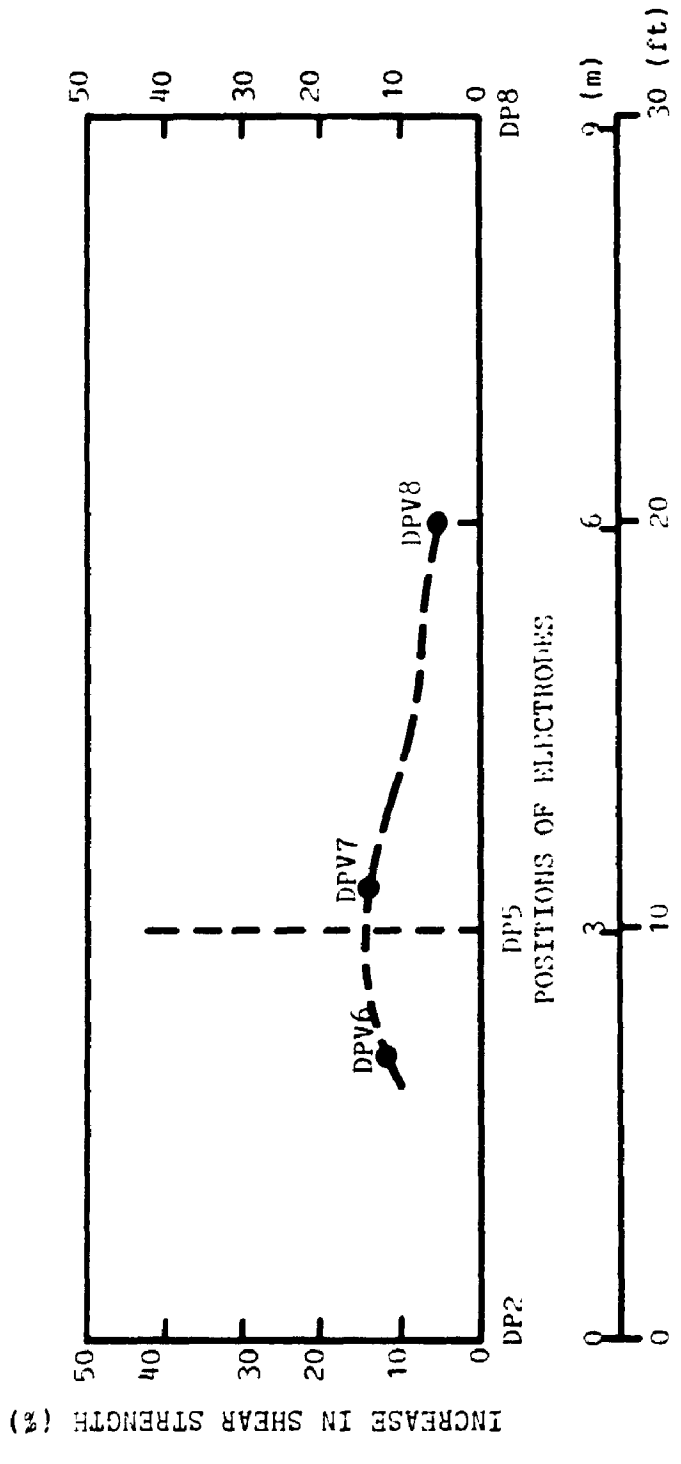

FIGURE 16.20 VARIATION OF SHEAR STRENGTH BETWEEN ELECTRODES DP2-DP5-DP8 AFTER TREATMENT

CHAPTER 17

FURTHER ANALYSIS OF ELECTRO-OSMOTIC TREATMENT

The field observations and monitoring test results of electro-osmosis were discussed in Chapter 15. The effects of electro-osmosis on the improvement of soil properties in the field as revealed by post-treatment laboratory tests are discussed in this chapter.

After the electro-osmotic treatment in the field, two 127 mm (5") diameter Osterberg tube samples (borehole EOS1 and EOS2) were recovered down to the depth of 6 m. Boreholes EOS1 and EOS2 located halfway between electrodes of 3.05 m spacing (electrodes EO1 and EO2) and electrodes of 6.1 m spacing (electrodes EO5 and EO6) respectively, as shown in Figure 15.17. Conventional laboratory tests such as moisture content, unconfined compression test, sensitivity, isotropically consolidated undrained triaxial test, one dimensional consolidation test, chemical analysis of soil, limits test and chemical analysis of water samples collected at cathodes were performed to investigate the effects of electro-osmosis to the soil properties in the field.

In the dielectrophoretic treatment, as discussed in the previous chapter, the average shear strength improvement was only 10 % which is so low that the factor of soil variation in the field may over-shadow the accuracy of any detailed analysis. It was therefore decided not to perform any sampling and

laboratory test in this test area.

17.1 Moisture Content

The distribution of moisture contents with depth before and after treatment are compared in Figure 17.1. The test results are summarized in Table 17.1. The average moisture content before treatment was 82.6 % and reduced to 70.6 % and 73.1 % as reflected by the tests in boreholes EOS1 and EOS2 respectively, corresponding to the average decrease of 14.6 % and 11.6 % respectively. From the field vane test results, the average shear strength increase were 50.8 % and 36.5 % for 3.05 m and 6.1 m electrode spacings respectively.

17.2 Stress-Strain Behaviour and Sensitivity

17.2.1 Unconfined Compression Test

In order to be consistent with the methodology used in the laboratory investigation of electro-osmosis (described in Part I of the thesis), unconfined compression tests were also performed on the tube samples recovered from the field for comparison. The unconfined compression tests were carried out on the tube samples EOS1 and EOS2 from the depth of 2 m to 5 m at 0.5 m interval. The test results are summarized in Table 17.2. The shear strength profiles are plotted in Figure 17.2. The laboratory shear strength profiles followed a similar

pattern of shear strength increase as those obtained by field vane tests. The average shear strength increased by 71.9 % and 54.6 % for EOS1 and EOS2 respectively. It can be seen that the average shear strength increase obtained by unconfined compression test is slightly higher than that by field vane test. This may be due to the anisotropic behaviour of the soft sensitive clay and the difference in test orientations (angle i) of the two test methods (Lo and Morin 1972, Law 1974). The ratios of peak shear strengths (by laboratory test) to field vane strengths are 1.42 and 1.50 for EOS1 and EOS2 respectively, which are similar to the ratio of 1.67 obtained by Law (1974).

Some typical stress-strain curves of unconfined compression tests performed on samples at 4.5 m depth before and after treatment are presented in Figure 17.3. It can be seen that the changes in stress-strain behaviour after treatment are similar to those obtained from laboratory investigation (Figure 7.4). The improvement of sensitivity was also investigated. The undisturbed and remoulded shear strengths were determined with the same method as in the field using a laboratory vane test equipment with an accuracy up to 0.1 kPa. The sensitivity test results are summarized in Table 17.2. The profiles are plotted in Figure 17.4. Table 17.2 indicates the decrease of sensitivity of clay from a nominal value of 100 to around 60, resulting in the average decrease of 35 % and 26 % for EOS1 and EOS2 respectively. The effect of electro-osmosis to soil sensitivity is therefore demonstrated.

17.2.2 Consolidated-Undrained Triaxial Test with Pore Pressure Measurement

The effect of electro-osmosis on the stress-strain behaviour of soft clay was investigated in terms of effective stress by performing isotropically consolidated undrained triaxial tests on specimen trimmed from the tube samples between 3 and 4 m depths. The standard sample sizes and test procedures were used as described by Bishop and Henkel (1962) with a constant strain rate of 0.017 % per minute. The test data obtained by Law (1974) is used as pre-treatment results (tests P2, P3, P4 and P5) together with test P1 which was performed by the writer to complete the failure envelope at lower consolidation pressure of 18 kPa. Another reason of performing test P1 is to verify the applicability of the past test results obtained by Law (1974). The post-treatment triaxial tests were performed with the same consolidation pressures for comparison. The plots of stress-strain variations and pore water changes are shown in Figures 17.5 to 17.8. The Test results of the consolidated-undrained triaxial tests of the specimen before and after treatment are compared in Figures 17.9a to 17.9c. In each of these figure, a general improvement in stress-strain behaviour and reduction of pore pressure as a result of treatment may be noted. The test results are summarized in Table 17.3 which shows that in the over-consolidated region, the peak axial stresses at failure of the clay after treatment are higher in EOS1 than in EOS2. The post-treatment stresses are also higher than those before treatment. While in the normally consolidated region, the peak axial

stresses at failure have no significant change.

Another important observation is the reduction of pore water pressure measured during the tests. As can be seen in Table 17.3 and in Figures 17.6 and 17.8, the pore water pressure reduced by 10 to 20 %. This may be explained that the clay in the test area is "over-consolidated" due to the generation of negative pore water pressure by electro-osmosis.

The changes in stress-strain behaviour of clay can be analyzed by comparing the failure envelope as shown in Figure 17.9d. Due to the increase in preconsolidation pressures after treatment (sections 7.6 and 17.3), the failure envelopes for EOS1 and EOS2 in the over-consolidated region are extended horizontally. Figure 17.9d also shows that the failure envelopes after treatment are significantly higher than the initial envelope further confirming that the strength in terms of effective stresses increased. When compared the p' and q' values in Table 17.3 and the p'-q' plot in Figure 17.9e, it can be seen that, in the over-consolidated region, both the p' and q' values increased after treatment, resulting in the shift of the failure envelope to the right. Whereas in the normally consolidated region, the p' and q' values decreased after treatment, causing a shift of failure envelope to the left. It is also interesting to note that, the failure envelopes after treatment have the tendency to merge to the origin of the graph as in the initial failure envelope. At consolidation pressure of triaxial test higher than the preconsolidation pressure, the two failure envelopes after treatment have the tendency to merge to the straight line portion

(unstructured portion of the envelope as described by Lo and Morin 1972) of the initial failure envelope.

17.3 Consolidation

One-dimensional consolidation tests were performed in the tube samples at depths 2.5 m and 4.5 m before and after treatment and the corresponding results are summarized in Table 17.4. Conventional consolidation curves are plotted with void ratio (e) against applied pressure (log scale) in Figures 17.10 and 17.11. For comparison purposes, the consolidation curves with the plot of the change of void ratio (Δe) against applied pressure (log scale) are plotted in Figures 17.12 and 17.13. The clay samples after treatment exhibited the reduction of void ratios and increase in preconsolidation pressures. These observations are similar to those discussed in section 7.5. The preconsolidation pressure increased from an initial value of 48.5 kPa at 2.5 m depth to 73 kPa and 63 kPa respectively for EOS1 and EOS2. For the test at 4.5 m depth, the preconsolidation pressure increased from 53 kPa to 98 kPa and 89 kPa respectively. The percentage increase ranges from 29.9 % to a maximum of 84.9 %. The increase in preconsolidation pressure in the field further supports the argument that the soft clay is actually consolidated by the electric potential which is analogous to a mechanical dead load.

17.4 Physical and Chemical Tests of Soil

Table 17.5 shows the test results of plastic and liquid limits tests of soil before and after treatment. The initial average values of plastic and liquid limits of clay were 23 % and 48.8 % respectively. After treatment, the liquid limits increased to the average of 51.7 % and 50.3 % for EOS1 and EOS2 respectively whereas the plastic limit has no appreciable change. As a result, the plasticity index increased with an average of 8 %. However, the reduction in moisture content by electro-osmosis should not affect the plastic properties of the clay. Bjerrum et al (1967) suggested that such effect may be due to certain changes in the chemical properties of the clay due to the passage of electric current. The measurement of carbonate content, salinity, pH value and cation exchange capacity (CEC) of the soil samples after treatment were then performed to investigate this effect. Table 17.6 summarizes these chemical test results and their profiles are plotted in Figures 17.14 to 17.16.

Similar to the laboratory investigation of electro-osmosis, the carbonate content and salinity of clay after treatment increased by 70 % as shown in the profiles in Figures 17.14 and 17.15. The carbonate content and salinity increased from the initial average of 4 % and 1.30 g/l to 7 % and 2.18 g/l respectively. As explained in section 7.7, the increase of carbonate content and salinity has the effect of stronger bonding in soil particles and thinner double layer in the soil-water system, resulting in higher strength, lower sensitivity and higher plasticity.

There was an impression in the past that the pH value of soil would increase due to electro-chemical reaction. As suggested by Mitchell (1976), the high pH value (alkalinity) of soil might have adverse effect to the soil properties. Surprisingly, the pH value of clay has practically not changed after treatment, as shown in Table 17.6 and Figure 17.16. This may be explained by the effect of electrode polarity reversal. During treatment with normal polarity, the pH value of the soil at the vicinity of anode is lower while that at cathode is higher, due to the electro-chemical reactions. When the electrode polarity is reversed, the variation of pH values are also reversed. Since the period of normal and reversal treatment were approximately the same (17 days and 15 days respectively), the effect of electro-chemical reaction is counter-balanced by the reversal of electric current. As a result, the pH value was unchanged. Another reason to this may be due to the effectiveness of the electrode design. In the past, the electrode system was inefficient and the migrated water accumulated around the cathode. More and more soluble hydroxide ions were produced due to electro-chemical reaction and consequently, increased the pH value of soil at vicinity of cathode. In the present electrode design, the expelled water can flow out through the electrode to the ground surface without difficulty and in the same manner, the soluble hydroxide ions are removed from the soil immediately after their formation. This explanation is further supported by the high pH value (about 10.5) obtained from the expelled water at cathode (see section 17.5).

Mitchell (1976) suggested that the high pH value in soil might be an indication of soil contamination or instability of soil structure. Although the pH values of soil after field treatment remained unchange, it was decided to carry out an extra test (cation exchange capacity test) to justify that the electro-osmosis would have no adverse effect to the soil properties. If the increase of pH value of soil together with an higher cation exchange capacity (higher CEC value) are obtained, the soil may be adversely affected. The spot check was performed on the soil samples at 2.5 m and 4 m depth before and after treatment. Table 17.6 shows that the post-treatment soil samples have slightly lower or no change in CEC values. Combining the pH value and CEC test results, it can be concluded that the electro-osmosis has no adverse effect to the soil properties, on condition that the process is properly manipulated and monitored.

17.5 Chemical Analysis of Water Samples

A series of chemical analysis of water samples were performed on the expelled water collected at cathode. The pH values of water were determined in the field immediately after sampling by paper indicator and the salinity test, cations concentration tests (copper, sodium, calcium, potassium and magnesium) and anions concentration tests (chloride and sulphate) were performed later in the laboratory. The test results are summarized in Table 17.7 and their variations with treatment time are plotted in Figures 17.1 / to 17.25.

As shown in Figures 17.17 and 17.18, both the pH value and salinity increased sharply one day after the power was switched on from the initial values of 8.5 and 1.4 g/l to 9.5 and 6.0 g/l respectively. From then on the values increased gradually to the maximum of 10 and 9.3 g/l respectively on day 18 (just before electrode polarity reversal). On day 19, one day after polarity reversal, the values dropped to 7.5 and 1.5 g/l and then increased gradually to 10.5 and 3.8 g/l respectively on day 33, iust before power shut off. Since the salinity measurement is basically the determination of sodium ion concentration, it can be seen that the variation of sodium ion concentration in Figure 17.19 has the similar trend as that of salinity variation.

In the field test, copper was used as electrode material. As shown in Figure 17.20, there was no trace of copper ion in the groundwater before treatment. A high concentration of copper ion of 1420 ppm (parts per million) in the expelled water was detected after polarity reversal. It is due to the fact that copper oxidized to copper ion and dissolved in the soil near anode during treatment with normal polarity and they were removed by the expelled water when the polarity was reversed. The anxiety of contamination of groundwater due to dissolved metallic ion of electrode can then be reduced by the present improvement of electro-osmotic treatment.

There is only low concentration of calcium, potassium and magnesium in the soil, as shown in Figures 17.21 to 17.23, and no important observation can be made on the variations of these ions. However, these figures give an

implication that certain metallic ions may be removed from the soil by electro-osmosis. Therefore, electro-osmosis may have a potential application in the remedy of some types of environmental hazardous site.

Certain anions such as chloride and sulphate are removed from the soil by electro-osmosis, as shown in Figures 17.24 and 17.25. During the treatment with normal polarity, no anions were detected from the expelled water at cathode since they were migrated towards anode. When the polarity was reversed, the accumulated anions near the new cathode (previously anode in normal treatment) were removed by the expelled water. Since chloride and sulphate may cause concrete deterioration, the removal of these anions by electro-osmosis may be advantageous to the underground concrete structures.

The knowledge of these chemical changes is quite inadequate but the applications are interesting. Some chemical changes due to electro-osmosis may be of potential usage in the future in different areas such as environmental and concrete engineering. The effects of electro-osmosis to the possible changes of clay fabric and chemical properties may be another branch of study as well. However, these are outside the scope of the present research.

Table 17.1 Summary of Moisture Content Test Results

Depth	Before Treatment	After Treatment			
		EOS 1		EOS 2	
m	ω_o %	ω_1 (%)	decrease (%)	ω_2 (%)	decrease (%)
2.0	81.2	71.9	11.5	73.6	9.4
2.5	65.7	54.6	16.9	58.8	10.5
3.0	91.1	78.4	13.9	82.2	9.8
3.5	86.2	74.2	13.9	77.6	10.0
4.0	83.6	70.3	15.9	73.8	11.7
4.5	84.9	73.4	13	72.1	15.4
5.0	85.6	71.6	16.4	73.5	14.1
		Average =	14.6 %	Average =	11.6 %

Table 17.2 Summary of Unconfined Compression Test Results

Depth	Before Treatment		After Treatment							
			EOS 1				EOS 2			
m	Cu kPa	S_t	Cu kPa	ΔCu %	S_t	ΔS_t %	Cu kPa	Cu %	S_t	ΔS_t %
2.0	15.9	11	28.8	81.1	9	-18	25.0	57.2	10	-9
2.5	15.2	15	23.8	56.6	14	-7	20.0	31.6	13	-13
3.0	16.5	23	24.9	50.9	14	-39	22.1	33.9	20	-13
3.5	17.9	100	26.3	46.9	40	-60	24.7	40.0	62	-38
4.0	13.9	100	24.2	74.1	60	-40	23.3	67.6	70	-30
4.5	12.6	100	23.6	87.3	47	-45	21.4	69.8	63	-37
5.0	12.8	96	26.4	106.3	60	-38	23.3	82.0	56	-40
			Average=	71.9 %		-35 %		54.6 %		-26 %

Notes:-
Cu = undrained shear strength obtained from unconfined compression test
S_t = sensitivity of soil measured by laboratory vane test equipment with accuracy up to 0.1 kPa

Table 17.3 Summary of Isotropically Consolidated Undrained Triaxial Test Results on Tube Samples after Electro-Osmosis Field Treatment

Borehole	Test No.	σ_c' kPa	$(\sigma_1-\sigma_2)_f$ kPa	$(\sigma_1-\sigma_2)_r$ kPa	ϵ_f %	E_u kPa	p_f' kPa	q_f' kPa	u_{max} kPa
pre-treatment sampling	P1	18	35.8	21.6	0.96	6200	25.3	17.9	11.2
after	P2	38	51.0	33.1	1.30	8280	43.5	25.5	30.0
Law	P3	88	56.0	--	2.30	8280	63.1	28.0	62.2
1974	P4	138	87.5	--	3.50	8690	93.2	43.8	102.3
	P5	207	129.4	--	4.60	18420	140.8	64.7	153.7
EOS1	101	18	51.0	37.4	1.44	8230	34.5	25.5	8.5
	102	38	66.8	47.5	1.71	11450	50.5	33.4	23.1
	103	88	78.4	--	1.97	12210	78.0	39.2	46.8
	105	207	114.6	--	3.79	18430	119.1	57.3	147.2
EOS2	201	18	41.6	27.1	1.83	5490	28.9	20.9	10.0
	202	38	59.6	41.1	1.43	9820	43.8	29.8	29.2
	203	88	71.2	63.7	3.05	9510	75.6	35.6	50.2
	204	138	79.6	--	2.23	13750	93.4	39.8	87.6
	205	207	123.8	--	4.20	19950	125.9	61.9	144.4

Notes:-

1. $(\sigma_1-\sigma_2)_f$ = peak axial stress at failure
2. $(\sigma_1-\sigma_2)_r$ = post-peak strength
3. E_u = secant modulus at $\frac{1}{2}(\sigma_1-\sigma_2)_f$
4. Rate of strain = 0.017 %/min
5. Sample type = 127 mm (5") diameter Osterberg tube sample
6. $p_f' = \frac{1}{2}(\sigma_1'+\sigma_2')_f$
7. $q_f' = \frac{1}{2}(\sigma_1-\sigma_2)_f$
8. Samples taken at 3 to 4 m for triaxial test

Table 17.4 Comparison of Pre-Consolidation Pressure of Soil Sample Before and After Electro-Osmotic Treatment

Borehole	Depth m	Pre-treatment kPa	Post-treatment kPa	Net Increase kPa	Percentage Increase %
EOS1	2.5	48.5	73	24.5	50.5
	4.5	53.0	98	45.0	84.9
EOS2	2.5	48.5	63	14.5	29.9
	4.5	53.0	89	36	67.9

Table 17.5 Summary of Plastic and Liquid Limits Test Results

Depth	Pre-treatment			EOS 1			EOS 2		
m	PL (%)	LL(%)	PI	PL (%)	LL (%)	PI	PL(%)	LL (%)	PI
2.0	21.1	54.3	33.2	23.9	55.9	32.0	23.3	58.5	35.2
2.5	22.6	48.8	26.2	21.8	51.6	29.8	23.1	49.5	26.4
3.0	21.1	45.6	24.5	21.4	45.2	23.8	22.4	46.1	23.7
3.5	23.1	47.2	24.1	24.8	53.8	29.0	21.3	50.2	28.9
4.0	25.3	56.5	31.2	27.5	58.7	31.2	25.1	53.6	28.5
4.5	22.7	42.9	20.2	23.2	47.9	24.7	20.1	46.1	26.0
5.0	25.7	46.3	20.6	25.0	48.8	23.8	22.1	48.4	26.3

Table 17.6 Summary of Chemical Test Results of Soil Samples

Depth	Carbonate Content (%)			Salinity (g/l)			Soil pH Value			C.E.C. (meq/100g soil)		
m	Pre-Treatment	EOS1	EOS2	Pre-Treatment	EOS1	EOS2	Pre-Treatment	EOS1	EOS2	Pre-Treatment	EOS1	EOS2
2.0	6.1	8.1	6.4	1.37	2.06	1.97	8.6	8.6	8.9	--	--	--
2.5	6.1	7.3	6.7	1.34	2.37	2.03	8.4	8.6	8.6	18.1	16.5	15.6
3.0	4.4	8.2	6.8	1.48	1.95	1.85	8.8	9.0	9.0	--	--	--
3.5	4.4	7.9	6.1	1.41	2.19	1.70	8.8	9.0	9.1	--	--	--
4.0	4.4	7.2	5.4	1.03	2.37	1.74	8.7	8.9	8.6	19.8	13.3	19.7
4.5	2.3	3.5	3.4	1.20	2.28	2.05	8.6	8.9	8.6	--	--	--
5.0	2.6	4.0	3.4	1.26	2.04	2.05	8.6	8.9	9.1	--	--	--

Table 17.7 Summary of Chemical Test Results of Water Samples Collected at Cathodes during Electro-Osmotic Treatment

Day No.	pH	Salinity g/l	Sodium ppm	Calcium ppm	Magnesium ppm	Potassium ppm	Copper ppm	Sulphate ppm	Chloride ppm	Remarks
1	8.5	1.4	520	63	66	25	0	450	240	initial values
2	9.5	6.0	1000	0	0	24	0	20	41	
3	9.5	7.5	1250	0	0	24	0	20	27	
4	9.5	8.0	1600	0	0	32	0	40	21	
5	9.5	7.8	1075	0	0	32	0	16	24	
8	9.5	8.0	1075	0	0	35	0	15	24	
9	10.0	8.2	1300	0	0	39	0	22	27	
10	10.0	8.5	1825	0	0	39	0	17	27	
11	10.0	8.6	1750	0	0	49	0	20	23	
12	10.0	8.7	1950	0	0	44	0	15	31	
16	10.0	9.0	2000	0	0	58	0	15	27	
17	10.0	9.0	2050	0	0	46	0	15	20	
18	10.0	9.3	2000	0	0	56	0	15	21	polarity reversal
19	7.5	1.5	182	200	83	24	520	1500	221	
22	7.5	2.8	240	400	200	27	330	2150	1637	
23	7.5	2.5	315	250	114	30	1420	2500	1247	
24	7.5	2.6	235	400	240	41	0	95	1947	
25	8.0	2.8	235	250	245	48	0	55	1460	
26	8.5	3.0	235	108	180	32	0	47	1018	
29	9.0	3.4	200	18	42	37	0	27	120	
31	9.5	3.5	185	4	7	40	0	30	46	
32	10.5	3.6	195	5	1	54	0	42	44	
33	10.5	3.8	875	0	0	120	0	42	73	treatment completed

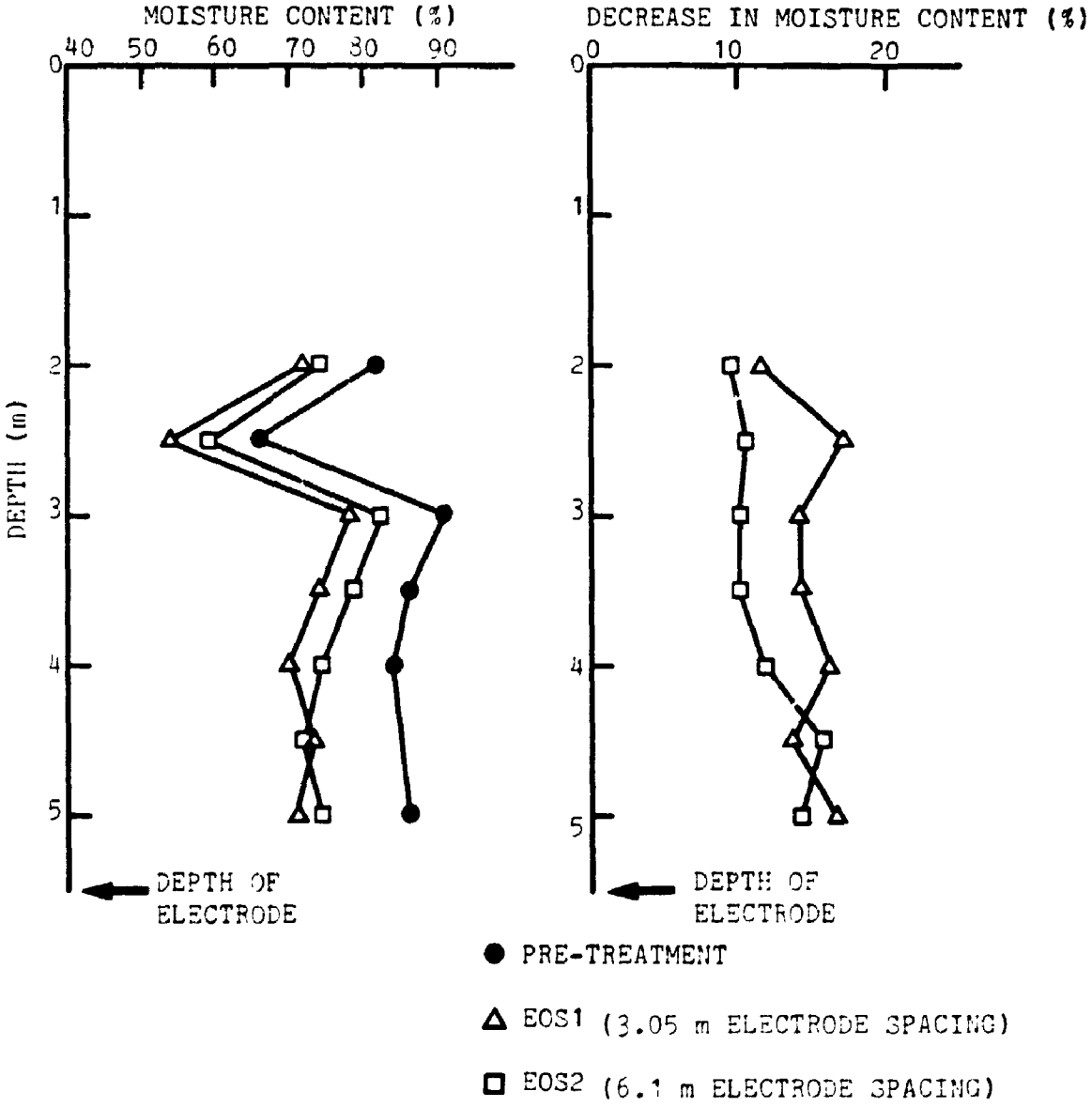

FIGURE 17.1 VARIATION OF MOISTURE CONTENT WITH DEPTH AFTER TREATMENT

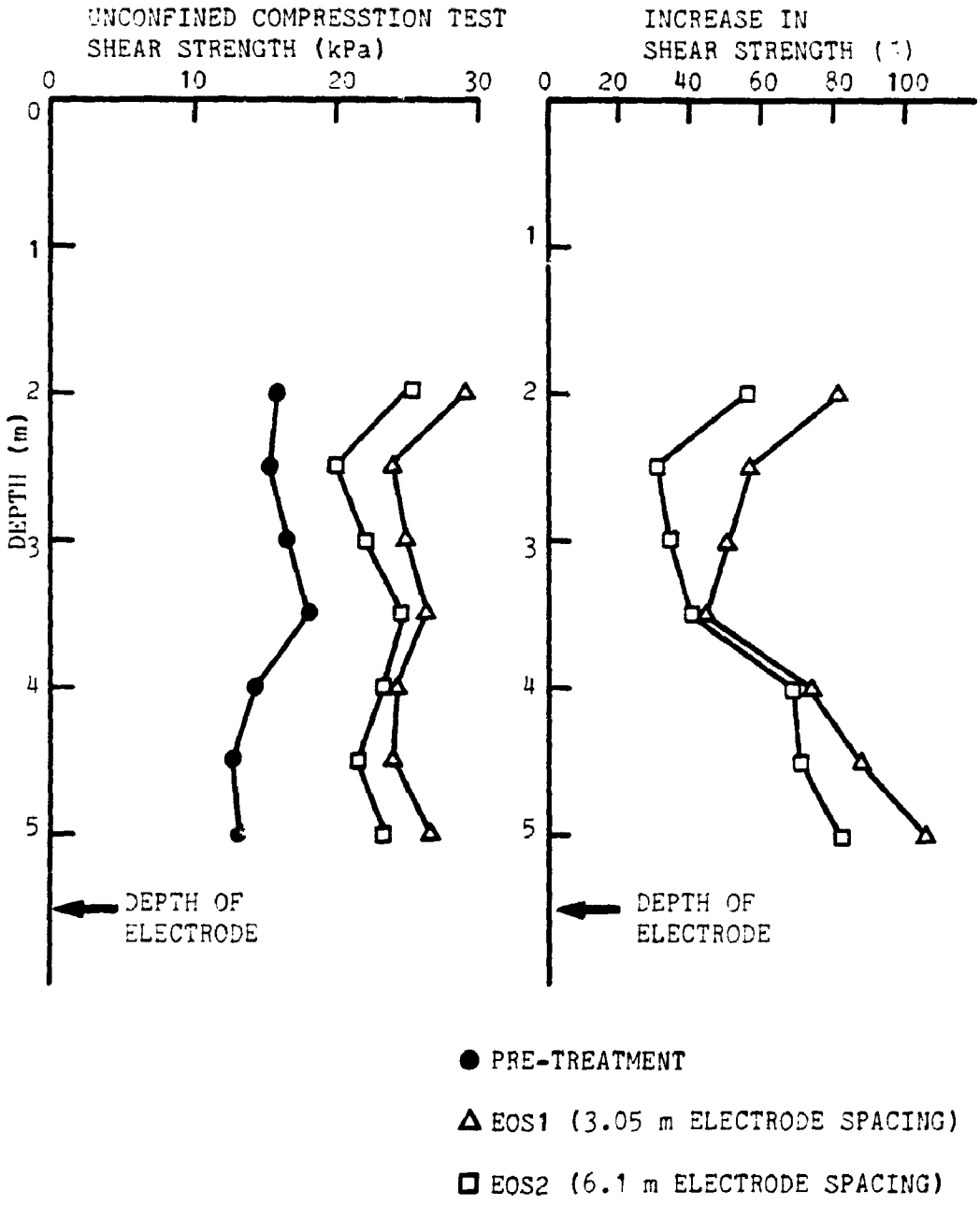

FIGURE 17.2 VARIATION OF SHEAR STRENTH PROFILES (UNCONFINED COMPRESSION TEST) BEFORE AND AFTER TREATMENT

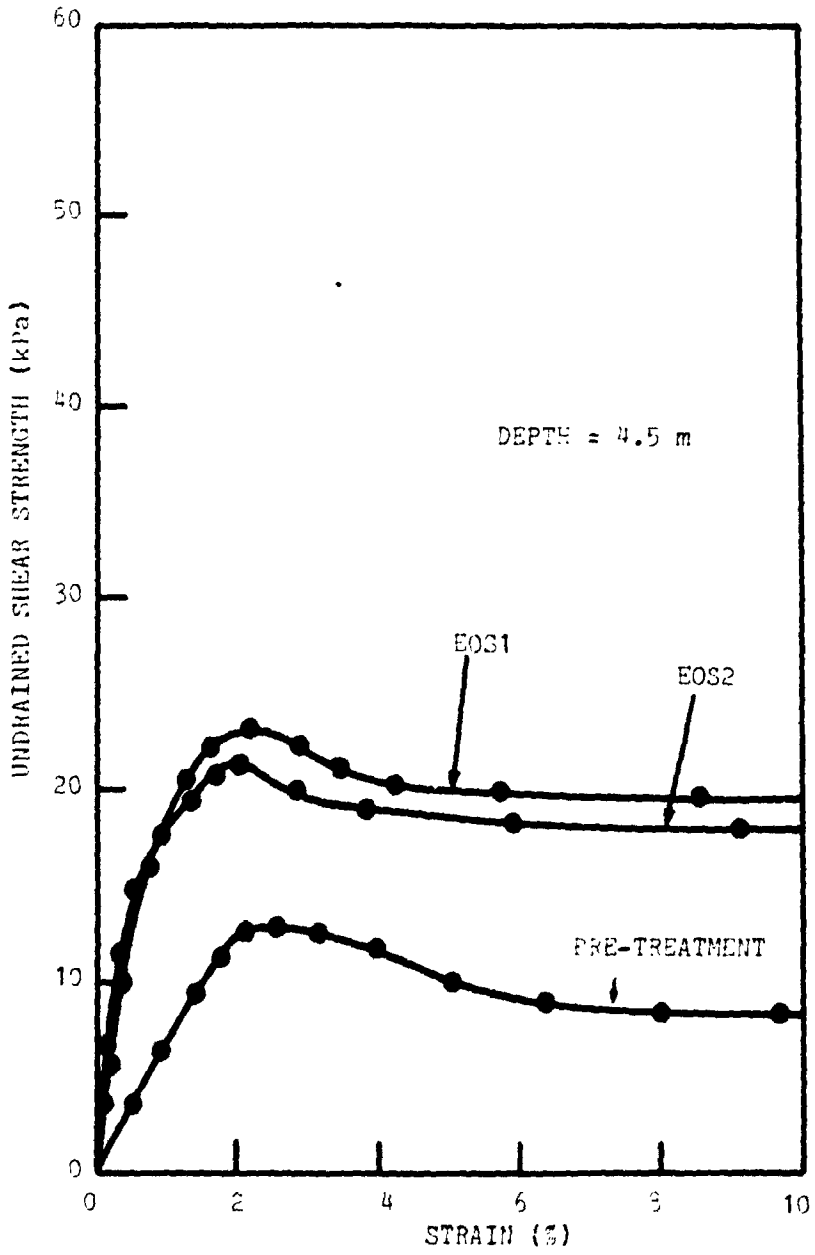

FIGURE 17.3 UNCONFINED COMPRESSION TEST OF SAMPLES BEFORE AND AFTER ELECTRO-OSMOTIC TREATMENT, TYPICAL CURVES FOR SAMPLE AT 4.5 m DEPTH

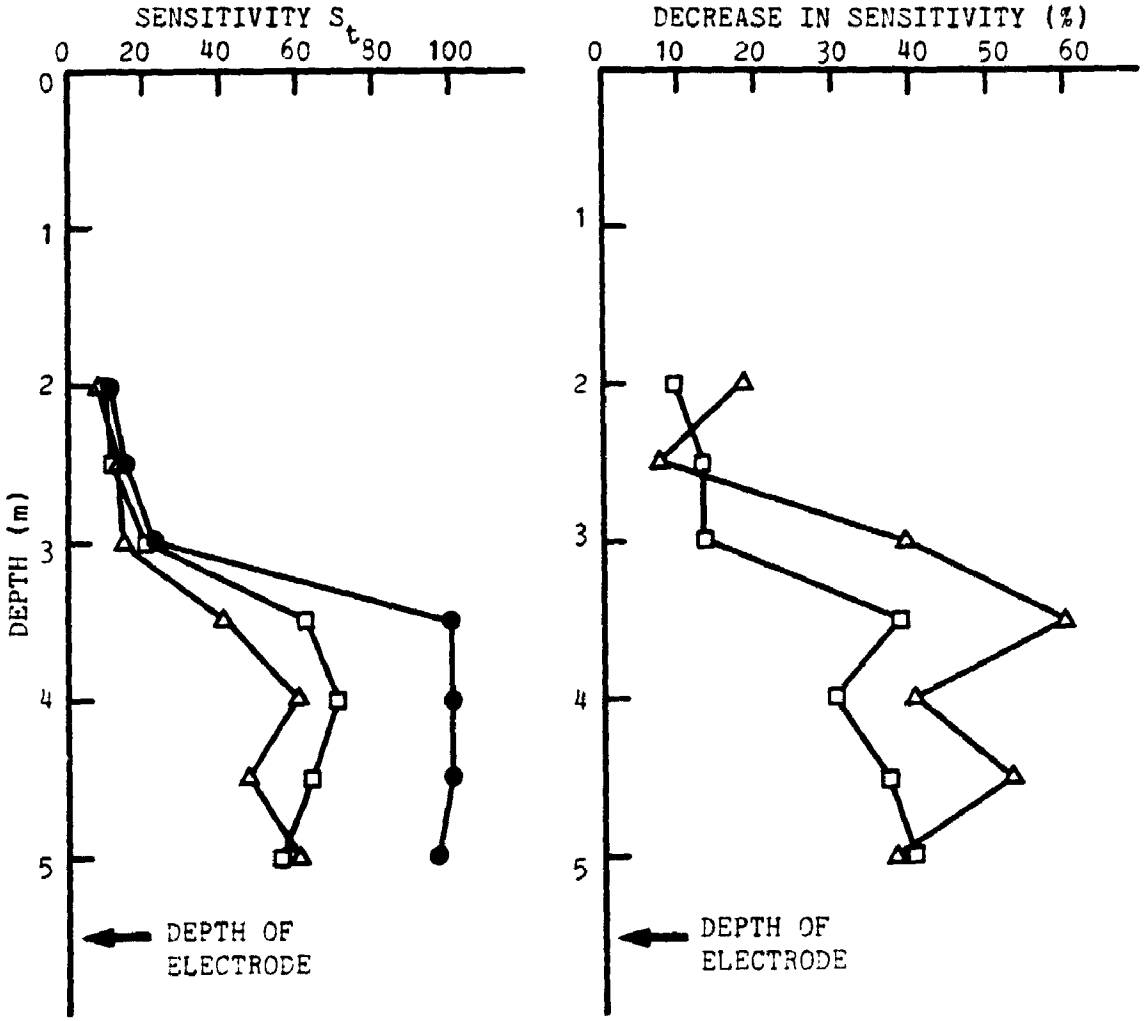

FIGURE 17.4 VARIATION OF SENSITIVITY OF SOIL BEFORE AND AFTER TREATMENT

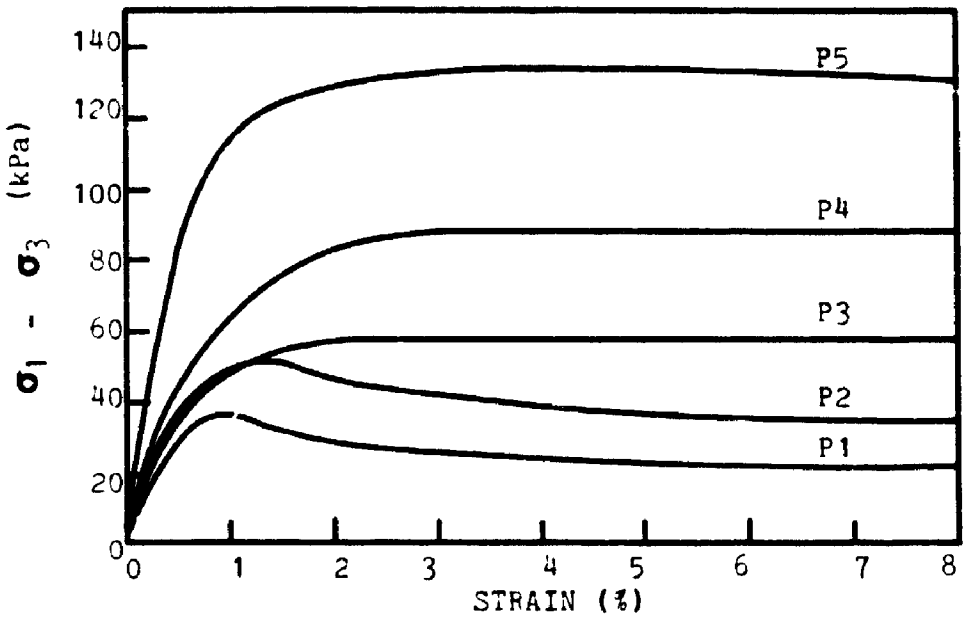

(a) PRE-TREATMENT

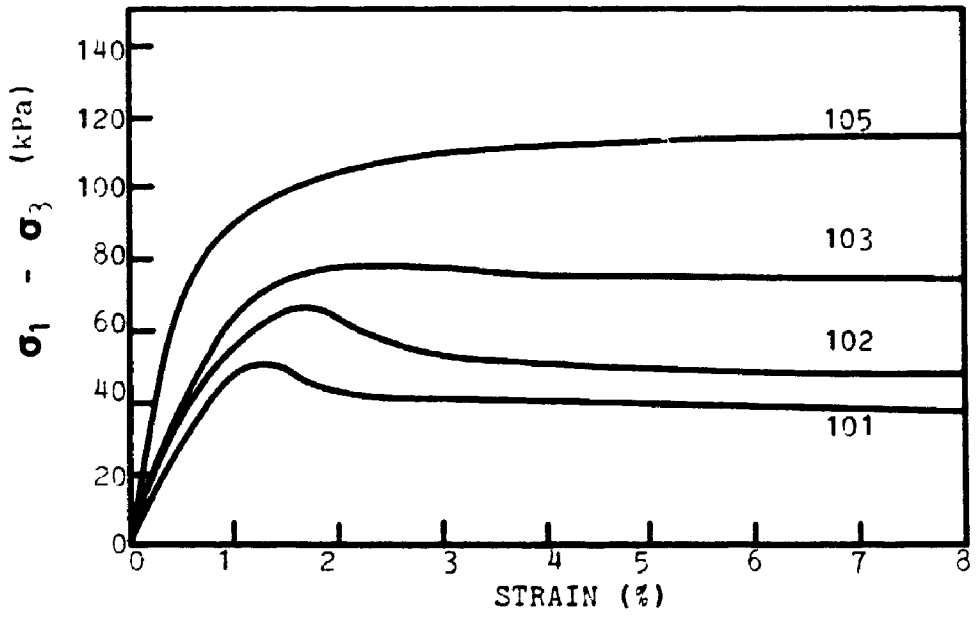

(b) BOREHOLE EOS1

FIGURE 17.5 STRESS-STRAIN PLOTS OF CONSOLIDATED-UNDRAINED TRIAXIAL TEST FOR BOREHOLE EOS1 BEFORE AND AFTER ELECTRO-OSMOTIC TREATMENT

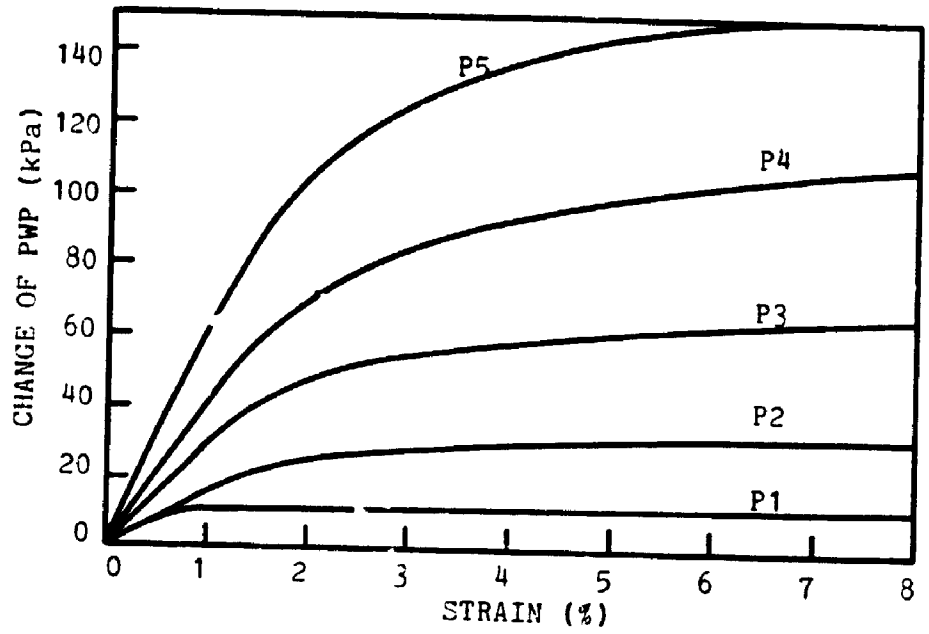

(a) PRE-TREATMENT

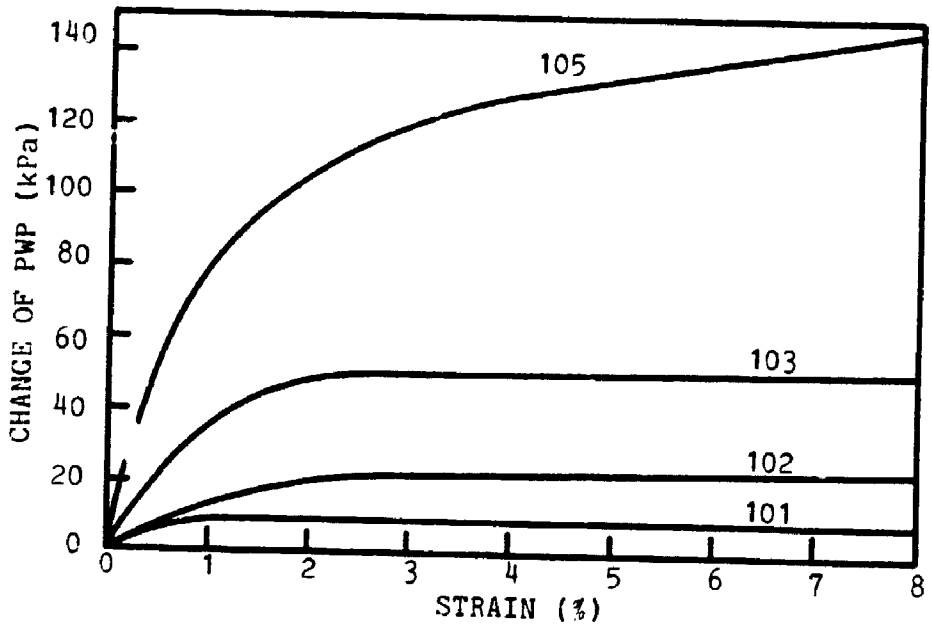

(b) BOREHOLE EOS1

FIGURE 17.6 PORE WATER PRESSURE CHANGES OF CONSOLIDATED UNDRAINED TRIAXIAL TEST FOR BOREHOLE EOS1 BEFORE AND AFTER ELECTRO-OSMOTIC TREATMENT

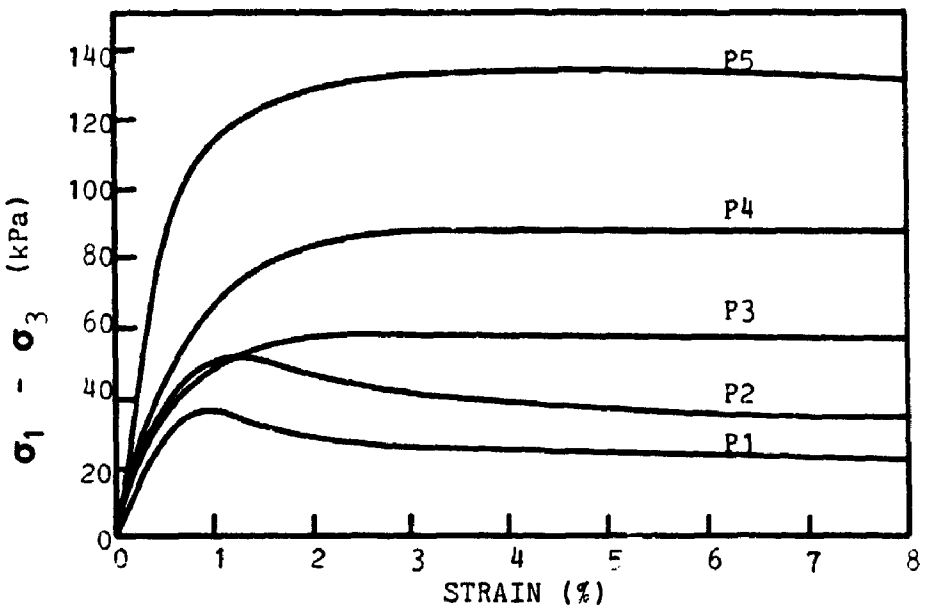

(a) PRE-TREATMENT

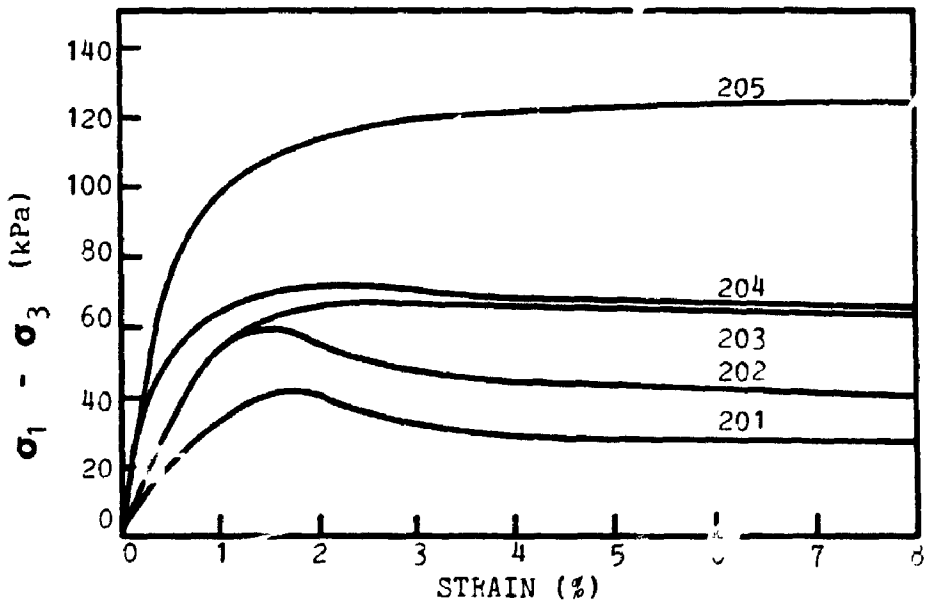

(b) BOREHOLE EOS2

FIGURE 17.7 STRESS-STRAIN PLOTS OF CONSOLIDATION-UNDRAINED TRIAXIAL TEST FOR BOREHOLE EOS2 BEFORE AND AFTER ELECTRO-OSMOTIC TREATMENT

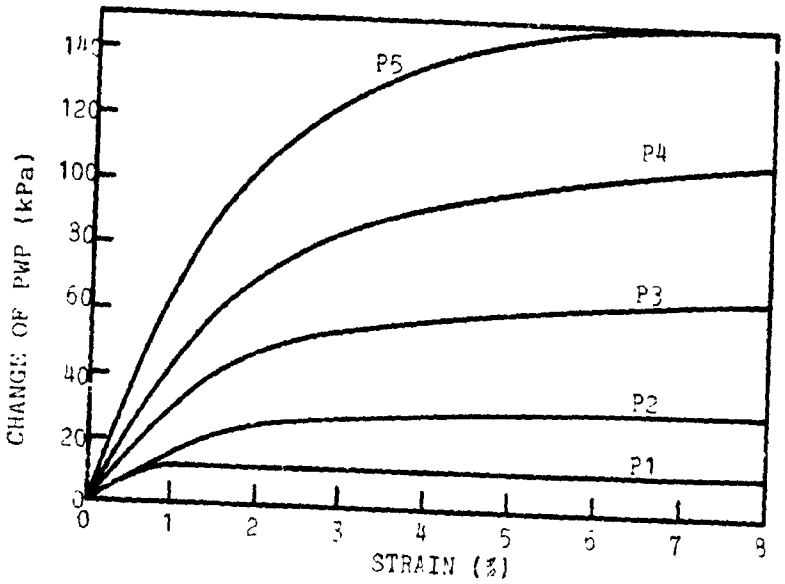

(a) PRE-TREATMENT

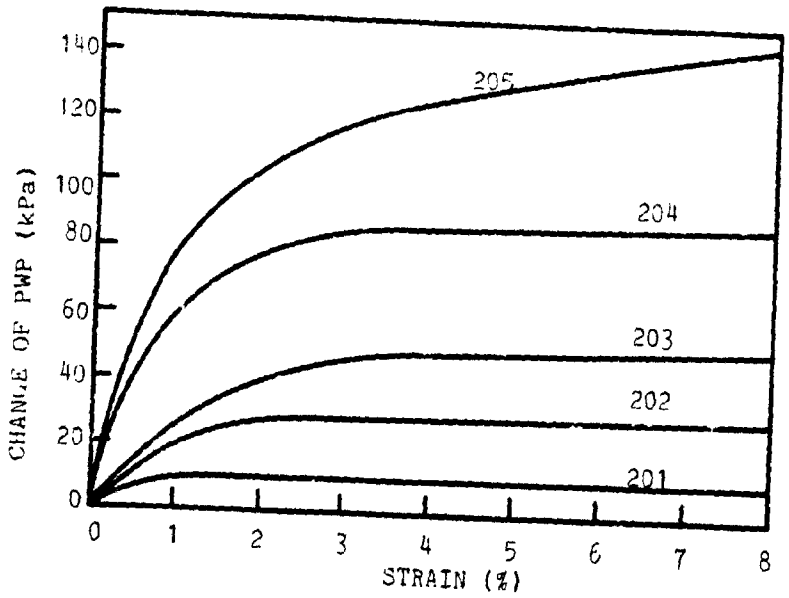

(b) BOREHOLE EOS2

FIGURE 17.8 PORE WATER PRESSURE CHANGES OF CONSOLIDATED UNDRAINED TRIAXIAL TEST FOR BOREHOLE EOS2 BEFORE AND AFTER ELECTRO-OSMOTIC TREATMENT

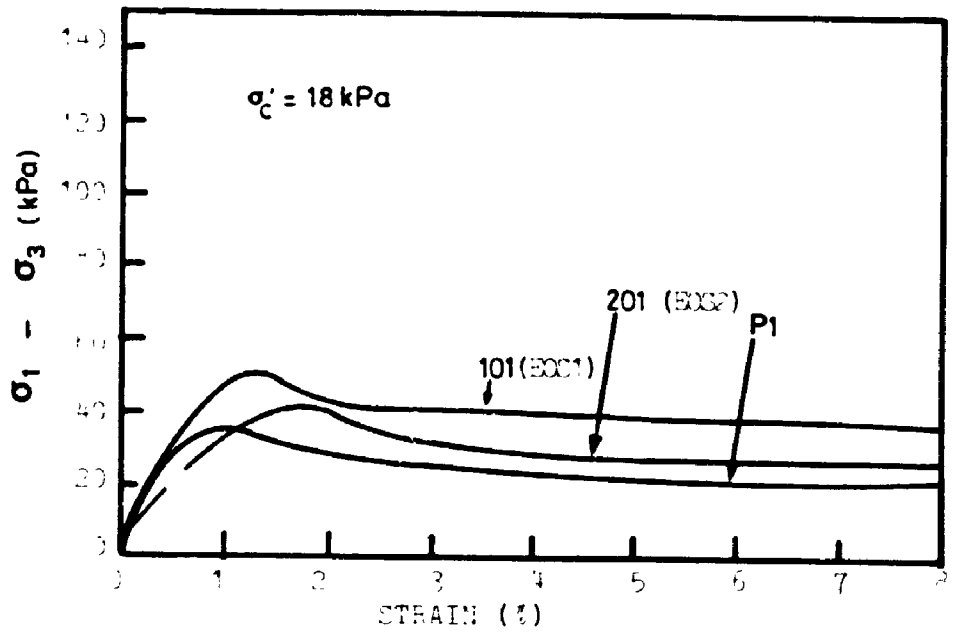

(i) DEVIATOR STRESS-STRAIN PLOT

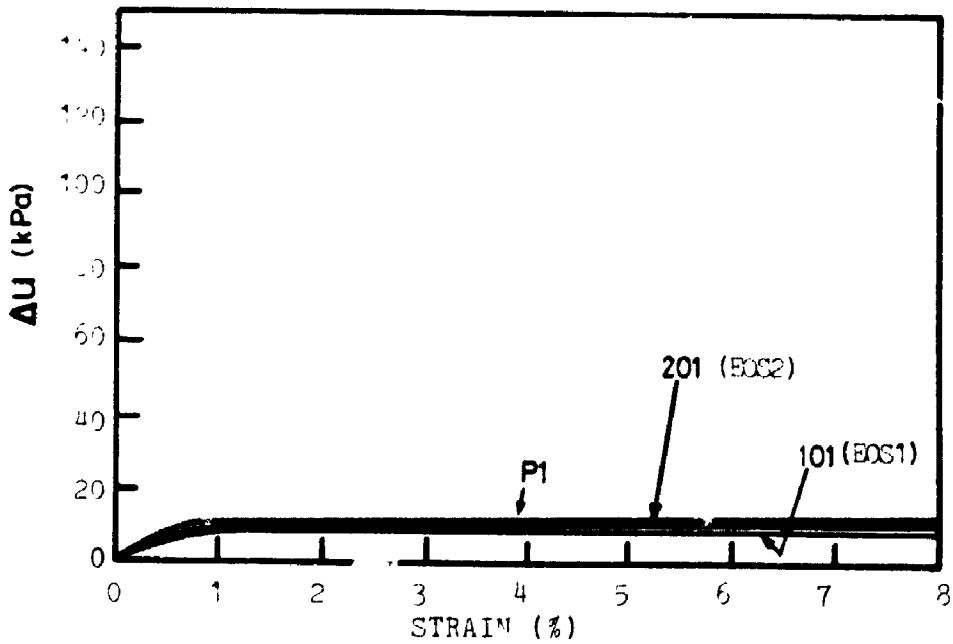

(ii) CHANGE OF PORE WATER PRESSURE

FIGURE 17.9a COMPARISON OF RESULTS OF CONSOLIDATED-UNDRAINED TRIAXIAL TESTS BEFORE AND AFTER TREATMENT FOR THE CONSOLIDATION PRESSURE OF 18 kPa

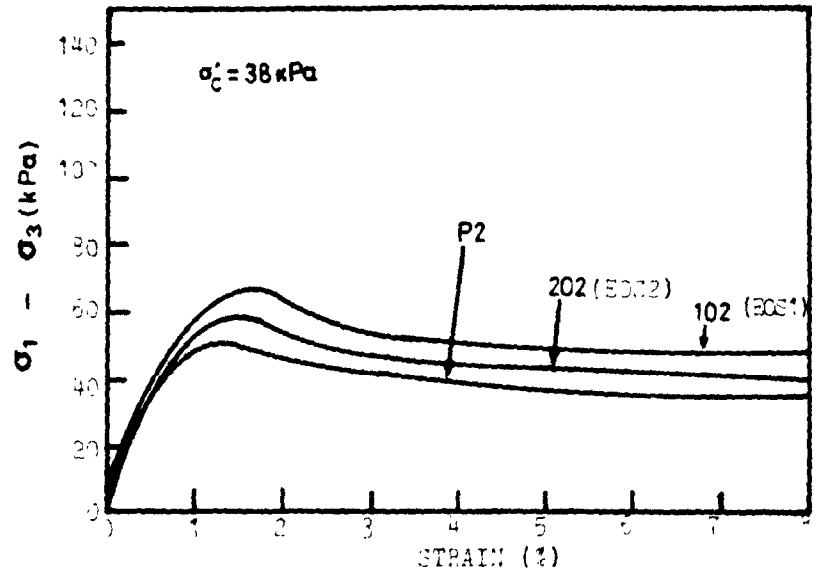

(i) STRESS-STRAIN PLOT

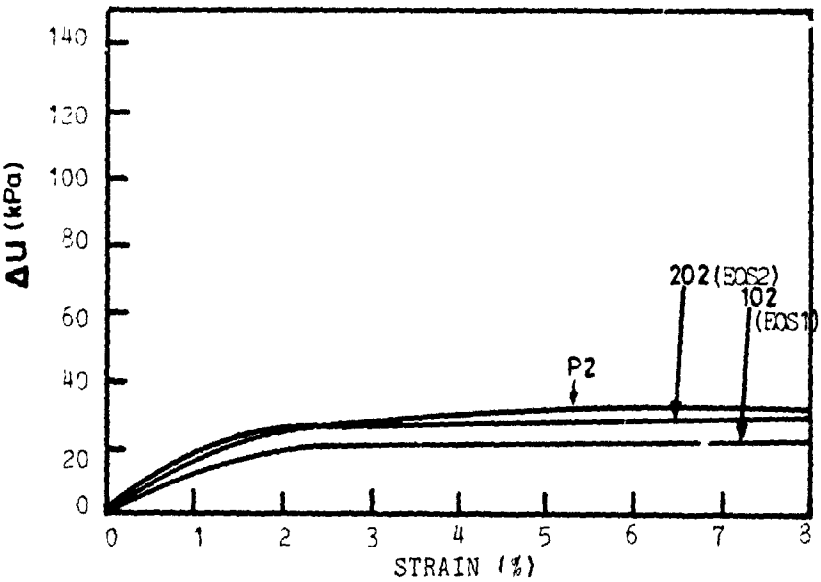

(ii) CHANGE OF PORE WATER PRESSURE

FIGURE 17.9b COMPARISON OF RESULTS OF CONSOLIDATED-UNDRAINED TRIAXIAL TESTS BEFORE AND AFTER TREATMENT FOR THE CONSOLIDATION PRESSURE OF 38 kPa

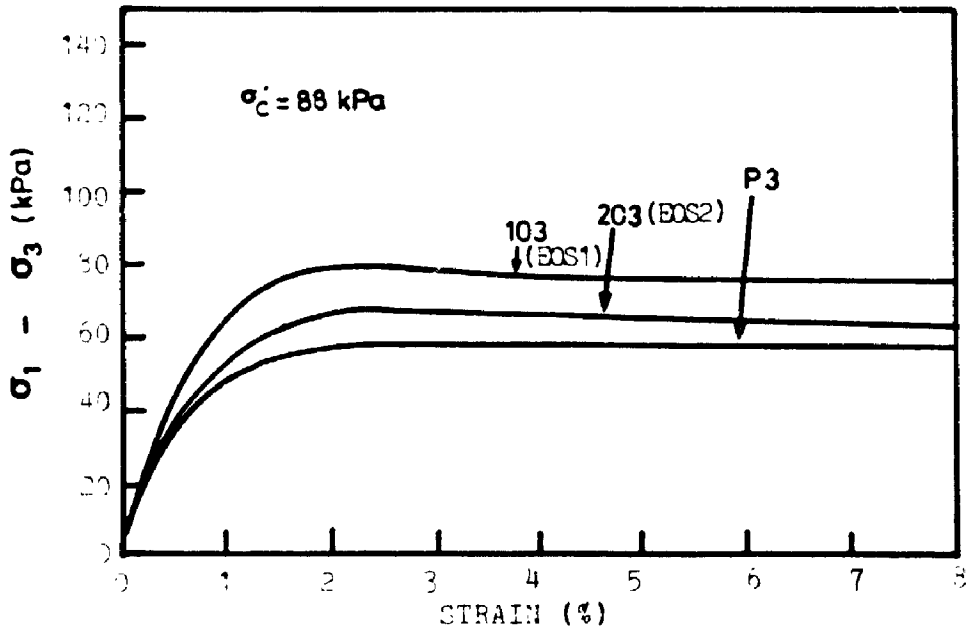

(i) STRESS-STRAIN PLOT

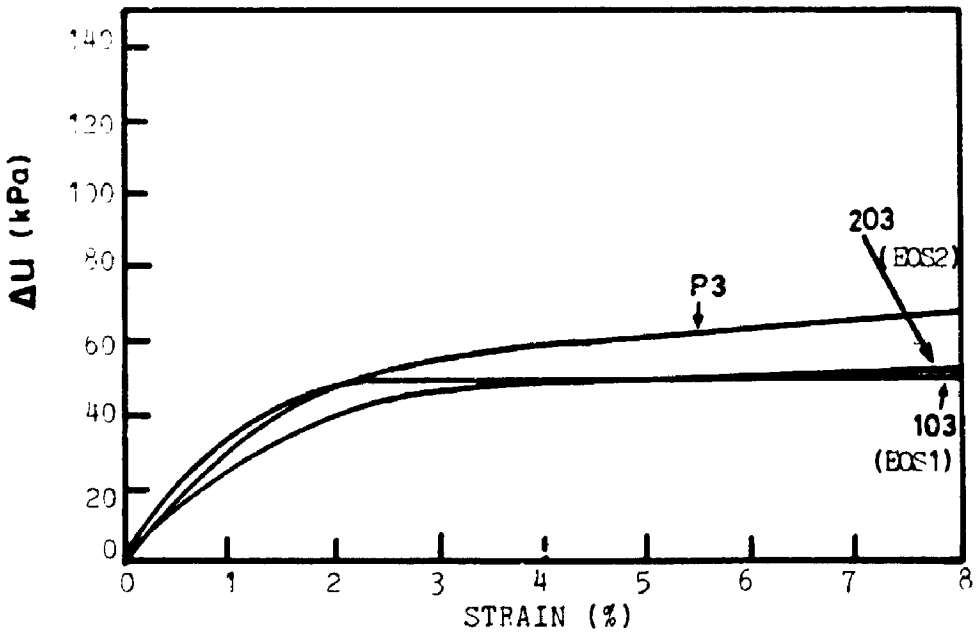

(ii) CHANGE OF PORE WATER PRESSURE

FIGURE 17.9c COMPARISON OF RESULTS OF CONSOLIDATED-UNDRAINED TRIAXIAL TESTS BEFORE AND AFTER TREATMENT FOR THE CONSOLIDATION PRESSURE OF 88 kPa

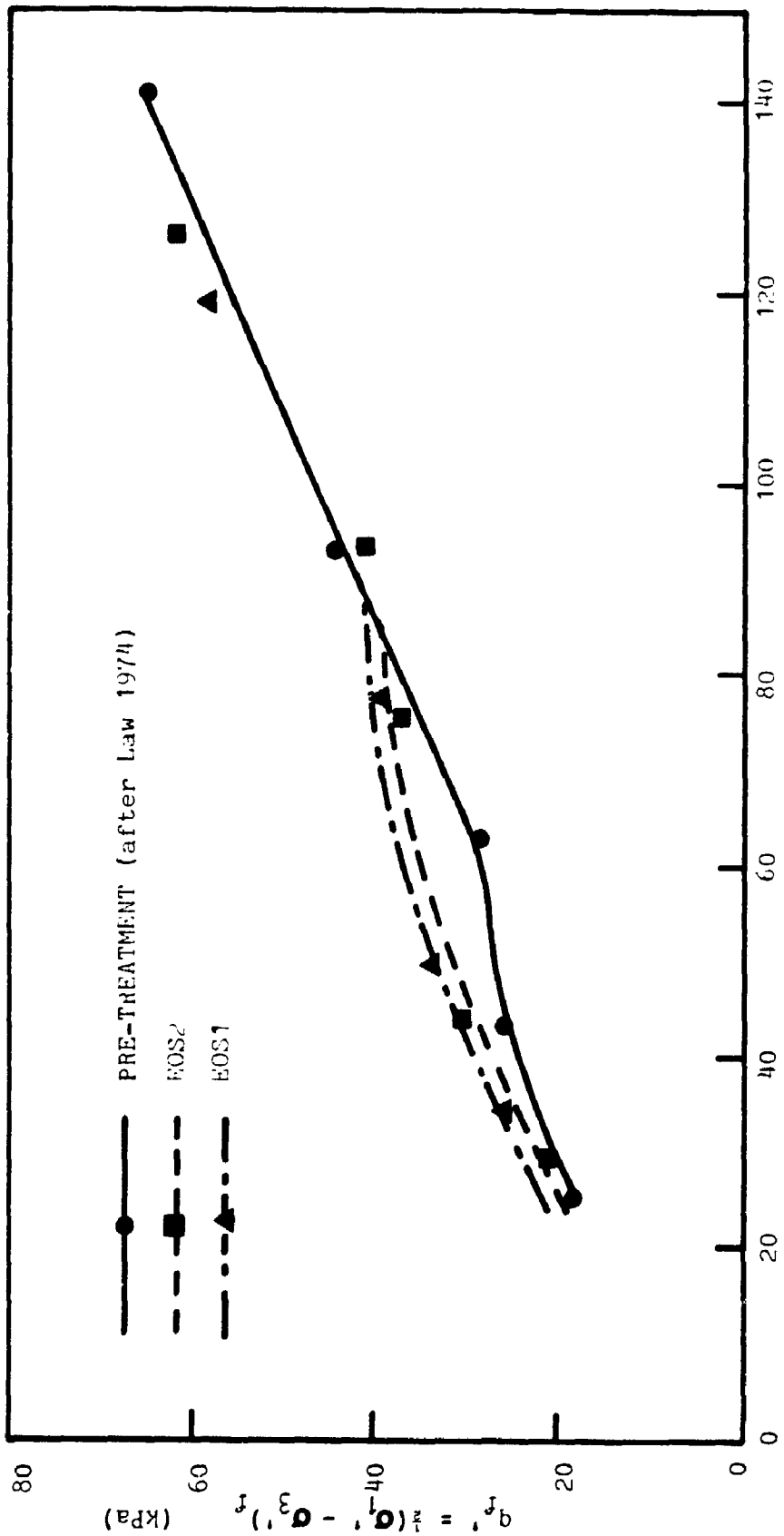

FIGURE 17.9d VARIATION OF STRENGTH ENVELOPE BEFORE AND AFTER ELECTRO-OSMOTIC TREATMENT

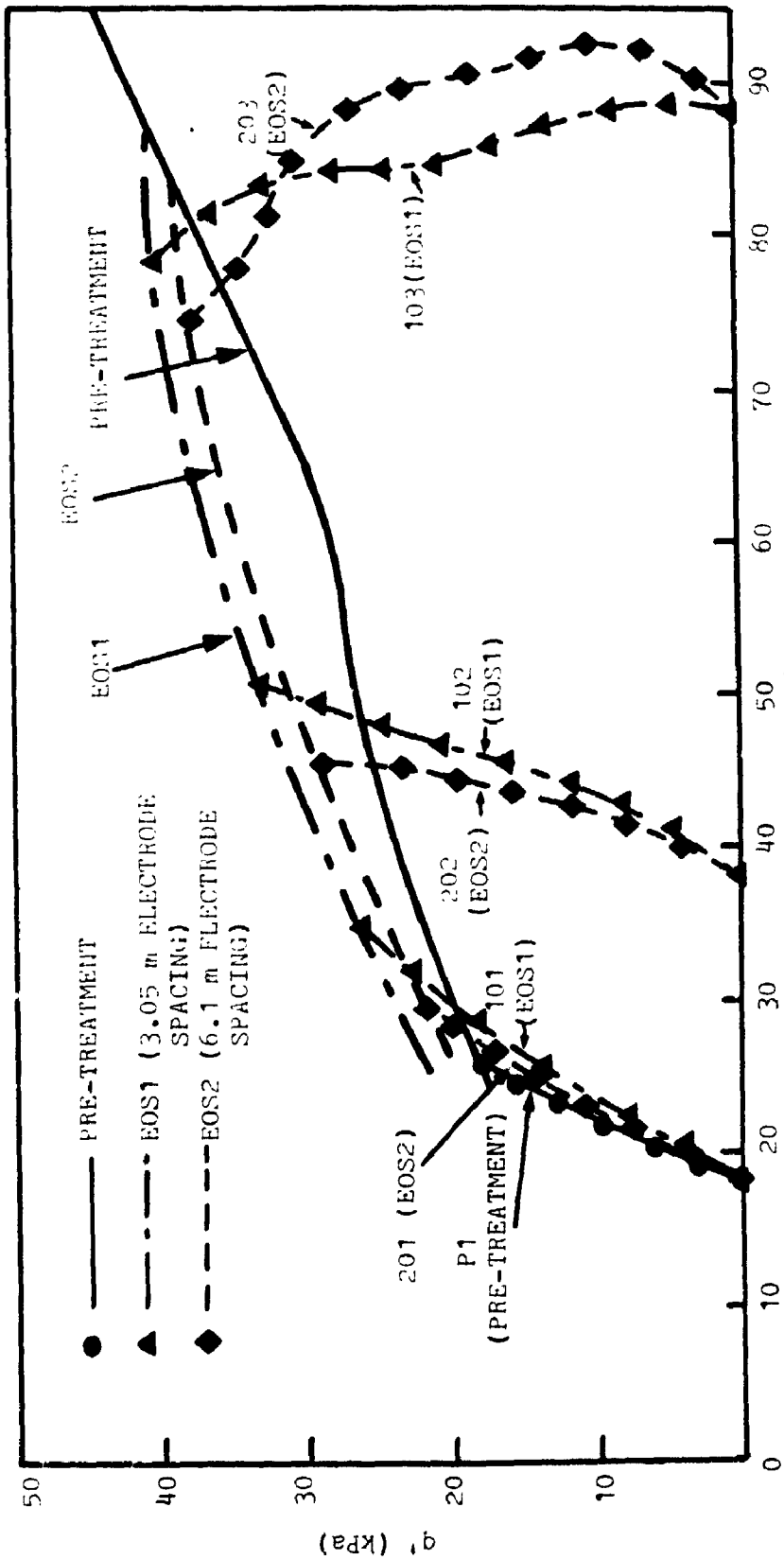

FIGURE 17.9e VARIATION OF STRESS PATHS BEFORE AND AFTER TREATMENT DURING CONSOLIDATION-UNDRAINED TRIAXIAL TEST WITH THE CONSOLIDATION PRESSURE OF 18, 38 AND 88 kPa

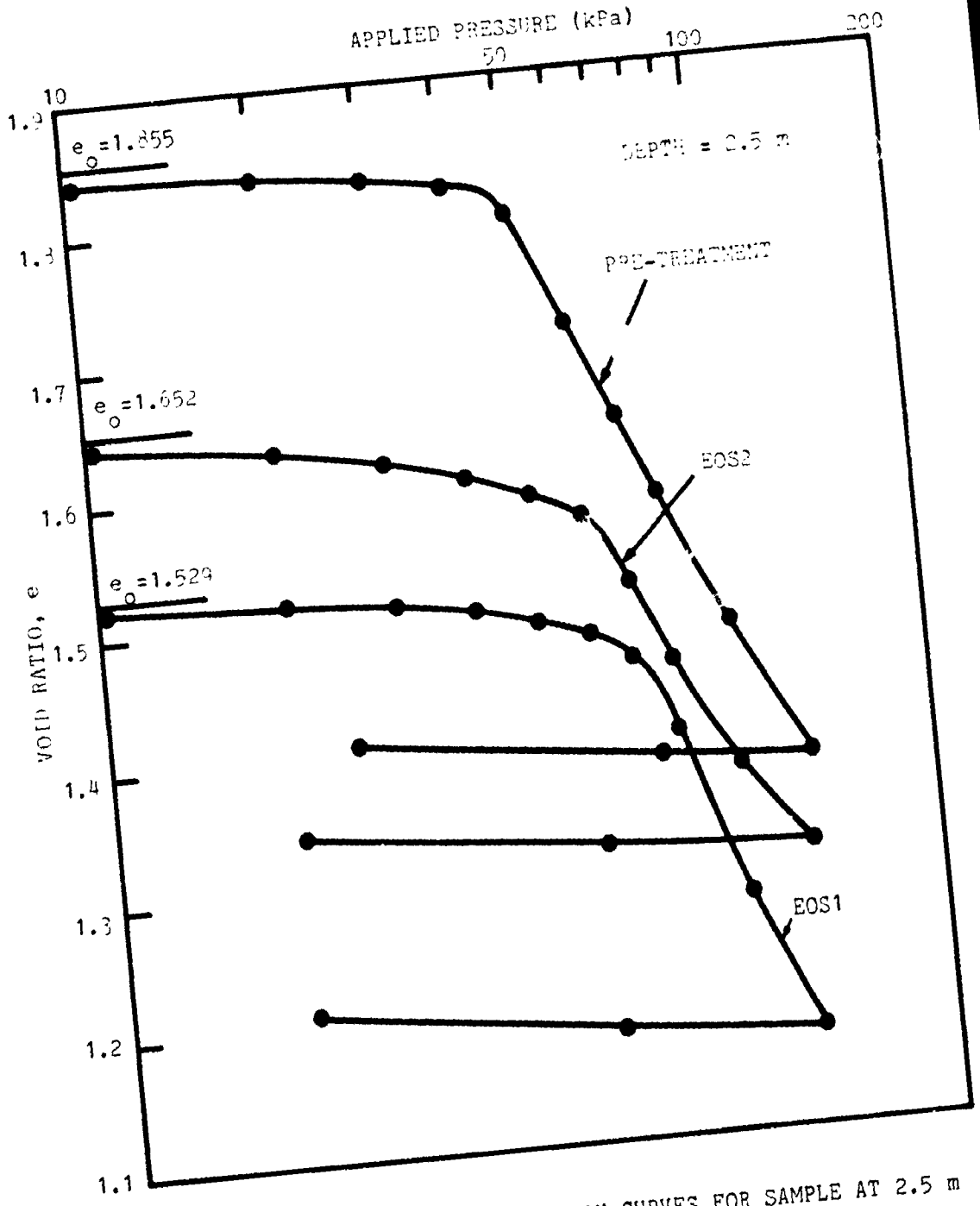

FIGURE 17.10 COMPARISON OF CONSOLIDATION CURVES FOR SAMPLE AT 2.5 m DEPTH BEFORE AND AFTER TREATMENT

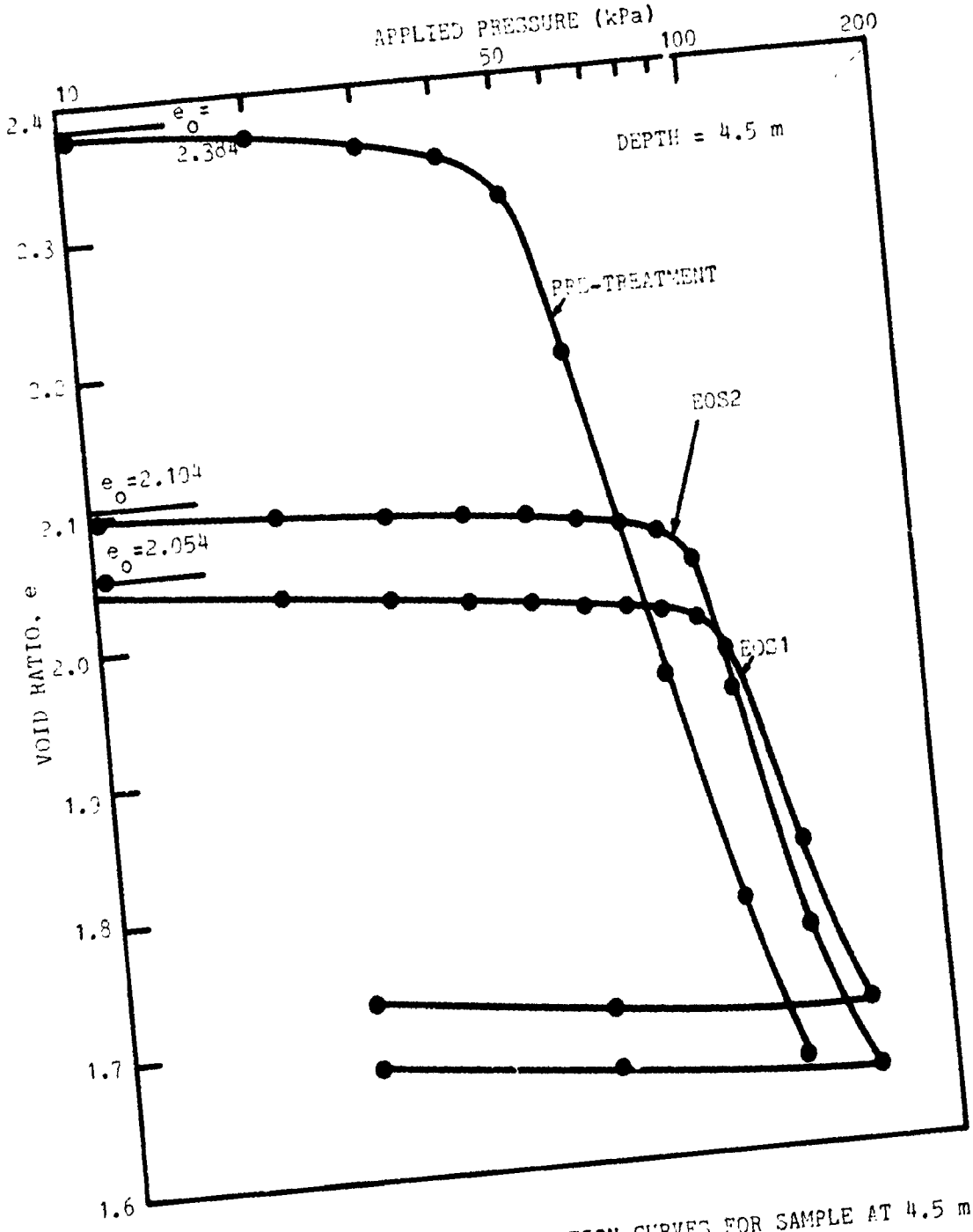

FIGURE 17.11 COMPARISON OF CONSOLIDATION CURVES FOR SAMPLE AT 4.5 m DEPTH BEFORE AND AFTER TREATMENT

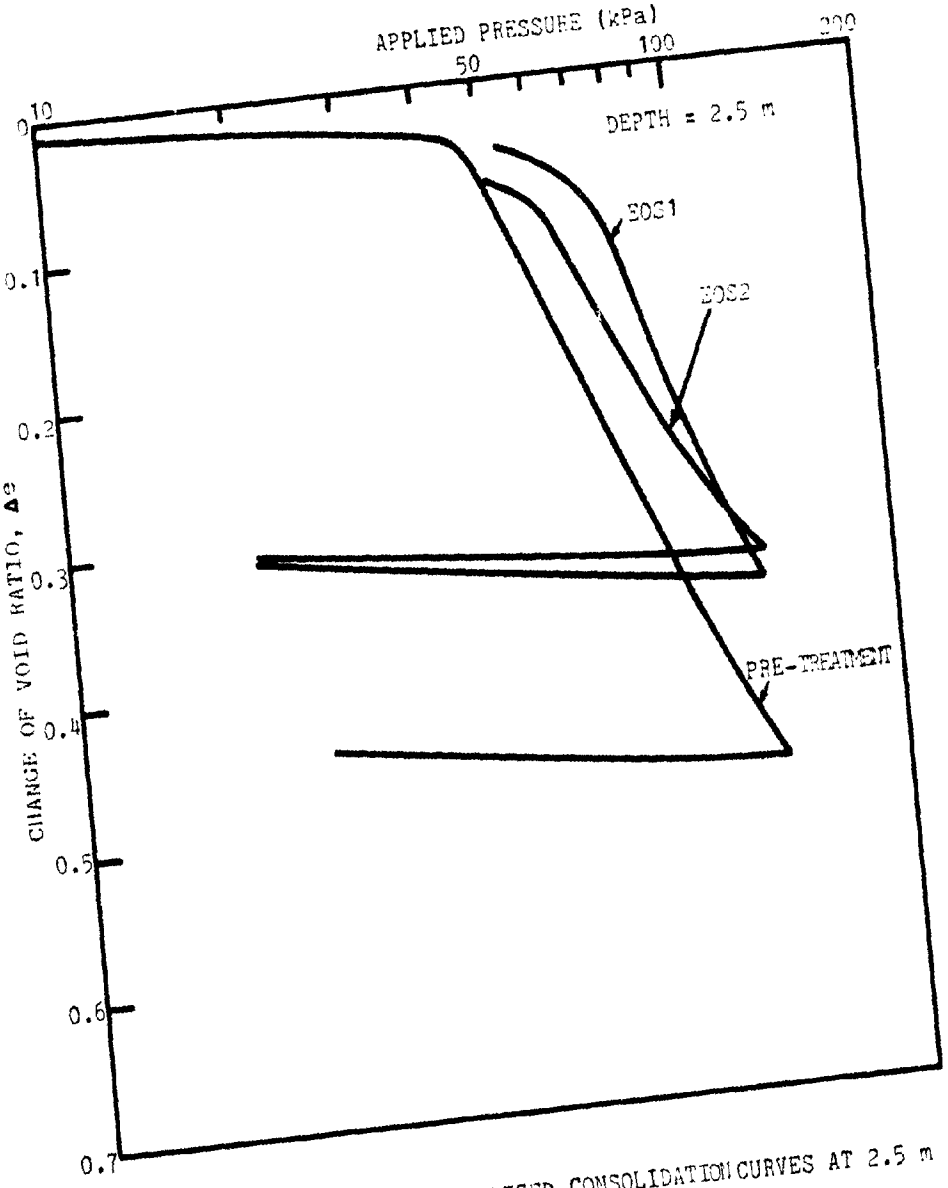

FIGURE 17.12 COMPARISON OF NORMALIZED CONSOLIDATION CURVES AT 2.5 m DEPTH BEFORE AND AFTER TREATMENT

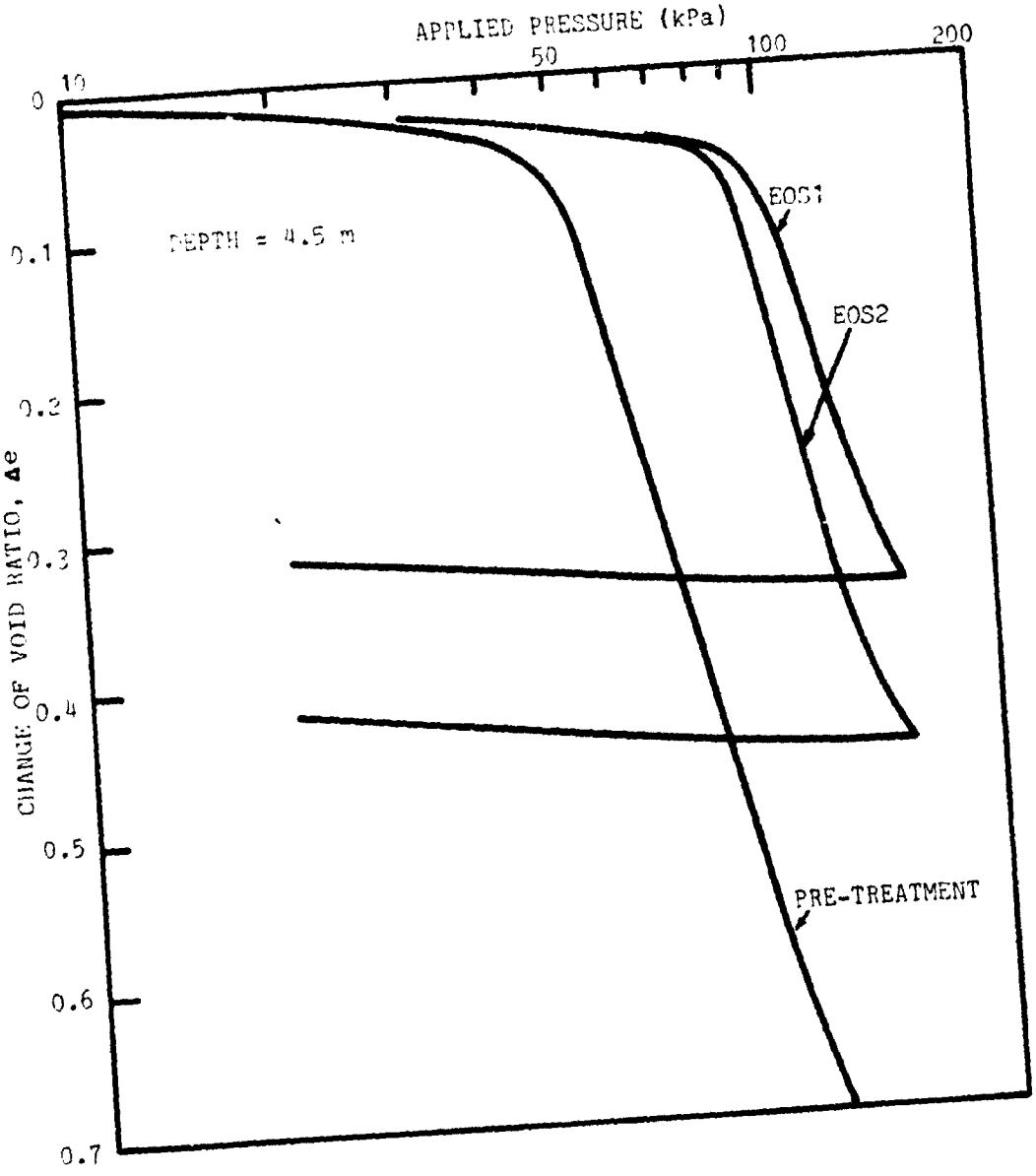

FIGURE 17.13 COMPARISON OF NORMALIZED CONSOLIDATION CURVES AT 4.5 m DEPTH BEFORE AND AFTER TREATMENT

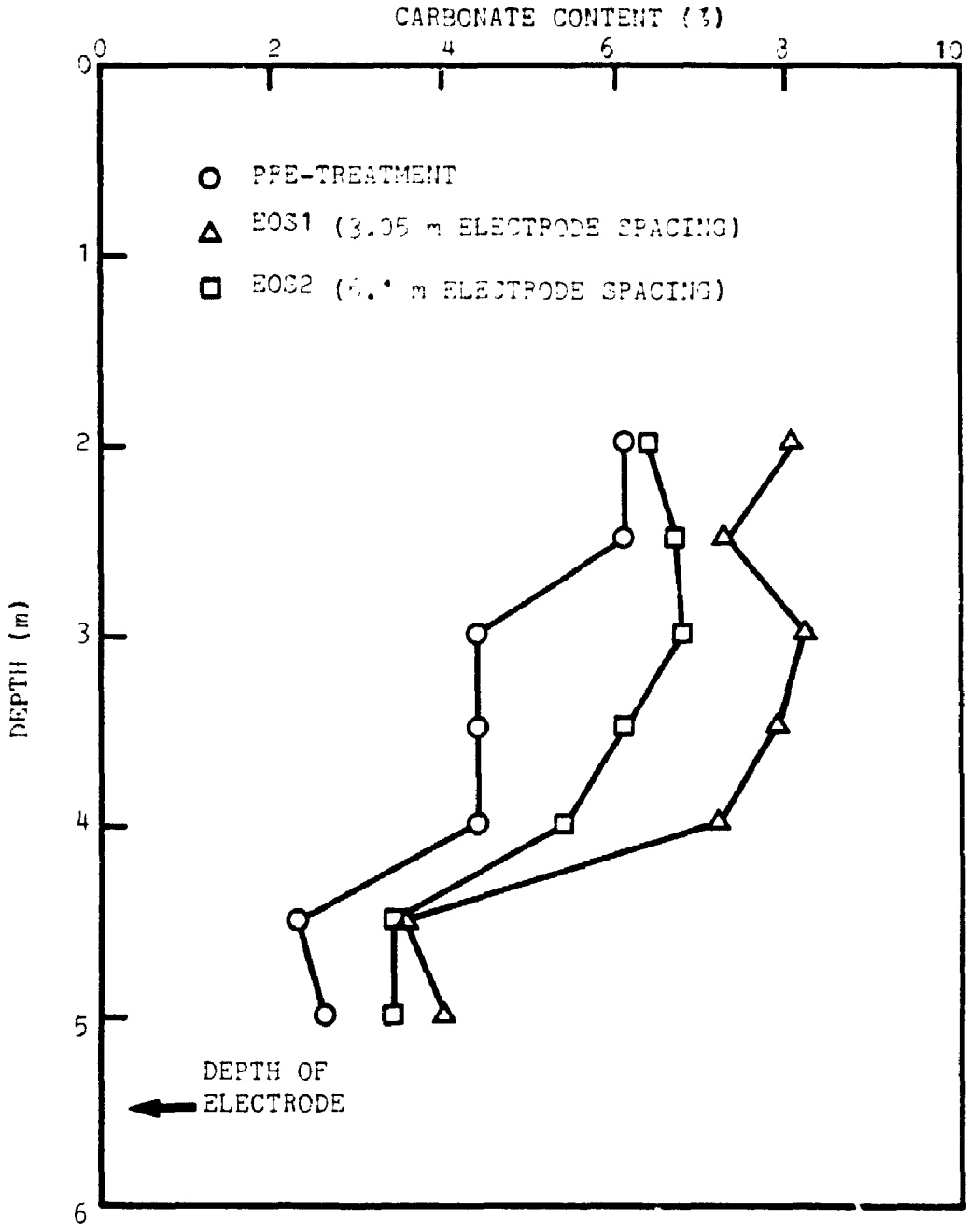

FIGURE 17.14 PROFILES OF CARBONATE CONTENT OF SOIL BEFORE AND AFTER TREATMENT

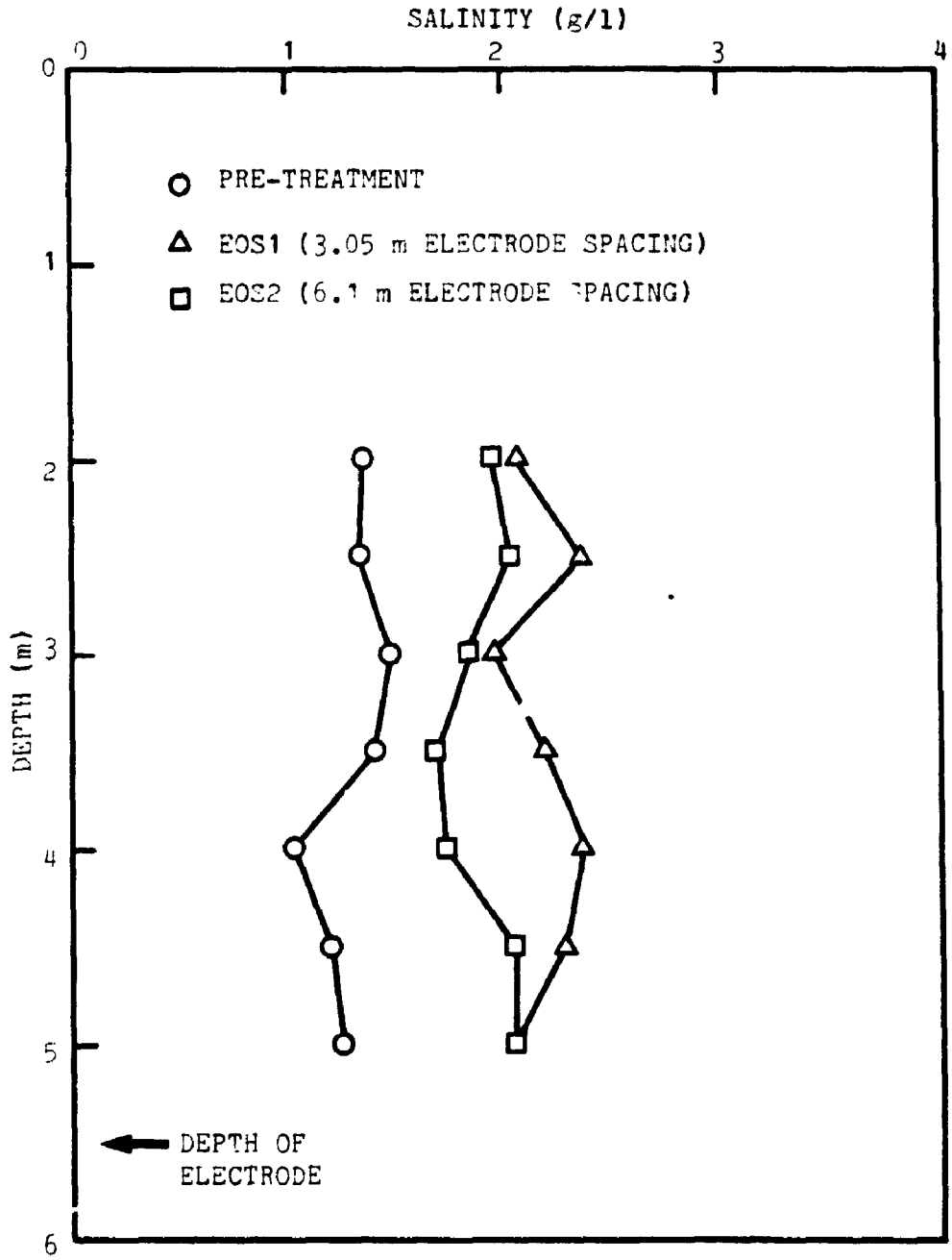

FIGURE 17.15 PROFILES OF SALINITY OF SOIL BEFORE AND AFTER TREATMENT

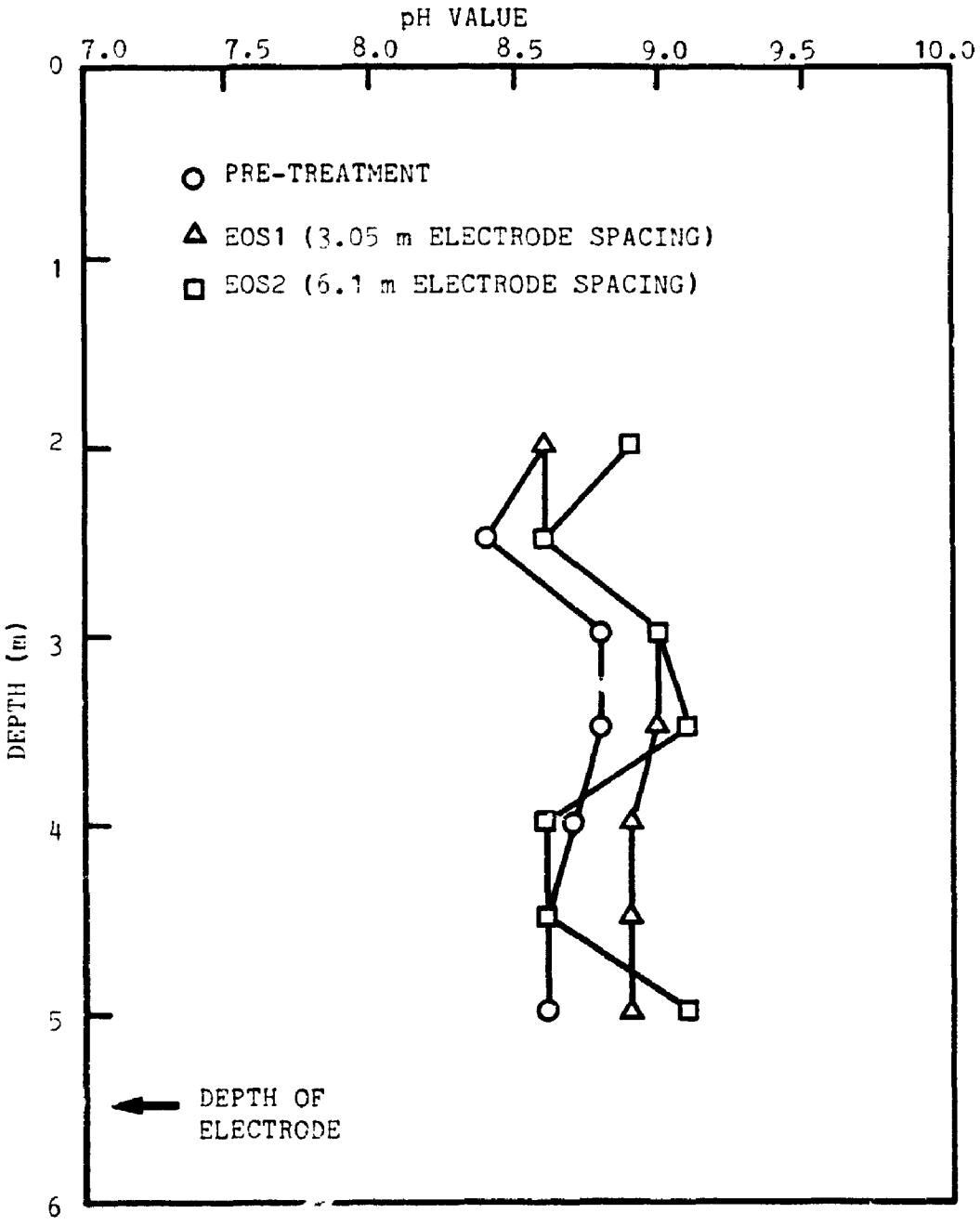

FIGURE 17.16 PROFILES OF pH VALUE OF SOIL BEFORE AND AFTER TREATMENT

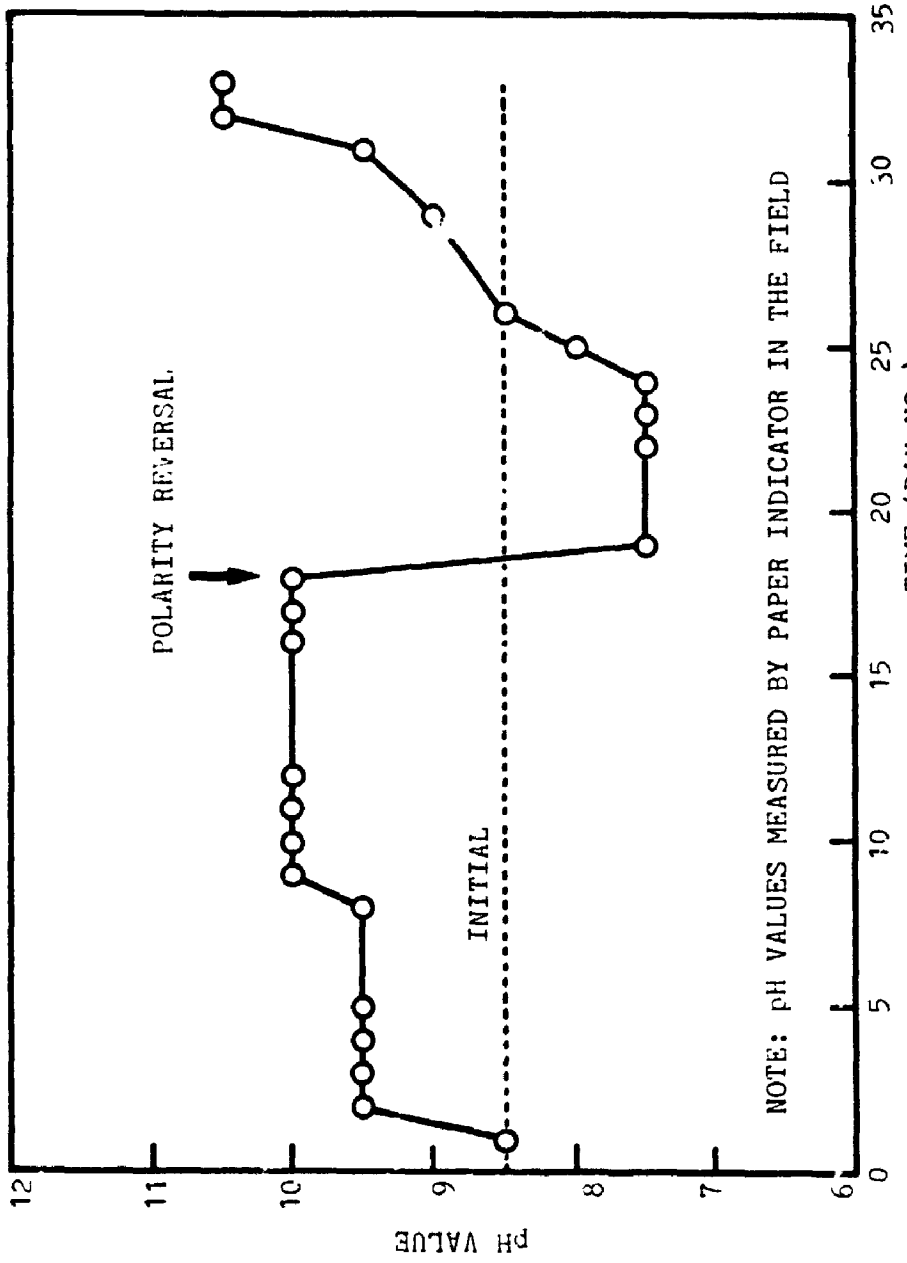

FIGURE 17.17 VARIATION OF pH VALUES OF WATER SAMPLE COLLECTED FROM CATHODE WITH TREATMENT TIME

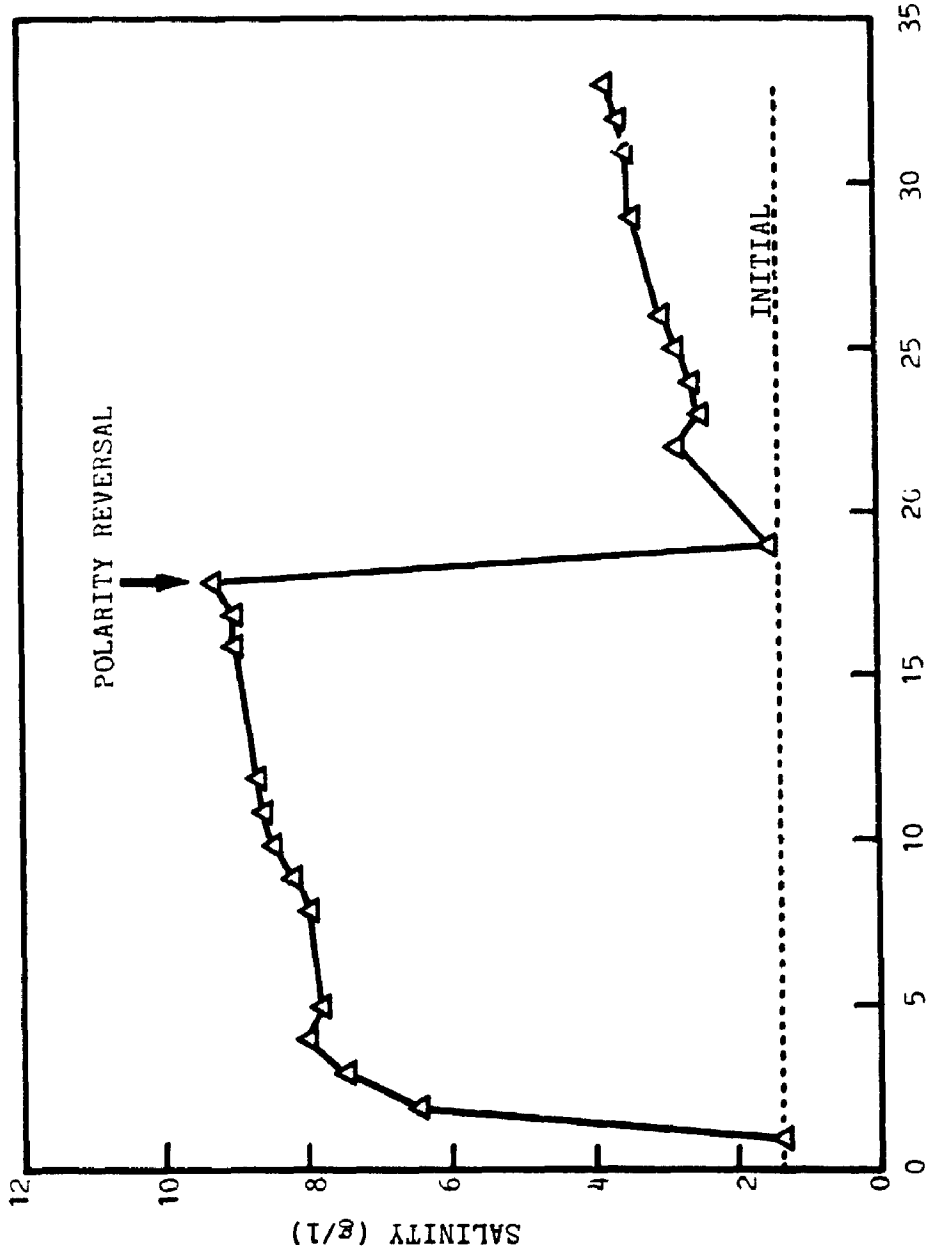

FIGURE 17.18 VARIATION OF SALINITY OF WATER SAMPLE COLLECTED FROM CATHODE WITH TREATMENT TIME

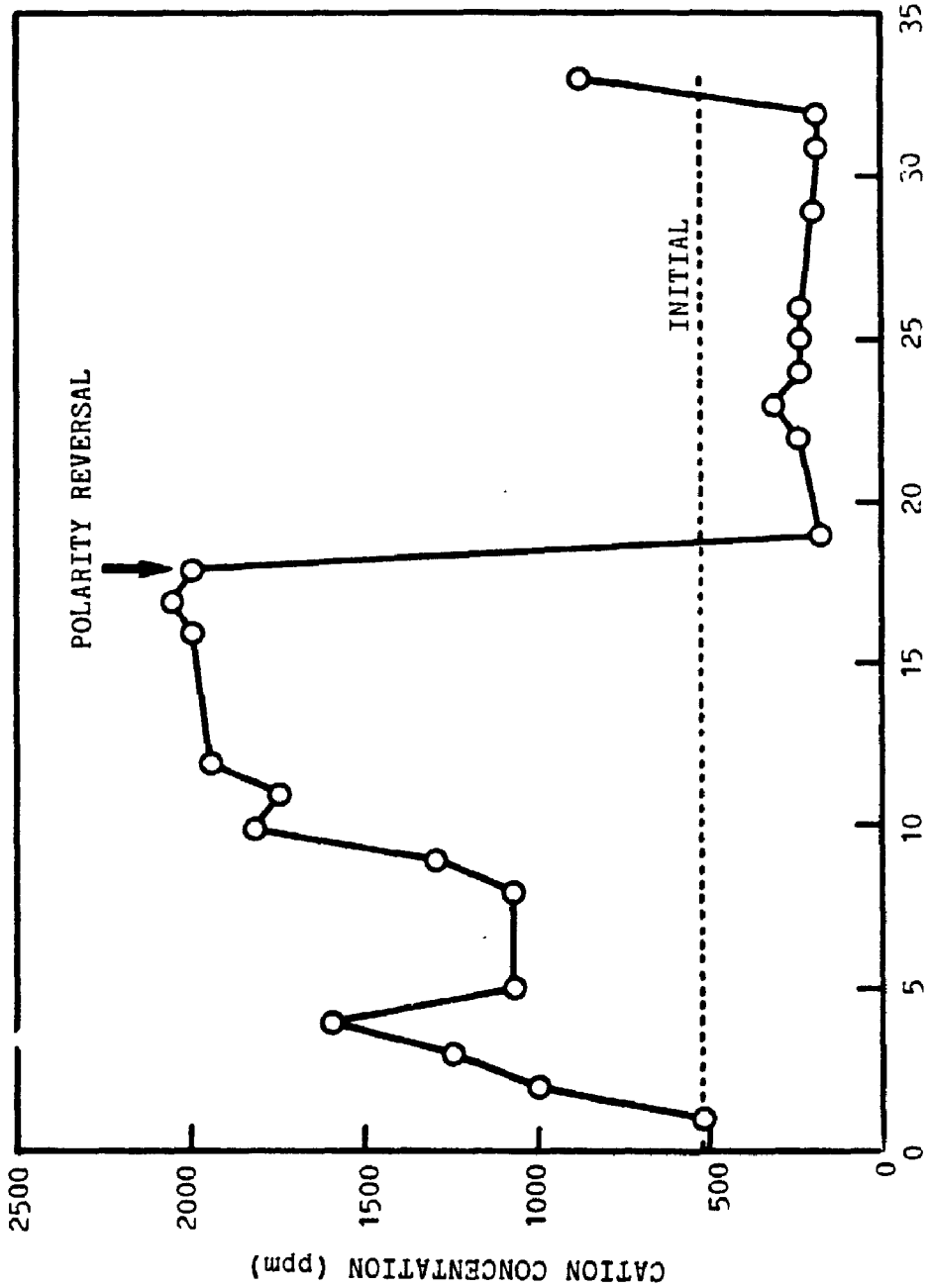

FIGURE 17.19 VARIATION OF SODIUM ION CONCENTRATION OF WATER SAMPLE COLLECTED FROM CATHODE WITH TREATMENT TIME

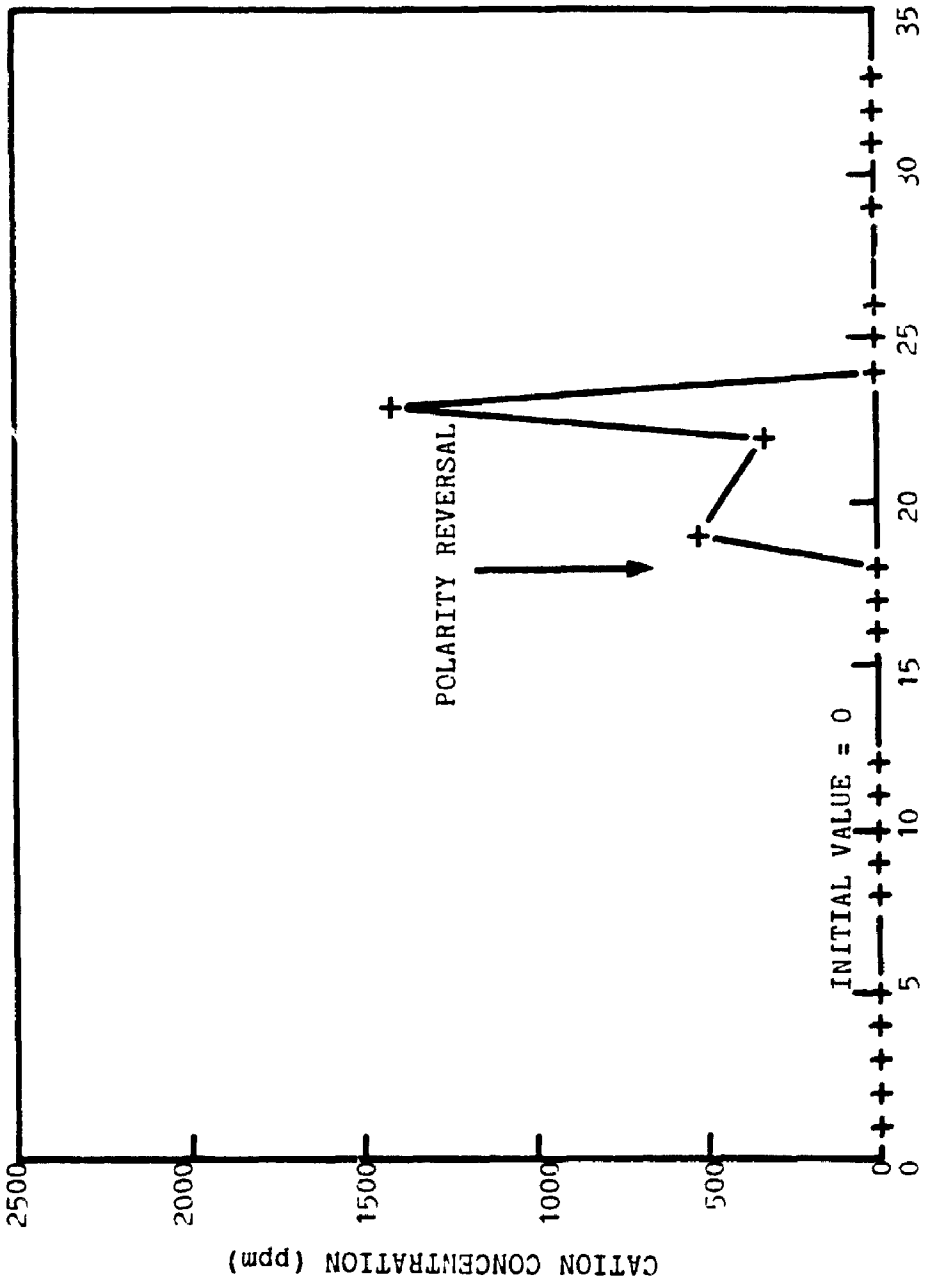

FIGURE 17.20 VARIATION OF COPPER ION CONCENTRATION OF WATER SAMPLE COLLECTED FROM CATHODE WITH TREATMENT TIME

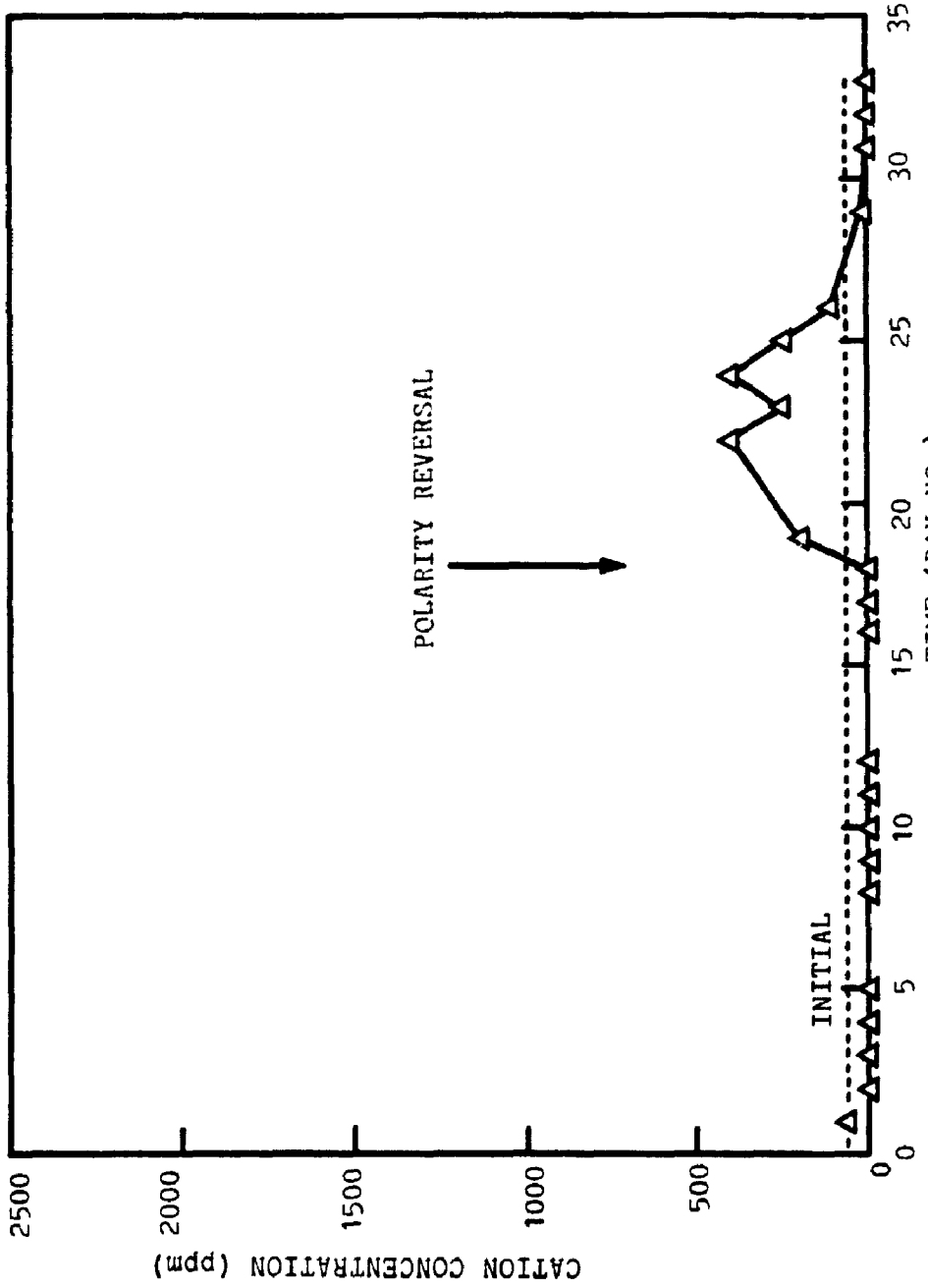

FIGURE 17.21 VARIATION OF CALCIUM ION CONCENTRATION OF WATER SAMPLE COLLECTED FROM CATHODE WITH TREATMENT TIME

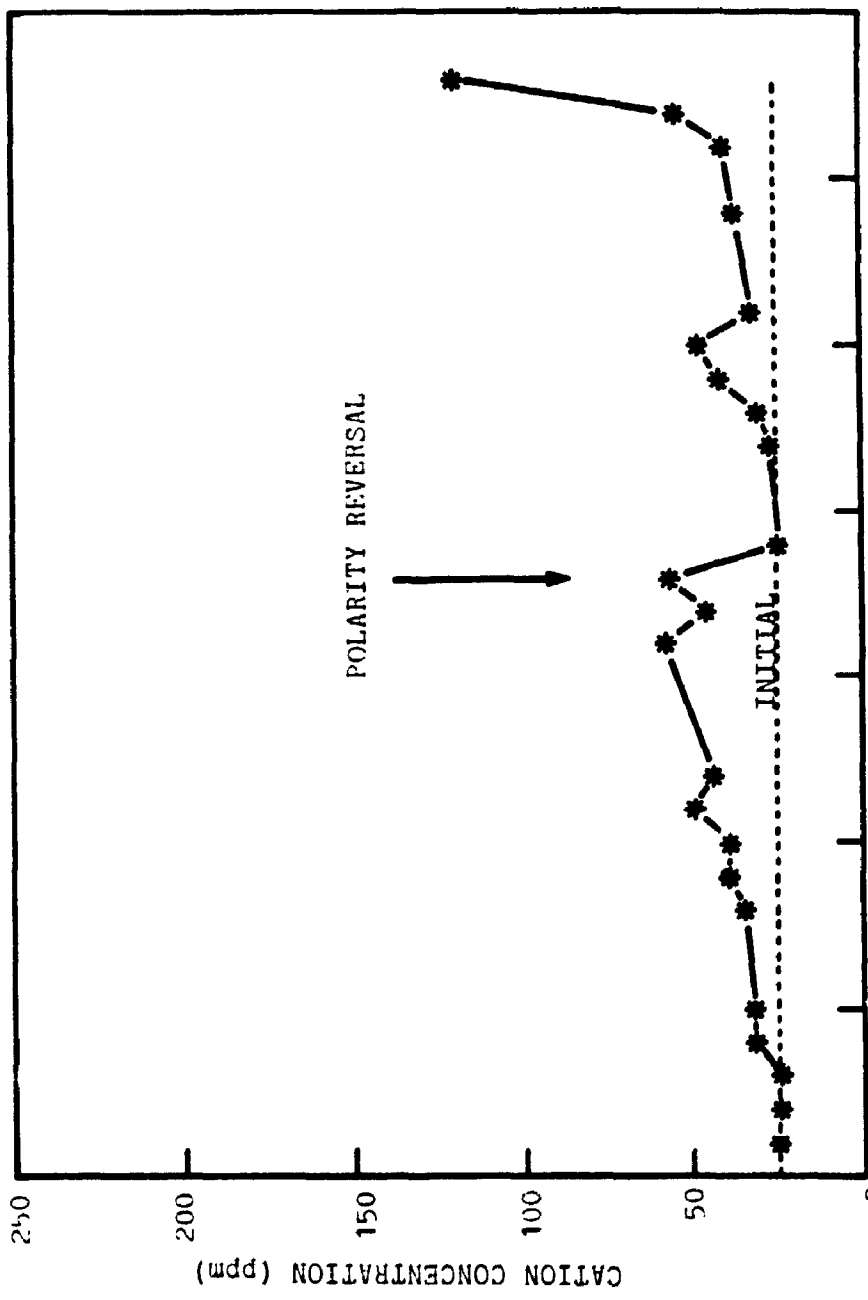

FIGURE 17.22 VARIATION OF POTASSIUM ION CONCENTRATION OF WATER SAMPLE COLLECTED FROM CATHODE WITH TREATMENT TIME

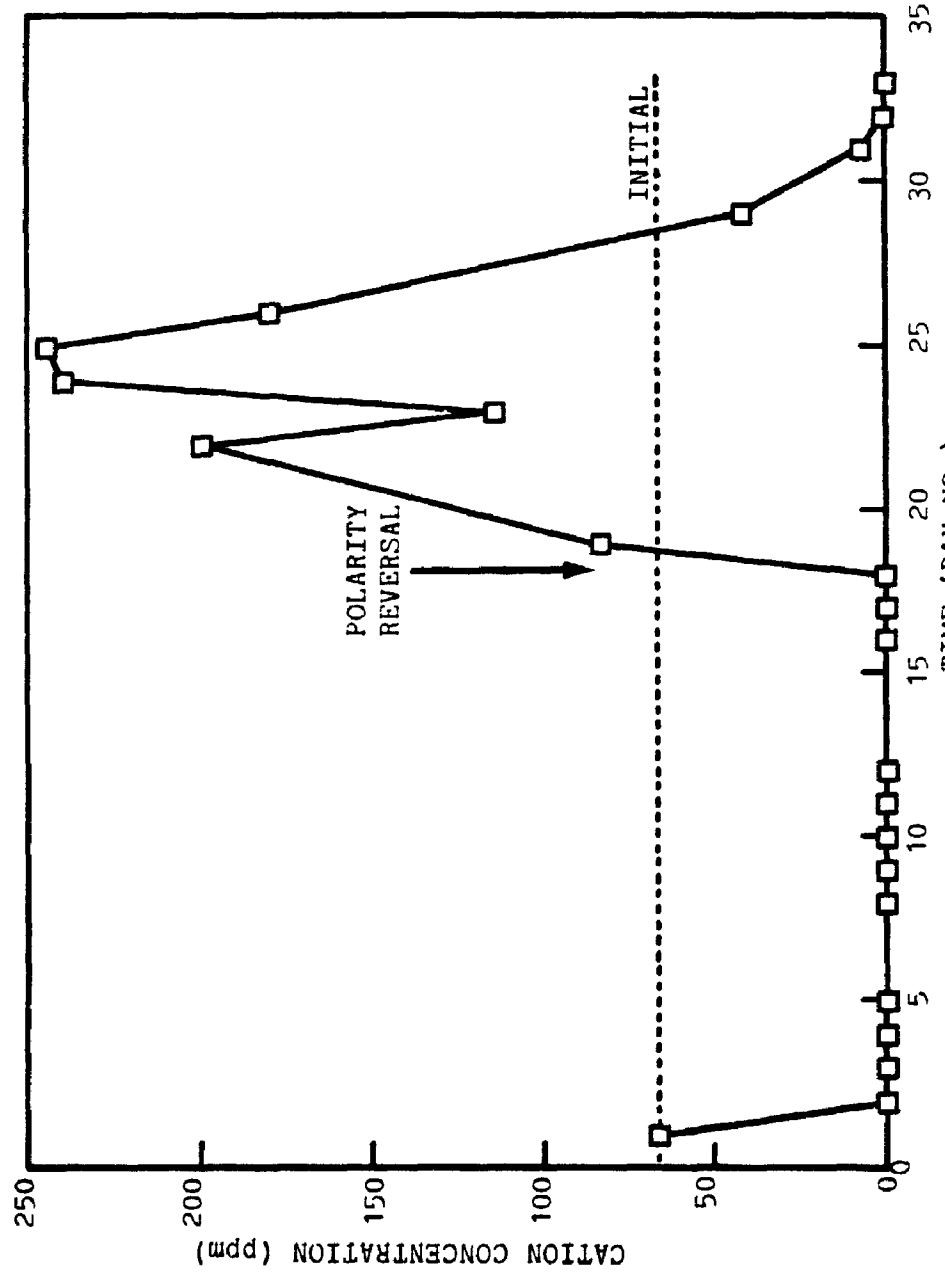

FIGURE 17.23 VARIATION OF MAGNESIUM ION CONCENTRATION OF WATER SAMPLE COLLECTED FROM CATHODE WITH TREATMENT TIME

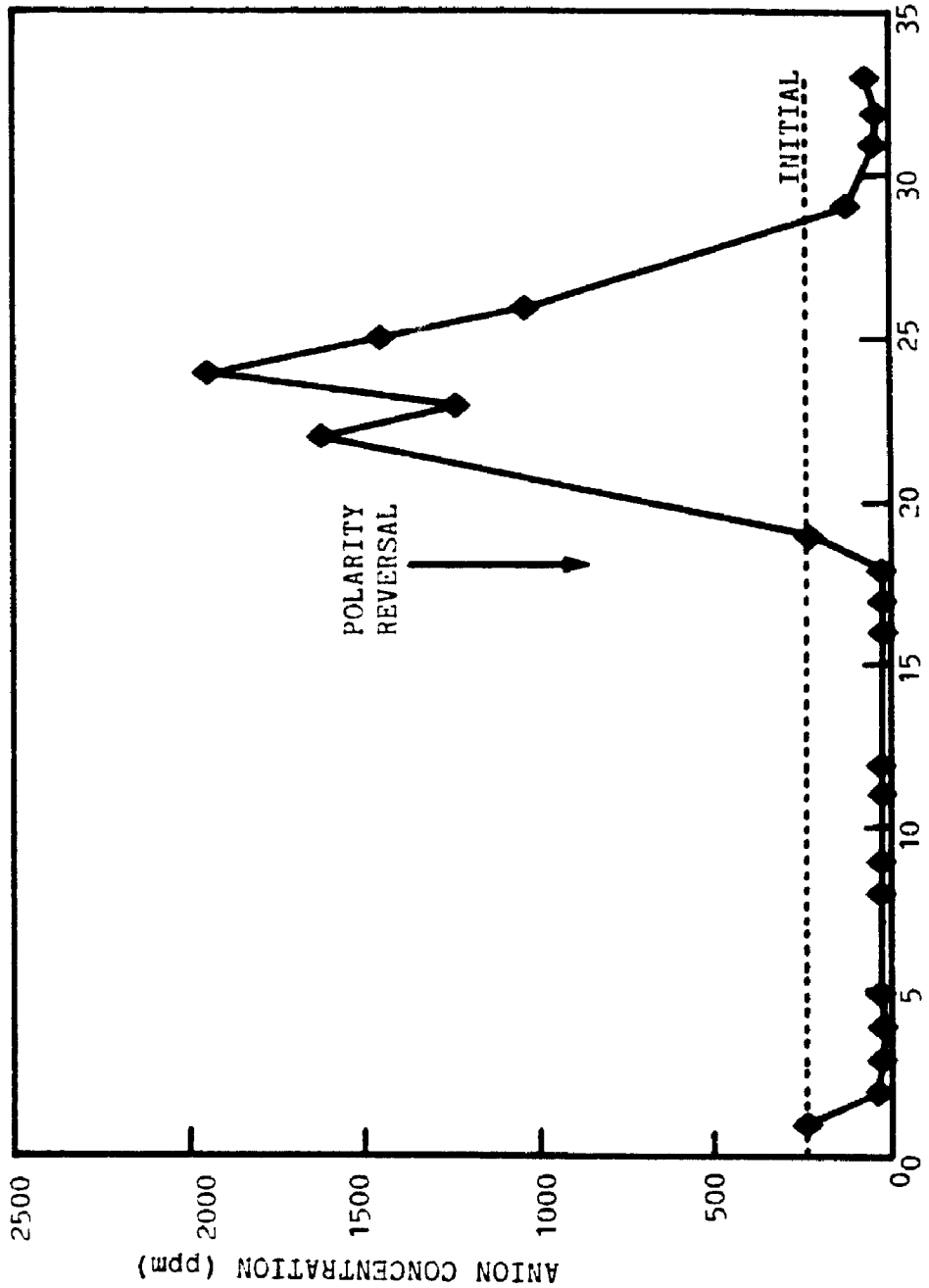

FIGURE 17.24 VARIATION OF CHLORIDE ION CONCENTRATION OF WATER SAMPLE COLLECTED FROM CATHODE WITH TREATMENT TIME

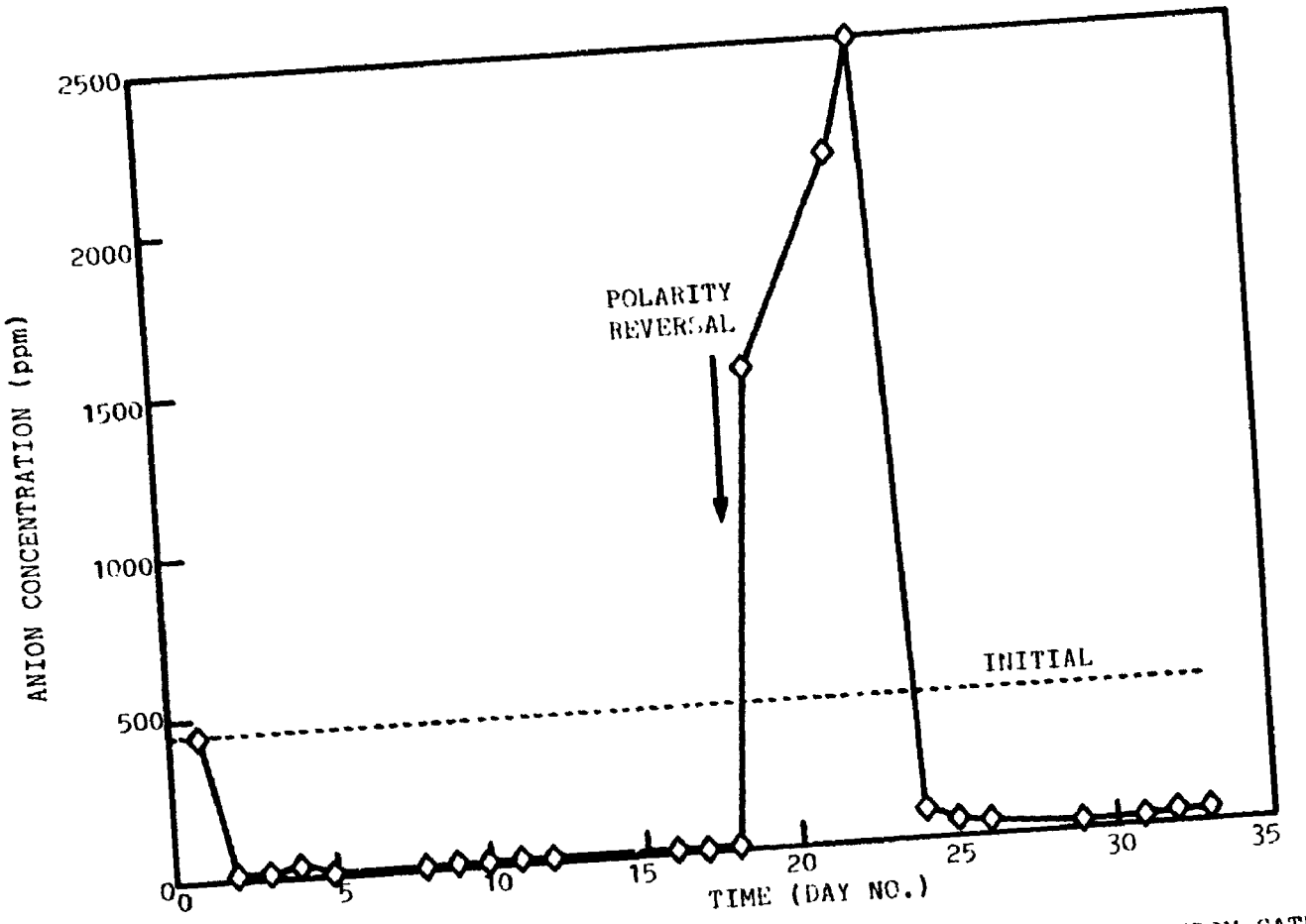

FIGURE 17.25 VARIATION OF SULPHATE ION CONCENTRATION OF WATER SAMPLE COLLECTED FROM CATHODE WITH TREATMENT TIME

CHAPTER 18

CONCLUSIONS ON FIELD TEST

A field test was undertaken to assess the effectiveness of the electro-osmosis and dielectrophoresis methods in strengthening the soft sensitive clay (Champlain Sea or Leda clay) in Gloucester test fill site. After the field and laboratory tests of soil samples, the following conclusions may be drawn.

18.1 Electro-osmosis

(1) The soft sensitive Champlain Sea clay, with an average initial undrained strength of 18 kPa, can be treated effectively by the electro-osmosis process. The increase in undrained shear strength was 60 % between electrodes of 3 m spacing and 40 % between electrodes of 6.1 m spacing in a treatment period of 32 days with a current of 40 amperes.

(2) The increase in strength is uniform throughout the entire depth of the electrodes and no "depth effect" was observed, as in some previous applications.

(3) Results of field vane tests at different times during treatment indicate that strength increase can be enhanced both in magnitude and uniformity by the technique of polarity reversal. This technique also eliminates the problem of no strength increase at cathode.

(4) Vane tests performed 10 months after treatment show that the strength

gained remain constant.

(5) The final settlement of the test area is approximately 50 mm, with a differential settlement of ± 20 %. The technique of electrode reversal is therefore a useful tool to reduce differential settlement.

(6) No pumping of expelled water is required in this "improved version" of electro-osmosis. Water flows out of the electrode 50 minutes after "switch-on". Both installation and electricity costs are reduced substantially with the electrodes developed.

(7) The process resulted in a decrease in sensitivity and the improvement of stress-strain behaviour of the soft sensitivity clay.

(8) Isotropically consolidated undrained triaxial tests showed that the failure envelope after treatment was significantly higher than the initial envelope indicating that the strength in terms of effective stresses increased.

(9) The mechanism of electro-osmosis is the consolidation of clay. As a result of the process the preconsolidation pressure increased by about 85 %, indicating that the soil is consolidated by the electric potential.

(10) The physical and chemical effects of electro-osmosis on the soft clay are the increase in plasticity, carbonate content and salinity, resulting in the increase in bonding of soil particles and the reduction in the thickness of double layer. As a result, the clay becomes more plastic and less sensitive. The pH value and cation exchange capacity of the soil have no appreciable change, implying that the process has no adverse effect to the soil properties.

(11) Some cations and anions are removed with the expelled water from the soil by the process. Electro-osmosis may have potential application in the remedy of some types of groundwater contamination.

From this field test, it is evident that substantial increase in strength and preconsolidation pressure as well as general improvement in soil properties can be achieved by this improved version of electro-osmosis. Furthermore, the elimination of pumping improved the economy of the process considerably. It is hoped that this effective and versatile process may receive wider application in soft sensitive clays.

18.2 Dielectrophoresis

(1) The design of high voltage electrode was shown to be suitable for field application, especially if a gap can be maintained between the electrode and soil.

(2) During the period of treatment, an unexpected electrical short circuiting was observed due to the water surrounding the high voltage electrode in the hole. The field intensity was drastically reduced resulting in a low efficiency of treatment.

(3) Field vane tests showed that the soil has 10 % average shear strength increase after treatment. The shear strength increase is maximum at the location nearest the electrode and minimum at halfway between electrodes.

(4) It is expected that the real electrical power consumption in

dielectrophoresis is lower than that of electro-osmosis due to the fact that there is no conduction current flowing between electrodes. Since the material costs of electrodes for dielectrophoresis are lower, this process would be potentially more economical than the electro-osmotic treatment.

It was demonstrated that dielectrophoresis can be applied in soil strengthening in the field. Due to the effect of water inside the hole, the effectiveness of the process was not as good as expected by the laboratory investigation. The process can still be considered to be successful since the soil is improved to some degree.

This pioneer research provides the opportunity to accumulate experience and to learn from any difficulties encountered. It is hoped that the experience gained in this field test may lead to a systematic research program in the laboratory towards a successful field application in the future.

CHAPTER 19

SUMMARY AND RECOMMENDATIONS FOR FURTHER RESEARCH

19.1 Summary

An extensive study on the effectiveness of electrical strengthening of soft sensitive clay was carried out. The study concentrated in three specific areas: laboratory investigation of electro-osmosis, laboratory investigation of dielectrophoresis and the field test. Summary and conclusions of the above three studies are discussed in the pertinent chapters and only the points of prime interest are summarized here.

(a) Laboratory Investigation of Electro-Osmosis

This investigation is directed with the aim to understand the mechanism of the process and the effects of electro-osmosis to the changes of soil properties. It was demonstrated that the newly developed electro-osmotic cell avoided the gas accumulating around the electrodes and improved the efficiency of treatment. Results of this study showed that the shear strength increased substantially concurrent with the reduction of moisture content. The technique of electrode polarity reversal enables the uniform treatment of soil and this technique can be applied in the field to minimize non-uniformity of improvement of soil properties.

The mechanism of the process was found to be the consolidation of soil

by the applied electric potential which is considered to be analogous to a mechanical dead load. The preconsolidation pressure increased after treatment and hence the soil is virtually "over-consolidated". In terms of soil chemistry, the bonding of soil particles are stronger as shown by the increase in carbonate content and salinity of the treated clay. The stress-strain behaviour of soil also improved with the decrease in sensitivity.

The induced maximum negative pore water pressure, percentage increase in undrained shear strength, settlement bear linear relationships with the applied voltage. The study showed that the induced negative pore water pressure is dependent on the effective voltage and independent of the sample size.

(b) Laboratory Investigation of Dielectrophoresis

This young science was studied for the first time in the laboratory in the area of geotechnical engineering. The objectives were to investigate the mechanism of this process and to explore the possibility of its application in electrical strengthening of soft sensitive clay. The preliminary results of this study showed that the process is more effective than electro-osmosis and the shear strength of treated clay increased drastically to 996 % with a reduction of moisture content by 24.9 %, at an applied electric potential of 20 kV for 28 days.

When compared with electro-osmosis, similar results are obtained in

dielectrophoresis such as the increase in preconsolidation pressure, decrease in sensitivity, improvement of stress-strain behaviour, increase in carbonate content and increase in salinity. The mechanism of dielectrophoresis is also due to the consolidation of clay by the alternating current unde high voltage in a converging field.

Linear relationships were also obtained among the parameters of settlement, shear strength increase, moisture content decrease, electrode depth to sample height ratio and the applied voltage.

(c) Field Test

The effectiveness of electrical strengthening of soft sensitive clay by electro-osmosis and dielectrophoresis was assessed in the field test. The improved version of electro-osmosis allows the pore water in the soil to flow out from the cathode without pumping and prevents gas accumulation around electrodes. It was shown that the new electrode design with the application of electrode polarity reversal improved the efficiency of treatment. The problems encountered in the past such as nonuniformity of soil treatment, heave of ground near the cathode, expensive electricity cost, pumping and the adverse effects of electro-chemical reactions are significantly reduced by this new version of electro-osmosis. It was therefore demonstrated that electro-osmosis is a useful and economical method for the improvement of soft sensitive clay.

Isotropically consolidated undrained triaxial tests showed that the failure

envelope of the treated clay was significantly higher than the initial envelope indicating that the strength in terms of effective stresses increased. The chemical analysis showed that there is no adverse effect due to the passage of electric current in the treated sample. From the long term field vane tests and consolidation tests, the soil strengthening effect of electro-osmosis was shown to be permanent.

In the field treatment by dielectrophoresis, it was shown that the design of high voltage electrode was suitable for field application, especially if a gap can be maintained between the electrode and soil. However, due to the effect of water in the hole, the field intensity was drastically reduced resulting in a low effectiveness of treatment.

From the signs of some increase in shear strength and ground settlement, the dielectrophoretic process is still considered to be successful. In the economy point of view, both the electricity and material costs of this process are found to be lower than those of electro-osmosis, giving a stimulation of the future development of this process. With the experience gained from this pioneer field test, it is expected a modified version of the process could be developed leading to a successful engineering application in the future.

19.2 Recommendations

(a) Electro-Osmosis

In the field treatment of electro-osmosis, it was found that the voltage at

vicinity to the electrodes dropped considerably and the efficiency of treatment was affected. Further study should be carried out to explain this and to improve the process.

The procedure of electrode polarity reversal needs to be applied several times during the treatment period to improve the uniformity of the treated soil and to avoid over-treatment. The time when the polarity should be reversed can be judged by monitoring the voltage distribution of the test area, current flow and the tendency of shear strength increase.

(b) Dielectrophoresis

The problems encountered in the field treatment of dielectrophoresis reflect that the fundamental aspects of the process have to be considered. Since the dielectric constant plays an important role in the dielectrophoretic force calculation, its effect to the process has to be studied.

The electric field intensity was drastically reduced by the water inside the hole. Modification of electrode installation such as the replacement of the gap in the hole by some slurry type material to avoid electric short circuiting. The effects of this filling material and its possible application have to be studied in greater detail in the laboratory.

A theory similar to that of electro-osmosis should be developed to relate the variation of pore water pressure with the dielectrophoretic force or with the applied voltage. With this theory, the performance of the process could be

predicted by a possible closed form solution or by numerical analysis.

As mentioned earlier, dielectrophoresis is a young science that requires more systematic and detailed study. With the encouraging results and fruitful experience obtained from both the laboratory and the field, a better understanding of the process and a successful field application are expected in the foreseeable future.

APPENDIX A

COMPLETE RECORD OF ELECTRO-OSMOSIS TESTS

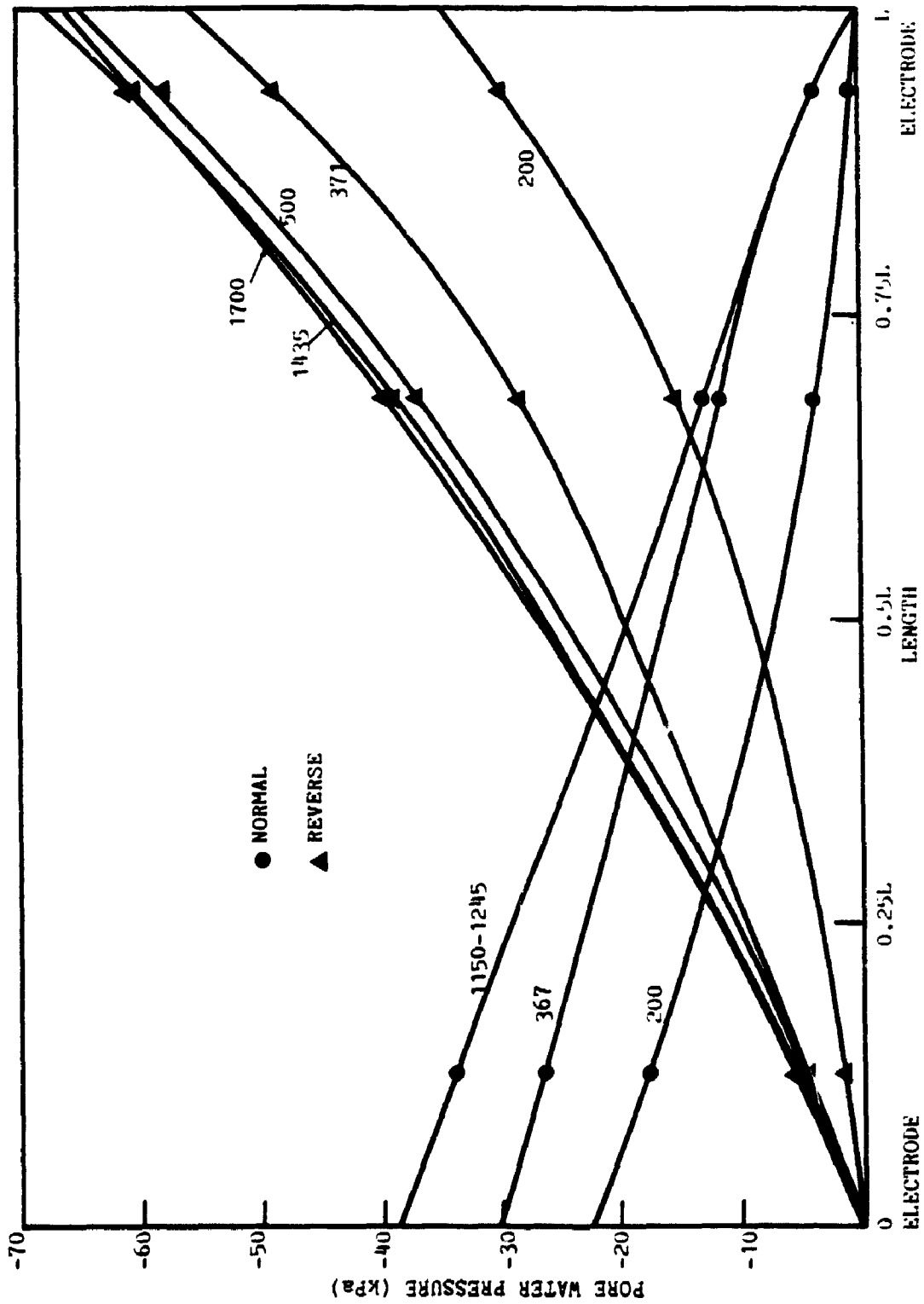

FIGURE A1 PORE WATER PRESSURE DISTRIBUTION WITH TIME (MINUTES), TEST WV-4, 2.5 V

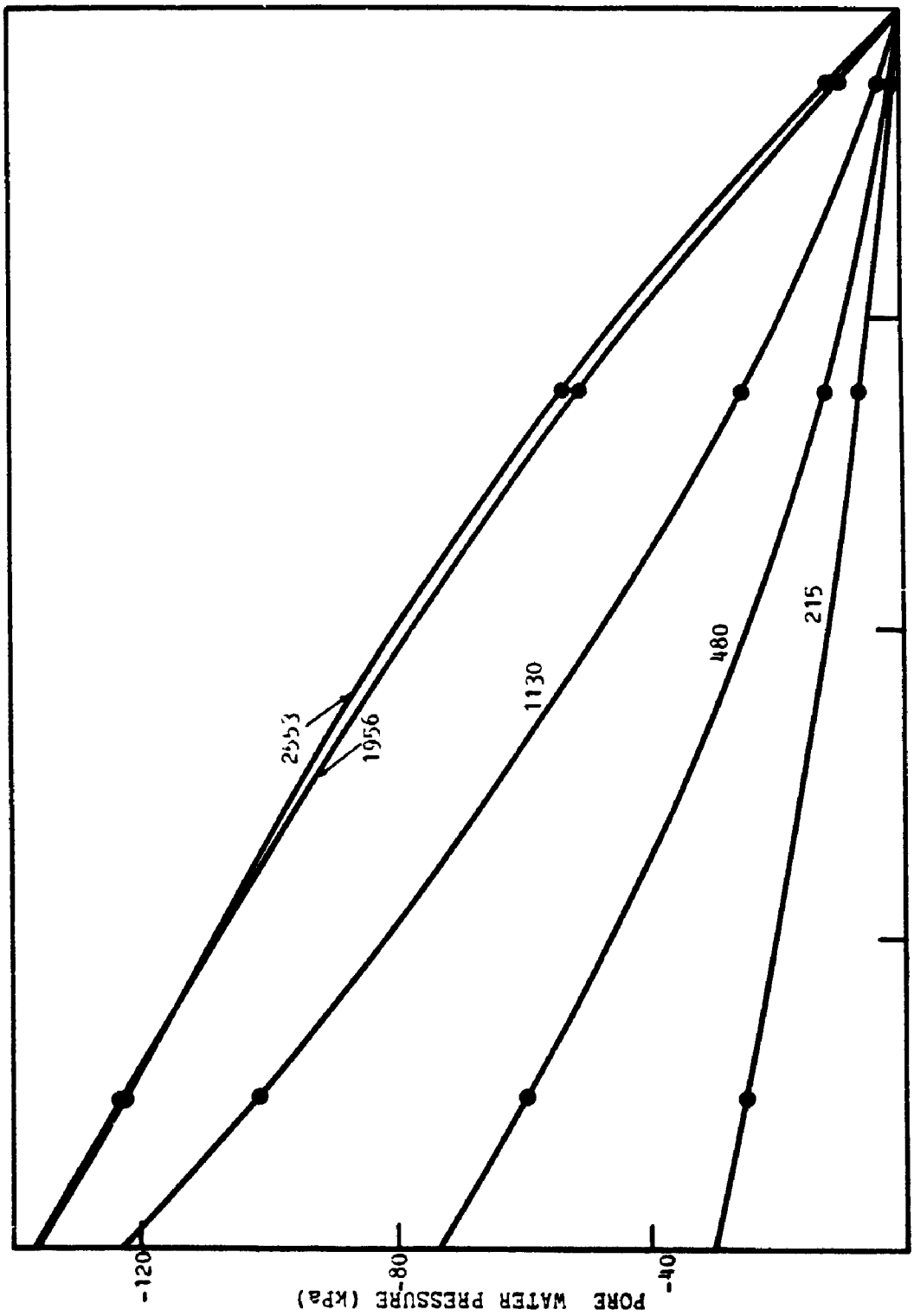

FIGURE A2 PORE WATER PRESSURE DISTRIBUTION WITH TIME (MINUTES), TEST WV-4, 4V

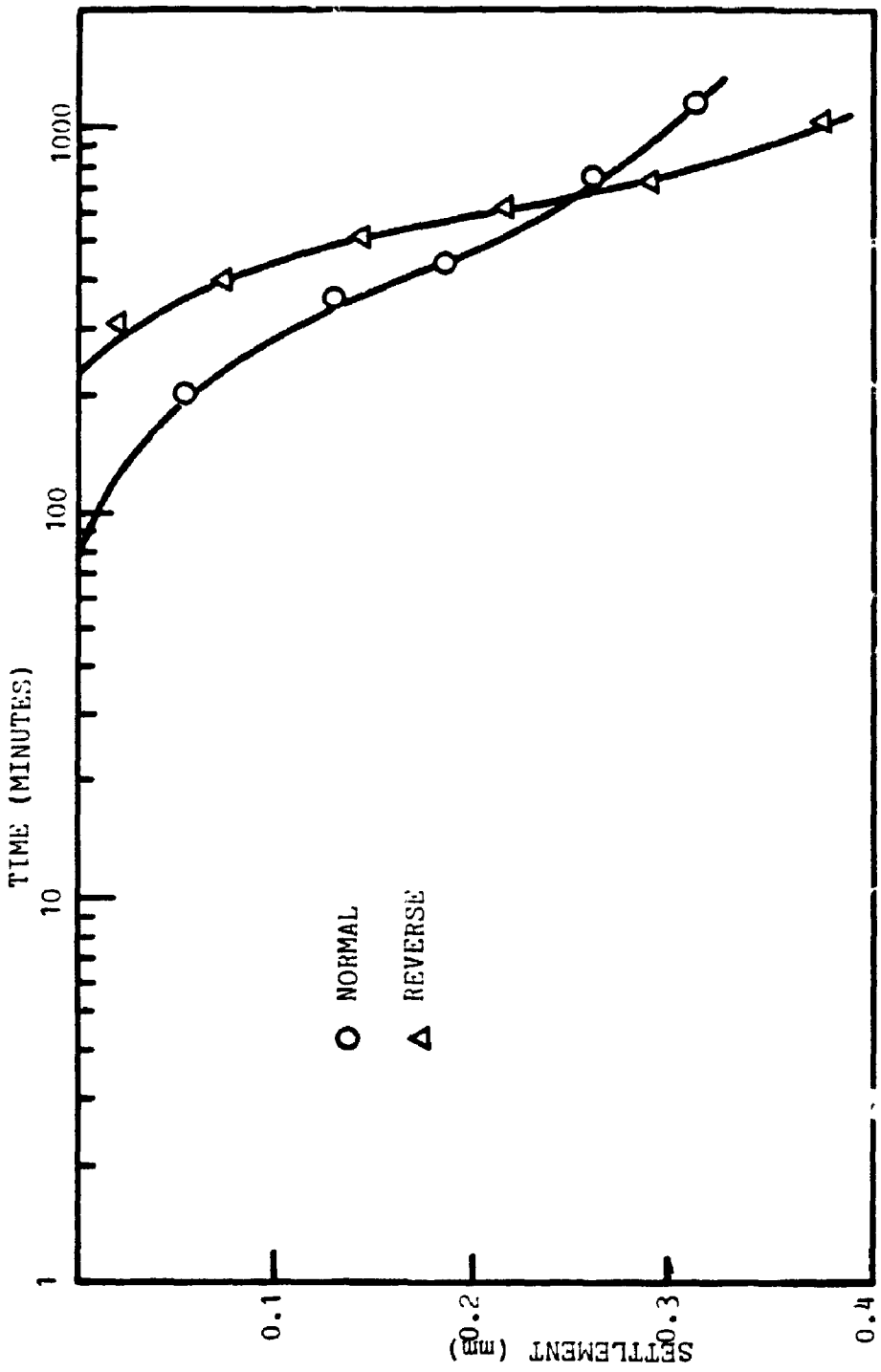

FIGURE A3 SETTLEMENT-TIME CURVE, TEST WV-4, 2.5 V

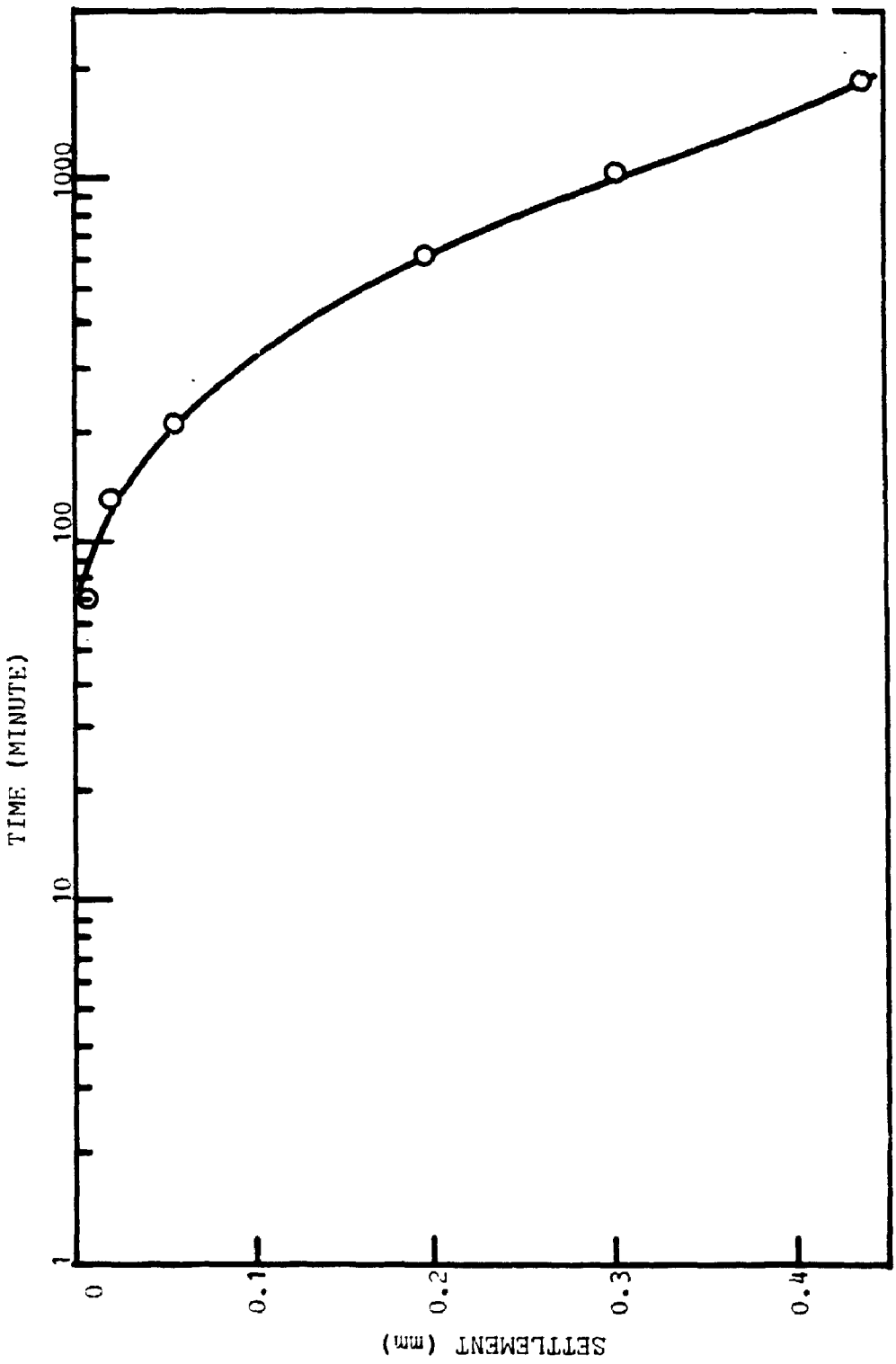

FIGURE A4 SETTLEMENT-TIME CURVE, TEST WV-4, 4 V

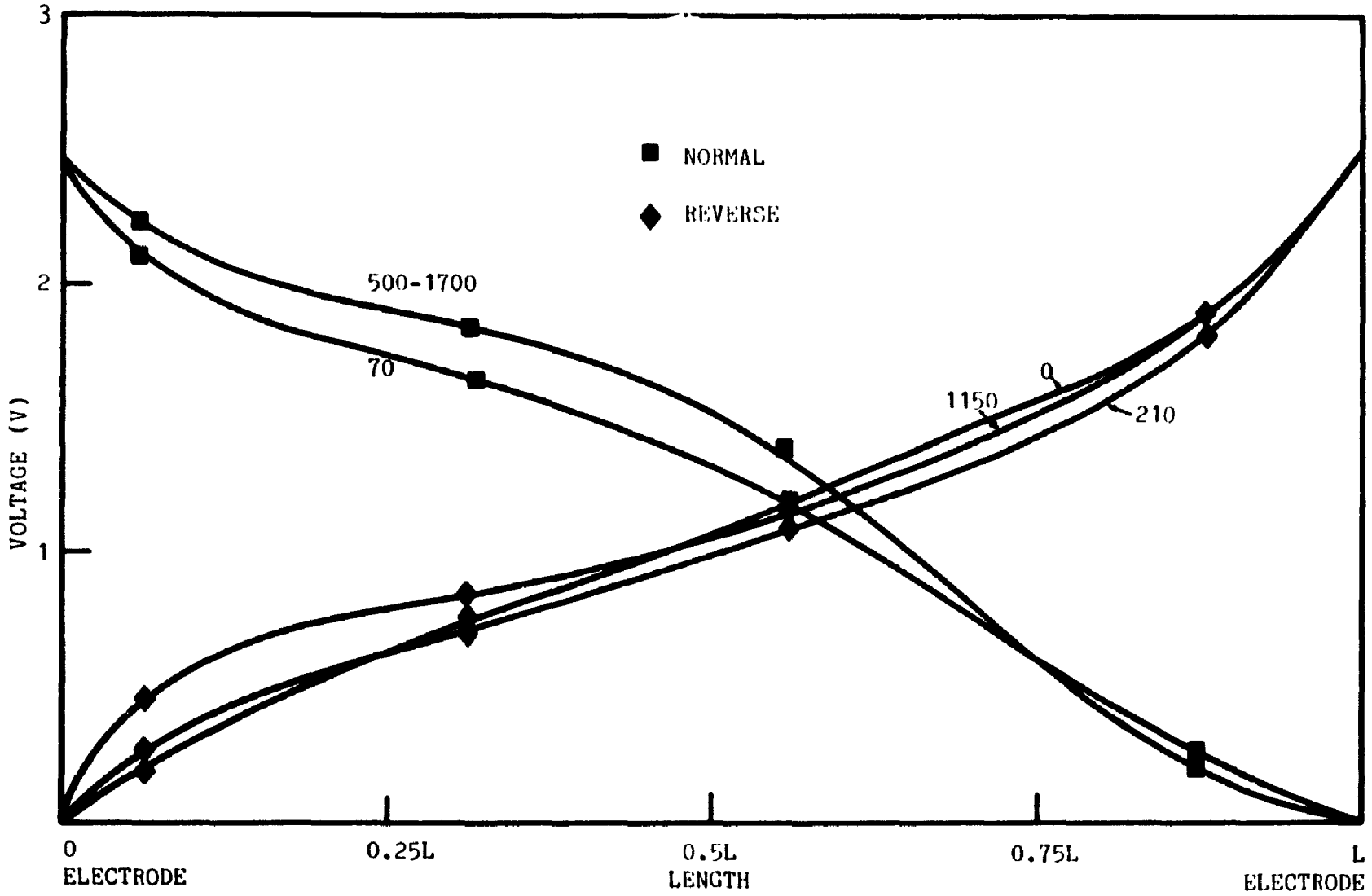

FIGURE A5 VOLTAGE DISTRIBUTION WITHIN SAMPLE WITH TIME (MINUTE), TEST WV-4, 2.5 V

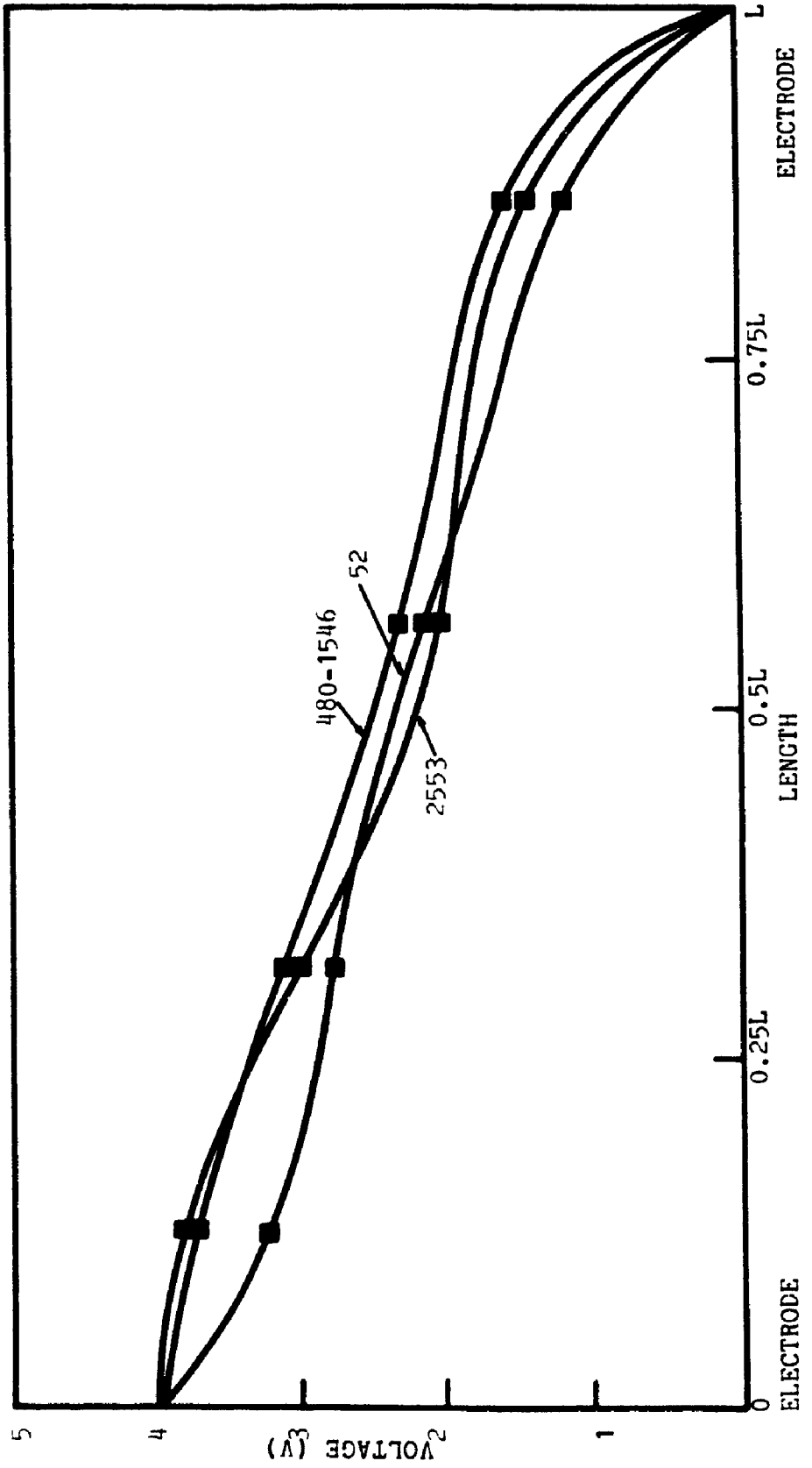

FIGURE A6 VOLTAGE DISTRIBUTION WITHIN SAMPLE WITH TIME (MINUTE), TEST WV-4, 4 V

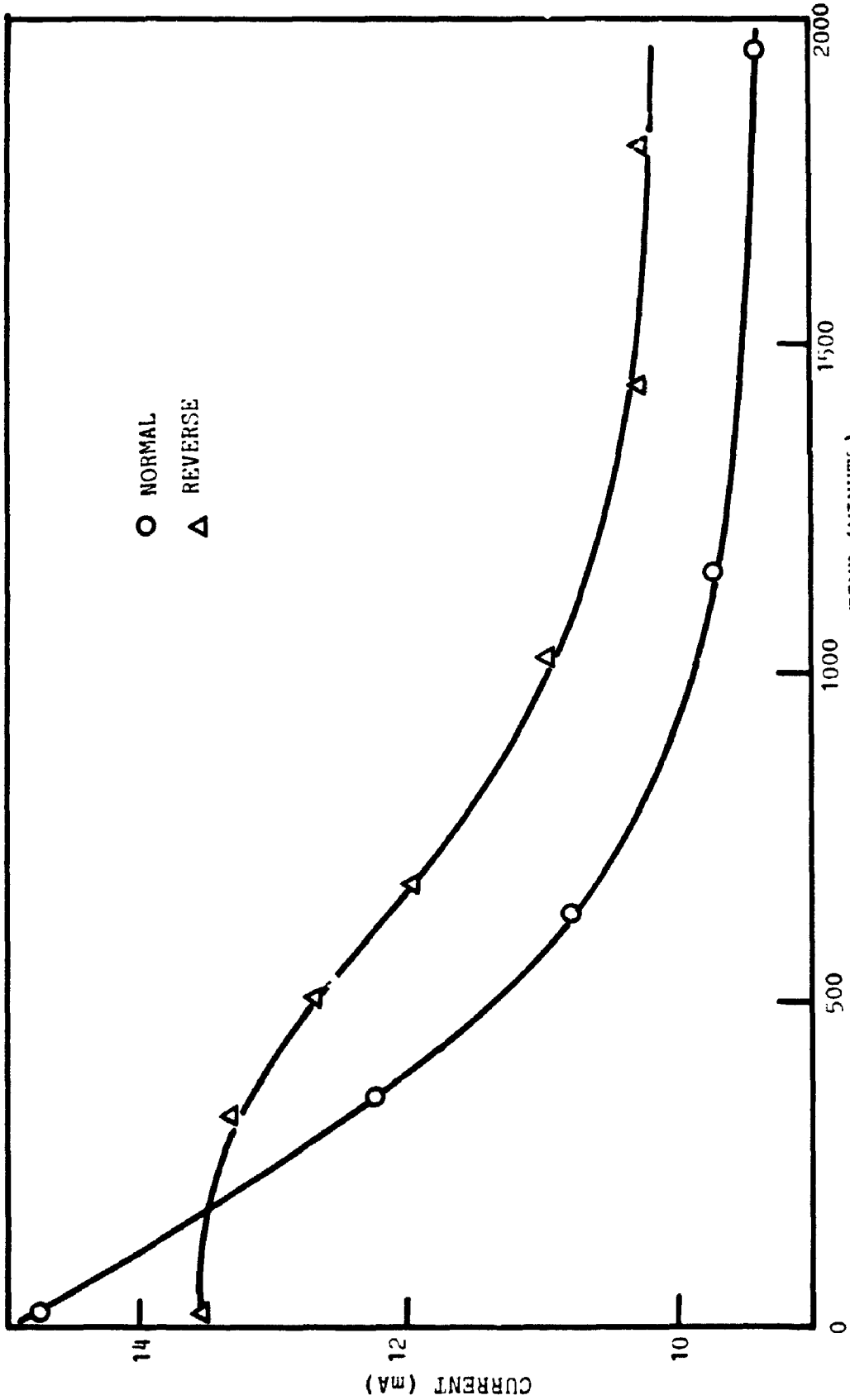

FIGURE A7 CURRENT VARIATION WITH TIME, TEST WV-4, 2.5 V

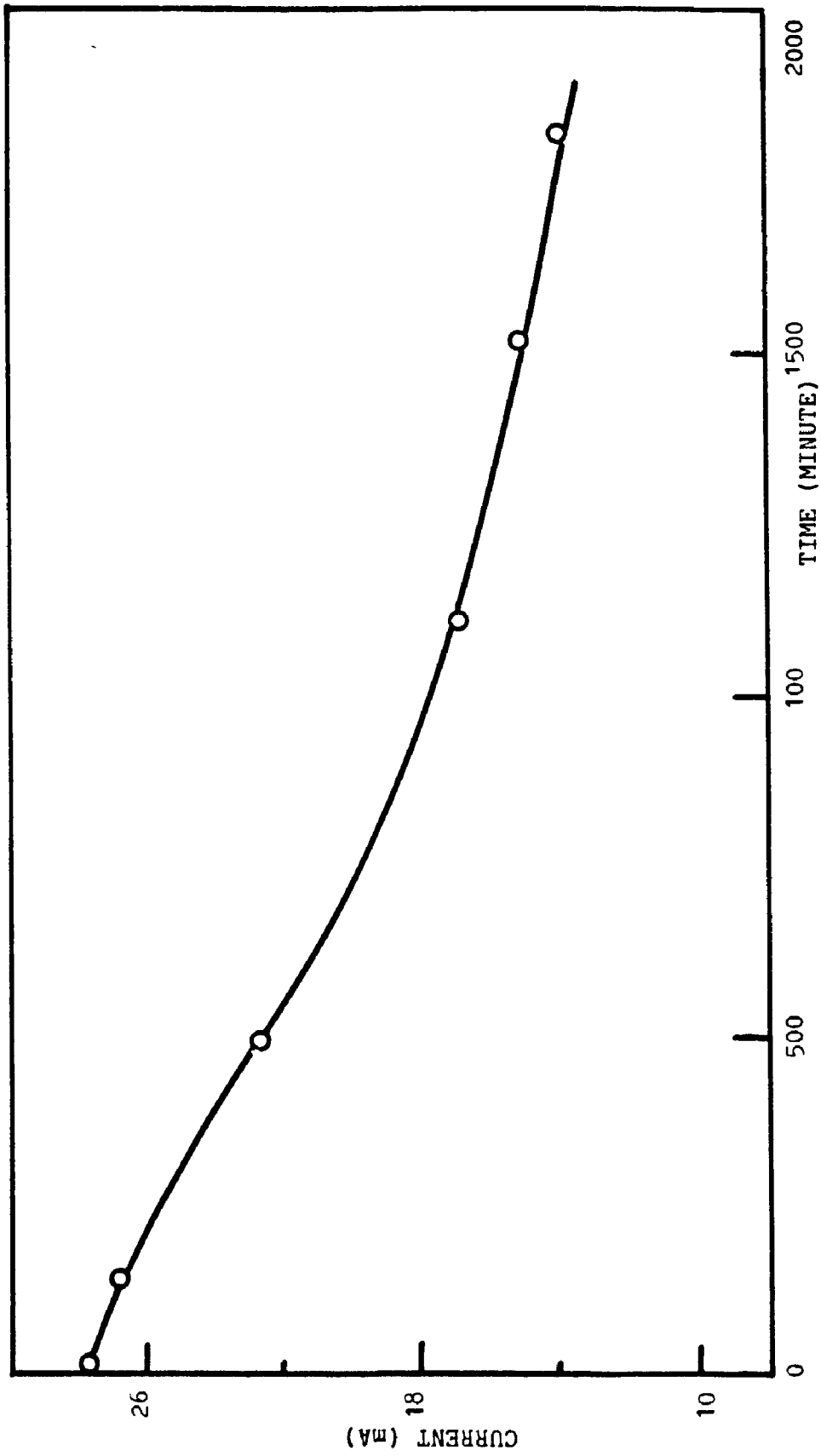

FIGURE A8 CURRENT VARIATION WITH TIME, TEST WV-4, 4 V

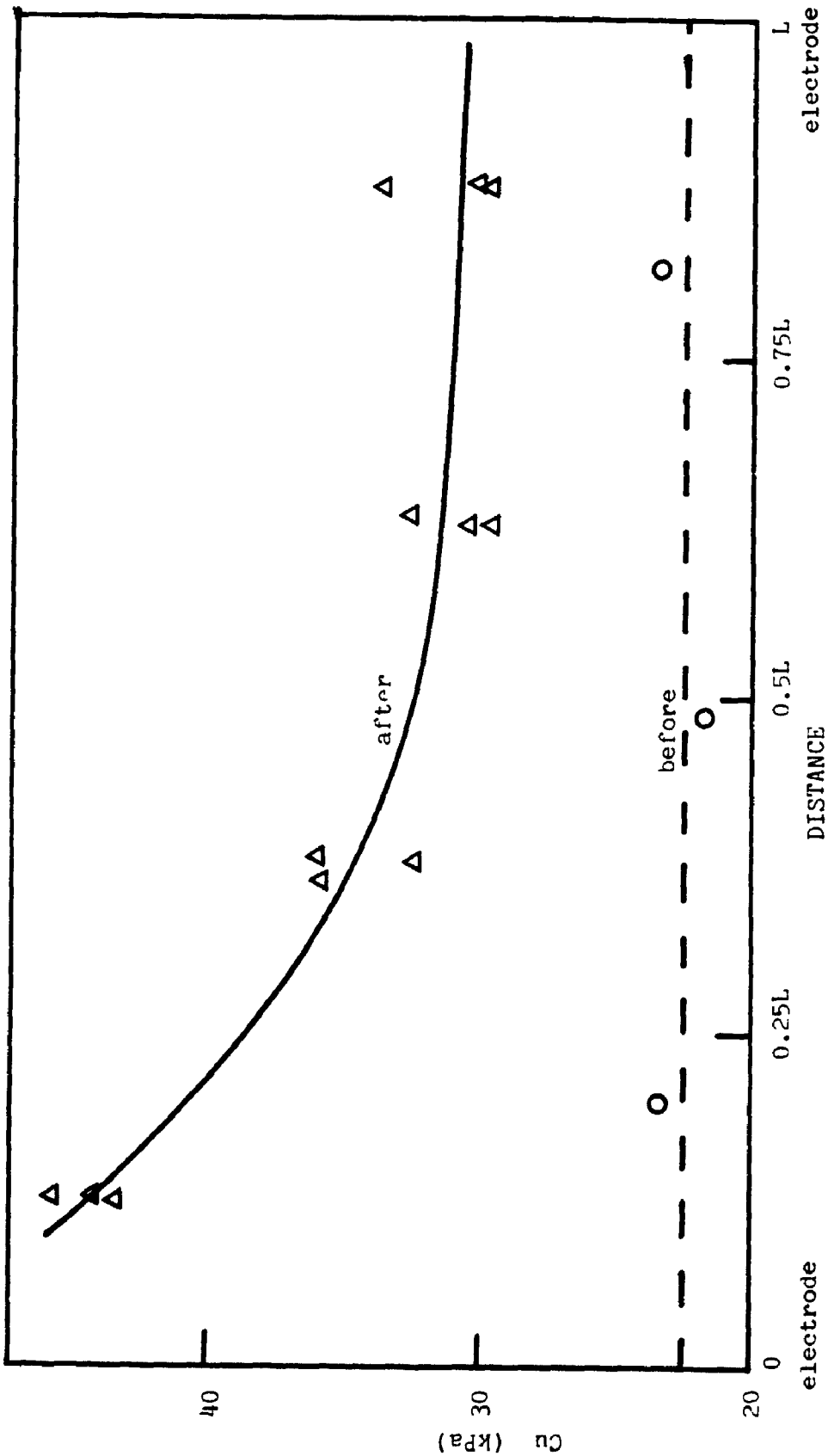

Fig. A9 VANE STRENGTH BEFORE AND AFTER TREATMENT TEST WV-4 2.5 V WITH ELECTRODE REVERSAL, 4.0 V WITHOUT ELECTRODE REVERSAL

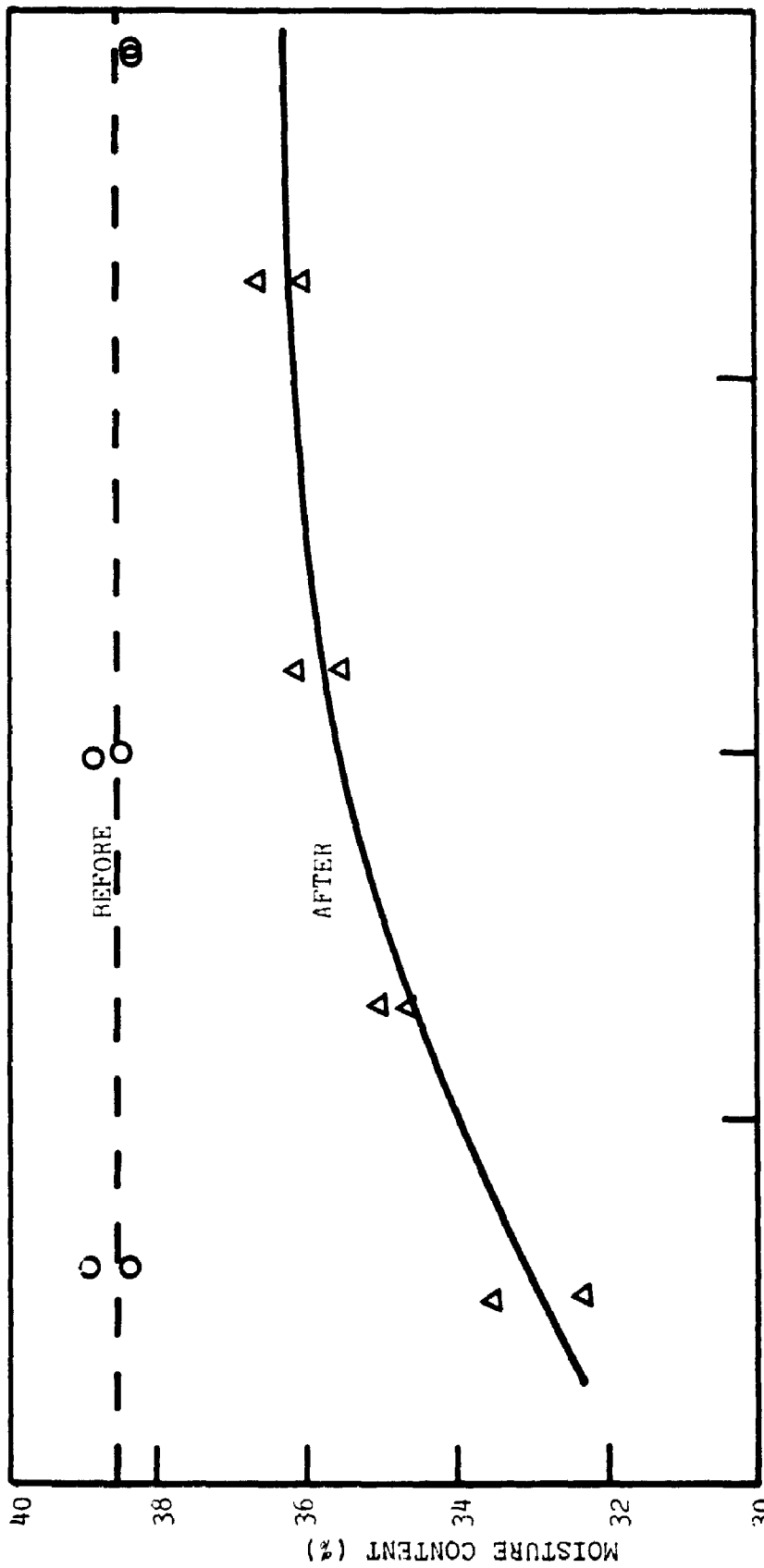

Fig A10 MOISTURE CONTENT BEFORE AND AFTER TREATMENT TEST WV-4, 2.5V WITH ELECTRODE REVERSAL, 4 V WITHOUT ELECTRODE REVERSAL

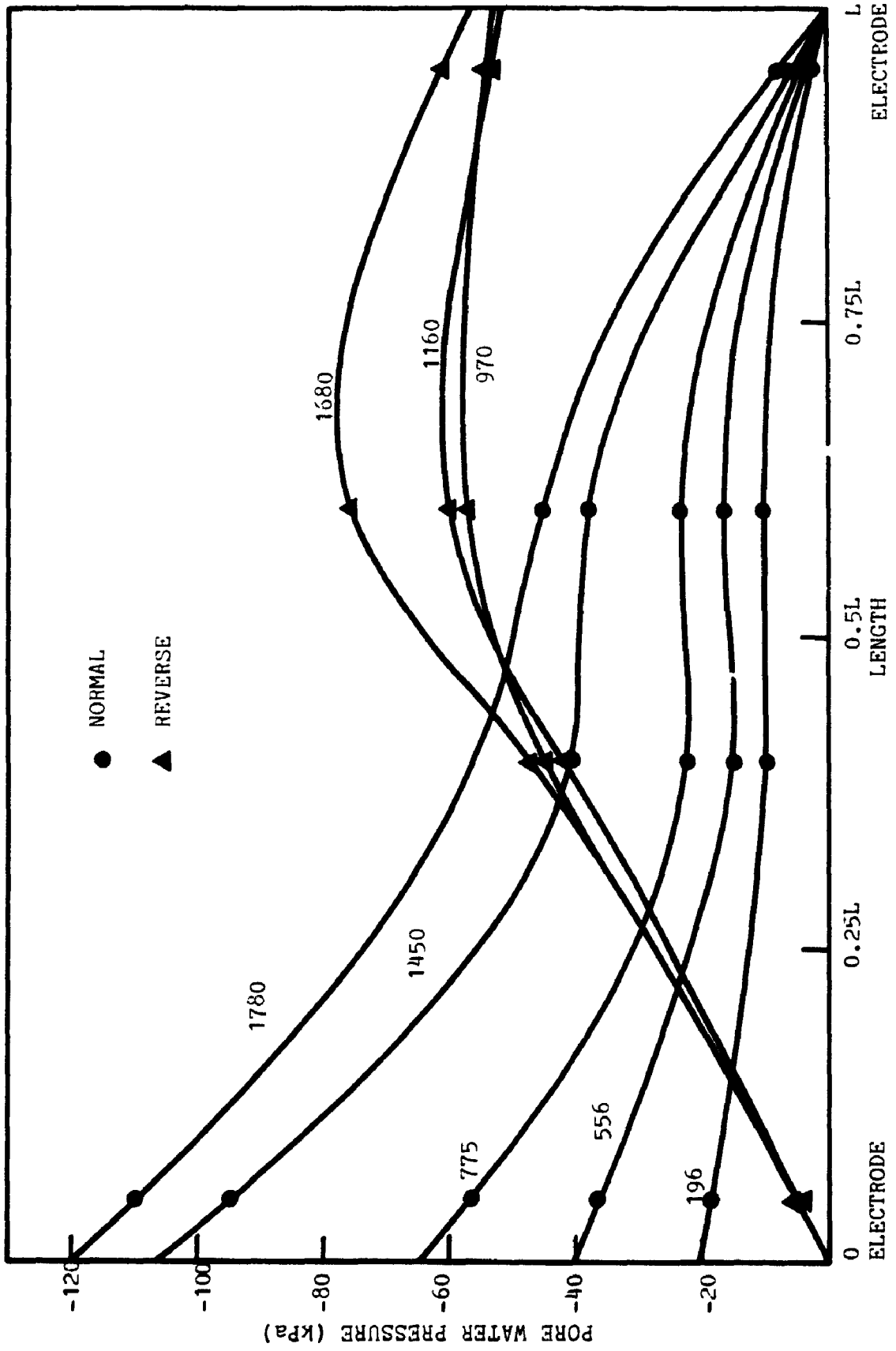

FIGURE A11 PORE WATER PRESSURE DISTRIBUTION WITH TIME (MINUTE), TEST WV-8V, 5 V

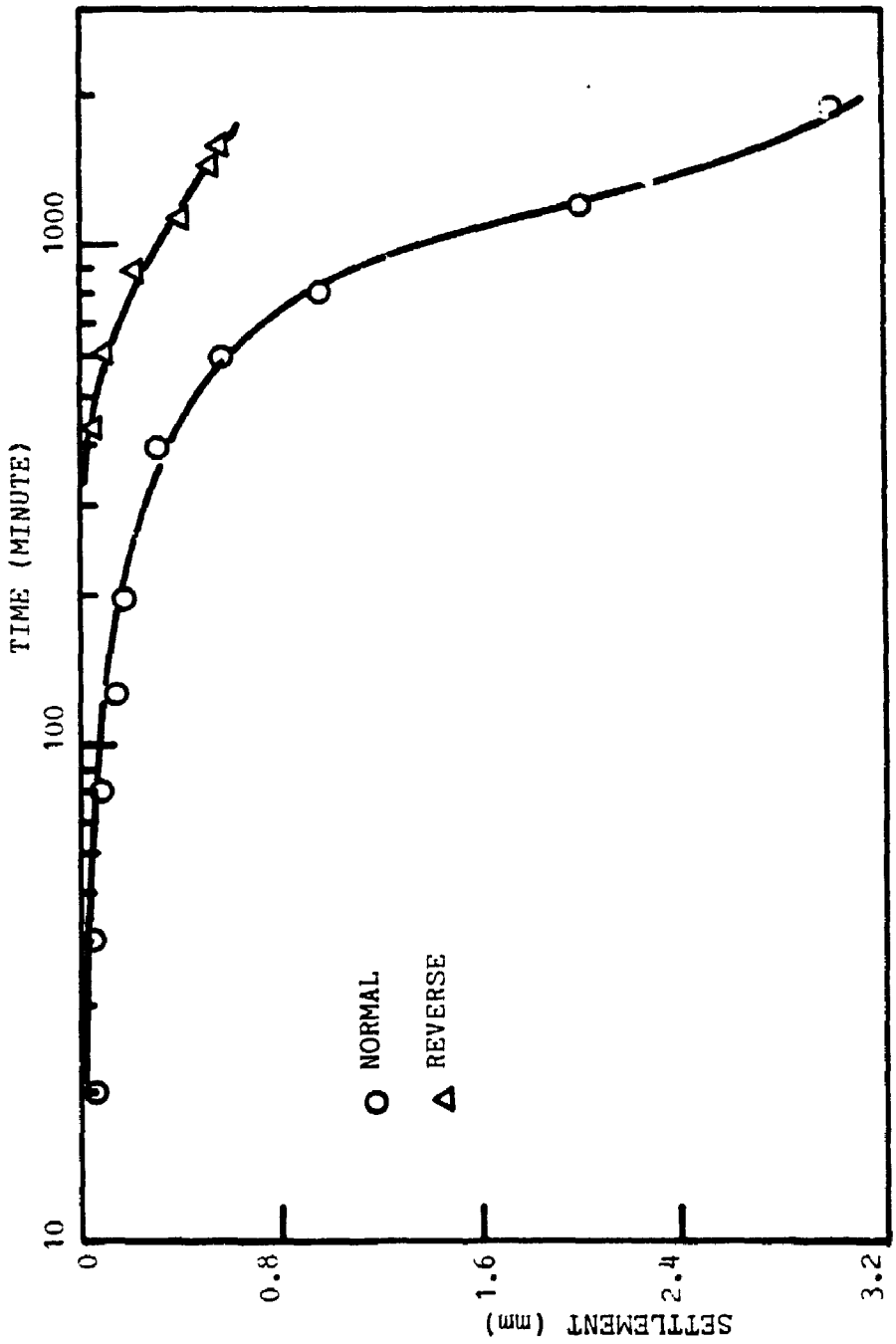

FIGURE A12 SETTLEMENT-TIME CURVE, TEST WV-8B, 5V

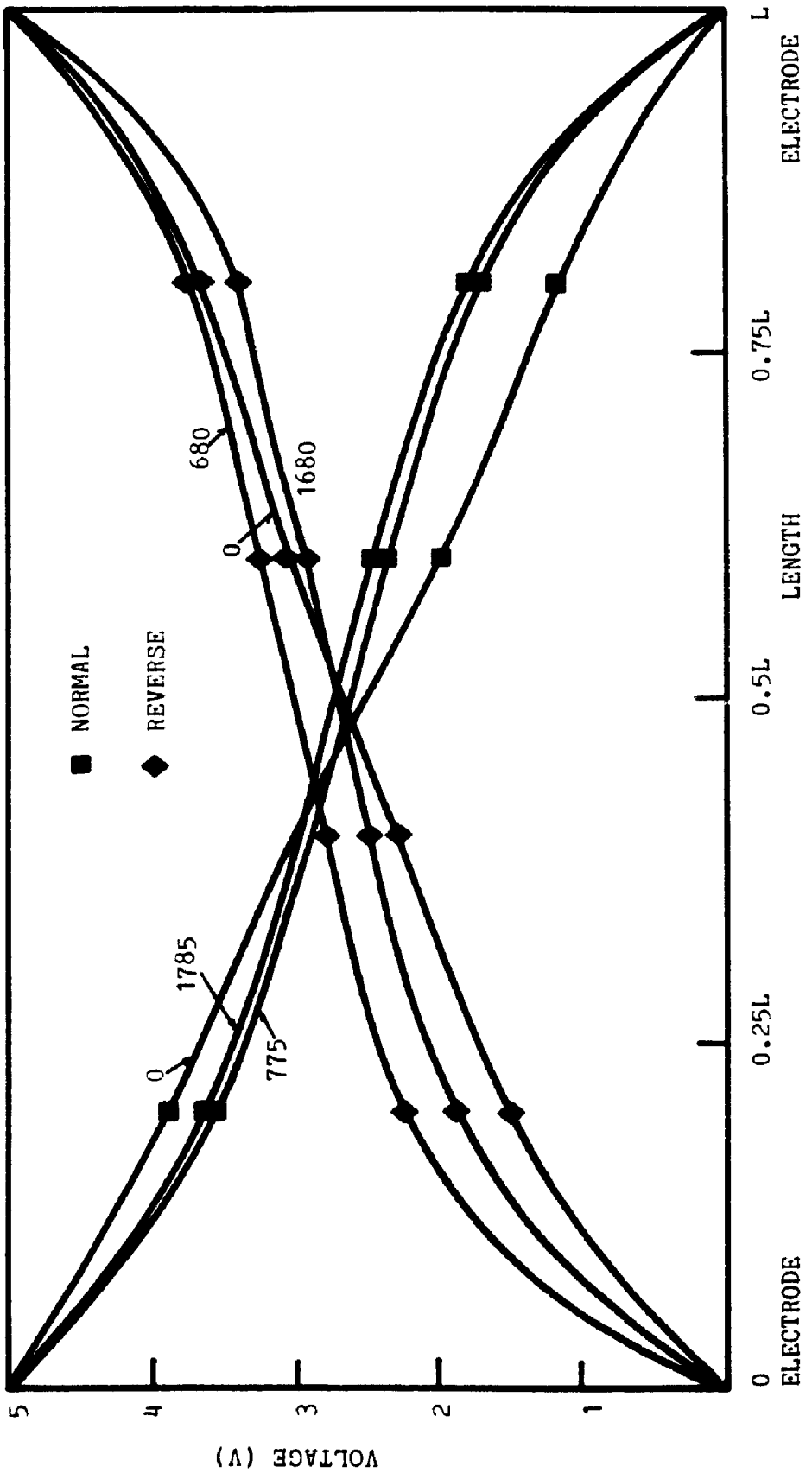

FIGURE A13 VOLTAGE DISTRIBUTION WITHIN SAMPLE WITH TIME, TEST WV-8B, 5 V

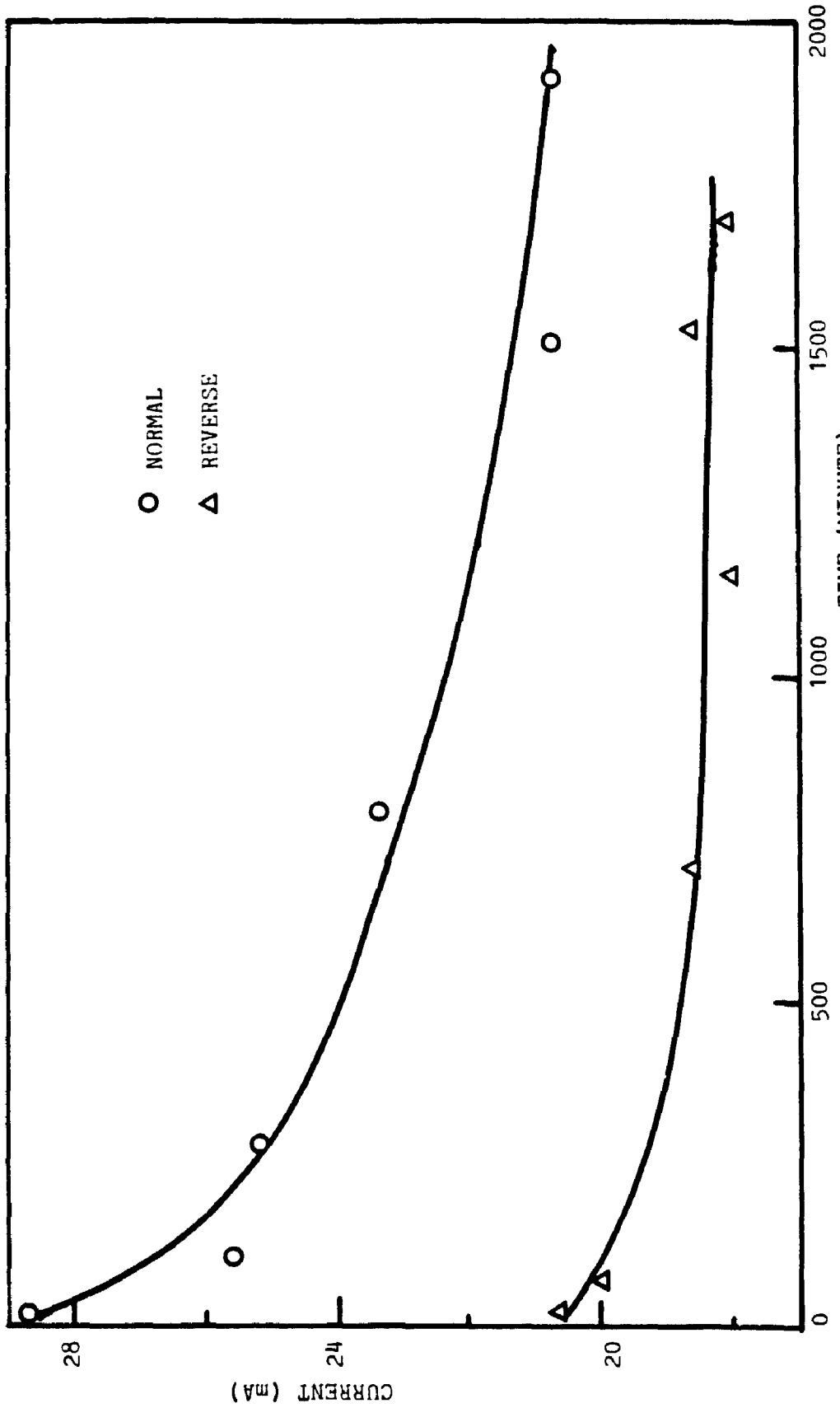

FIGURE A14 CURRENT VARIATION WITH TIME, TEST WV-8B, 5 V

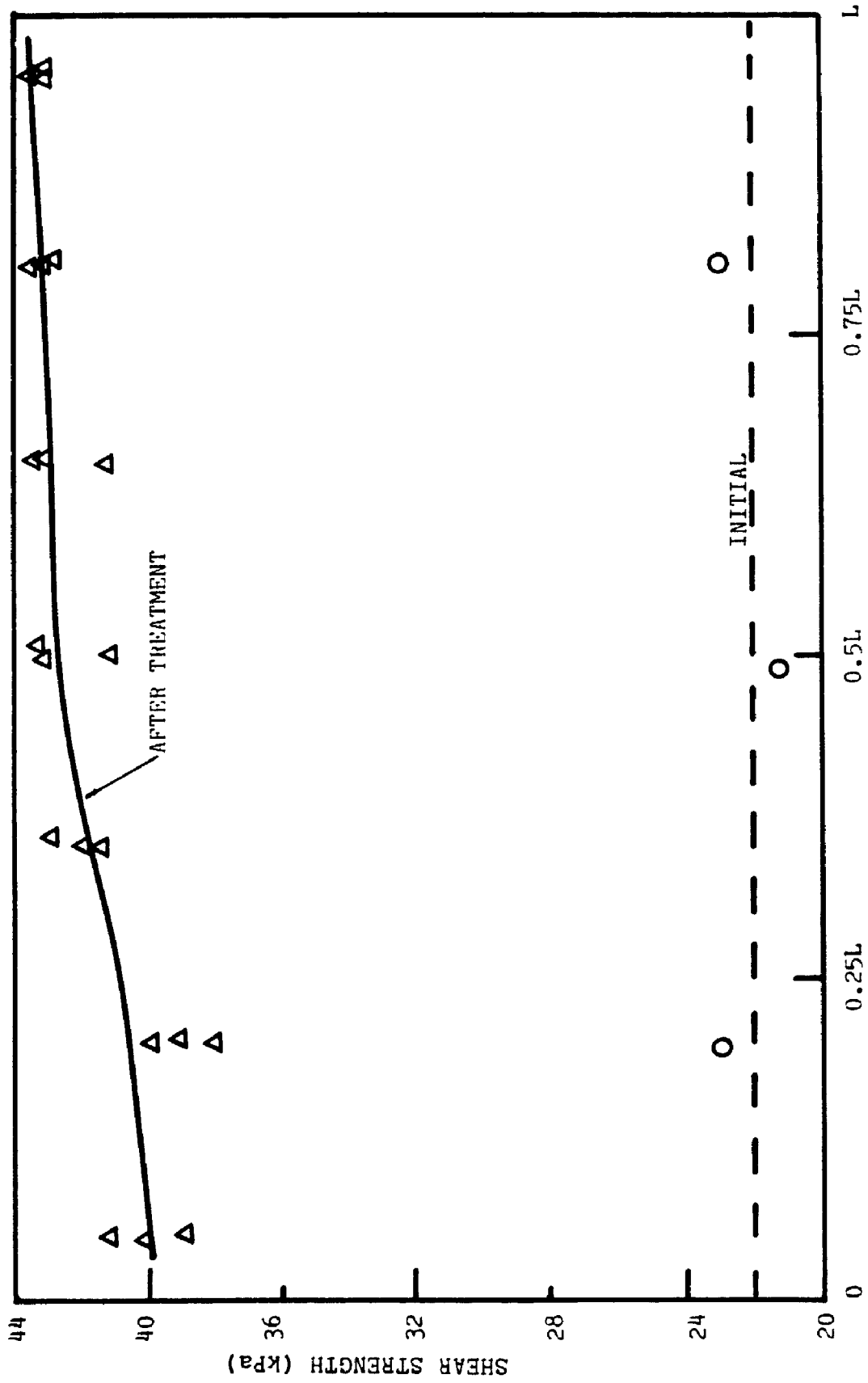

FIGURE A15 VANE STRENGTH BEFORE AND AFTER TREATMENT, TEST WV-8V, 5 V WITH ELECTRODE REVERSAL

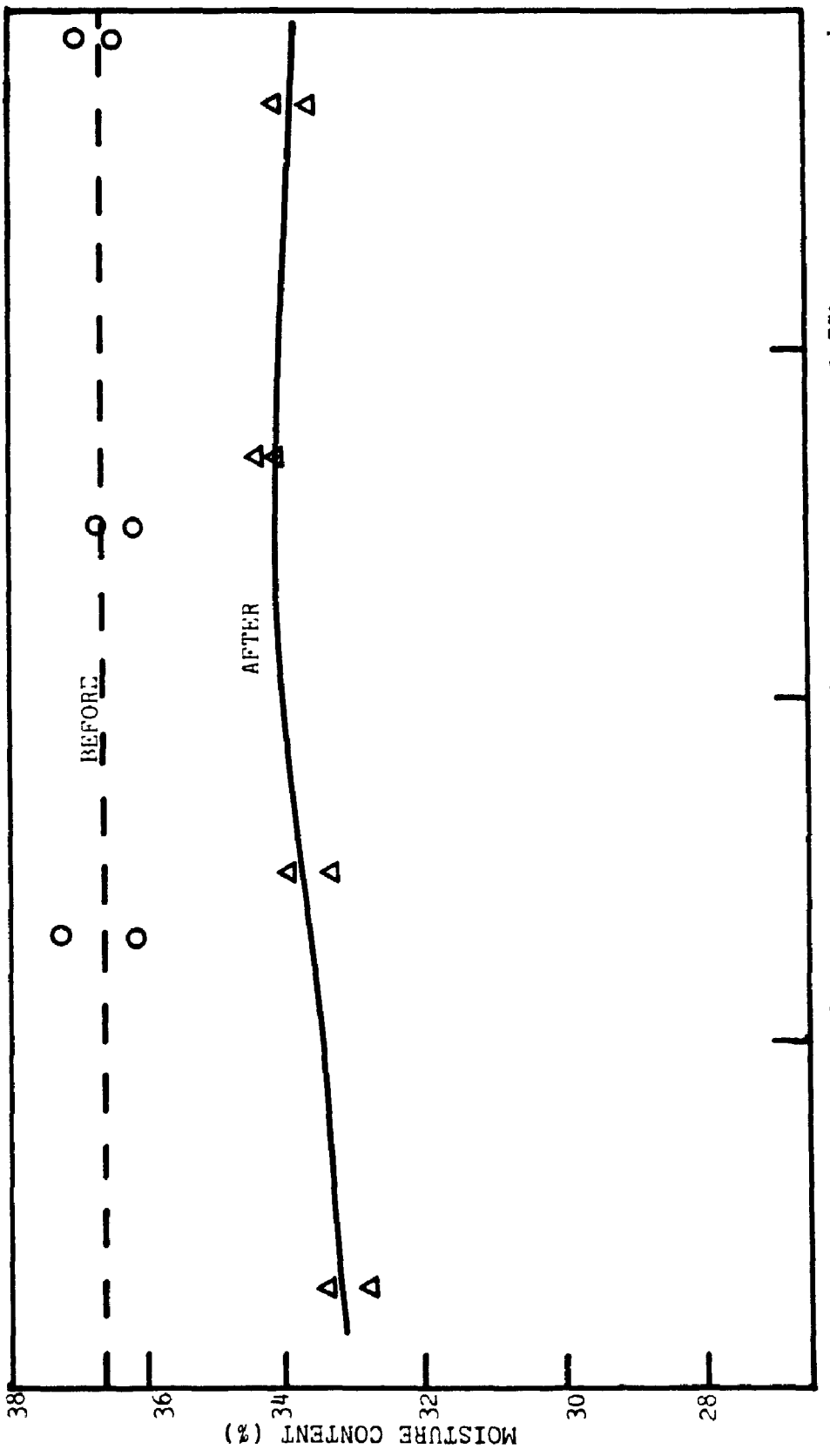

FIG. A16 MOISTURE CONTENT BEFORE AND AFTER TREATMENT, TEST WV-8B, 5 V WITH ELECTRODE REVERSAL

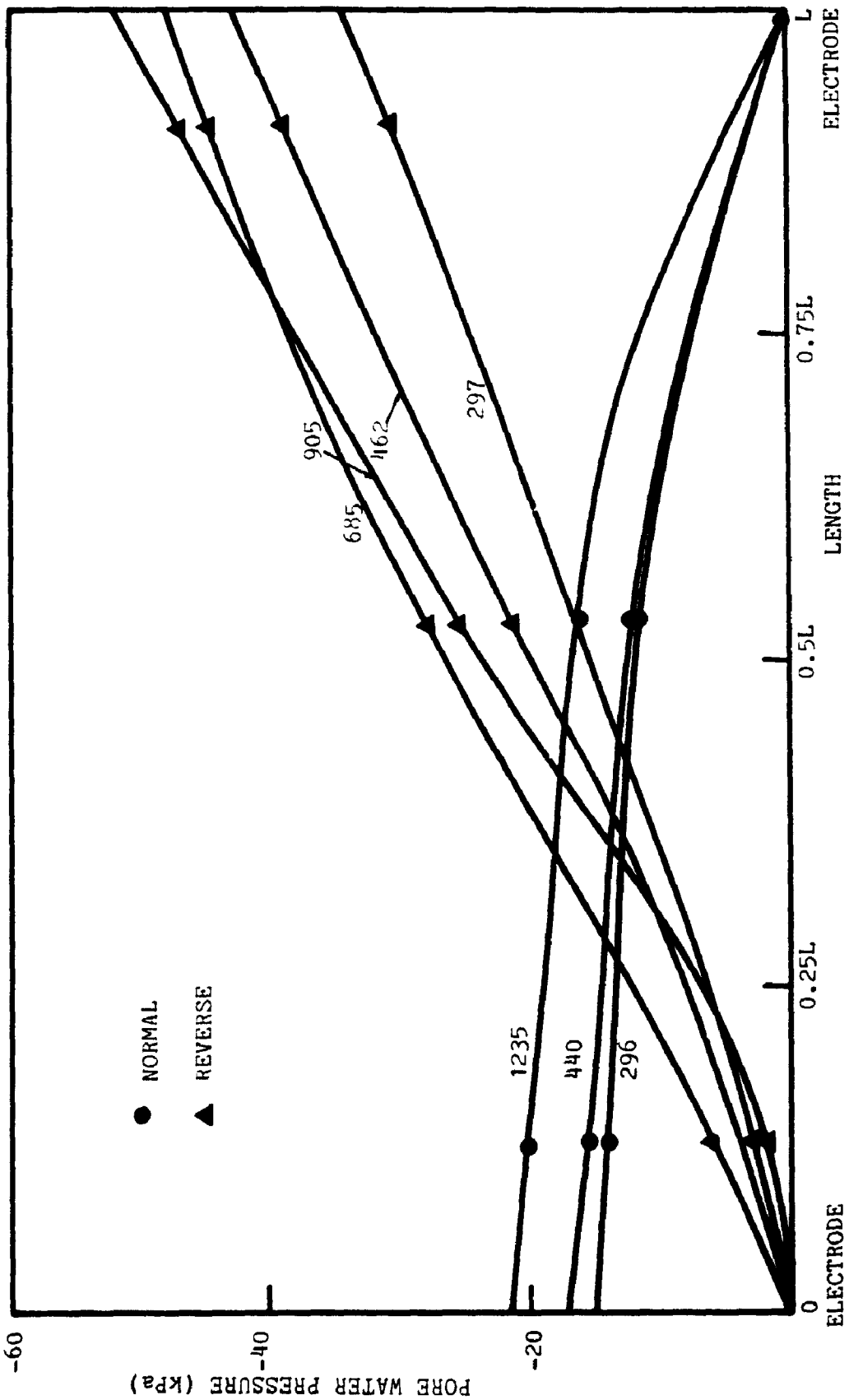

FIGURE A17 PORE WATER PRESSURE DISTRIBUTION WITH TIME (MINUTE), TEST WH-3, 2 V

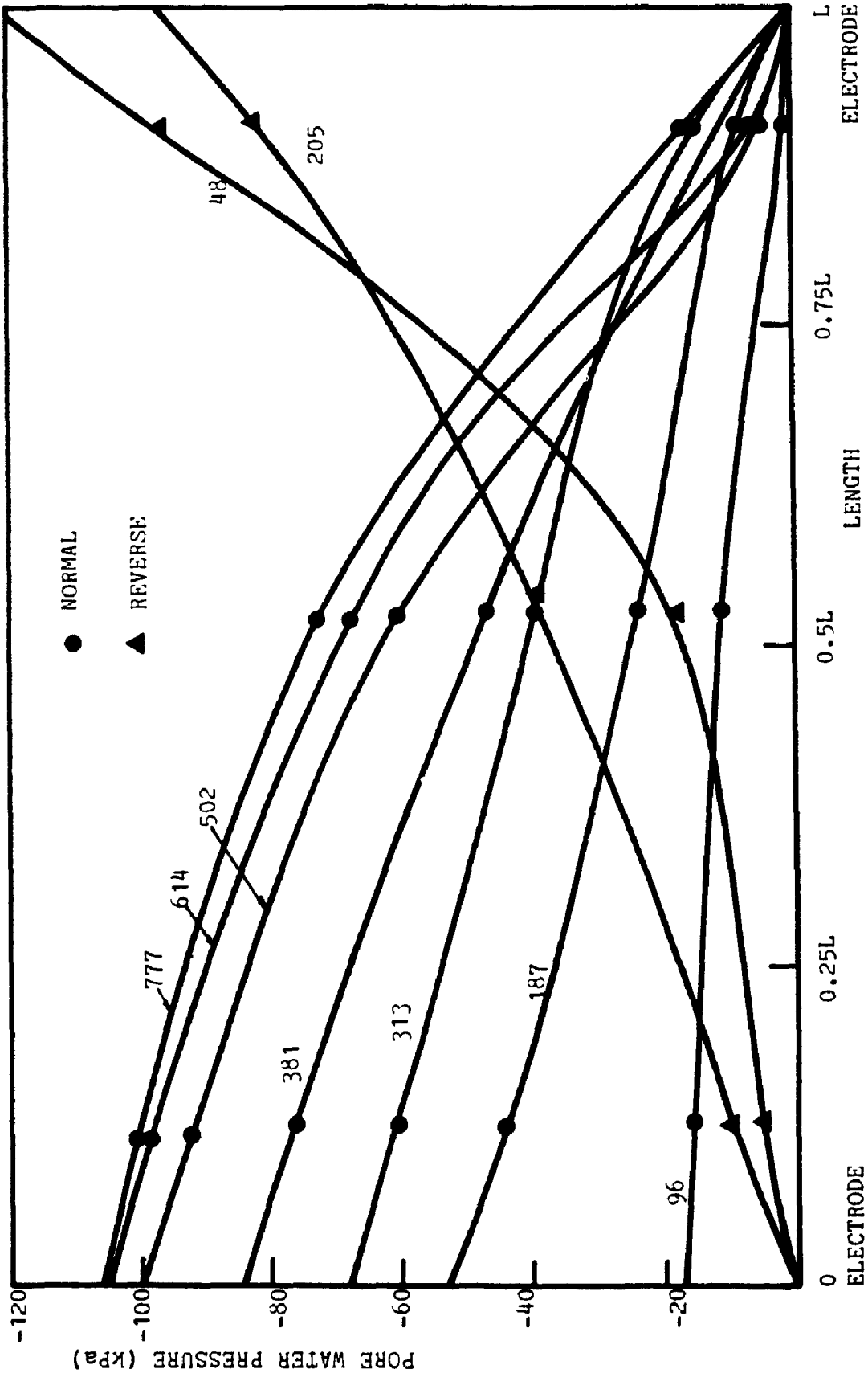

FIGURE A18 PORE WATER PRESSURE DISTRIBUTION WITH TIME (MINUTE), TEST WH-3, 4 V

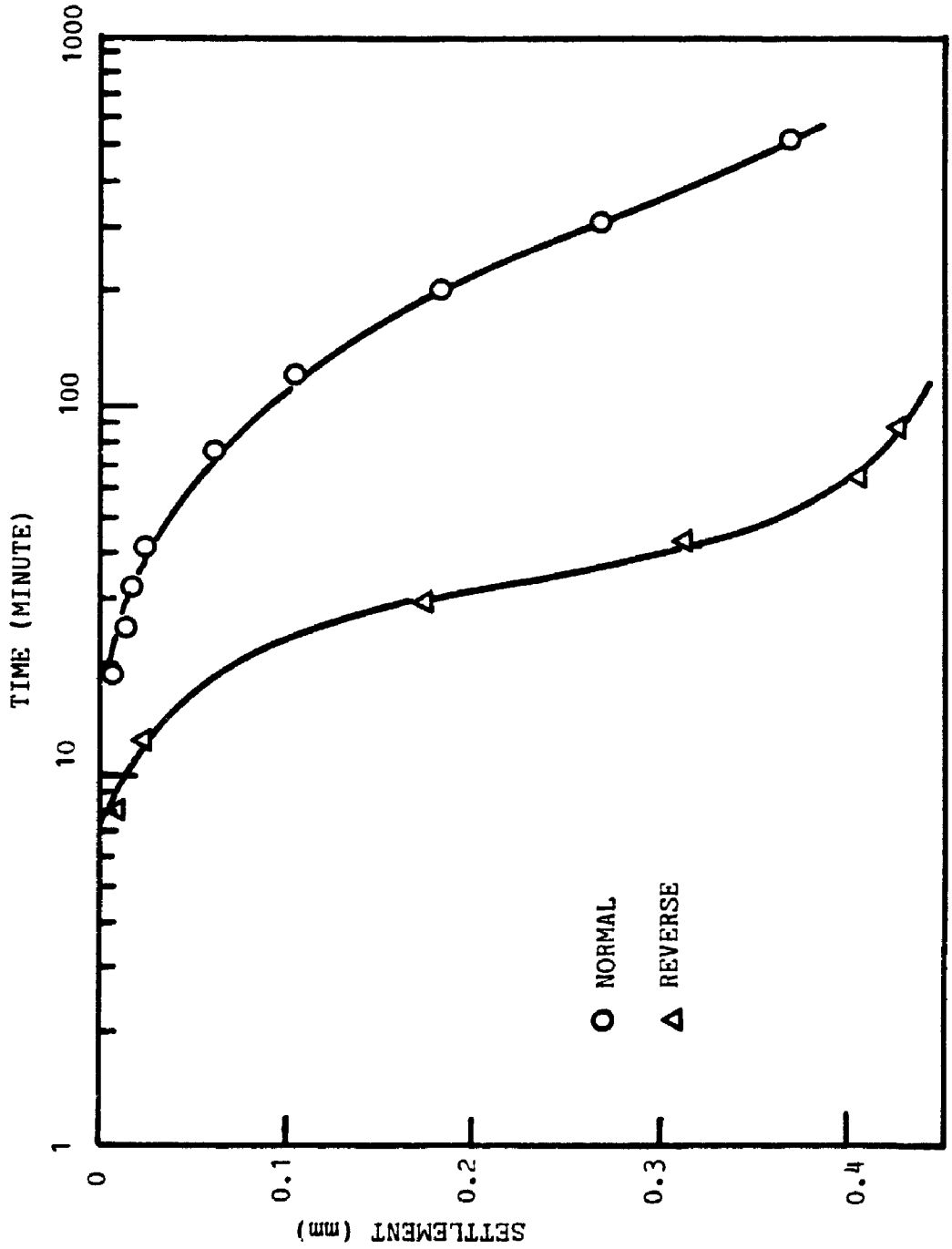

FIGURE A19 SETTLEMENT-TIME CURVE, TEST WH-3, 2 V

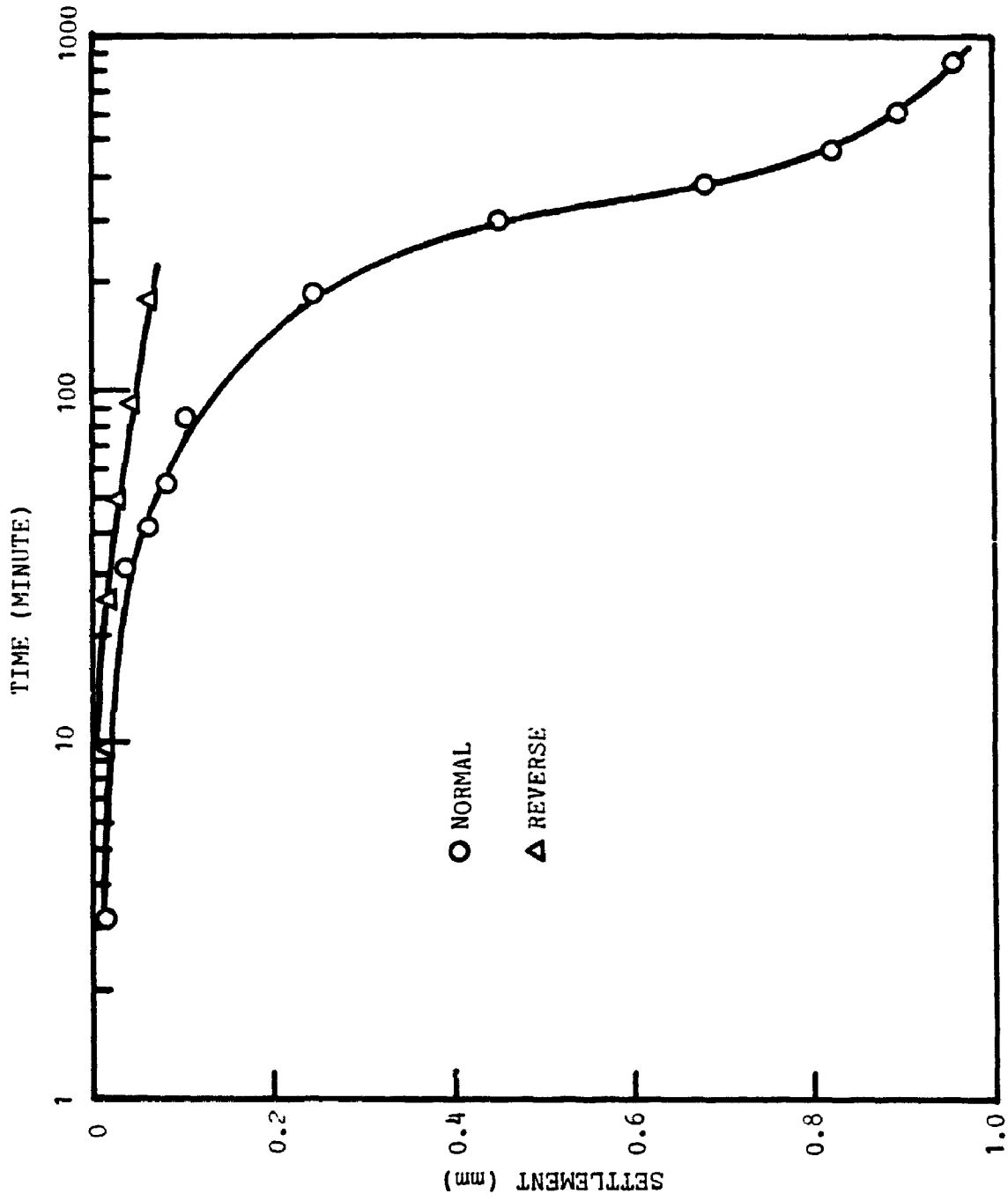

FIGURE A20 SETTLEMENT-TIME CURVE, TEST WH-3, 4 V

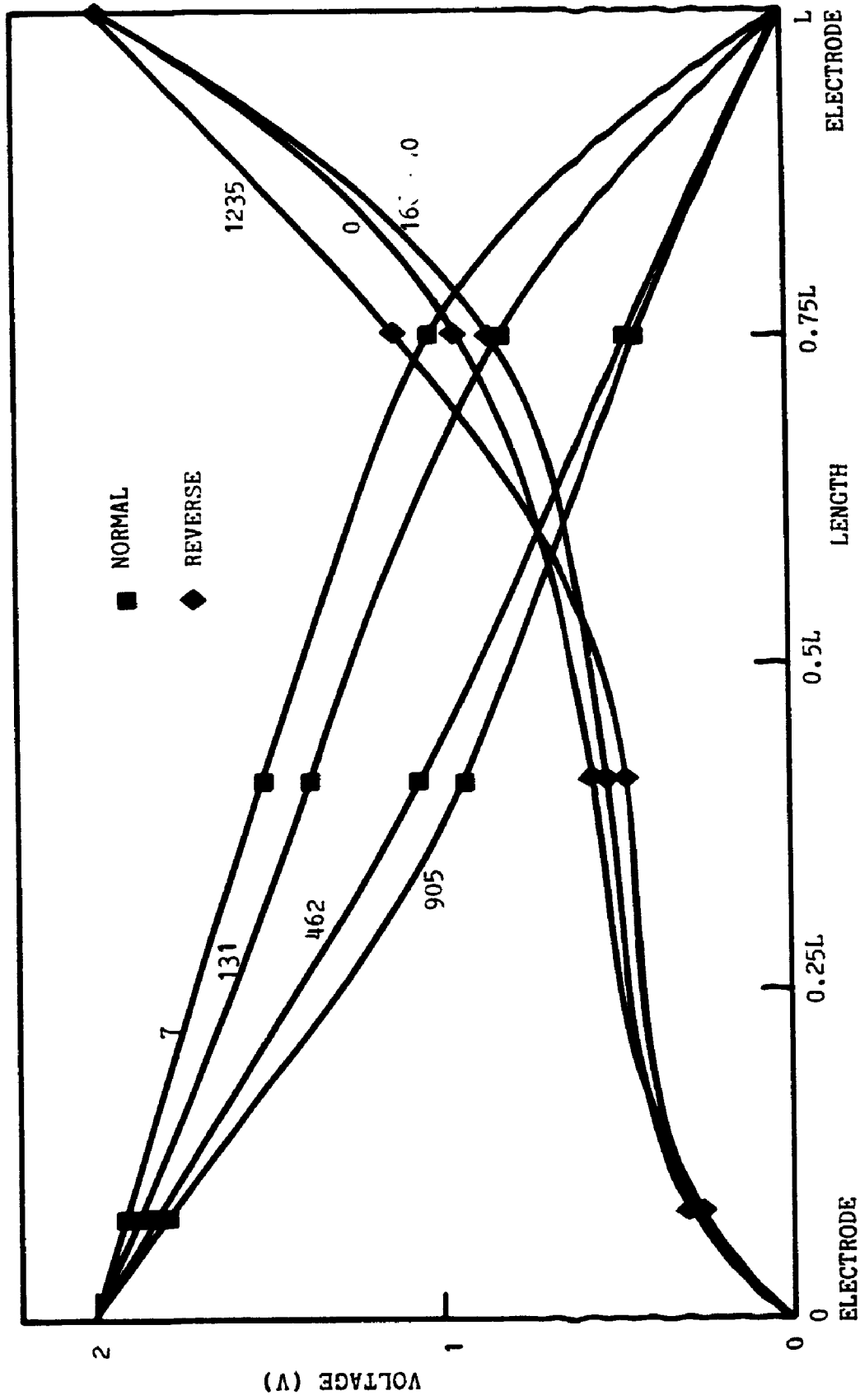

FIGURE A21 VOLTAGE DISTRIBUTION WITHIN SAMPLE WITH TIME (MINUTE), TEST WH-3, 2 V

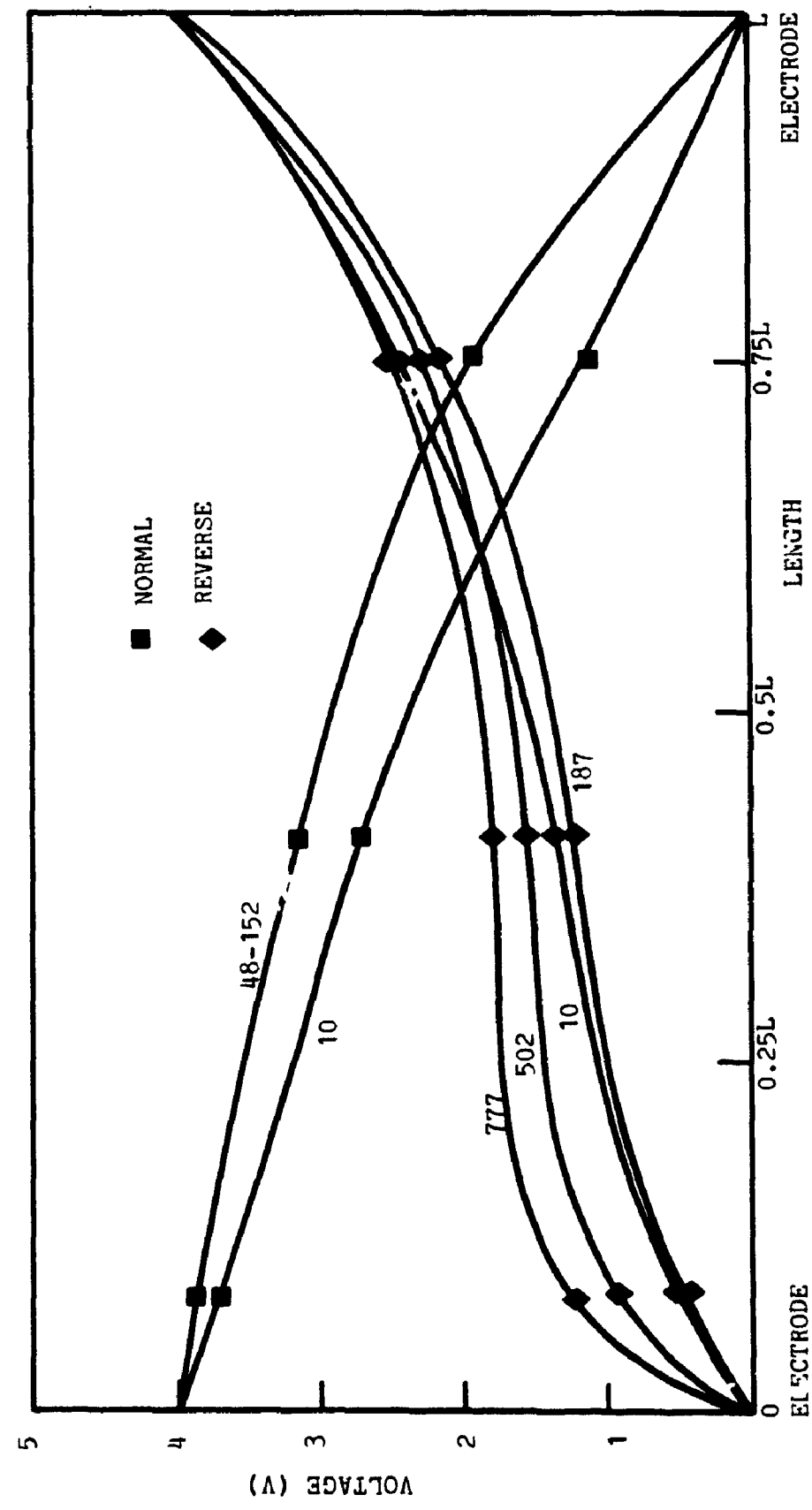

FIGURE A22 VOLTAGE DISTRIBUTION WITHIN SAMPLE WITH TIME (MINUTE), TEST WH-3, 4 V

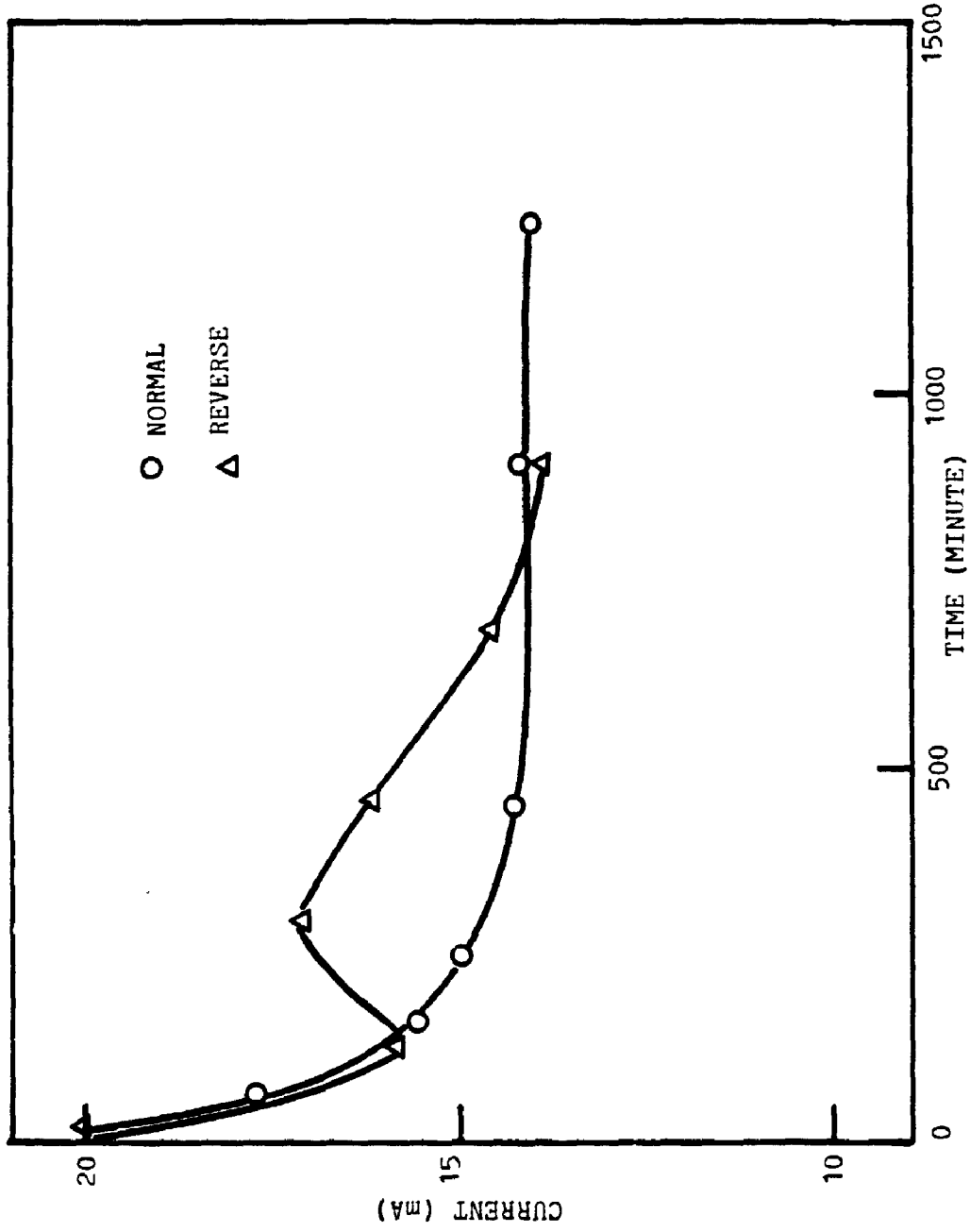

FIGURE A23 CURRENT VARIATION WITH TIME, TEST WH-3, 2 V

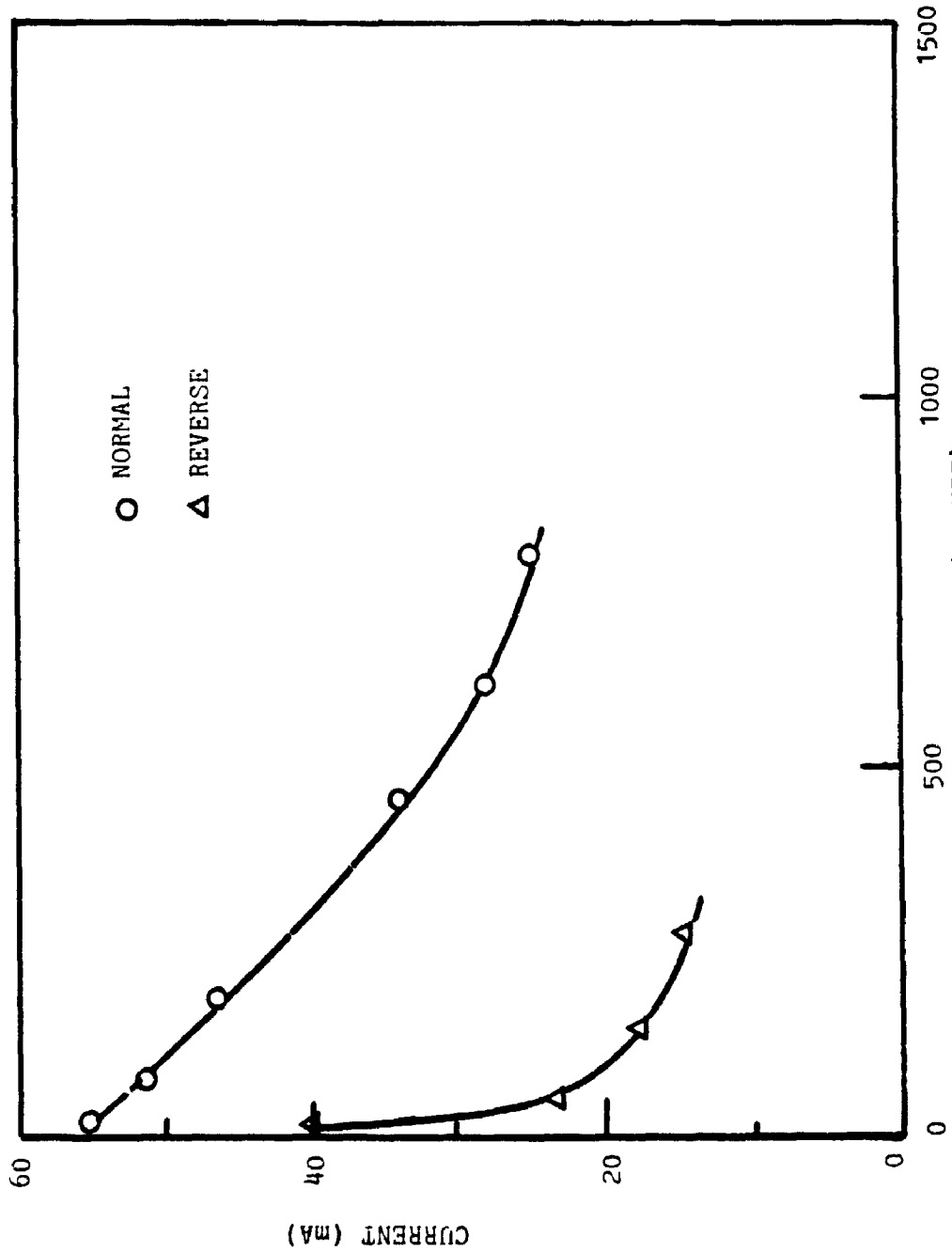

FIGURE A24 CURRENT VARIATION WITH TIME, TEST WH-3, 4 V

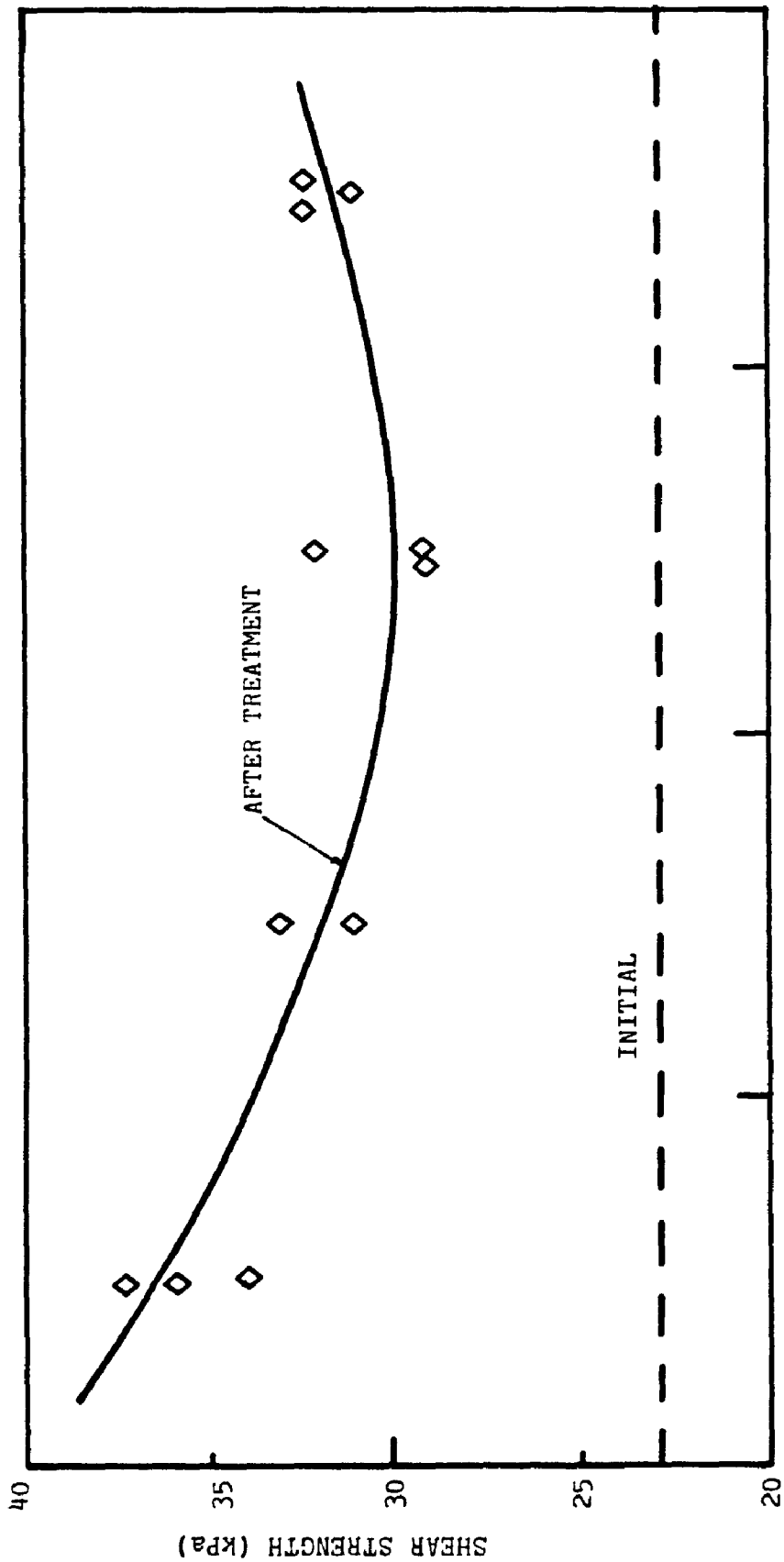

FIGURE A25 VANE STRENGTH BEFORE AND AFTER TREATMENT, TEST WH-3, 2 and 4 V WITH ELECTRODE REVERSAL

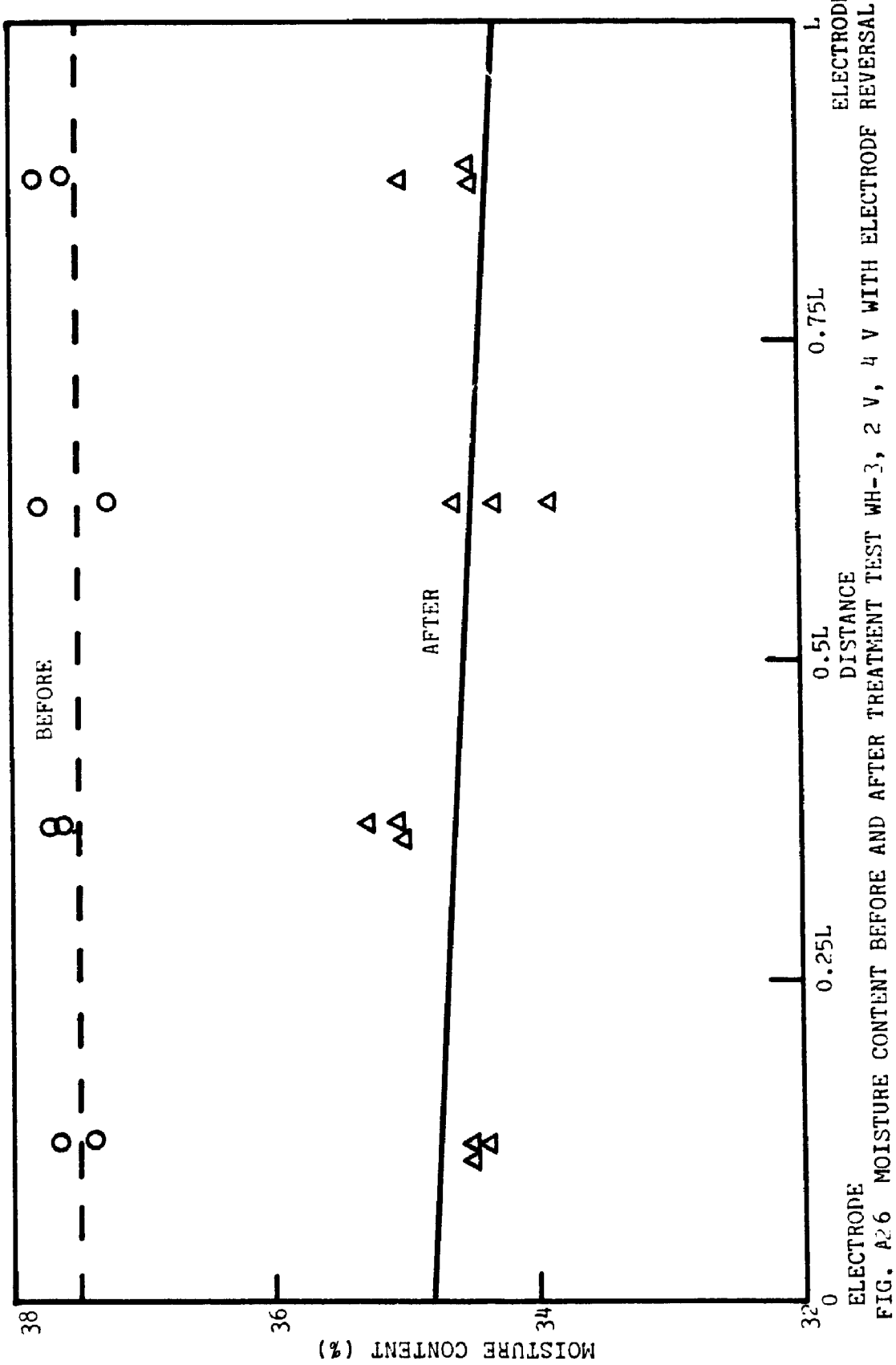

FIG. A26 MOISTURE CONTENT BEFORE AND AFTER TREATMENT TEST WH-3, 2 V, 4 V WITH ELECTRODE REVERSAL

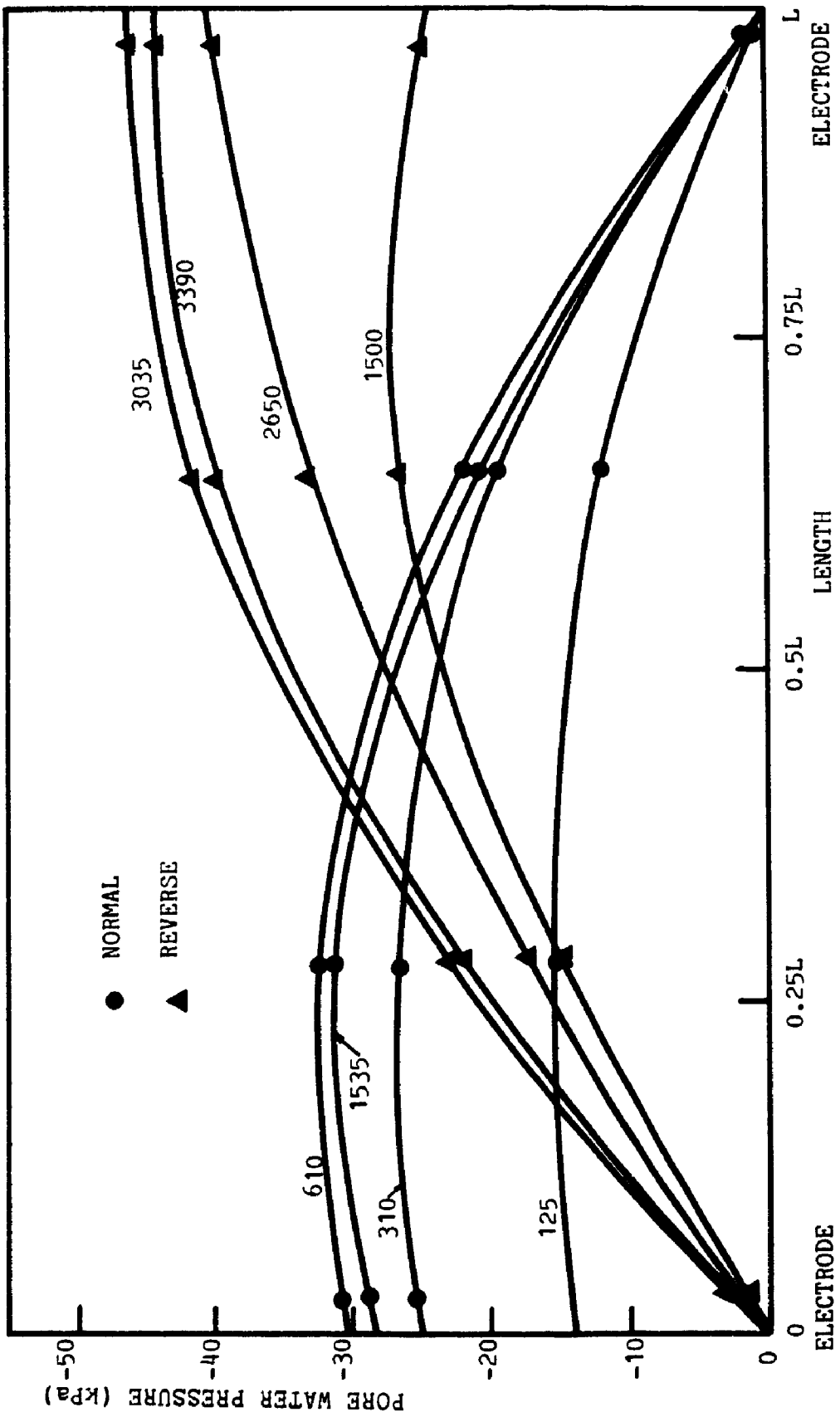

FIGURE A27 PORE WATER PRESSURE DISTRIBUTION WITH TIME (MINUTE), TEST WH-9, 2 V

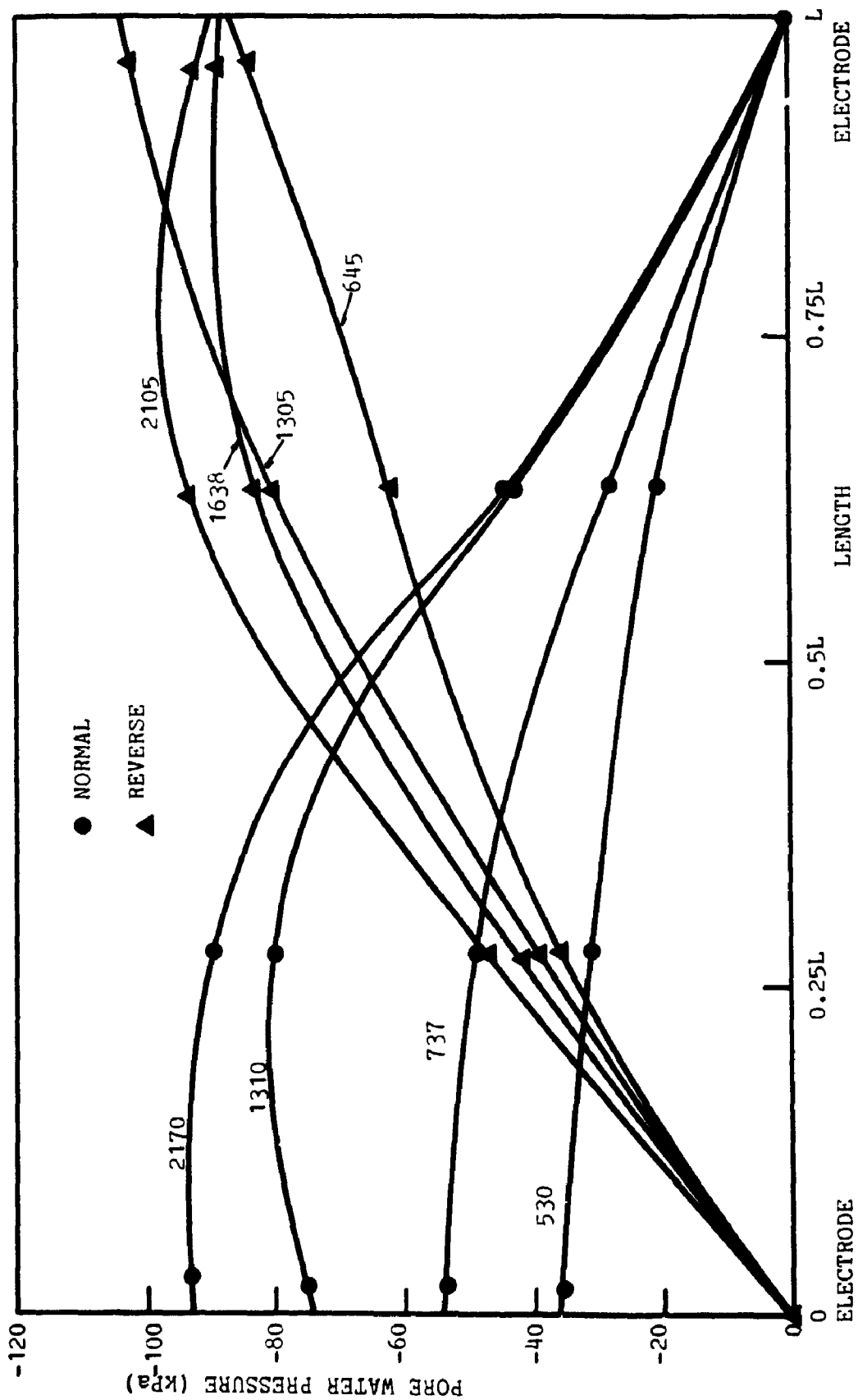

FIGURE A28 PORE WATER PRESSURE DISTRIBUTION WITH TIME (MINUTE), TEST WH-9, 4 V

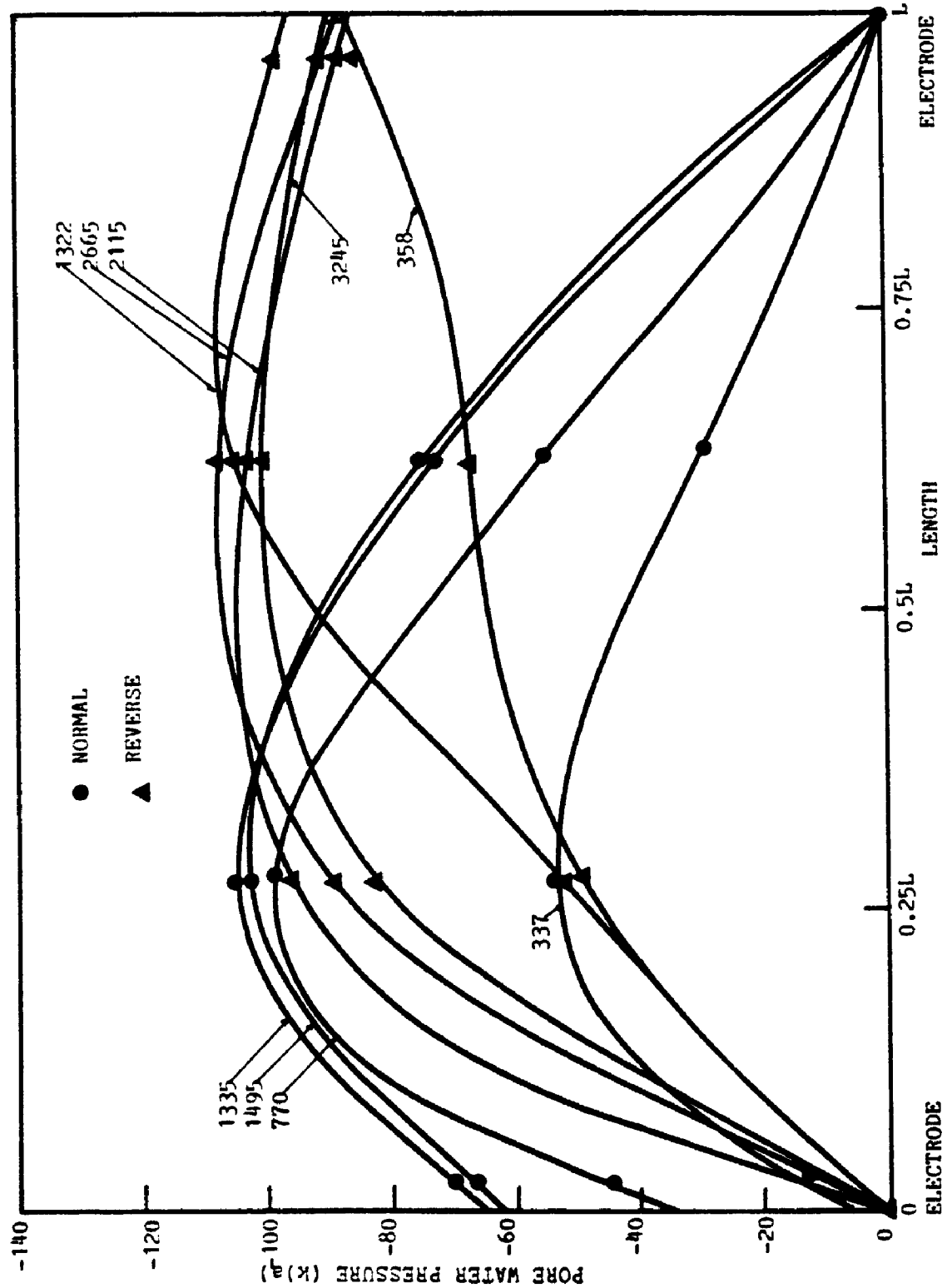

FIGURE A29 PORE WATER PRESSURE DISTRIBUTION WITH TIME (MINUTE), TEST WH-9, 6 V

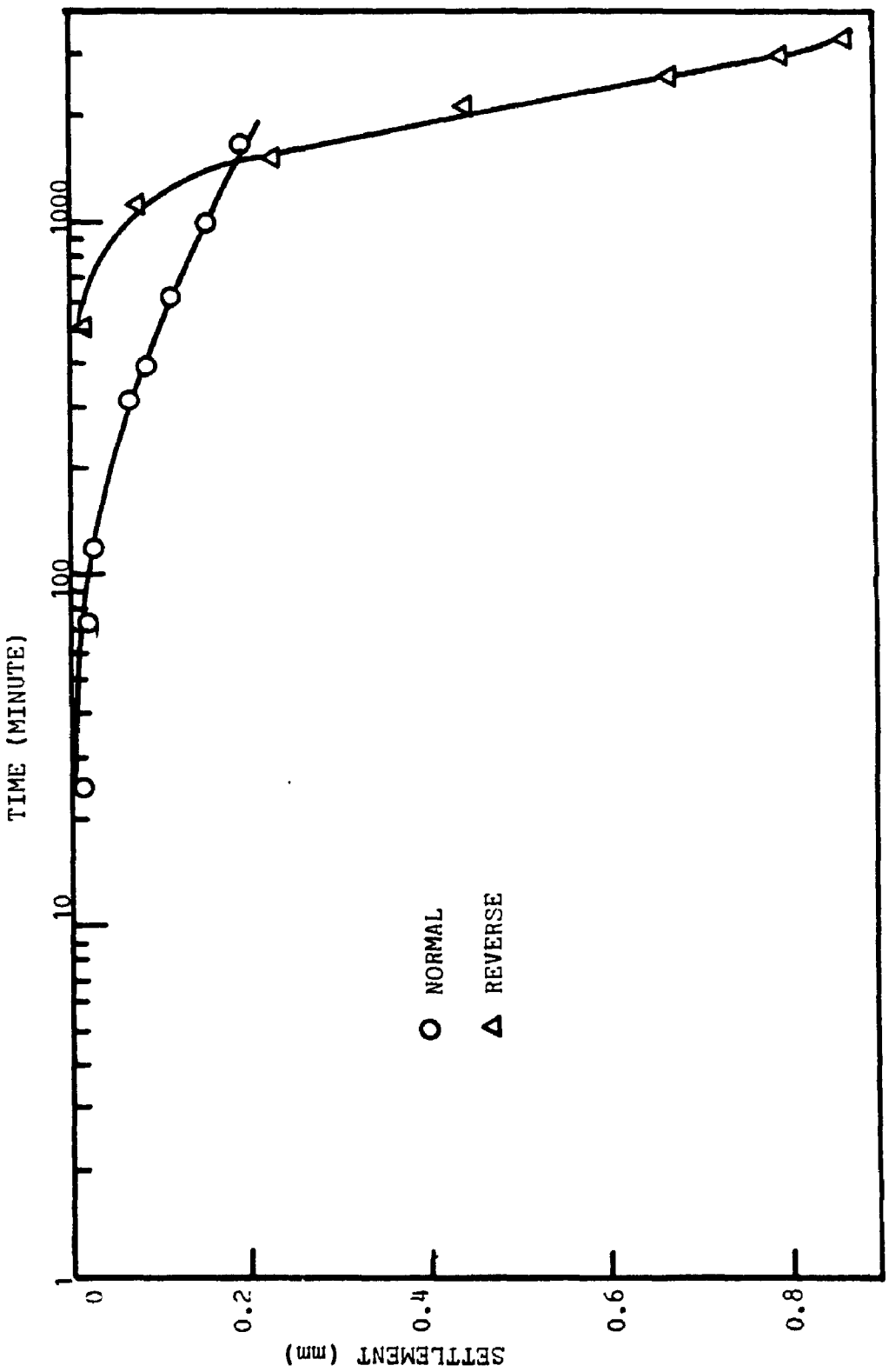

FIGURE A30 SETTLEMENT-TIME CURVE, TEST WH-9, 2 V

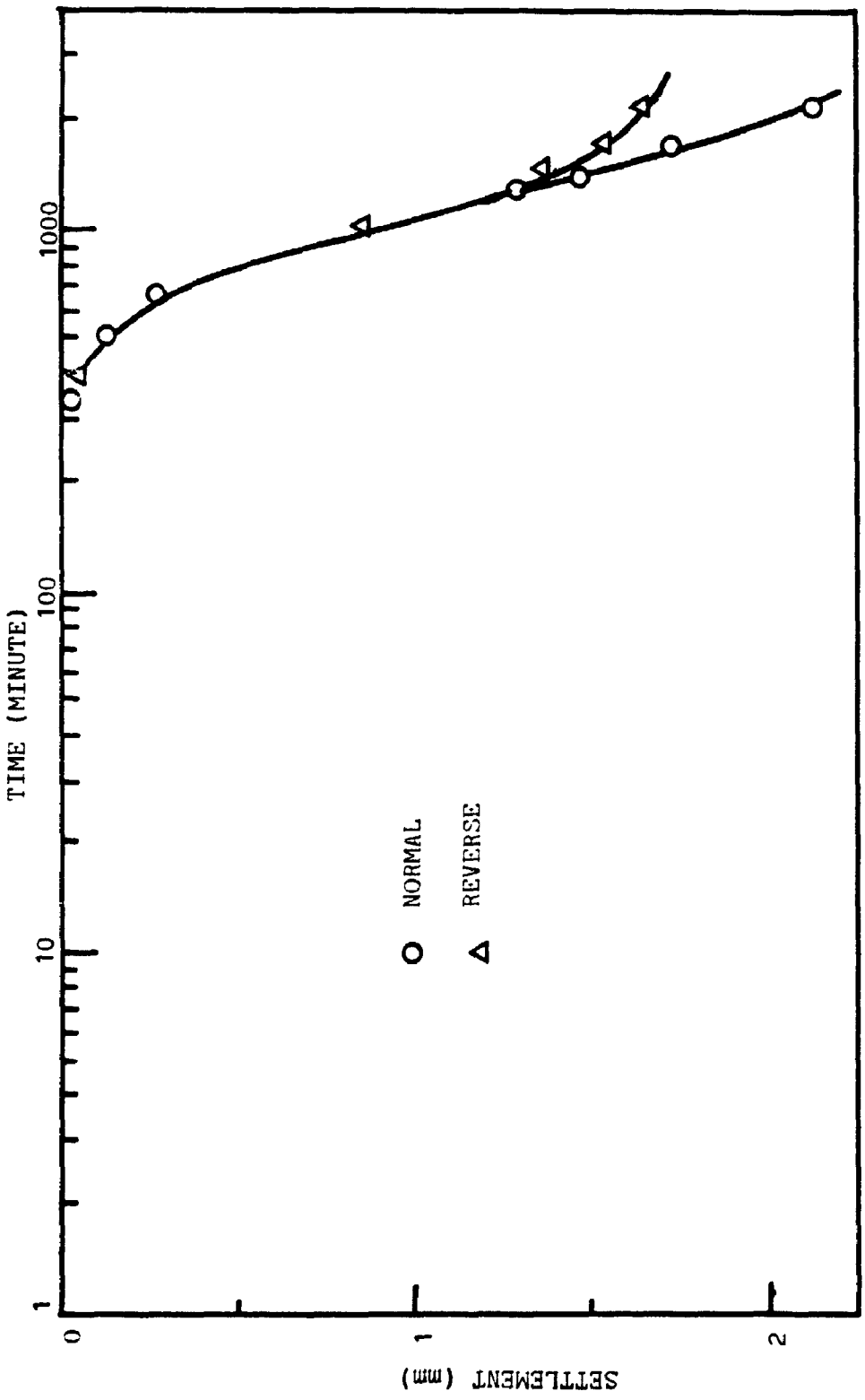

FIGURE A31 SETTLEMENT-TIME CURVE, TEST WH-9, 4 V

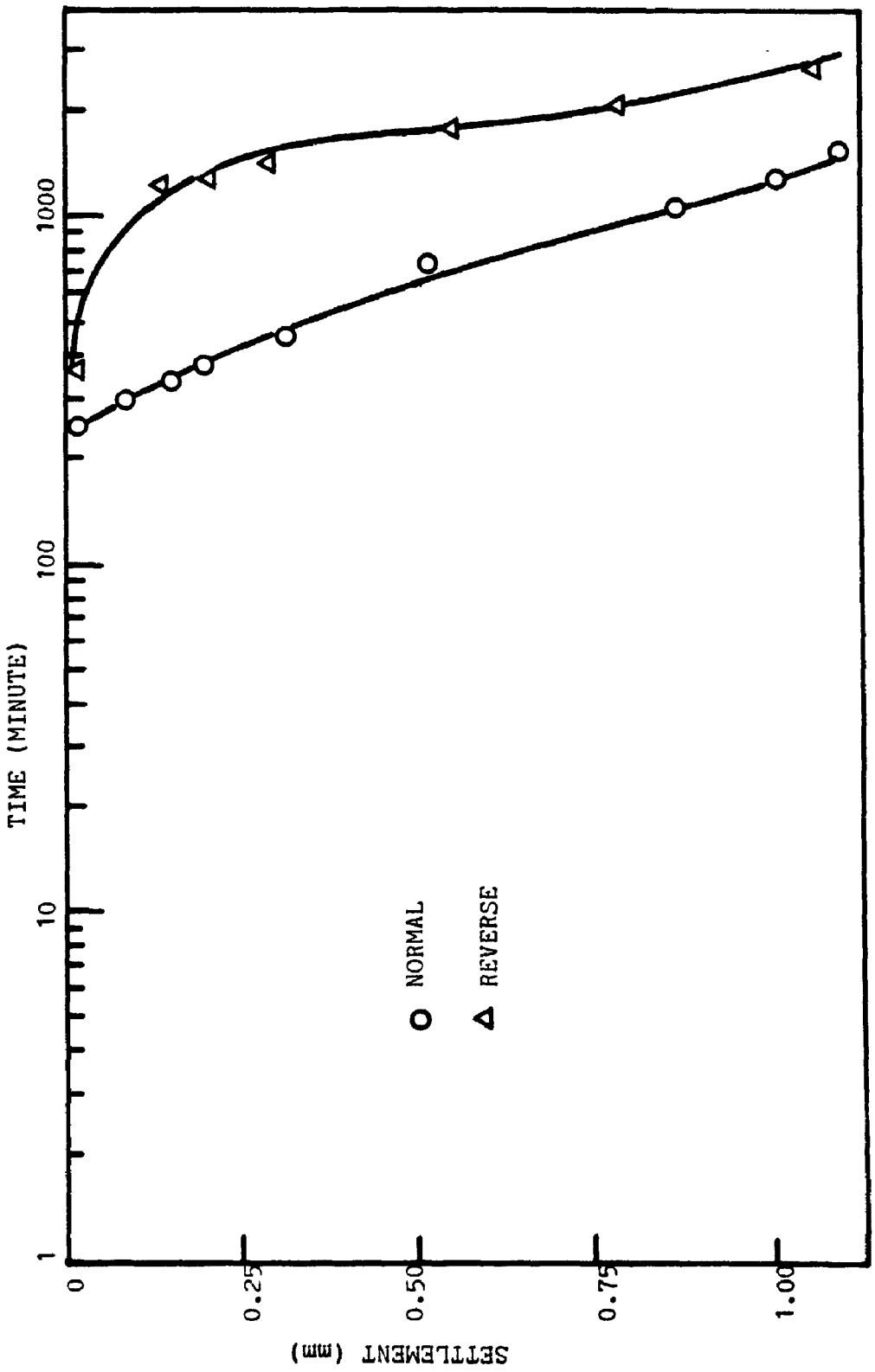

FIGURE A32 SETTLEMENT-TIME CURVE, TEST WH-9, 6 V

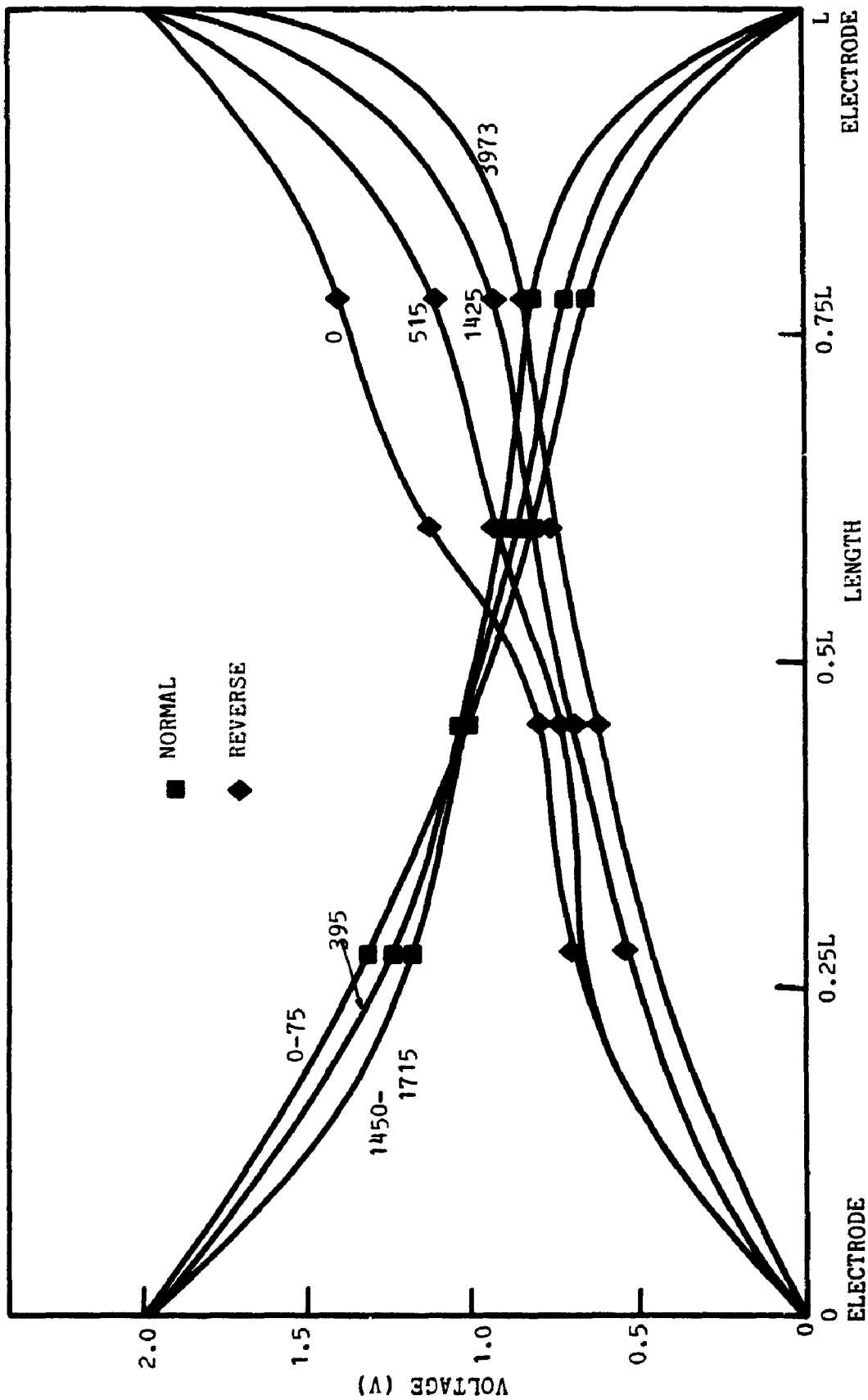

FIGURE A33 VOLTAGE DISTRIBUTION WITHIN SAMPLE WITH TIME (MINUTE), TEST WH-9, 2 V

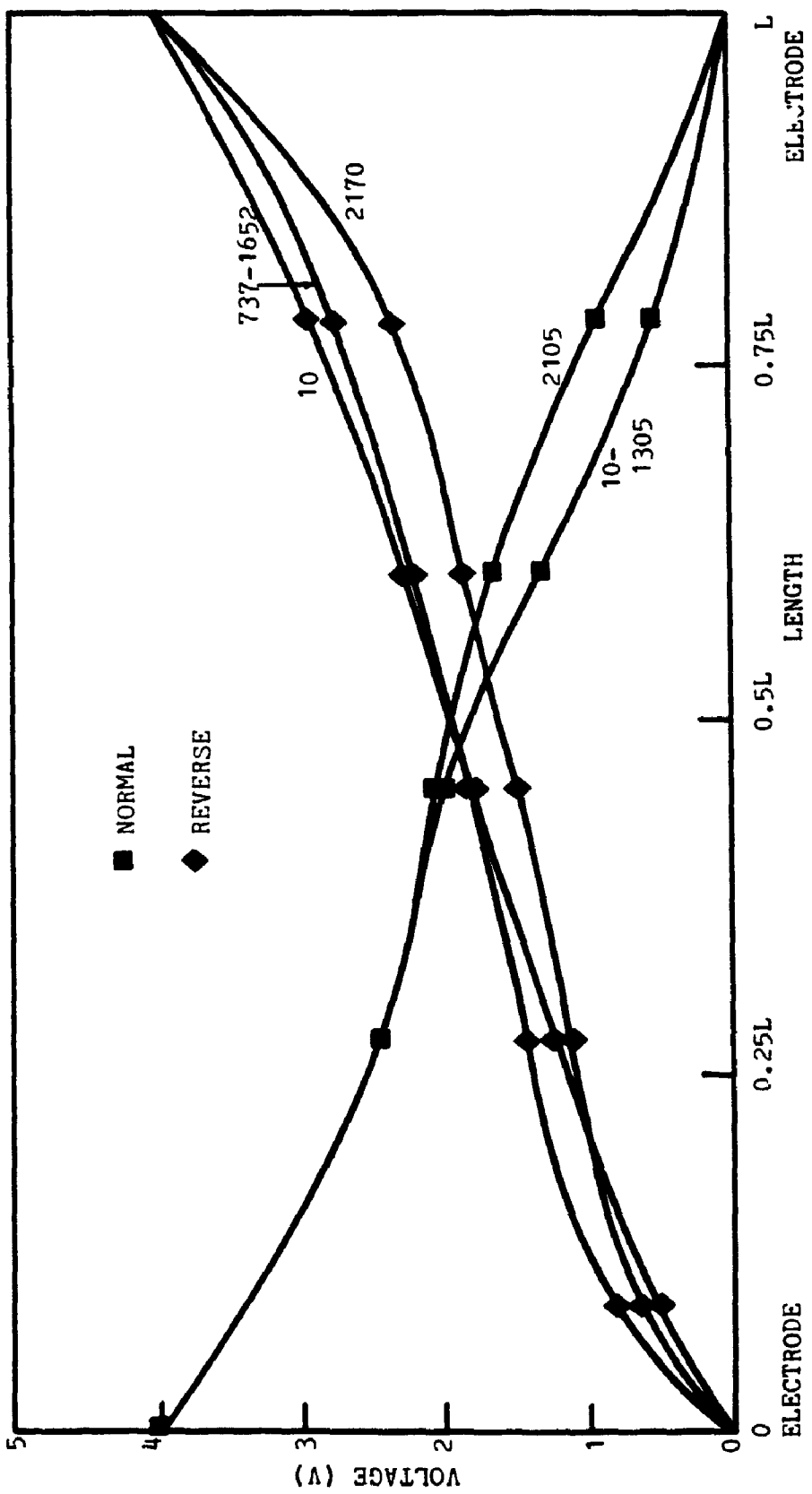

FIGURE A34 VOLTAGE DISTRIBUTION WITHIN SAMPLE WITH TIME (MINUTE), TEST WH-9, 4 V

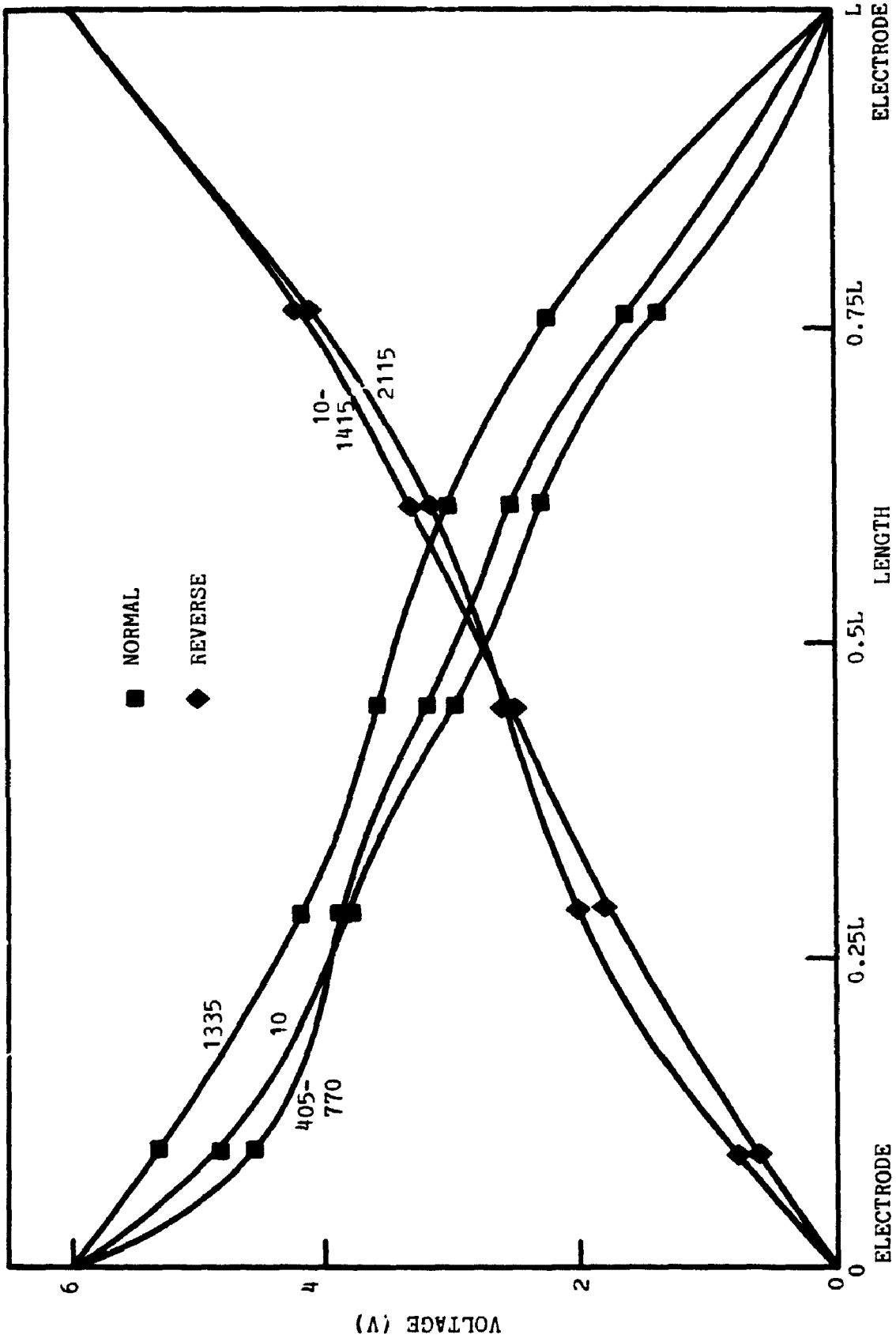

FIGURE A35 VOLTAGE DISTRIBUTION WITH SAMPLE WITH TIME (MINUTE), TEST WH-9, 6 V

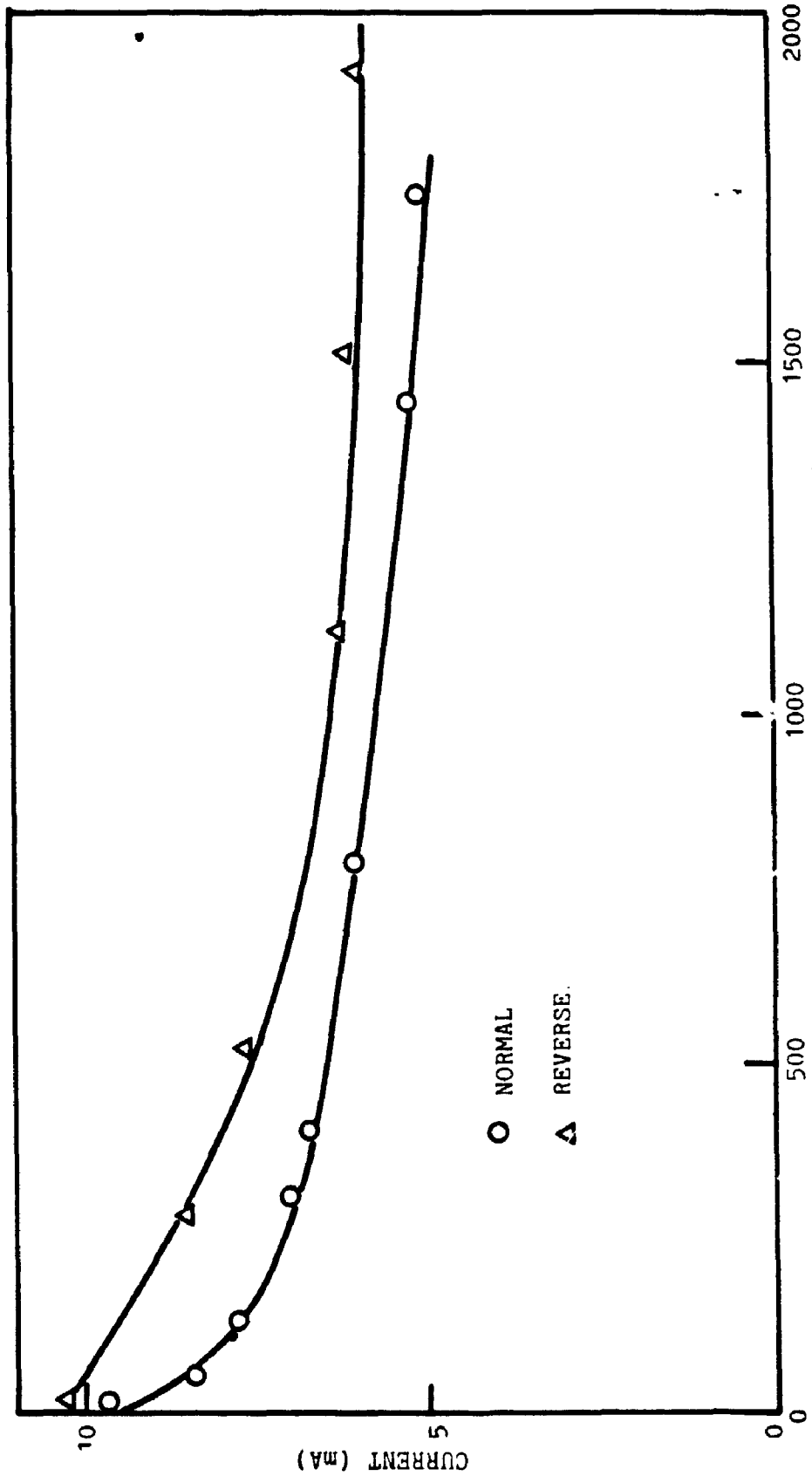

FIGURE A36 CURRENT VARIATION WITH TIME, TEST WH-9, 2 V

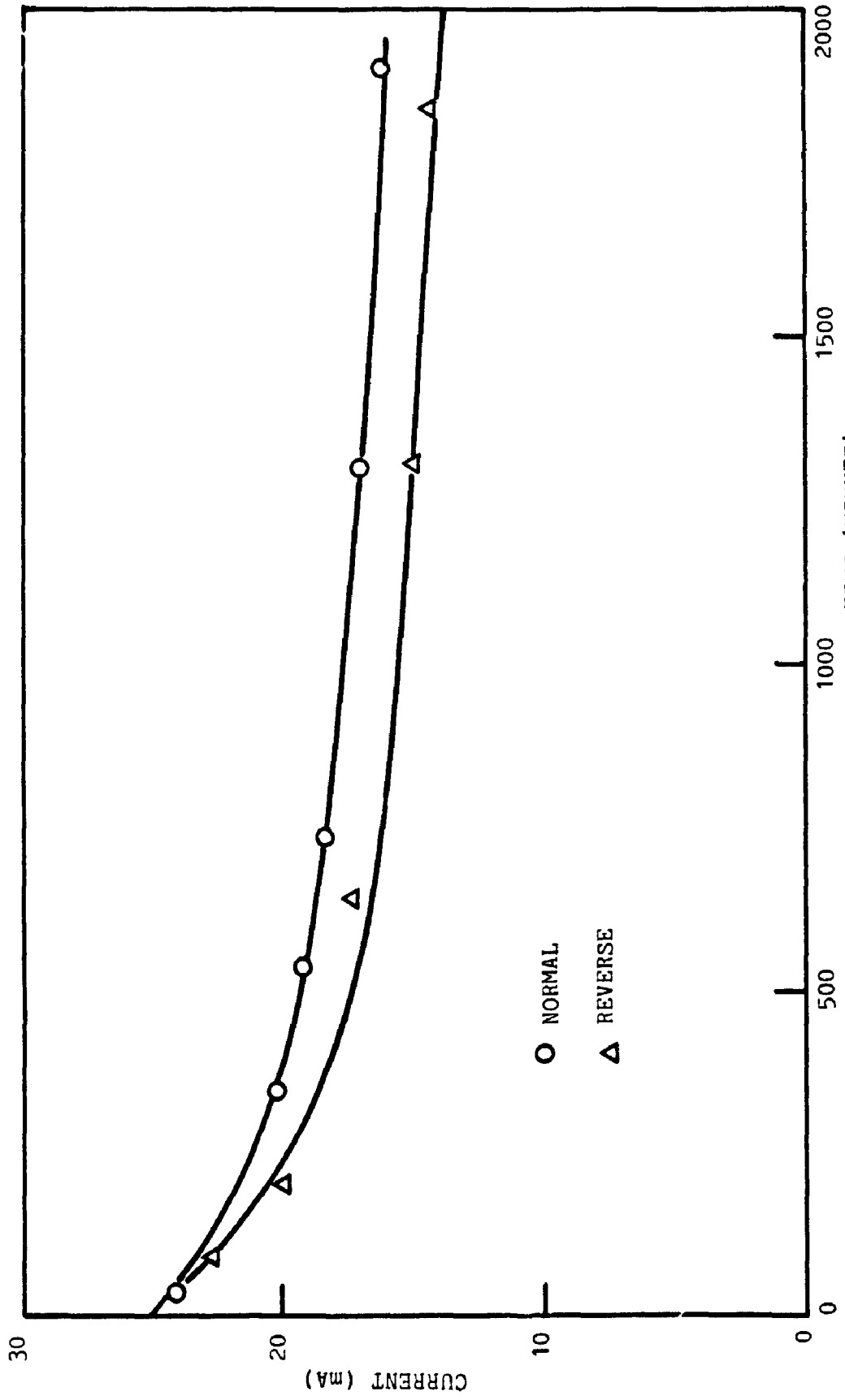

FIGURE A37 CURRENT VARIATION WITH TIME, TEST WH-9, 4 V

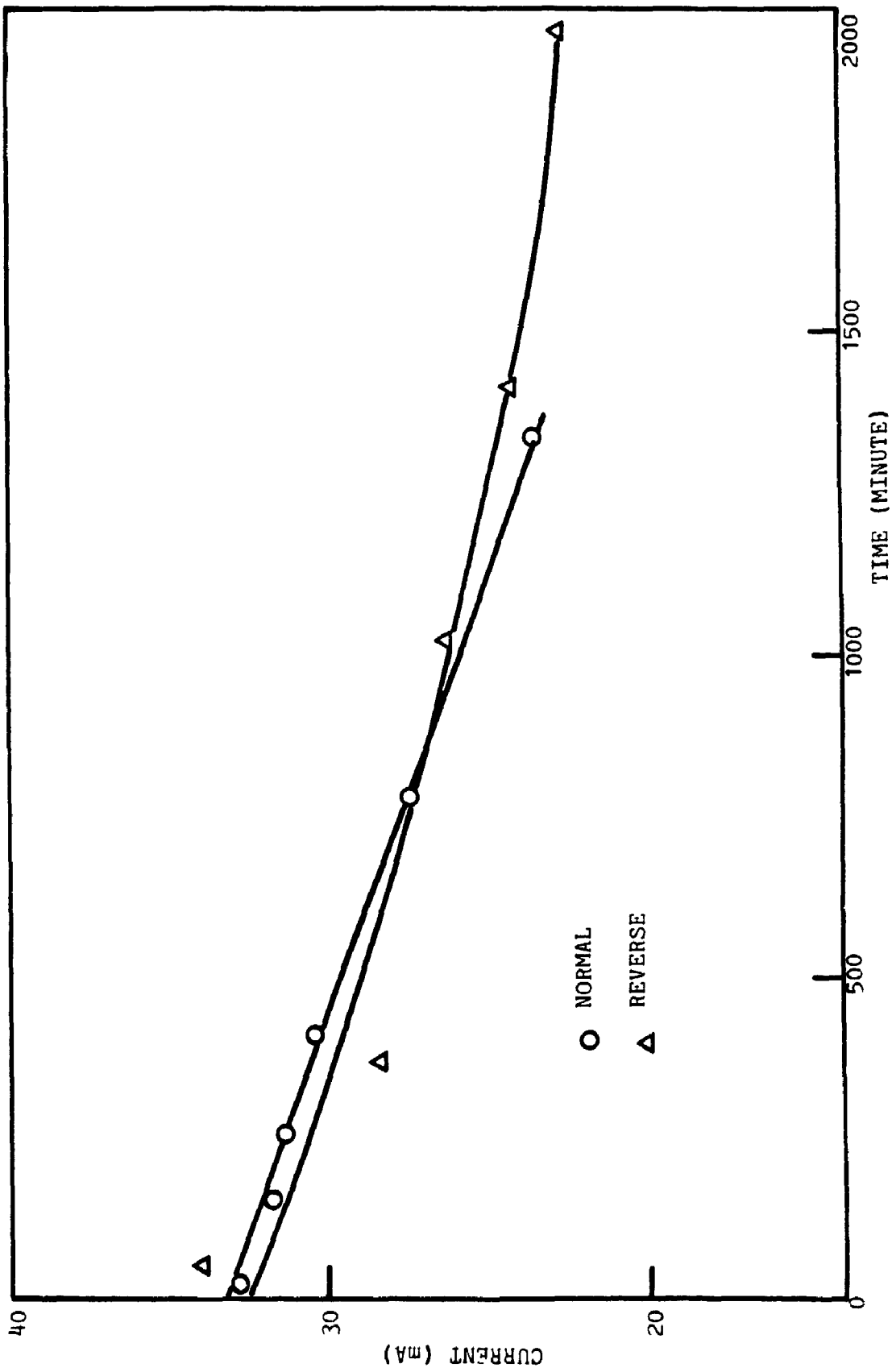

FIGURE A38 CURRENT VARIATION WITH TIME, TEST WH-9, 6 V

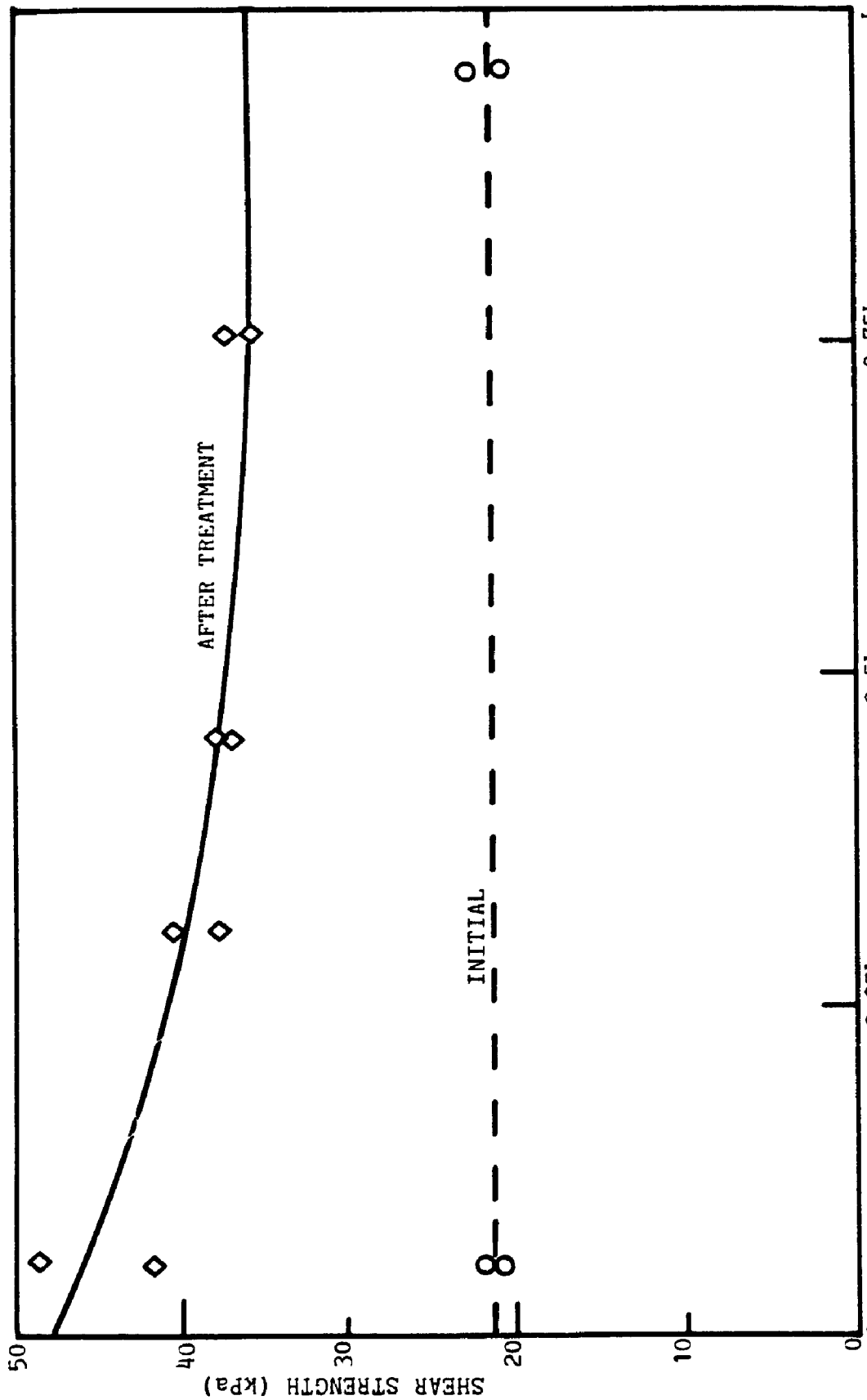

FIGURE A 39 VANE STRENGTH BEFORE AND AFTER TREATMENT, TEST WH-9, 2, 4 and 6 V WITH ELECTRODE REVERSAL

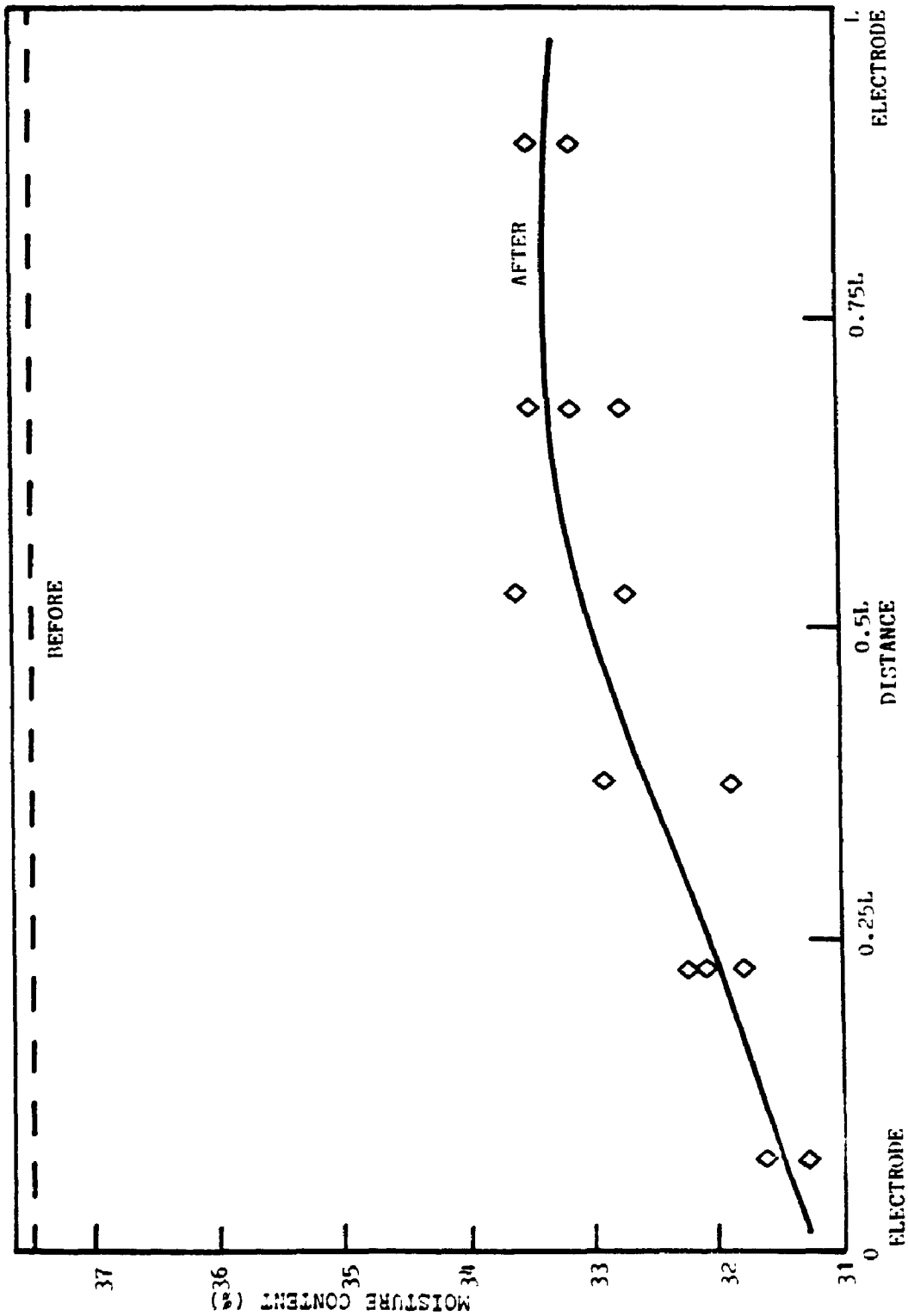

FIG. A40 MOISTURE CONTENT BEFORE AND AFTER TREATMENT TEST WH-9, 2, 4, 6 volts WITH ELECTRODE REVERSAL

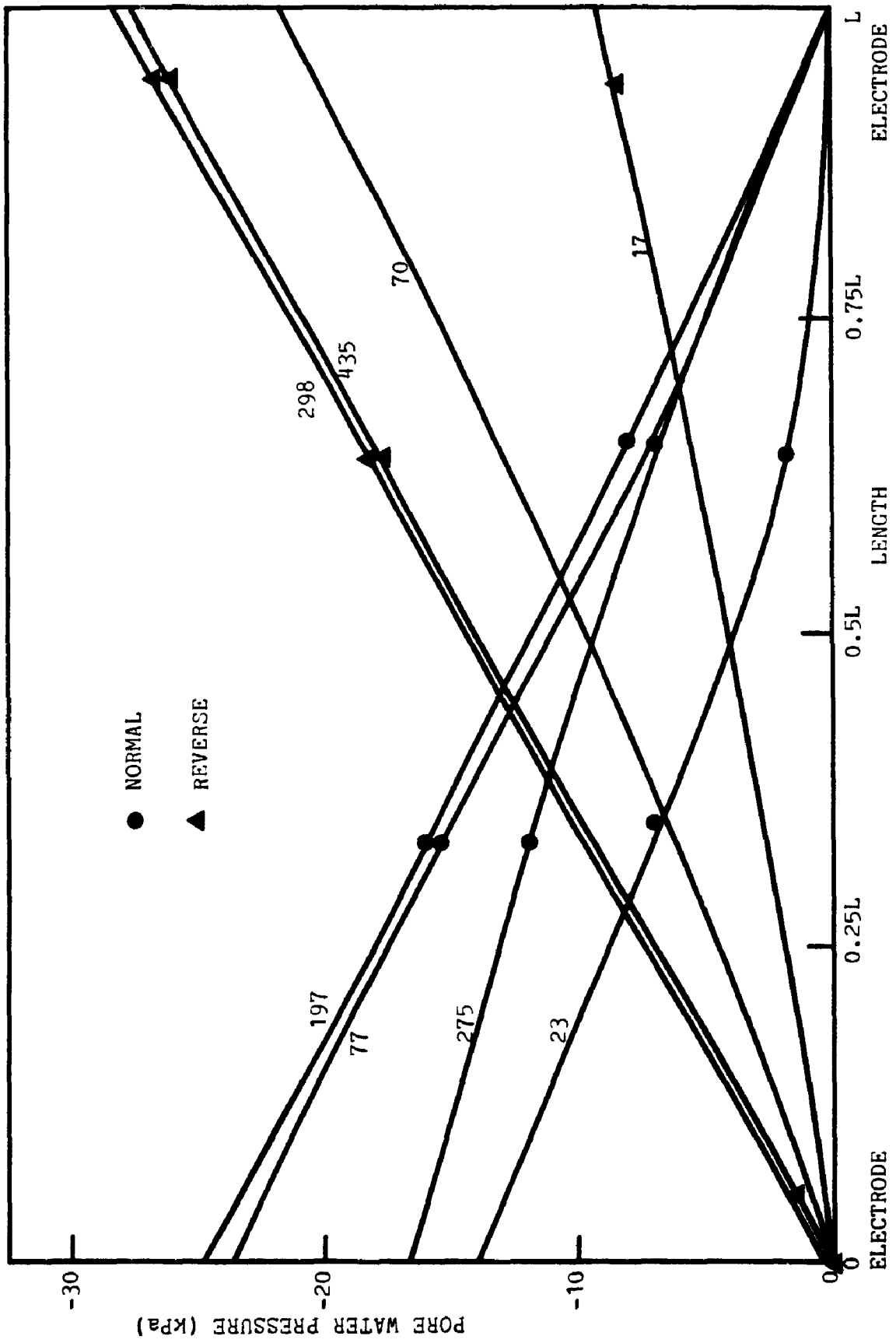

FIGURE A41 PORE WATER PRESSURE DISTRIBUTION WITH TIME (MINUTE), TEST GV-4A, 3 V

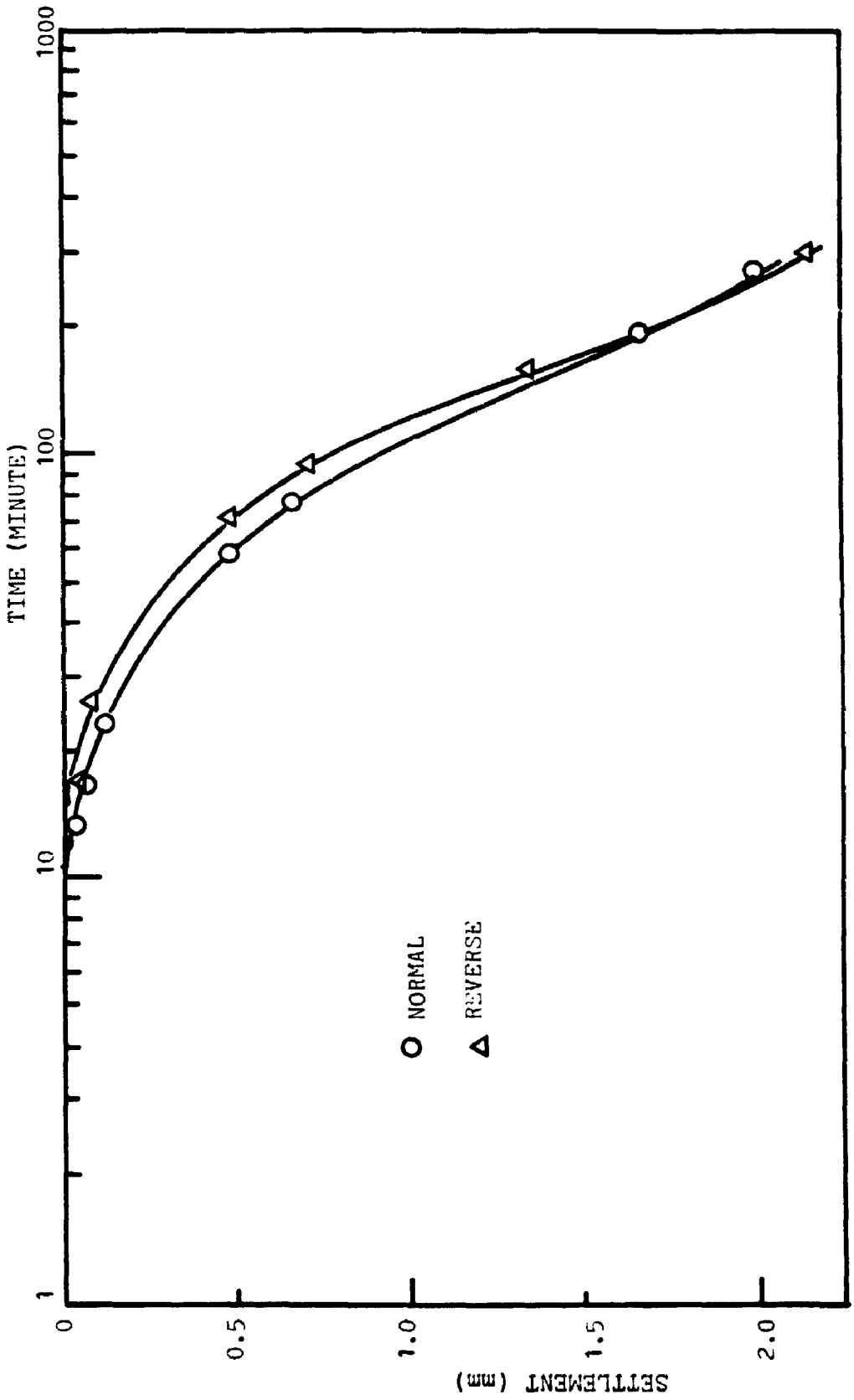

FIGURE A42 SETTLEMENT-TIME CURVE, TEST GV-4A, 3 V

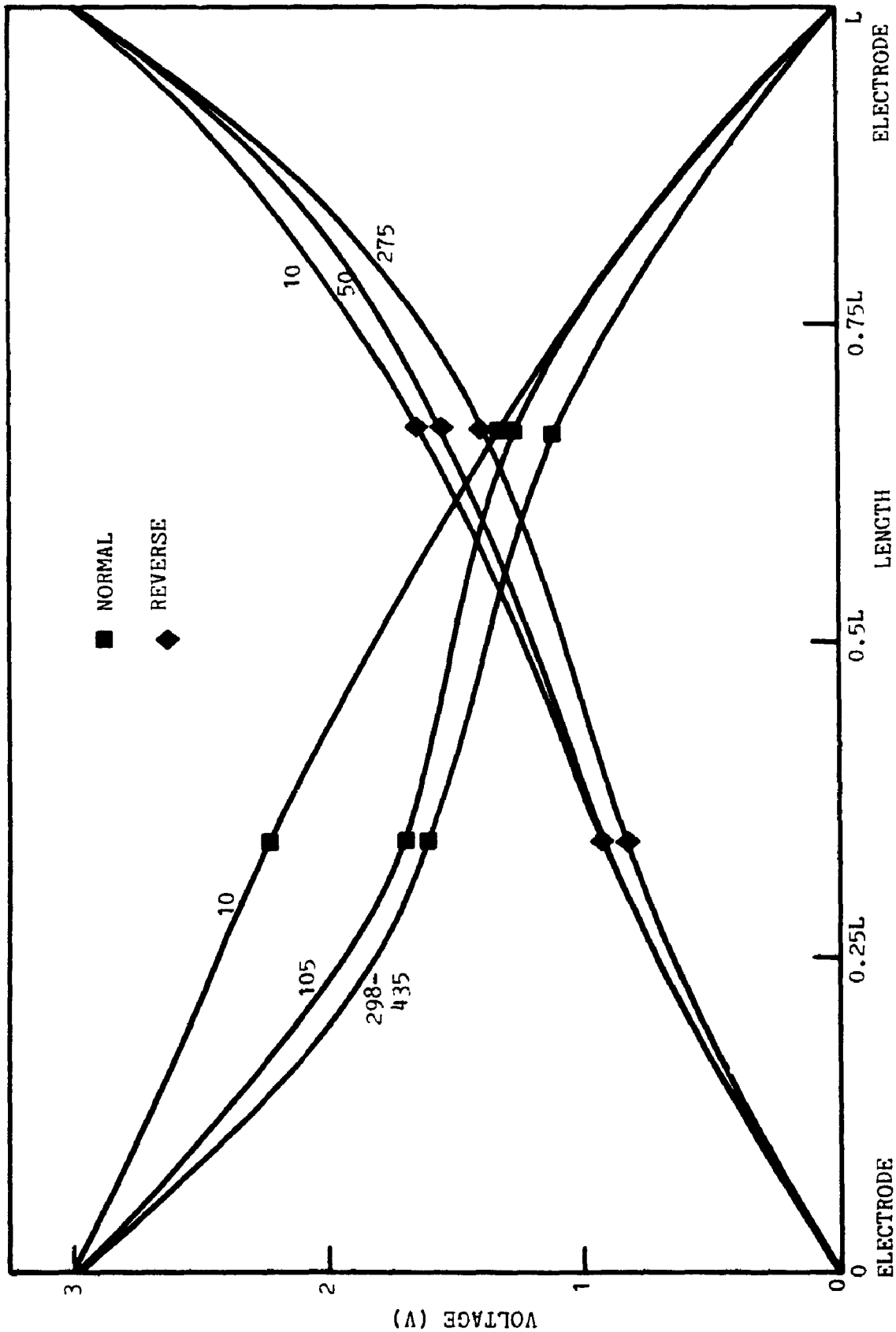

FIGURE A43 VOLTAGE DISTRIBUTION WITHIN SAMPLE WITH TIME (MINUTE), TEST GV-4A, 3 V

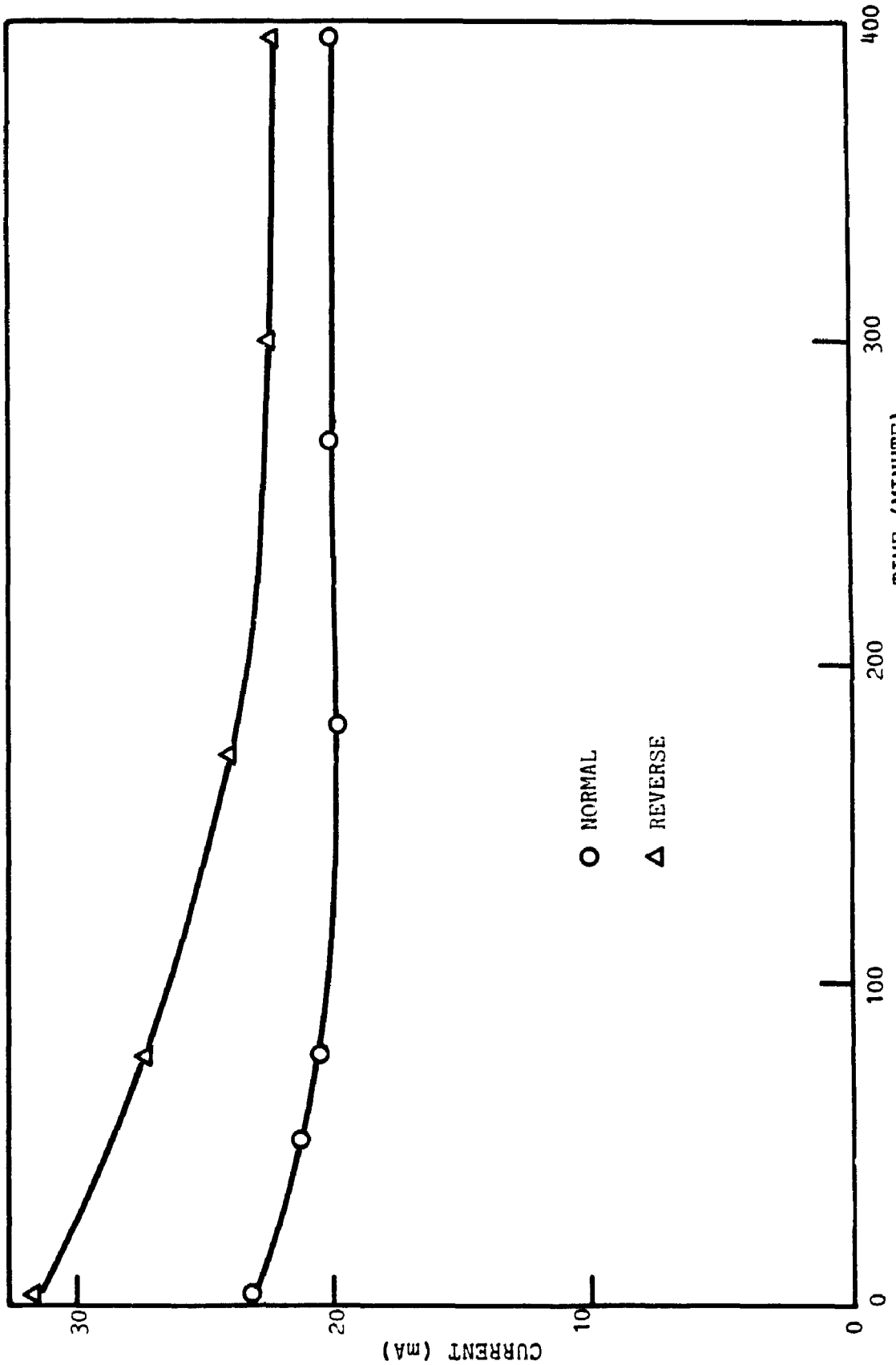

FIGURE A44 CURRENT VARIATION WITH TIME, TEST GV-4A, 3 V

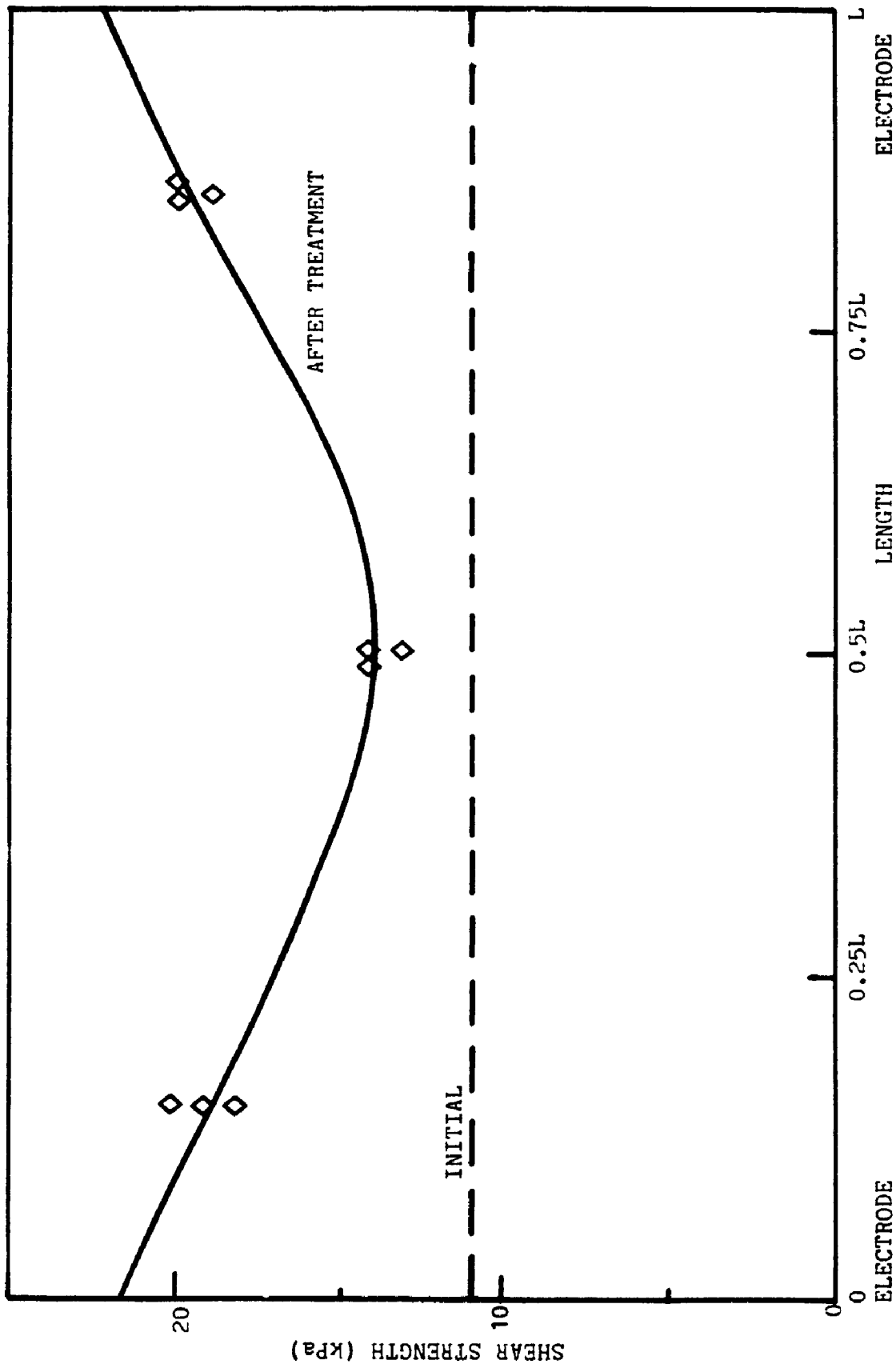

FIGURE A45 VANE STRENGTH BEFORE AND AFTER TREATMENT, TEST GV-4A, 3 V WITH ELECTRODE REVERSAL

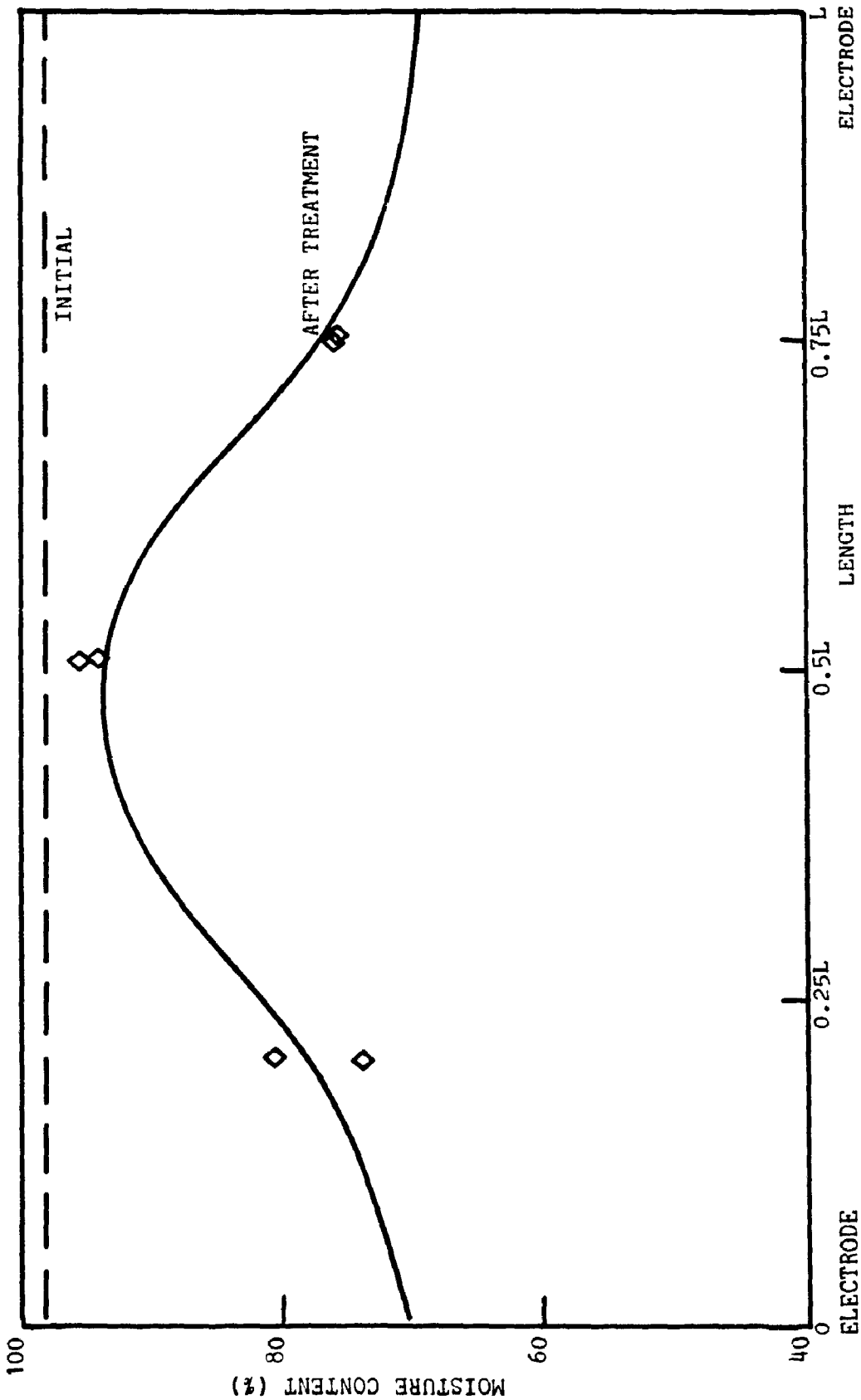

FIGURE A46 MOISTURE CONTENT BEFORE AND AFTER TREATMENT, TEST CV-4A, 3 V WITH ELECTRODE REVERSAL

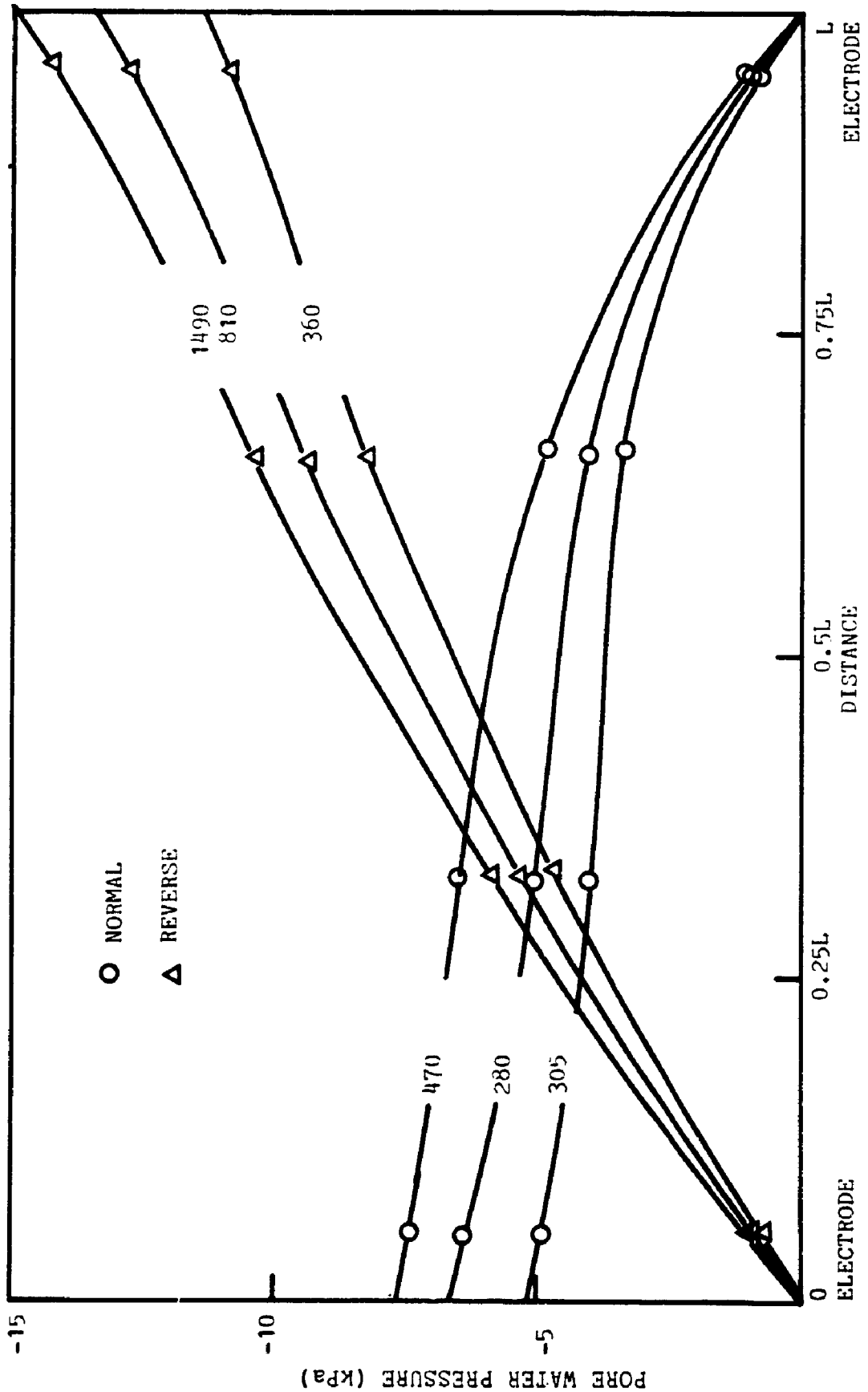

FIG. A47 PORE WATER PRESSURE DISTRIBUTION WITH TIME (MINUTES), TEST GV-4B 1.5 V

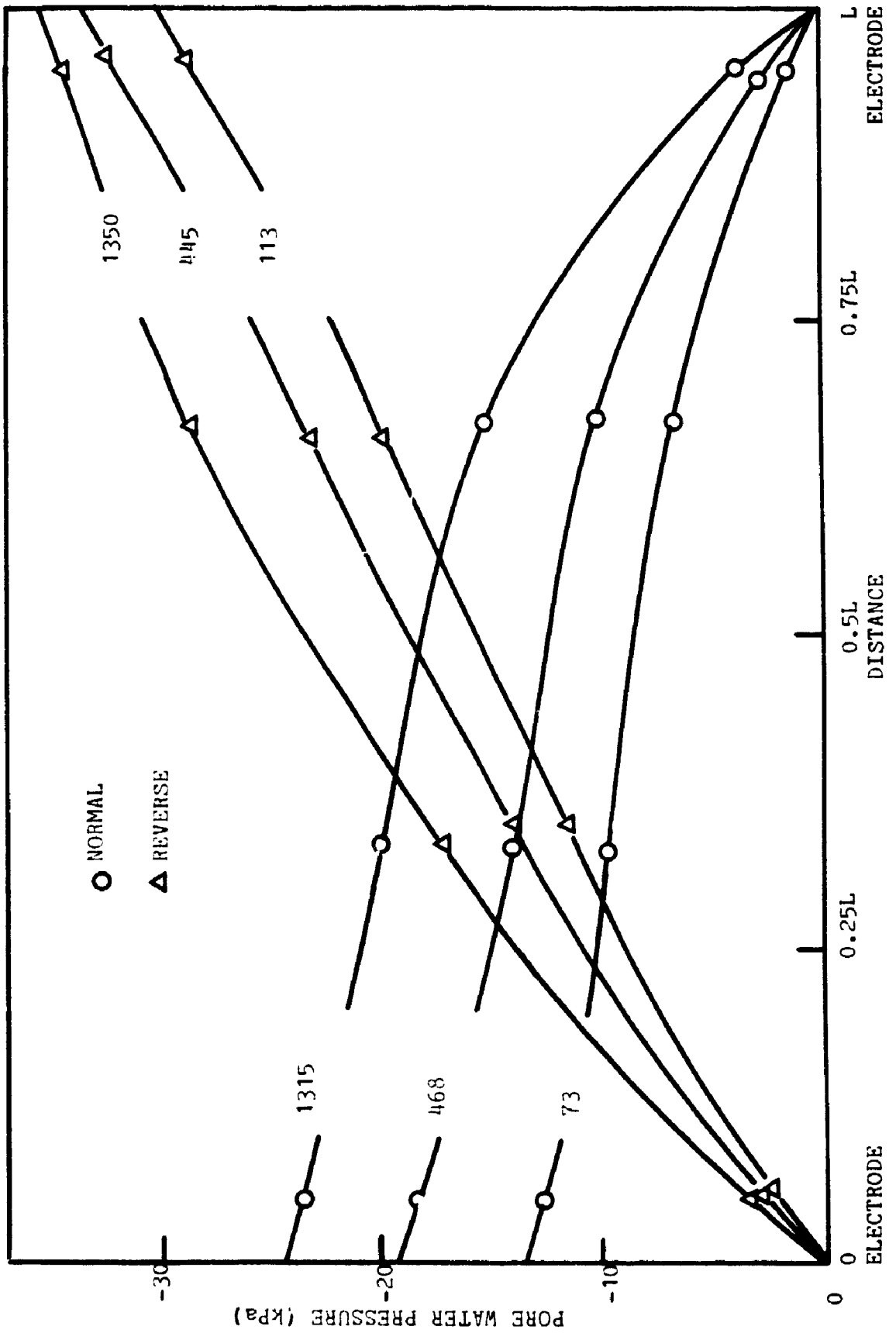

FIG. A48 PORE WATER PRESSURE DISTRIBUTION WITH TIME (MINUTES) TEST GV-4B 2.4 V

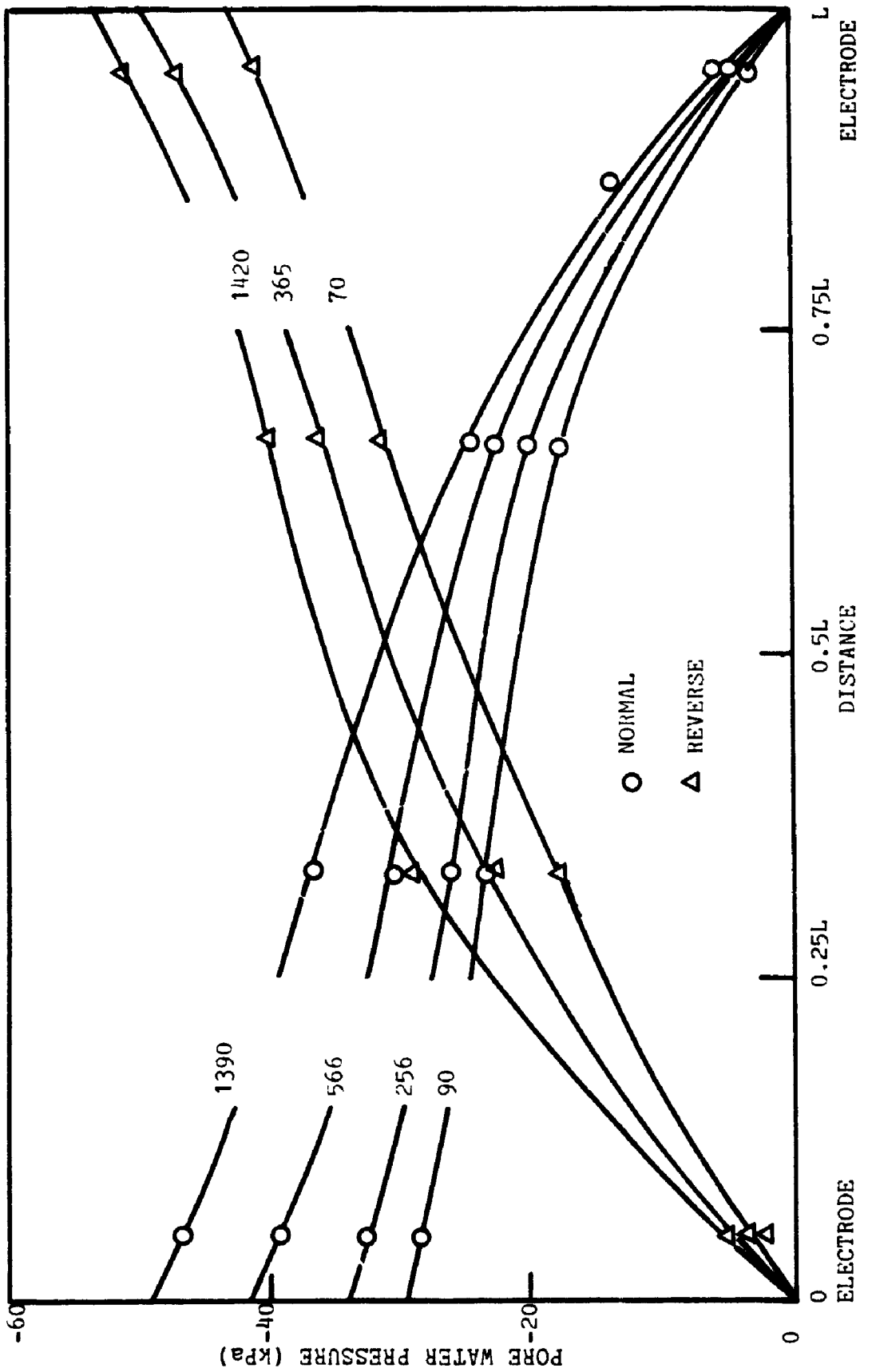

FIG. A49 PORE WATER PRESSURE DISTRIBUTION WITH TIME (MINUTES), TEST GV-4B, 4 V

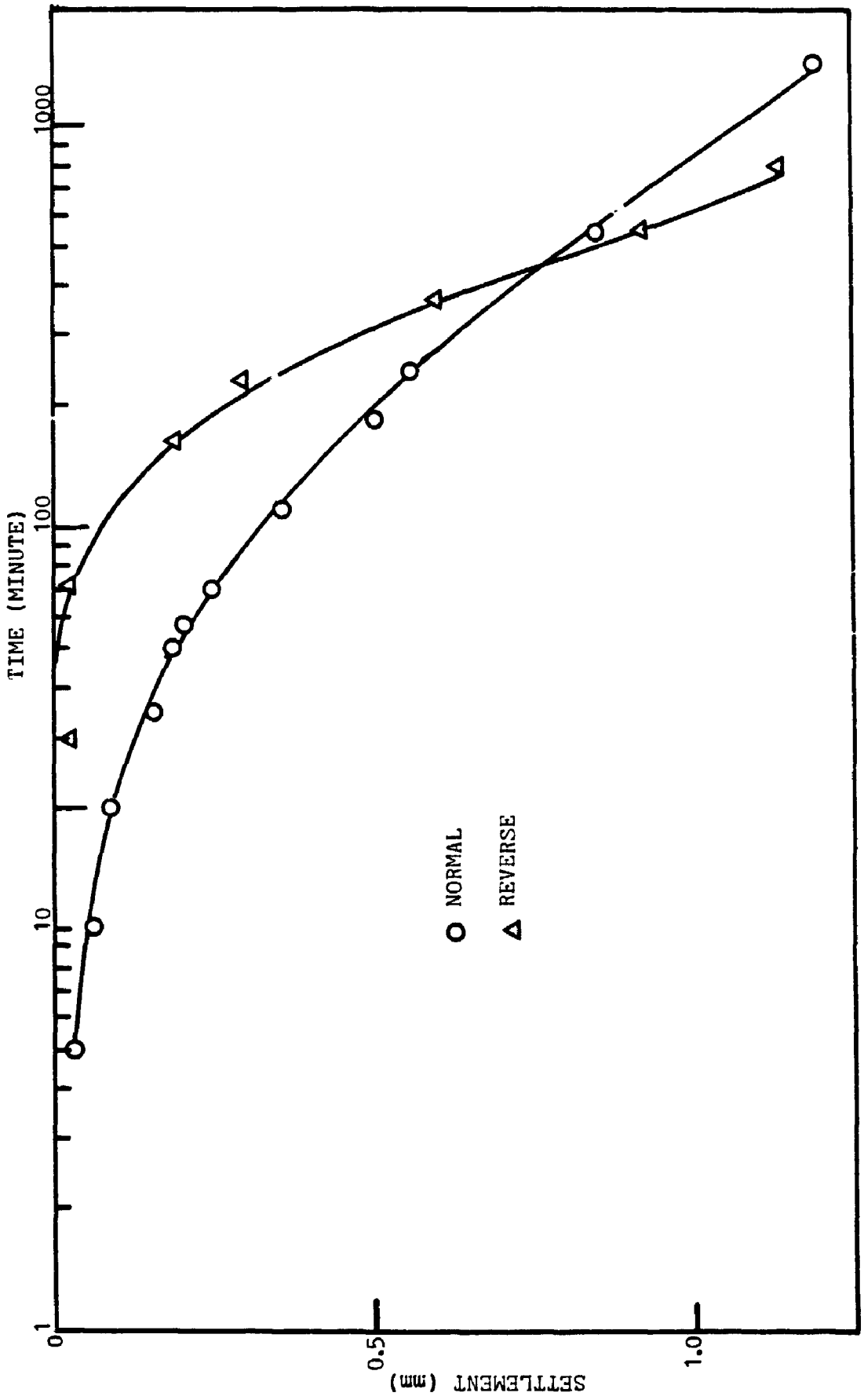

FIGURE A50 SETTLEMENT-TIME CURVE, TEST GV-4B, 1.5 V

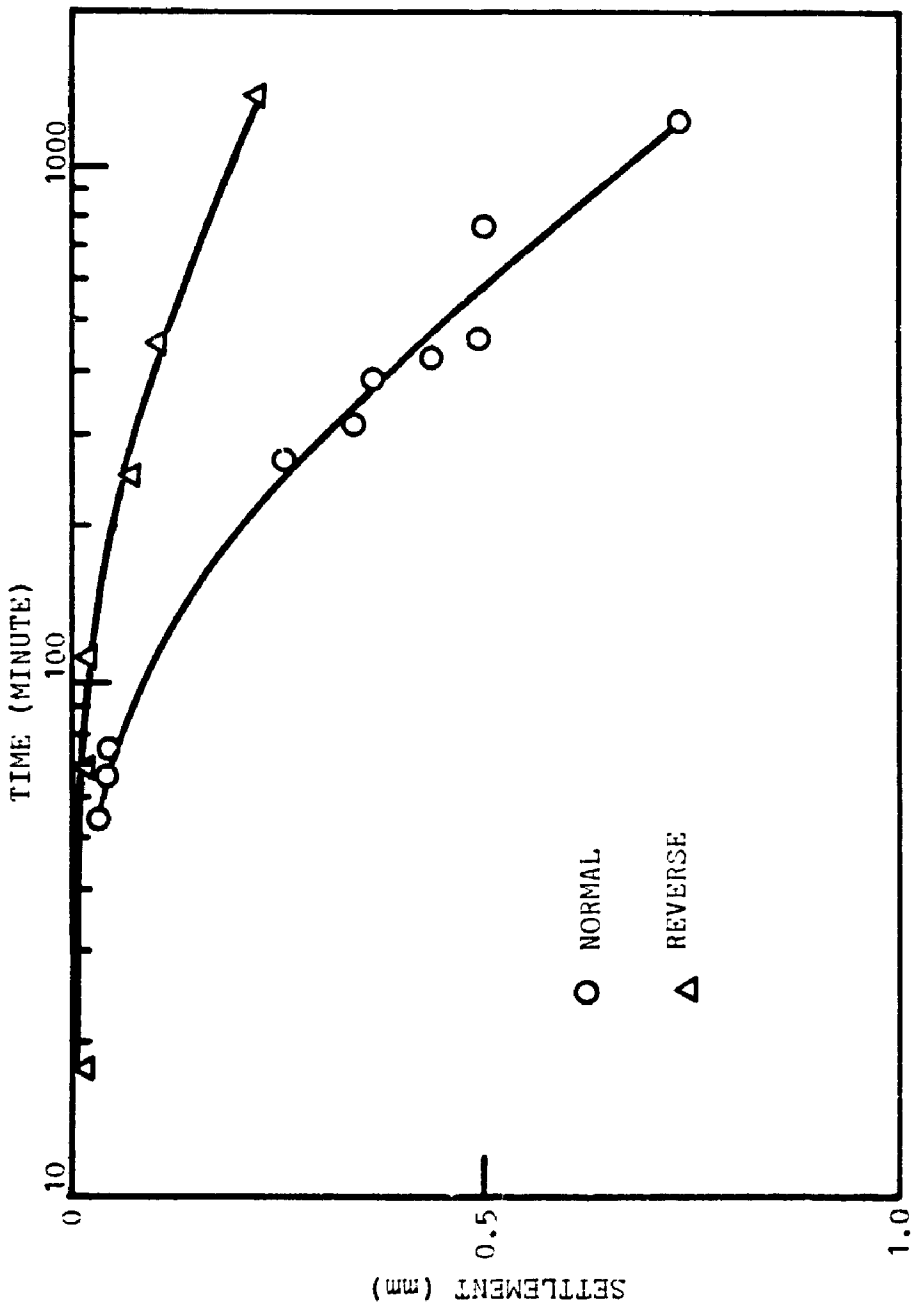

FIGURE A51 SETTLEMENT-TIME CURVE, TEST GV-4B, 2.4 V

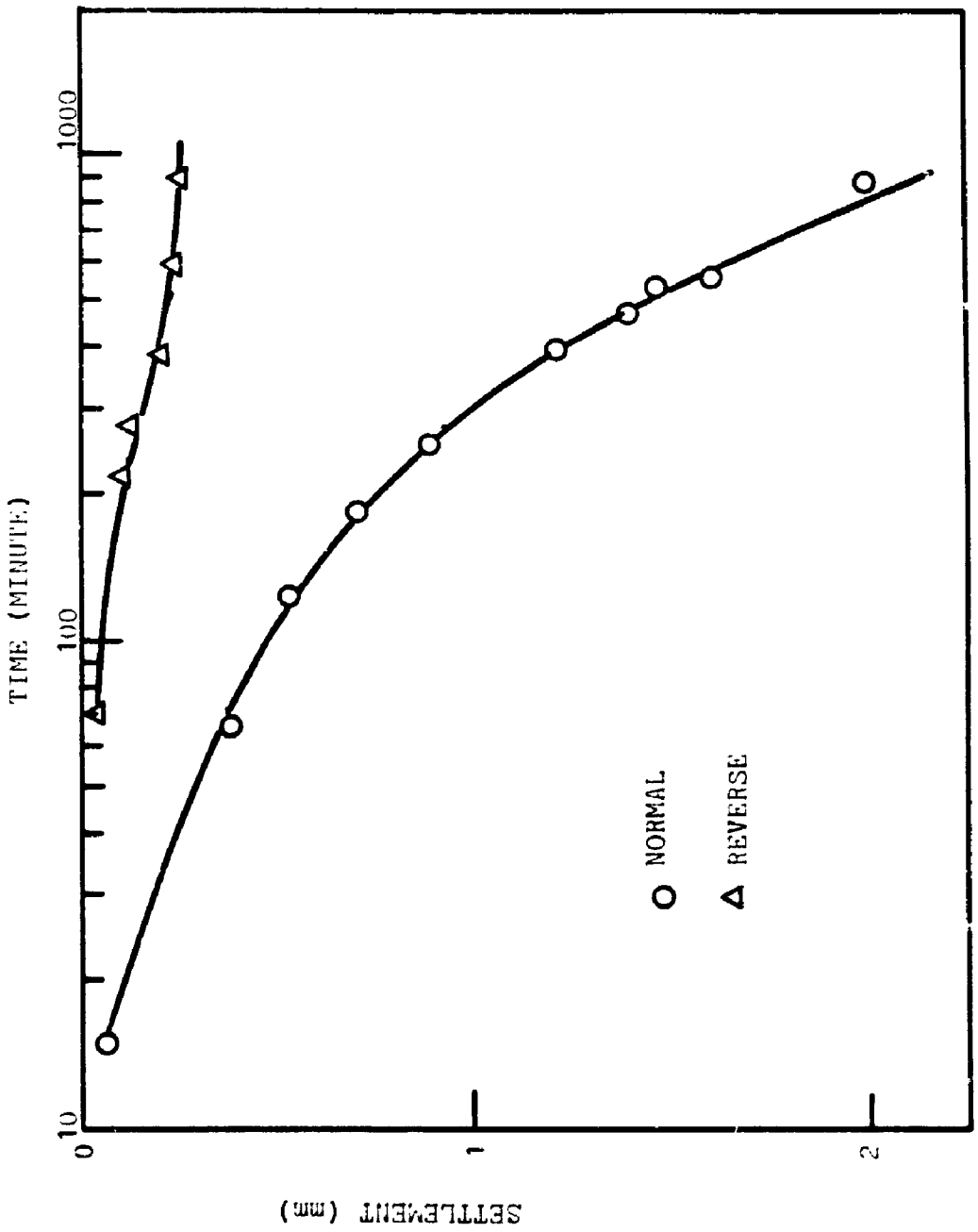

FIGURE A52 SETTLEMENT-TIME CURVE, TEST GV-4R, 4 V

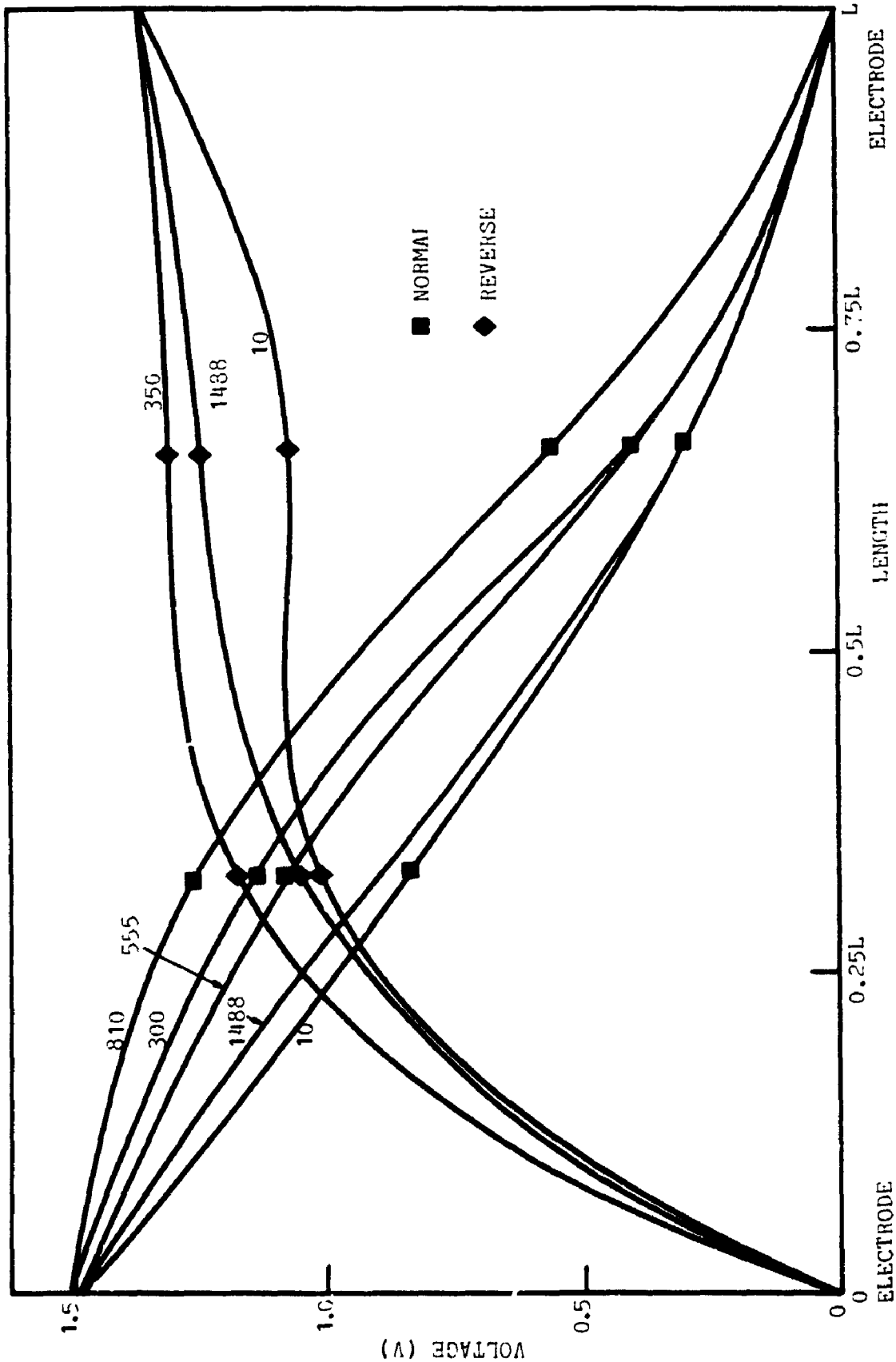

FIGURE A53 VOLTAGE VARIATION WITHIN SAMPLE WITH TIME (MINUTE), TEST GV-4B, 1.5 V

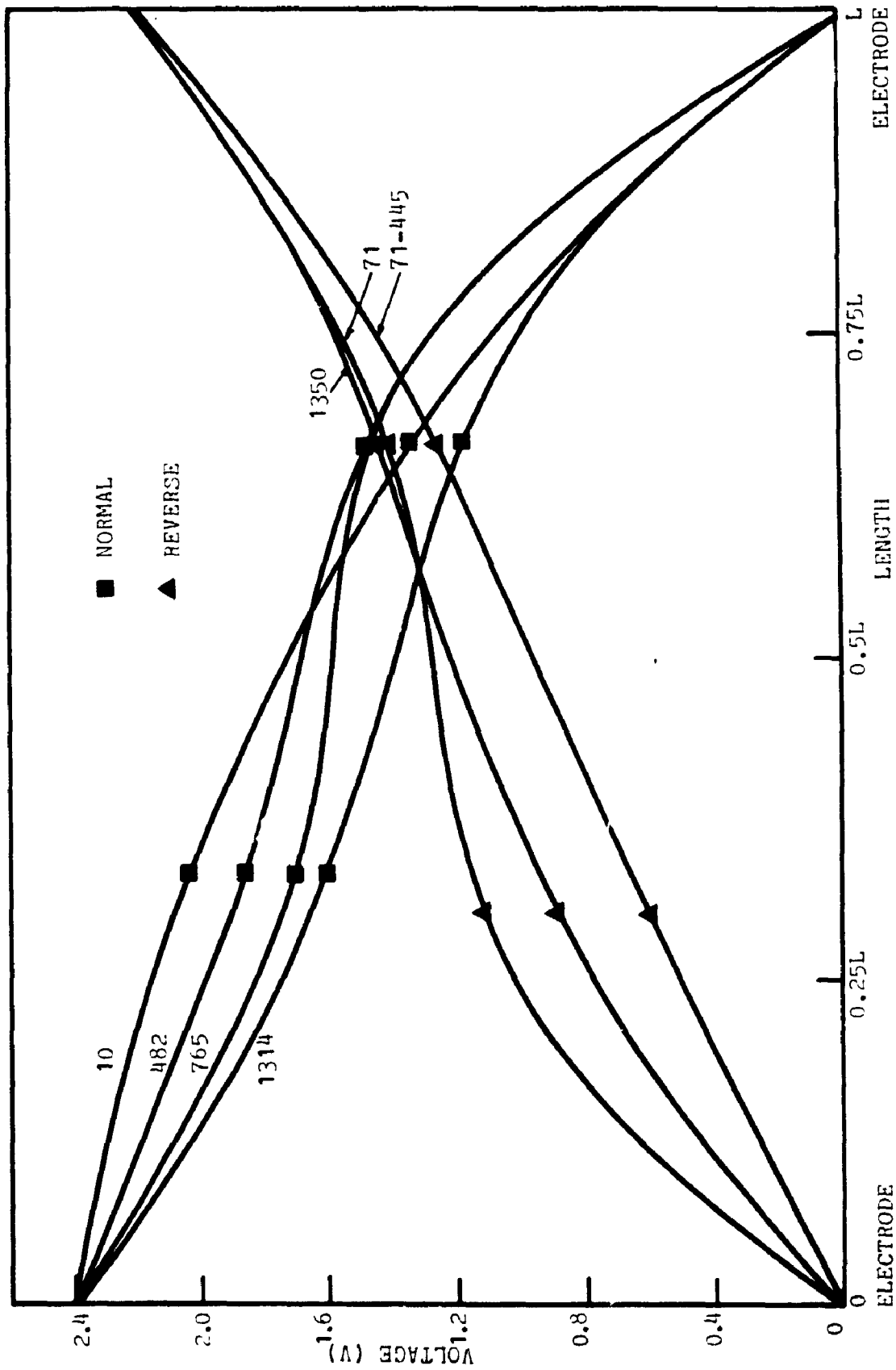

FIGURE A54 VOLTAGE VARIATION WITHIN SAMPLE WITH TIME (MINUTE), TEST GV-4B, 2.4 V

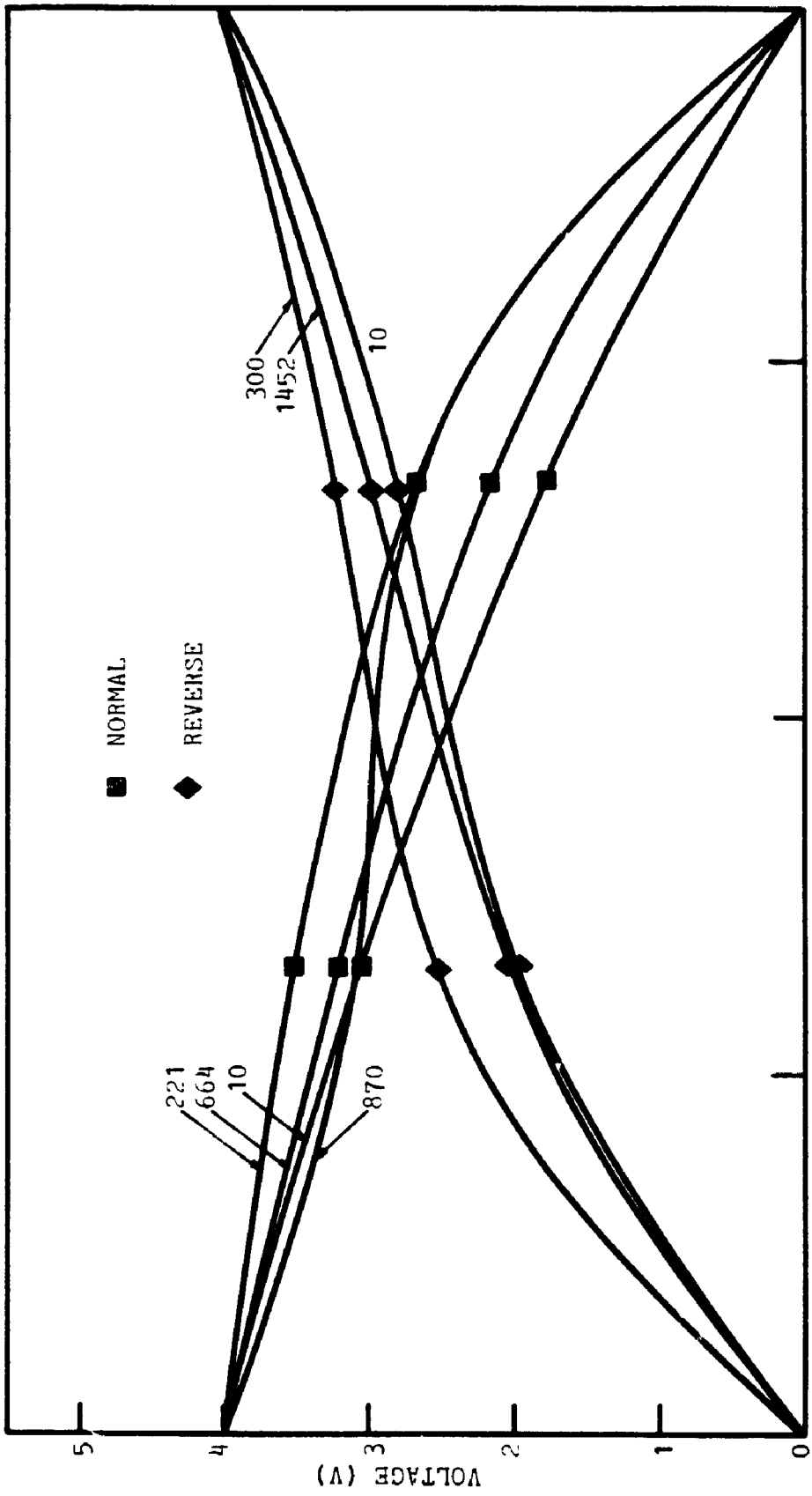

FIGURE A55 VOLTAGE VARIATION WITHIN SAMPLE WITH TIME, TEST GW-4B, 4 V

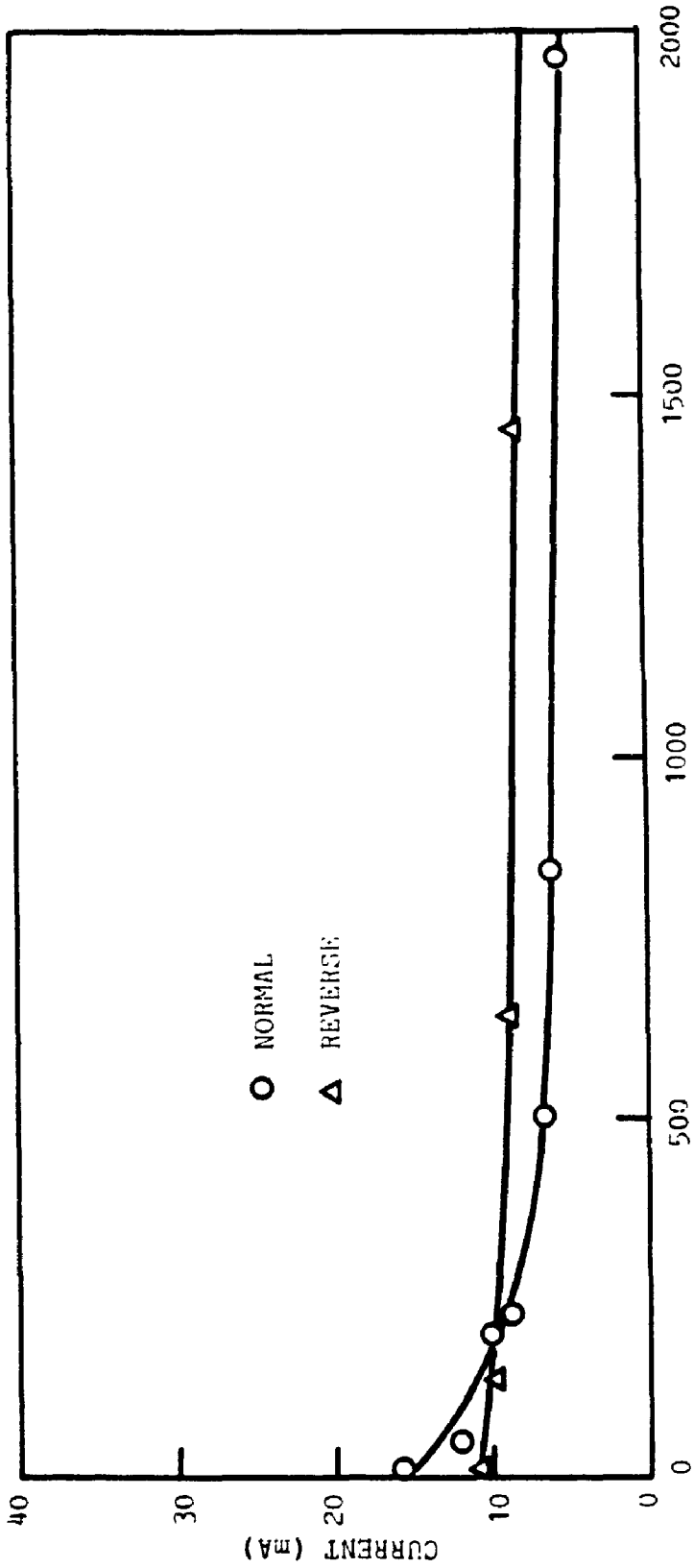

FIGURE A56 CURRENT VARIATION WITH TIME, TEST GV-4B, 1.5 V

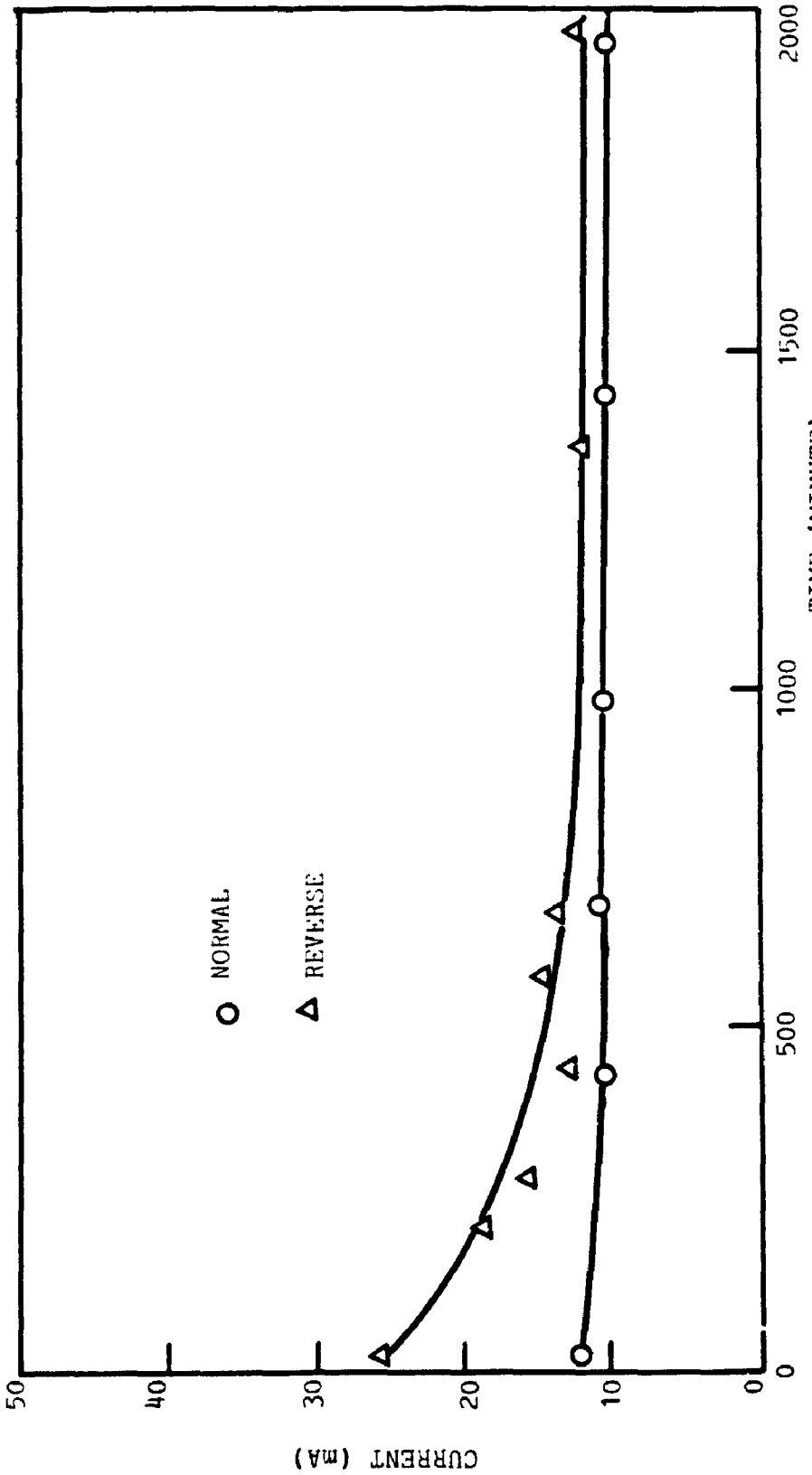

FIGURE A57 CURRENT VARIATION WITH TIME, TEST GV-4B, 2.4 V

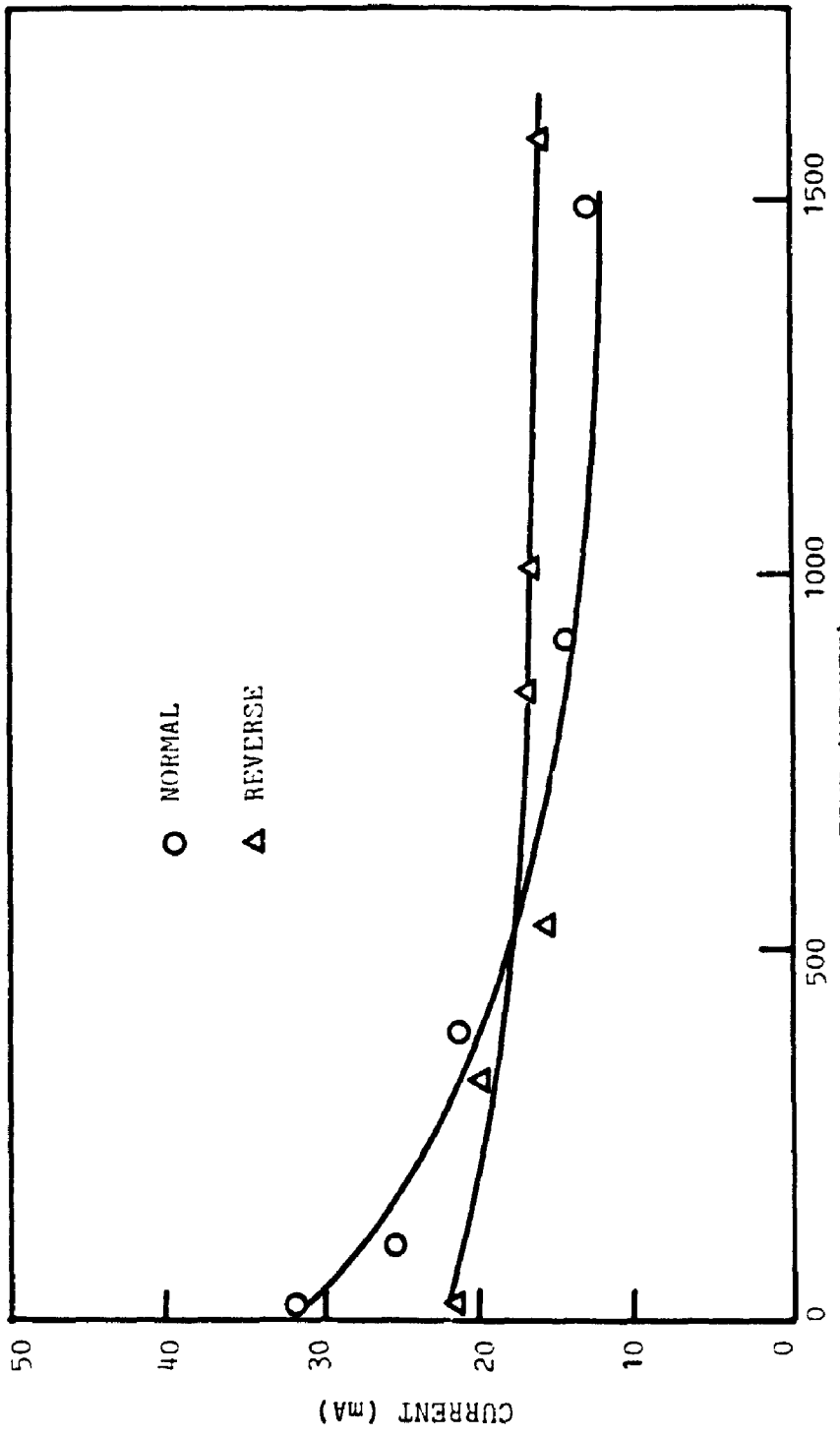

FIGURE A58 CURRENT VARIATION WITH TIME, TEST GV-4B, 4 V

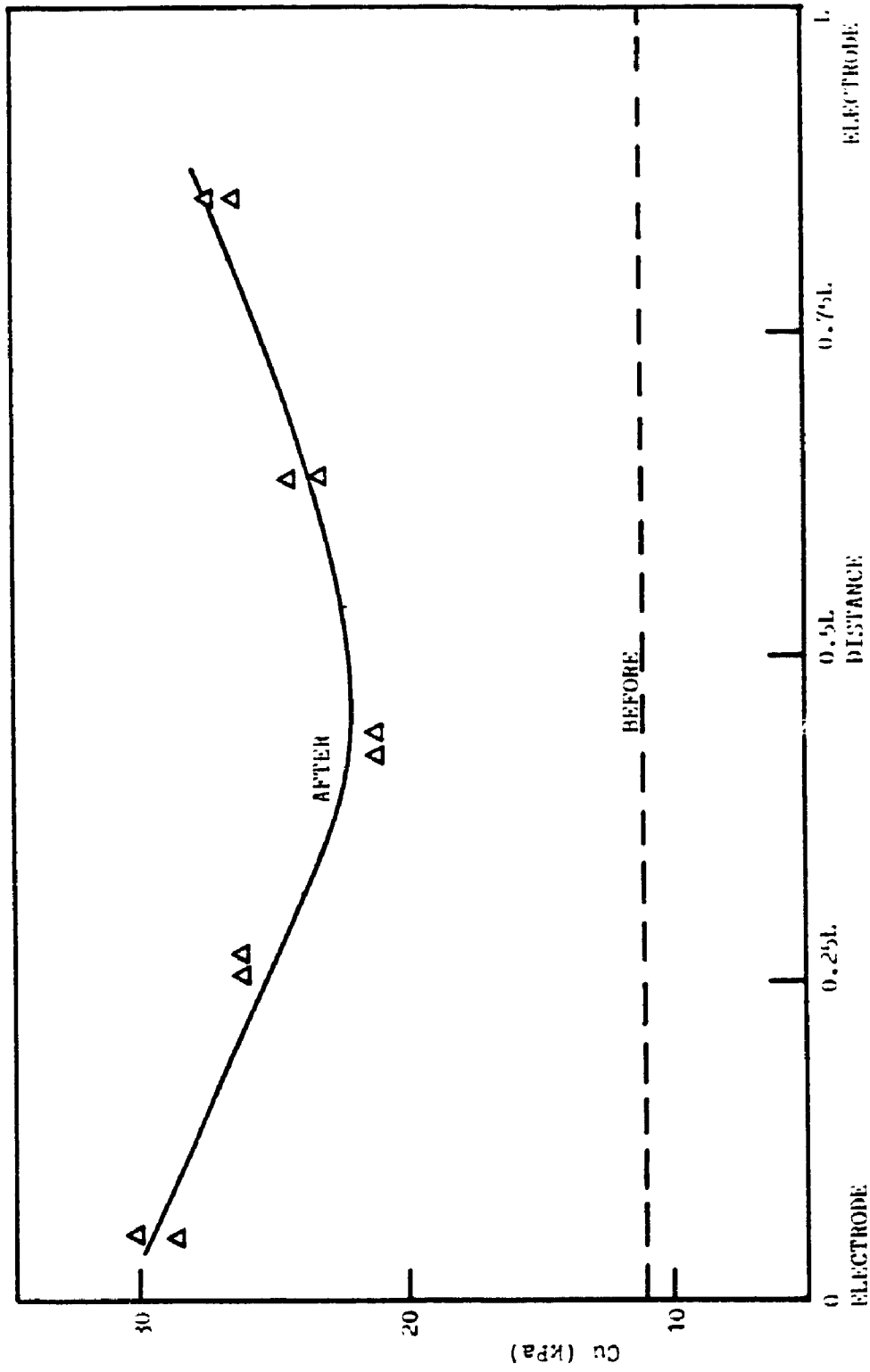

Fig. A59 VANE STRENGTH BEFORE AND AFTER TREATMENT TEST GV-48, 1.5, 0.4, 4 V WITH ELECTRODE REVERSAL

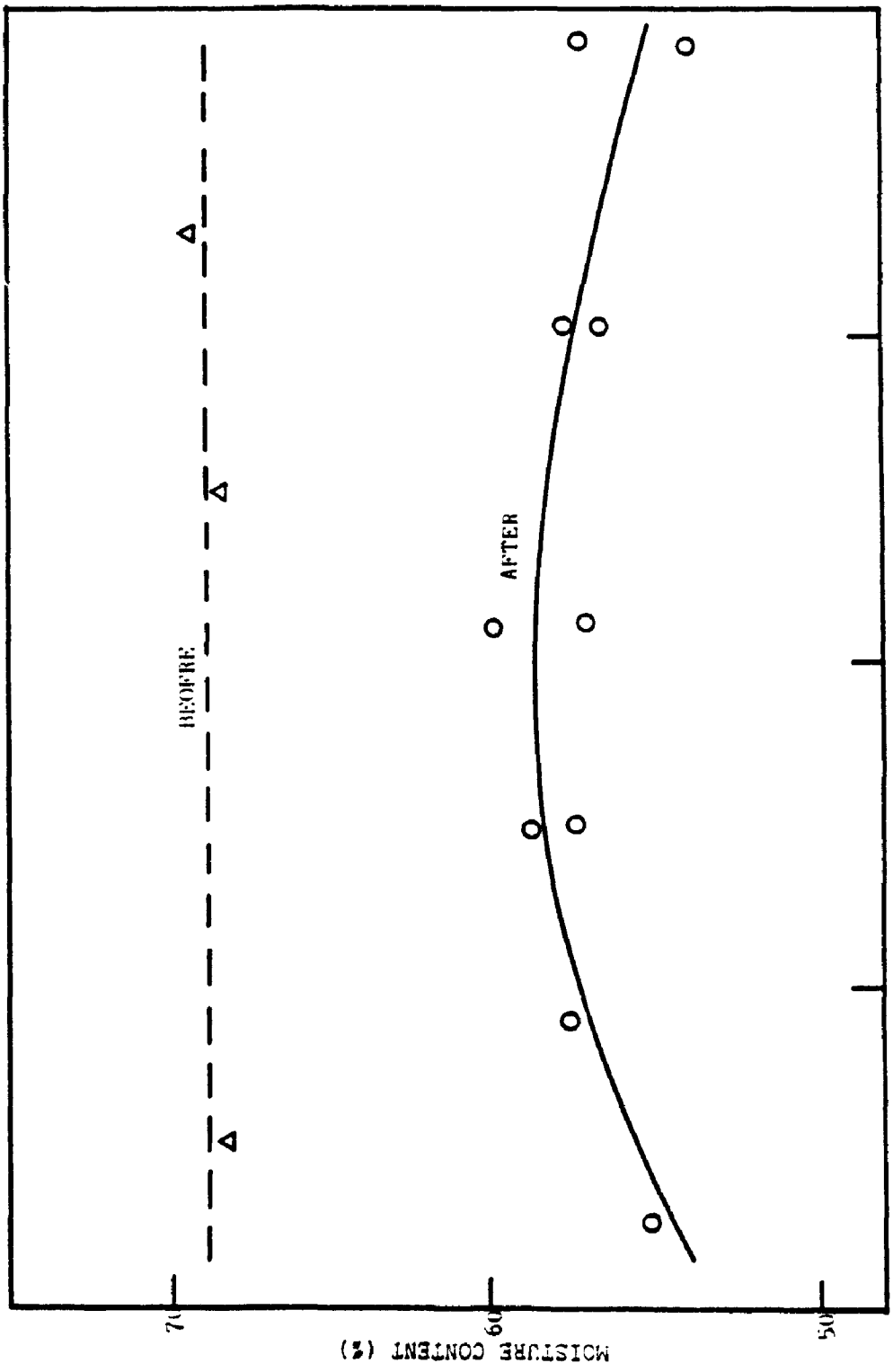

FIG. A60 MOISTURE CONTENT BEFORE AND AFTER TREATMENT, TEST GV-4B, 1.5, 2.4, 4 V WITH ELECTRODE REVERSAL

BIBLIOGRAPHY

Arnold, M. 1973. Laboratory determination of the coefficient of electro-osmotic permeability of a soil. Geotechnique, Vol. 23, No. 4, pp.581-588.

Arulanandan, K. 1969. Hydraulic and electrical flows in clays. Clays and Clay Minerals, Vol. 17, pp.63-76.

Ballou, E.V. 1955. Electroosmotic flow in homoionic kaolinite. Journal of Colloid Science, Vol. 10, pp.450-460.

Bally, R-J. and Antonescu, I.P. 1961. Application de l'électro-osmose à l'étude des sols et à leur consolidation. Proceedings, 5th International Conference on Soil Mechanics and Foundation Engineering, Vol. 1, pp.7-11.

Banerjee, S. and Mitchell, J.K. 1980a. In-situ volume-change properties by electro-osmosis - theory. Journal of the Geotechnical Engineering Division, ASCE, Vol 106, GT4, pp.347-365.

Banerjee, S. and Mitchell, J.K. 1980b. In-situ volume-change properties by electro-osmosis - evaluation. Journal of the Geotechnical Engineering Division, ASCE, Vol. 106, GT4, pp.367-384.

Banerjee, S. and Vitayasupakorn, V. 1984. Appraisal of electro-osmotic oedometer tests. Journal of the Geotechnical Engineering, ASCE, Vol. 110, GT8, pp.1007-1023.

Becker, D.E. and Lo, K.Y. 1981. Settlements under intermittent loading. Proceedings, 10th International Conference on Soil Mechanics and Foundation Engineering, Vol. 1, pp.35-40.

Begemann, Ir H.K.S.Ph. 1953. The influence of a direct current potential on the adhesion between clay and metal objects. Laboratory and full scale tests. Proceedings, 3rd International Conference on Soil Mechanics and Foundation Engineering, Vol. 1, pp.89-93.

Benguigui, L. and Lin, I.J. 1988. Dielectrophoresis in two dimensions. Journal of Electrostatics, Vol. 21, pp.205-213.

Bernatzik, W. 1948. Electro-osmosis, contribution to the problem of the seepage pressure in electro-osmosis. Proceedings, 2nd International Conference on Soil Mechanics and Foundation Engineering, Vol. 7, pp.65-66.

Bishop, A.W. 1967. Progressive failure-with special reference to the mechanism causing it. Panel discussion. Proceedings, Geotechnical Conference, Oslo, Vol. 2, pp.142-150.

Bishop, A.W. and Henkel, D.J. 1962. The measurement of soil properties in the triaxial test. 2nd Edition, Edward Arnold & Co., London.

Bjerrum, L. 1967. Engineering geology of Norwegian normally-consolidated marine clays as related to settlements of buildings. Geotechnique, Seventh Rankine Lecture, Vol. 17, pp.81-118.

Bjerrum, L., Moum, J. and Eide, O. 1967. Application of electro-osmosis to a foundation problem in a Norwegian quick clay. Geotechnique, Vol. 17, pp.214-235.

Boast, W.B. 1948. Principles of electric and magnetic fields. Harper & Brothers, New York.

Bozozuk, M. and Labrecque A. 1969. Down drag measurements on 270-ft composite piles. ASTM Special Technical Publication No. 444, pp.15-40.

Bozozuk, M. and Leonards, G.A. 1972. The Gloucester test fill. Special Conference on Performance of Earth and Earth-Supported Structures, ASCE, Purdue University, Vol. 1, Part 1, pp.299-317.

Butterfield, R., and Johnston, I.S. 1980. The influence of electro-osmosis on metallic piles in clay. Geotechnique, Vol. 30, No. 1, pp.17-38.

Cambefort, H. and Caron, C. 1961. Electro-osmose et consolidation électro-chimique des argiles. Geotechnique, Vol. 11, No. 3, pp.203-223.

Caron, C. 1971a. Consolidation électrochimique du sol de la Culée Rive Droite du Pont de la Basse-Chaine a Angers. Annales I.T.B.T.P., Paris, France, No. 66, pp.11-13.

Caron, C. 1971b. Consolidation des terrains argileus par électro-osmose. Annales I.T.B.T.P., Paris, France, No. 82, pp.75-92.

Casagrande, L. 1935. Method of hardening soils. U.S. Patent No. 2,099,328,1937 (Application, Jan. 7, 1935).

Casagrande, L. 1941. Die Elektrische Entwasserung Feinkorniger Boden. Die Strasse, No.19-20.

Casagrande, L. 1947. The application of electro-osmosis to practical problems in foundations and earthworks. Building Research Technical Paper No.30, Her Majesty Stationery Office, London.

Casagrande, L. 1948. Electro-osmosis. Proceedings of the Second International Conference on Soil Mechanics and Foundation Engineering. Rotterdam, Vol. 1, pp.218-223.

Casagrande, L. 1949. Electro-osmosis in Soils. Geotechnique, Vol. 1, No. 3, pp.159-177.

Casagrande, L. 1952a. Electro-osmosis stabilization of soils. Journal of Boston Society of Civil Engineers, January, Vol. 39, pp51-83.

Casagrande, L. 1952b. Electrical Stabilization in earthwork and foundation engineering. Proceedings of Conference on Soil Stabilization, Massachusetts Institute of Technology, Cambridge, pp.84-106.

Casagrande, 1953. Review of past and current work on electro-osmosis stabilization of soils. Report to the Bureau of Yards and Docks, Harvard Soil Mechanics Series No. 45, Massachusetts.

Casagrande, L. 1959. Practical aspects of electro-osmosis in foundation engineering. Proceedings, Pan American Conference on Soil Mechanics and Foundation Engineering, Vol. 1, pp.217-233.

Casagrande, L. 1962. Electro-osmosis and related phenomena. Harvard Soil Mechanics Series No. 66, Massachusetts, pp.51-62.

Casagrande, L. 1983. Stabilization of soils by means of electro-osmosis, State-of-the-Art. Journal of the Boston Society of Civil Engineers, Vol. 69, No.2, pp.225-302.

Casagrande, L., Longhney, R.W. and Matich, A.J. 1961. Electro-osmotic stabilization of a high slope in loose saturated silt. Proceedings, 5th International Conference on Soil Mechanics and Foundation Engineering, Paris, Vol. 2, pp.555-561.

Casagrande, L., Wade, N., Wakely, M. and Loughney, R.W. 1981. Electro-osmosis projects, British Columbia, Canada. Proceedings, 10th International Conference on Soil Mechanics and Foundation Engineering, Rotterdam, pp.607-610.

Chandler, J.E. and Wilkinson, R.J. 1979. Chemistry. Charles Letts & Co. Ltd.

Chapman, L.J. and Putnam, D.F. 1951. The Physiography of Southern Ontario. University of Toronto Press.

Chappell, B.A. and Burton, P.L. 1975. Electro-osmosis applied to unstable embankment. Journal of Geotechnical Engineering Division, ASCE, Vol. 101, GT8, pp.733-739.

Conway, B.E. 1965. Theory and Principles of Electrode Processes. The Ronald Press Co.

Crawford, C.B. 1961. Engineering studies of Leda clay. Soils in Canada. The Royal Society of Canada, pp.200-217.

Crawford, C.B. 1963. Cohesion in an undisturbed sensitive clay. Canadian Geotechnical Journal, Vol. 13, pp.132-146.

Crawford, C.B. 1967. Stability of natural slopes in sensitive clay. Journal of the Soil Mechanics and Foundations Division, ASCE, Vol. 93, SM4, pp.419-436.

Crawford, C.B. 1968. Quick clays of eastern Canada. Engineering Geology, Vol. 2, No. 4, pp.239-265.

Crowley, J.M. 1984. Fundamentals of applied electrostatics. John Wiley & Sons, New York.

Dawson, R.F. and McDonald, R.W 1948. Some effects of electric current on the consolidation characteristics of a soil. Proceedings, 2nd International Conference on Soil Mechanics and Foundation Engineering, Vol. 5, pp.51-57.

Esrig, M.I. 1968a. Pore pressures, consolidation and electrokinetics. Journal of the Soil Mechanics and Foundations Division, ASCE, Vol.94, SM4, pp.899-921.

Esrig, M.I. 1968b. Applications of electrokinetics in grouting. Journal of the Soil Mechanics and Foundations Division. Proceedings, ASCE, Vol.94, SM5, pp.1143-1157.

Esrig, M.I. and Gemeinhardt, J.P. 1967. Electrokinetic stabilization of an illitic clay. Journal of the Soil Mechanics and Foundations Division, ASCE, Vol.93, SM3, pp.109-128.

Esrig, M.I. 1971. Electrokinetics in soil mechanics and foundation engineering. Transactions of New York Academy of Sciences, Vol. 33, Series II, No.2, pp.234-245.

Evans, H.E. and Lewis, R.W. 1966. Application of electro-osmosis to the direct measurement of negative pore water pressures during triaxial compression testing of soils, Civil Engineering and Public Works Review, March, pp.299-304.

Ferguson, J.F. and Nelson, P. 1986. Migration of inorganic contaminants in groundwater under the influence of an electrical field. Workshop on Electrokinetic Treatment for Hazardous Waste Site Remediation, Cincinnati, August, Section V, pp.1-27, unpublished.

Fetzer, C.A. 1967. Electro-osmotic stabilization of West Branch Dam. Journal of the Soil Mechanics and Foundations Division, ASCE, Vol.93, SM4, pp.85-106.

Foecke, H.A. 1961. Introduction to electrical engineering science. Prentice-Hall, Inc. New Jersey.

Franceschini, A. 1975. Method for the electro-osmotic conversion of the scaly structure of a moist clay mass into a granular structure. U.S. Patent No. 3,915,826 (Application Oct. 28, 1975).

Geuze, E.C.W.A., De Bruyn, C.M.A. and Joustra, K. 1948. Results of laboratory investigation of the electrical treatment of soils. Proceedings, 2nd International Conference on Soil Mechanics and Foundation Engineering, Vol. 3, pp.153-157

Gilbert, W. 1600. De Magnete. Peter Short, London.

Gray, D.H. 1979. Electrochemical hardening of clay soils. Geotechnique, Vol. 20, No. 1, pp.81-93.

Gray, D.H. and Somogyi, F. 1977. Electro-osmotic dewatering with polarity reversals. Journal of the Geotechnical Engineering Division, ASCE, Vol. 103, GT1, pp.51-54.

Gray, D.H. and Mitchell, J.K. 1967. Fundamental aspects of electro-osmosis in soils. Journal of the Soil Mechanics and Foundations Division, ASCE, Vol. 93, SM6, pp.209-236.

Gray, D.H. and Olsen, H.W. 1986. Physics and Chemistry of electrokinetic processes. Workshop on Electrokinetic Treatment for Hazardous Waste Site Remediation, Cincinnati, August, Section III, pp.1-25, unpublished.

Gray, D.H. 1969. Prevention of moisture rise in capillary systems by electrical short circuiting. Nature, Vol.223, No. 5204, pp.371-374.

Gouy, M. 1910. Sur la constitution de la charge électrique à la surface d'un électrolyte. Journal de Physique, 4e série, tome IX, pp.457-468.

Helmholtz, H.L.F. 1879. Wiedemanns Annalen D. Physik, Vol. 7, Leipzig, Germany, pp.337-382. (Translated by Bocquet, P.E., "Studies of electric boundary layers", Two Monographs on Electrokinetics, University of Michigan Engineering Research Institute, Ann Arbor, Bulletin No. 33, October 1951, pp.5-47.)

Hicky, W.E. and Loughney, R.W. 1959. Electricity stabilizes bridge subsoil. Engineering News-Record, April 16.

Hippel, A.R. Von. 1954. Dielectrics and Waves. Wiley, New York.

Inculet, I.I. and Lo, K.Y. 1988. Dielectrophoretic consolidation of clays. Conference Record of the IEEE Industry Applications Society Annual Meeting, Part II, October 2-7, pp.1574-1577.

Javid, M. and Brown, P.M. 1963. Field analysis and electromagnetics. McGraw-Hill Book Co., New York.

Johnston I.W. and Butterfield, R. 1977. A laboratory investigation of soil consolidation by electro-osmosis. Australian Geomechanics Journal, G7, pp.21-32.

Jones, T.B. 1979. Dielectrophoretic force calculation. Journal of Electrostatics, Vol. 6, pp.69-82.

Jones, T.B. 1986. Dielectrophoretic force in axisymmetric fields. Journal of Electrostatics, Vol. 18, pp.55-62.

Karrow, P.F. 1961. The Champlain Sea and its sediments. Soils in Canada, The Royal Society of Canada, Edited by R.F. Legget, pp.97-108.

Law, K.T. 1974. Analysis of embankment on sensitive clays. Ph.D. Thesis, University of Western Ontario, London, Ontario.

Lewis, R.W. 1967. Effects of electro-kinetic phenomenon on soil stabilization. Proceedings, 12th Canadian Soil Mechanics Conference, Quebec City.

Lewis, R.W. and Garner, R.W. 1972. A finite element solution of coupled electro-kinetic and hydrodynamic flow in porous media. International Journal for Numerical Methods in Engineering, Vol. 5, pp.41-55.

Lewis, R.W. and Humpheson, C. 1973. Numerical analysis of electro-osmotic flow in soils. Journal of the Soil Mechanics and Foundations Division, ASCE, Vol. 99, SM8, pp.603-616.

Lo, K.Y. and Becker, D.E. 1979. Pore-pressure response beneath a ring foundation on clay. Canadian Geotechnical Journal, Vol. 16, No. 3, pp.551-566.

Lo, K.Y. and Becker, D.E. 1980. Settlement analysis of intermittently-loaded structures. Research Report GEOT-4-80, Faculty of Engineering Science, University of Western Ontario.

Lo, K.Y., Bozozuk, M. and Law, K.T. 1976. Settlement analysis of the Gloucester test fill. Canadian Geotechnical Journal, Vol. 13, pp.339-354.

Lo, K.Y., Inculet, I.I. and Ho, K.S. 1990a. Laboratory investigation of electro-osmotic strengthening of soft sensitive clays. Canadian Geotechnical Journal, Vol. 27, No.6 (in print).

Lo, K.Y., Inculet, I.I. and Ho, K.S. 1990b. Field test of electro-osmotic strengthening of soft sensitive clays. Proceedings, 43rd Canadian Geotechnical Conference, October 10-12, Quebec, P.Q., (in print).

Lo, K.Y. and Morin, J.P. 1972. Strength anisotropy and time effects of two sensitive clays. Canadian Geotechnical Journal, Vol. 9, pp.261-277.

Lomizé, G.M., Netushil, A.V. and Rzmanitzin, B.A. 1957. Electro-osmotic processes in clayey soils and dewatering during excavations. Proceedings, 4th International Conference on Soil Mechanics and Foundation Engineering. Vol. 1, London, pp.62-68.

Ministry of Transportation and Communications, Ontario. 1981. Pile load and extraction tests 1954 - 1980. Report EM-48. 297p.

Mise, T. 1961. Electro-osmotic dewatering of soil and distribution of the pore water pressure. Proceedings, 5th International Conference on Soil Mechanics and Foundation Engineering, Vol. 1, pp.255-258.

Mitchell, J.K. and Wan, T.Y. 1977. Electro-osmotic consolidation - Its effects on soft soils. Proceedings, 9th International Conference on Soil Mechanics and Foundations Engineering, Vol.1, pp.219-224.

Mitchell, J.K. 1967. Fundamentals of soil behavior. John Wiley & Sons, New York.

Mitchell, J.K. 1970. In-place treatment of foundation soils. Journal of the Soil Mechanics and Foundations Division, ASCE, Vol. 96, SM1, pp.73-110.

Mitchell, J.K. 1986. Potential uses of electro-kinetics for hazardous waste site remediation. Workshop on Electro-Kinetic Treatment and Its Application in Environmental-Geotechnical Engineering for Hazardous Waste Site Remediation, Cincinnati, August, Section II, pp.1-20, unpublished.

Morris, D.V., Hillis, S.F. and Caldwell, J.A. 1985. Improvement of sensitive silty clay by electro-osmosis. Canadian Geotechnical Journal, Vol. 22, pp.17-24.

Mugeraya, S. and Prabhakar, B.R. 1986. Measurement of resistivity and dielectric constant of beach-sand minerals. Journal of Electrostatics, Vol. 18, pp.109-112.

Murayama, S. and Mise, T. 1953. On the electrochemical consolidation of soil using aluminium electrodes. Proceedings, 3rd International Conference of Soil Mechanics and Foundation Engineering, Vol. 1, pp.156-159.

Nicholls, R.L. and Herbst, R.L. 1967. Consolidation under electrical pressure gradients. Journal of the Soil Mechanics and Foundations Division, ASCE, Vol. 93, SM5, pp.139-151.

Piaskowski, A. 1957. Investigations on electro-osmotic flow in soils in relation to different characteristics. Proceedings, 4th International Conference on Soil Mechanics and Foundation Engineering, Vol. 1, pp.89-92.

Pickard, W.F. 1965. Progress in Dielectrics, Vol. 6.

Pohl, H.A. 1951. The motion and precipitation of suspensoids in divergent electric fields. Journal of Applied Physics, Vol. 22, pp.869.

Pohl, H.A. 1978. Dielectrophoresis, The behavior of neutral matter in nonuniform electric fields. Monographs on Physics, Cambridge University Press.

Pohl, H.A. and Pickard, W.F. 1969. Dielectrophoretic and electrophoretic deposition. The Electrochemical Society, Inc. New York.

Potter, E.C. 1956. Electrochemistry - Principles and Applications. Cleaver-Hume Press Ltd.

Priestley, J. 1769. The history and present state of electricity with original experiments, 2nd Edition, London.

Probstein, R.F. and Renaud, P.C. 1986. Quantification of fluid and chemical flow in electrokinetics. Workshop on Electro-Kinetic Treatment and Its Application in Environmental-Geotechnical Engineering for Hazardous Waste Site Remediation, Cincinnati, August, Section IV, pp.1-48, unpublished.

Quigley, R.M. 1980. Geology, mineralogy, and geochemistry of Canadian soft soils: a geotechnical perspective. Canadian Geotechnical Journal, Vol. 17, pp.261-285.

Quigley, R.M., Fernandez, F. and Ohikere, C. 1989. Compatibility of Leda clay with municipal solid waste leachate. Research Report No. GEOT-6-89, Faculty of Engineering Science, University of Western Ontario.

Quigley, R.M. and Ogunbadejo, T.A. 1976. Till geology, mineralogy and geotechnical behaviour, Sarnia, Ontario. In Glacial till. Edited by R.F. Legget, Royal Society of Canada Special Publication 12, pp.336-345.

Renaud, P.C. and Probstein, R.F. 1987. Electroosmotic control of hazardous wastes. PCH PhysicoChemical Hydrodynamics, Vol. 9, No. 1/2, pp.345-360.

Reuss, F.F. 1809. Sur un nouvel effet de l'électricité galvanique. Memoires de la Societé Imperiale des Naturalists de Moscow, Moscow, Vol.2, pp.327-337.

Schmidt, G. 1950, 1951. Zur Elektrochemie Feinporiger Kapillarsystems. Zhurnal fur Elektrochemie, Vol. 54, p.425, Vol. 55, p.684.

Selig, E.T. and Mansukhani, S. 1975. Relationship of soil moisture to the dielectric property. Journal of the Geotechnical Engineering Division, ASCE, Vol. 101, GT8, pp.755-770

Segall, B.A., O'Bannon, C.E. and Judson, A.M. 1980. Electro-osmosis chemistry and water quality. Journal of the Geotechnical Engineering Division, ASCE, Vol. 106, GT10, pp.1148-1152.

Shalom, A.L. and Lin, I.J. 1984. A study of the mechanisms of particle build-up on single rods in dielectrophoretic separation. Proceedings, IEEE - Industry Application, Annual Meeting, Chicago, October, pp.1125-1129.

Shukla, K.P. 1953. Electro-chemical treatment of clays. Proceedings, 3rd International Conference on Soil Mechanics and Foundation Engineering, Vol. 1, pp.199-202.

Smoluckowski, M. 1914. Handbuch der Elektrizitat und Magnetismus. L.Graetz, Ed., Vol. 2, J.A. Barth, Leipzig.

Soderman, L.G. and Milligan, V. 1961. Capacity of friction piles in varved clay increased by electro-osmosis. Proceedings, 5th International Conference on Soil Mechanics and Foundation Engineering, Vol.II, Paris, pp.143-147.

Soderman, L.G. and Quigley, R.M. 1965. Geotechnical properties of three Ontario clays. Canadian Geotechnical Journal, Vol. 11, No. 2, pp.167-189.

Spiegler, K.S. 1958. Transport processes in ionic membranes. Transactions of the Faraday Society, Vol. 54, pp.1408-1428.

Sundaram, P.N. 1979. Hydraulic and electro-osmosis permeability coefficients. Journal of the Geotechnical Engineering Division, ASCE, Vol. 105, GT1. pp.89-92.

Titkov, N.I., Petrov, V.P. and Neretina, A. 1961. Mineral formation and structure in the electrochemical induration of weak rocks. Translation from Russian by Consultants Bureau, New York, 70pp.

Van Doren, E.P. and Bruell, C.J. 1987. Electro-osmotic removal of benzene from a water saturated clay. Proceedings of the NWWA/API Conference on Petroleum Hydrocarbons and Organic Chemicals in Groundwater - Prevention, Detection and Restoration, Houston, Texas, November 17-19, pp.107-126.

Vey, E. 1949. The mechanics of soil consolidation by electro-osmosis. Proceedings, Highway Research Board, Vol. 29, pp.578-589.

Wade, M.H. 1976. Slope stability by electro-osmosis. Proceedings, 29th Canadian Geotechnical Conference, Vancouver, Section X, pp.44-66.

Wan, T.Y. and Mitchell, J.K. 1976. Electro-osmotic consolidation of soils. Journal of the Geotechnical Engineering Division, ASCE, Vol. 102, Gt5, pp.473-491.

Wan, T.Y. and Mitchell, J.K. 1975 New apparatus for consolidation by electro-osmosis. Journal of the Geotechnical Engineering Division, ASCE, Vol. 101, GT5, pp.503-507.

Wang, N.S. and Vey, E. 1953. Stresses in a saturated soil mass during electro-osmosis. Proceedings, 3rd International Conference on Soil Mechanics and Foundation Engineering, Zurich, Switzerland, pp.76-79.

Winckler, F.H. 1748. Essai sur la nature; Effects et les cause de l'électricité, Vol. 1, Sebastian Jorry, Paris.

Yoshida, H., Shinkawa, T. and Yukawa, H. 1985. Water content and electric potential distributions in gelatinous bentonite slidge with electro-osmotic dewatering. Journal of Chemical Engineering, Japan, Vol. 18, No. 4, pp.337-342.